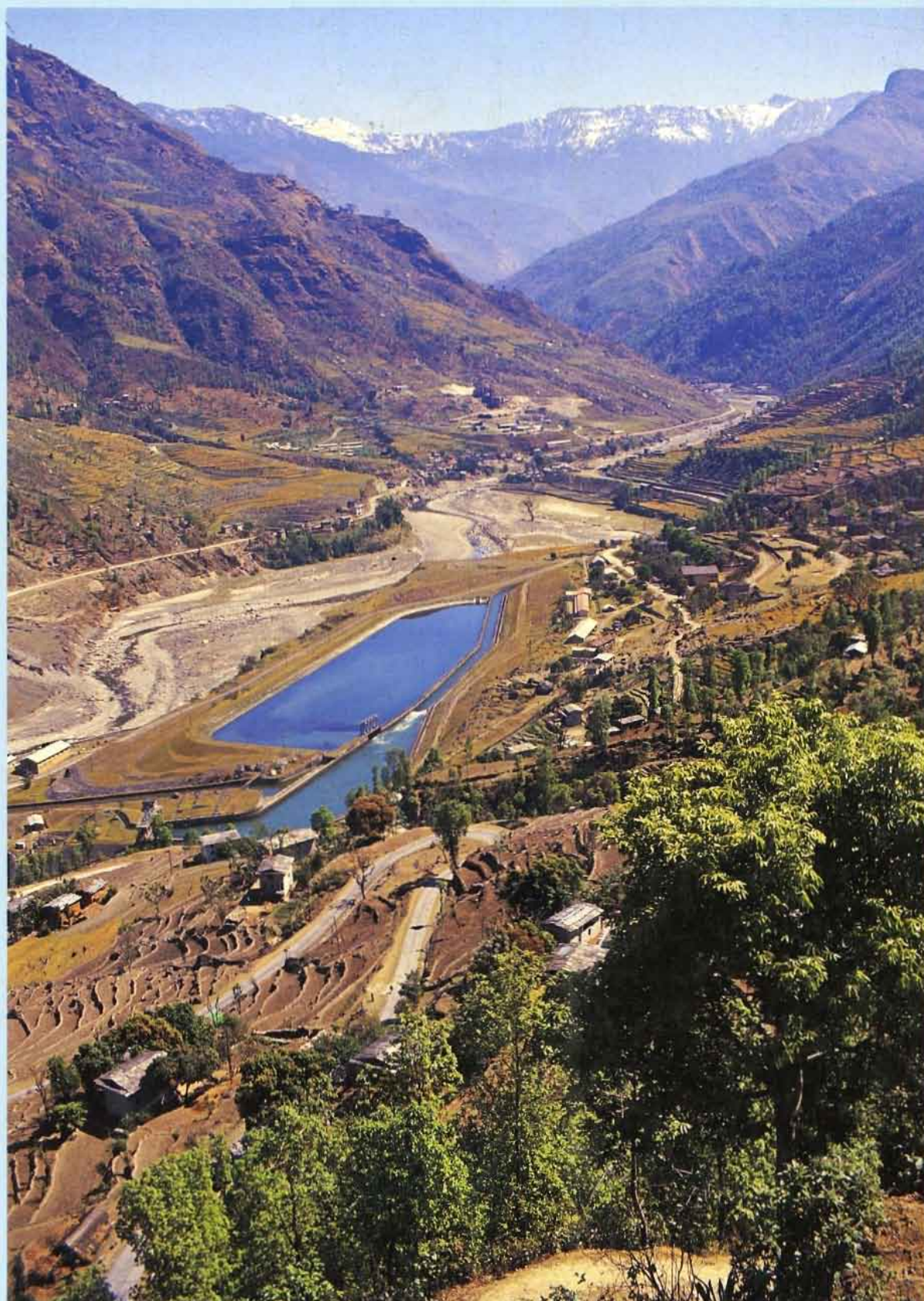


MOUNTAIN RISK ENGINEERING HANDBOOK

SUBJECT BACKGROUND: Part I



Cover Photographs : B. Deoja

**Front : Damages to a mountain road
along a river.**

Arniko Highway, Nepal, March 1991.

**Back : A road blending with the
environment - Lamosangu-Jiri Road.**

Mountain Risk Engineering Handbook - Part I

Subject Background

Principal Editors : **B. Deoja, M. Dhital, B. Thapa, A. Wagner**

Published by
International Centre for Integrated Mountain Development
Kathmandu, Nepal

Copyright © 1991

International Centre for Integrated Mountain Development

All rights reserved

Cover Photographs : B. Deoja

Front : Damages to a mountain road along a river.
Aniko Highway, Nepal, March 1991

Back : A road blending with the environment.
Lamosangu-Jiri Road. Nepal, March 1991

Citation:

International Centre for Integrated Mountain Development, 1991.

Mountain Risk Engineering Handbook : Part I - Subject Background

G.P.O. Box 3226, Kathmandu, Nepal

Typesetting : ICIMOD Computer Centre

Please direct all enquiries and comments to:

International Centre for Integrated Mountain Development

G.P.O. Box 3226, Kathmandu, Nepal

Telephone: (977-1) 525313

Telex: 2439 ICIMOD NP

Fax: (977-1) 524509

Cable: ICIMOD, NEPAL

PREFACE

The progressive and effective development of mountain communities through an integrated approach is the principal perspective in ICIMOD's mandate. Infrastructural establishment, therefore, being one of the primary needs for development, has to be carried out, taking into consideration this integrated, holistic perspective. Notwithstanding, experiences indicate that integration of essential modern development technologies with effective and sustainable resource management has not received sufficient attention.

In the Hindu Kush-Himalayan (HKH) Region, failures and washouts of roads, irrigation canals, and power plants have resulted in considerable losses of life and property. In addition, the vulnerability of mountain ecosystems has been exacerbated by the techniques applied in establishing infrastructure. Development with conservation is, therefore, essential.

The impacts of artificial structures and human interventions on mountain slopes can only be understood adequately within the context of a broader-based knowledge and understanding of the inherent properties of the materials constituting the mountains themselves and the dynamics that influence the surface and sub-surface processes and environments. Traditional civil engineering education and practices are not adequate to fulfill this requirement.

Geology, the science of the earth, can help to provide the requisite understanding so that civil engineers will have a clear picture of what can be done to keep a structure in place throughout its expected life. This knowledge, however, is only useful to the engineer provided the time horizon, material, and process characterisation provided by geology are adequately scaled, quantitatively ascertained, and clearly presented to facilitate their direct input into civil engineering analysis and design.

The application of engineering-geological inputs is not new in the case of major projects such as dams, tunnels, and mines, but in the case of linear infrastructure, such as roads and canals, scant attention has been paid to engineering-geological inputs, especially in the developing countries. As the pressure of population increases in the mountains, there will be a need for more roads and canals throughout these areas. The additional impacts caused by their construction are bound to accelerate natural destabilization and processes caused by people will add to the forces of nature. This presents us with a choice, i.e., people as a positive force, friendly to nature, or as a negative force that is hostile to nature.

The devegetation and deforestation associated with infrastructural establishment have created an extremely important role for soil conservation, forestry, and ecology so that establishment of plantations and vegetation within the watershed areas that influence roads has become an integral part of normal engineering practice. Long-term, sustainable protection of mountain slopes influences infrastructural stability and, in this respect, plantations and vegetation are crucial because engineering solutions alone are neither cost-effective nor hospitable to mountain ecosystems.

Infrastructural development is no longer the domain of a single discipline, i.e., civil engineering, and mountain infrastructural engineering cannot be separated from a basic knowledge of the geology, environment, and other related disciplines. The Mountain Risk Engineering (MRE) Programme introduced by ICIMOD is a step forward in the process of the integration of various disciplines in order to induce the establishment of sustainable mountain infrastructural institutions.

This handbook is a synthesis of selected practical experiences and up-to-date literature, and its objective is to provide a working basis for training institutions and practising engineers and geologists involved in the development of infrastructure in mountainous areas, in general, and in the mountainous areas of developing countries, in particular.

The question arises, in the case of developing countries with low per capita income, of the additional costs incurred by MRE approaches. How much room is realistically available in fragile mountain terrains for site selection? how compatible is the concern for resource conservation over the long term with the immediate needs of a subsistence economy? and so on.

A comprehensive response to all of these concerns is outside the scope of this Handbook. Nevertheless, experience has shown that there is ample room for the minimisation of hazards and that the cost of rehabilitating failed infrastructures will easily offset the one or two per cent of additional expenditure needed for proper investigation and analysis. In addition, the benefits accruing from soil loss reduction and reduction in the loss of productive land, caused by hazards incurred by infrastructures designed within a narrow framework, are additional bonuses.

This handbook is a combination, of an earlier draft version and incorporates inputs and comments received from several resource persons and institutions, both in the Region itself and from other parts of the world. For this reason, and because of the limited time period permitted for its completion, the general spelling style has, by and large, had to follow the most common usage prevailing in the case of each term and word. Had we standardised to one of the principal dictionary styles (Websters or Oxford) the document would not have been completed within the time-frame required, given the facilities available. In short, the amount of material to be edited, and the degree of editing prohibited by this, is a fact regretted by the editor.

The complete MRE approach has been used to conduct a feasibility study for, and to design a road project in, Nepal. Obviously, there will be more inputs of this nature in future and the Handbook will need revision from time to time until Mountain Risk Engineering establishes itself as a discipline in its own right and until it is fully institutionalised within the infrastructural agencies of the developing mountain nations. In this respect, an Expert Group Meeting, International Consultative Meeting, Pilot Training, and individual visits from academicians, policy makers, and donor agencies have served to indicate the sizeable degree of enthusiasm already existing as a result of the establishment of the Mountain Risk Engineering Project.

Thanks are due to all those who helped us to achieve this task; those who inspired ICIMOD and who became inspired by ICIMOD about Mountain Risk Engineering. The mountains, which remained seemingly silent, but nonetheless dynamic, will give more to mountain inhabitants than they will receive provided we handle them with care.

These mountains, seemingly silent but truly dynamic, have a lot to give to the people of the mountains as well as to the people of the plains provided we start to understand and appreciate them. MRE, thus, begins this process.

Birendra Deoja

MRE Project Coordinator

ACKNOWLEDGEMENTS

This handbook on Mountain Risk Engineering (MRE) is the product of the contributions of many people. I am grateful to all of them. In particular, I wish to record my deep appreciation and thanks to Dr. Colin Rosser, the Previous Director, for the initiation of Mountain Risk Engineering (MRE) work at ICIMOD and Dr. E. F. Tacke, the current Director, for his encouragement and untiring support throughout the work on the completion of MRE Phase I and for initiating MRE Phase II which has resulted in the first full-scale publication of this Handbook.

The generous financial support of the Commission of the European Economic Community (EEC), for Phase I, and the Swiss Development Cooperation (SDC) and German Technical Assistance (GTZ), for Phase II, are gratefully acknowledged. This is indicative of their growing concern for the deteriorating mountain environment and the increasing impoverishment of its inhabitants.

Alexis Wagner of ITECO International, Switzerland, Dr. Mahesh Banskota, Chief Programme Coordinator, Mr. Surendra Shrestha, the Chief Administrator, and Dr. M. Abdullah, the former Head of the Mountain Infrastructure and Technology Division of ICIMOD, assisted in the development of the project proposal and also helped in many ways in the completion of this work. Similarly, N.D. Sharma, Director General of the Department of Roads, HMG, Nepal provided his enthusiastic support and guidance. There were also several institutions that have been supportive throughout the whole period and a few of these are: The Department of Roads, HMG, Nepal; ITECO International, Switzerland; The University of Roorkee, India; The Transport and Road Research Laboratory (TRRL), U.K.; The Public Works' Department, Bhutan; The Ministry of Communication, NWFP, Pakistan; The Chinese Academy of Sciences, Beijing; Tribhuvan University, Kirtipur, Kathmandu; The Department of Mines and Geology, HMG, Nepal; and ITECO-Nepal, Kathmandu.

Professor H. Einstein of the Massachusetts Institute of Technology (MIT), U.S.A., Dr. Robert Schuster, USGS, Professor Tien Wu of Ohio University, and Dr. G. C. Nayak of the University of Roorkee, deserve unlimited thanks for devoting so much of their time and attention to provide valuable comments on the draft of the Manual and for attending the Consultative Meeting in February 1990. Also Dr. Donald H. Gray provided invaluable comments on biotechnical stabilizations.

Cliff Lawrance of TRRL, U.K., and Jane Clark and John Howell of Roughton and Partners, U.K., provided their valuable inputs in the field of geomorphology and biotechnical stabilizations.

The Handbook would never have been completed, within the short period of time given, without the untiring efforts of its team of contributors, Dr. R. Anbalagan, Dr. Dominique Chapellier, Dr. M. Dhital, Tom Heah, K.C. Manandhar, Dr. Tej Partap, Urs Schaffner, Dr. Bhawani Singh, Bhaskar Thapa, and Alexis Wagner.

Uday Tegi, Usha Tamang, Sudas Sharma, Prerna Rana, and Rajendra Shah have put in an unlimited number of hours in order to type several versions of the manuscript. They have been supportive, patient, and tireless throughout this whole endeavour.

Greta Rana, the editor of ICIMOD, undertook the task of editing this voluminous manuscript in such a short period of time and made our task easier in preparing this manuscript which is now lucid and readable.

The figures for the handbook have been painstakingly prepared by three excellent draughtsmen, Bipin Ghimire, P.B. Shaky, and S. B. Phainju.

There are many others who have given their support both within and outside ICIMOD and, although they have not been listed here because of paucity of space, they are gratefully and duly acknowledged. Finally, we are grateful to all those authors whose generous contributions have made it possible to bring out this Handbook on Mountain Risk Engineering.

Birendra Deoja

MRE Project Coordinator

CONTRIBUTORS

Dr. R. Anbalagan	Lecturer in Geology, Department of Earth Sciences, University of Roorkee, Roorkee, U.P. India. (Chapters 8 and 12)
Dr. D. Chapellier	Department of Geophysics, University of Lausanne, Lausanne, Switzerland. (Chapter 11)
B. B. Deoja	Project Coordinator, Mountain Risk Engineering Project, International Centre for Integrated Mountain Development (ICIMOD), Jawalakhel, Nepal. (Chapters 1, 9, 10, 13, 14, 15, 17, 18, and 20)
Dr. M. Dhital	Lecturer, Central Department of Geology, Tribhuvan University, Kirtipur, Nepal. (Chapters 2, 3, 4, 5, 7, 8, and 12)
Tom Heah	The University of British Columbia, Vancouver B.C., Canada. (Chapters 3, 4, and 6)
K. C. Manandhar	Consulting Engineer, Sub-Structural Consult, Kathmandu, Nepal. (Chapter 19)
Dr. Tej Partap	Ecologist, Mountain Farming Division, ICIMOD, Nepal. (Chapter 16)
Urs Schaffner	I&D Consult Ltd. Habsburgstrasse 6, CH-3006 Bern, Switzerland.
Dr. Bhawani Singh	Professor of Rock Mechanics, Department of Civil Engineering, University of Roorkee, U.P., India. (Chapters 9, 10, 13, and 17)
Bhaskar Thapa	Research Engineer, ICIMOD, Nepal. (Chapters 16 and 20)
A. Wagner	Consulting Engineering-Geologist, ITECO International, Afoltern a/A Switzerland. (Chapters 2 and 12)

FOREWORD

Infrastructural development in the Hindu Kush-Himalayan Region is a formidable task with considerable problems caused by washouts and failures resulting from landslides, erosion, and gullyng. Such problems are, to a significant extent, triggered by faulty planning and designing of mountain infrastructure which also have ramifications on their construction and maintenance. These problems are compounded by mass movements caused by natural processes, deforestation, and other human interventions. They constitute a huge challenge for the building and maintenance of sound physical infrastructure. Therefore, there is an urgent need to develop guidelines for the construction of infrastructure that is ecologically stable and economically viable. It is in this context that the mountain risk engineering programme was started in January 1988 with financial support from the European Economic Community (EEC).

The first draft manual on Training in Mountain Risk Engineering was tested during a nine week pilot training programme from February-April 1989. Twenty participants, mainly engineers and geologists from Bhutan, China, Nepal, and Pakistan, participated in the training sessions. Subsequently the manual was revised and put into folder form for convenient distribution. The preparation of the manual was undertaken by ICIMOD staff in close collaboration with short-term professional inputs from Europe and the Regional countries.

The manual was sent to international experts in this field for their comments. This was followed by the organisation of an International Consultative Meeting on Mountain Risk Engineering in February 1990 in Kathmandu. Some 40 experts, representing government agencies, consultants, donor agencies, and university professors, participated and commented on the content and utility of the manual. There was a general consensus that the MRE Manual was an extremely useful document in the context of providing guidance for sound infrastructural development and that its wider application is urgently needed. It has already been used by the Department of Roads and several foreign consultants in Nepal. As a follow up to the recommendation of the Consultative Meeting, the Swiss Development Cooperation (SDC) and the German Technical Cooperation Agency (GTZ) were approached for funding for the preparation of this Handbook for wider dissemination and for the organisation of an eight week training programme in Kathmandu on Mountain Risk Engineering; and this they have generously supported.

This Handbook is being produced in two parts and will provide useful reference materials to field engineers engaged in building ecologically and economically sound infrastructure in the mountains. It can also provide useful course material for students who are being trained as civil engineers and geologists.

Finally, Mr. Birendra Deoja, Coordinator of this activity deserves special mention, along with his colleagues, who worked extremely hard to bring out this very useful Handbook on Mountain Risk Engineering.

Dr. E. F. Tacke

Director

LIST OF CONTENTS

PREFACE	Page (i)
ACKNOWLEDGEMENTS	(iii)
FOREWORD	(v)
Chapter 1: INTRODUCTION	1
1.1 MOUNTAIN RISK ENGINEERING (MRE)	1
1.2 PURPOSE OF THE MRE HANDBOOK	1
1.3 STRUCTURE OF THE MRE HANDBOOK	2
1.4 CONTENTS OF THE MRE HANDBOOK	2
1.5 EVOLUTION OF THE MRE HANDBOOK	3
1.6 USING THE MRE HANDBOOK	4
1.6.1 Users of the MRE Handbook	4
1.6.2 Use of the MRE Handbook	4
1.7 TRAINING CURRICULUM	5
1.7.1 Field-based Practical Training Using Application Guide	5
1.7.2 Equipment and Trainers Required for MRE Training	6
Chapter 2: GEOLOGICAL PROCESSES	7
2.1 INTRODUCTION	
2.1.1 Branches of Geology	7
2.1.2 The Earth's Outer Zones	8
2.1.3 The Earth's Inner Zones	8
2.1.4 The Shape of the Earth	9
2.1.5 Isostasy	9
2.1.6 Plate Tectonics	11
2.1.7 The Geological Time Scale	13
2.2 EXOGENOUS AND ENDOGENOUS PROCESSES	14
2.2.1 Exogenous Processes	14
2.2.2 Endogenous Processes	15
2.3 WEATHERING	15
2.3.1 Physical Weathering	16
2.3.2 Chemical Weathering	16

Tables and Figures are with their relevant sections and are not listed here. The index and references are included in Part II Applications.

2.4	GEOLOGICAL ACTION OF RIVERS	18
2.4.1	<i>River Erosion</i>	18
2.4.2	<i>Transport of Particles</i>	18
2.4.3	<i>Accumulation</i>	19
2.4.4	<i>Geomorphological Features of Rivers</i>	19
2.5	GEOLOGICAL ACTIVITY OF GLACIERS	22
2.5.1	<i>Types of Glacier</i>	22
2.5.2	<i>Deposits of a Glacier: Moraines</i>	22
2.6	HYDROGEOLOGY	22
2.6.1	<i>Types of Water in Rocks</i>	24
2.6.2	<i>Water Tables</i>	24
2.6.3	<i>Reservoir Properties of Rocks</i>	24
2.6.4	<i>Aquifer</i>	25
2.6.5	<i>Spring</i>	25
2.6.6	<i>Water and Soil Slope Movements</i>	26
2.7	ORIGIN AND DESCRIPTION OF SOIL	28
2.7.1	<i>Alluvium</i>	28
2.7.2	<i>Alluvial Fan or Delta</i>	30
2.7.3	<i>Eluvial Soils or Regoliths</i>	30
2.7.4	<i>Colluvium</i>	31
2.7.5	<i>Moraine</i>	31

Chapter 3: MINERALOGY AND PETROLOGY

3.1	MINERALS AND THEIR PROPERTIES	33
3.1.1	<i>Properties of Rocks</i>	33
3.2	PETROLOGY	40
3.2.1	<i>Igneous Rocks</i>	40
3.2.2	<i>Metamorphic Rocks</i>	44
3.2.3	<i>Sedimentary Rocks</i>	50

Chapter 4: STRUCTURAL GEOLOGY

4.1	INTRODUCTION	53
4.2	DEFINITIONS	53
4.2.1	<i>Strike and Dip</i>	53
4.2.2	<i>Trend and Plunge</i>	53
4.3	PRIMARY STRUCTURES	53
4.4	SECONDARY OR TECTONIC STRUCTURES	57
4.4.1	<i>Folds</i>	57
4.4.2	<i>Fractures</i>	59

Chapter 5: TECTONIC SETTING OF THE HIMALAYA

5.1	GANGETIC PLAIN	64
5.2	MAIN FRONTAL THRUST (MFT)	64

5.3	SIWALIKS	64
5.4	MAIN BOUNDARY THRUST (MBT)	65
5.5	THE LESSER HIMALAYA	65
5.5.1	<i>The Sedimentary Belt</i>	65
5.5.2	<i>The Metamorphic Belt</i>	67
5.6	MAIN CENTRAL THRUST (MCT)	68
5.7	THE HIGHER HIMALAYA	68

Chapter 6: THE GEOLOGICAL COMPASS AND ITS FIELD USES

6.1	THE GEOLOGICAL COMPASS	70
6.2	MAGNETIC DECLINATION	70
6.2.1	<i>Definition</i>	70
6.2.2	<i>Adjustment for Declination</i>	70
6.3	FIELD MEASUREMENTS	70
6.3.1	<i>Bearing (or Azimuth)</i>	71
6.3.2	<i>Measuring Geological Structures</i>	72

Chapter 7: STEREOGRAPHIC PROJECTION

7.1	INTRODUCTION	77
7.2	PROJECTION OF A LINE	77
7.3	PROJECTION OF A PLANE	83
7.4	PROJECTION OF A CONE	83
7.5	PLOTTING TECHNIQUES	83
7.5.1	<i>Plotting a Line</i>	85
7.5.2	<i>Plotting a Plane</i>	85
7.5.3	<i>Plotting a Line Contained in a Plane</i>	88
7.5.4	<i>Plotting a Pole</i>	88
7.5.5	<i>Plotting the Line of Intersection of Two Planes</i>	90
7.5.6	<i>Determination of the Angle between Two Lines</i>	90
7.5.7	<i>Plotting the Line of Intersection of Two Planes from Their Poles</i>	91
7.6	POLE NET	93
7.6.1	<i>Plotting the Pole on a Pole Net</i>	93
7.7	CONTOURING FIELD DATA AND STATISTICAL ANALYSIS	93
7.8	DETERMINATION OF EXTENT OF SCATTER AROUND THE MEAN POLE OR GREAT CIRCLE POSITION	99

Chapter 8: AERIAL PHOTO INTERPRETATION

8.1	INTRODUCTION	101
8.2	ELEMENTS OF AERIAL PHOTO INTERPRETATION	101
8.2.1	<i>Topography</i>	101
8.2.2	<i>Drainage</i>	101
8.2.3	<i>Gray Tone</i>	102
8.2.4	<i>Erosion</i>	102
8.2.5	<i>Vegetation</i>	103
8.2.6	<i>Miscellaneous Features</i>	103
8.3	INTERPRETATION OF ROCK TYPES	103

Chapter 9: SOIL MECHANICS

9.1	DEFINITIONS	109
9.1.1	<i>Solid-Air-Water Phase Relationship</i>	109
9.1.2	<i>Gradation of Soils</i>	110
9.1.3	<i>Plasticity of Fine-grained Soils</i>	111
9.1.4	<i>Soil Density</i>	112
9.1.5	<i>Flow of Water</i>	113
9.1.6	<i>Stresses in a Soil Mass</i>	115
9.1.7	<i>Shear Strength</i>	116
9.1.8	<i>Consolidation</i>	116
9.1.9	<i>Bearing Capacity</i>	117
9.1.10	<i>Lateral Earth Pressure</i>	117
9.2	FIELD IDENTIFICATION OF SOILS	118
9.2.1	<i>Test Methods</i>	118
9.3	UNIFIED CLASSIFICATION SYSTEM	125
9.3.1	<i>Soil Properties Used in Classification</i>	125
9.3.2	<i>Definition of Soil Components</i>	125
9.3.3	<i>The Plasticity Chart</i>	128
9.3.4	<i>Summary of the Unified Classification System</i>	128
9.4	ENGINEERING PROPERTIES	130

Chapter 10: ROCK MECHANICS

10.1	SHEAR STRENGTH OF ROCKS	136
10.1.1	<i>Peak and Residual Shear Strength</i>	137
10.1.2	<i>Shear Strength of Rocks with Single Discontinuity - Plane Surface</i>	138
10.1.3	<i>Shear Strength of Single Discontinuity</i>	139
10.1.4	<i>Shear Strength of Filled Discontinuities</i>	143
10.1.5	<i>Shear Strength of Closely Jointed Rock Mass</i>	143
10.2	DETERMINATION OF SHEAR STRENGTH	144
10.3	ROCK MASS CLASSIFICATION	146

Chapter 11: GEOPHYSICS

11.1	INTRODUCTION	153
11.2	SEISMIC REFRACTION METHOD	154
11.2.1	<i>Uses of Seismic Refraction</i>	154
11.2.2	<i>Definitions</i>	154
11.2.3	<i>Data Acquisition</i>	156
11.2.4	<i>Seismic Wave Propagation</i>	160
11.2.5	<i>Parallel Interfaces</i>	161
11.2.6	<i>Analysis of Time-distance Graphs</i>	162
11.2.7	<i>Examples of Geological Models Inferred from Seismic Refraction</i>	166
11.3	ELECTRICITY RESISTIVITY METHOD	175
11.3.1	<i>Resistivity of Rocks</i>	175
11.3.1a	<i>The Quality of the Electrolyte</i>	175
11.3.1b	<i>The Quantity of Electrolyte</i>	175
11.3.2	<i>Darcy's Law</i>	176
11.3.3	<i>Point Current Electrode on Homogeneous Earth</i>	177
11.3.4	<i>Apparent Resistivity</i>	179
11.3.5	<i>Current Penetration</i>	179
11.3.6	<i>Depth of Investigation</i>	179
11.3.7	<i>Heterogeneous Medium</i>	180
11.3.8	<i>Electrical Profiling or Mapping</i>	180
11.4	ELECTRICAL SOUNDING	183
11.4.1	<i>Field Procedure</i>	183
11.4.2	<i>Plotting</i>	183
11.4.3	<i>Quantitative Interpretation</i>	184
11.4.4	<i>Interpretation by Curve Matching</i>	187

Chapter 12: MASS WASTING

12.1	INTRODUCTION	188
12.2	TYPES OF MASS MOVEMENT	188
12.2.1a	<i>Falls</i>	188
12.2.1b	<i>Topples</i>	188
12.2.1c	<i>Slides</i>	188
12.2.1d	<i>Spreads</i>	189
12.2.1e	<i>Flows</i>	189
12.2.1f	<i>Complex Movements</i>	190
12.3	CAUSES OF LANDSLIDES	191
12.3.1	<i>Natural Factors</i>	191
12.3.2	<i>Anthropogenic Factors</i>	191
12.4	MAIN TRIGGERS OF MAJOR LANDSLIDES AND THEIR CONTROL	192
12.4.1	<i>Earthquake-induced Landslides</i>	192
12.4.2	<i>Rainfall-induced Landslides</i>	192
12.5	PREVENTION AND CONTROL OF LANDSLIDES	193
12.6	LANDSLIDE-DAMS	194
12.6.1	<i>Causes of Landslide-Dams</i>	194
12.6.2	<i>Failure of Landslide-Dams</i>	195

12.6.3	<i>Floods from Landslide-Dam Failure</i>	195
12.6.4	<i>Methods of Preventing Landslide-Dam Failure</i>	195
12.7	GLACIAL LAKE OUTBURST FLOODS	196

Chapter 13: STABILITY ANALYSIS OF SLOPES AND PROBABILITY OF SLOPE FAILURE

13.1	PURPOSE OF SLOPE STABILITY ANALYSIS	200
13.2	LEVELS OF SLOPE STABILITY ANALYSIS	200
13.2.1	<i>Network Level Planning</i>	200
13.2.2	<i>Project Level Planning</i>	201
13.2.3	<i>Implementation Level</i>	201
13.3	STABILITY ANALYSIS OF SOIL SLOPES	201
13.3.1	<i>Total Stress and Effective Stress</i>	202
13.3.2	<i>Analysis of Infinite Slope and Plane Translation Failures</i>	202
13.3.3	<i>Debris Flow</i>	207
13.3.4	<i>Finite Slope Failure on Curved Surface</i>	208
13.3.5	<i>Soil Slope Analysis by Method of Slices</i>	211
13.4	ROCK SLOPE STABILITY	227
13.4.1	<i>Plane Failure</i>	228
13.4.2	<i>Wedge Failure</i>	237
13.5	LANDSLIDES	248
13.5.1	<i>Causes of Landslides</i>	257
13.5.2	<i>Mechanics of Landslides</i>	259
13.5.3	<i>Back Analysis of Landslides</i>	260
13.5.4	<i>Design Factors of Safety</i>	260

Chapter 14: HAZARDS AND RISKS

14.1	INTRODUCTION	262
14.1.1	<i>Natural Variability</i>	262
14.1.2a	<i>Measurement Errors</i>	262
14.1.2b	<i>Simplification Errors</i>	262
14.2	HAZARDS	262
14.3	RISKS	263
14.4	USE OF HAZARDS AND RISKS IN DECISION-MAKING ON HILL ROADS	263
14.4.1	<i>Prefeasibility and Feasibility Assessments</i>	263
14.4.2	<i>Detailed Design Stage Assessments</i>	264
14.5	ASSESSMENT OF HAZARDS AND RISKS	268

Chapter 15: CONSTRUCTION MATERIALS

15.1	PURPOSE AND USES OF AGGREGATES	271
15.1.1	<i>Aggregates Used without the Addition of a Cementing Material</i>	271

15.1.2	<i>Aggregates for Bituminous Pavement Layers</i>	271
15.1.3	<i>Aggregate in Fresh, Plastic Concrete</i>	272
15.1.4	<i>Aggregates in Hardened Concrete</i>	272
15.2	AGGREGATE QUALITIES OF CONCERN	273
15.2.1	<i>Test for the Evaluation of the Quality of Aggregates</i>	273
15.2.2	<i>Maximum Size Aggregate in Concrete</i>	276
15.3	PROPERTIES OF AGGREGATES	282
15.3.1	<i>Physical Properties</i>	283
15.3.2	<i>Chemical Properties</i>	287
15.4	SPECIFICATIONS AND PROPERTIES	288
15.4.1	<i>Local Specifications and Their Importance</i>	289
15.4.2	<i>Quality Requirements for Aggregates</i>	289
15.5	AGGREGATE CALCULATIONS	293
15.5.1	<i>Sieve Analysis Data</i>	293
15.5.2	<i>Combining Aggregate Gradings</i>	293
15.5.3	<i>Two Graphical Methods for Blending Aggregates</i>	295
15.6	AGGREGATE PROPERTIES AND BEHAVIOUR PECULIAR TO BITUMINOUS MIXTURES	299
15.7	SUMMARY OF PHYSICAL PROPERTIES, ENGINEERING PROPERTIES, AND MINERAL COMPOSITION OF ROCKS (See Tables 15.10, 15.11, and 15.12)	308
15.8	SOME COMMONLY USED GEOLOGICAL AND MINERALOGICAL TERMS	311

Chapter 16: ECOLOGY AND BIOTECHNICAL STABILIZATIONS

16.1	ECOLOGICAL CONCERNS OF ROADSIDE PLANTATIONS	314
16.1.1	<i>Introduction</i>	314
16.1.2	<i>Contributions for Restoration, Maintenance, and Conservation of Ecosystems</i>	316
16.1.3	<i>Contributions Supporting the Sustainability of Agroecosystems</i>	318
16.1.4	<i>Contributions to Maintain the Quality of Physical Health of Ecosystems</i>	321
16.1.5	<i>Pattern of Changes in Roadside Plantation Approaches</i>	323
16.1.6	<i>Engineering Angles on the Orientation of Plantation</i>	324
16.1.7	<i>Choice of Species for Planting</i>	325
16.2	BIOTECHNICAL STABILIZATION	341
16.2.1	<i>Introduction</i>	341
16.2.2	<i>Surface Erosion</i>	341
16.2.3	<i>Increase in Shearing Strength</i>	356
16.2.4	<i>Moisture Content and Groundwater Table Reduction</i>	368

Chapter 17: RETAINING WALLS

17.1	INTRODUCTION	377
17.2	LATERAL EARTH PRESSURE	377
17.2.1	<i>Equations for Static Conditions for Stresses in a Two-dimensional Case</i>	380
17.2.2	<i>Lateral Earth Pressure for At-rest Condition</i>	381
17.2.3	<i>Active and Passive Earth Pressure</i>	384

17.3	RIGOROUS DESIGN OF RETAINING WALLS	389
17.3.1	<i>Design of Gravity Type Retaining Wall</i>	389
17.3.2	<i>Crib Walls</i>	403
17.3.3	<i>Tieback Wall</i>	404
17.3.4	<i>Design of Reinforced Earth Walls-Empirical Method</i>	406

Chapter 18: PAVEMENT DESIGN

18.1	TRAFFIC CONVERSION TO EQUIVALENT SINGLE AXLE LOAD	411
18.2	LAND DISTRIBUTION OF TRAFFIC	414
18.3	DESIGN LOAD	414
18.4	DESIGN METHODS	415
18.4.1	<i>CBR Method</i>	415
18.4.2	<i>U.S. Corps of Engineers' Method</i>	416
18.4.3	<i>The TRRL Method</i>	416
18.4.4	<i>R-Value Method</i>	416
18.4.5	<i>Structural Number (AASHTO 1985) Method</i>	416
18.4.6	<i>Mechanistic Empirical Method</i>	417
18.4.7	<i>Criteria for Failure</i>	417
18.4.8	<i>Advantages of Disadvantages of Mechanistic Design</i>	417
18.4.9	<i>Existing Computer Programmes for Layered-Elastic Analysis</i>	418
18.5	EXAMPLE OF NEW PAVEMENT DESIGN BY DIFFERENT METHODS	424
18.5.1	<i>Corps of Engineers CBR Method</i>	424
18.5.2	<i>TRRL Road Note 31</i>	424
18.5.3	<i>TRRL Road Note 29</i>	424
18.5.4	<i>Structural Number (SN) - AASHTO, 1985, Method</i>	424
18.5.5	<i>Asphalt Institute Method</i>	426
18.5.7	<i>TRRL Laboratory Report 1132</i>	427
18.5.7	<i>Mechanistic - Empirical Design Using CHEVPC Computer Programme</i>	427
18.5.8	<i>R-Value Method</i>	427
18.6	OVERLAY DESIGN	458
18.6.1	<i>Overlaying Design by Component Analysis Based on the Asphalt Institute</i>	459
18.6.2	<i>Overlay Design Based on AASHTO Design Guide</i>	465
18.6.3	<i>Overlay Based on Deflection Criteria</i>	465
18.6.4	<i>Overlay Design by Mechanistic Analysis</i>	469

Chapter 19: DRAINAGE

19.1	INTRODUCTION	486
19.2	HYDROLOGY	486
19.2.1	<i>Intensity, Frequency, and Duration of Rainfall</i>	486
19.2.2	<i>Design Flood and Its Frequency</i>	488
19.2.3	<i>Method of Runoff Prediction</i>	489
19.3	HYDRAULICS	495
19.3.1	<i>Hydraulics of Drainage Channels</i>	495
19.3.2	<i>Hydraulic Design of Culverts</i>	505

Chapter 20: TRANSPORTATION ECONOMICS

20.1	INTRODUCTION	524
20.2	BASIC CONCEPTS	524
20.2.1	<i>Time Value of Money</i>	524
20.2.2	<i>Common Terms in Economic Analysis</i>	525
20.2.3	<i>Costs and Benefits</i>	526
20.2.4	<i>Methods of Economic Evaluation</i>	529
20.2.5	<i>Terms Related to Cash Flow Analysis Method</i>	532
20.2.6	<i>Equations Relating to Cash Flow Analysis</i>	533
20.2.7	<i>Sensitivity Analysis and Risk Analysis</i>	538
20.3	ANALYTICAL FRAMEWORK FOR ECONOMIC ANALYSIS USING LONG-RUN ECONOMIC PLANNING (LREP)	539
20.3.1	<i>Long-Run Economic Planning (LREP)</i>	539
20.4	CASH FLOW ANALYSIS AND REVISED RULES FOR THE IRR METHOD	
20.4.1	<i>Revised IRR Decision Rules for Determining Project Acceptability</i>	549
20.4.2	<i>Revised Procedure for Ordering Mutually Exclusive Alternatives</i>	554
20.4.3	<i>Revised Decision Rules for Determining the Best Alternative</i>	555
20.4.4	<i>Determining the Best Acceptable Alternative</i>	556
20.5	GENERALIZED HEURISTICS	557

Chapter 1

INTRODUCTION

1.1 MOUNTAIN RISK ENGINEERING (MRE)

Mountain Risk Engineering may be defined as "the science and art of engineering mountain infrastructure giving due consideration to natural and human processes, and the tolerable risks to and from infrastructures". Infrastructural engineering practices in hill and mountain areas are deficient in their approaches to solving problems specific to slope environments. This deficiency is a consequence of the following facts:

- o traditional engineering education is not adequately oriented to the hills and mountains,
- o traditional geological education is not oriented to problem-solving skills specific to civil engineering needs for linear infrastructures such as roads, railways, and canals,
- o a comprehensive treatise or integrated material (for training and reference on hill infrastructural activities at the various stages of a project cycle) does not exist at present, and
- o environmental aspects, not traditionally considered, require that solutions to hill road problems use a multi-disciplinary approach.

Mountain Risk Engineering is an integrated approach to solving the infrastructural engineering problems of hilly and mountainous areas. Its aim is to evolve cost-effective and site-specific designs, as well as environmentally conscious construction and maintenance practices. This can be achieved by basing engineering analysis and design on techniques to transform the constraints of hazards into tolerable risks.

1.2 PURPOSE OF THE MRE HANDBOOK

Mountain Risk Engineering must be practised to minimize the large economic and environmental costs (that will be experienced by infrastructural agencies and beneficiary groups) wherever the gaps in the traditional engineering practices for slope environments are likely to cause substantial loss. The first and foremost necessity of the process involved in updating current engineering practices to fit the MRE approach is a comprehensive handbook on MRE for application and training. This handbook contributes to the MRE adoption process by providing engineering approaches based on geological, environmental, and economic considerations specific to the mountain environments of developing countries.

The contents of this handbook will serve to establish a common ground for engineers and geologists involved in infrastructural projects in mountainous areas. Professionals in each of these disciplines have developed expertise in one or several of the areas covered by the handbook, depending upon the strength of their previous education and experience. However, familiarity with each of the topics included in the

handbook will allow each discipline to appreciate the need of the other discipline and gear them towards making more effective contributions to sustainable mountain infrastructure through either the direct application of their skills or through soliciting the services of experts from respective disciplines to promote the development of environmentally sound and safe infrastructures in the mountainous areas of the Hindu Kush-Himalayan (HKH) countries.

1.3 STRUCTURE OF THE MRE HANDBOOK

The MRE Handbook consists of two parts, i.e., 1) Subject Background and 2) Application Guide, and these have the following characteristics.

- o The contents are mainly derived from a compilation of existing literature. These have been selected, interpreted, synthesized, and laid out by using experiences of hill road problems in the middle mountains of Nepal. The contents provide ready reference material on relevant problems to practitioners and teachers.
- o Although problem definitions and subsequent recommendations are based on Nepalese hill roads, the handbook is believed to be applicable, to a large extent, to all linear infrastructural works in all hilly regions of the HKH and other mountainous areas.
- o The suggested techniques in the handbook are based on state-of-the-art reviews and their relevance to developing countries.

1.4 CONTENTS OF THE MRE HANDBOOK

There are twenty chapters under Subject Background-Part I. Chapters 2 to 8 are on geology. Knowledge of geological processes (Chapter 2) helps civil engineers to understand the variability in the forces and material properties over time so that the stability analysis is fully cognisant of these facts and so that the hazards and risks involved over the life of the infrastructure are well considered. The knowledge of the origin of rocks and soils (Chapter 2 and Chapter 3) helps in understanding the strength and behaviour of such rocks and soils over a longer time period. Chapters 4 and 5 give an introduction to Structural Geology and the Tectonic Setting of the *Himalaya* respectively.

Understanding of geological measurements and stereographic projections (Chapters 6 and 7) for rocks are essential to civil engineers because the joints and their orientations in the rocks determine the stability, conditions, and type of likely failure of these rocks. Slope stability analysis of rocks is not possible unless the direction and inclination of joints vis-a-vis the direction and inclination of the slope, along with the joint roughness, type of material filling the joints, and presence of water in the joints are measured in the field and plotted in the figure.

Airphoto Interpretation (Chapter 8) enables the identification of various features, in a larger area, influencing road stability. Many of these features are difficult to observe in the field without the help of air photos.

Chapter 9, Soil Mechanics, although generally familiar to civil engineers, is included in the handbook to serve as a refresher to civil engineers and as an introduction to geologists. Chapter 10, Rock Mechanics, is intended to provide concepts of rock slope analysis to civil engineers and geologists.

Chapter 11, Geophysics, is included because measurements of surface conditions alone do not provide sufficient insight into the type of rock, soil, and the presence of water below the surface. Major slope stability analysis requires geophysical investigations on the surface supported by some drilling to ascertain the properties of the material deep below the ground.

Chapters 12 and 13 provide insight into various types of landslides, mechanisms of landslides, and methods of stability analysis for slopes and landslides.

Chapter 14 provides concepts of hazards and risks for the predication of landslides from the existing conditions of the materials and the processes, and assessment of likely damage to infrastructure by the occurrence of landslides. Hazard and risk assessment is a tool for decision-making under uncertainty. It is a planning tool at the prefeasibility stage assessment, a management tool at the feasibility stage, and a design optimization tool at the detailed design stage of a project cycle.

Chapters 15, 17, 18, and 19 are intended to provide specific skills in evolving a cost-effective and durable design of various components of mountain roads, in particular, and other mountain infrastructures, in general.

Chapter 16 provides an introduction to roadside ecological concerns along with methods of biotechnical stabilization designs. The section on biotechnical stabilization is aimed at providing a clear concept of the role of plantation and vegetation in slope stabilizations.

Chapter 20 outlines basic concepts and methods of economic analysis to engineers and geologists engaged in infrastructural projects.

Part II - Application Guide-consists of six chapters (Chapters 21 to 26).

Chapter 22 deals with various aspects of the selection process at the prefeasibility stage and Chapter 23 deals with the site-selection process at the feasibility stage. Since the rigor of investigation and analysis depends upon the scale of work; the minor, medium, and major roads are treated separately. Chapter 24 deals with problem identification, practical guidelines, and illustrative examples for the various activities in the detailed survey and design of a mountain road.

Chapters 25 and 26 provide a brief outline of problems and approaches during the construction and maintenance of a road project.

1.5 EVOLUTION OF THE MRE HANDBOOK

The handbook is an outcome of several stages of feedback and improvement.

1. A draft manual was prepared by ICIMOD under a two year (1988-89) Mountain Risk Engineering Programme sponsored by the Commission of the European Communities. This draft version was tested through a nine-week pilot training programme, involving 20 mid-career engineers and geologists from the HKH countries, which took place from February 6 to April 10, 1989, at ICIMOD.

2. Within the two year MRE programme framework the 1988 draft manual was improved after receiving feedback from the 1989 pilot training course and the final version was a two volume, four part manual in folder form which was circulated for restricted use.
3. As a final stage of the two year MRE Programme, a 3 day international consultative meeting was held at ICIMOD in February 1990 to solicit review of the manual by international academicians, decision-makers from infrastructural agencies in the HKH countries, and international and local consultants practising in Nepal.
4. Practical use of the MRE approach by the Department of Roads, HMG, Nepal in 1990.
5. A six month MRE Phase II Project, under the sponsorship of the Swiss Development Cooperation (SDC) and the German Technical Cooperation Office (GTZ), in Nepal, has enabled further improvement and revision of the 1989 manual and resulted in the present version entitled " The Mountain Risk Engineering Handbook"

1.6 USING THE MRE HANDBOOK

1.6.1 *Users of the MRE Handbook*

The primary target groups for the MRE Handbook are practising engineers and geologists in mid-career. The secondary target groups are undergraduate and graduate level students in academic institutions. The tertiary target groups are donor agencies, decision-makers, and consulting firms. Last, but not least, prospective researchers may find the handbook useful for identifying new areas of research on mountain road issues.

The tertiary group will find the handbook of value in framing the terms of reference for studies relating to hill roads in developing countries. The primary and secondary target groups may use the handbook as follows.

1.6.2 *Use of the MRE Handbook*

This handbook may be used for the following purposes:

- integrated MRE training to teachers/practising engineers and geologists for 8 to 9 weeks;
- teaching a one quarter (2.5 months) course of 12 to 15 credits or 125 hours of lectures, laboratory, and field exercises, and 47 hours of classroom or home exercises on mountain engineering to undergraduate or graduate students in civil engineering;
- practical field-based training as a project exercise for engineers already familiar with the subject background; the three stages of a road project cycle for 3 weeks to road engineers;
- one to two weeks' modular training on specific aspects of MRE to trainers/practising civil engineers and geologists;

- preparation of an institution or agency-specific application guide, code-oriented to specific infrastructures in the hill areas of developing countries; and
- preparation of terms of reference for consultants' services for various stages of mountain roads.

1.7 TRAINING CURRICULUM

Chapter	Lecture hrs.	Lab. hrs.	Field hrs.	Exercise/Home work hrs.	Total hrs
2	1.5	-	-	-	1.5
3	3.0	18.0	-	-	21.0
4	1.5	-	-	-	1.5
5	1.0	-	-	-	1.0
6	1.0	-	3.0	-	4.0
7	2.5	8.0	-	8	18.5
8	1.0	4.0	-	-	5.0
9	2.0	-	-	-	2.0
10	2.5	-	4	-	6.5
11	8.0	8.0	-	12	28.0
12	2.0	-	-	-	2.0
13	3.0	12.0	-	-	15.0
14	1.0	4.0	8	-	13.0
15	1.0	2.0	4	-	7.0
16	3.0	-	5	-	8.0
17	2.0	4.0	4	-	10.0
18	2.0	4.0	8	-	14.0
19	2.0	-	6	-	8.0
20	2.0	-	5	-	7.0
	42	64	47	20	173
					= 5 weeks of 7 hours/day

The training can be organized as: 5 weeks' training with daily classroom lectures and exercises for 4 to 5 hours and daily homework for 2 to 3 hours, or 5 weeks' training at 7 hours a day.

1.7.1 Field-based Practical Training Using Application Guide

Project Work

- Prefeasibility stage assessments of a 50 to 100 km long road, based upon desk work - only 3 days.

- ii) Sample feasibility stage assessments of a 5 km stretch - 7 days.
- iii) Design of three sections of 1km long each representing valley, climb, and ridge sections of a sample road - 10 days. Total 3 weeks.

1.7.2 *Equipment and Trainers Required for MRE Training*

The equipment needed for training in Part I is as follows:

- geologic hammer,
- geologic compass,
- rock samples,
- acid,
- stereoscopes,
- air photos,
- topographic maps, and
- personal computers.

Teachers needed for training in Part I are:

- 1 training coordinator (civil engineer) for 5 weeks
- 1 engineering-geologist for three to four weeks,
- 1 geotechnical engineer for 3 weeks,
- 1 civil engineer for two weeks,
- 1 geophysicist for one week,
- 1 natural resource specialist for one week, and
- 1 economist for one week.

Teachers needed for Part II are:

- 1 training coordinator (civil engineer for 3 weeks),
- 2 engineering-geologists for 3 weeks,
- 1 geotechnical engineer for 3 weeks, and
- 1 civil engineer for 3 weeks.

The equipment needed for Part II is as follows:

- electrical resistivity meter,
- seismograph,
- stereoscope,
- geologic compass,
- geologic hammer,
- altimeter
- a field camping equipment distomat
- air photos,
- topo maps, and
- drawing sets.

Chapter 2

GEOLOGICAL PROCESSES

2.1 INTRODUCTION

2.1.1 Branches of Geology

Geology is the science that studies the earth. Geology (from the Greek, *gia* or *ge*, the Goddess Earth, and *logos*, denoting logical speech or science) deals not only with landforms but also with the structure and behaviour of the earth. Modern geology tries to explain the whole evolution of the earth and its inhabitants from the time of the earliest record, which can be recognized in the rocks, right down to the present day (Holms 1986).

Geology has several branches. Geomorphology (from the Greek, *ge*- earth, *morpha*- shape, *logos*-science) is that branch of geology which deals mainly with the landforms and processes of the earth's surface. The geological processes that are responsible for the changes in the features of the earth's surface are studied in physical geology. Hydrogeology evaluates the geological controls on the occurrence and movement of groundwaters. The architecture of the rocks is studied by structural geology. The earth's structure, the arrangement and form of materials composing it, the movements of the earth's crust, and deformations caused by them are studied in geotectonics or tectonics (from the Greek, *teutonikos*- builder). Geophysics applies physical methods to study rocks and the globe as a whole. Seismology (*seisma*- tremor) is the science of earthquakes.

The materials of the earth's rocky crust are studied by mineralogy (from the French- *minéral*) and petrology (from the Greek *petra*- rock). Magmatism (*magma*- dough) deals with the composition of magma, its role and activity. Metamorphism (*meta*- after; *morpha*- appearance, shape) concerns itself with the changes that rocks undergo in the interior of the earth under high temperature and pressure.

The erosion and deposition of rock fragments as well as the processes involved are studied in sedimentology. The study of various layers of rocks in space and time and their relationship with rocks of other regions is called stratigraphy (from the Latin, *stratum* - cover). The science that deals with the origin and evolution of life on earth, and the classification of fossil records, is called paleontology (*paleo*-ancient, *ontos*- existence, *logos*- science). The dating of rocks by radioactive and other methods is studied under geochronology (*ge*- earth, *chronos*-time). Historical geology studies the history of evolution of the organisms, our continents, and the oceans.

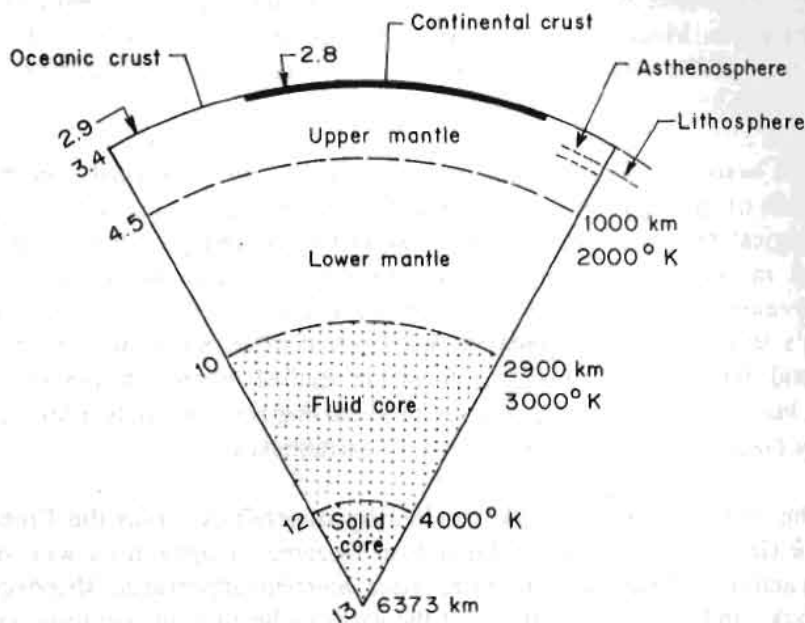
Engineering geology is a part of applied geology and is more closely related to civil engineering. It deals with the identification and assessment of the problems due to the inherent geologic setting that may arise during the planning, design, and construction of engineering structures in order to evolve suitable remedial measures.

Figures and Tables without credit lines in this Chapter are compiled by the author.

2.1.2 The Earth's Outer Zones

The earth can be described as a ball of rock (the crust), partly covered by water (the hydrosphere) and wrapped in an envelope of air (the atmosphere). The biosphere (*bio-* life) is another important aspect of the earth's crust. It is the site of organic activity. This system of crust, hydrosphere, atmosphere, and biosphere is a closed system. This means that losses from any part of the system are balanced by additions to others (Holms 1986).

The crust is the outer shell (Fig. 2.1) of the earth. It is made up of various kinds of rock. The uppermost part of the cover is composed of loose soil which is a product of the disintegration of the rocks themselves.



Source: Blyth and de Freitas 1985

Fig. 2.1 Composition of the earth

2.1.3 The Earth's Inner Zones

Apart from the outermost envelope called the crust, the earth's interior is divided into mantle and core as inferred from the seismological data (Fig. 2.1). The boundary between the crust and the mantle is called the Moho Discontinuity. It was discovered by Mohorovicic in 1909 by observing the break in the velocity of seismic waves. In passing through the rocks immediately above this surface, earthquake waves reach a velocity of about 7.2 km/sec, whereas in the rocks below the Moho Discontinuity the velocity jumps to about 8.1 km/sec. The core is divisible into two parts - the outer fluid core and the inner solid core, having a very high density (10.72 gm/cm³).

2.1.4 *The Shape of the Earth*

The earth is more or less shaped like a sphere. The reason for this shape is that the gravitational force pulls all the particles towards the centre. Because of the earth's daily rotation, its matter is also affected by the centrifugal force. The opposing centrifugal force pulls in a direction perpendicular to the axis of rotation. It is proportional to the distance of the object from the axis of rotation, and, therefore, is maximum at the equator and minimum (almost zero) at the poles. Hence, the earth has an equatorial bulge, and the equatorial axis is 42.8 km longer than the polar axis.

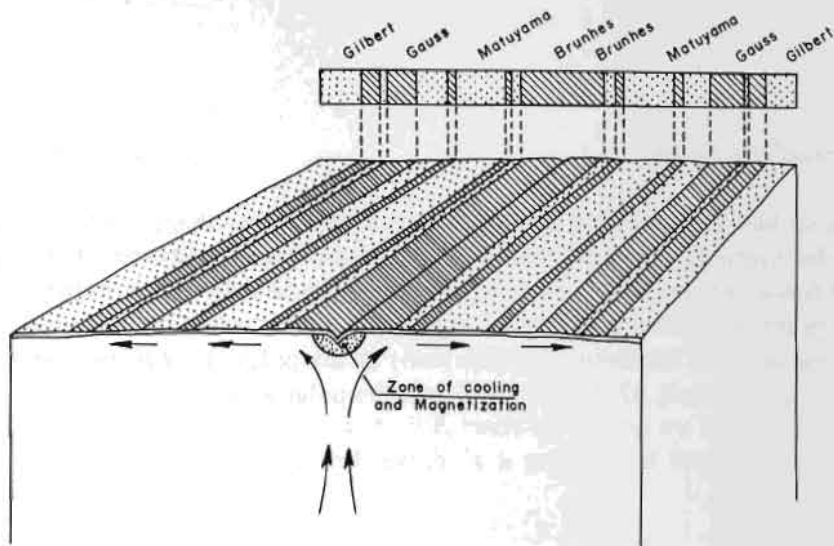
2.1.5 *Isostasy*

The ideal condition of gravitational equilibrium that controls the heights of continents and ocean floors in accordance with the densities of their underlying rocks is called isostasy.

If a wooden block is put into water, it floats, but a part of the block remains under water. The height of the submerged part of the block is proportional to the buoyant height of the block. The same concept is applicable to the mountains. In other words, as the mountains are raised there should be a proportional part of that mountain in the earth's crust. This is called the root of the mountain. Then what about the oceans? How to explain the depressions on the earth's crust? This problem is solved if we consider several wooden blocks of different heights floating together. The shorter block will have a lower level than the higher one.

Continents and mountains are composed of low-density rock, and they stand high because they are thick and light; ocean basins are topographically low because the thin oceanic crust is composed of dense rock. Isostasy and difference in the density of rocks beneath the continents and oceans, therefore, are the reasons why the earth has two pronounced topographic levels. The depth at which rock is weak enough to flow like a viscous fluid in order to produce the buoyancy effects of isostasy is called the **depth of compensation**. It is defined as that depth above which segments of crust and upper mantle act as blocks that rise or sink depending upon the mass and density of the individual blocks. The depth of compensation corresponds approximately to the bottom of the lithosphere where rock is hot enough to be weak and easily deformed (Skinner and Porter 1987).

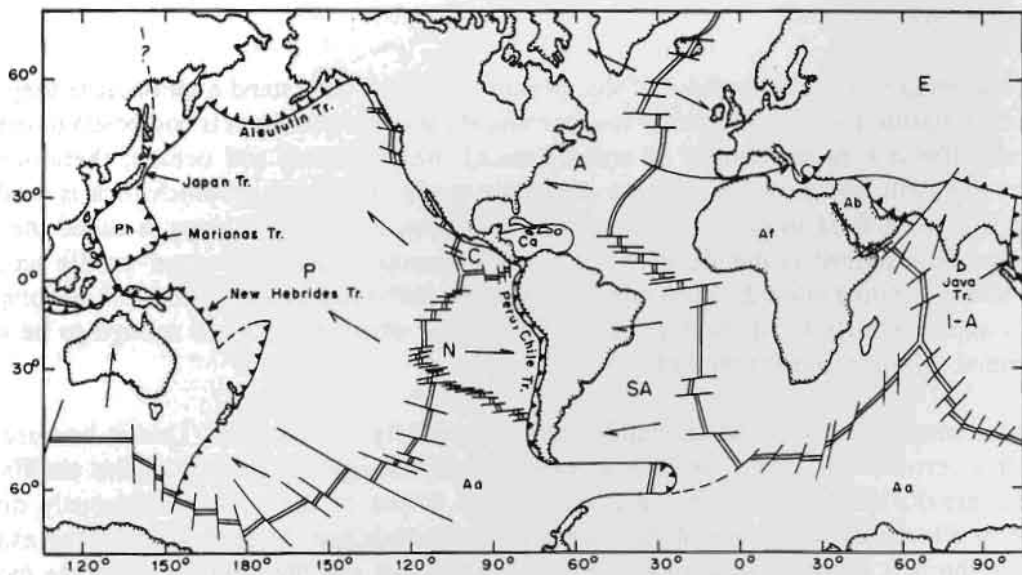
Under natural conditions, the isostatic equilibrium is generally not reached. This is because external forces, such as erosion and mass movement, continuously change the heights of the earth's crust to maintain the gravitational equilibrium, and the internal forces of the earth continuously disturb the equilibrium. It clearly shows the possibility of vertical movements in the earth's crust. For example, in the *Himalaya* the isostatic equilibrium has not yet been reached and the lighter root of the mountain is 'pushing' the mountain chain upwards, and the rivers and glaciers are eroding the mountain slopes. There are some rivers such as the Ganges and Brahmaputra which are older than the Himalayan mountains and have been cutting through them from the time of origin. The mountains are rising so rapidly that these rivers do not have enough time to cut wide valleys and can only make very narrow gorges. The *Himalaya* is a young (about 40 million years old in comparison to the earth which is 4.5 billion years) mountain chain, and the steep mountain slopes are basically caused by the faster speed of uplift and slower erosion rates.



Source: Cox et al. 1967

Fig. 2.2 Sea floor spreading and magnetic anomaly patterns

Convection currents bring molten material up under the mid-ocean ridge, where it cools, becomes magnetized and then spreads laterally away from the ridge. Symmetrical bands of normal and reversed magnetic anomalies in rocks would be produced by the combined effect of field reversal and spreading.



Source: Modified from Oxburgh 1974 in Blyth and de Freitas 1985

Fig. 2.3 Plate boundaries in the earth's crust

Plate boundaries in the Earth's crust. P. Pacific Plate. A. North American Plate. SA. South American Plate. Af. African Plate. E. Eurasian Plate. I-A. Indo-Australian Plate. Aa. Antarctica. Ph. Philippine. Ca. Caribbean. N. Nazca. C. Cocos. Ab. Arabian. The plate boundaries largely coincide with zones of seismic and volcanic activity. Oceanic ridges shown by double lines, transcurrent faults by single lines. ▲▲▲ = zones of subduction.

2.1.6 Plate Tectonics

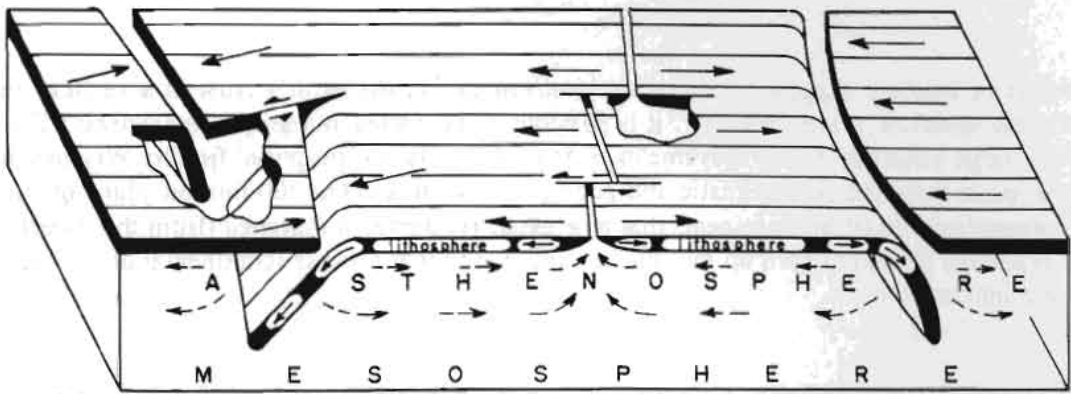
The principle of isostasy suggests that there are movements in the earth's crust in a vertical direction. Obviously, the question arises whether it is possible to have some horizontal movements. The answer is yes. Very large-scale horizontal movements of the continents was proposed first by Wegener in 1912. He tried to prove from the paleoclimatic and geological data that about 300 million years ago there was a supercontinent joining all the continents that now exist. He named it *Pangaea* (from the Greek : whole earth). It gradually started to split up into pieces, and due to that process (continental drift), the Atlantic Ocean came into existence.

Many geologists and geophysicists did not believe in this hypothesis until 1960. The geophysical and geological findings of the 1960s showed that the ocean floor is quite young (about 150 million years). Scientists also discovered that the magnetic poles flip back and forth from N to S after a certain interval. This property is called the **magnetic reversals**.

If we make a geological map of the magnetic reversals in the ocean, it will look like a zebra crossing (Fig. 2.2). The youngest of the strips are found in the central portion of the ocean and are called the mid-oceanic ridge. They become successively older away from the ridge. This clearly shows that the ocean floor is spreading. In other words, a new oceanic crust, formed by eruption of lava at the ridges, slowly moves away on either side. But a question arises concerning what happened to the ocean floor that was older than 150 million years (as there is no floor older than that)? It means that there is some way of destroying the ocean floor. This destruction occurs at the margins of the continents where we find deep trenches. The depth of some of the trenches is more than 10,000 m. The moving ocean floor vanishes down the trenches. This process is called **subduction**. The hypotheses dealing with all these interpretations are called **plate tectonics**.

According to plate tectonics, the earth can be subdivided into six large rigid plates and several smaller ones (Fig. 2.3). The boundary of the plates is fixed by the foci of the earthquake epicentres. The plates, about 100 km thick, consist of crust and the uppermost part of the mantle and together are called the **lithosphere** (Fig. 2.1). The lithosphere moves along a more or less ductile zone called the **asthenosphere** (Fig. 2.1). As the lithosphere moves, a new crust is generated at the mid-oceanic ridges, and the older crust is partly destroyed at the trenches (Fig. 2.4). Thus the ocean floor is continuously renewed. In other words, the ocean floor is slowly moving away from both sides of the mid-oceanic ridge and disappearing in the trenches, like a conveyer belt. The continental crust, being lighter than the oceanic crust, floats and generally cannot be subducted. Sometimes, two continental blocks come close to each other and collide. A typical example of a collided mountain range is the Himalayan Range where the Indian subcontinent collided with the Eurasian continent about 40 million years ago (Fig. 2.5). The process of convergence is still continuous and, therefore, earthquakes are frequent in this region.

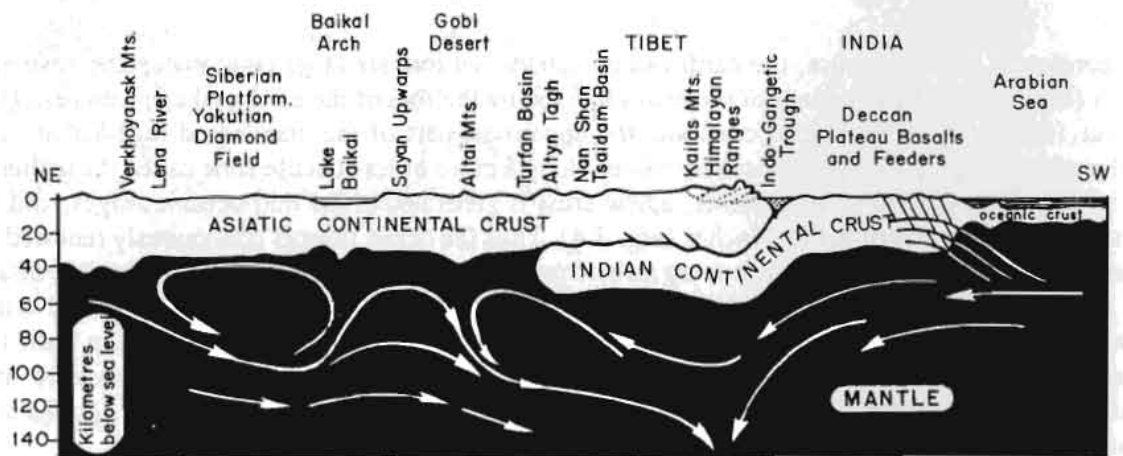
The mechanism that drives a moving plate is not known. Probably it results from a combination of convection currents in the mantle and the forces that act on a plate of lithosphere. The convective mixing was probably vigorous in the early earth and it resulted in a less clear distinction between continental and oceanic crust than is the case for the present-day earth.



Source: Isacks et al. 1968

Fig. 2.4 Block diagram illustrating schematically the configurations and roles of the lithosphere, asthenosphere, and mesosphere

Arrows on lithosphere indicate relative movements of adjoining blocks. Arrows in asthenosphere represent possible compensating flow in response to downward movement of segments of lithosphere.



Source: Holms 1986

Fig. 2.5 Schematic cross-section across Asia illustrating continental collision and partial under thrusting

2.1.7 The Geological Time Scale

Since the earth came into existence about 4,600 million years ago, its outer layer, called the crust, has changed significantly. As soon as the atmosphere and hydrosphere were formed, the earth's outer surface was subjected to an endless cycle of erosion and deposition. This interaction between the earth's crust, atmosphere, and hydrosphere led to the creation of the first organisms in the sea. The traces of the primitive organisms were subsequently lost in the sediments as they did not possess any resistant skeleton or shell.

The long timespan taken for the evolution of life on earth gave rise to successively more and more complex animal and plant species. Owing to natural selection, the old species that could not survive in a changing environment were lost and new, more advanced ones, appeared. As the evolution of life progressed, unicellular and multicellular organisms with hard shells or skeletons came into existence. The observation that sedimentary rocks deposited at various time intervals contain the remains of organisms that flourished during that period and the principle of superposition of strata (i.e., that in an undisturbed rock succession, the beds lying below are older than those lying above) make it possible to prepare a relative time scale. That means relative in the sense that it is possible only to say, for example, that the Cambrian period is older than the Ordovician as the latter overrides the former in undisturbed rock succession.

The discovery of radioactivity in 1896, by French physicist Becquerel, made it possible to get precise data concerning the formation of igneous and some sedimentary rocks containing radioactive isotopes. From these 'fossil watches' we can date the rocks in terms of the time that has elapsed after their formation. The common radioactive elements found in rocks are uranium (U), radium (Ra), thorium (Th), rubidium (Rb), potassium (K), and their isotopes. With time, they undergo spontaneous decay and change into other elements such as lead (Pb) and helium (He) as given below:



The process of decay is constant and not affected by external forces. The decay of some radioactive elements continues for a long time. For example, a half of all the uranium atoms decay over 7×10^8 years. A precise count of new atoms of lead or helium together with the parent uranium present in the rock enables us to determine the absolute age of that rock.

Geologists have sub-divided the geological time scale into larger and smaller time units termed respectively era, period, epoch, and age. A short description of eras and periods with corresponding duration and age and organisms of that time is presented in Table 2.1.

Table 2.1 The geological time scale

ERA		PERIOD	DURATION AND AGE (million years)		EVOLUTION OF LIFE
CAINOZOIC (CENOZOIC) (<i>Kainos</i> = recent <i>zoe</i> = life)	Quaternary		2	2	Homo sapiens
	Tertiary	Neogene	23	25	Ancestral pigs and apes
		Paleogene	40	65	Ancestral horses and elephants
MESOZOIC (<i>Mesos</i> = middle)	Cretaceous		79	144	Flowering plants
	Jurassic		69	213	Early mammals
	Triassic		35	248	Birds, flying reptiles, dinosaurs
PALAEOZOIC (<i>Palaios</i> = ancient)	Permian		38	286	Conifers and beetles
	Carboniferous		74	360	Abundant plants, early reptiles
	Devonian		48	408	Ammonites, trees
	Silurian		30	438	Plants, jawed fish
	Ordovician		67	505	Early fish
	Cambrian		85	590	Brachiopods, Trilobites, Corals
PRE-CAM-BRIAN	PROTEROZOIC (<i>Proteros</i> = earlier)		~ 1910	~ 2500	Worms, Algae, Bacteria
	ARCHAEAN (<i>Archaeos</i> = primaeval)		~ 2100	~ 4600	Oldest algae and bacteria

Source: Modified from Holms 1986

2.2 EXOGENOUS AND ENDOGENOUS PROCESSES

From the beginning of its existence, the earth has gone through a continuous series of changes. These changes are never ending. The first group of processes causing the changes is known as exogenous (from the Greek *exo*- outside) processes and they take place on the surface of the earth. The second group of processes takes place inside the globe and they are governed by the forces inherent in the earth. These are the endogenous processes.

2.2.1 Exogenous Processes

Exogenous processes consist of continuous movements of water and air masses, of the circulation of water in the atmosphere, on the surface, and inside the earth. These processes also include the chemical and physical transformation of matter under the action of weathering reactions, destruction, transportation and redeposition of rocks, the life activity of organisms, and the like.

The exogenous processes can be divided into three stages. They are: (1) the breakdown of the primary rock exposed on the surface, (2) the stripping and transport of the liberated particles, and (3) the accumulation of the material or sedimentation. The totality of the processes involving the disintegration of rocks and the stripping of decomposed products and transport down to low-lying areas is called denudation (from Latin, *denudare*- to lay bare).

2.2.2 Endogenous Processes

The sediments deposited in the ocean, sea, or lake show horizontal or nearly horizontal layers. This property is related to the gravitational force of the earth. But, as soon as the sediments are deposited, they begin to undergo a series of changes in their geometry and composition.

At first they gradually become compact and solid without much change in mineral composition or internal arrangement of the grains. This kind of change is called **diagenesis**. Later, due to **tectonic movements**, as well as higher temperatures in the earth's crust and the pressure of the overlying rocks, the **sedimentary rocks** gradually transform into **metamorphic rocks**. Further change in temperature and pressure may lead to melting and formation of **magma**.

Crystallization of magma in the interior of the earth gives rise to **intrusive igneous rocks** and if the magma pours out from volcanoes it solidifies into **volcanic igneous rocks**. Thus, the three major rock groups (1) sedimentary, (2) metamorphic, and (3) igneous come into existence. They are discussed in Chapter Three.

The process of transformation of sedimentary, metamorphic, and igneous rocks into one another is called the rock cycle. The rock cycle is continuously taking place in the earth's crust (Fig. 2.6a and Fig. 2.6b).

When the rocks undergo deformation, folds may be generated. But when the rock cannot be deformed, it ruptures and the fracture is called the fault. Folds and faults are discussed in Chapter Four.

2.3 WEATHERING

Weathering is an aggregate of exogenous processes involving the physical destruction and chemical decomposition of minerals and rocks at the site of their occurrence and caused by the variations in temperature, by the chemical action of water, by gases (e.g., oxygen and carbon dioxide), by the biochemical action of organisms in the course of vital activity, and by the products of their decomposition after they have died off (Gorshkov and Yakushova 1977).

Weathering processes can be divided into two types: (1) physical weathering and (2) chemical weathering. However these two types always work together in nature and there is no sharp boundary between them.

2.3.1 Physical Weathering

Physical weathering is caused by a variety of factors that lead to the mechanical breakdown of rocks into smaller and smaller fragments. One type of physical weathering is caused by variations of temperature (thermal weathering). The periodic contraction and expansion of rocks, due to the diurnal variations of temperature, lead to the formation of cracks parallel to the heated surface and later to the flaking off of the upper layer. The process of temperature breakdown in rocks is called **exfoliation**.

Temperature weathering may also occur because of intensive heating, by sunshine, of rocks of different coloured minerals. Since the dark minerals are more intensely heated than the light ones, the difference in their volumetric expansion leads to the development of cracks.

Another form of physical weathering is mechanical weathering. One of the examples is frost weathering in which rocks are broken down by the freezing and thawing of water that has penetrated pores and cracks. The roots of plants, capillary water, and crystallization of minerals have the same effect.

2.3.2 Chemical Weathering

Chemical weathering is the chemical decomposition of rocks by the effect of atmospheric factors. The most important factors are the oxygen, carbon dioxide, and water contained in the atmosphere and the active role of organisms. The main reactions causing chemical weathering are oxidation, hydration, dissolution, and hydrolysis.

An example of oxidation is the change of sulfides into oxides:



Hydration consists of the formation of new minerals containing water of crystallization: CaSO_4 (anhydrite) + $2\text{H}_2\text{O} = \text{CaSO}_4 \cdot 2\text{H}_2\text{O}$ (gypsum). Hydrolysis is the chemical decomposition or alteration of minerals into other compounds by taking up molecules of water.



All the processes involving physical and chemical weathering result in the formation of various weathering products. These may be (1) mobile ones, which are transported over varying distances under the action of gravity, sheet flow, erosion by water, etc and (2) residual products that remain on the site of destruction of the parent rocks.

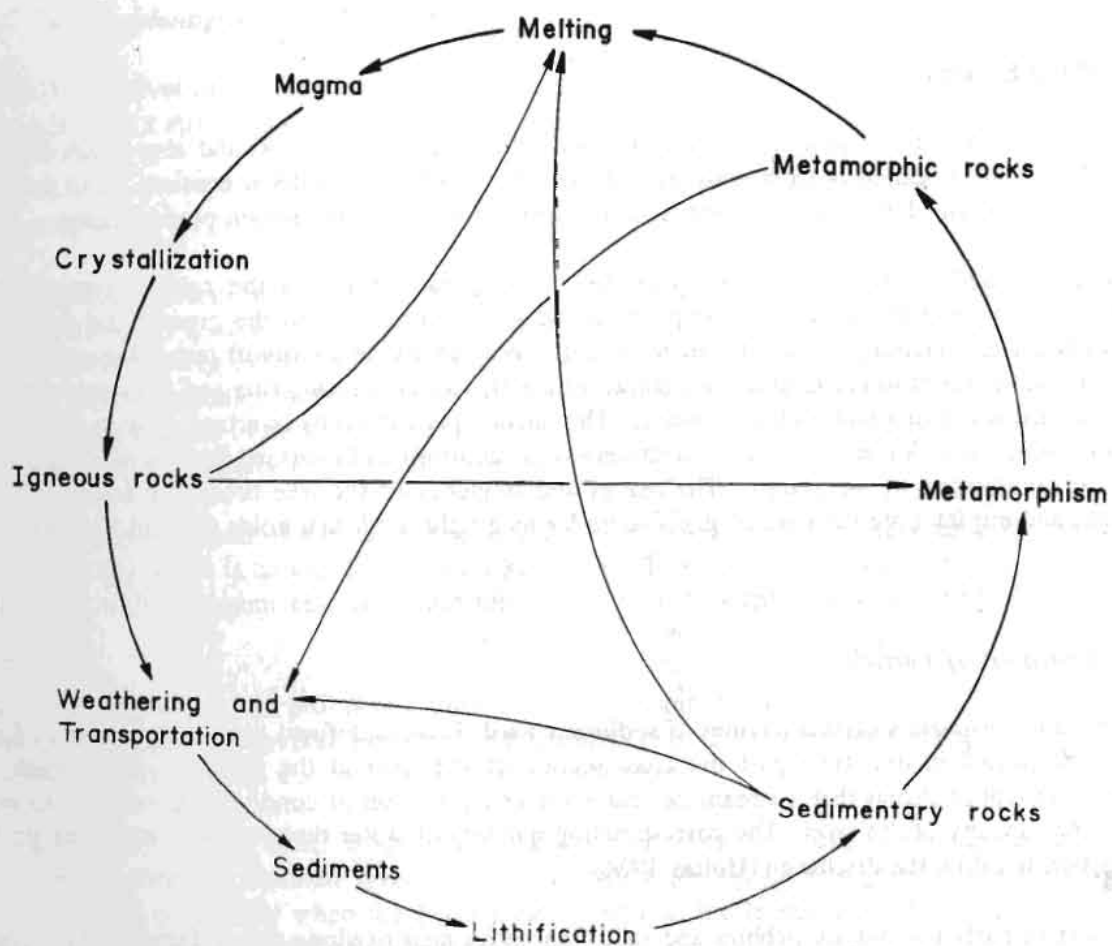


Fig. 2.6 Rock cycle

2.4 GEOLOGICAL ACTION OF RIVERS

A river or stream is a body of water which carries rock particles and dissolved substances and which flows down a slope along a clearly defined path called the stream's channel (Skinner and Porter 1987). The material the stream moves or carries is called the load.

Rivers and streams shape the continents. The work done by rivers is of three kinds: the destruction of rocks (erosion), the transport of particles by water, and their subsequent deposition (accumulation).

2.4.1 *River Erosion*

Rivers erode the bottom of their channels, gradually cutting into the bedrock, and also break down the banks. The former is called **bottom erosion** and the latter is known as **lateral erosion**. Both processes always take place together, but, in the initial stages of the river, bottom erosion predominates.

The water supplied to streams and rivers comes from rainfall. Some of the rainfall returns to the atmosphere through evaporation and transpiration and some infiltrates into the ground and remains as groundwater. The remaining portion forms the runoff. We can divide the runoff into (1) overland flow, the movement of runoff in broad sheets or groups of small, interconnecting rills and (2) streamflow, the flow of surface water in a well-defined channel. The erosion performed by overland flow is called **sheet erosion** (Skinner and Porter 1987). The effectiveness of raindrops and overland flow in eroding the land are greatly diminished by vegetation. The leaves and branches of the tree break the force of falling raindrops, and the intricate network of grass roots forms a tight mesh that holds the soil in place.

2.4.2 *Transport of Particles*

Every stream transports a certain amount of **sediment load**. Load is defined as the total weight of solid detritus transported in unit time past the cross-section of the river at the place of observation. The maximum amount of debris that a stream can carry under a given set of conditions is referred to as the transporting capacity of the river. The corresponding quantity of water that passes in unit time past the cross-section is called the discharge (Holms 1986).

The amount of particles (mainly pebbles and sand) that move near or along the surface of a river bed is called **bed load**. The quantity of fine particles that are carried away in suspension is called the **suspended load**. However, there is no sharp boundary between the two categories. The third load, in the form of dissolved substances, is called the **dissolved load**.

The particles of bed load generally move down current by saltation, a forward movement of the particles by intermittent jumps. In this process, the particles spin and bounce. As a result, the pebbles of the river become well rounded in contrast to the angular fragments of colluvium. The suspended load is diffused in water due to turbulence. The upward moving currents within a turbulent stream hold the particles in suspension as long as the energy, that the silt and clay particles settle, is less than that of the turbulent eddies.

2.4.3 Accumulation

The process of erosion and transport is accompanied by accumulation or deposition. Even in the early stages, when erosion and transport prevail over accumulation, the material carried by the river is deposited in some of its sections. As the river loses its transporting capacity, the bed load and the suspended load begin to accumulate. The deposits accumulating in river valleys are called alluvial deposits or simply alluvium (from the Latin, *alluvius*).

2.4.4 Geomorphological Features of Rivers

The water of a river or stream moves along a channel and the channel continuously modifies its course. Downcutting by a stream is called **vertical erosion**.

Channel Pattern

Depending upon geological conditions the stream may have **straight**, **meandering**, or **braided channels**. Straight channels (Fig. 2.7) are rare and, if present for a long distance, are probably controlled by joints or faults. The **thalweg** is the line connecting the deepest part of a stream along its direction of flow. Generally it is not parallel to the banks. A bar (or point bar) is the feature produced by the deposition of sediments at the side of the stream due to decrease in stream velocity. The deepest part of the channel, called the pool, is generally found opposite the bar.

A smooth, loop-like bend of a river channel is called a meander (from the Latin name for the Meander River in Turkey which is famous for its loop-like course). The meandering pattern (Fig. 2.8) is the result of the flow with minimum resistance and the energy is distributed almost uniformly along the river course.

If a river is overloaded with sediment it cannot transport material downstream in which case the material is deposited as bars with several interconnected channels (Fig. 2.9). This braided pattern is observed in rivers with highly variable discharge and easily erodible banks.

A **flood plain** is that area which is inundated in flood. Generally the banks of a stream are bordered by a small rise called the **natural levée**. The levees are made up of fine-grained sediments, and the deposition takes place only when the flood plain as well as the levees are submerged in flood and a temporary lake is formed on the flood plains.

River Terrace

In the process of lateral and vertical erosion, the river channel abandons its older flood plain which then becomes a river terrace. In some areas, the terraces occur at a number of levels. The lowest part of the river terrace is made up of coarse gravel with rounded pebbles representing the channel and/or bar deposits. The highest part of the terrace is composed of fine sand, silt, and clay representing the deposits of the natural levee and flood plain. If the river occasionally changes its course laterally and vertically, the terraces show a cyclic deposition of coarse and fine sediments (Fig. 2.10).

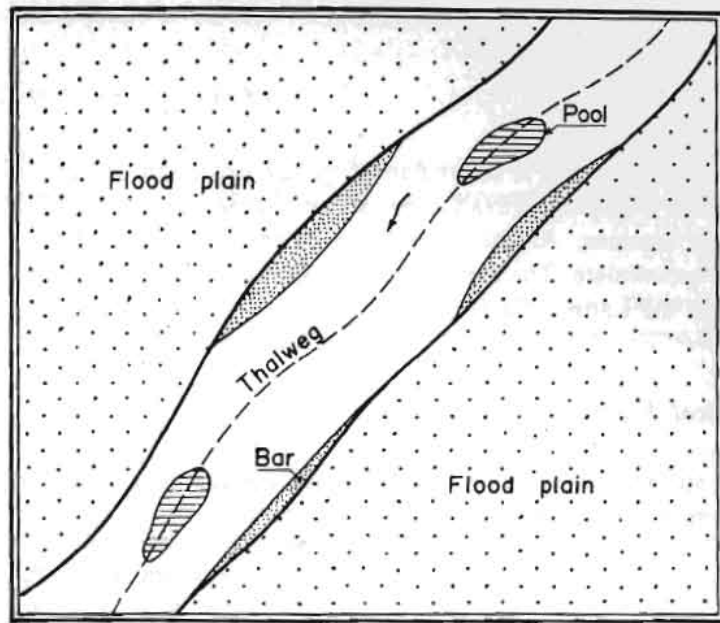


Fig. 2.7 Features of a straight channel

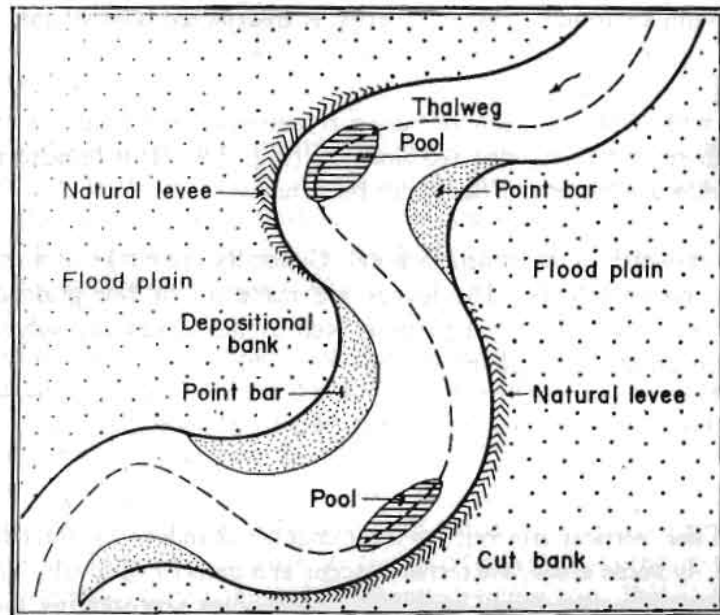


Fig. 2.8 Features of a meandering channel

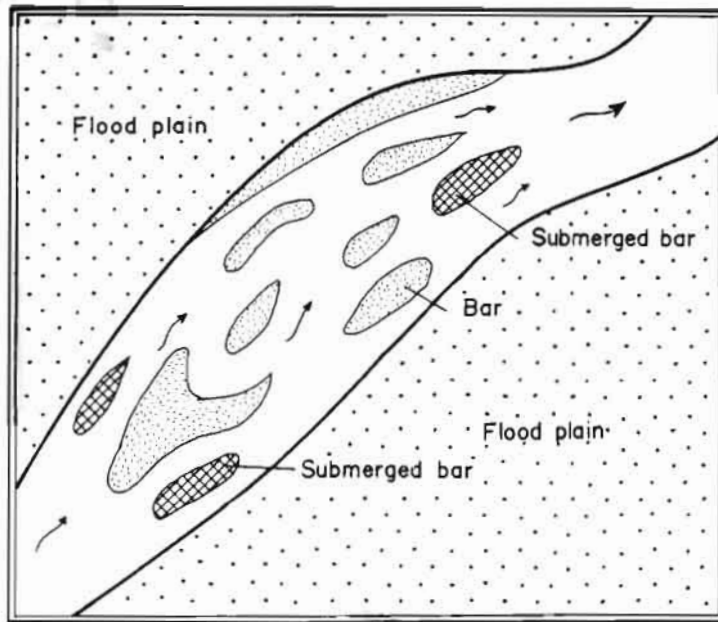


Fig. 2.9 Features of a braided channel

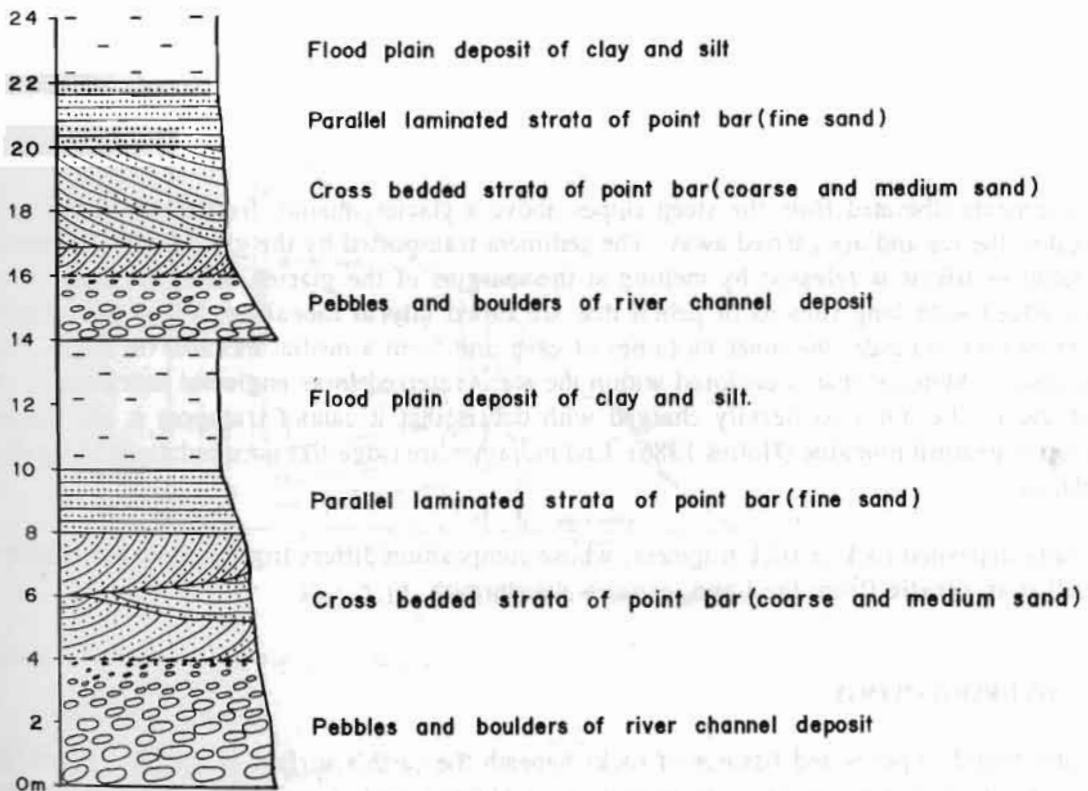


Fig. 2.10 Cyclic deposition in a river terrace

2.5 GEOLOGICAL ACTIVITY OF GLACIERS

A glacier is a large natural body of crystal ice, formed as a result of accumulation and subsequent transformation of snow. A glacier moves constantly down a slope.

Transformation of snowflakes into glacier ice is a kind of low-temperature metamorphism. As the loose feathery snow is buried by later falls it gradually passes into neve, a closely compact form with a density of from 0.8 units of air free ice to 0.917 units. With further compaction more air is squeezed out until the deeper layers are transformed into ice (Holms 1986). The loss of glacier ice by evaporation, melting, or calving is called **ablation** (from the Latin *auferre-ablatum*- to carry away). As the ice moves down slowly the glacier exhibits a tongue-like shape. The glacier advances until its front reaches a point where the accumulation is balanced by ablation.

2.5.1 *Types of Glacier*

Generally glaciers are classified into three major groups: (1) ice-sheets or thin sheets of ice which are spread over the flat surfaces of continents and plateaux, (2) mountain or valley glaciers occupying the valleys of high mountains, and (3) piedmont glaciers resulting from the coalescence of several valley glaciers (Holms 1986).

Glaciers erode rock by plucking, quarrying, and abrasion. They transport the waste and deposit it as glacial drift. Mountain glaciers erode the valley floor into U-shaped troughs with hanging tributaries (Refer to Section 2.7.5).

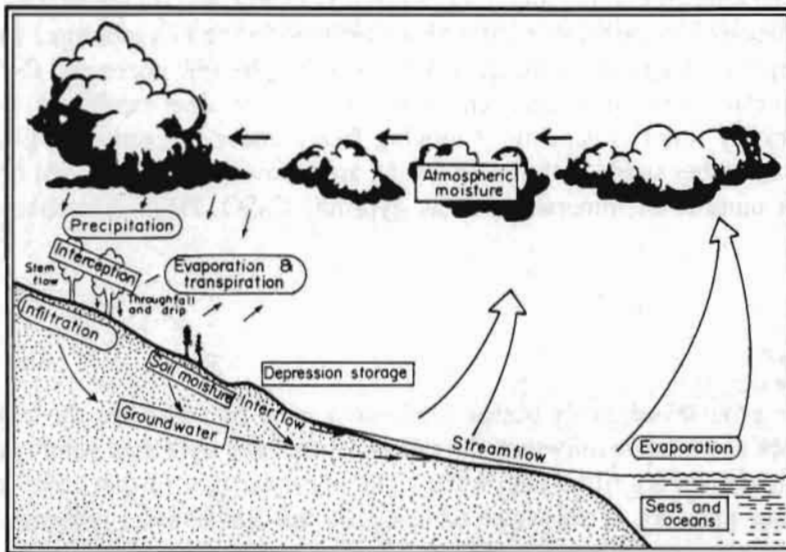
2.5.2 *Deposits of a Glacier: Moraines*

Rock fragments liberated from the steep slopes above a glacier, mainly from frost shattering, tumble down on to the ice and are carried away. The sediment transported by the glacial ice is plastered on to the ground as **till** or is released by melting at the margins of the glacier. Thus the sides of a glacier become edged with long ribbons of debris that are called **lateral moraines**. When two glaciers from adjacent valleys coalesce, the inner moraines of each unit form a medial moraine on the surface of the united glacier. Material that is enclosed within the ice is referred to as **englacial moraine**. If the lower part of the ice becomes so heavily charged with debris that it cannot transport it all, the excess is deposited as **ground moraine** (Holms 1986). End moraines are ridge-like accumulations along the margin of a glacier.

A glacially deposited rock or rock fragment, whose composition differs from that of the bedrock beneath it, is called an **erratic** (from the Latin, *erratus*- wandering).

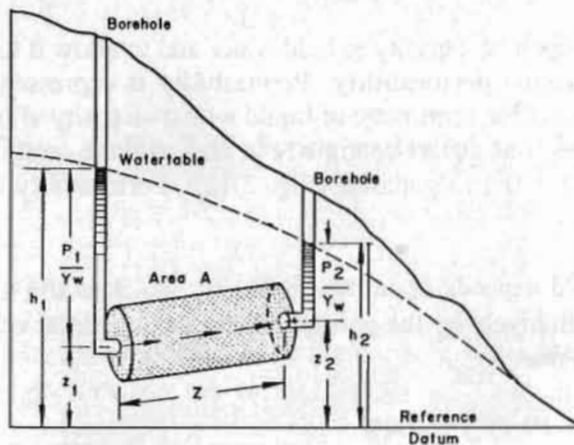
2.6 HYDROGEOLOGY

The water found in pores and fissures of rocks beneath the earth's surface is studied by hydrogeology. This covers their origin, distribution, migration, qualitative and quantitative variations in time, and geological effects (Gorshkov and Yakushova 1977). The hydrological cycle is shown in Fig. 2.11.



Source: Selby 1982

Fig. 2.11 The hydrological cycle



Source: Hoek and Bray 1981

Fig. 2.12 Definition of permeability

Permeability $K = Ql/A(h_1 - h_2)$ (see Fig. 2.12), where:

- K = permeability coefficient,
- Q = discharge (m^3),
- A = cross-sectional area of the sample (m^2),
- $(h_1 - h_2)$ = head, i.e., difference in water table (m)
- l = length of the sample (m).

2.6.1 *Types of Water in Rocks*

Water in the form of vapour is contained in the air that fills pores and fissures. It is in a dynamic equilibrium with other types of water. **Hygroscopic water** forms when molecules of water vapour are adsorbed (from the Latin (*ad*)*sorbere*- to swallow up) or retained on the surface of minerals. It forms a thin monomolecular envelope around the mineral grain and is firmly held on the surfaces of the particles. Film water forms a thicker envelope around the rock particles and the hygroscopic layer. It can move from one particle to another. Capillary water fills fully or partly the fine pores and fissures in rocks and is held in them by surface tension forces. The water rises over fine capillaries upwards from the groundwater table. Gravity water is capable of moving freely under the action of gravity through and along pores, fissures, and other voids in the rocks which are below the melting point of ice. Crystallized water forms part of a number of minerals such as gypsum: $\text{CaSO}_4 \cdot 2\text{H}_2\text{O}$ (Gorshkov and Yakushova 1977).

2.6.2 *Water Table*

A hole penetrating the ground ordinarily passes first into a **zone of aeration**, the zone in which open spaces in soil or bedrock are filled mainly with air and moisture. The hole then enters the saturated zone, the zone in which all openings are filled with water. The upper surface of that zone is called the water table and the pore water pressure at the water table equals the atmospheric pressure. The water table generally slopes towards the nearest river or stream (Skinner and Porter 1987).

2.6.3 *Reservoir Properties of Rocks*

The water content of rock depends upon its capacity to hold water and to allow it to pass through it. This capacity for transmitting fluids is called **permeability**. Permeability is expressed in darcy or units of permeability equal to the flow of one cubic centimetre of liquid with a viscosity of one centipoise through the cross-section of a porous medium, one square centimetre in area and one centimetre in length, within one second at a pressure differential of 0.1 megapascal (Fig. 2.12). Permeability is generally expressed in millidarcies.

The capacity of rocks to hold liquid depends upon their porosity, which is the total volume of all the voids in them. It is measured quantitatively by the porosity ratio, i.e., the total void space expressed as a percentage of the rock's total volume:

$$n = (V_p/V_o) \times 100\%$$

where,

n is the porosity ratio; V_p is the total pore space in the rock; and V_o is the volume of the rock.

Permeability and porosity play a major role in slope movement. The rate of infiltration and percolation (slow infiltration) of surface runoff depends mainly on the permeability and porosity of materials. Based on the permeability and porosity, the rocks and soils can be broadly classified into three categories.

1. Pervious and non-porous: a. hard rocks with tight fractures - igneous and metamorphic rocks,
b. hard rocks with wide fractures and solution cavities-limestone.
2. Pervious and porous: porous rocks and soils - sandstone, conglomerate, sand, gravel, and cobble.
3. Impervious and porous: impervious and porous rocks and soils - claystone, siltstone, clay, marl, and fine silt.

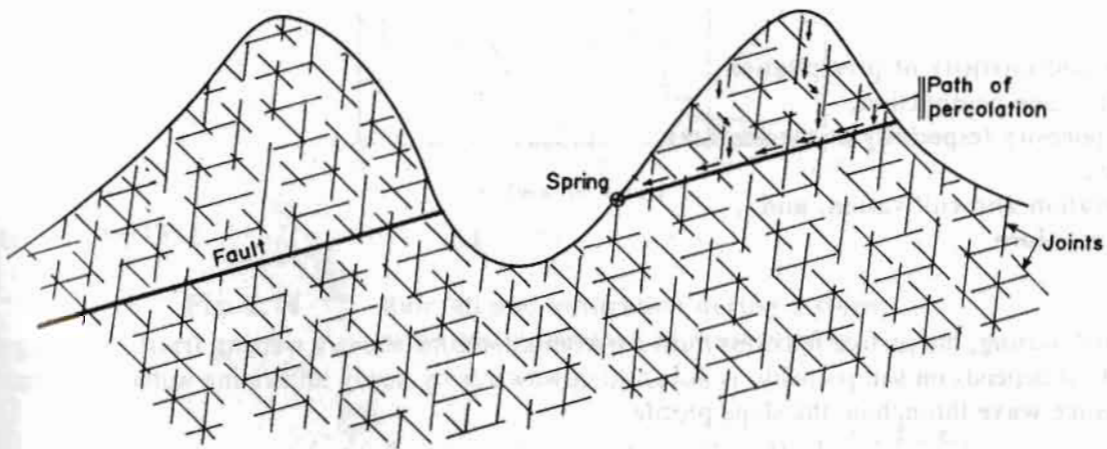


Fig. 2.13 Spring controlled by a fault

2.6.4 Aquifer

An aquifer is a layer of rock or soil in which the pores, cavities, and fissures are saturated with water and through which the groundwater moves.

2.6.5 Spring

A spring is the natural outflow of underground water on to the surface. Often springs are confined to depressed sectors of the relief where the aquifers outcrop on the surface. The quantity of water discharged by a spring is called its yield.

A general emission of water along the line of interception is called **seepage**. The diagram in Figure 2.13 illustrates an example of structures favouring the development of springs.

2.6.6 Water and Soil Slope Movements

Before the infiltration process, rainfall may be intercepted by the leaves of trees or shrubs or may become stem flow as it runs down the trunks of plants. This phase occurs at the beginning of a storm, during which water may be directly absorbed or evaporated from the plant surface. The capacity of the plant to store and lose water by evaporation declines with the increasing duration of the storm. Under prolonged rainfall the canopy may become saturated, the interception loss declines to virtually nothing, and the infiltration process starts.

Infiltration is a process by which water enters the surface horizon of soil. **Percolation** down to the water table occurs beneath the surface horizons. Infiltration may be controlled by a variety of factors. The most important are:

- type and intensity of precipitation,
- surface soil compaction,
- soil porosity (especially at the surface),
- slope,
- vegetation and cultivation, and
- soil moisture.

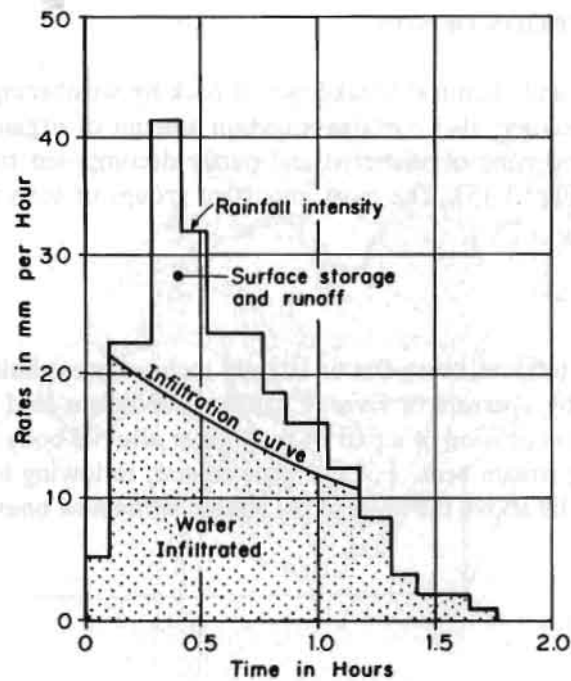
After initial wetting, the surface horizons form a transmission zone above a **wetting front**. Existing soil water, which depends on soil porosity, is displaced downwards by newly infiltrating water which moves as a **pressure wave** throughout the slope profile.

In multi-layered soils, **permeabilities** vary so that saturated layers may form above each less permeable horizon. A steady rate of infiltration is achieved when the entire profile is transmitting water at the maximum rate permitted by the least permeable horizon. This infiltrated water then forms the water table through percolation.

Excess water which cannot infiltrate is stored initially in surface depressions and once these are filled the excess spills downslope as **overland flow**. The changing rate of infiltration may be represented by a curve (Fig. 2.14).

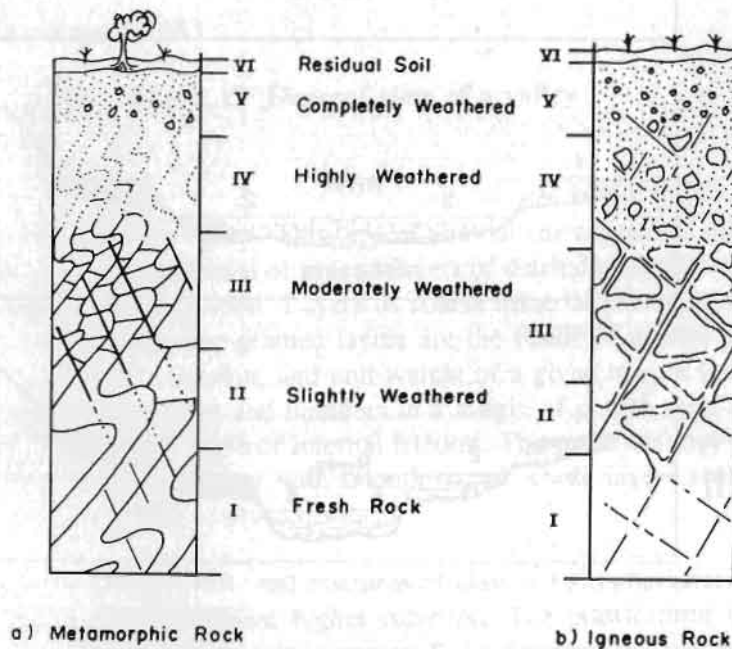
When rainfall is intense, runoff and storage is high. The intensity of a storm is therefore one of the main causes of erosional processes such as **sheet erosion**, **rilling**, **gullying**, and other slope movements.

Infiltration and, therefore, runoff is strongly influenced by the texture of the soil as sands and gravels may be several times more permeable than clays. Permeability alone, however, does not control infiltration. It is also controlled by land use practices, vegetation cover, and slope. Compaction by animals or machinery may reduce the porosity and permeability. The range of infiltration in relation to vegetation, slope, and antecedent moisture content has to be taken into account when erosion hazard is assessed.



Source: Selby 1982

Fig. 2.14 Rainfall and infiltration during a storm
At low rainfall intensities, all water infiltrates.



Source: Deere and Patton 1971

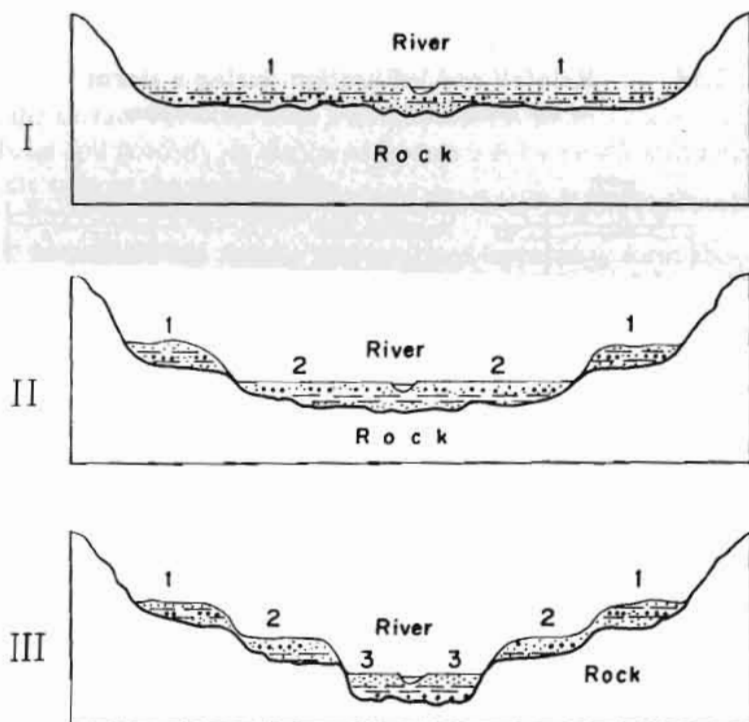
Fig. 2.15 Typical weathering profiles in igneous and metamorphic rocks

2.7 ORIGIN AND DESCRIPTION OF SOIL

Soil is formed by the physical and chemical breakdown of rock by weathering processes. However, the soil (topsoil in engineering geology) also contains a certain amount of organic matter. The soil passes gradually downwards through a zone of shattered and partly decomposed rock (called subsoil) to the bedrock, which is still fresh (Fig. 2.15). The most important groups of soils are described below.

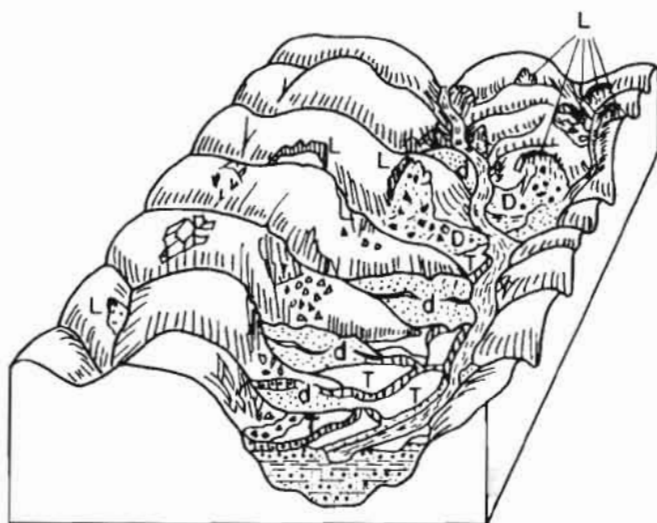
2.7.1 Alluvium

Alluvial soil is found on river terraces or on flat or slightly inclined areas built up over a period of time by detrital material deposited by a stream or river. Changing conditions lead to shifts in the position of the stream bed and to consequent erosion of a part of the former alluvial body. This is why alluvial cliffs are frequently found bordering stream beds. For the same reason, following long periods of erosion and uplift, former alluvial terraces lie above the level of the stream while new ones are deposited below (Fig. 2.16).



Source: Krähenbuhl and Wagner 1983

Fig. 2.16 Deposition of successive alluvial terraces



- d delta
- D facing deltas (may dam the main river)
- T alluvial terraces
- l landslide
- L landslide (may dam tributary)

Source: Krähenbuhl and Wagner 1983

Fig. 2.17 General view of a valley

Fig. 2.17 depicts a general view of a valley. This type of alluvial site represents one or more successive terraces, each of which is usually composed of several layers of detrital material which vary in thickness and in the size of the elements they contain. Layers of coarse material correspond to periods of strong current and heavy erosion, whereas fine-grained layers are the result of quieter periods. The physical parameters such as friction angle, cohesion, and unit weight of a given terrace consequently vary from one layer to another. Layers of pebbles and boulders in a matrix of coarse sand are very porous, pervious, cohesionless, and have a high angle of internal friction. The materials they contain are generally rounded but can frequently be semi-angular with smooth edges. These layers are often poorly graded, particularly when the material is very coarse.

Layers of fine material such as sand, silt, and mixtures of clay and silt characteristically have a rather low angle of internal friction but somewhat higher cohesion. The plastic limit is sometimes critical. Because layers of fine material vary from semi-pervious to impervious, the seepage of water is slowed down or stopped altogether, which sometimes leads to the formation of more or less perennial aquifers. These aquifers frequently determine the stability of alluvial cliffs and adjacent areas and influence the unit weight of the material.

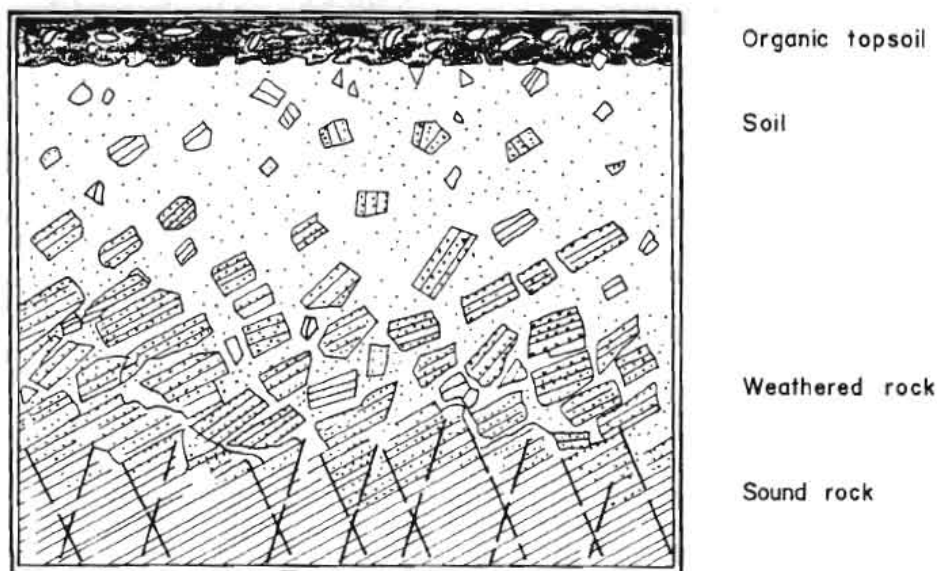
2.7.2 Alluvial Fan or Delta

An alluvial fan or delta (Fig. 2.17) is an alluvial deposit, triangular in shape, at the mouth of a tributary stream emerging into a larger river. Like the alluvial terrace an alluvial fan consists of eroded material brought to the tributary. The bulk of the alluvial material is considerably increased when the catchment area of the tributary is affected by landslides and gully erosion. In such cases, during the monsoon periods, heavy rains and the swelling of the tributary cover the fan with angular pebbles and blocks. Damming may also alter the tributary's course. Should two fan terminals of such eroded basins face both banks of a main river, they may temporarily dam the latter and thus dangerously threaten the downstream channel of the river when the dam bursts. Except when such events take place, the material of the fan is rounded to sub-angular but is poorly graded, rather coarse, and poor in fines. A strong increase in the water level of the main river where the fan emerges may destroy important features of the fan's body.

2.7.3 Eluvial Soils or Regoliths

Eluvial soils originate from the weathering of the underlying rock. For our purpose, only thick eluvial soils are considered. In the case of thin eluvial soils, when rock can be reached by excavation, the site must be considered a rocky site (Fig. 2.18). Thick regoliths appear on rather weak slopes into which surface water may penetrate deeply leading to weathering of the rock. Near the surface, these soils contain small rock debris. The grain size of this debris frequently increases with depth below the surface.

Because the composition of the soil matrix depends on the nature of the parent rock, parameters such as cohesion, permeability, friction angle, and unit weight may vary greatly from one soil to another.

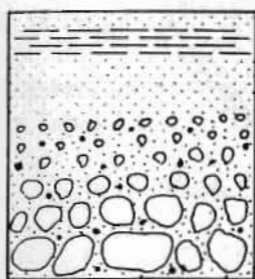


Source: Krähenbuhl and Wagner 1983

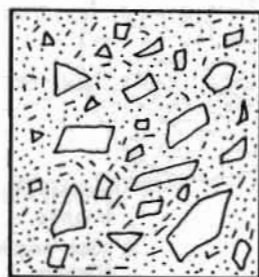
Fig. 2.18 Eluvial soil or regoliths

2.7.4 Colluvium

These soils originate from landslides or transported eluvial soils. They are characterized by angular stones and blocks in a matrix of clay, silt, sand, or gravel. No grading or horizontal continuity is visible (except for weathered, rock-rotational slides where relicts of lamination remain). This is the main criterion distinguishing colluvium from alluvial soils (Fig. 2.19).



a. Alluvium



b. Colluvium

Fig. 2.19 Alluvium and colluvium.

Parameters such as cohesion and friction angle are highly dependent on the rock from which they originate and on the type of movement which has occurred. These types of soil are often unstable and should be considered with caution. Due to weathering, impervious horizons may be formed in the colluvium which leads to the formation of perched water tables. This water table may control rotational slides. In general, the colluvium is thicker at the toe of the slope.

2.7.5 Moraine

A moraine (Fig. 2.20) is a drift deposited by glacial action having a topography different from that of the surface on which it lies. Morainic soils are confined to relatively high altitudes in the Himalayan terrain, though they may be present down to 2,000 m and lower. Moraine consists of gravels, pebbles, and boulders (the latter sometimes reaching large proportions), within a clayey, silty, or sandy matrix. The edges of material are frequently polished by glacial action, distinguishing them from old stabilized landslides. The stones and boulders sometimes exhibit glacial striae or scratches due to the friction and compression they underwent while being transported by the glacier. Often huge boulders (erratic boulders) appear within or on the surface of the moraine. As only glaciers are capable of displacing such material, the presence of huge boulders, especially if they bear striations, is proof of deposits of glacial origin. Moraines sometimes reach great thickness. They generally have poor grading and horizontal continuity, except where they have been reworked by stream action during the glacial period. Glacial valleys characteristically have U shapes, cirque-shaped catchment areas, and horns (Fig. 2.20). As the morainic soils on the slopes are rather unstable, they should be surveyed and tested carefully.

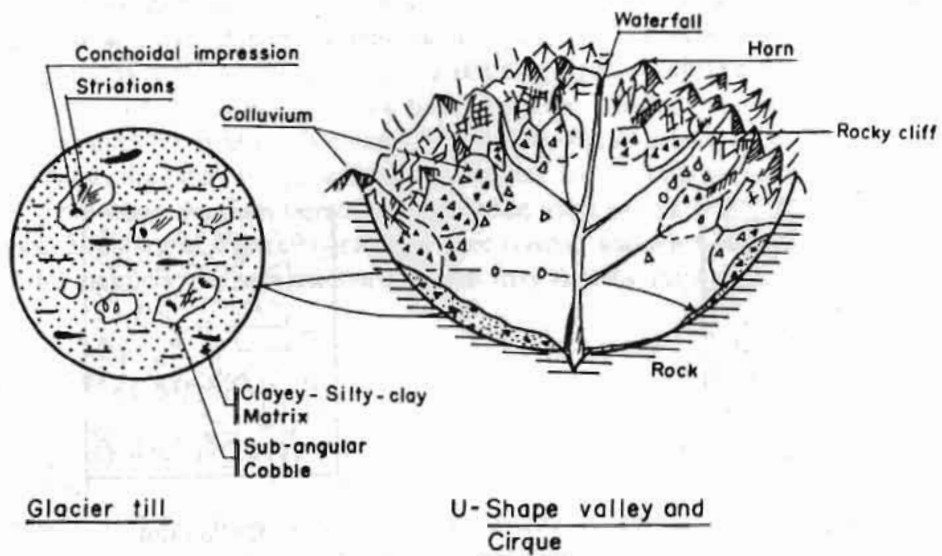


Fig. 2.20 Moraine and Glacial Valley Features

MINERALOGY AND PETROLOGY

3.1 MINERALS AND THEIR PROPERTIES

Rocks are composed of **minerals** which are natural inorganic substances with particular chemical compositions, or ranges of compositions, and regular atomic structures.

Mineralogy involves the study of these minerals. The average composition of rocks in the earth's crust is given in the Table 3.1.

Table 3.1 Average composition of crustal rocks

SiO ₂	59.26 %	Na ₂ O	3.81 %
Al ₂ O ₃	15.35 %	K ₂ O	3.12 %
Iron Oxides	6.88 %	H ₂ O	1.26 %
CaO	5.08%	Others	1.78 %
MgO	3.46 %	Total	100.00 %

Source: Blyth and de Freitas 1985

3.1.1 *Properties of Rocks*

From Table 3.1, it can be observed that silicon and oxygen are the most abundant elements. These combine to form silicates, the main rock-forming minerals. Some common silicates are: feldspar, quartz, mica, amphibole, and garnet. Also commonly found in minerals are oxides such as hematite and limonite. Common sulfide minerals include pyrite, chalcopyrite, and sphalerite.

Minerals are most commonly distinguished by physical properties such as crystal form, colour, streak, lustre, cleavage, fracture, hardness, specific gravity, tenacity, electrical properties, such as magnetism and conductivity, and special properties such as taste (rock salt) and feel (talc).

- Form** describes the shapes of groups of minerals and individual crystal shapes. Figures 3.1 and 3.2 show common mineral forms, and Figure 3.3 illustrates crystal forms.
- Colour** can be misleading, as many minerals assume different colours from the content of impurities. However, certain minerals are identified on the basis of their typical colours.
 - . Jasper - red
 - . Malachite - green
 - . Pyrite - bronze yellow

Figures and Tables without credit lines in this Chapter are compiled by the author(s).

- c. **Streak** is the colour of a mineral's powder which is produced by rubbing on an unglazed porcelain tile or streak plate, or other rough surface. It is useful in distinguishing metallic minerals. This property is more diagnostic than colour in a mineral's identification.

<u>Mineral</u>	<u>Colour</u>	<u>Streak</u>
Haematite	Black	Cherry Red
Magnetite	Black	Greyish black

- d. **Lustre** is a mineral's appearance under reflected light and can be described as metallic or non-metallic. The non-metallic minerals can be classified as vitreous or glassy, resinous or greasy, pearly, silky, dull, etc.

vitreous	-	quartz
pearly	-	biotite
silky	-	asbestos

- e. **Cleavage** is the tendency of a mineral to part easily in directions parallel to crystal faces producing cleavage planes. It can be described as perfect, good, moderate, or poor, and often the number of cleavage directions is also given. For example, biotite mica has one perfect cleavage, whereas calcite has three perfect cleavages.
- f. **Fracture** refers to the nature of the surface of a mineral in a direction other than that of cleavage in crystallised minerals and in any direction in massive minerals.

The terms **conchoidal**, **hackly**, **uneven**, and **even** describe the various types of fracture (Fig. 3.4).

Examples:

conchoidal	-	quartz
even	-	chart
uneven	-	tourmaline

- g. **Hardness** is the resistance offered by the mineral when it is scratched. It is measured on Moh's Scale which gives a relative scale of 10 minerals.

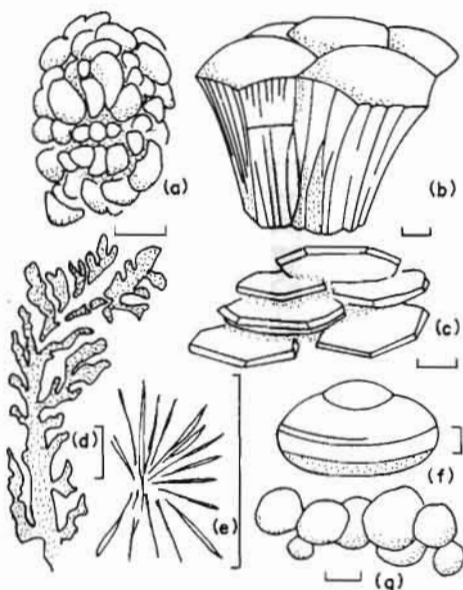
1.	Talc	6.	Orthoclase
2.	Gypsum	7.	Quartz
3.	Calcite	8.	Topaz
4.	Fluorite	9.	Corundum
5.	Apatite	10.	Diamond

The other tools, often used for testing hardness, are the finger nail ($H=3$), window glass ($H=5$), and a knife ($H=6$).

- h. **Specific gravity** (Table 3.2) is the density of a mineral and expressed as:

$$SG = \frac{\text{weight in air}}{(\text{weight in air} - \text{weight in water})}$$

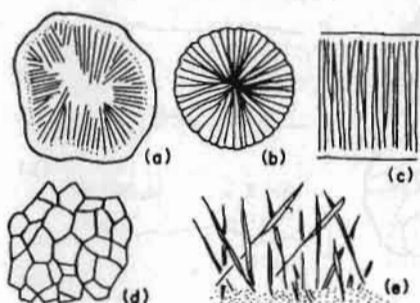
- i. **Tenacity** denotes the response of a mineral to cutting by a knife. For example, **malleable** minerals are gold and copper, **brittle** minerals include quartz and feldspar, **sectile** minerals, such as copper, can be sliced with a knife, and **elastic** minerals, such as muscovite, spring back after bending.



Source: Blyth and de Freitas 1985

Fig. 3.1 Common shapes of mineral clusters

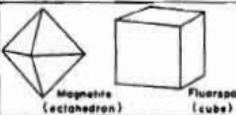
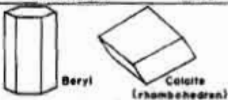
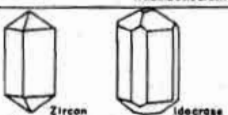
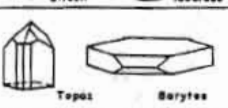
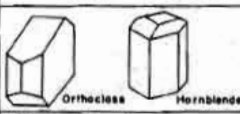
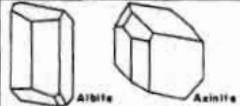
- a. Botryoidal b. Reniform c. Tabular
d. Dendritic e. Acicular f. and g. Concretionary



Source: Blyth and de Freitas 1985

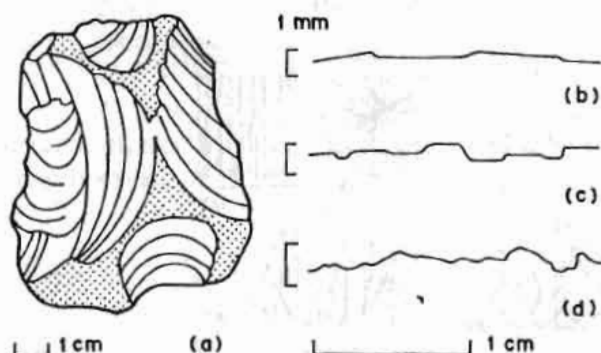
Fig. 3.2 Relationship between minerals in clusters

- a. Drusy b. Radiating c. Fibrous
d. Granular e. Reticulated

Crystal system	Crystal form	
Cubic	 Magnetite (octahedron) Fluorite (cube)	Examples
		Garnet, leucite, fluorite, rock salt, zinc-blende, pyrite
Hexagonal and trigonal	 Beryl Calcite (rhombohedral)	Beryl, nepheline, apatite, tourmaline, calcite, quartz
Tetragonal	 Zircon Idocrase	Zircon, cassiterite (tin-stone), idocrase
Orthorhombic	 Topaz Barytes	Olivine, enstatite, topaz, barytes
Monoclinic	 Orthoclase Hornblende	Orthoclase, feldspar, hornblende, augite, biotite, gypsum
Triclinic	 Albite Axinite	Plagioclase feldspars, axinite

Source: Modified after Blyth and de Freitas 1985

Fig. 3.3 Common crystal forms and systems



Source: Blyth and de Freitas 1985

Fig. 3.4 Fracture of minerals

a. Conchoidal b. Even c. Uneven d. Hackly

Table 3.2 Specific gravity of common minerals

Feldspar	2.56 - 2.7
Caetite	2.7
Quartz	2.65
Dolomite	2.85
Chlorite	2.2 - 3.3
Muscovite	2.8 - 3.0
Hornblende	3.2
Tourmaline	3.0 - 3.2

Source: Anbalagan 1991

Table 3.3 Non-metallic Minerals

Mineral	Hardness	Lustre	Cleavage	Colour	Remarks
Talc $\text{Mg}_3\text{Si}_4\text{Al}(\text{OH})_2$	1	Greasy	1 perfect	White, light green	Usually as alteration in mafic/ultramafic rocks. Often with serpentine, sometimes with magnesite.
Chlorite (Fe,Mg) ₅ $\text{Si}_3\text{Al}_2\text{O}_{10}(\text{OH})_2$	2-2.5	Dull to resinous	1 perfect	Clear to white	In low to medium grade metamorphic and igneous rocks.
Muscovite K Al ₂ $(\text{AlSi}_3)\text{O}_{10}(\text{OH})_2$	2-2.5	Pearly	1 perfect	Clear to white	Occurs in granites and felsic rocks, gneisses, schists, and sedimentary rocks. Sericite is a fine-grained secondary alteration.
Biotite K (Mg,Fe) ₃ $(\text{Si}_3\text{Al})\text{O}_{10}(\text{OH})_2$	2.5-3	Pearly to submetallic	1 perfect	Brown to black	In igneous rocks, gneisses and schists. Commonly alters to chlorite.
Plagioclase feldspar -Albite ($\text{NaAlSi}_3\text{O}_8$) -Anorthite ($\text{CaAl}_2\text{Si}_2\text{O}_8$)	6-6.5	Vitreous	2 good at 90°, 1 poor	White, grey, blue, yellow	Twining striae common on cleavages. Often occurs with orthoclase. Common in igneous and some metamorphic and sedimentary rocks.
Dolomite $\text{CaMg}(\text{CO}_3)_2$	3.5	Pearly to vitreous	3 perfect	White to brown	Effervesces in warm HCl, or when powdered. Major constituent of dolostone deposits.

Mineral	Hardness	Lustre	Cleavage	Colour	Remarks
Garnet Group $X_3 Y_2 (SiO_4)_3$ where X = Ca, Mg, Fe^{+2} , Mn^{+3} and Y = Al, Fe^{+3} , Cr	6.5-7.5	Vitreous to resinous	Conchoidal fracture	Red, brown, yellow, green	Dodecahedron or trapezohedron form. Most of metamorphic origin, some of igneous origin. Also occurs in hydrothermal deposits such as skarns.
Quartz SiO_2	7	Vitreous none	Conchoi- dal	Colour- white, yellow, brown, grey	Hexagonal prismatic crystals. In granitic rocks as clear, glassy crystals. Also as phenocrysts and in veins and infillings. Abundant in gneisses, schists, and arenaceous sandstones.
Tourmaline $Na (Mg P_1 Fe)_3$ $Al_6 (BO_3)_3 (Si_6 O_{18})$ $(OH_1 F)_4$	7-7.5	Vitreous	Conchoi- dal fracture	Black (most common), blue, pink, yellow, multi- coloured	Hexagonal or trigonal crystals, sometimes radiating. In igneous and metamorphic rocks. Often in hydrothermal deposits.
Amphibole Group- Hornblende $(Ca Mg Na Al)_3$	5-6	Vitreous to resinous	2 perfect at 56° and 124°	Brown to greenish black	Usually as monoclinic bladed crystals. Common in igneous and metamorphic rocks. Alteration to chlorite.
Pyroxene Group- Monoclinic pyroxene e.g. Augite $(CaMgFeAl)_2 (SiAl)O_3$	5-6	Vitreous to resinous	2 good at 93° & 87°	Brown to greenish black	Usually as 8-sided prisms in mafic to ultramafic rocks.
Orthorhombic e.g. Hypersthene $(Mg Fe)SiO_3$ Enstatite $MgSiO_3$	5-6	Vitreous to resinous	2 good at 93° & 87°	Dark to green	8-sided prisms in mafic igneous and some ultramafic rocks.
Epidote $Ca (FeAl)_3$ $(SiO_4)_3 (OH)_2$	6-7	Vitreous	2 moderate	Pistachio green	Monoclinic crystals, generally in radial clusters. Alteration product of anorthitic plagioclase, pyroxenes or hornblendes. Also a metamorphic mineral, in igneous veins, and as volcanic rock vesicles.
Orthoclase feldspar $KAlSi_3O_8$	6-6.5	Vitreous	2 good at 90° 1 poor	White, pink, grey, blue, brown	Perthitic intergrowth common. In granites, gneisses, and sand- stones. Often as porphyroblasts in gneissic rocks. Alters to kaolinite and sericite.

Source: Dhital 1991

Table 3.4 Metallic Minerals

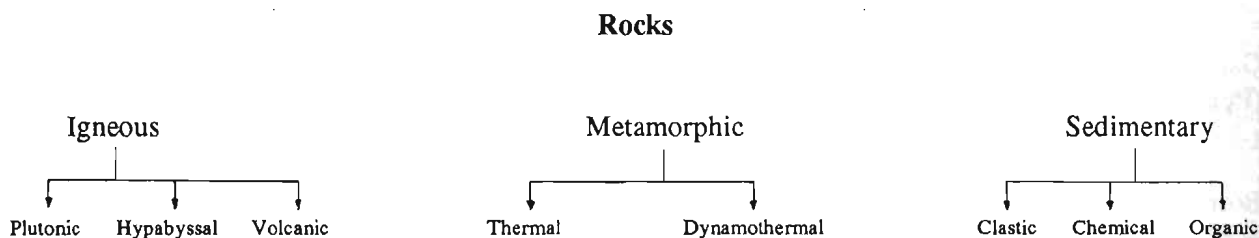
Mineral	Hardness	Streak	Colour	S.G.	Lustre	Comments
Graphite (C)	1	Black	Black	2.2	Metallic	Layered mineral. Marks paper, slippery feel. In veins, metamorphic rocks.
Copper (Cu)	2.5	Copper-red	Copper-red	8.9	Metallic	Malleable. Native copper is rare.
Gold (Au)	2.5	Yellow	Yellow	19.3	Metallic	Malleable. Usually as fine disseminations with sulfides such as pyrite and in quartz veins.
Galena (PbS)	2.5	Lead-grey	Lead-grey	7.4 - 5.1	Metallic	Dense feel. Perfect cubic cleavage. Infillings and fractures, skarn replacements.
Bornite (Cu ₅ FeS ₄)	3	Greyish black	Bronze-brown, Iridescent peacock tarnish	4.9-5.1	Metallic	Common with other copper minerals in hydrothermal deposits & veins.
Malachite Cu ₂ (OH) ₂ CO ₃	3.5	Dull to silky	-		Green	Copper ore produced by weathering of copper minerals. Appears as staining. Botryoidal form common.
Sphalerite (ZnS)	3.5-4	Brown-yellow	Yellow, brown, red, black	4	Resinous	In sedimentary and hydrothermal replacement deposits.
Chalcopyrite (CuFeS ₂)	3.5-4	Greenish black	Brass yellow	4.2	Metallic	Main source of Cu in varied environments. Usually with pyrite and other Cu minerals in veins. Also in metamorphic rocks.
Limonite Fe ₂ O ₃ (3H ₂ O)	5	Yellow brown	Yellow to brown	3.8	Earthy	Along fractures, weathered surfaces as weathering deposits.
Hematite (Fe ₂ O ₃)	5 - 6	Red	Cherry red	5.3	Metallic	Common source of iron ore. Also in igneous rocks, metamorphic rocks, in hydrothermal deposits.
Magnetite (Fe ₃ O ₄)	5.5-6.5	Black	Black	5.2	Metallic	Strongly magnetic. Igneous and clastic sedimentary rocks. Also in metamorphic and hydrothermal deposits.
Pyrite (FeS ₂)	6.5	Black	Brass - yellow	4.9 - 5.2	Metallic	Similar to gold. Disseminated crystals common in veins, quartzites, igneous and metamorphic rocks. The most widespread sulfide.

Source: Dhital 1991

3.2 PETROLOGY

Petrology studies the origin, distribution, and composition as well as alterations of rocks occurring in the earth's crust. Rock is an aggregate of minerals, and there are three main categories of it according to origin. They are igneous, metamorphic, and sedimentary rocks. Texture is an important property in identifying the types of rock. Texture is defined as the relationship among the mineral grains of which the rock is constituted. The texture includes size, shape, and arrangement of constituent particles. Table 3.5 provides a general classification of rocks.

Table 3.5 General classification of rocks



Source: Anbalagan 1991

3.2.1 *Igneous Rocks*

Igneous rocks are the product of solidification of lava or magma on or below the earth's surface.

Plutonic rocks have cooled deeper below the earth's surface and are also known as **intrusive** rocks. **Volcanic, effusive, or extrusive** rocks are formed due to ejection of magma through volcanic pipes and vents and cool on the earth's surface. They can be classified as **flows** or **pyroclastics** depending upon their mode of extrusion. While extremely rare in Nepal, these rocks are common in North Western India, in the Deccan traps, in South-central Tibet, and Northern Burma, to mention a few places.

a. *Intrusive (or plutonic) Rocks*

These rocks are formed by cooling of magma at greater depth beneath the earth's surface. They differ in texture from other rocks because of their cooling history. Depending on their size they are classified as major or minor intrusions.

i. Major intrusions

These are classified as **batholiths** (Fig. 3.5) and **stocks** in decreasing order of size. It is generally accepted that major intrusions are the result of forceful injection, that is, they physically push aside the

surrounding rocks. Evidence in the form of **xenoliths**, which are remains of the country rock present within the intrusions, supports this theory. However, in some areas, intrusions grade gradually into country rocks, with no apparent break. This kind of evidence supports the theory of partial melting of country rocks and solid state diffusion known as **granitisation** (i.e., becoming granite).

ii. Minor intrusions

Leading from major intrusions are often fingers of magma, forming dykes, veins, sills, laccoliths, and lopoliths.

Dykes (Fig. 3.5) are tabular bodies which cross-cut country rock. They vary in width from several cm to about 5m and may be continuous over several kilometres. **Dyke swarms** are groups of dykes arrayed either in a parallel or radiating manner.

Sills are approximately parallel to the layers of rocks they intrude and are usually fed by vertical and sub-vertical dykes (Fig. 3.5).

b. *Hypabyssal Rocks*

The rocks that are formed by solidification of magma at shallow depth are called hypabyssal rocks. They are characterised by the inequigranular size of minerals ranging from coarse to fine. This type of texture is called 'porphyry'. These rocks generally occur as minor intrusions.

c. *Volcanic Rocks*

The rocks that crystallise on or very near the surface are known as volcanic rocks. They are formed as a result of the eruption of lava along conduits leading from the earth's surface down to a magma chamber. Usually, a crater is formed on eruption (Fig. 3.5). The type of volcanic eruption, violent or quiet, depends upon the viscosity, chemical composition, and gas content of the magma. Normally, mafic magmas, such as basalts, which have low silica contents, extrude quietly as lava flows. Highly siliceous rocks are generally viscous and commonly contain high amounts of gases. These erupt violently to form glowing avalanches of debris and lava called *nuées ardentes*. **Pyroclastic** rocks are formed as a result of violent eruptions. The plateau basalts of the Deccan Plateau in India are examples of quiet eruptions, while Krakatoa in Java, in 1883, erupted so forcefully that dust from the eruption circled the earth's upper atmosphere for a year after the explosion. Hot springs are often, though not always, associated with the warning phases of a volcanic area.

i. Engineering considerations

Because of the complex processes involved, volcanic rocks can produce very complicated associations. Periods of volcanism are interrupted by quiescence, during which different rocks are formed. Volcanic episodes may also produce different rocks depending upon the magma's chemical and fluid composition, both of which are highly variable.

The inter-trappean beds, which include the sediments deposited between successive volcanic activities, have different engineering properties compared to the rocks above and below. When major structures such as dams are planned on these rocks, the non-homogeneity of the foundation condition causing differential settlements may be studied in detail.

Pyroclastic rocks (breccia and tuff) are generally quite porous, but rhyolitic lavas are not. Thus, weathering zones may be hidden by strong basaltic lavas and large variations in thickness are to be expected.

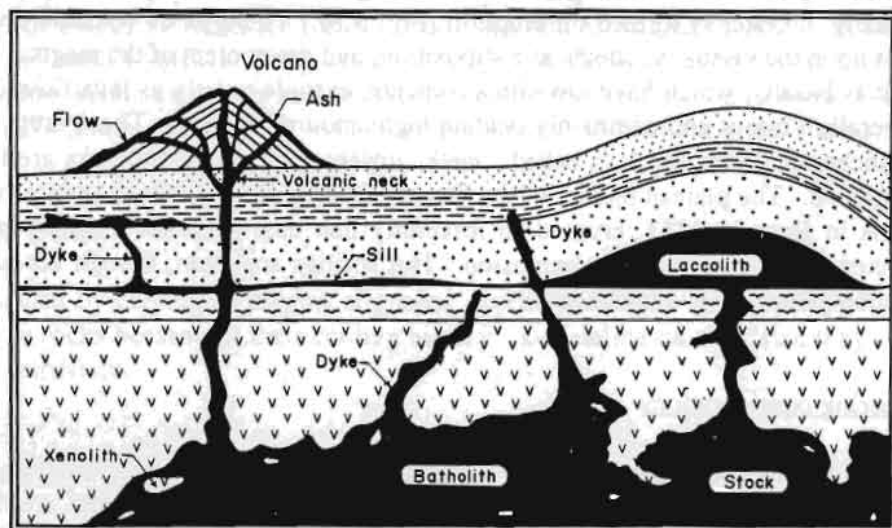
These considerations highlight the importance of detailed mapping and careful interpretation in volcanic terrain. Proper selection of representative samples for laboratory and field tests are required due to the possible variability of these rocks. Cross sections are essential in the case of detailed studies.

d. Classification

Igneous rocks are classified by their texture and mineral composition. Table 3.6 shows the common textures of igneous rocks and Table 3.7 provides a detailed classification of igneous rocks.

The texture of an igneous rock depends upon its mode of emplacement. Thus, a volcanic rock, which cools quickly on the earth's surface, is finer grained than a plutonic rock which solidifies over long periods in the earth's crust.

The texture and composition of an igneous rock has great bearing on its engineering characteristics. A highly vesicular basalt, with many holes, called **vesicles**, is highly porous and weak and weathers readily to clay. On the other hand, a dense, quartz-rich rhyolite flow is harder than any granite and is highly resistant to weathering. It is thus imperative that an engineer recognizes the different rock types and is able to classify their texture. As many descriptive terms as possible should be used in describing a rock's physical characteristics.



Source: Skinner and Porter 1987

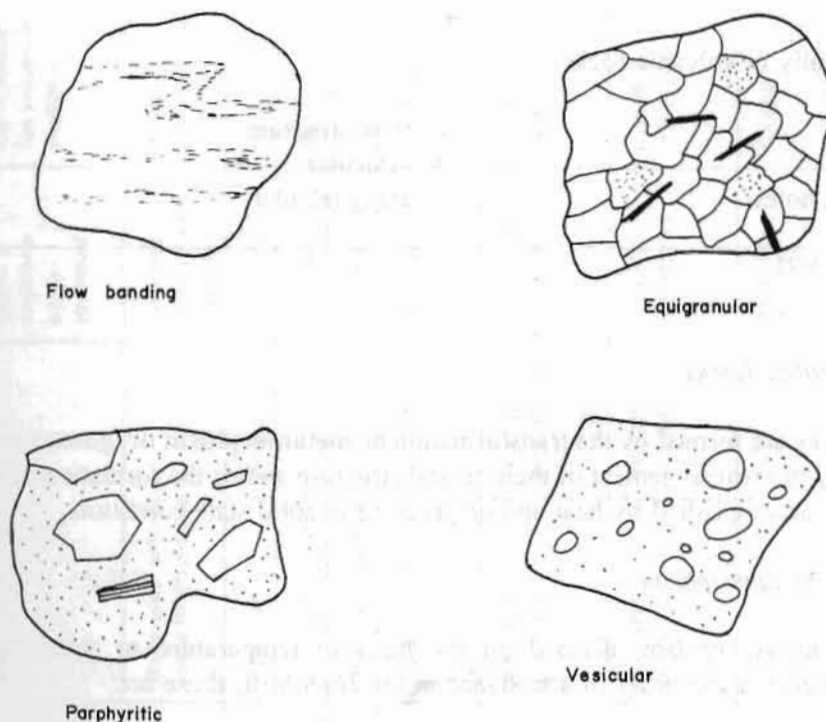
Fig. 3.5 Block diagrams illustrating a pluton, dykes, and sills

The common textures seen under a microscope are shown in Fig. 3.6. The mineral composition of a rock is dependent upon its chemistry. Broadly, igneous rocks are classified as felsic (or acidic) and mafic (or basic) depending upon their silica (SiO_2), alkali (Na_2O , K_2O , and CaO) and ferromagnesian content. Felsic rocks are lighter in colour than mafic ones. Ultramafic rocks are very dark coloured.

e. *Engineering Considerations*

The mineral composition of igneous rocks affects their weathering and other properties. Pyroxenes and amphiboles, both high-temperature minerals, are unstable on the earth's surface and decompose readily to chlorite and other clays. These minerals are common in veins and dykes, basalt tuffs and flows, and mafic plutonic rocks such as gabbro. The engineer should be alerted to these rocks as potentially unstable units and use discretion in construction, excavation, and blasting.

On the other hand, granites are generally quite strong, although their feldspars can weather to clays under tropical and sub-tropical conditions. The interrelationship between igneous rocks and their country rocks should also be observed. Horizontal sills may have a destabilizing effect on a hillslope by allowing ground water to accumulate above it, giving rise to perched water tables. Interlayered, impervious igneous sills and sedimentary rocks have also been blamed for piping failures due to the preferential movement of water above the sills.



Source: Blyth and de Freitas 1985

Fig. 3.6 Common igneous rock textures described in Table 3.6.

Table 3.6 Commonly used terms for describing igneous rock texture

1. Crystal size

Intrusive rocks	> 2 mm	= coarse-grained	Phaneritic
	0.06 - 2 mm	= medium-grained	(crystals visible)
	< 0.06 mm	= fine-grained	
Volcanic rocks	< 0.06 mm	= aphanitic	(crystals not visible)
Crystals not present		= glassy	

2. Crystal Shape

Well-defined	= euhedral
Ill-defined	= anhedral

3. Relative crystal size

Same size	= equigranular
Some larger than others	= inequigranular
Large crystals set among small crystals	= porphyritic

4. Others (generally in volcanic rocks)

Banding	= flow structure
With holes	= vesicular
With in-filled holes	= amygdaloidal

Source: Dhital 1991

3.2.2 Metamorphic Rocks

Metamorphic rocks are formed by the transformation or **metamorphism** of igneous or sedimentary rocks into new rocks by the rearrangement of their crystal structure and/or the formation of new minerals. This transformation is accomplished by heat and/or pressure in solid state condition.

a. Types of Metamorphism

Three types of metamorphism, divided on the basis of temperature or pressure controls, can be distinguished. In decreasing order of abundance in the *Himalaya*, these are:

- i. regional metamorphism, divided on the basis of temperature and pressure has affected a large area due to confinement of overlying rocks, shearing stresses due to plate movements, and large igneous intrusions;

Table 3.7 Classification of Igneous Rocks

MINERAL COMPOSITION														
Dark Minerals	Subordinate (biotite and/or amphibole, less commonly pyroxene)	Abundant (biotite and/or amphibole and/or pyroxene)	Dominant (pyroxene and/or olivine less commonly amphibole)	Predominant (olivine and/or pyroxene; less commonly amphibole)	Lava flows Volcanic explosion (pyroclastic)	Extrusive	Volcanic	Hypabyssal	Plutonic					
Feldspars	Predominant orthoclase, minor Na Plagioclase	Dominant (mostly Na-Ca plagioclase)	Abundant (Ca-plagioclase)	Little or no feldspar										
Quartz	With quartz	No quartz	No quartz	No quartz	Small or tabular shallow bodies and lava flows	Intrusive	Medium to large, deep-seated masses							
Fragmental	TUFF (lithified ash)	VOLCANIC	BRECCIA											
Glassy	OBSIDIAN (dark glass)	PUMICE			UNCOMMON									
Aphanitic (< 0.06 mm) (micro crystalline)	RHYOLITE TRACHYTE FELSITE	ANDESITE	BASALT											
Porphyritic (Phenocrysts in aphanitic groundmass)	RHYOLITE PORPHYRY	ANDESITE PORPHYRY	BASALT PORPHYRY											
Porphyritic (Phenocrysts in phenitic groundmass)	GRANITE PORPHYRY	DIORITE PORPHYRY	GABBRO PORPHYRY											
Phenitic (coarsely crystalline) (> 2 mm)	GRANITE	DIORITE	GABBRO	PERIDOTITE PYROXENITE HORNBLENDITE										
Light Coloured		Intermediate		Dark Coloured						Basic	Ultrabasic			
Acidic														
T E X T U R E														

Source: Anbalagan 1991

- ii. dynamic or cataclastic metamorphism, where pressure (in the form of stress) is the dominant control, in fault and shear zones, and
- iii. contact or thermal metamorphism, where heat is the most important control, as in contact aureoles around igneous bodies.

Each of the above metamorphic types has distinct textural and mineralogical features which affect its physical properties.

i. Regional Metamorphism

As the name suggests, this process acts over large areas, typically hundreds to thousands of square kilometres, and develops due to the heat and stresses arising from burial, shearing, and igneous intrusions.

With increasing depth, pressure and temperature increase. As rocks are subjected to ever-increasing pressure and temperature regimes, they undergo facies changes (Fig. 3.7). Each **facies** is distinguished by sets of index minerals and particular textural types. The first occurrence of any one of these minerals marks the beginning of a particular facies.

For instance, during the metamorphism of a shale, the following rocks and corresponding facies are observed:

Rock name	shale	slate	phyllite	gneiss	migmatite
Metamorphic facies	unmeta-morphosed	zeolite	green-schist	amphibolite	partial melt

As metamorphism increases the **texture** of a rock changes. At very low metamorphic grades, shale will preserve its bedding and other sedimentary textures. As pressure increases, it is transformed into slate which possesses both bedding and cleavage (Fig 3.8). In some places, slaty cleavage may be parallel to bedding but, in others, it may be perpendicular to it (Fig 3.8).

With increasing metamorphism, a highly foliated, shiny rock named **phyllite** results. Micas such as chlorite and muscovite begin to grow along foliation planes perpendicular to the principal stress. This rock cleaves easily along its foliation planes and, together with quartzite, causes mass movements. **Schists** are crystalline, foliated rocks whose minerals can be distinguished in hand specimens (Fig 3.9). They are composed of micas, quartz, and hornblende, depending upon the original rock. Generally, metamorphosed clay-rich sedimentary rocks are rich in micas. Likewise quartzites are rich in quartz and meta-volcanics are rich in chlorite and hornblende. **Gneisses** (Fig 3.10) are coarse-grained, crystalline rocks with thick, sometimes indistinct, bands of quartz, feldspar, and mafic minerals. Breakages along foliation are sometimes accompanied by breakages across it.

In the *Himalaya*, augen (eye-shaped) gneisses are common (Fig 3.10), in which the foliation wraps around elongated feldspar and quartz-feldspar masses. These rocks may behave unexpectedly during loading because of their heterogeneous nature. On further application of heat and pressure, partial melting occurs and a rock called **migmatite** forms. Migmatite is a mixed rock of plutonic and gneissic components and has the properties of both.

ii. Cataclastic Metamorphism

During movement along faults, the mechanical breaking and shearing of rock occurs, resulting in fine-grained rocks known as **mylonite**. With further shearing, partial fusion occurs giving rise to **cataclasite**. These rocks contain large amounts of hydrous minerals, such as mica and amphibole, because of the abundance of hydrothermal solutions found along fault zones. **Mylonite zones** occupy large areas and are common along the Main Central Thrust and Main Boundary Thrust, as well as other thrusts. In Southern Tibet, they are also present in the Indus-Tsangpo Suture Zone.

iii. Contact Metamorphism

Contact metamorphism is produced by the intrusion of hot igneous bodies into country rocks. Here the increased temperature is the dominant agent producing changes and the degree of crystallization bears a simple relation to it. Hornfels and allied rocks are formed in the contact aureoles bordering the bodies of plutonic rocks (Fig. 3.11). Hornfels are hard and granular rocks with no preferred orientation of minerals.

b. Classification

Metamorphic rocks are classified by their texture and structure, crystal size, and mineral composition. Most metamorphic rocks have pronounced preferred orientations in which the foliations are very well developed. Some rocks, however, such as quartzites and marbles, which contain a low amount of clay minerals, have little or no foliation.

i. Texture and Structure

Foliation describes the lining up of platy minerals and/or surfaces due to differential stress regimes.

Lineation describes a series of aligned minerals or traces of foliation on a rock surface.

Porphyroblasts are coarser grained minerals within a finer grained matrix. When sheared, these give rise to **augens** (Fig. 3.10).

Crystal size - Contact metamorphic rocks are very fine grained to microscopic. Cataclastic rocks are also very fine grained.

Regionally metamorphosed rocks range in grain size from microscopic to very coarse grained depending on metamorphic grade.

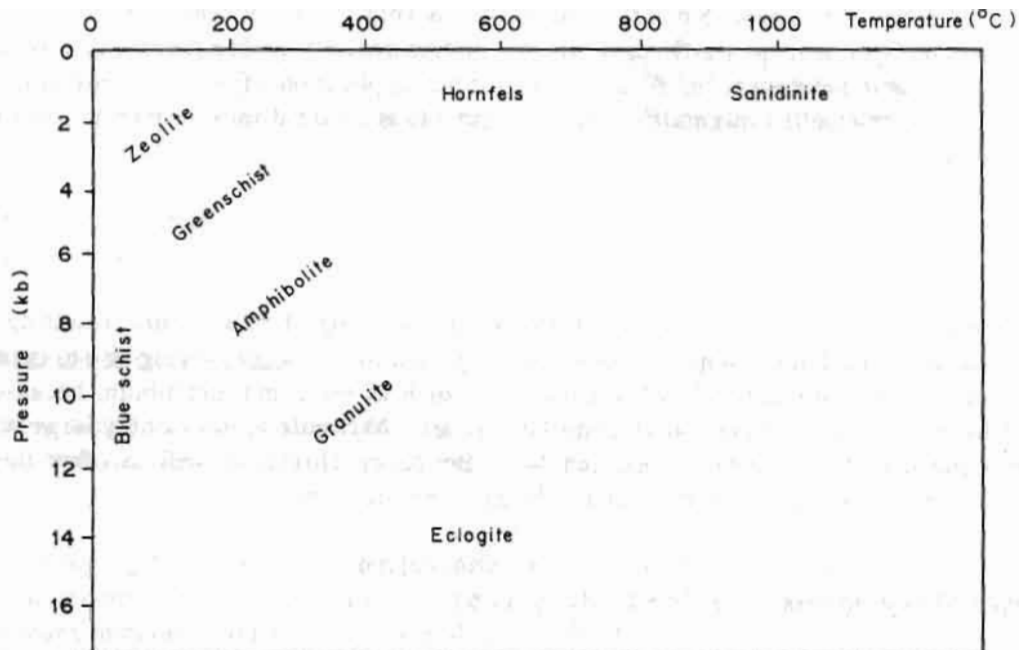


Fig. 3.7 Metamorphic facies according to pressure temperature regimes

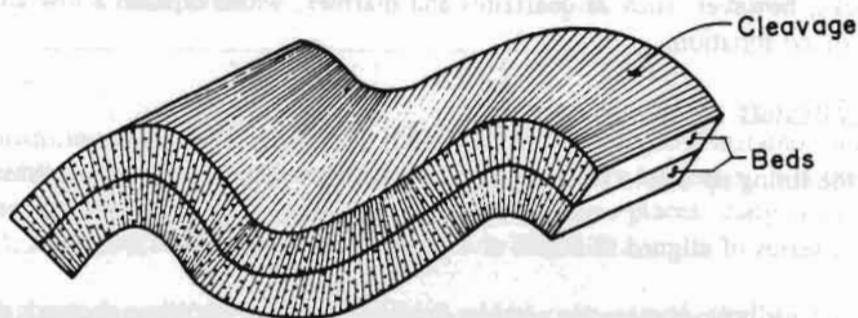


Fig. 3.8 Slaty cleavage and bedding

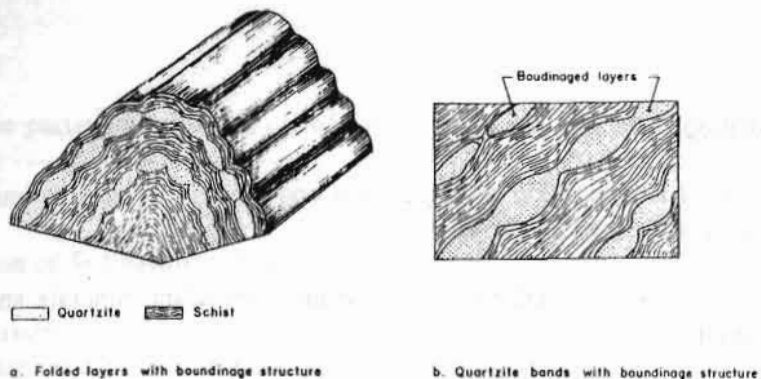


Fig. 3.9 Boudinage structure in gneiss with schistose layers

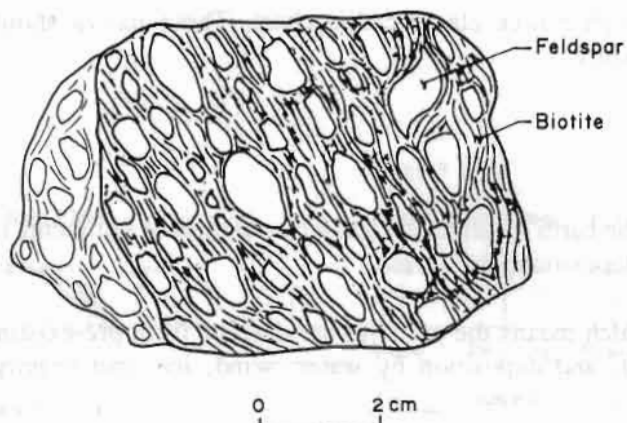


Fig. 3.10 Augen gneiss with 'stretched' porphyroblasts

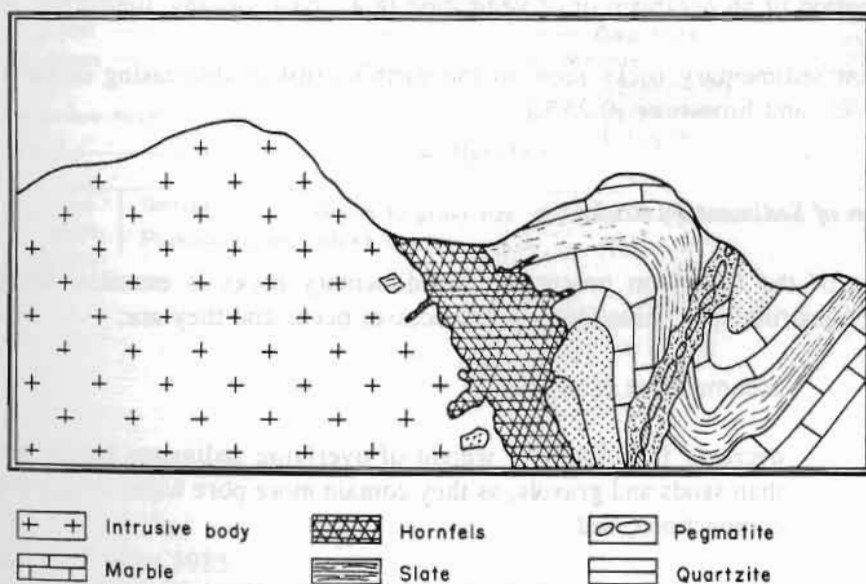


Fig. 3.11 Contact aureoles around igneous intrusion

ii. Mineral Composition

The mineral composition of metamorphic rocks depends upon their original composition, metamorphic grade, and presence of hydrothermal solutions.

Generally, a metamorphic rock is named by listing the most abundant minerals and rock name, e.g., quartz-biotite-garnet schist.

iii. Rock Name

Figure 3.12 gives a metamorphic rock classification chart. These names should be preceded by the predominant minerals and texture.

3.2.3 *Sedimentary Rocks*

These are formed at or near the earth's surface by the accumulation of sediments in a basin of deposition. According to their mode of deposition, they are:

- **detrital** or **clastic** which means the particles are derived from pre-existing rocks by mechanical weathering, transport, and deposition by water, wind, ice, and gravity (e.g. sandstones and conglomerates);
- **chemical** which implies precipitation of minerals from solution (e.g., dolomite, various types of limestone, salt), and
- **organic** which implies that they are formed by the action, fossilization, preservation, or transformation of an organism or of vegetation (e.g., coal, organic limestone, and oil shale).

The most common sedimentary rocks seen on the earth's crust in decreasing order are **shale** (4%), **sandstone** (0.75 %), and **limestone** (0.25 %).

a. *Formation of Sedimentary Rocks*

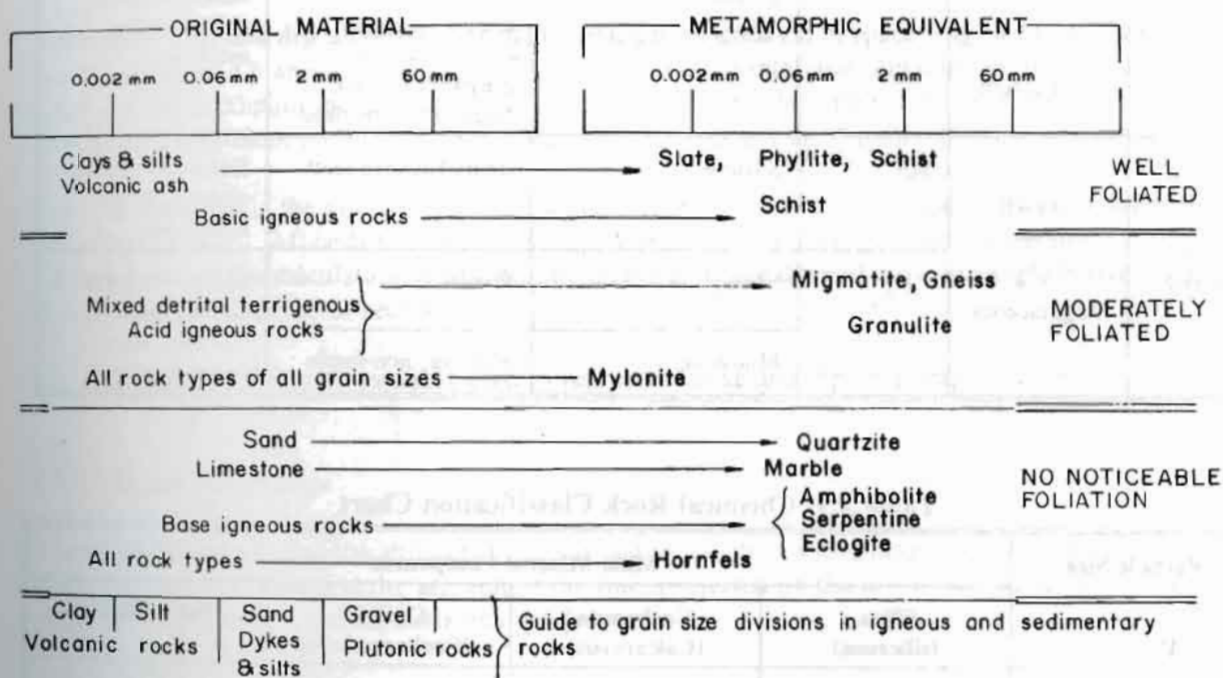
An understanding of the formation processes of sedimentary rocks is essential for predicting their behaviour during construction. Three important processes occur and they are:

1. **deposition** - accumulation of sediments,
2. **compaction** - decrease in volume by weight of overlying sediments (muds are more affected than sands and gravels, as they contain more pore water which is extruded during compaction), and
3. **cementation** - subsequent cementation of particles due to precipitation of minerals (cement) by percolating waters.

The change of loose particles to rock is called **lithification**. It is a chemical process that reduces the original porosity.

b. *Classification of Sedimentary Rocks*

In Table 3.8, the classification of detrital sediments is based on the grain size of the particles. Chemical sedimentary rocks are classified differently, the size limits not being the standards (Table 3.9).



Source: Blyth and de Freitas 1985

Fig. 3.12 Metamorphic rock classification chart

Table 3.8 Detrital sedimentary rock classification chart

Particle size (mm)	Unconsolidated Sediment		Sedimentary rock name	Field identification	Environment of deposition
200	Rudaceous	Boulder	Conglomerate	Rounded fragments in fine-grained matrix; indicates long transport	Glacial moraine, storm beaches, landslide colluvium
		Cobble			
60		Gravel	Breccia	Angular fragments in fine-grained matrix; indicates short transport	River bottoms and banks, deltas, glacial streams
60	Arenaceous	Sand	Sandstone (arkose, greywacke, arenite)	Predominant minerals arkose - feldspar arenite - quartz greywacke - rock fragments with fines	Beaches, river banks, deserts, deltas, glacial moraine
0.06	Argillaceous	Silt	Siltstone	Gritty between teeth	Estuaries, glacial outwash plains, mudflows
0.002		Clay	Shale	Fissile	Glacial outwash plains, till, sea-bottoms, lakes, and mudflows
			Mudstone	Massive, non-fissile	

Table 3.9 Chemical Rock Classification Chart

Particle Size	Main Mineral Component			
	Silica (siliceous)	Carbonate (Calcareous)	Carbon (Carbonaceous)	Salts (Saline)
Megacrystalline > 2 mm		Limestone, Dolomite		Evaporites (after diagenesis)
Mesocrystalline 0.6 - 2 mm			Peat, Coal	Evaporites - rock salt, gypsum, anhydrite
Microcrystalline < 0.06 mm	Flint, chert, jasper, radiolarite, diatomite			

Chapter 4

STRUCTURAL GEOLOGY

4.1 INTRODUCTION

Structural geology deals with rock features of the earth's crust. The geological structures formed during the deposition or emplacement of rock are known as **primary structures**, and those formed later are called **secondary structures**.

4.2 DEFINITIONS

4.2.1 *Strike and Dip*

The **strike**, **dip**, and **dip direction** of a plane define its orientation in space (Fig. 4.1). Figure 4.1 shows that the strike of a plane is the direction (bearing) of a horizontal line contained in that plane and the dip is the line of maximum inclination which is perpendicular to the strike line. It is defined by angle and direction of maximum inclination. For simplicity, the dip and the dip direction are measured.

The **apparent dip** is the dip of any line on a plane other than the true dip and is always smaller than the true dip (Fig. 4.2). All beds have horizontal apparent dips in any vertical section parallel to their strike. Table 4.1 shows the calculation of true dip, given the apparent dip and the acute angle between the strike of the plane and the line of section.

Fig. 4.3 indicates different symbols used to represent strike and dip on a map.

4.2.2 *Trend and Plunge*

Trend and **plunge** define the attitude of a linear feature, such as a fold hinge, mineral lineation, or plane-plane intersection. **Trend** is the azimuth of the line, projected on the horizontal plane, and **plunge** is the angle between the line and its horizontal projection.

4.3 PRIMARY STRUCTURES

Primary structures include those features that are formed concurrently with rock formation. These include the sedimentary structures as well as flow contacts of volcanic rocks. The most important sedimentary structure is **bedding** which separates strata of different composition and texture. Other features, such as ripple marks, cross-bedding, and flute casts are related to bedding. These may affect the behaviour of the bedding surface due to their roughness or waviness. Generally, sediments are deposited horizontally. Subsequent tectonic movements cause these layers to be uplifted, tilted, and warped (Fig. 4.4a).

Figures and Tables without credit lines in this Chapter are compiled by the author(s).

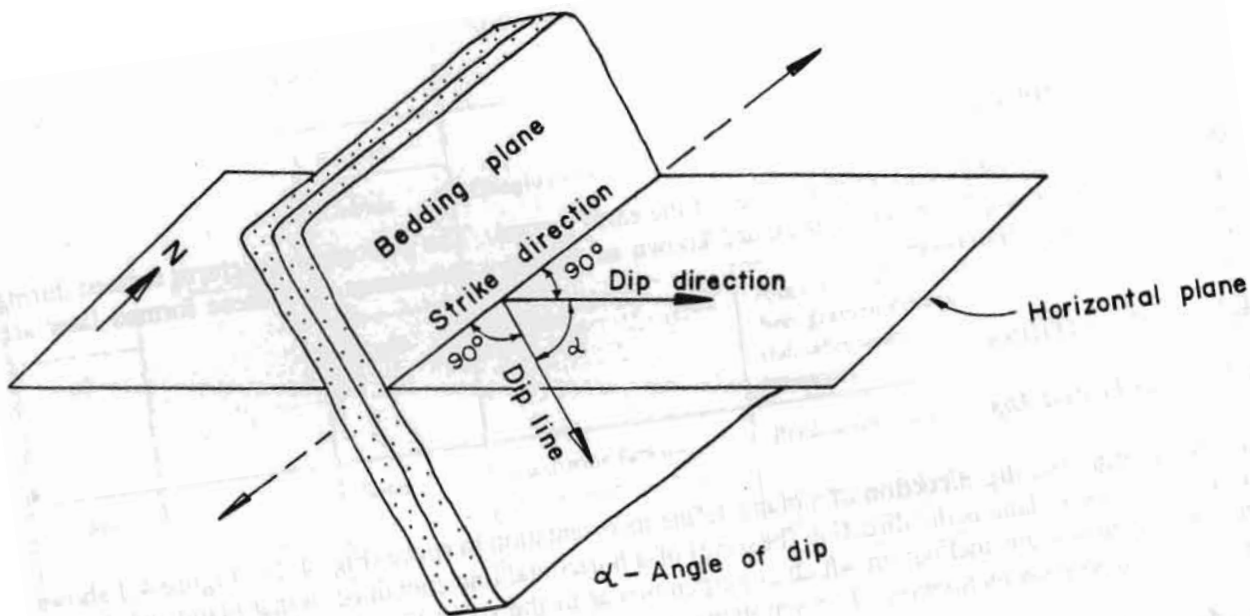


Fig. 4.1 Strike and dip of a plane

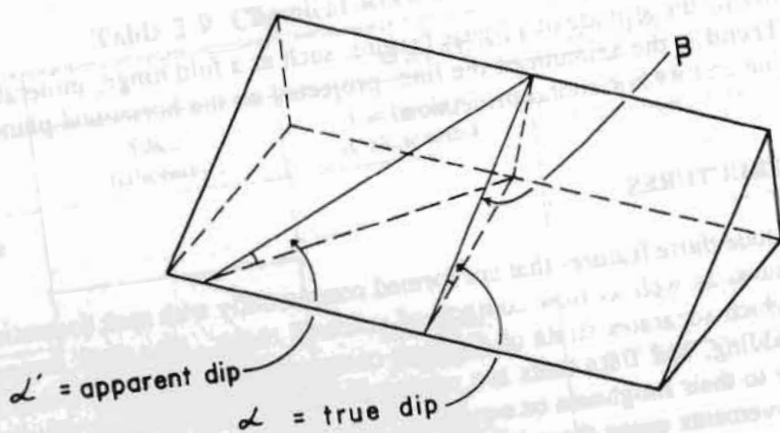
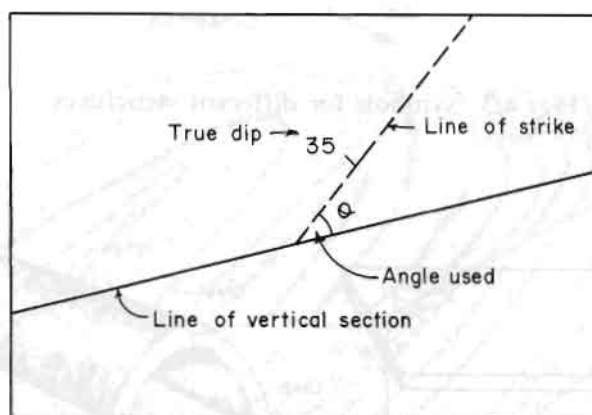


Fig. 4.2 Apparent dip of a plane

Table 4.1 Table for conversion of true dips to apparent dips

$$\tan A = \tan \alpha \cdot \sin \theta$$

A = apparent dip (in degrees)
 α = true dip (in degrees)
 θ = angle between the line of cross-section and the strike line (degrees)



True Dip α	ACUTE ANGLE θ BETWEEN STRIKE AND LINE OF VERTICAL SECTION															
	2.5	5	10	15	20	25	30	35	40	45	50	55	60	65	70	80
5	0.0	0.5	1.0	1.5	2.0	2.0	2.5	3.0	3.0	3.5	4.0	4.0	4.5	4.5	5.0	5.0
10	0.5	1.0	2.0	2.5	3.5	4.0	5.0	6.0	6.5	7.0	8.0	8.0	8.5	9.0	9.5	10.0
15	1.0	1.5	3.0	4.0	5.0	6.5	8.0	9.0	10.0	11.0	11.5	12.5	13.0	13.5	14.0	15.0
20	1.0	2.0	3.5	5.5	7.0	9.0	10.0	12.0	13.0	14.5	15.5	16.5	17.5	18.0	19.0	20.0
25	1.0	2.0	4.5	7.0	9.0	11.0	13.0	15.0	17.0	18.0	20.0	21.0	22.0	23.0	24.0	25.0
30	1.5	3.0	6.0	8.0	11.0	14.0	16.0	18.5	20.5	22.0	24.0	25.0	26.5	27.5	28.5	29.5
35	2.0	3.5	7.0	10.5	13.5	16.5	19.5	22.0	24.0	26.5	28.0	30.0	31.0	32.5	33.5	35.5
40	2.0	4.0	8.0	12.0	16.0	19.5	23.0	26.0	28.5	30.5	33.0	34.0	36.0	37.0	38.5	39.5
45	2.5	5.0	10.0	14.5	19.0	23.0	26.5	30.0	33.0	35.0	37.0	39.0	41.0	42.0	33.0	44.5
50	3.0	6.0	11.5	17.0	22.0	27.0	31.0	34.5	37.5	40.0	42.5	44.0	46.0	47.0	48.0	49.5
55	4.0	7.0	14.0	20.0	26.0	31.0	35.5	39.5	42.5	45.0	47.5	49.5	51.0	52.5	53.5	54.5
60	4.5	8.5	16.5	24.0	30.5	36.0	41.0	45.0	48.0	51.0	53.0	55.0	56.0	57.5	58.5	59.5
65	5.5	10.5	20.5	29.0	36.0	42.0	47.0	51.0	54.0	56.5	58.5	60.0	62.0	63.0	63.5	64.5
70	6.5	13.0	25.5	35.0	43.0	49.0	54.0	57.5	60.5	63.0	64.5	66.0	67.0	68.0	69.0	69.5
75	9.0	18.0	33.0	44.0	52.0	57.5	62.0	65.0	67.5	69.0	70.5	72.0	73.0	73.5	74.0	75.0
80	13.5	26.5	44.5	56.0	63.0	67.5	70.5	73.0	74.5	76.0	77.0	78.0	78.5	79.0	79.5	80.0
85	26.0	45.0	63.5	71.5	75.5	78.0	80.0	81.5	82.0	83.0	83.5	84.0	84.0	84.5	84.5	85.0

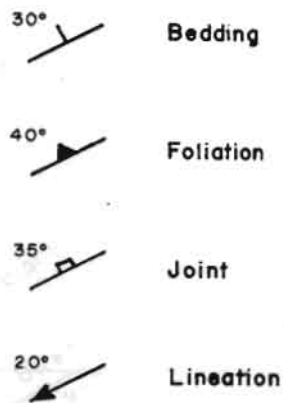


Fig. 4.3 Symbols for different structures

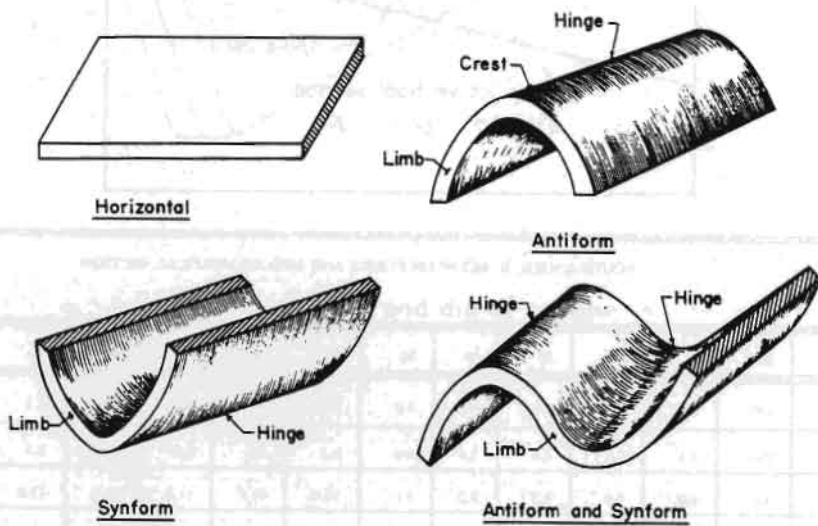


Fig. 4.4a Folded single layer

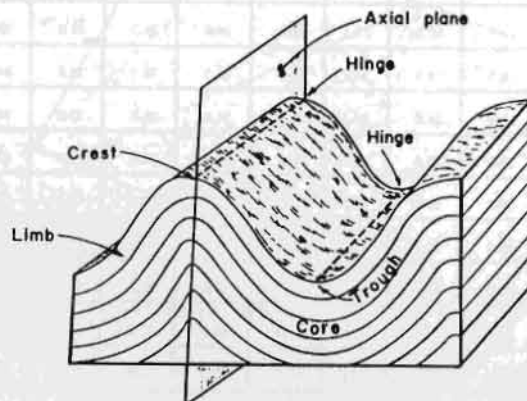


Fig. 4.4b Parts of a fold

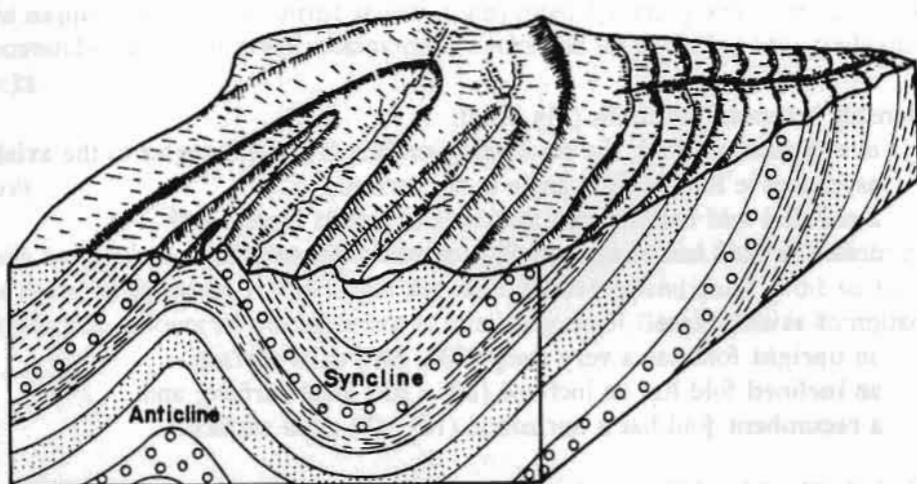


Fig. 4.5 Folded multilayers

4.4 SECONDARY OR TECTONIC STRUCTURES

4.4.1 Folds

A fold is a non-planar configuration of rocks resulting from deformation. When layers are subjected to stress they buckle or fold.

Parts of a Fold

A single fold can be divided into several important parts as follows (Fig 4.4a, 4.4b).

The hinge lines are lines along points of maximum curvature.

The axial plane (or axial surface) is the locus of hinge lines of beds in a fold.

The crest is the highest part of an antiform

The trough is the lowest part of a synform

Folds can be classified as **antiforms** and **synforms** (Fig 4.4a, 4.5). An antiform is a fold with limbs dipping away from each other. When rocks at the core are older than on the outside, this is called an **anticline** (Fig. 4.5). A synform is a fold with limbs dipping towards each other. A **syncline** contains younger rocks at its core (Fig. 4.5).

Geometry of Folds

Folds can have different shapes and orientations. Some important terms describing them are illustrated in Figure 4.6.

- i. Relationship between fold limbs (Fig 4.6a):
 - in a **symmetric** fold, the enveloping surface is at right angles to the axial surface; in an **asymmetric** fold, a right angle is not formed,
 - a **parallel** fold has constant thickness of folded layers, and
 - a **similar** fold has a constant dip, vertically downwards.
- ii. Inclination of axial surface
 - an **upright** fold has a very steep ($90^\circ - 80^\circ$) axial surface,
 - an **inclined** fold has an inclined ($80^\circ - 10^\circ$) axial surface, and
 - a **recumbent** fold has a horizontal ($10^\circ - 0^\circ$) axial surface.

- iii. Interlimb Angle (Fig. 4.6b)

The **interlimb** angle is the angle between the limbs of a fold.

- an **isoclinal fold** has an interlimb angle of about 0° ,
- a **tight fold** has an interlimb angle of less than $< 30^\circ$,
- a **close fold** has an interlimb angle between $30^\circ - 70^\circ$,
- an **open fold** has an interlimb angle between $70^\circ - 120^\circ$, and
- a **gentle fold** has an interlimb angle between $120^\circ - 180^\circ$.

- d. *Small-Scale Structures*

These are generally several millimeters to a few metres in scale and include cleavage, boudinage, and small-scale folds.

- i. Cleavage

Cleavage consists of parallel to sub-parallel fractures often oriented normal to the principal stress. Although cleavage may fan out sometimes about the hinge of a fold, it is generally parallel to the hinge line. On the earth's surface, cleavage is more open in antiforms and closed in synforms (Fig. 3.9).

ii. Boudinage

Boudinage structure results from deformation of a hard or competent layer by stretching into sausage-like boudins. The intervening gaps are filled by incompetent material (refer to Fig. 3.9).

e. *Major Fold Structures*

These may cover several tens to hundreds of square kilometres in area.

In the *Himalaya nappe* structures or thrust-sheets, transported for many kilometres, are common (Fig. 4.7). These commonly have high-grade metamorphic rocks and they overlay low-grade metamorphic or sedimentary rocks.

4.4.2 *Fractures*

When a rock fails by brittle deformation, it **fractures**. If one block moves laterally relative to the other, it is said to have failed by **faulting**. If movement has taken place perpendicular to the surface, it is known as a **joint**. In joints, the amount of displacement is relatively small (less than a few cm).

a. *Faults*

Faults are surfaces parallel to which the movement of rock blocks has taken place. They can be classified into **dip**, **strike**, and **oblique-slip faults**, depending upon the direction of movement (Fig. 4.8). Faults in which the movement is along the dip of the fault are **dip-slip faults**. The apparent vertical displacement of layers is known as the **vertical throw**. When the movement is parallel to the strike of the fault, the faults are called **strike-slip faults**. Faults in which movement is neither parallel to the strike, nor to the dip, are called **oblique-slip faults**. Dip-slip faults are either **normal** or **reverse**.

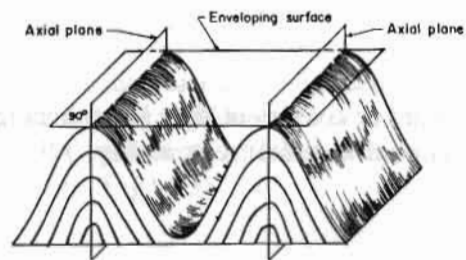
Normal faults are those where the **hangingwall** has moved down relative to the **footwall** (Fig 4.9a). This situation develops during the extension of a layer.

Reverse faults are those along which the footwall moves down relative to the hangingwall along a steeper inclined fault plane (Fig 4.9b). This results in a shortening of the horizontal extent of the rock formation.

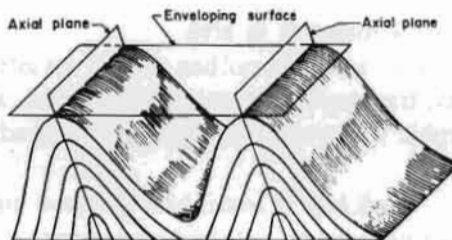
Thrust faults are reverse faults in which planes dip at less than 30°.

A thrust fault develops due to horizontal tectonic stresses. This results in great shortening of the layers, and the resulting **imbrication** appears in the stacking up of successive layers (Fig. 4.10). Nappes are thrust faults with large horizontal displacements. This phenomenon is in the *Himalaya* where complex thrust sheets are piled on top of each other successively giving rise to thrust faults such as the Main Central Thrust (MCT), Main Boundary Thrust (MBT), and large nappes.

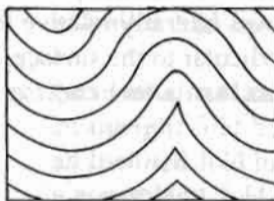
a)



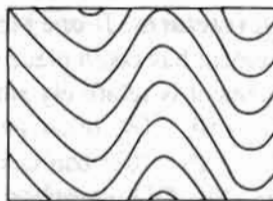
Symmetric



Asymmetric

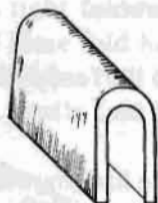


Parallel



Similar

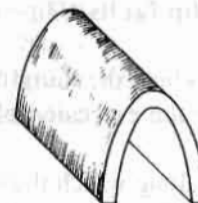
b)



Isoclinal



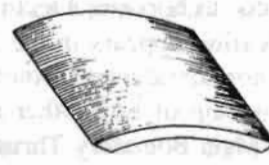
Tight



Close



Open



Gentle

Fig. 4.6 Fold geometry

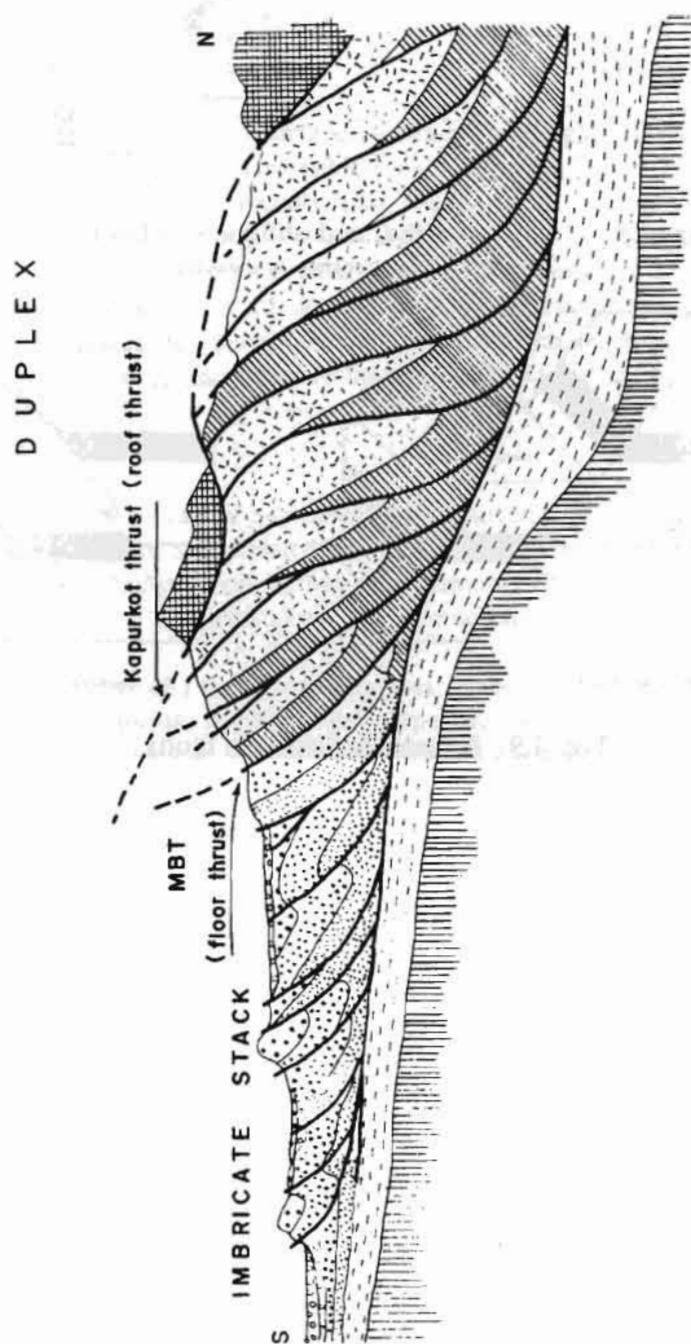


Fig. 4.7 Example of nappes in West-Central Nepal

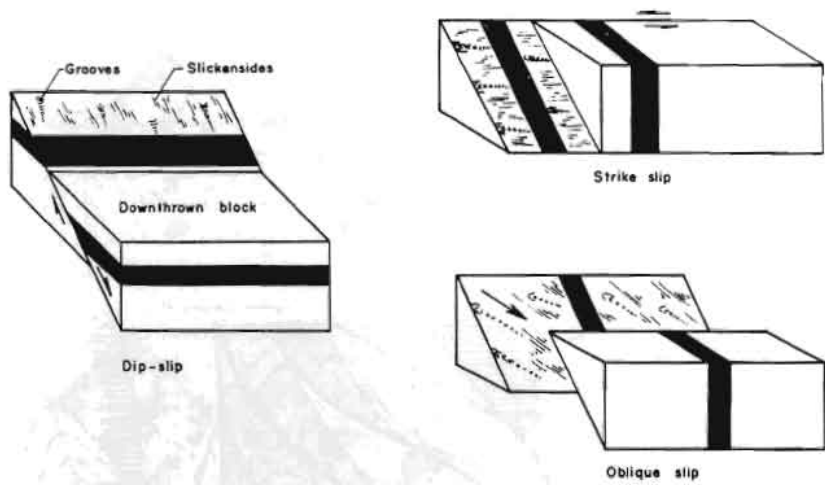


Fig. 4.8

Dip, strike, and oblique slip faults
Arrows show direction of movement.

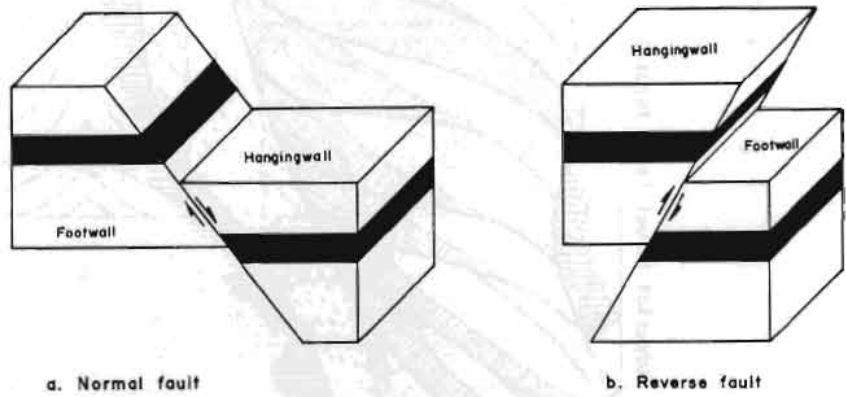


Fig. 4.9 Normal and reverse faults

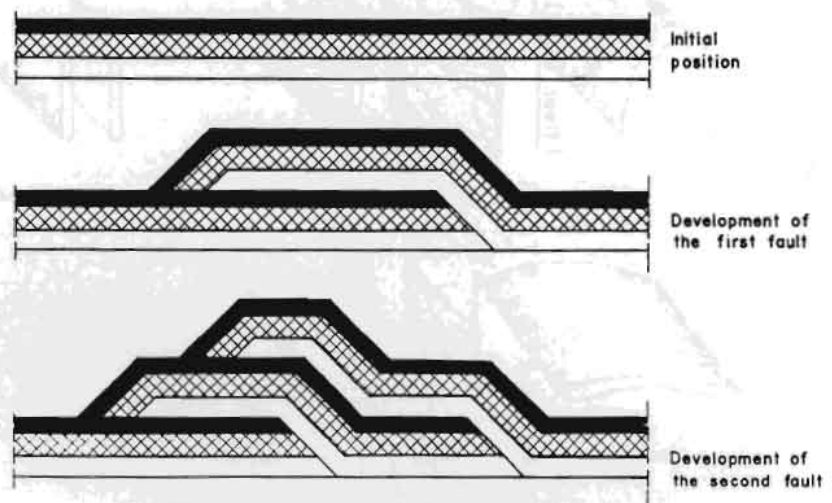


Fig. 4.10 Development of thrust faults and imbricate structure

iii. Engineering Considerations in Faulted Terrain

Faulted terrain is generally very friable and crushed. Because the faults may have tapped deep layers of the earth, hydrothermal fluids may have invaded them, resulting in further weakening of the rocks. The increased surface area of materials in fault zones makes these more susceptible to attack by rain, river, and frost action.

Fault zones can be recognized by several features.

1. **Breccia** - angular, crushed rock fragments.
2. **Gouge** - highly crushed, soft clayey mass.
3. **Slickensides** - smooth, polished hard surfaces, often with straight grooves.
4. **Mylonite** - fine-grained, sheared metamorphic rock.
5. **Cataclasite** - partially fused, dense metamorphic rock.

Construction on or near a fault is asking for trouble if due consideration is not given to their unstable nature. In the *Himalaya*, many faults are still active. Many of the region's largest landslides are located on or near fault zones. Earthquake-triggered landslides have also caused abundant damage in the region. In the *Himalaya* most of the historic earthquakes have epicentres located between the MCT and MBT.

b. Joints

Joints are surfaces along which no lateral movement has occurred and are found in practically all rocks. Commonly, they are found in **joint sets**, related by their orientation with respect to the stresses operating in an area. Because joints are relatively open, they are commonly filled with minerals. The infilling tends to reduce shearing resistance and cohesion along the joint surfaces. Some important joints are:

Joints in Folded Rocks: formed due to regional stresses. Some are parallel to the axial plane and are called **longitudinal** or **tension joints**. Joints formed perpendicular to the hinge line are called **transverse** or **dip joints**. Joints which are neither parallel to or perpendicular to the hinge line are called **diagonal joints**. **Conjugate joints** are sets of joints oriented roughly perpendicular to each other and are bisected by the principal stress (Fig. 4.11)

Columnar Joints in basaltic rocks give rise to a hexagonal pattern when these rocks contract on cooling at the earth's surface (Fig. 4.12).

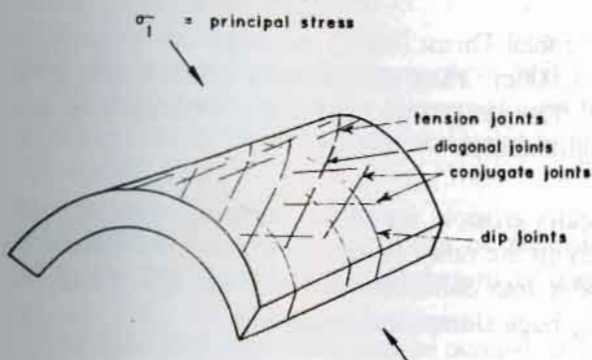


Fig. 4.11 Joints in folded rocks

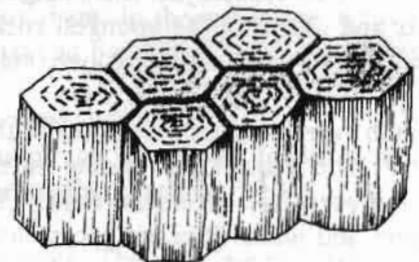


Fig. 4.12 Columnar joints in basalt

TECTONIC SETTING OF THE HIMALAYA

Most of the Asiatic mountain belts begin from the Pamir Plateau which acts as a knot. The Kun-Lun and Tien-Shan belts divert to E and NE from the Pamir Knot, respectively. While the Karakoram Range runs to SE from the Pamirs, the Hindu Kush Range continues up to SW of the Pamirs. The Himalayan Arc extends to SE of the Pamir Knot and lies between the Tibetan Plateau and the Indian Shield. The Himalayan arc is about 2,400 km long and convex towards the Indian Shield. After two conspicuous syntaxial bends, at Kashmir and Assam, the Himalayan Range is followed by the Baluchistan Arc in the west and the Arakan Yoma Arc in the east (Fig. 5.1)

The Himalayan Range with its NW-SE general trend was formed by the collision of the Indian Plate with Eurasian Plate. This collision, which began with first contact about 40 million years ago, caused the sediments of the intervening Tethys Sea and the Indian Shield to be folded and faulted into the lofty peaks and odd outliers visible in the *Lesser Himalaya*. From south to north, the Himalayan Mountains can be divided into the following major tectonic zones, which trend northwest to southeast perpendicular to the direction of plate collision (Fig 5.2).

5.1 GANGETIC PLAIN

The Gangetic Plain lies south of the Himalayan Range and is covered by alluvium several hundred metres thick eroded from the *Himalaya*.

5.2 MAIN FRONTAL THRUST (MFT)

This more or less conspicuous fault surface separates the Siwalik Hills from the Gangetic Plain, which it overrides.

5.3 SIWALIKS

The Siwalik rocks are exposed to the north of the Main Frontal Thrust (MFT) and constitute the southern foothills of the *Himalaya*. Their height rarely exceeds 1,000m. They are generally covered with thick forests and comprise the youngest rocks in the range. The soft, loose, and easily erodible rocks are represented by sandstone, siltstone, mudstone, and conglomerate.

Common types of mass movement in the Siwaliks are gully erosion, mudflow, slumping, toppling, and rockfall. The frequency of sliding increases considerably in the rainy season, as the soft rock saturated with rainwater acts like semi-fluid. The water penetrates into colluvium and into the rock along the fractures and joints. It exerts enormous pressure causing huge slumps and mudflows.

* Figures and Tables without credit lines in this Chapter are compiled by the author.

Steep river banks with the exposed Siwalik rocks should be avoided if possible, as in this region the side-cutting action of rivers is very fast. Better alignment could be the upper river terraces, occasionally found on the river banks, the ridge, spur, shoulder, or saddle. If the road runs along the river valley, it should be aligned at least 50m up the river bed and the material from side cutting should not be disposed of along the natural slope into the river.

Generally, the Siwaliks have inverse relief. It means that the synclines are found along the ridges and the anticlines in the valleys. The synclines are often open and the anticlines are tight to close. Steep faults may run along the foothills of the Siwaliks.

The conglomerate beds of the Upper Siwaliks are fairly stable if they are not alternating with thin claystone and sandstone beds. The interbedded mudstone and sandstone rocks of the Middle Siwaliks are rather unstable, and the Lower Siwaliks, which are composed predominantly of green-grey sandstone with a minor amount of claystone, are moderately stable. However, the above-mentioned factors are largely modified by such local conditions as rainfall, land use, vegetation, groundwater, and seismicity.

5.4 MAIN BOUNDARY THRUST (MBT)

The Main Boundary Thrust is one of the most conspicuous faults in the *Himalaya*. It marks the boundary between the Siwaliks and valley deposits to the south and the older rocks of the *Lesser Himalaya* to the north. The MBT is an active fault.

5.5 THE LESSER HIMALAYA

The *Lesser Himalaya* is a rugged and highly dissected mountain region reaching altitudes of 4,000 m. Morphologically it can be divided into the southernmost part called the Mahabharat Range and the more depressed Midland Zone further North. Both zones consist of a thick sequence of unmetamorphosed or weakly metamorphosed rocks on top of which can be seen the high grade metamorphics called 'Lesser Himalayan Crystallines'. The *Lesser Himalaya* is also intricately folded and faulted. From the engineering as well as from the geological point of view, the *Lesser Himalaya* can be divided into the sedimentary belt and the metamorphic belt.

5.5.1 The Sedimentary Belt

The vast territory immediately north of MBT in Central and West Nepal and Kumaon is covered by sedimentary rocks with a few klippen of metamorphics resting on them. In the inner part of the *Lesser Himalaya* the sedimentary rocks are found in the windows in East and Far West Nepal, Darjeeling, and elsewhere.

The MBT Zone is tectonically one of the most active regions of the *Himalaya*. In this zone many imbricate faults, tight folds, and various systems of joints are occasionally encountered.

The rocks range from weak slate to massive and thick-bedded dolomite. The most common types of mass movement are wedge failure, rockslide, rockfall, rock toppling, debris avalanche, deep gully erosion, debris flow, debris and alluvial fans, and slump.

To highlight the engineering-geological problems related to the various rock types, the following rock types are treated separately.

a. *Very Fractured and Crumbly Slate*

These types of rocks cover a large territory in the inner part of the Nepal *Lesser Himalaya* and they are also found immediately north of the MBT. Their typical property is that they easily break into long, pencil-shaped, or small polygonal, flat chips which cleave off the bed even in dry season. There is a high risk of gully erosions, debris fans and debris flows, toppling, wedge failures, and the occurrence of huge talus cones and slumps. A possible way of controlling this mode of mass wasting is not to disturb the natural slope and to balance the cut and fill. It is recommended that the vegetation cover should not be destroyed and the cut slope should be made as close to the natural slope as possible. It is suggested that the alignment along the ridge be followed, rather than the valley with bare rock. The road alignment must maintain the vegetation cover up as well as down slope.

b. *Interbedded Quartzite and Shale*

These types of rocks are found near the MBT as well as in the inner part of the *Lesser Himalaya*. The anisotropy inherent to the interbedding of resistant quartzite or sandstone with weak shale or mudstone may contribute significantly to mass movement. In this situation, even the slightest disturbance of natural slope may lead to huge rockslides parallel to the bedding plane. If the quartzite is very thickbedded and heavily jointed, there is always a strong possibility of wedge failure. On the other hand, if the shale or mudstone predominates, slumping may be expected.

c. *Medium to Thick-bedded Dolomite or Calcareous Quartzite with Thin Beds or Partings of Claystone or Slate*

The most common types of mass movement in this kind of rock are rockslides parallel to the bedding plane and wedge failure. Thick beds of dolomite fail along the thin clay partings if the natural slope (which is in most cases the dip of the bedding plane) is disturbed by the steeper cut slope of the road. Steep gullies cut through and a lot of debris is unloaded on the road. The side-casting further worsens the situation and triggers off the rocksliding and wedge failure down the road. Preventive measures against the loss of vegetation cover and the penetration of rainwater must be taken. It is better to avoid the wet areas and the areas with paddy grounds.

d. *Massive and Cliff-forming Dolomite, Limestone, and Quartzite*

In normal conditions, these rocks are fairly stable and generally do not create any problems. When they are joined, wedge failure can be expected.

e. *Deeply-weathered Soil, Colluvium, and Loose Mass*

After weathering and disintegration of rocks, various kinds of soil and colluvium of varying thicknesses

are seen in the *Lesser Himalaya*. Rotational slides (slumps) are common in this soil. If the slope is not very steep (less than 25°) it may be fairly stable. But steep, natural slopes combined with rainwater or irrigation water may create catastrophic conditions.

Apart from this, a special kind of 'soil' which is nothing but fault breccia, fault gouge, or crushed zone, developed by the thrusts and faults, is also encountered. Generally, the fault zone stretches from a few metres to 50 metres wide. It may happen that two imbricate faults run close to each other, and the zone may be wider, up to 100m and more. In such 'soil', occasionally, big exotic boulders of limestone, dolomite, quartzite, fragments of slate, phyllite, and gneiss are encountered. The 'soil' is unstable on the steep slopes, and the situation is further aggravated if the road runs along the river valley, as the rivers are prone to follow the path of least resistance which is nothing but the fault itself. It is recommended that such areas be avoided if possible.

5.5.2 *The Metamorphic Belt*

The metamorphic belt of the *Lesser Himalaya* is mainly represented by low-grade metamorphic rocks with some high-grade metamorphics such as gneisses.

The metamorphic rocks constitute klippen resting on the sedimentary rocks and these are also present in the inner part of the *Lesser Himalaya*. They are represented by phyllite, marble, quartzite, schist, and gneiss.

a. *Phyllite and Quartzite Alternation*

Generally, it is a monotonous very thick succession. There may be major anticlines and synclines with numerous small-scale folds. Generally the terrain is less rugged than the Mahabharat Range. Numerous rivers flowing from north to south with river terraces of various levels are encountered. Alluvial deposition and lateral shift of the rivers are common. Occasionally they have a braided course. Most of the tributaries make torrent fans with terrace cultivation. But some are very active, especially where their drainage basins are being deforested and opened to cultivation.

Major mass wasting processes are debris slides, debris flows, and slumping. There may be some large-scale slides present and the area may be further aggravated by cultivation, irrigation, deforestation, and the toe-cutting action of older slides by rivers. In rainy season, deep slumps may occur in weathered phyllite or soil. If the slump occurs in very wet material, it may grade downslope into debris flow. The size of the slumps ranges from hundreds of metres in width and length and tens of metres in depth. Sometimes very thick colluvium, or tillitic material with huge slides, is encountered along the river banks.

b. *Thick-bedded Quartzite, Marble, or Limestone*

Generally these are found in the form of a narrow band of about 500m in thickness, together in a vast territory covered with phyllites. In the quartzites, the rivers become narrower and have steeper gradients. The rock is quite stable and could provide good sites for bridge construction. If fractured, there is a possibility of wedge failures.

5.6 MAIN CENTRAL THRUST (MCT)

This tectonic boundary separates the *Lesser Himalaya* from the *Higher Himalaya* to the north.

5.7 THE HIGHER HIMALAYA

North of the MCT, high-grade metamorphic rocks such as gneisses, migmatites, schists, and marbles are prevalent. They are competent and massive. They produce very rugged and high mountain terrain. Altitude increases steadily northwards ranging up to 8,000m and more. Due to the high rugged terrain there is little human activity. The rocks can be divided into two major units: (a) **The Central Crystallines**, comprised of high grade metamorphics such as gneisses, migmatites, and granite rocks, and (b) **The Tibetan-Tethys Zone** which is made up of fossiliferous, sedimentary rocks. With increasing relief, rock and debris falls become dominant and coarse and mixed colluvium, talus cones, and mantles of waste are encountered on the lower slopes. At higher altitudes, gentle slopes contain mantles of colluvium and/or glacial till which are acted upon by solifluction and gelifluction processes. This material is prone to gullying and sliding adjacent to torrents. The steep upper slopes are dominated by more rapid forms of alpine denudation, especially avalanches and rock and debris falls. Most of these upper slopes contain structural scarps and cliffs. Extensive glacial deposits and cirques, outside the area now undergoing glaciation, give evidence of former more extensive glaciers than at present. On the other hand, the glacier lakes found in this region create a high hazard for the areas below the region, as sudden glacier lake outbursts are not uncommon in this region.

The Tibetan or Tethys Zone is composed of incompetent rocks such as shale, sandstone, siltstone, and conglomerate with competent limestone and quartzite interbeds. There are also many river terraces. Occasionally, the rocks are intensely folded and faulted. The river channels, during the periods of high flood, erode adjacent terrace scarps and torrent fans entering the floodplain, subsequently causing slumps and slides along the floodplain margins. Several slump areas are found associated with poorly consolidated, alluvial and lacustrine deposits. Where cliffs and structural scarps occur, rapid mass wasting occurs and downslope piles of colluvium are typical. At higher altitudes, both glaciation and periglaciation are intense. In them ice and rock avalanches are common. Similarly, rockfalls and debris slides are also common on the steeper slopes.

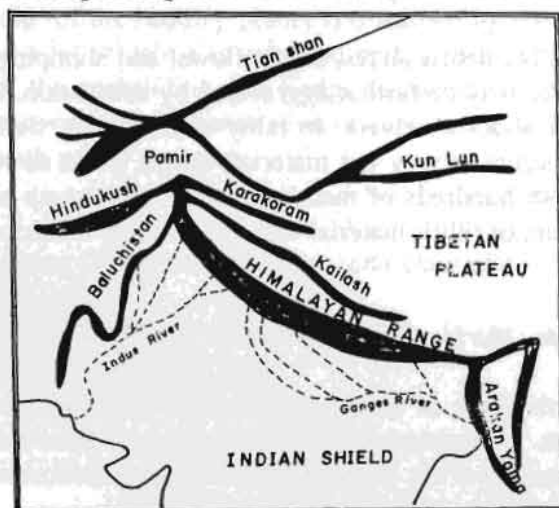
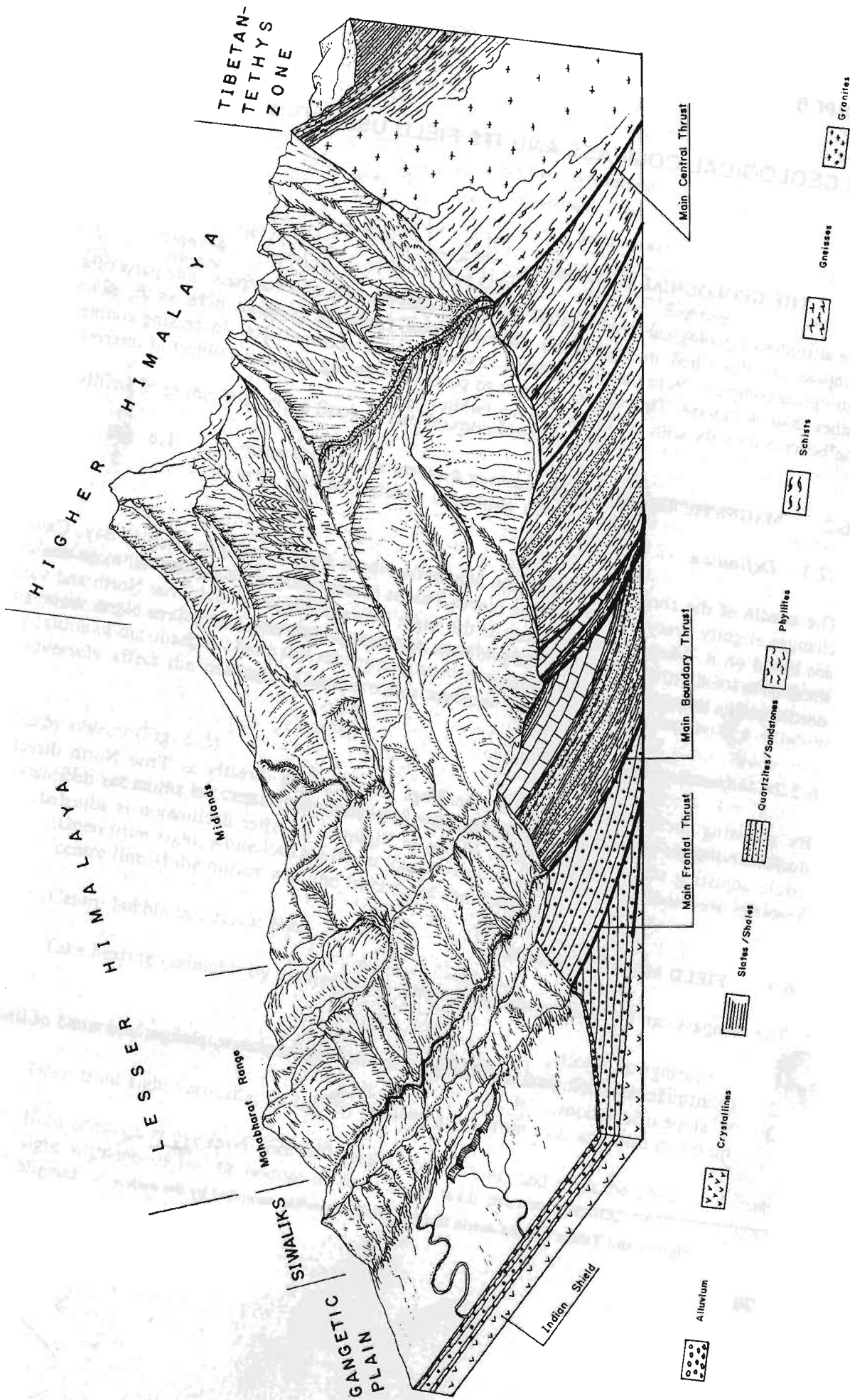


Fig 5.1 Sketch map of Asiatic mountain ranges



THE GEOLOGICAL COMPASS AND ITS FIELD USES

6.1 THE GEOLOGICAL COMPASS

The attitudes of geological structures are measured with the help of a compass. The parts of a geological compass are described in Figure 6.1. The **Brunton Compass** is taken here as an example of the geological compass. Note that the compass circle is numbered from 0-360° increasing counter clockwise rather than clockwise. This allows the user to point the sighting arm at the object of interest and to read the bearing directly with the north seeking (white) tip.

6.2 MAGNETIC DECLINATION

6.2.1 Definition

The needle of the compass points to the **Magnetic North Pole**, located in Hudson Bay, Canada. This changes slightly every year. The **True North Pole** is located geographically and all maps and directions are based on it. **Magnetic declination** is the angle between Magnetic and True North and varies from location to location. For example, the grid lines on a topographic map locate True North, but the compass needle points towards Magnetic North.

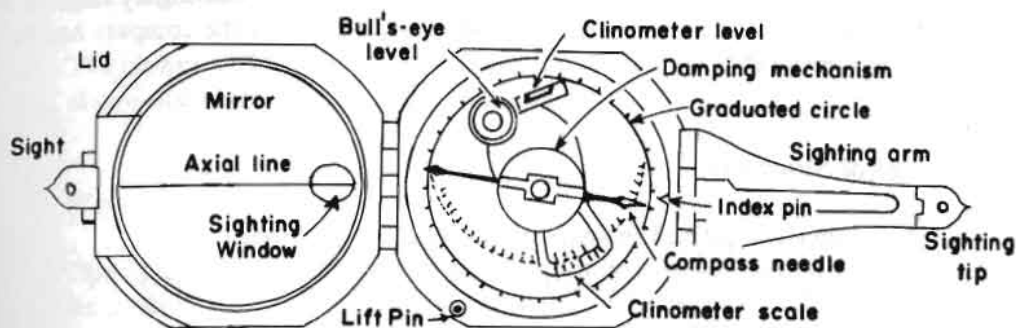
6.2.2 Adjustment For Declination

By adjusting declination, all compass readings can be taken directly as True North directions. The declination angle is given on the margins of the topographic maps. To adjust for declination, use the circle adjusting screw and turn it as shown in Figure 6.2. After declination is adjusted, all compass readings are based on True North.

6.3 FIELD MEASUREMENTS

The compass can be used for measuring:

1. bearings of objects,
2. attitudes of geological structures: strike and dip of planes, plunge, and trend of lines, and
3. slope orientations.



Source: Modified from the Instruction Book of the Brunton Company, 1980

Fig. 6.1 View directly down on a geological (Brunton) compass with lid and sighting arm fully open

6.3.1 *Bearing (or Azimuth)*

A bearing is the angle in degrees, between True North and the object, measured in a horizontal plane from the position of the observer. Note that nearby magnetic materials (watches, hammers, belt buckles, etc) can adversely affect the reading. There are two methods for taking a bearing with a Brunton Compass.

a. *Nearby objects (Fig. 6.3)*

1. Hold compass horizontally at waist level with mirror lid opened at 45° towards you.
2. Open front sight, while looking down into the mirror lid, until you can line up the black centre line of the mirror with the front sight and the object.
3. Centre bubble in circular level.
4. Take bearing (azimuth) by reading north-seeking end of needle.

b. *Far Away Objects; for Greater Accuracy, or Objects Below or Above Operator (Fig. 6.4)*

1. Open front sight vertically, or slightly inclined away from eye, and turn its tip up.
2. Hold compass at eye level with front sight close to you, and align the object and front sight with top of lid; or bottom of front sight with mirror opening, with the object aligned.

3. Adjust mirror of lid so that compass needle and level bubble can be seen.
4. Centre the bubble and, when the needle has come to rest, take the bearing by reading the **black end** of the needle. This is because the sighting direction of the compass has been reversed by this method.

6.3.2 *Measuring Geological Structures*

Geological structures can be completely defined in space either by planes or lines.

a. *Planes*

A planar structure can be bedding, foliation, joint, cleavage, axial plane, or fault, and is completely defined by its **strike** and **dip** (Fig. 6.5), or **dip** and **dip direction** (Fig. 6.6). The **strike** is the horizontal direction of a slope, and the **dip** is the inclination of the line of maximum slope angle of the plane and is perpendicular to the strike. Several conventions for expressing dip direction, strike, and dip exist, e.g., 110/45° NE denotes a plane with a strike of 110° and a dip of 45° in the northeast compass quadrant; 200/30° is another convention denoting a dip angle of 30° towards azimuth 200°.

To measure the dip direction of a plane (Fig. 6.6):

1. Open the Brunton Compass and place it with mirror side on the plane.
2. Level the **Bull's-eye level** (Fig. 6.1) and steady the needle with the lift pin.
3. The dip direction is the azimuth on the dial indicated by the needle.

Note that for irregular surfaces an average reading may be required and can be obtained by laying a flat surface, such as a clipboard, on the plane to be measured and then taking the azimuth of that surface.

To measure the dip amount of a plane:

1. After measuring the dip direction, lay the compass with its long side on the plane to be measured.
2. Suspend the compass in the dip direction.
3. Level the clinometer level with the lever at the back of the compass.
4. Take the reading on the inside dial in degrees.

b. *Lines*

A linear structure can be a fold axis, mineral lineation, or foliation/plane intersection. The attitude of a line is expressed by its trend and plunge. This completely defines the line in space, for example, a fold axis can be said to plunge at 20° towards 45°.

To measure the attitude of a line:

1. Align a non-magnetic object, such as a pen or pencil, parallel to the linear structure.

2. Holding the compass level, align the long sight with the pencil in the plunge direction, and take the reading with the white end of the needle when the Bull's-eye level bubble is steady. This gives the **trend** which is the direction of the **plunge** of the line.
3. The plunge is obtained by determining the inclination of the pencil or any other object (described above) for measuring the dip of a plane.

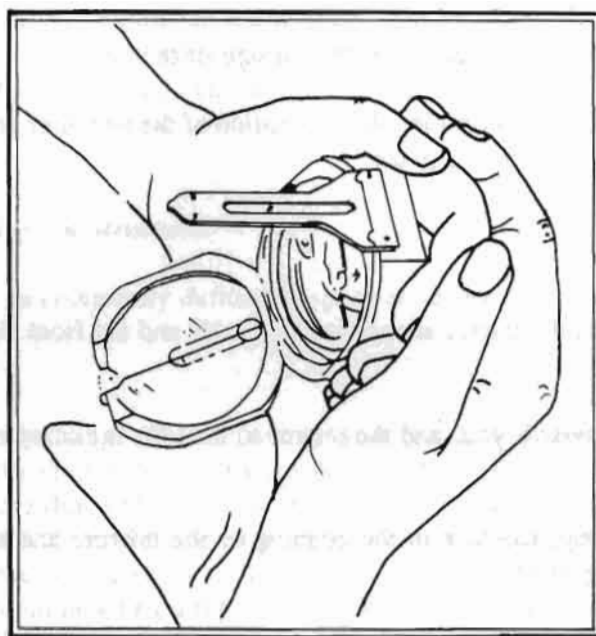
c. *Slopes*

1. Open the compass with the mirror at approximately 45° and the front sight all the way open with its tip up.
2. With the front sight towards you, and the mirror to the left, the compass is held vertically in the right hand.
3. Align the front sight tip, the hair in the opening of the mirror, and an object up or down the slope at eye level (Fig. 6.7).
4. With the right hand, move the **vernier level** until the long level bubble (as reflected in the mirror) is centred and read the **vernier scale**. The reading is either in degrees or percentages on the vernier scale.
5. Measure the direction of the slope by treating it as a plane and getting the azimuth of the dip direction.



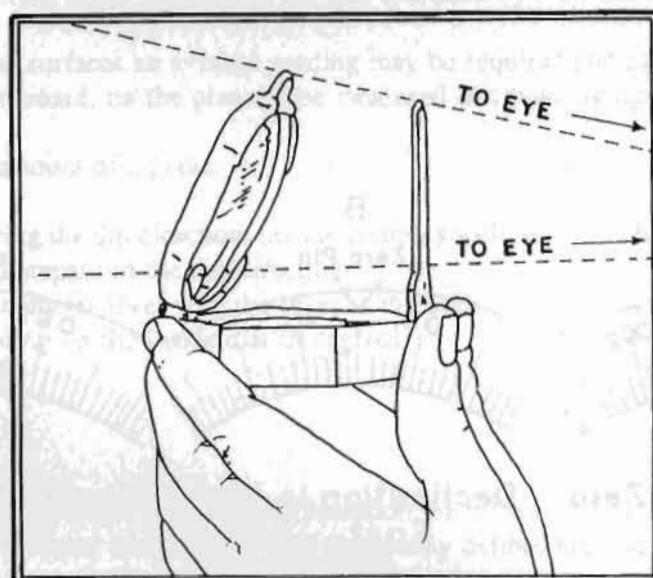
Source: Instruction Book of the Brunton Company, 1980

Fig. 6.2 Declination adjustment



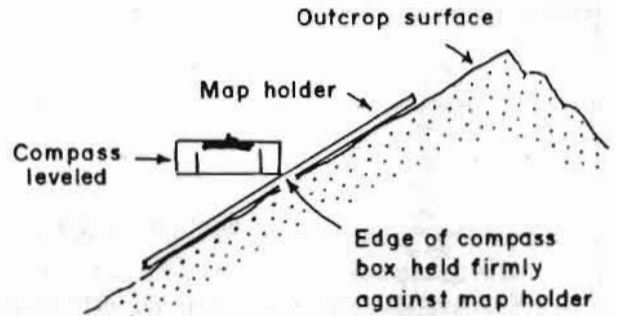
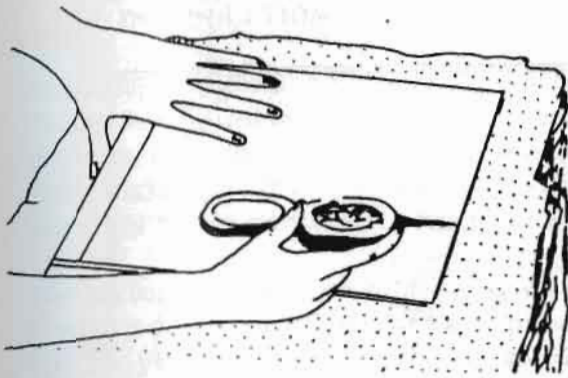
Source: Instruction Book of the Brunton Company, 1980

Fig. 6.3 Taking azimuths of nearby objects



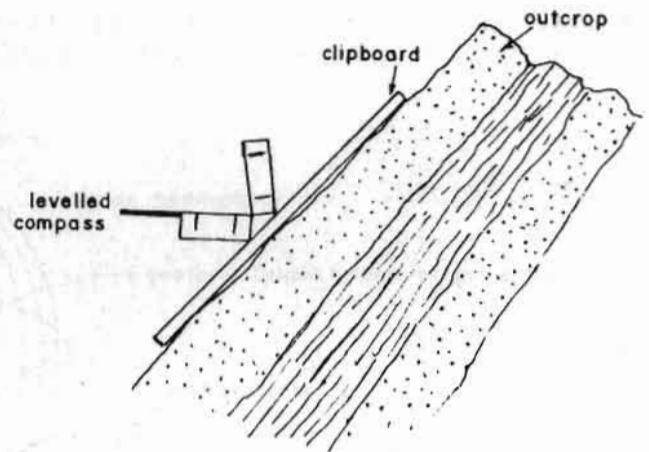
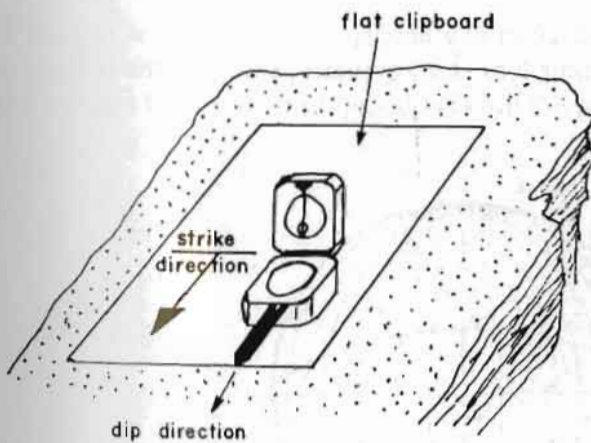
Source: Instruction Book of the Brunton Company, 1980

Fig. 6.4 Taking azimuth of far-away objects



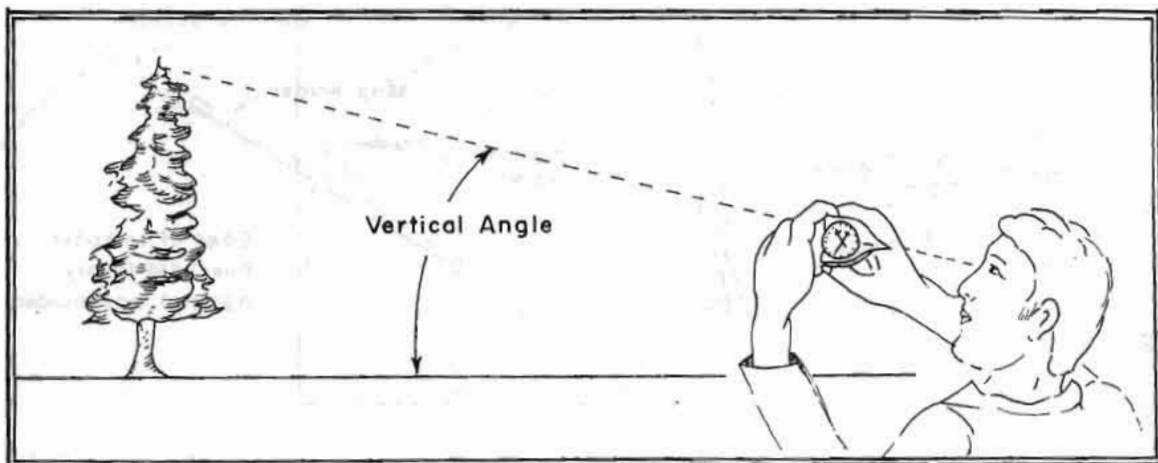
Source: Instruction Book of the Brunton Company, 1980

Fig. 6.5 Measuring strike of a planar surface by placing the compass against a map holder that is held against the surface
The map holder must not have iron or steel parts.



Source: Instruction Book of the Brunton Company, 1980

Fig. 6.6 Measurement of dip direction



Source: Instruction Book of the Brunton Company, 1980

Fig. 6.7 Measuring a vertical angle

STEREOGRAPHIC PROJECTION

7.1 INTRODUCTION

Stereographic projection is one of the convenient methods of projecting the linear and planar features. This method is used exclusively for the determination of the angular relationship among the lines as well as planes. In geotechnical engineering, it provides a quick and reliable picture of the discontinuities and their intersections. It is also used for the estimation of cut slope angle, for the preparation of hazard maps, and for the estimation of safety factors.

The stereographic projection is a projection of the sphere. The sphere is divided into two equal hemispheres by a horizontal (equatorial) plane and the upper and lower poles are fixed as shown in Figure 7.1. The plane of projection is the equatorial plane itself. The circumference of the equatorial plane is called the primitive circle. For the stereographic projection one of the hemispheres is chosen. Here the technique of projection on the upper hemisphere is discussed. The principle of projection is the same for the lower hemisphere.

7.2 PROJECTION OF A LINE

Any required line l is moved parallel to itself in such a way that it passes through the centre of the sphere. In doing so the line will pierce the sphere in two diametrically opposite points A and B (Fig. 7.2). For the upper hemispherical projection, the upper point is projected down to the equatorial plane as the point of intersection A' of the line joining the point A with the lower pole Z (Fig. 7.2).

If the line is vertical, the projection will be at the centre O of the sphere. If the line is horizontal, the projection will be at the primitive circle in diametrically opposite points n' and n'' (Fig. 7.3a). All the inclined lines will be projected between the primitive circle and its centre (Fig. 7.2 and 7.3b).

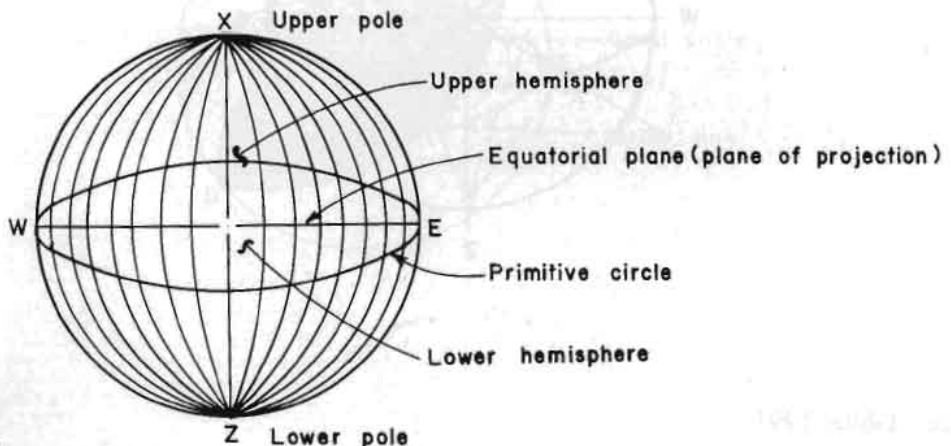
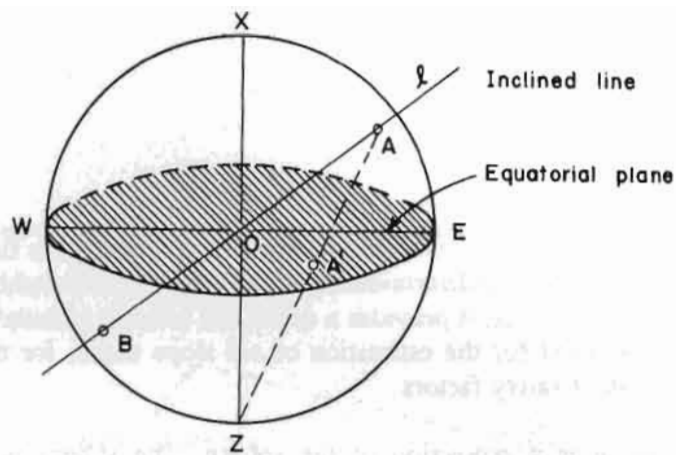
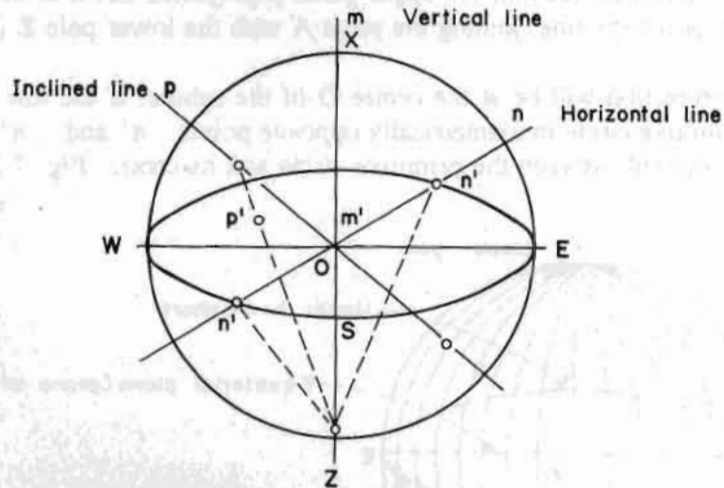


Fig. 7.1 Projection sphere



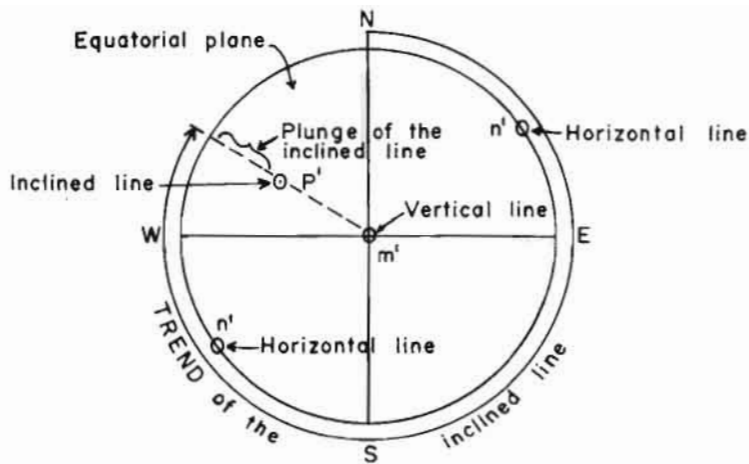
Source: Dhital 1991

Fig. 7.2 Projection of an inclined line on the upper hemisphere



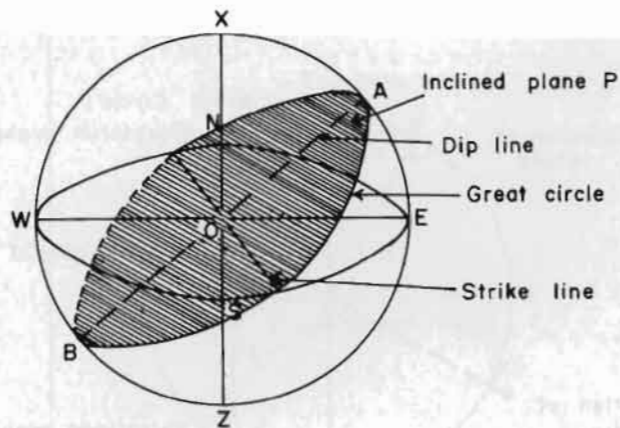
Source: Dhital 1991

Fig. 7.3(a) Projection of vertical, horizontal, and inclined lines on the upper hemisphere



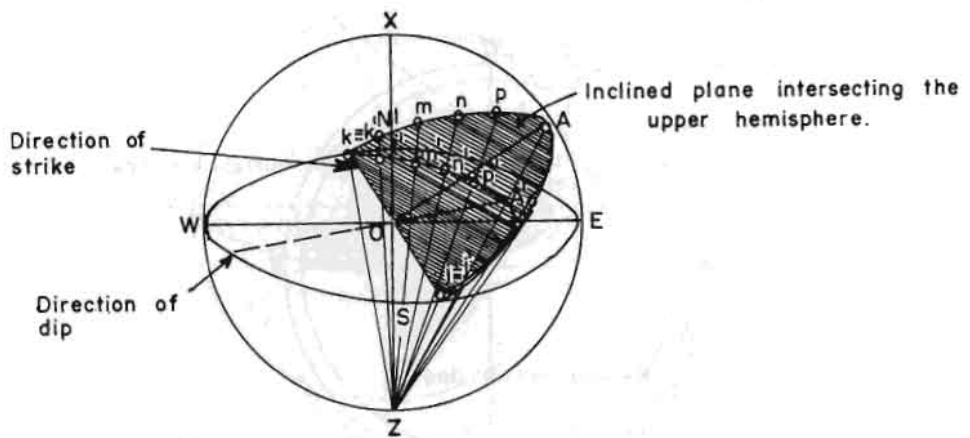
Source: Dhital 1991

Fig. 7.3(b) Stereographic projection of the horizontal, vertical, and inclined lines of Fig. 7.3(a)



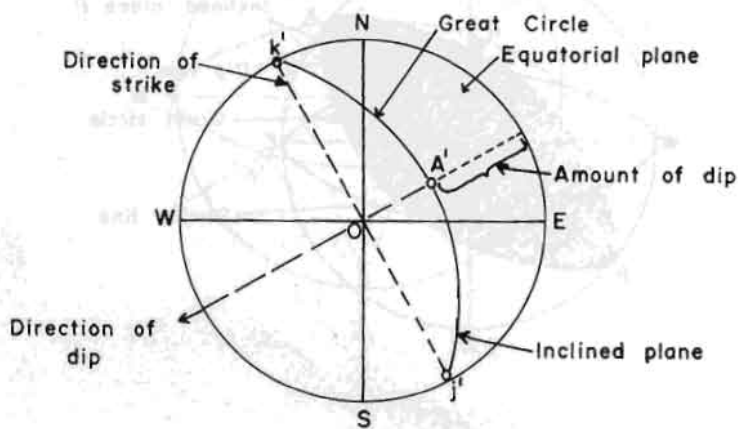
Source: Dhital 1991

Fig. 7.4 Intersection of an inclined plane



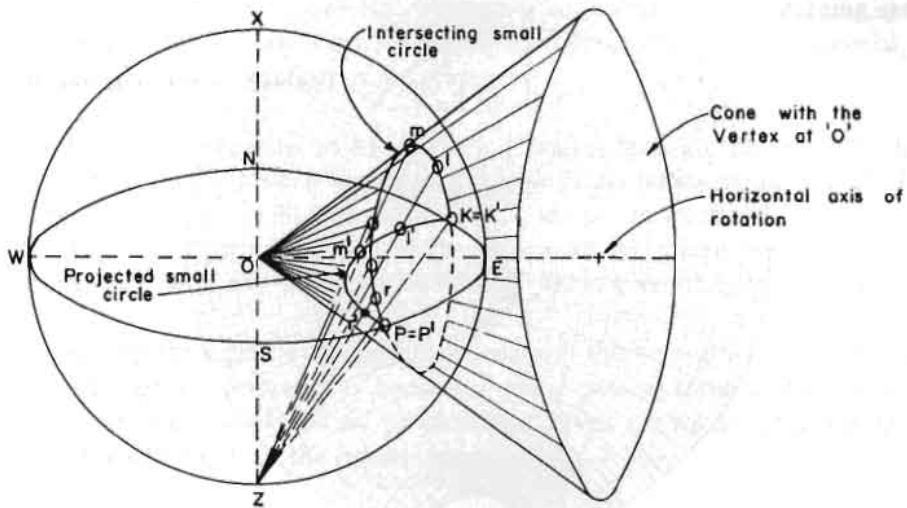
Source: Dhital 1991

Figure 7.5a Projection of an inclined plane, intersecting the upper hemisphere



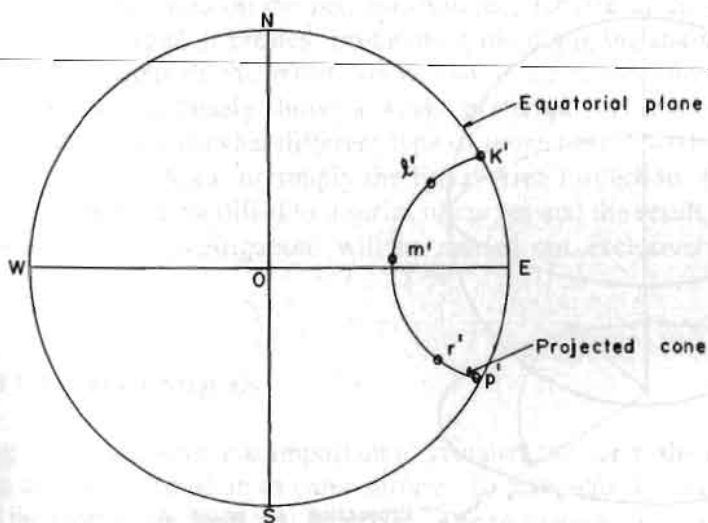
Source: Dhital 1991

Fig. 7.5(b) The stereographic projection of an inclined plane of Fig. 7.5(a)



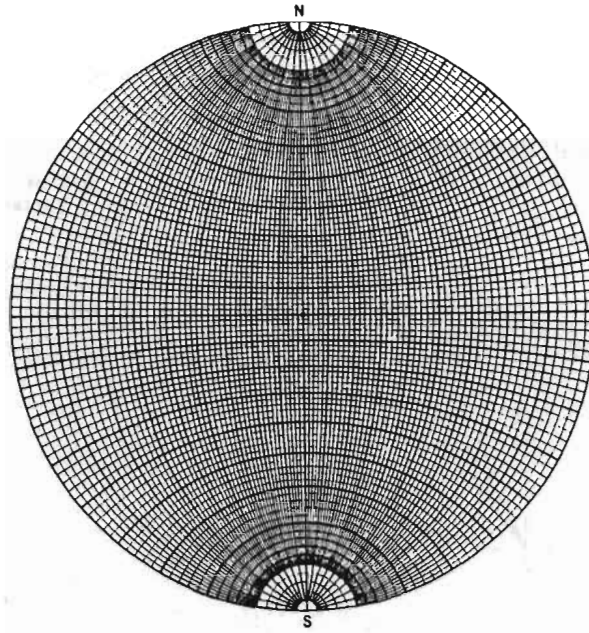
Source: Dhital 1991

Fig. 7.6(a) Projection of a cone on the upper hemisphere



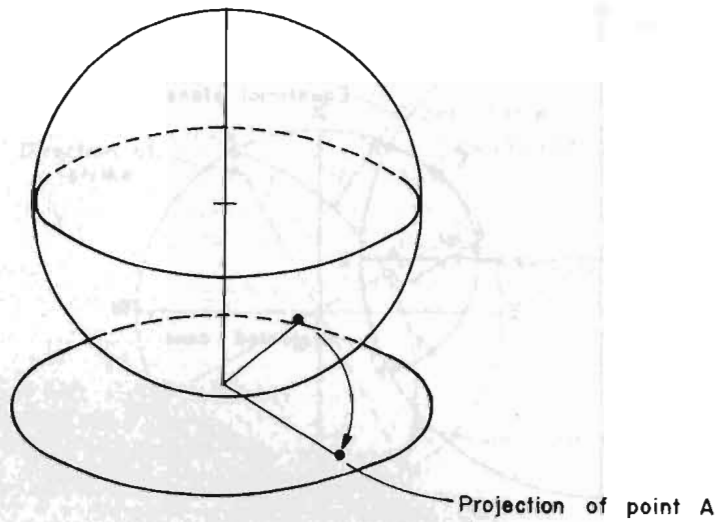
Source: Dhital 1991

Fig. 7.6(b) The stereographic projection of the cone



Source: Krähenbuhl and Wagner 1983

Fig. 7.7 Wulff Stereographic Net



Source: Rockslides; USDT 1981

Fig. 7.8 Method of projection for equal-area net

7.3 PROJECTION OF A PLANE

A plane is projected in the same way as the line. We can imagine the plane containing several lines that pass through the centre of the sphere. Each of the lines is projected on the equatorial plane and the trajectory of them will give the projection of the plane.

In general, a plane **P** is moved parallel to itself unless it passes through the centre of the sphere. The intersection of the plane with the sphere is a great circle with the radius equal to that of the sphere or primitive circle (Fig. 7.4). Then, each of the points, **k**, **l**, **m**, **n**, etc from the upper hemispherical part of the great circle (Fig. 7.5a), is joined by straight lines with the lower pole **Z** and the trace of the intersecting points, **k'**, **l'**, **m'**, **n'**, etc on the equatorial plane, gives the projection (Fig. 7.5a and b).

Any vertical plane passing through the centre will bisect both the hemispheres. Its projection will be a straight line passing through the centre. Any horizontal plane passing through the centre is projected as the primitive circle itself. Inclined planes are projected as curves known as great circles with the ends at the diametrically opposite points in the primitive circle (Fig. 7.5b).

7.4 PROJECTION OF A CONE

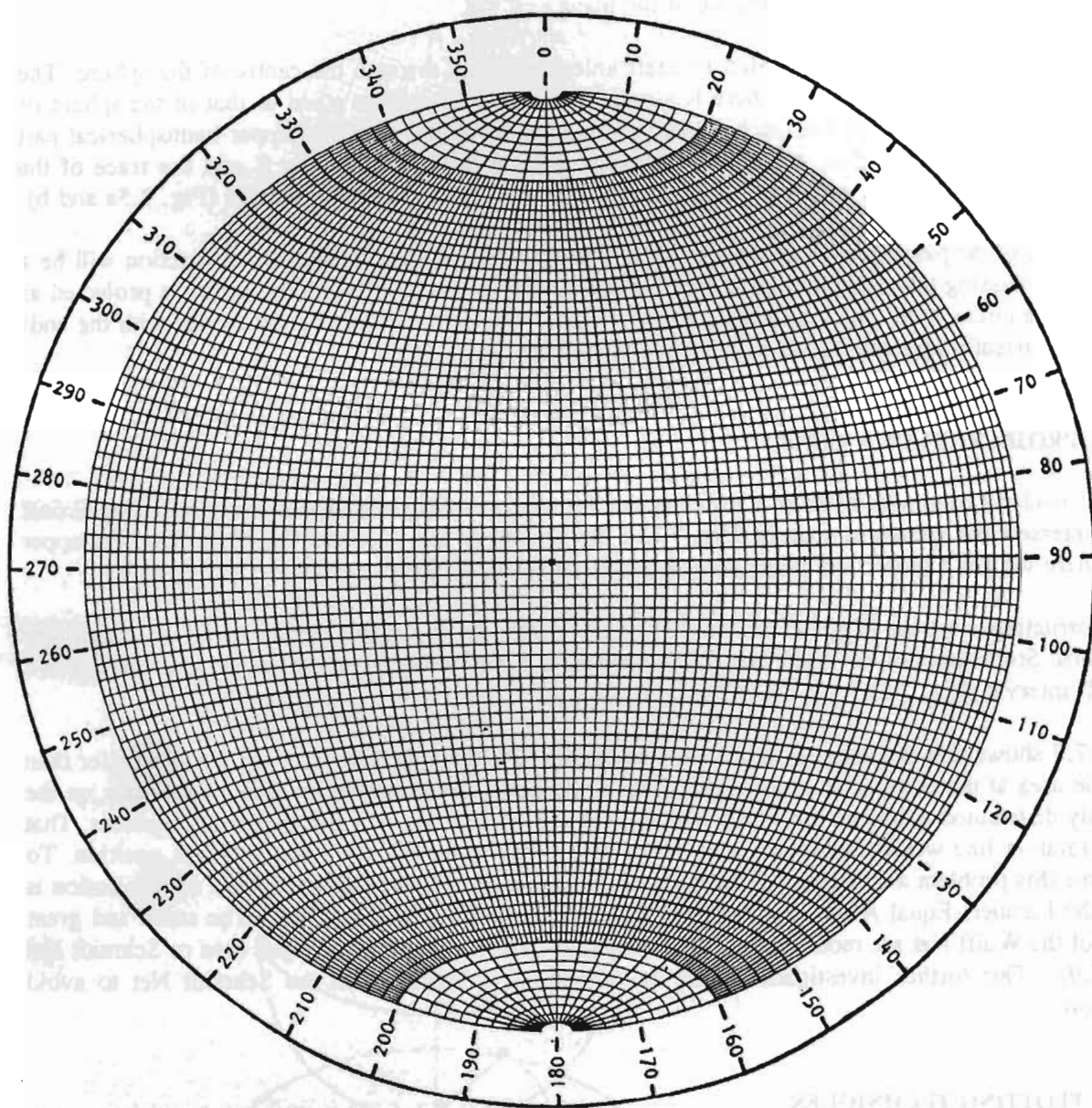
Let us consider a cone with a vertex at the centre of the sphere and horizontal axis of rotation (Fig. 7.6a). It will intersect the sphere in a circle (Fig. 7.6a). By joining all the points of the circle from the upper hemisphere we get a projection of the cone as small circles (Fig. 7.6b).

By constructing a series of great circles and small circles on the upper hemisphere, we obtain the Meridional Stereographic, or Wulff Net, or Stereonet. In it the two types of curves are generally drawn every 2° interval (Fig. 7.7).

Figure 7.7 shows that the area on the net, for example, 10°x10° in the centre of the net is smaller than the same area at the margin. It creates problems while doing the statistical analysis of the data, as the randomly distributed points on the Wulff Net will show a concentration of the points at the centre. That is, the random line would falsely show a weak preferred orientation in the vertical position. To overcome this problem a somewhat different type of projection is needed. This method of projection is called the Lambert Equal Area, or simply the Equal Area Projection. (Fig. 7.8). The small and great circles of the Wulff Net are modified to a series of curves and the result is the equal area or Schmidt Net (Fig. 7.9). Our further investigations will be carried out exclusively on the Schmidt Net to avoid confusion.

7.5 PLOTTING TECHNIQUES

When plotting on the stereonet it is important to visualize the net as the convex-upwards hemisphere and to imagine the curves inscribed on its outer surface. To make the plotting visual, several figures are given together with the plotting on the Equal Area Net. The techniques discussed here are modified after Ragan (1985).



Source: Rock Slopes: USDT 1981

Fig. 7.9 Equal Area or Schmidt Net

7.5.1 *Plotting a Line* (Fig. 7.10)

Given a line with trend = 40° and plunge = 46° :

1. with the tracing paper on the Equal Area Stereonet trace the primitive circle and make a small tick mark and label it N; this is the first step in all works on the stereonet;
2. to locate the trend of the line, count off 40° clockwise from N and make the second small mark on the primitive circle at this point;
3. revolve this trend mark about the centre of the net to the north point (or any other straight line such as East-West and North-South) of the net;
4. count off 46° from the primitive, inwards along the diametrically opposite (Southern) end of the North-South straight line and mark the point P; and
5. restore the overlay to the starting position and recheck by visualization.

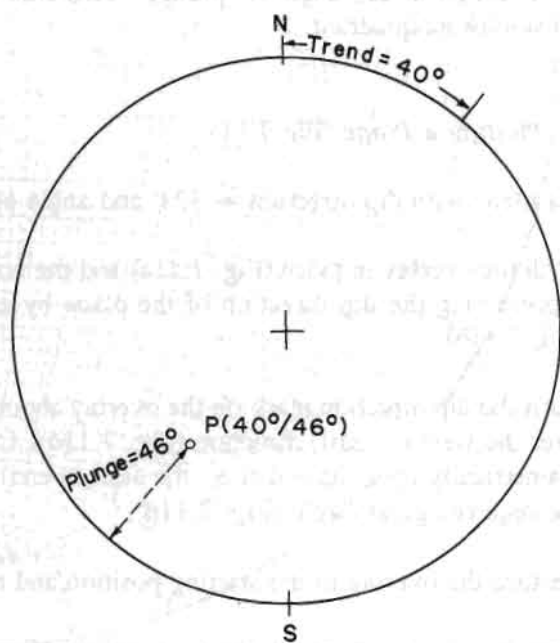
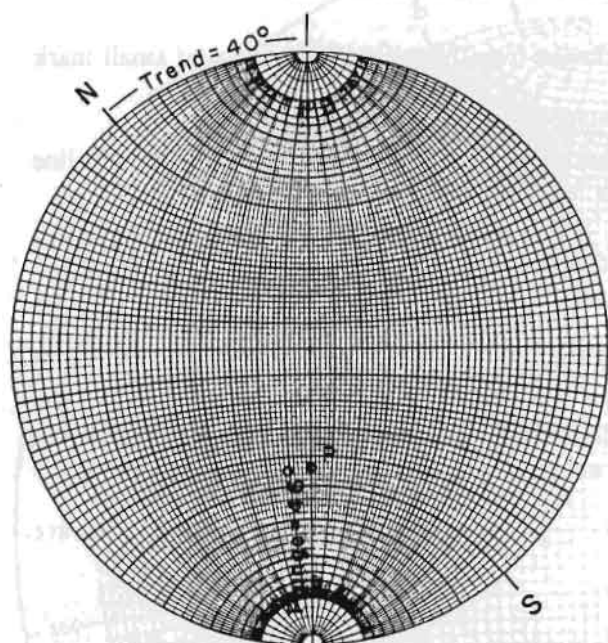
Visualization: Hold a pencil over the centre of the stereonet in the direction of the given trend direction at the angle of plunge. Visualize its intersection with the upper hemisphere in the southwest quadrant.

7.5.2 *Plotting a Plane* (Fig 7.11)

Given a plane with dip direction = 324° and angle of dip = 40°

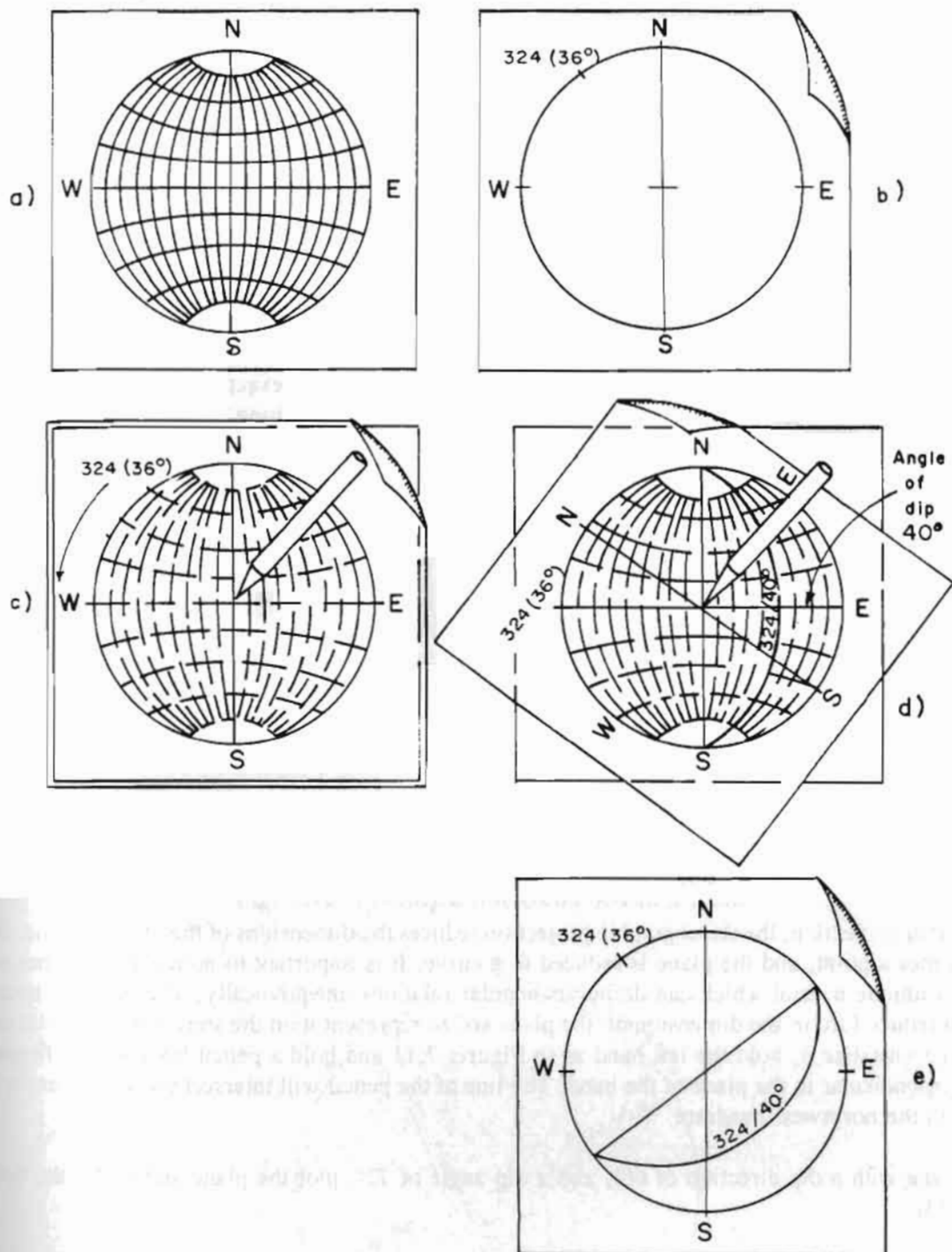
1. With the overlay in place (Fig. 7.11a) and the north index marked N, locate a point on the primitive representing the dip direction of the plane by counting 324° clockwise or 36° counter clockwise. (Fig. 7.11b).
2. Turn the dip direction mark on the overlay about the centre of the net (Fig. 7.11c) until it is exactly over the west (or east) direction (Fig. 7.11d). Count off 40° from the primitive, inwards along the diametrically opposite end (i.e., the eastern end) of the East-West straight line of the net, and trace the required great circle (Fig. 7.11d).
3. Restore the overlay to the starting position and recheck by visualization (Fig. 7.11e).

Remarks: Do not forget to begin counting off inwards from the diametrically opposite end of the marked position. If you count off directly inwards from the marked position, it will be the projection on the lower hemisphere. Visualization: Hold the right hand palm upwards, over the centre of the stereonet with the fingers pointing towards $324^\circ + 90^\circ = 414^\circ = 54^\circ$ NE and the plane of the hand inclined 40° to the northwest (324°). The plane of the hand in this position can be imagined to extend into the upper hemisphere and intersect its surface. Its trace cuts the southeast quadrant and this is where the final plot must be.



Source: Dhital 1991

Fig. 7.10 Plotting a line



Source: Krähenbuhl and Wagner 1983

Fig. 7.11 Plotting a plane

7.5.3 Plotting a Line Contained in a Plane

Given a plane (sandstone bed) with a dip direction of 130° and a dip amount 55° and a line (intersection of the vertical cut slope with the sandstone bed) with a trend of 78° and lying in that plane. Find the plunge of the line (apparent dip of the bed along that cut slope).

Note: The apparent dip is the angle between the line of intersection of the sandstone bed with the vertical cut slope and any horizontal line parallel to the slope.

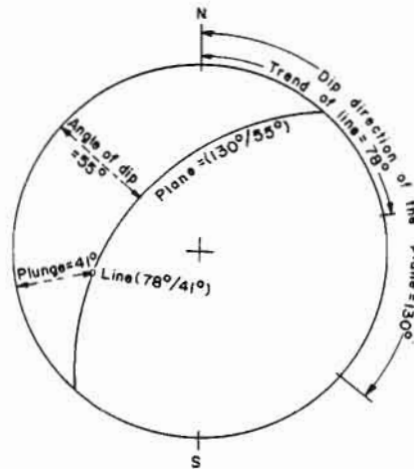
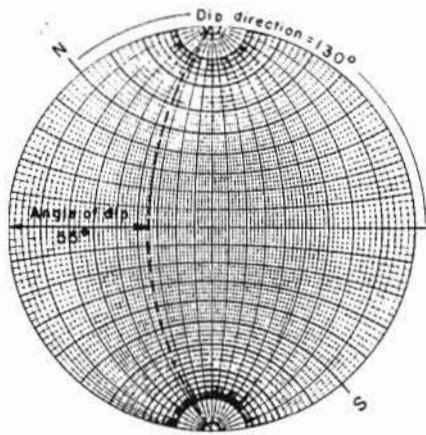
1. With the overlay in place (Fig. 7.12), and the north index marked N, locate a point on the primitive representing the dip direction of the plane by counting 130° clockwise from N.
2. Turn the dip direction mark about the centre of the net until it is exactly over the east (or west) direction (Fig. 7.12). Count off 55° from the primitive, inwards along the diametrically opposite end (i.e., the western end) of the East-West straight line, and trace the required great circle.
3. Restore the overlay to its starting position and count off 78° clockwise from N and make a tick mark.
4. Rotate the overlay about the centre and coincide the tick mark with the nearby diameter and locate the required point (line) in the previously traced great circle. In the same position count off the plunge of the line which is equal to the angle between the tick-marked point in the primitive and point (line) located in the great circle.
5. Restore the overlay to the starting position and recheck by visualization (Fig. 7.12).
Result: the plunge is 41°

7.5.4 Plotting a Pole

Like any other projection, the stereographic projection reduces the dimensions of the object by one. Here, a line becomes a point, and the plane is reduced to a curve. It is important to notice the fact that every plane has a unique normal which can define its angular relations unequivocally. Therefore, it becomes possible to reduce further the dimension of the plane and to represent it on the stereonet by a point called the pole. To visualize it, hold the left hand as in Figure. 7.11 and hold a pencil between the fingers so that it is perpendicular to the plane of the hand. The line of the pencil will intersect the upper hemisphere at a point in the northwest quadrant.

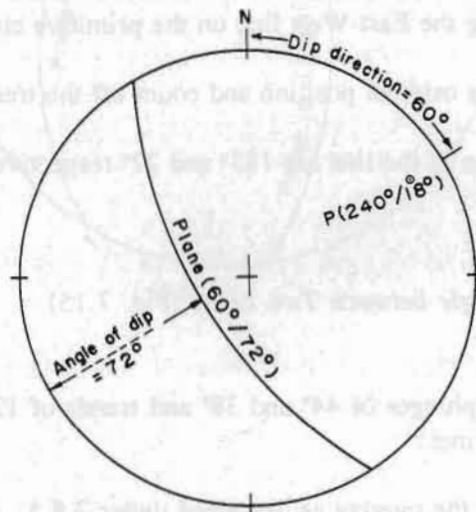
Given a plane with a dip direction of 60° , and a dip angle of 72° , plot the plane and locate the pole to it (Fig. 7.13).

1. With the overlay in place and the north index marked N, locate a point on the primitive circle equal to the dip direction of the plane by counting off 60° clockwise from N and tick mark it.
2. Rotate the overlay about the centre until the tick mark is over the East-West diameter of the net and, by counting off 72° inwards from the opposite end of the diameter, trace the required great circle.



Source: Dhital 1991

Fig. 7.12 Plotting a line contained in a plane



Source: Dhital 1991

Fig. 7.13 Plotting the pole to a plane

3. As the pole is everywhere located 90° from the plane, count off 90° towards the tick-marked point from the great circle and locate the pole (Fig. 7.12).
4. Restore the overlay to its original position and visualize the plotting by holding the left hand over the centre of the net and tilting it towards NE (60°) by 72° , while the fingers will point towards $60^\circ - 90^\circ = -30^\circ = 330^\circ$ NW (the strike). In this position, the plane will be plotted in the SW quadrant and the pole in the NE quadrant.

Note that it is easier to plot the pole by rotating the overlay so that the dip direction mark coincides with any nearby diameter and by counting off the dip amount (here, 70°) from the centre of the net towards the tick mark (dip direction). Check the previous results with this method.

Result: The position of the pole is $240^\circ/18^\circ$.

7.5.5 *Plotting the Line of Intersection of Two Planes* (Fig 7.14)

Given two intersecting planes (joints), having dip amounts of 40° and 60° and a dip direction of 120° and 260° respectively, it is required to find the plunge and the trend of the line of intersection (wedge axis).

1. With tracing paper over the stereonet trace the primitive circle and mark the north point. Measure off the dip direction of 120° clockwise from N and mark this position on the primitive.
2. Rotate the overlay about the centre of the net until the dip direction mark lies on the East-West diameter of the net. Measure 40° from the primitive and trace the required great circle.
3. Rotate back the tracing paper to its original position and repeat the same for the second plane.
4. The point of intersection of two great circles defines the required line. Rotate the overlay until the intersection of the two great circles lies along the East-West diameter of the stereonet and measure the plunge of the line of intersection. Also mark with a tick on the overlay at the diametrically opposite direction (trend) along the East-West line on the primitive circle.
5. Rotate the tracing back to its original position and count off the trend of the line.

Result: The trend and plunge of the line are 183° and 22° respectively.

7.5.6 *Determination of the Angle between Two Lines* (Fig. 7.15)

Given: Two lines in space with plunges of 44° and 38° and trends of 120° and 220° respectively. Find the angle between these lines:

1. mark the points A and B on the overlay as described under 7.5.1;
2. now rotate the overlay until these two points lie on the same great circle of the stereonet; and

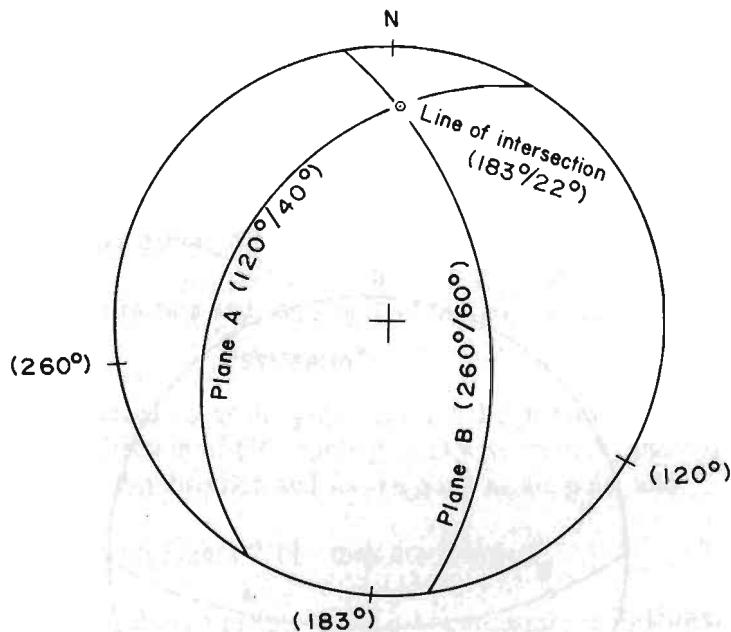
3. determine the angle between the two lines by counting the small circle divisions between A and B along the great circle.

Note that the great circle on which A and B lie defines the plane that contains these two lines.

Result: The angle is found to be 72° and the dip direction and dip amount of the plane containing the line are 165° and 54° respectively.

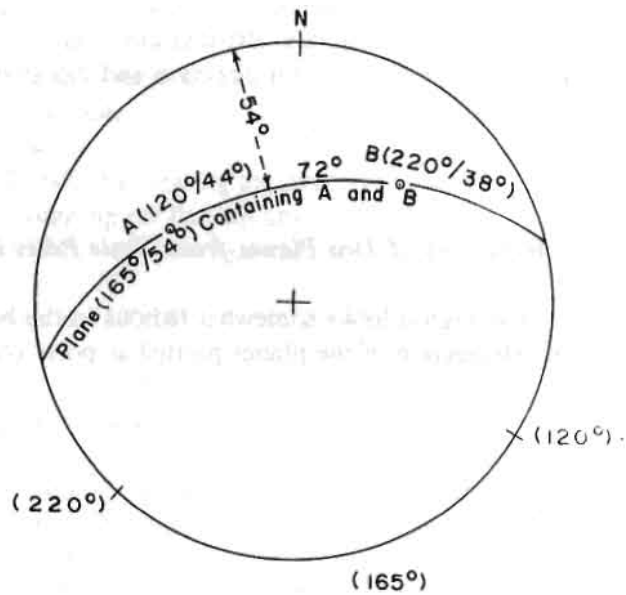
7.5.7 Plotting the Line of Intersection of Two Planes from Their Poles (Fig. 7.16)

This is an alternative to 7.4.4. Although it looks somewhat tedious in the beginning, it is a very useful method for plotting the lines of intersection of the planes plotted as poles obtained from the field data.



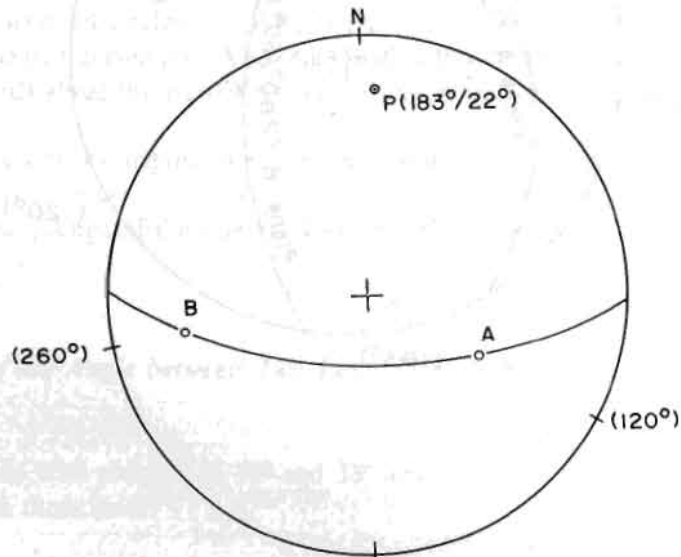
Source: Dhital 1991

Fig. 7.14 Plotting the line of intersection of two planes



Source: Dhital 1991

Fig. 7.15 Determination of the angle between two lines



Source: Dhital 1991

Fig. 7.16 Plotting the line of intersection of two planes from their poles

Given: the same two planes of 7.5.5 with dips of 40° and 60° and dip directions of 120° and 260° respectively. Plot their poles and find their line of intersection:

1. plot the poles to the planes as discussed in 7.5.4 and mark them as **A** and **B**;
2. rotate the overlay until both poles lie on the same great circle. This great circle defines the plane that contains the two normals to the planes; and
3. find the pole of this plane by measuring the dip on the East-West diameter of the net, locate it as described in 7.5.4., and mark it as **P**.

Note that this pole **P** is a pole to a plane which passes through the poles of two other planes and, therefore, is a common normal to both poles **A** and **B**. But, as the pole **P** is normal to **A** and **B**, it must be parallel to the given planes and hence to their line of intersection.

Result: The trend and plunge of the line of intersection are 183° and 22° respectively.

7.6 POLE NET

A pole net is used for plotting a large number of poles to the planes measured from the field. To plot several planes on the same diagram is very difficult. The diagram looks very cumbersome and there is no way of statistical analysis. On the other hand, the poles provide a quick and convenient way of plotting the field data and carrying out their statistical analysis.

A polar stereonet or pole net (Fig. 7.17) is obtained by projecting, on the equatorial plane the vertical planes of varying strike and the small circles of varying radius centred in the upper pole.

7.6.1 Plotting the Pole on a Pole Net (Fig 7.18)

Given a plane with a dip direction and dip angle of 60° and 72° respectively, plot its pole on the pole net:

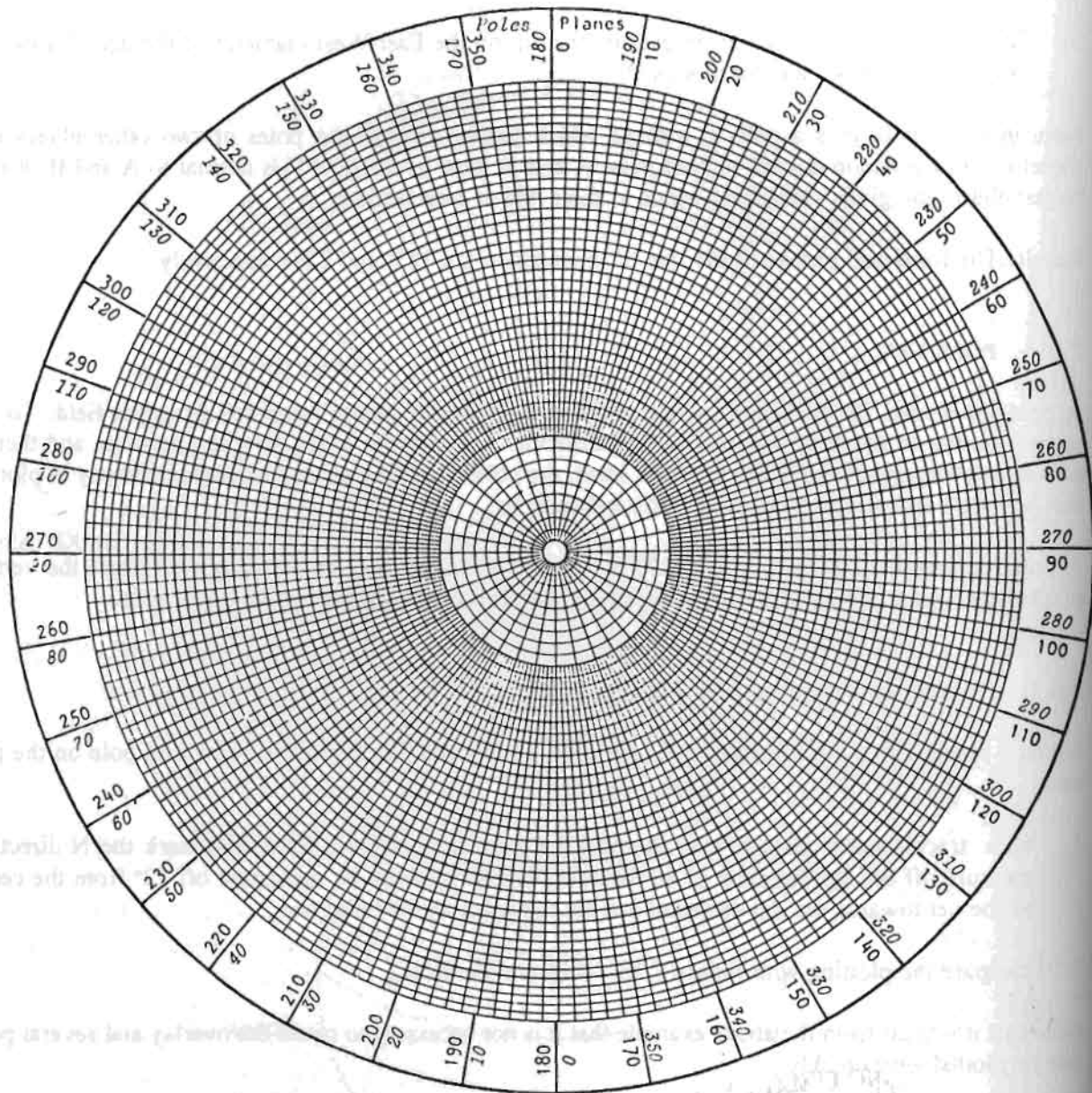
1. with tracing paper placed over the pole net trace the primitive circle and mark the N direction, measure off the dip direction of 60° counting clockwise from N, and count off 72° from the centre of the net towards the dip direction and fix the point as the pole; and
2. compare the plotting with Figure 7.13 - they are identical.

Note that it is clear from the above example that it is not necessary to rotate the overlay and several poles can be plotted very quickly.

7.7 CONTOURING FIELD DATA AND STATISTICAL ANALYSIS

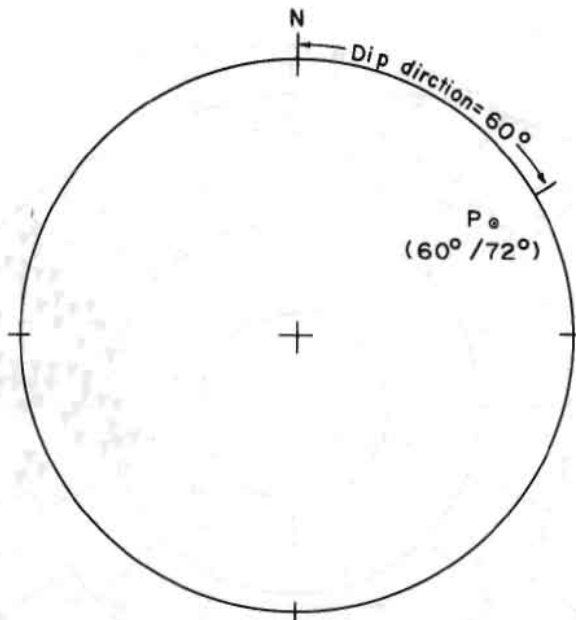
Occasionally it is necessary to plot the discontinuity pattern accurately. For that purpose, pole concentrations need to be contoured in order to obtain the statistical mean for each set of the discontinuity.

A plot of 351 poles of bedding planes and joints and of one fault (United States Department of Transport [USDT] 1981) in a hard rock mass is given in Figure 7.19.



Source: USDT 1981

Fig. 7.17 The pole net



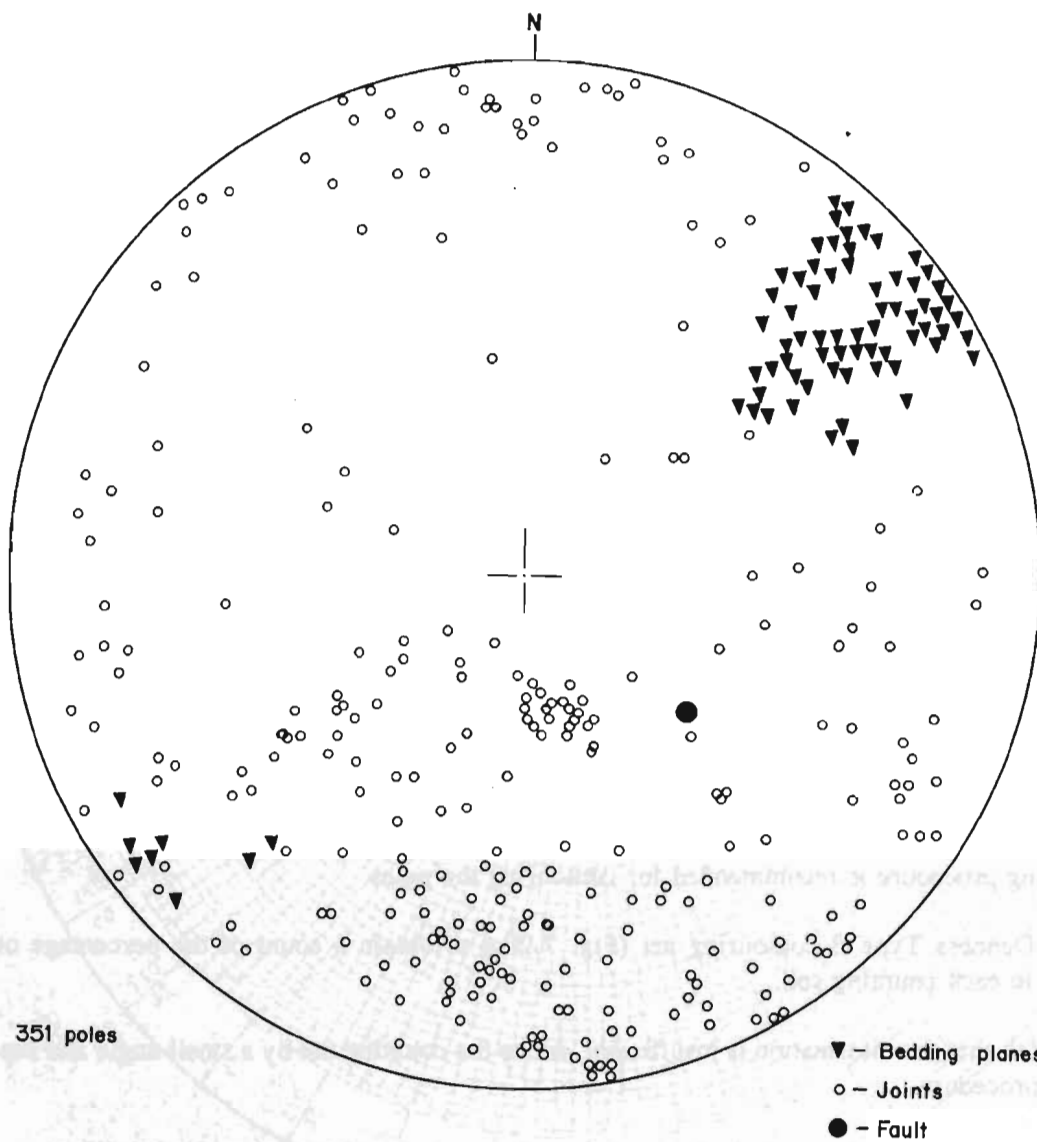
Source: Dhital 1991

Fig. 7.18 Plotting the pole on a pole net

The following procedure is recommended for contouring the poles.

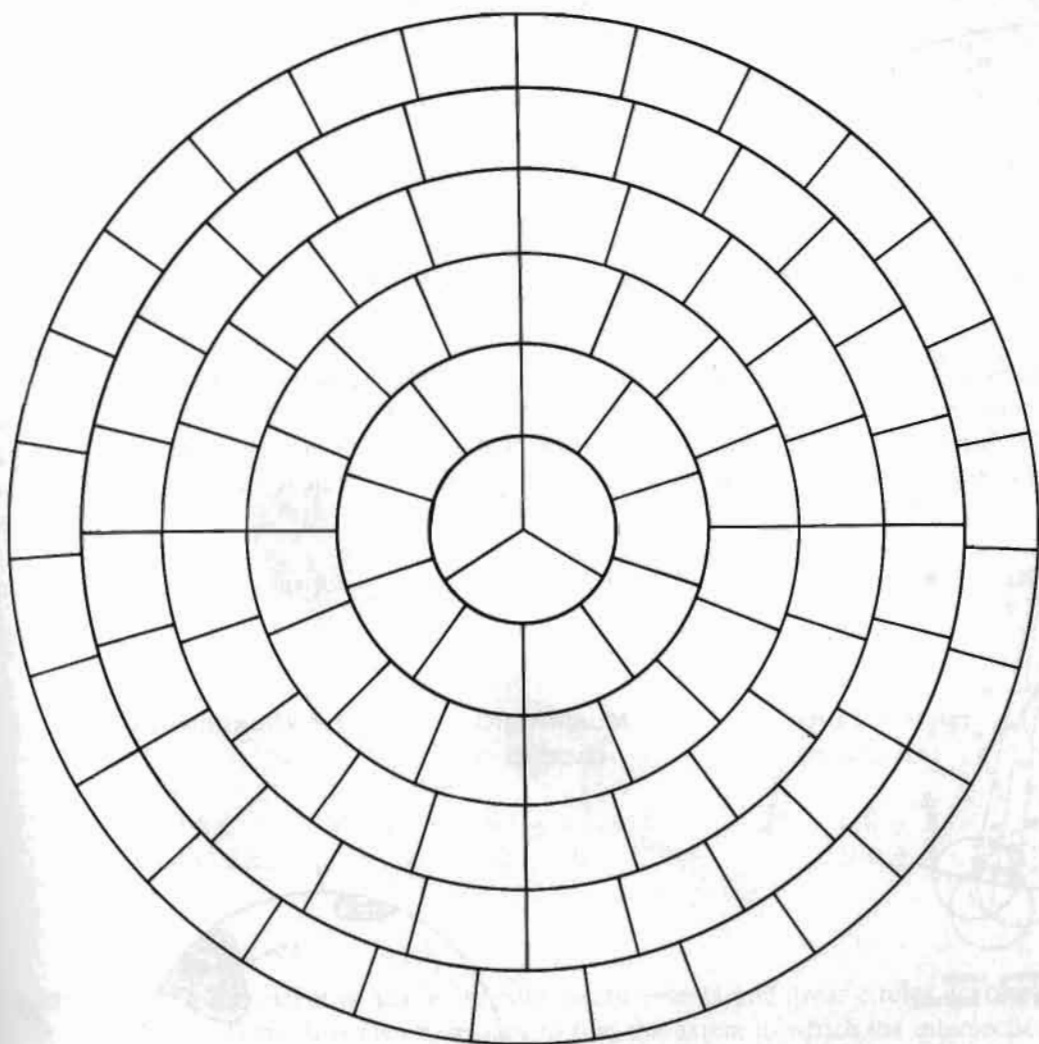
1. Use a Denness Type B contouring net (Fig. 7.20a) to obtain a count of the percentage of poles falling in each counting cell.
2. If it is felt that the information is insufficient, rotate the counting net by a small angle and repeat the above procedure.
3. Draw very rough contours on the basis of the pole counts noted on the tracing paper.
4. Use the circle counter (Fig. 7.20b) to refine the contours starting with low value contours and working inwards towards the maximum pole concentration.

Note: In order to construct a circle counter, trace the pattern given in Figure 7.20b on to a transparent plastic sheet. Make two little holes at the centre of each circle and draw a straight line through the centres of the two circles.



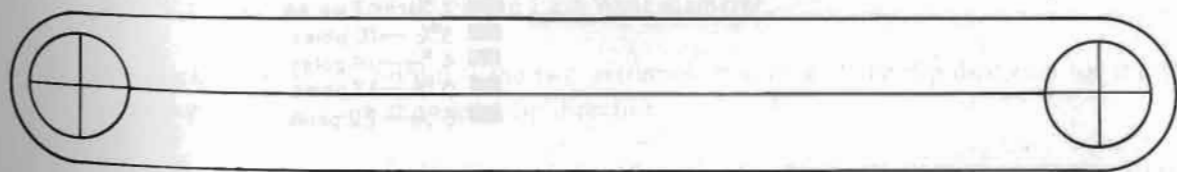
Source: USDT 1981

Fig. 7.19 Plot of poles of discontinuities



Source: USDT 1981

Fig. 7.20(a) Denness Type B curvilinear cell mounting net



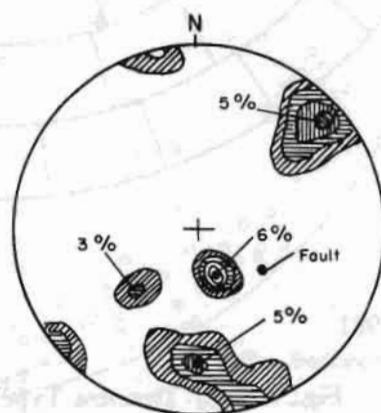
Source: USDT 1981

Fig. 7.20(b) Counting circles for use in contouring pole plots



Source: USDT 1981

Fig. 7.21 Contouring by counting circles



- 2% — 7 poles
- 3% — 10 poles
- 4% — 14 poles
- 5% — 17 poles
- 6% — 22 poles

Source: USDT 1981

Fig. 7.22

Contour diagram obtained from contouring of poles in Figure 7.19

Figure 7.21 illustrates the use of the circle counter for the construction of 3 per cent or 10 to 11 poles. Move one of the small circles around the poles, until 10 to 11 poles are enclosed by it, and mark the centre of the circle by a pencil. Continue this process till a complete contour is drawn by the locus of the points. If the circle lies partly out of the primitive circle, the total number of poles falling in the circle is added to the number of poles reappearing at the diametrically opposite end (Fig. 7.21).

Figure 7.22 is the contour diagram obtained from the contouring of 351 poles given in Figure 7.19.

7.8 DETERMINATION OF EXTENT OF SCATTER AROUND THE MEAN POLE OR GREAT CIRCLE POSITION

When the mapping covers a large area the scatter in the dip and dip direction measurements is considerable and must be taken into account in the analysis. After contouring the diagram as explained in Figure 7.7, a mean pole position for more than one set of discontinuities is determined. The procedure for the determination of the scatter of the line of intersection of two sets of discontinuities is obtained as follows:

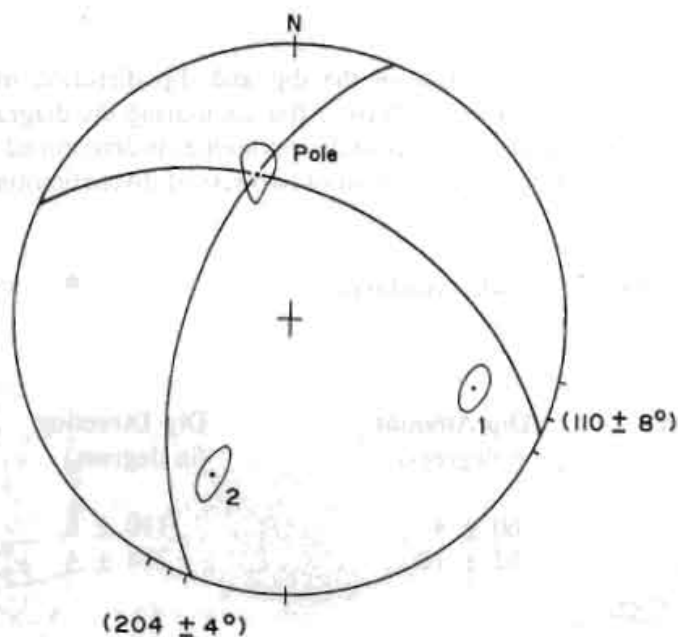
Given the mean pole positions for two sets of discontinuity:

Discontinuity Set	Dip Amount (in degrees)	Dip Direction (in degrees)
First Set	60 ± 4	110 ± 8
Second Set	52 ± 10	204 ± 4

It is necessary to plot the extent of scatter in pole measurements and great circles corresponding to the most probable pole positions. It is also necessary to find the extent to which the intersection point (line) is influenced by the scatter around the pole points (Fig. 7.23).

1. Plot the mean pole positions and corresponding great circles of the two sets of discontinuity according to 7.5.4.
2. Tick mark the two extremes of scatter in the dip angle of dip for the first set by counting off $\pm 4^\circ$ from the mean pole position on the East-West diameter.
3. Also tick mark on the primitive the two extremes of scatter in the dip direction for the first set by counting off $\pm 8^\circ$ from the mean dip direction.
4. Determine the corresponding mean pole positions for the above dip directions and join all the scatters with a smooth curve.
5. Repeat 2,3, and 4 for the second set and determine the scatter.

- To obtain the influence of scatter of poles around the intersection point, rotate the overlay to coincide with a great circle containing simultaneously any outer point of the great circle. The locus of the poles, thus marked around the intersection point, defines the required influence area (Fig. 7.23).



Source: Dhital 1991

Fig. 7.23 Determination of extent of scatter in pole measurements

Chapter 8

AERIAL PHOTO INTERPRETATION

8.1 INTRODUCTION

Aerial photographs provide an overview of both the regional conditions and local site features. Since aerial photographs are generally available for most parts of the world, the aerial photo interpretation may provide very useful information at virtually no cost. Examination of stereopairs under a stereoscope enables the interpretation of geological and geomorphological features. Geological information such as recognition of rock types and their distribution, as well as bedding, jointing, and fault zones, may supplement the study of regional conditions with particular reference to the feasibility of the engineering structures. The study of landforms provides information on the geological history of the area. Even where the ground surface is obscured by dense vegetation, the nature of cover may reflect the nature of the underlying rocks and landslide activity. If aerial photographs are available for an area over a period of time, it may help in identifying the extent of recent mass wasting processes. The inferences obtained from the aerial photograph are often checked at important locations by field investigations.

8.2 ELEMENTS OF AERIAL PHOTO INTERPRETATION

The important elements of aerial photo interpretation are i) topography, ii) drainage, iii) gray tone, iv) erosion, v) vegetation, and vi) miscellaneous features resulting from man-made activities on the landscape (Keser 1979). All these patterns are not always well expressed on a given photograph as the expression varies with the nature of the photograph and its scale.

8.2.1 Topography

The study of topographic characteristics, such as relief, size, and surface configurations, helps to identify the landforms. The boundary characteristics are observed in the plan view in order to assess the nature of the landforms. These landform characteristics may be:

- terraced, e.g., fluvial, glaciofluvial, and marine terraces
- ridged, e.g., lateral moraines,
- lobate, e.g., mass movements, especially flows and spreads,
- conical, e.g., fans and talus cones, and
- linear, e.g., streams.

8.2.2 Drainage

Drainage patterns refer to the spatial arrangement of stream channels and show a close relationship to lithology, structure, and the geological history of the area. The basic drainage patterns (Fig. 8.1) are:

- **dendritic** - a drainage pattern having a branch-like form with an acute angle between tributaries and mainstreams - inference: homogeneous crystalline or flat-layered sedimentary rock; homogeneous soil texture;
- **rectangular** - a drainage pattern having a right-angled system of streams with abrupt bends - inference: intersecting joints and faults;
- **parallel** - a drainage pattern in which the streams and tributaries are nearly parallel - inference: tilted rocks with parallel faults and joints; lava flows; alluvial aprons.
- **trellis** - a drainage pattern having short parallel tributaries joining the long streams flowing parallel for the most part to the regional strike - inference: parallel folds in strata of varying resistances; parallel faults;
- **radial** - a drainage pattern having streams radiating from a central area like spokes on a wheel - inference: dome-shaped intrusions; and
- **annular** - a drainage pattern having ring-like tributaries - inference: volcanic craters; rocks of different erosional resistance in a domed structure.

8.2.3 *Gray Tone*

Gray tone is basically the result of reflected light from terrains of soil and vegetation cover and varies between absolute black and absolute white. Gray tone is considered in contexts of the following elements:

- **tone variation** is due to inherent colour differences of various units, e.g., gabbro and basalt-black colour, granite and sandstone -light black; sand and gravels-white to light gray;
- **tone uniformity** indicates the nature of distribution of the material both laterally and vertically;
 - e.g., uniform - coarse, well-drained material such as coarse alluvium and fans,
 - mottled - due to changes in soil texture and moisture,
 - banded - sedimentary rocks consisting of dark and light strata, e.g., alternating shale-sandstone beds; and
- **boundary sharpness** is identified by the nature of variation of the tones;
 - e.g., sharp - abrupt change of contrasting rock types,
 - gradual - textural changes of clayey materials.

8.2.4. *Erosion*

Erosional features are produced as a result of the interaction of erosional agents and the nature of the geologic materials. Some of the well-known erosional features are gullies and landslides. Figures 8.2, 8.3, 8.4, and 8.5 show the resultant slope geometrics when resistant and non-resistant beds of the hill slopes are subjected to surface erosion.

8.2.5 Vegetation

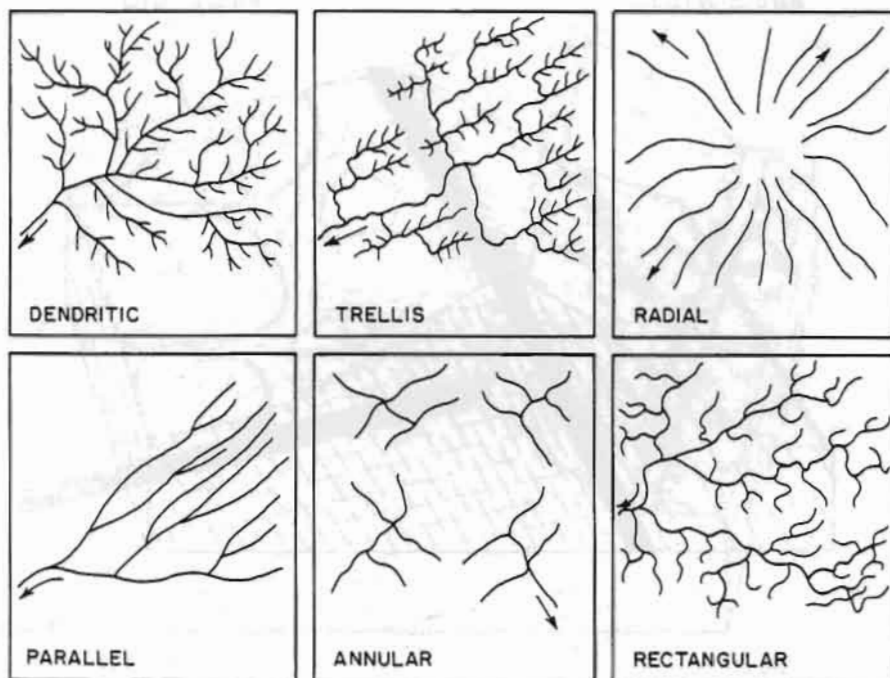
Proper identification and evaluation of vegetation require a good knowledge of the vegetation patterns of the area as well as the regional geological setting. The distribution of vegetation is affected by soil, slope, and relief. Identification of vegetation pattern involves the evaluation of elements such as tone, texture, shape, and size. The general factors affecting tone have already been discussed under 'Gray Tone'. Texture is the orderly arrangement of tone patterns. The shape and size of the species are often important although they may vary with age.

8.2.6 Miscellaneous Features

In both forested and non-forested areas man-made features may reflect characteristic changes in the landscape. Some features, such as dams, channels, roads, and industrial developments, can be easily identified on the photographs.

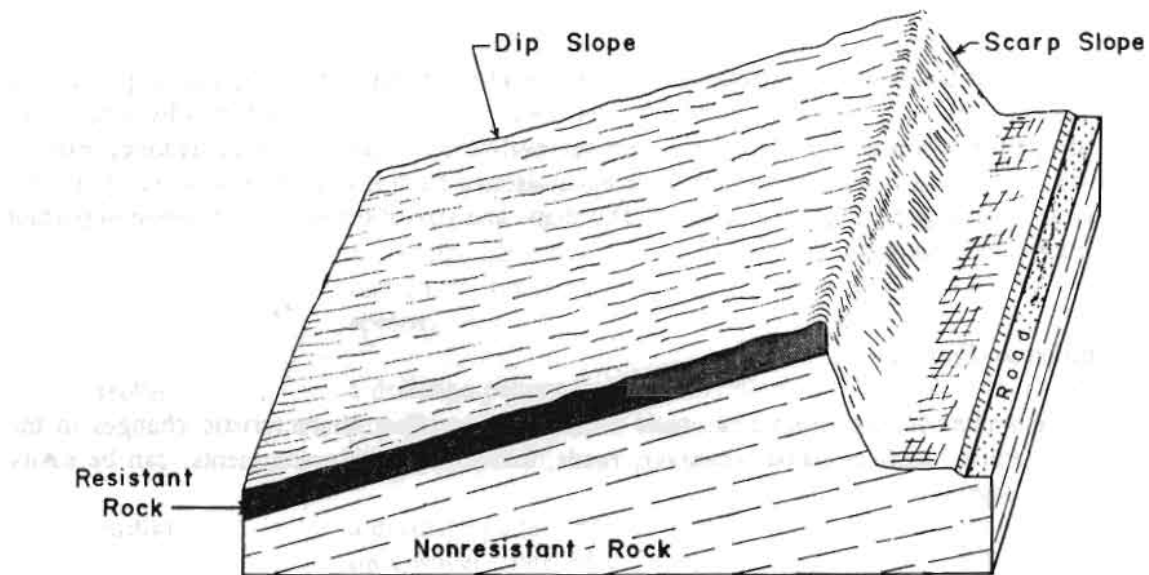
8.3. INTERPRETATION OF ROCK TYPES

The interpretation of rock types involves a careful evaluation of the various identifiable elements of photointerpretation described above. In areas where the overlying surficial material is deep or the surface covered with dense forest, the interpretation may be difficult. Tables 8.1, 8.2, and 8.3 provide the nature of photo features generally associated with igneous, metamorphic, and sedimentary rocks.



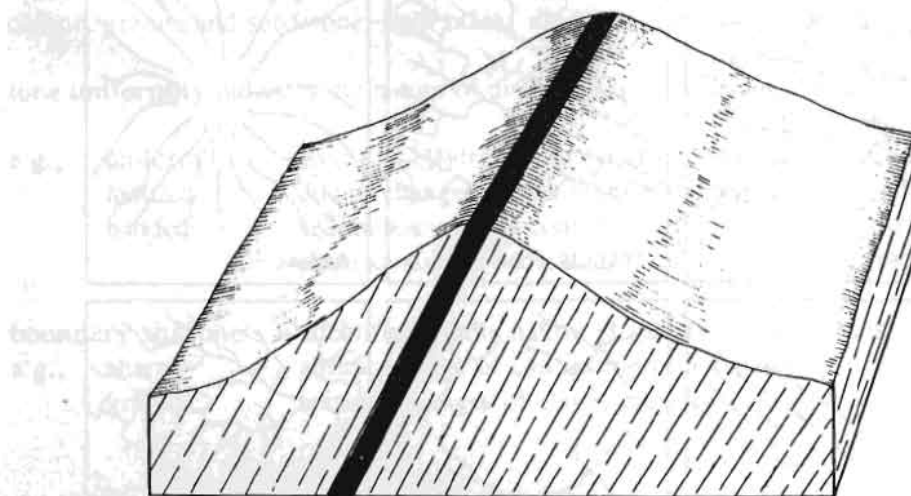
Source: Keser 1976

Fig. 8.1 Basic drainage patterns



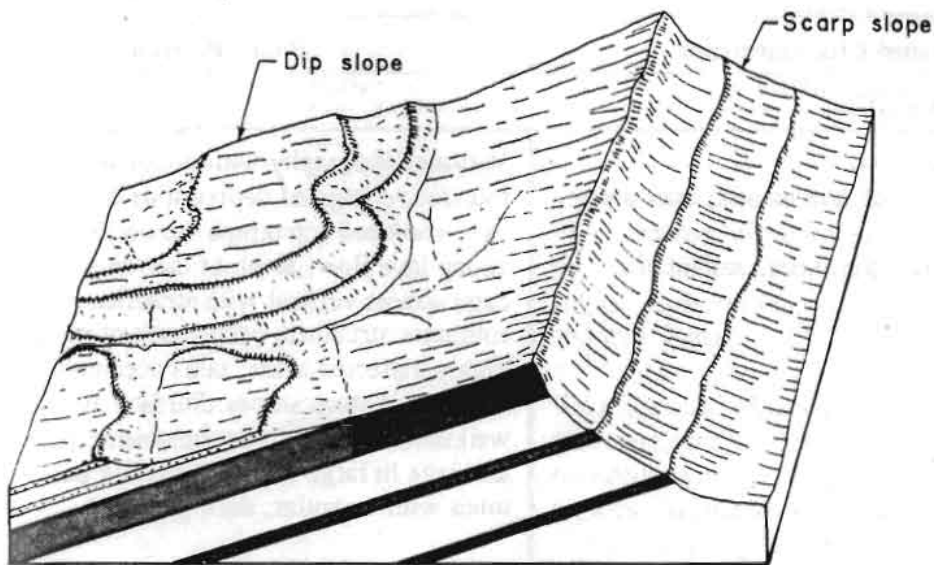
Source: Modified from Miller 1962

Fig. 8.2 Dip slope and scarp slope represented by resistant rock on top non-resistant rock



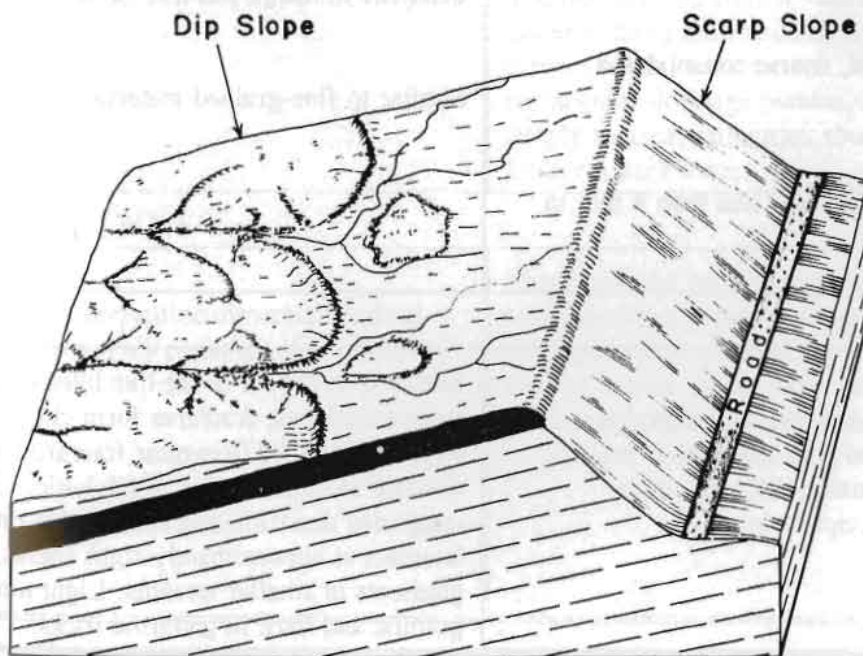
Source: Modified from Miller 1962

Fig. 8.3 Steeply dipping resistant and non-resistant beds without distinct dip slopes and scarp slope



Source: Modified from Miller 1962

Fig. 8.4 Interbedding of resistant and non-resistant strata with dip and scarp slopes



Source: Modified from Miller 1962

Fig. 8.5 Dip slope drainage pattern in soft rock on top of hard rock

Table 8.1. Identification of igneous rocks

Type and Characteristics	Photo Pattern
EXTRUSIVE ROCKS:	
<p>Lava and related rocks: very fine-grained (grains seen only under microscope) major minerals: quartz, feldspar, mica, pyroxene, amphibole</p>	<p>Varying topography with minor irregularities; rounded, elongated depressions common; rope-like, scalloped topography towards terminus of young lava flow; slope of canyon walls (river cuts) almost vertical with stratification and columnar structure; occurrence of mesas in highly dissected areas; talus accumulation at the base of steep slopes. Surface drainage not well developed and may be absent; parallel drainage in large areas. Generally dull, dark tones with irregular, dark patches.</p> <p>Lack of drainage - white tone.</p>
<p>Ash: uncemented, fine pyroclastic fragments</p>	<p>Rough dissected topography - uniform, dense, dendritic drainage pattern; variable tone.</p>
<p>Breccia: highly angular, coarse consolidated fragments</p>	<p>Similar to fine-grained material.</p>
<p>Tuff: compacted fragments less than 4 mm in diameter</p>	
INTRUSIVE ROCKS:	
<p>Plutonic rocks: medium to coarse-grained (grains distinguished with naked eye) major minerals: quartz, feldspar, mica, pyroxene, amphibole</p>	<p>Massive, rounded, dome-like hills with fairly steep sideslopes; fractures form choppy surface with minor relief (irregular fracture patterns); absence of stratification and foliation. Well-integrated dendritic and rectangular lines intersect at approximately right angles; high gradients in smaller streams. Light tones in granitic and dark in gabbroic rocks.</p>

Source: Keser 1976

Table 8.2 Identification of metamorphic rocks

Type and Characteristics	Photo Pattern
FOLIATED ROCKS:	
<p>Gneissic: coarse-grained alternating bands of granular and micaceous minerals</p>	<p>Sub-parallel, steep-sided, sharp-crested ridges. Fine-textured, angular dendritic drainage pattern; tributaries join main trunk at near right angles. Uniform light tones or alternating light and dark bands.</p>
<p>Schistose: medium to coarse-grained micaceous minerals dominant</p>	<p>Well dissected topography; humid regions - moderate relief, ridges are usually smooth and rounded; in arid, subarctic and glaciated regions - scattered, irregular banding (foliation). Long, steep, closely-spaced, sub-parallel gullies and ravines common; contorted drainage pattern in some areas. Contour farming and terracing common. Uniform light or banded tones.</p>
<p>Slate: fine-grained; well-developed fissility</p>	<p>Uniform size, comparatively small, randomly distributed hills; similar lateral and height dimensions to numerous hills produces a distinctive airphoto pattern. Fine-textured rectangular drainage pattern - highly developed; deeply incised; numerous short, steep gullies. Uniform dark tones.</p>
NON-FOLIATED ROCKS:	
<p>Serpentinite: contains serpentine minerals; derived from previous existing olivine and pyroxene</p>	<p>Sharp contrast with bordering rock types; sinuous ridges connect conically-shaped hills; scalloped ridge outlines; smoothly, rounded convex slopes. Short steep gullies. Light tone ('creamy') often has soft mohair-like sheen.</p>

Source: Keser 1976

Table. 8.3 Identification of sedimentary rocks

Type and Characteristics	Photo Pattern
MASSIVE ROCKS	
Limestone: fine to medium-textured, cemented dominant mineral - calcite	Commonly hummocky surface expression in glaciated terrain; karst topography may not have developed; few valleys - steep, nearly vertical sides with flat floor. Few streams with many short, steep tributaries; sinkhole depressions, often ponds or swamps with swallowhole drainage pattern. Humid regions - vegetated except in sinkholes. Arid regions - vegetated in sinkhole depressions. Light gray tone overall, broken by tone changes in sinks; erosion scars appear as short, light streaks on hillsides.
THIN BEDDED ROCKS:	
Shale: indurated and consolidated clays and silts; impervious, fine-textured classified for the impurity that is dominant (argillaceous, siliceous)	Humid regions - rounded hills. Arid regions - rough topography with steep to vertical sideslopes on hills. Well developed, fine, dendritic drainage pattern. Humid regions - mottled light and dark tones. Arid regions - uniform light tone (with banding in the rock).
INTERBEDDED ROCKS:	
Flat-lying: alternating layers with differing resistances to erosion Tilted: alternating layers with differing resistances to erosion	Faint (thin beds) to well-defined, stepped (structural benches and terraces) contour breaks on sideslopes; hilltops are at same general elevation. Dendritic drainage pattern; may be rectangular if cap rock is jointed; more intense drainage with many gullies - thicker beds; less intense drainage with few gullies - thinner beds. Banding along contours, with more distinctive banding in thicker beds. Alternating light and dark bands. Series of straight, nearly parallel ridges (escarpments), forms include cuestas and hogbacks. Definite trellis drainage pattern. Parallel light and dark bands.
THICK BEDDED TO MASSIVE ROCKS:	
Flat-lying (sandstone): fine to coarse-grained principal constituents: quartz, feldspar, rock fragments, silt and clay cemented together; classified according to cementing agent (calcareous, ferruginous, siliceous)	Arid regions - rugged topography with deep valleys, isolated hills with banding evident. Humid regions - rolling to hilly topography with bold massive hills and steep slopes. Widely-spaced rectangular pattern - few gullies. Arid regions - short, dark, straight lines indicate joint pattern. Humid regions - light tone.
Tilted: as in THIN BEDDED	AS IN THIN BEDDED.

Source: Keser 1976

SOIL MECHANICS

9.1 DEFINITIONS

9.1.1 Solid-Air-Water Phase Relationship

Water Content or Moisture Content

$$w = \frac{\text{Weight of water}}{\text{Weight of solids}} = \frac{W_w}{W_s}$$

Degree of Saturation

$$S_r = \frac{\text{Volume of water}}{\text{Total volume of void space}} = \frac{V_w}{V_v} = \frac{wG_s}{e}$$

Void Ratio

$$e = \frac{\text{Volume of voids}}{\text{Volume of solids}} = \frac{V_v}{V_s} = \frac{n}{1-n}$$

Porosity

$$n = \frac{\text{Volume of voids}}{\text{Total volume of soil}} = \frac{V_v}{V} = \frac{e}{1+e}$$

Air Content

$$A = \frac{\text{Volume of air}}{\text{Total volume of soil}} = \frac{V_a}{V} = \frac{e - wG_s}{1+e} = n(1 - S_r)$$

Figures and Tables without credit lines in this chapter have been compiled by the author(s) for this handbook.

Bulk Density

$$\begin{aligned}\rho &= \frac{\text{Total weight of soil}}{\text{Total volume of soil}} = \frac{W}{V} = \frac{G_s (1 + w) \rho_w}{1 + e} \\ &= \frac{G_s + S_r e}{1 + e} \rho_w\end{aligned}$$

$S_r = 1$, for fully saturated soil

$S_r = 0$, for completely dry soil

Specific Gravity of Solid Particles

$$G_s = \frac{\text{Weight of solids}}{\text{Volume of solids} \times \text{density of water}}$$

$$\begin{aligned}&= \frac{W_s}{V_s \times \gamma_w} \\ \gamma_w &= \text{unit weight of water}\end{aligned}$$

Unit Weight of Soil

$$\begin{aligned}\gamma &= \frac{\text{Total weight (force)}}{\text{Total volume}} = \frac{W}{V} = \frac{G_s (1 + w)}{1 + e} \gamma_w \\ &= \frac{G_s + S_r e}{1 + e} \gamma_w\end{aligned}$$

9.1.2 Gradation of Soils

Coarse-grained Soils

Soils in which the properties are mainly influenced by sand and gravel-sized particles (0.06 mm to 60 mm).

Fine-grained Soils

Soils in which the properties are mainly influenced by clay and silt-sized particles (0.001 mm to 0.06 mm).

Well-graded Soils

Coarse-grained soil which have no excess of particles in any size range and do not lack intermediate-sized particles. Represented by a smooth, concave grain size distribution curve (i.e., a semi-logarithmic plot of particle size versus percentage by weight of particles smaller than the given size).

Poorly-graded Soils

Uniformly-graded - has a high proportion of particles having sizes within narrow limits. Represented by an S type curve on the grain size distribution curve plotted on a semi-logarithmic graph.

Gap-graded - has both large and small sizes but with a relatively low proportion of particles of intermediate sizes. Represented by an almost flat curve at the middle of the grain size distribution curve.

9.1.3 Plasticity of Fine-grained Soils

Plasticity is the ability of a soil to undergo plastic (unrecoverable) deformation at constant volume without cracking or crumbling. Plasticity is due to the presence of clay minerals or organic material.

Liquid Limit, LL or w_L

The upper limits of the range of water content over which a soil exhibits little strength.

Plastic Limit, PL or w_p

The lower limit of the range of water content over which a soil exhibits plastic behaviour.

Plasticity Index, PI or I_p

The difference between liquid limit and plastic limit.

Liquidity Index

$$\begin{aligned} \text{LI or } I_L &= \frac{\text{Water content of soil} - \text{plastic limit}}{\text{Plasticity Index}} \\ &= \frac{w - w_p}{PI} \end{aligned}$$

Shrinkage Limit

This is the water content stage at which the volume of a soil reaches its lowest value as it dries out.

9.1.4 Soil Density

Compaction is the process of increasing the density of a soil by packing the particles closer together with a reduction in the volume of air: there is no significant change in the volume of water in the soil. The degree of compaction is measured in terms of dry density, i.e., the mass of solids per unit volume of soil.

$$\begin{aligned}\text{Bulk density of a soil, } \rho &= \frac{W}{V} = \frac{W_s + W_w}{V_s + V_v} \\ \rho &= \frac{W_s + W_s \times w}{V_s + V_v} = \frac{W_s (1 + w)}{V_s + V_v} \\ &= \frac{G_s \times V_s \times \rho_w (1 + w)}{V_s + V_v} = \frac{G_s (1 + w) \rho_w}{1 + e}\end{aligned}$$

$$\begin{aligned}\text{Dry density of soil, } \rho_d &= \frac{G_s (1 + w) \rho_w}{1 + e} = \frac{G_s (1 + 0) \rho_w}{1 + e} \\ &= \frac{G_s \rho_w}{1 + e}\end{aligned}$$

$$\rho = \frac{G_s (1 + w) \rho_w}{1 + e} = \rho_d (1 + w)$$

$$\text{Therefore, } \rho_d = \frac{\rho}{1 + w}$$

Thus, the dry density of a soil can be found, if we know the bulk density and water content of the soil. Dry density, after compaction (at water content w) to an air content A , can be calculated by,

$$\rho_d = \frac{G_s (1 - A)}{1 + wG_s} \cdot \rho_w$$

9.1.5 *Flow of Water*

Seepage

Soils under the water table may be under static water pressure, depending upon the depth below the water table, or under seepage pressure due to water flowing through the pores under a hydraulic gradient. Normally, the seepage velocities in soils are so small that the velocity head can be neglected. The total head, thus, is the sum of elevation head and pore pressure head caused by seeping water. The energy of water is used up in flowing through the soil.

Water Table or Phreatic Surface

The uppermost level of water at which the pressure is atmospheric.

Pore-Water Pressure

Water pressure at any point in the pores of a soil mass, due to static or seeping water, measured relative to atmospheric pressure. Thus the pore-water pressure at atmospheric pressure is zero.

Permeability of Soil

In accordance with Darcy's empirical law, it is the discharge velocity of water through a soil divided by the hydraulic gradient. The coefficient of permeability is a function of void ratio. If a soil deposit is stratified, the permeability for flow, parallel to the direction of stratification, is higher than that for flow perpendicular to the direction of stratification.

Degree of Saturation of Soil

The degree of saturation of soil below the water table is assumed to be a hundred per cent, i.e., fully saturated.

Perched Water Table

Local water table, caused by water contained by soil of low permeability, above the normal water table level.

Artesian Condition

A condition where an inclined sand layer of high permeability is confined locally by an overlying layer of low permeability. The pressure in the confined layer is governed not by the local water table level but by a higher water table at a distant location where the layer is unconfined.

Total Head

The total head at any point in a soil mass is the sum of elevation head from a datum and the head, caused by pore-water pressure in the soil, at the point in question. In other words, it is the elevation, from a given datum, of free water in a tube (manometer or piezometer) inserted in the soil at the point for which the total head is being determined. The head caused by pore-water pressure is the ratio of pore-water pressure at the point and the unit weight of water.

Flow Net

This is the family of flow lines and family of **equipotentials** drawn, by graphical representation of groundwater flow, to solve the problem of seepage in a soil. Flow lines or stream lines are just a few of the flow paths selected, from among an infinite number, of flow paths of water, flowing through all the interconnecting pore spaces in a soil. **Equipotential lines** or equipotentials are the lines joining points at which the total head is the same. These lines intersect the flow lines approximately at right angles in an isotropic soil. Figure 9.1 illustrates the flow net in two dimensions in a slope.

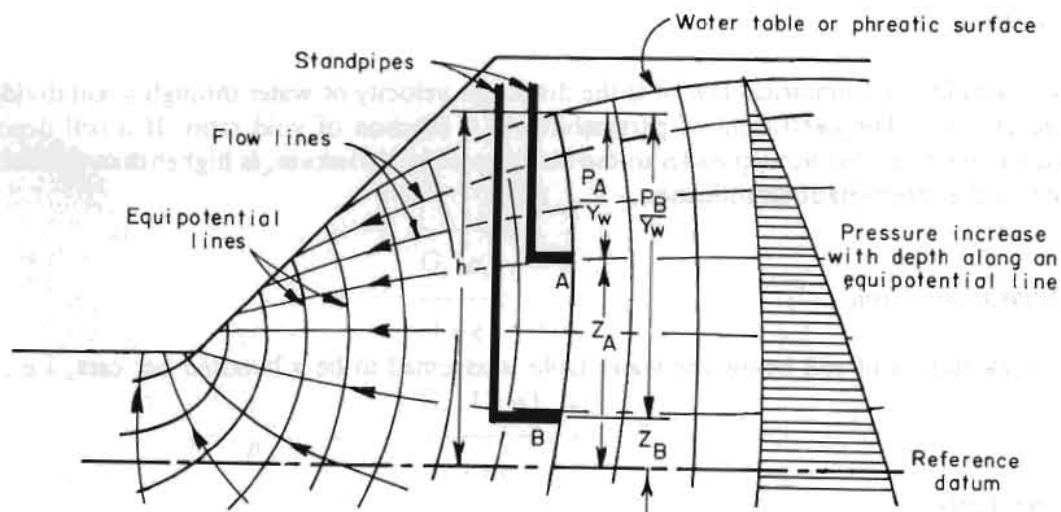


Figure 9.1 : Two-dimensional flow net in a slope.

Source: USDT 1981

Fig. 9.1 Two-dimensional flow net in a slope

Effective Stress

The effective stress on a plane in a fully saturated soil mass, according to Terzaghi's Principle of Effective Stress, is the stress transmitted through the soil skeleton only. This can be expressed by the following relationship:

$$\sigma' = \sigma - u$$

where,

- σ' = effective normal stress,
- σ = total normal stress, i.e., the force per unit area normal to the plane, and
- u = pore-water pressure, i.e., the pressure of the water filling the void space between solid particles.

Seepage Force

This is a force corresponding to the transfer of energy from water to solid particles, when water is seeping through the pores of a soil, dissipating the total head as **viscous friction** producing a **frictional drag**, acting in the direction of flow, on the solid particles.

Seepage Pressure (j) is defined as the seepage force per unit volume, i.e:

$$j = i \gamma_w \quad \text{where, } i = \text{hydraulic gradient, and} \\ \gamma_w = \text{unit weight of water.}$$

Resultant Body Force

Resultant body force in a soil mass is the combination of the forces in a soil mass due to gravity and seeping water.

Quick (Liquefaction) Condition

This is a condition caused when the contact forces between the soil particles are zero and the soil will have no strength. It occurs when there is an upward seepage in soil and the hydraulic gradient corresponds to zero resultant body force. The condition is said to be 'boiling' when the hydraulic gradient exceeds the gradient for zero resultant body force.

Piping

This is the process of internal erosion due to seeping water under a high hydraulic gradient.

9.1.7 Shear Strength

The strength (τ_f) of a soil at a point on a particular plane was originally expressed by Coloumb as a linear function of the normal stress (σ) on the plane at the same point:

$$\tau_f = c + \sigma \tan \phi$$

where,

$$\begin{aligned} c &= \text{cohesion, and} \\ \phi &= \text{angle of internal friction.} \end{aligned}$$

According to Terzaghi's fundamental concept, the shear stress in a soil can be resisted only by the skeleton of solid particles. Shear strength is expressed as a function of effective normal stress:

$$\tau_f = c' + \sigma' \tan \phi'$$

where,

$$\begin{aligned} c' &= \text{effective cohesion, and} \\ \phi' &= \text{effective angle of internal friction.} \end{aligned}$$

Mohr-Coloumb Failure Criterion

The relationship between effective principal stresses (ϕ_1' = major principal stress at failure and ϕ_3' = minor principal stress at failure) at failure and shear strength can be expressed by:

$$\sigma_1' = \sigma_3' \tan^2 \left(45^\circ + \frac{\phi'}{2} \right) + 2c' \tan \left(45^\circ + \frac{\phi'}{2} \right)$$

This relationship is referred to as the **Mohr-Coloumb Failure Criterion**.

9.1.8 Consolidation

Consolidation is the gradual reduction in volume of a fully saturated soil of low permeability due to drainage of some of the pore-water. The process continues until the excess pore-water pressure set up by an increase in total stress has been completely dissipated.

Degree of consolidation (U_z) at a particular instant of time, at depth z ($0 \leq U_z \leq 1$):

$$U_z = \frac{e_o - e}{e_o - e_1} = \frac{\sigma' - \sigma'_o}{\sigma_1' - \sigma'_o} = 1 - \frac{u}{u_i}$$

- where,
- e_o = void ratio before the start of consolidation,
 - e_i = void ratio at the end of consolidation,
 - e = void ratio at the time in question during consolidation,
 - σ_o' = effective normal stress before the start of consolidation,
 - σ_i' = effective normal stress at the end of consolidation,
 - u = pore-water pressure in excess of u_o (pore-water pressure before the increase in total stress), and
 - u_i = increase in pore-water pressure above u_o (pore-water pressure before the increase in total stress) immediately after the increase in total stress.

9.1.9 *Bearing Capacity*

Ultimate Bearing Capacity (q_f or q_u)

This is the least soil pressure which would cause shear failure of the supporting soil immediately below and adjacent to a foundation.

Allowable Bearing Capacity (q_a)

This is the maximum soil pressure which may be applied to the soil such that 1) the factor of safety against shear failure of the supporting soil must be adequate, a value between 2.5 and 3 normally being specified, and 2) the settlement of the foundation should be tolerable and, in particular, differential settlement should not cause any unacceptable damage or interference with the function of the structure.

9.1.10 *Lateral Earth Pressure*

Earth Pressure at Rest (P_o)

This is the earth pressure associated with no lateral strain in soil:

$$P_o = K_o \gamma' z$$

- where,
- K_o = coefficient of earth pressure at rest, in terms of effective stress,
 - γ' = effective unit weight of soil, and
 - z = depth of soil.

Active Earth Pressure (P_a)

This is earth pressure, associated with lateral expansion of the soil and is a minimum value. It is applicable in the case of a retaining wall moving away from the backfill.

Passive Earth Pressure (P_p)

This is the earth pressure associated with lateral compression of the soil and is a maximum value. It is applicable in the case of a retaining wall moving into the backfill.

9.2 FIELD IDENTIFICATION OF SOILS

The soil classification system is so devised that it is possible, with experience, to classify most soils correctly on the basis of field identification methods alone. The easiest way to learn field identification is under the guidance of an experienced man. While learning the procedures, one should systematically compare the laboratory test results for typical soils in each group with the feel of these soils while performing the field identification tests.

The following tests were developed largely by Professor A. Casagrande, Graduate School of Engineering, Harvard University, and have been widely adopted for use in identification of soils. These tests can be performed without equipment and are simple in nature. Do not make a decision on the basis of a single test. Use all applicable tests, then identify the soil.

9.2.1 Test Methods

Grain Shape By Visual Examination

Observe and classify the sand and gravel particles according to degree of angularity or roundness (Fig. 9.2).

Grain Size and Gradation by Visual Examination

Sand and gravel sizes are readily identified by visual inspection. Individual grains below the smallest sand size cannot be seen by the naked eye and must be identified by other tests.

To estimate the gradation of **coarse-grained soils**, spread a representative sample out on a flat surface and observe the distribution or uniformity of grain sizes (Fig. 9.3a and b). Observe the proportion of fines and subject the **fine-grained fraction** to all tests described for fine-grained soils.

For gradation of **fine-grained soils**, shake the sample in a jar of water and allow it to settle out. Approximate gradation is indicated by the separation of the particles in the jar from top to bottom. Silt remains in suspension for at least one minute; clay, one hour or more. Table 9.1 can be used for soil classification based on these visual tests and other tests described below.

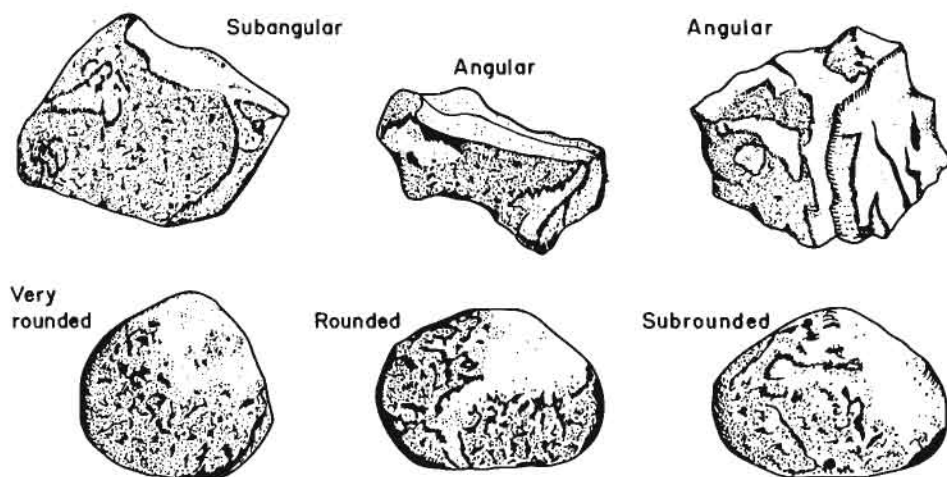
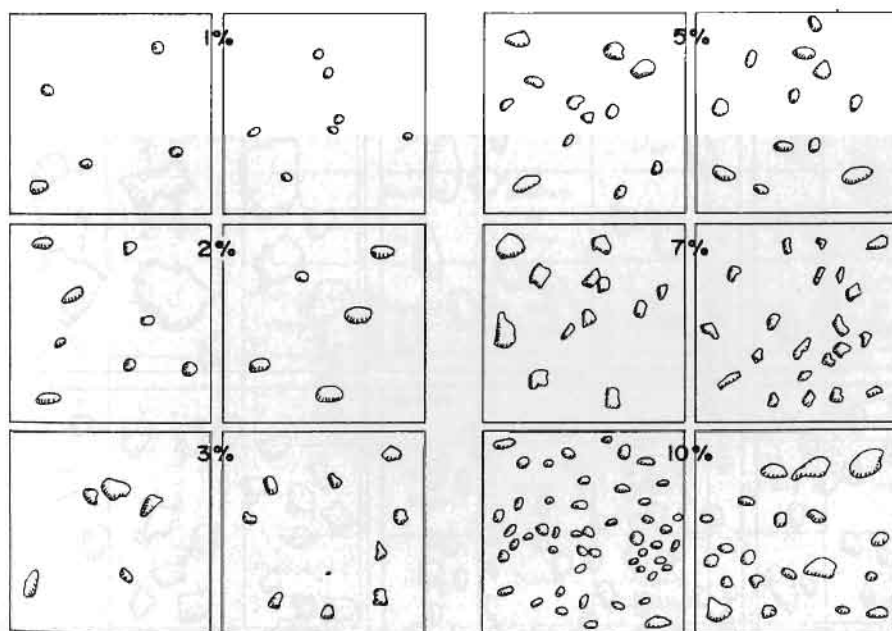


Fig. 9.2 Grain shape



Source: Krähenbuhl and Wagner 1983

Fig. 9.3a Visual estimation of percentage of material larger than 0.6 mm.

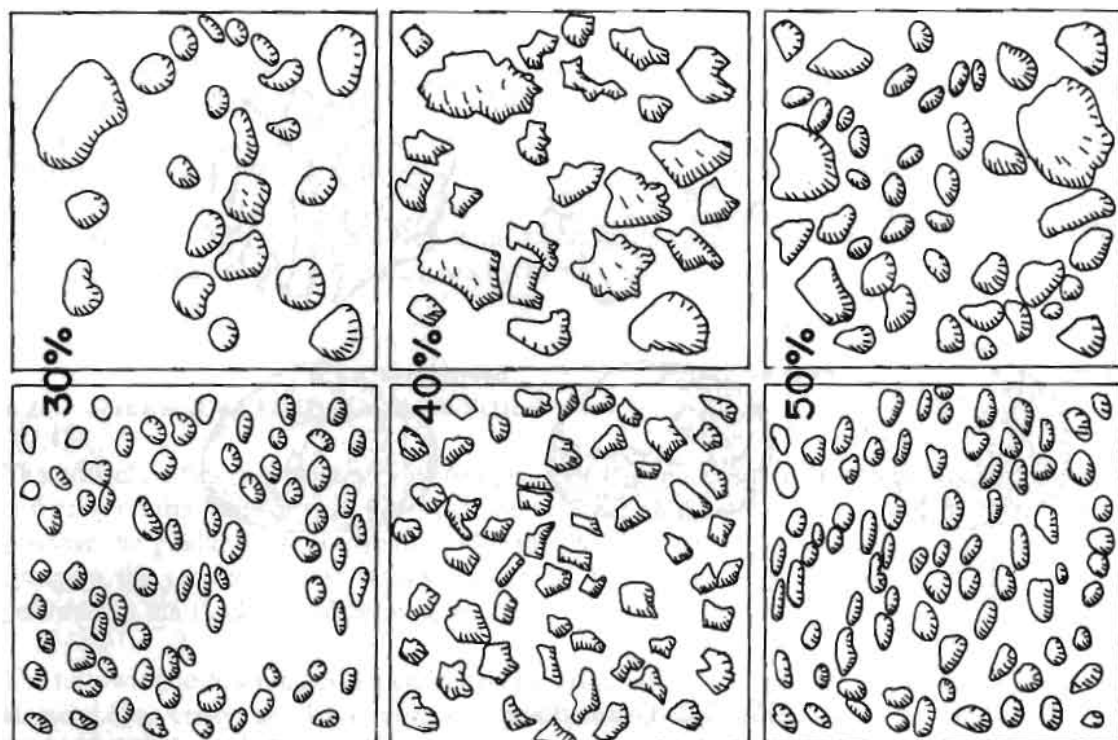
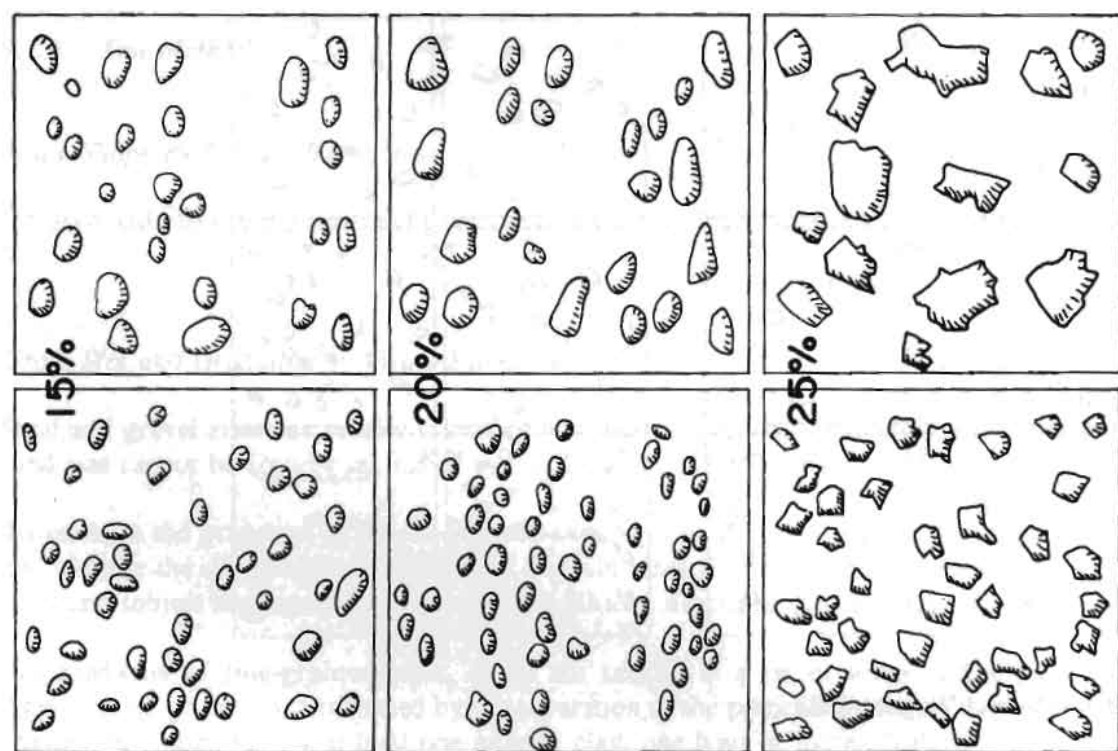


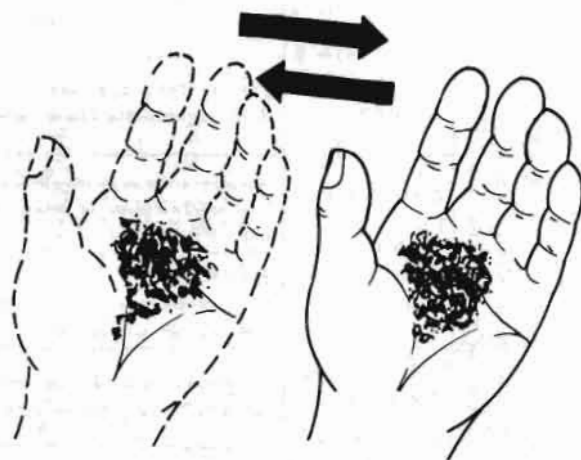
Fig 9.3b

Table 9.1 Field identification

FINE-GRAINED SOILS		COARSE-GRAINED SOILS											
More than half of the material (by weight) is of individual grains not visible to the naked eye		More than half of the material (by weight) is of individual grains visible to the naked eye											
No. 200 sieve size is about the smallest particle visible to the naked eye													
SILTS AND CLAYS (High liquid limit)	SILTS AND CLAYS (Low liquid limit)	See identification procedures	SAND AND SANDY SOILS More than half of coarse Fraction (by weight) is smaller than 6mm size		GRAVEL AND GRAVELLY SOILS More than half of coarse Fraction (by weight) is larger than 6mm size								
			Pronounced Organic										
			Pronounced Organic										
			Pronounced Organic										
		ODOUR		DRY STRENGTH		DILATANCY (SHAKE) REACTION		TOUGHNESS		RIBBON (NEAR THE PL)		SHINE (NEAR THE PL)	
		Pronounced Organic		Medium		Slight		Rapid		None		Dull	
		Medium		Medium to High		Medium to Slow		Medium		Weak		Slight to Shiny	
		Medium		Medium		Slow to None		Low (Spongy)		None		Dull to Slight	
		Medium		Medium		Very slow to None		Medium to High		Weak to Strong		Slight	
		High		Very High		None		High		Strong		Shiny	
		None		None		None		Low to Medium (Spongy)		Weak		Dull to Slight	
HIGHLY ORGANIC SOILS													
Readily identified by color, odour, spongy feel and frequently by fibrous texture													

Shaking Test (Dilatancy)

The shaking test aids in the identification of fine-grained soils. After removing particles larger than No. 40 sieve size, prepare a pat of moist soil with a volume of about 10 cc. Add enough water, if necessary, to make the soil soft but not sticky.



Method of Shaking

Fig. 9.4 Shaking test

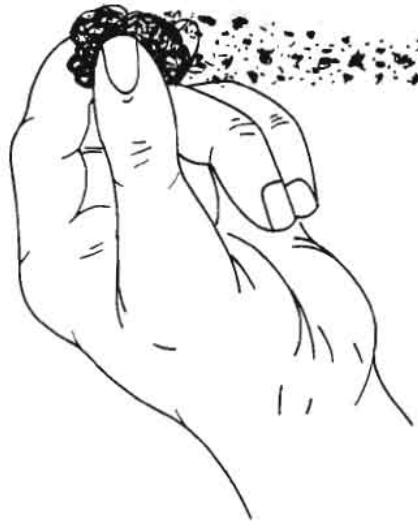
Place the pat in the open palm of one hand and shake horizontally, striking vigorously against the other hand several times (Fig. 9.4). A positive reaction consists of the appearance of water on the surface of the pat which becomes glossy. When the sample is squeezed between the fingers, the water and gloss disappear from the surface, the pat stiffens, and finally it cracks or crumbles. Shake the broken pieces until they flow together again. Distinguish between slow, medium, and rapid reactions to the shaking test.

A **rapid reaction** indicates a lack of plasticity, such as is the case with a typical inorganic silt, a rock flour, or a very fine sand. A **slow reaction** indicates a slightly plastic silt or silty clay. **No reaction** indicates a clay or a peaty (organic) material. Use these results with Table 9.1.

Breaking Test (Dry Strength)

The breaking test may be used to determine the dry strength of a soil, and this is a measure of its cohesiveness.

After removing particles larger than No. 40 sieve size, mould a pat of soil to the consistency of putty, adding water if necessary. Allow the pat to dry completely by oven, sun, or air drying, and then test its strength by breaking and crumbling between the fingers (Fig. 9.5). This strength is a measure of the character and quantity of the colloidal fraction contained in the soil. The dry strength increases with increasing plasticity.



Method of crumbling soil between fingers

Figure 9.5 Breaking Test

Low dry strength indicates an inorganic silt, a rock flour, or a silty sand. However, the sand feels gritty when the sample is powdered. The dried soil pat can be powdered with slight finger pressure.

Medium dry strength indicates a low to medium plastic inorganic clay. Considerable finger pressure is required to powder the sample.

High dry strength indicates a highly plastic, inorganic clay. The dried sample may be broken but cannot be powdered by finger pressure.

Cohesion or high dry strength may be furnished by some cementing materials such as calcium carbonate or iron oxide. For example, non-plastic lime rock or coral may develop high dry strength.

Odour Test

Freshly sampled organic soils usually have a distinctive odour which aids in their identification. The odour can be made more apparent by heating a wet sample.

Acid Test

Drop a little hydrochloric acid on a piece of soil. A fizzing reaction indicates calcium carbonate.

Shine Test

Rub a dry or slightly moist sample with the fingernail or a knife blade. A shiny surface indicates a highly plastic clay; a dull surface indicates a silt or clay of low plasticity (Fig. 9.6).

- A. Method of rolling thread
- B. Thread of soil above plastic limit
- C. Crumbling thread as plastic limit is reached

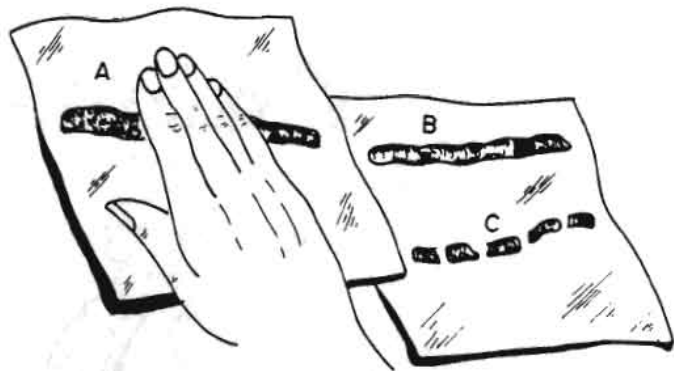


Fig. 9.6 Plasticity Test

Colour

The colour of a soil in both moist and dry conditions should be described as accurately as possible by use of standard colour designations. Acceptable soil colour descriptions are: white, gray, black, brownish-black, reddish-gray, brownish-gray, orange, red-brown, yellowish-brown, olive-brown, yellow, olive, blue, green, etc. These terms should be further modified by the adjectives light, medium, dark, or vivid. Use of the Munsell soil colour charts and plates is recommended when more precise soil colour descriptions are desired.

Mottles or streaks should be indicated and their description should follow the main colour designation of the soil; for example - stiff clay, plastic when moist, friable when dry; medium blue, mottled with brown when moist; light green, mottled with brown when dry.

Texture

The term texture refers to the distinctive appearance and feel of the soil, which are direct indications of the fineness and uniformity of the soil. Texture should be described by a standard adjective as listed below.

- Sharp - typical of gravelly or sandy soils
- Gritty - typical of coarse silts or sandy silts and clay
- Floury - typical of fine silts
- Smooth - typical of clays or fine silty clays

Consistency

The term consistency refers to the degree of adhesion between soil particles or the resistance to deformation or rupture under applied pressure. Consistency of the moist soil in both the undisturbed and remoulded states should be described by standard adjectives in Table 9.1 as listed below:

(1) Cohesionless Soils (Sands and Silts)

- Loose - poorly-graded, lacks binder or cementing agent, not well compacted.
- Dense - well-graded, well compacted, may contain binder or cementing agent.

(2) Cohesive Soils (Clays)

Very Soft	- easily penetrated several centimetres by fist.
Soft	- easily penetrated several centimetres by thumb.
Medium	- can be penetrated by thumb with moderate effort.
Stiff	- readily indented by thumb; penetrated only with great effort.
Very Stiff	- readily indented by thumbnail.
Hard	- indented with difficulty by thumbnail.

Additional adjectives used in connection with the terms listed above in describing the consistency of cohesive soils are: sticky, plastic, friable, brittle, jointed, stratified, and varved.

Moisture Content

The apparent moisture content of the soil should be described by such terms as dry, moist, wet, saturated, etc.

9.3 UNIFIED CLASSIFICATION SYSTEM

9.3.1 *Soil Properties Used in Classification*

This system identifies soils according to their textural and plasticity qualities and on their groupings with respect to behaviour. The system is based on those characteristics of a soil that indicate how it will behave as an engineering construction material.

The soil properties that have been found most useful for this purpose and form the basis of soil identification are:

- percentage of gravel, sand, and fines (fraction passing No. 200 sieve),
- shape of grain size distribution curve, and
- plasticity and compressibility characteristics.

These properties are determined by mechanical analysis, liquid limit, and plastic limit tests.

9.3.2 *Definition of Soil Components* (Fig. 9.7)

<u>Component</u>	<u>Size Range</u>
Boulders	Larger than 300 mm in diameter
Cobbles	Between 80 mm and 300 mm in diameter
Gravel	Between No.4 mesh (4.76 mm) and 80 mm in diameter
Sand	Between No. 200 mesh (.074 mm) and No. 4 mesh
Fines*	Smaller than No. 200 mesh

A comparison of the size of the soil components as defined in the UNIFIED, the American Association of State Highway and Transportation Officials (AASHTO), and the United States Department of Agriculture (USDA) textural classification systems is shown in Figure 9.8.

* Fines include silt and clay. A material is called a silt if it is non-plastic or very slightly plastic and exhibits little or no strength when air-dried. Silt fines fall below A-line, Figure 9.7. A material is called a clay if the fines exhibit plasticity within a range of water contents and if it has considerable strength when air-dried. Clay fines fall above the A-line (Fig. 9.6).

LABORATORY CRITERIA FOR UNIFIED SOIL CLASSIFICATION SYSTEM									
LABORATORY CLASSIFICATION CRITERIA ¹					GROUP SYMBOLS	TYPICAL NAMES ²			
	GRAVELS								
Coarse Grained Soils Less than 50% passing No. 200 sieve	Less than half of the coarse fraction passes the No. 4 sieve size	Less than 5% passing the No. 200 sieve size	Borderline cases requiring the use of dual symbols (i.e. SW-SC)	$C_u = D_{60}/D_{10}$ Greater than 4; $C_c = (D_{30})^2/D_{10} \times D_{60}$ Between 1 and 3		GW	Well graded gravels, gravel-sand mixtures, little or no fines		
		More than 12% passing the No. 200 sieve size		Not meeting both C_u and C_c requirements above		GP	Poorly graded gravels, gravel-sand mixtures, little or no fines		
	Sands and Gravels	More than half of the coarse fraction passes the No. 4 sieve size		Less than 5% passing the No. 200 sieve size	Above "A" line with PI between 4 and 7 requires the use of dual symbols (GC-GM)		GM	Silty gravels, gravel-sand-silt mixtures	
					Atterberg limits below "A" line, or $PI < 4$		GC	Clayey gravels, gravel-sand-clay mixtures	
Fine Grained Soils More than 50% passing No. 200 sieve	GO TO PLASTICITY CHART	Silty and Clays		5% to 12% passing the No. 200 sieve size	$C_u = D_{60}/D_{10}$ Greater than 4; $C_c = (D_{30})^2/D_{10} \times D_{60}$ Between 1 and 3		SW	Well-graded sands, gravelly sands, little or no fines	
					Not meeting both C_u and C_c requirements above		SP	Poorly graded sands, gravelly sands, little or no fines	
					Above "A" line with PI between 4 and 7 requires the use of dual symbols (SC-SM)		SM	Silty sands, sand-silt mixtures	
					Atterberg limits below "A" line, or $PI < 4$		SC	Clayey sands, sand-clay mixtures	
					Atterberg limits above "A" line, and $PI > 7$		ML	Inorganic silts and very fine sands, rock flour silty or clayey fine sands with slight plasticity	
							CL	Inorganic clays of low to medium plasticity, gravelly clays, silty clays, lean clays	
							MH	Inorganic silts, micaceous or diatomaceous, fine sandy or silty soils, elastic silts	
							CH	Inorganic clays of high plasticity, fat clays	
							OL	Organic silts and organic silt-clays of low plasticity $LL < 50$	
							OH	Organic clays of medium to high plasticity $LL > 50$	
				$\frac{LL \text{ (oven dry soil)}}{LL \text{ (air dry soil)}} < 0.75$		PI	Peat or other highly organic soils		
				Visual identification only					

¹ Work from left to right across chart
² Typical names not necessarily appropriate for individual soil description

Source: Krahenbuhl and Wagner 1983
 Fig. 9.7 Laboratory criteria for unified soil classification system

9.3.3 *The Plasticity Chart* (Fig. 9.7)

The plasticity chart is based on a plot of the plasticity index versus the liquid limit. The A-line on the plasticity chart is an important empirical boundary.

In general, soils with Atterberg limits that fall above the A-line behave as typical non-organic clays. Soils falling below the A-line behave as plastic soils containing organic colloids, or as typical inorganic silts. An exception to the above rule is the shaded area above the A-line with PI greater than 4 and less than 7. Soils with Atterberg limits falling in this zone may behave as a clay or as a silt.

The U-line on the plasticity chart represents the upper limit of the LL and PI plots for soils. The plasticity chart is very useful in classifying soils for engineering purposes. The soil groupings of the unified soil classification system are shown on a plasticity chart in Figure 9.7. Much useful information about the behaviour of a soil can be inferred from the plasticity chart.

If a mineral is ground up and the Atterberg limits of the various grain size fractions determined, the points representing such test results plot along a straight line roughly parallel to the A-line. Depending upon the mineralogical compositions of the grains, the plot may be above or below the A-line.

The points representing the limits of soils from a geologically well-defined sedimentary deposit will plot along a line roughly parallel to the A-line.

9.3.4. *Summary of the Unified Classification System*

- a. Designates soils as fine or coarse according to median size. Soil is coarse if the median size is larger than 0.074 mm (No. 200 mesh) and fine-grained if the median size is smaller than 0.074 mm (No. 200 mesh).
- b. Coarse-grained soils are classified on the basis of:
 - grain size and distribution,
 - quantity of fines, and
 - character of fines
- c. Fine-grained soils are classified on the basis of:
 - liquid limit - high if LL is greater than 50, Low if LL is less than 50,
 - plasticity index - clay if above A-line, silt if below A-line, and
 - grading is of minor importance.

d. Soil groups and group symbols of the Unified Classification System.

Basic Symbols

Modifying Symbols

G - gravel	W - Well-graded
S - sand	P - poorly-graded
C - clay	C - with clay fines
M - silt	M - with silt fines
O - organic	L - low liquid limit
Pt - peat	H - high liquid limit

Each soil is classified and identified with a verbal description and a group symbol consisting of two of the above letters. The letters may be considered to be initials of the name of the most typical soil in the group.

Sub-division of Coarse-grained Soils

- gravel and gravelly soils; symbol G, and
- sands and sandy soils; symbol S.

Sand and Gravel Groups

The gravels and the sands are each divided into four groups.

- Well-graded, fairly clean material; symbol W, in combinations GW and SW.
- Poorly-graded, fairly clean material; symbol P, in combinations GP and SP.
- Coarse material with clay fines, symbol C, in combinations GC and SC.
- Coarse materials with silt fines, symbol M, in combinations GM and SM.

Fine-grained Soil Groups

Fine-grained soils are sub-divided into three groups.

- The inorganic silty and very fine sandy soils; symbol M, used for fine-grained, non-plastic, or slightly plastic soils.
- The inorganic clays; symbol C.
- The organic silts and clays; symbol O.

Each of these types of fine-grained soils is grouped according to its liquid limit as:

- fine-grained soils having liquid limits less than 50; symbol L, in combinations ML, CL, and OL, and
- fine-grained soils having liquid limits greater than 50: symbol H, in combinations MH, CH, and OH.

Highly organic soils, usually fibrous, such as peat and swamp soils having high compressibility, are not sub-divided and are placed in one group; symbol Pt. The sequence of the group symbols need not be memorized but meanings of the symbols and sequence of the major divisions, i.e., G-S-L-H, should be learned. When a material does not clearly fall into one group, boundary classifications such as GW-SW or CL-ML should be used.

9.4 ENGINEERING PROPERTIES

Assessment of soil slope instability hazards during the feasibility stage requires at least an approximate estimation of soil strength parameters such as unit weight, friction angle, cohesion, moisture conditions, and water table depths. These parameters may be estimated in the field by visual identifications and index tests. The estimated values of these parameters should account for the worst conditions during the life of the proposed road or structures.

Tables 9.1 to 9.6 and Figure 9.9 are presented to facilitate the right classification of transported soils and soil strength parameters from rapid field tests. Residual soils (eluvial soils) are likely to have higher strength parameters than those for transported soils.

An alternative method to determine shear strength of slope material is to back-analyse existing slope failure in order to determine the shear strength parameters that must have been mobilized at the time of failure. It may be noted that back-analysis cannot determine both c and ϕ . It is, therefore, necessary to determine cohesion from laboratory tests on fine material or run back analyses for several slope failures in the same material. In case of boulder deposits, back-analysis is very fruitful because cohesion may be negligible.

Table 9.2 Compressibility

Term	Compression Index	Liquid Limit
Slight or low compressibility	0 - 0.19	0-30
Moderate or intermediate	0.20 - 0.39	31-50
High compressibility	0.40 and over	51 and over

Example for :-

GP - Poorly-graded gravel

Dr - Dense (from table)

Moisture content = 6%

Find

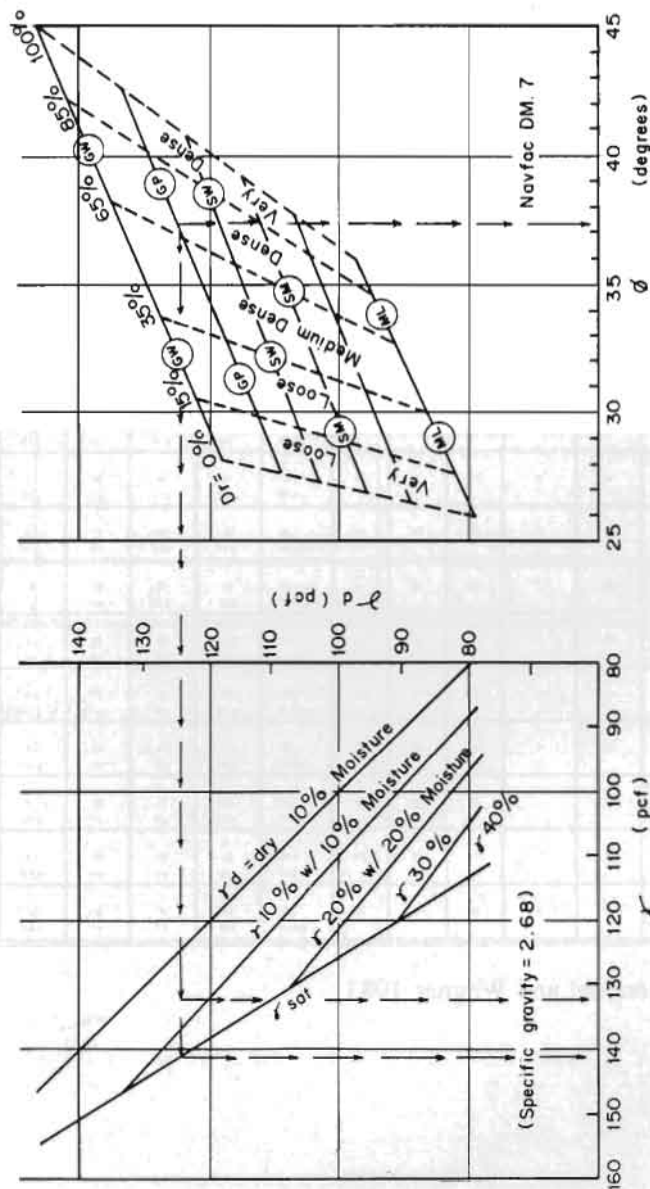
$$\phi' = 37.4^\circ$$

$$\gamma_d = 125 \text{ pcf}$$

$$\gamma' = 133 \text{ pcf (6\% Moisture)}$$

$$\gamma_{sat} = 141.5 \text{ pcf}$$

$$\gamma_{sub} = 141.5 - 62.4 = 79 \text{ pcf}$$



Field test with No. 4 rebar	Dr %
Can be driven only a few inches with 5 lb. hammer	100
Can be driven only one foot with a 5 lb. hammer	90
Easily driven with 5 lb. hammer	70
Easily pushed by hand	50

Fig. 9.9 Cohesionless soil - D_r v.s. γ and ϕ

Table 9.4 Typical strength characteristics of soil

Group Symbol	Cohesion of soil t/m ²		ϕ' (Effective stress envelope) degrees	$\tan\phi'$
GW	0	0	> 38	> 0.79
GP	0	0	> 37	> 0.74
GM	-	-	> 34	> 0.67
GC	-	-	> 31	> 0.60
SW	0	0	38	0.79
SP	0	0	37	0.74
SM	0.5	0.2	34	0.67
SM-SC	0.5	0.15	33	0.66
SC	0.75	0.1	31	0.60
ML	0.7	0.1	32	0.62
ML-CL	0.65	0.2	32	0.67
CL	0.9	0.15	28	0.54
OL	-	-	-	-
MH	0.75	0.21	25	0.47
CH	1.0	0.1	19	0.35

Source: Driscoll 1979

Table 9.5 Engineering use chart for soils classified by Unified Soil Classification System (USCS)

DESCRIPTION					
Typical Names of Soil Groups	Group Symbol	Permeability when compacted	Shearing strength when compacted and saturated	Compressibility when compacted and saturated	Workability as a construction material
Well-graded gravel, gravel-sand mixtures little or no fines.	GW	Pervious	Excellent	Negligible	Excellent
Poorly-graded gravel, gravel-sand mixtures, little or no fines.	GP	Very pervious	Good	Negligible	Good
Silty gravel, poorly-graded gravel-sand-silt mixtures.	GM	Semi-pervious to impervious	Good	Negligible	Good
Clayey gravel, poorly-graded gravel-sand mixtures.	GC	Impervious	Good to fair	Very low	Good
Well-graded sands, gravelly sands, little or no fines.	SW	Pervious	Excellent	Negligible	Excellent
Poorly-graded sands, gravelly sands, little or no fines.	SP	Pervious	Good	Very low	Fair
Silty sands, poorly-graded sand-silt mixtures.	SM	Semi-pervious to impervious	Good	Low	Fair
Clayey sands, poorly-graded sand-clay mixtures.	SC	Impervious	Good to fair	Low	Good
Inorganic silt, poorly-graded sand, rock flour, silty or clayey fine sands with slight plasticity.	CL	Semi-pervious to impervious	Fair	Medium	Fair
Inorganic clays of low to medium plasticity: gravelly sandy and lean clays.	CL	Impervious	Fair	Medium	Good to fair
Organic silts and organic silt clays of low plasticity.	OL	Semi-pervious or impervious	Poor	Medium	Fair
Inorganic silts, micaceous or diatomaceous fine sandy or silt soils, elastic silts.	MH	Semi-pervious to impervious	Fair to Medium	High	Poor
Inorganic clays of high plasticity, fat clays.	CH	Impervious	Poor	High	Poor
Organic clays of medium to high plasticity.	OH	Impervious	Poor	High	Poor
Peat and other highly organic soils.	Pt				

Source: Adapted from Krähenbuhl and Wagner 1983

Table 9.6 Relative desirability for various uses

	Canal Sections		Foundations		Roadways		
	Erosion resistance	Compacted earth lining	Seepage important	Seepage not important	Fills		Surfacing
					Frost	Heave	
					Important	Possible	
GW	1	-	-	1	1	1	3
GP	2	-	-	3	3	3	-
GM	4	4	1	4	4	9	5
GC	3	1	2	6	5	5	1
SW	6	-	-	2	2	2	4
SP	7	-	-	5	6	4	-
SM	8	5	3	7	8	10	6
SC	5	2	4	8	7	6	2
ML	-	6	6	9	10	11	-
CL	9	3	5	10	9	7	7
OL	-	7	7	11	11	12	-
MH	-	-	8	12	12	-	-
CH	10	8	9	13	13	8	-
OH	-	-	10	14	14	14	-

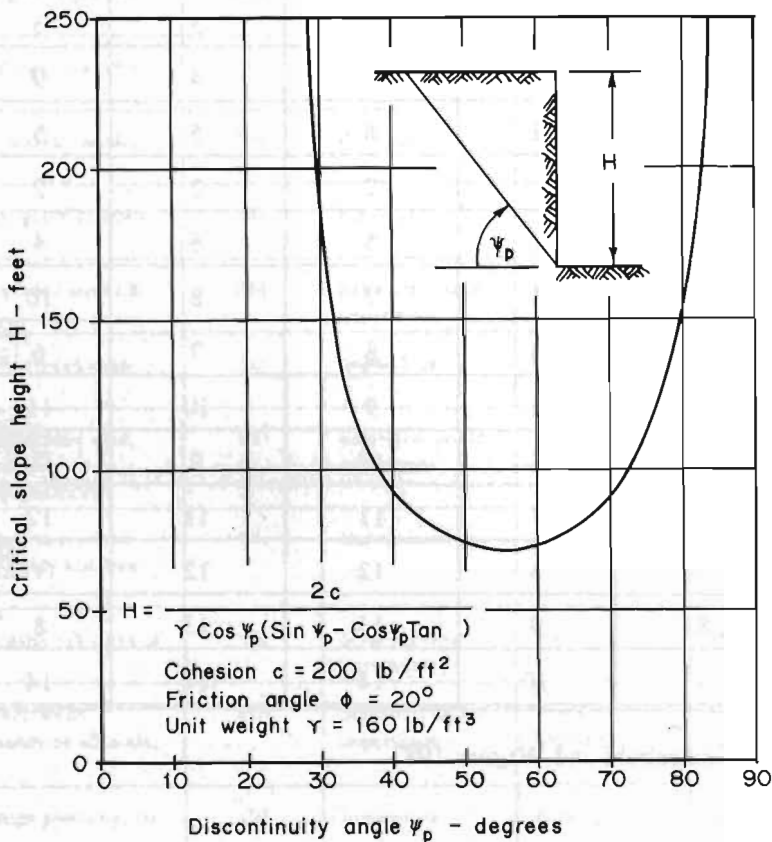
Source: Adapted from Krähenbuhl and Wagner 1983

Note: 1 is most desirable and 14 is least desirable.

ROCK MECHANICS

10.1 SHEAR STRENGTH OF ROCKS

The planning and design of structures in mountainous areas require understanding of the geological and mechanical behavior of rock masses.



Source: United States Department of Transportation (USDOT) 1981

Fig. 10.1 Critical height of a drained vertical slope containing a planar discontinuity dipping at an angle ψ_p

Unless otherwise stated all Figures and Tables in this chapter are based on "Rock Slopes" published by the United States Department of Transportation (USDOT) Federal Highway Agency (FHA) in 1981.

Analysis of rock slope stability has been approached by a number of investigators based on the assumption that rock mass behaves as an elastic continuum. The most analysis of practical rock slope problems is currently based on a **discontinuum approach**. The discontinuum approach emphasizes that the behavior of rock mass is dominated by discontinuities such as faults, joints, and bedding planes.

The stability analysis of rock slopes requires an understanding of the discontinuities, effect of the discontinuities on a failure plane, shear strength properties of rock masses, and the mechanics of stability. Rock mechanics is a subject that includes all these areas concerned with the engineering of structures in a rocky terrain.

The shear strength of rocks along a single discontinuity surface is influenced by friction angle and roughness of discontinuity, uniaxial compressive strength of joint surface, and type of infilling and water pressure in the joint. Figure 10.1 illustrates the influence of a discontinuity on critical slope height.

Shear strength of rock mass with a number of closely spaced joint sets is influenced by confining pressure, uniaxial compressive strength, water pressure, and constants defining the Mohr Failure Envelope.

10.1.1 *Peak and Residual Shear Strength*

Peak Shear Strength

This is the maximum shear strength or shear stress at yield point given by a curve obtained by plotting shear displacement against shear stress at constant normal stress (Fig. 10.2a).



Fig. 10.2 (a) Peak shear strength

Peak Friction Angle

This is the friction angle given by the slope of a straight line representing the relationship between normal stress and peak shear strength from shear strength tests carried out at varying normal stresses (Fig. 10.2b).

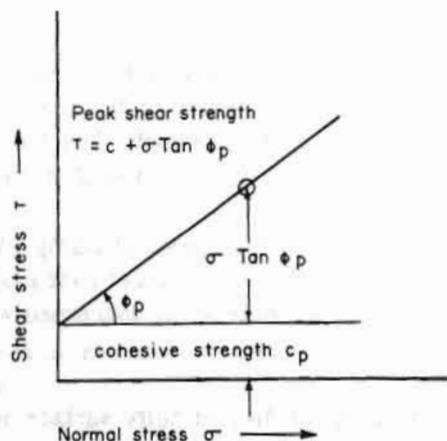


Fig 10.2(b) The relationship between normal stress and shear stresses

Residual Shear Strength

This is the shear stress that levels out at a constant value with increasing shear displacement in a shear test at constant normal stress (Fig. 10.2a)

Residual Friction Angle

This is the friction angle represented by the slope of a straight line obtained by a plot of normal stress against residual shear strength from shear tests at different normal stresses (Fig. 10.2c).

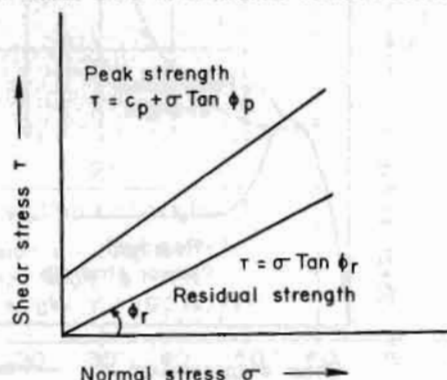


Fig. 10.2(c) Residual strength

10.1.2 Shear Strength of Rocks with Single Discontinuity - Plane Surface

The shear strength of rocks with even bedding planes having no surface undulation or roughness, can be expressed in a simple linear relationship. There are two cases, and these are given below.

In dry conditions, the peak shear strength $\tau = C_p + \sigma \tan \phi_p$,

and the residual shear strength $\tau = \sigma \tan \phi_r$.

In conditions of water-filled discontinuity, peak shear strength $\tau = c_p + (\sigma - u) \tan \phi_p$,
 and residual shear strength $\tau = (\sigma - u) \tan \phi_r$

where,

u = water pressure in the discontinuity.

10.1.3 Shear Strength of Single Discontinuity

Barton's Equation

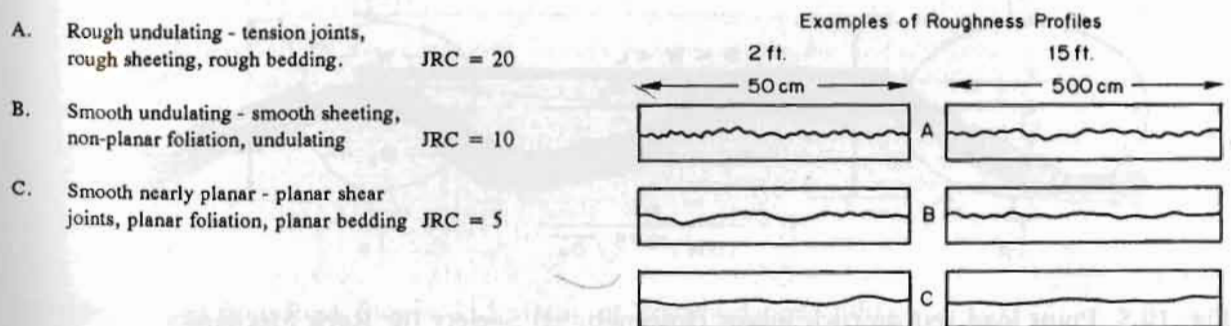
Barton (Barton and Chaubey 1977) proposed the following equations for predicting the shear strength of rough joints

$$\tau = \sigma \tan (\phi_r + JRC \log_{10} [\frac{JCS}{\sigma}])$$

$$\phi = \phi_r + i$$

where, JRC = joint roughness coefficient,
 JCS = joint-wall compressive strength,
 ϕ_r = basic friction angle of a smooth diamond saw-cut surface,
 σ = normal stress across a joint surface,
 i = angle of dilation or primary as parities, and
 ϕ = friction angle of rough joints.

Barton's equation is for low values of normal stress and is probably most applicable in the range of $0.01 < \sigma/JCS < 0.3$. Figures 10.3 and 10.4 illustrate Barton's definition of joint roughness, JRC, and the prediction of shear strength of rough discontinuities.



Source: Barton and Chaubey 1977

Fig. 10.3 Barton's definition of joint roughness coefficient (JRC)

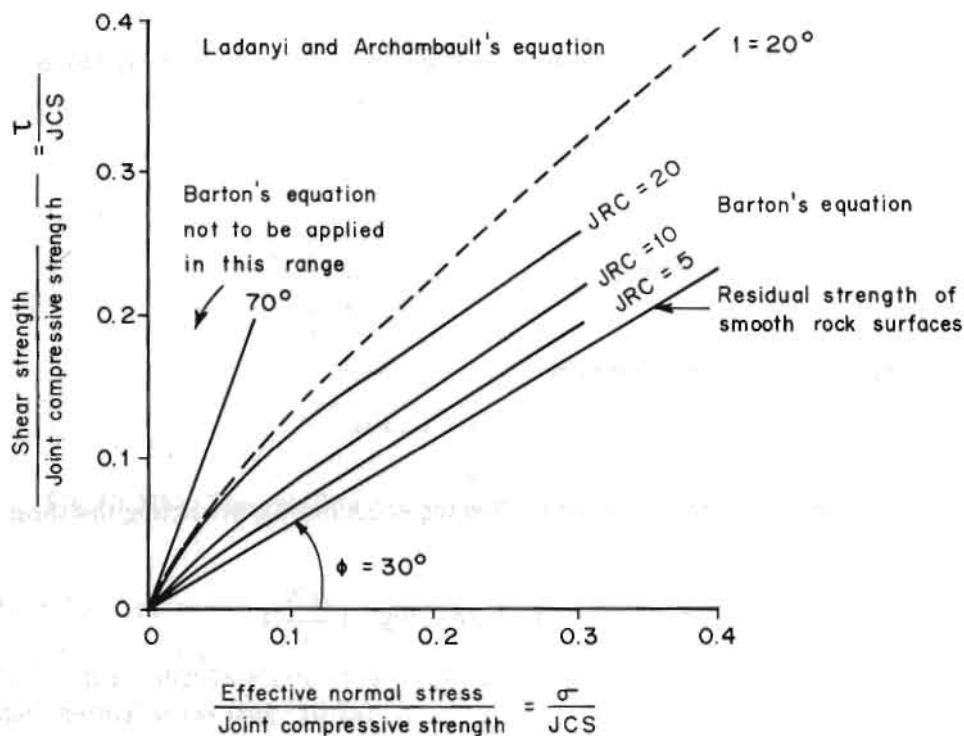


Fig. 10.4 Barton's prediction for the shear strength of rough discontinuities

The uniaxial compressive strength of the joint wall material can be obtained in a simpler manner by point load testing of a lump specimen by the following relationship (Fig. 10.5):

$$\sigma_c = 15 I_L$$

where,

σ_c = uniaxial compressive strength, and
 I_L = point load lump strength index.

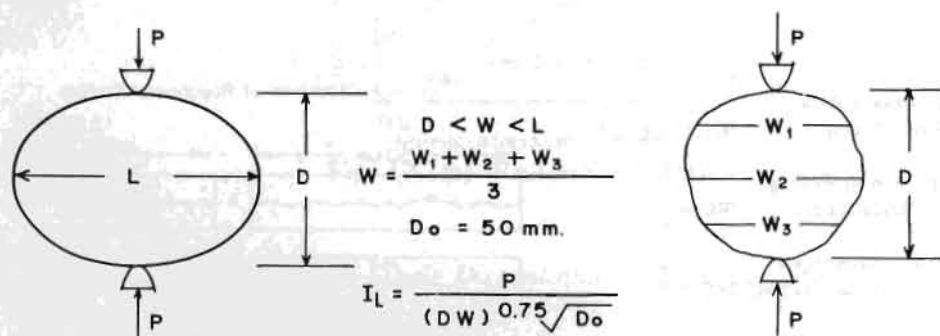


Fig. 10.5 Point load test on rock lumps (International Society for Rock Mechanics [ISRM])

Note that Joint Compressive Strength (JCS) is the compressive strength of the rock material adjacent to the joint surface and may be lower than σ_c as a result of weathering of the surface.

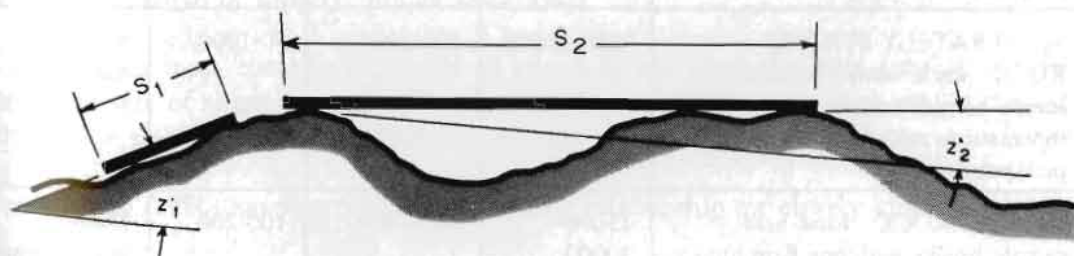
Table 10.1 gives the approximate basic friction angle for different rocks. Table 10.2 gives the approximate values of uniaxial compressive strength for cohesive soils and rocks. Surface roughness i can be measured as shown in Figure 10.6.

Table 10.1 Approximate values for the basic friction angle for different rocks

Rock	Degrees
Amphibolite	32
Basalt	31-38
Conglomerate	35
Chalk	30
Dolomite	27-31
Gneiss (schistose)	23-29
Granite (fine grain)	29-35
Granite (coarse grain)	31-35
Limestone	33-40
Porphyry	31
Sandstone	25-35
Shale	27
Siltstone	27-31
Slate	25-30

Source: Barton and Chaubey 1977

Lower value is generally given by tests on wet rock surfaces



Source: adapted from Rock Slopes, U.S. Dept. of Transportation, 1981

Fig. 10.6

Measurement of surface roughness with different lengths

Short base length give high values for the effective roughness angle, while long bases give smaller angles.

Table 10.2 Approximate classification of cohesive soil and rock

No.	Description	Uniaxial <i>lb/in²</i>	Compressive strength		Examples
			<i>kg/cm²</i>	<i>MPa</i>	
S1	VERY SOFT SOIL - easily moulded with fingers, shows distinct heel marks	< 5	< 0.4	< 0.04	
S2	SOFT SOIL - moulds with strong pressure from fingers, shows faint heel marks	5-10	0.4-0.8	0.04-0.08	
S3	FIRM SOIL - very difficult to mould with fingers, indented with finger nail, difficult to cut with hand spade	10-20	0.8-1.5	0.08-0.15	
S4	STIFF SOIL - cannot be moulded with fingers, cannot be cut with hand spade, requires hand picking for excavation	20-80	1.5-6.0	0.15-0.60	
S5	VERY STIFF SOIL - very tough, difficult to move with hand pick, requires a pneumatic spade for excavation	80-150	6-10	0.6-1.0	
R1	VERY WEAK ROCK - crumbles under sharp blows with geological pick point, can be cut with pocket knife	150-3500	10-250	1-25	Chalk, rocksalt
R2	MODERATELY WEAK ROCK - shallow cuts or scraping with pocket knife with difficulty, pick point indents deeply with firm blow	3500-7500	250-500	25-50	Coal, schist, siltstone
R3	MODERATELY STRONG ROCK - knife cannot be used to scrape or peel surface, shallow indentations under firm blow from pick point	7500-15000	500-1000	50-1000	Sandstone, slate, shale
R4	STRONG ROCK - hand-held sample breaks with one firm blow from the hammer head of a geological pick	15000-30000	1000-2000	100-200	Marble, granite, gneiss
R5	VERY STRONG ROCK - requires many blows from geological pick to break intact sample	> 30000	> 2000	> 200	Quartzite, dolerite, gabbro, basalt

10.1.4 Shear Strength of Filled Discontinuities

Often there are no rock-to-rock contacts in discontinuities. They can be filled with detrital material or gouge from previous shear movements, or material deposited by the movement of water through the rock mass.

Shear strength decreases with the increase in thickness of infilling; once the thickness exceeds the amplitude of surface projections, the shear strength of the joint is controlled only by the strength of the filling material (Fig. 10.7).

Filled joints influence the permeability of the rock mass. The permeability of clay gouge and similar joint filling material may be three or four orders of magnitude lower than that of the surrounding rock mass, and this can give rise to the damming of groundwater into compartments within the rock mass. The building of water pressure and also the very low shear strength of filling materials drastically weakens the stability of slopes. Table 10.3. gives shear strength of filled discontinuities from tests carried out by various persons.

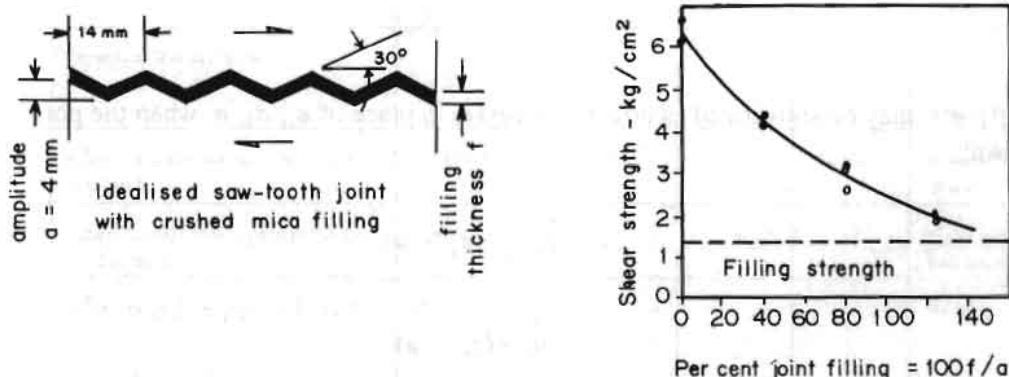


Fig. 10.7 Influence of joint filling thickness on the shear strength of an idealised saw-tooth joint

10.1.5 Shear Strength of Closely Jointed Rock Mass

When a hard rock mass contains a number of joint sets and when the joint spacing is very close, in relation to the size of slope being considered, the behaviour of the rock mass may differ significantly from that of the single discontinuity discussed earlier.

Hoek and Brown (1980) have proposed the following relationship for closely jointed rock masses:

$$\tau = A \sigma_c (\sigma/\sigma_c - T)^b$$

$$T = \frac{1}{2} (m - \sqrt{m^2 + 4s})$$

where,

A,B = constants defining the shape of the Mohr Failure Envelope,

or,

$$\sigma_1 = \sigma_3 + \sqrt{m \sigma_c \sigma_3 + s \sigma_c^2}$$

where,

σ_1	=	axial failure stress,
σ_3	=	confining pressure,
σ_c	=	uniaxial compressive strength of the intact rock pieces, and
m and s	=	dimensionless constants which depend upon the shape and degree of interlocking of the individual pieces of rock within the mass.

σ_1' , σ_3' , σ' may be substituted as effective stresses in place of σ_1 , σ_3 , σ when the pore-water pressure is known:

$$\sigma_1' = (\sigma_1 - u)$$

$$\sigma_3' = (\sigma_3 - u)$$

$$\sigma' = (\sigma - u).$$

Table 10.4 may be used to estimate the values of m, s, A, B, and T approximately when *in situ* test data are not available.

10.2 DETERMINATION OF SHEAR STRENGTH

Shear strength of rock masses may be determined for minor structures without major tests by the use of the tables and equations in the preceding sections. Major structures require large-scale field tests and laboratory tests to accurately determine the shear strength.

An alternative method to determine shear strength is to back-analyze existing slope failure, to determine the shear strength parameters that must have been mobilized in the full-scale rock mass at the time of failure. It may be noted that back analysis cannot determine both c and ϕ . It is, therefore, necessary to either determine one of these, usually ϕ , from direct shear tests or run back analyses for several failures in the same material.

Table 10.3 Shear strength of filled discontinuities

Rock	Description	Peak strength		Residual strength		Tested by
		$c' \text{ kg/cm}^2$	ϕ'	$c' \text{ kg/cm}^2$	ϕ'	
Basalt	Clayey basaltic breccia, wide variation from clay to basalt content	2.4	42			Ruiz, Camargo, Midea, and Nieble
Bentonite	Bentonite seam in chalk Thin layers Triaxial tests	0.15 0.9-1.2 0.6-1.0	7.5 12-17 9-13			Link Sinclair and Brooker
Bentonitic shale	Triaxial tests Direct shear tests	0-2.7	8.5-29	0.3	8.5	Sinclair and Brooker
Clays	Over-consolidated slips, joints, and minor shears	0-1.8	12-18.5	0-0.03	10.5-16	Skempton and Petley
Clay shale	Triaxial tests	0.6	32			Sinclair and Brooker
Clay shale	Stratification surfaces			0	19-25	Leussink and Muller-Kirchenbauer
Coal measure rocks	Clay mylonite seams, 1.0 to 2.5 cm thick	0.11-0.13	16	0	11-11.5	Stimpson and Walton
Dolomite	Altered shale bed, approximately 15 cm thick	0.41	14.5	0.22	17	Pigot and Mackenzie
Diorite, granodiorite and porphyry	Clay gouge (2% clay, PI = 17%)	0	26.5			Brawner
Granite	Clay-filled faults Weakened with sandy-loam fault filling Tectonic shear zone, schistose and broken granites, disintegrated rock and gouge	0-1.0 0.5 2.42	24-45 40 42			Rocha Nose Evdokimov and Sapegin
Greywacke	1-2 mm clay in bedding planes			0	21	Drozdz
Limestone	6 mm clay layer 1-2 cm clay fillings < 1 mm clay fillings	 1.0 0.5-2.0	 13-14 17-21	0	13	Krsmanovic et al. Krsmanovic & Popovic
Limestone, marl and lignites	Interbedded lignite layers Lignite/marl contact	0.8 1.0	38 10			Salas and Uriel
Limestone	Marlaceous joints, 2 cm thick	0	25	0	15-24	Bernaix
Lignite	Layer between lignite and underlying clay	0.14-0.3	15-17.5			Schultze
Montmorillonite clay	8 cm seams of bentonite (montmorillonite) clay in chalk	3.6 0.16-0.27	14 7.5-11.5	0.8	11	Eurenus Underwood
Schists, quartzites, and siliceous schists	10-15 cm thick clay filling Stratification with thin clay Stratification with thick clay	0.3-0.8 6.1-7.4 3.8	32 41 31			Serafim and Guerreiro
Slates	Finely laminated and altered	0.5	33			Coates, McRorie and Stubbins
Quartz/kaolin/pyrolusite	Remoulded triaxial tests	0.42-0.9	36-38			

Care must be taken in applying the results obtained from back analysis of a particular slope to the design of a slope of different dimensions in which the normal stress levels may be different. This is because many rough discontinuity surfaces or shear zones in a closely jointed rock mass exhibit strongly non-linear Mohr envelopes.

Figure 10.8 presents the relationship between the friction angles and cohesive strengths mobilized at failure from the results of back analysis of the slope failures. This will be useful as a starting point for stability analysis or as a check on the reasonableness of assumed shear strength data.

10.3 ROCK MASS CLASSIFICATION

Rock mass classification systems have been developed in order to relate the performance of excavations made in different rock masses. These empirical systems quantify those factors that affect the performance of rock and they are then added to produce a rating number. The relationship between this rating number and the strength of rock mass is given in Tables 10.4 and 10.5 (see Section D). Unlike in soils, the friction angle of rock mass tends to increase with cohesion.

Almost all these classification systems are applicable to tunnels and not to slopes. Bieniawski's Rock Mass Rating (RMR)(1979) and Romana's Slope Mass Rating (SMR)(1988) classification systems are perhaps the ones most applicable to slopes.

Rock Quality Designation (RQD) is the ratio of the sum of lengths of cores longer than 10 cm and the total length of the drill-run. When borehole core is unavailable, RQD can be estimated from the number of joints per unit volume, in which the number of joints per metre for each joint set are added.

A simple relationship can be used to convert this number to RQD for the case of clay free rock masses:

$$RQD = 115 - 3.3 J_v \text{ (approx.)}$$

where,

$$\begin{aligned} J_v &= \text{total number of joints per m}^3 \text{ (volumetric joint count), and} \\ RQD &= 100 \text{ for } J_v < 4.5. \end{aligned}$$

Table 10.5 presents the Council for Scientific and Industrial Research in South Africa (CSIR), Bieniawski (1979), or Rock Mass Rating (RMR) System. Table 10.6 (a,b, and c) extends it for slopes and gives slope mass ratings.

Table 10.4 Approximate relationship between rock mass quality and empirical constants

Empirical failure criterion	CARBONATE ROCKS WITH WELL-DEVELOPED CRYSTAL CLEAVAGE	LITHIFIED ARGILLACEOUS ROCKS	ARENACEOUS ROCKS WITH STRONG CRYSTALS AND POORLY DEVELOPED CRYSTAL CLEAVAGE	FINE-GRAINED POLYMINERAL, IGNEOUS AND METAMORPHIC CRYSTALLINE ROCKS	COARSE-GRAINED POLYMINERAL, IGNEOUS AND METAMORPHIC CRYSTALLINE ROCKS
$\sigma_1 = \sigma_3 + \sqrt{m\sigma_3\sigma_3 + \sigma_3^2}$ $T = A\sigma_3 \left(\frac{\sigma_1}{\sigma_3} - T \right) B$ <p>Where $T = \frac{1}{2} (m - \sqrt{m^2 + 4})$</p>	dolomite, limestone, and marble	sludstone, siltstone, shale, and slate (normal to cleavage)		andesite, dolerite, diabase, and rhyolite	amphibolite, gabbro, gneiss, granite, norite, and quartz-diorite
INTACT ROCK SAMPLES <i>Laboratory size specimens free from joints</i> CSIR rating 100 NGI rating 500	$m = 7.0$ $s = 1.0$ $A = 0.816$ $B = 0.658$ $T = -0.140$	$m = 10.0$ $s = 1.0$ $A = 0.918$ $B = 0.677$ $T = -0.099$	$m = 15.0$ $s = 1.0$ $A = 1.044$ $B = 0.692$ $T = -0.067$	$m = 17.0$ $s = 1.0$ $A = 1.086$ $B = 0.696$ $T = -0.059$	$m = 25.0$ $s = 1.0$ $A = 1.720$ $B = 0.705$ $T = -0.040$
VERY GOOD QUALITY ROCK MASS <i>Tightly interlocking undisturbed rock with unweathered joints at $\pm 3m$</i> CSIR rating 85 NGI rating 100	$m = 3.5$ $s = 0.1$ $A = 0.651$ $B = 0.679$ $T = -0.28$	$m = 5.0$ $s = 0.1$ $A = 0.759$ $B = 0.692$ $T = -0.020$	$m = 7.5$ $s = 0.1$ $A = 0.848$ $B = 0.702$ $T = -0.013$	$m = 8.5$ $s = 0.1$ $A = 0.883$ $B = 0.705$ $T = -0.012$	$m = 12.5$ $s = 0.1$ $A = 0.998$ $B = 0.712$ $T = -0.008$
GOOD QUALITY ROCK MASS <i>Fresh to slightly weathered rock, slightly disturbed with joints at 1 to 3m</i> CSIR rating 65 NGI rating 10	$m = 0.7$ $s = 0.004$ $A = 0.369$ $B = 0.669$ $T = -0.006$	$m = 1.0$ $s = 0.004$ $A = 0.427$ $B = 0.683$ $T = -0.004$	$m = 1.5$ $s = 0.004$ $A = 0.501$ $B = 0.695$ $T = -0.003$	$m = 1.7$ $s = 0.004$ $A = 0.525$ $B = 0.698$ $T = -0.002$	$m = 2.5$ $s = 0.004$ $A = 0.603$ $B = 0.707$ $T = -0.002$
FAIR QUALITY ROCK MASS <i>Several sets of moderately weathered joints spaced at 0.3 to 1m</i> CSIR rating 44 NGI rating 1.0	$m = 0.14$ $s = 0.0001$ $A = 0.198$ $B = 0.662$ $T = -0.0007$	$m = 0.20$ $s = 0.0001$ $A = 0.234$ $B = 0.675$ $T = -0.0005$	$m = 0.30$ $s = 0.0001$ $A = 0.280$ $B = 0.688$ $T = -0.0003$	$m = 0.34$ $s = 0.0001$ $A = 0.295$ $B = 0.691$ $T = -0.0003$	$m = 0.50$ $s = 0.0001$ $A = 0.346$ $B = 0.700$ $T = -0.0002$
POOR QUALITY ROCK MASS <i>Numerous weathered joints at 30 to 500 mm with some gouge - clean waste rock.</i> CSIR rating 23 NGI rating 0.1	$m = 0.04$ $s = 0.00001$ $A = 0.115$ $B = 0.646$ $T = -0.00002$	$m = 0.05$ $s = 0.00001$ $A = 0.129$ $B = 0.655$ $T = -0.00002$	$m = 0.08$ $s = 0.00001$ $A = 0.162$ $B = 0.672$ $T = -0.00001$	$m = 0.09$ $s = 0.00001$ $A = 0.172$ $B = 0.676$ $T = -0.00001$	$m = 0.13$ $s = 0.00001$ $A = 0.203$ $B = 0.686$ $T = -0.00001$
VERY POOR QUALITY ROCK MASS <i>Numerous heavily weathered joints spaced < 50 mm with gouge - waste with fines.</i> CSIR rating 3 NGI rating 0.01	$m = 0.007$ $s = 0$ $A = 0.042$ $B = 0.534$ $T = 0$	$m = 0.010$ $s = 0$ $A = 0.050$ $B = 0.539$ $T = 0$	$m = 0.015$ $s = 0$ $A = 0.061$ $B = 0.546$ $T = 0$	$m = 0.017$ $s = 0$ $A = 0.065$ $B = 0.548$ $T = 0$	$m = 0.025$ $s = 0$ $A = 0.078$ $B = 0.556$ $T = 0$

Note: The CSIR method of classifying rock masses is described in Section 10.3

CSIR = Council for Scientific and Industrial Research in South Africa
 NGI = Norwegian Geotechnical Institute

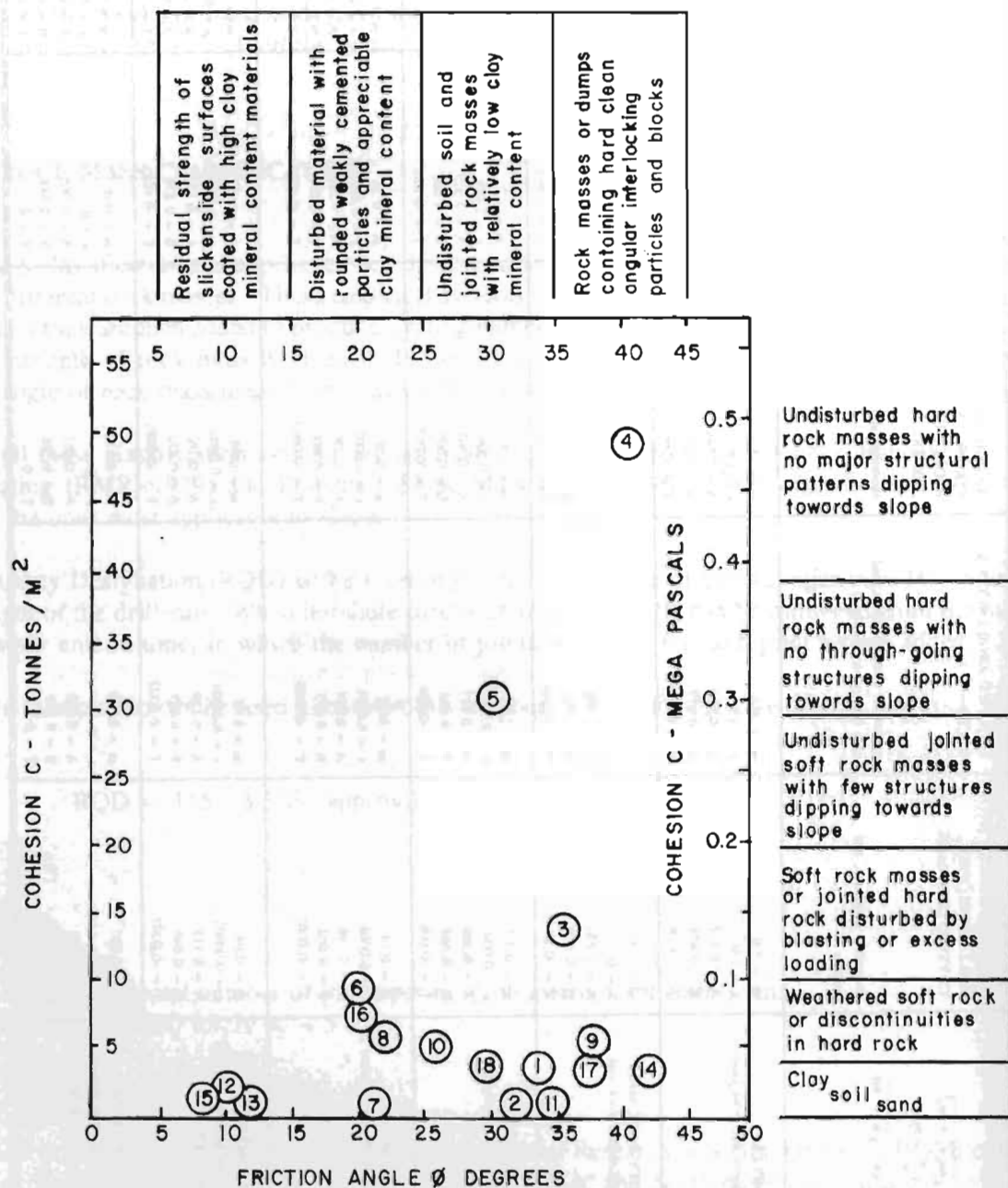


Fig. 10.8 Relationship between the friction angles and cohesive strengths from back analysis of failed slopes

First of all RMR (basic) is estimated by adding ratings for the first five parameters from Part A of Table 10.5. Then SMR is obtained from RMR (basic) by adding a negative frictional adjustment factor as follows:

$$\text{SMR} = \text{RMR (basic)} + (F1.F2.F3) + F4.$$

The adjustment ratings for factors F1,F2,F3, and F4 are given in Tables 10.6a and b. Table 10.6c gives a description of the stability of cut slopes/natural slopes.

It may be mentioned here that wedge failures may also be taken into account by substituting the dip of planes by the dip of the intersection of joint planes in Table 10.6a.

The following remedial measures are recommended as the basis of SMR (Romana 1988):

Ia.	91-100	:	None
Ib.	81-90	:	None. Scaling
IIa.	71-80	:	None. Toe ditch or fence. Spot bolting.
IIb.	61-70	:	Toe ditch or fence. Nets. Spot or systematic bolting.
IIIa.	51-60	:	Toe ditch and/or nets Spot systematic bolting Spot shotcrete
IIIb.	41-50	:	(Toe ditch and/or nets) Systematic bolting. Anchors Systematic shotcrete. Toe wall and/or dental concrete.
IVa.	31-40	:	Anchors. Systematic shotcrete. Toe wall and/or concrete. Re-excavation. Drainage.
IVb.	21-30	:	Systematic reinforced shotcrete Toe wall and/or concrete Re-excavation. Deep drainage.
Va.	11-20	:	Gravity or anchored wall. Re-excavation.

Table 10.5 Geomechanics' classification of jointed rock masses

A. CLASSIFICATION PARAMETERS AND THEIR RATINGS

	PARAMETER		RANGE OF VALUES					
1.	Strength of intact rock material	Pointload strength index	> 8 MPa	4-8 MPa	2-4 MPa	1-2 MPa	For this low range, uniaxial compressive test is preferred	
		Uniaxial compressive strength	> 250 MPa	100-200 MPa	50-100 MPa	25-50 MPa	5-25 MPa	1-5 MPa
	Rating		15	12	7	4	2	1
2.	Drill core quality RQD (%)		90%-100%	75%-90%	50%-75%	25%-50%	< 25%	
	Rating		20	17	13	8	3	
3.	Spacing of joints		> 2 m	0.6-2 m	0.2-0.6 m	60-200 mm	< 60 mm	
	Rating		20	15	10	8	5	
4.	Condition of joints		Very rough surface. Not continuous. No separation. Unweathered.	Slightly rough surfaces. Separation < 1 mm. Slightly weathered.	Slightly rough surfaces. Separation < 1 mm. Highly weathered.	Slickenside surface OR Gouge < 5 mm thick OR separation 1-5 mm. Continuous.	Soft gouge > 5 mm thick OR separation > 5 mm. Continuous.	
	Rating		30	25	20	10	0	
5.	Groundwater	Inflow per 10m tunnel length	None	1-10 l/min	10-25 l/min	25-125 l/min	> 125 l/min	
		Joint water pressure ratio. Major principal stress	OR	OR	OR	OR	OR	
			0	0-0.1	0.1-0.2	0.2-0.5	> 0.5	
			OR	OR	OR	OR	OR	
	General conditions		Dry	Damp	Wet or water under moderate pressure	Dripping or severe water problem	Flowing	
Rating		15	10	7	4	0		

B. RATING ADJUSTMENT FOR JOINT ORIENTATIONS

Strike and dip orientations of joints		Very Favourable	Favourable	Fair	Unfavourable	Very Unfavourable
Ratings	Tunnels	0	-2	-5	-10	-12
	Foundations	0	-2	-7	-15	-25
	Slopes	Use slope mass rating				

Note: RMR is sum of all ratings for parameters 1-6.

C. ROCK MASS CLASSES DETERMINED FROM TOTAL RATINGS

Rock Mass Rating (RMR)	100-81	80-61	60-41	40-21	< 20
Class No.	I	II	III	IV	V
Description	Very good rock	Good rock	Fair rock	Poor rock	Very poor rock

D. MEANING OF ROCK MASS CLASSES

Class No.	I	II	III	IV	V
Average stand-up time	10 years for 5m span	6 months for 4m span	1 week for 3m span	5 hours for 1.5m span	10 min for 0.5m span
Cohesion of rock mass	> 400 kPa	300-400 kPa	200-300 kPa	100-200 kPa	< 100 kPa
Friction angle of the rock mass	> 45°	35-45°	15-25°	15-25°	< 15°
Allowable bearing pressure (t/m ²) (Indian Code)	440-600	280-440	55-145	145-280	40-55

Source: Bieniaswski 1979

Table 10.6a Adjustment rating for joints for slope mass rating

CASE	--	Very Favourable	Favourable	Fair	Unfavourable	Very Unfavourable
P T P/T	$[\alpha_j - \alpha_s]$ $[\alpha_j - \alpha_s - 180^\circ]$ F_1	$> 30^\circ$ 0.15	$30^\circ - 20^\circ$ 0.40	$20^\circ - 10^\circ$ 0.70	$10^\circ - 5^\circ$ 0.85	$< 5^\circ$ 1.00
P P T	β_j F_2 F_2	$< 20^\circ$ 0.15 1	$20^\circ - 30^\circ$ 0.40 1	$30^\circ - 35^\circ$ 0.70 1	$35^\circ - 45^\circ$ 0.85 1	$> 45^\circ$ 1.00 1
P T P/T	$\beta_j - \beta_s$ $\beta_j + \beta_s$ F_3	$> 10^\circ$ $< 110^\circ$ 0	$10^\circ - 0^\circ$ $110^\circ - 120^\circ$ -6	0° $> 120^\circ$ -25	$0^\circ - (-10^\circ)$ -- -50	$< -10^\circ$ -- -60

P Plane failure

T Toppling failure

 α_s Slope dip direction β_s Slope dip α_j Joint dip direction β_j Joint dip

Table 10.6b Adjustment rating for methods of excavation of slopes for SMR

Method	Natural slope	Presplitting	Smooth blasting	Blasting or Mechanical	Deficient blasting
F_4	+ 15	+ 10	+ 8	0	-8

Table 10.6c Tentative description of SMR classes

Class No	V	IV	III	II	I
SMR	0-20	21-40	41-60	61-80	81-100
Description	Very bad	Bad	Normal	Good	Very good
Stability	Completely Unstable	Unstable	Partially stable	Stable	Completely stable
Failures	Big planar or soil-like	Planar or Big wedges	Some joints or Many wedges	Some blocks	None
Support	Reexcavation	Important/ Corrective	Systematic	Occasional	None
Probability of failure	0.9	0.6	0.4	0.2	0

Source: Romana 1988

GEOPHYSICS

11.1 INTRODUCTION

This Chapter is intended to be a guide to the applications of seismic refraction and resistivity on engineering sites. Many civil engineers and geologists have some acquaintance with these basic geophysical tools, but few apply them frequently. The primary purpose of this Chapter is to provide the reader with a working knowledge of the methods and a basis to judge the applicability of these methods and the results to his particular exploration problem. In common with other indirect methods of sub-surface exploration, there are no rigid and inflexible approaches to making sense of the data nor are there any handbooks that infallibly lead the engineer, geologist, or geophysicist to the correct answer. The general case will require thought and care, ambiguities and uncertainties are not uncommon. Some foreknowledge of the site conditions and an understanding of what is geologically plausible will always assist in resolving the raw data into meaningful information.

Two methods are based on the measurement of different physical properties of the sub-surface material, i.e., the **resistivity method** and the **seismic refraction method**. The resistivity method shows up variations in the resistivity of each material and this is largely dependent upon the amount of salinity in the water contained in the material. This method is capable of detecting water tables, of distinguishing between porous and non-porous materials, or of distinguishing fresh from salty water. The seismic refraction method displays the variations in **seismic velocity** of earth materials, and these are largely dependent upon hardness and degree of consolidation. With this method it is possible to distinguish between rock and soil, between consolidated and unconsolidated materials, between compacted soils and loose, and between fresh rock and weathered rock.

For example, both dry sand and bedrock show high resistivity but the seismic velocity of bedrock is usually considerably greater than that of sand. A resistivity survey could therefore be used to outline the limits of sand deposit and a few seismic lines could separate sand from bedrock. As another example, badly weathered bedrock may show the same seismic velocity as a gravel lens. In this case, a distinction can be made between them with the help of their differences in resistivity.

Exploratory drilling is almost always done in a site investigation; its value, in terms of the quality of information gathered, will be enhanced if geophysical surveys are carried out first and the results used to guide the drilling operations. To this end, results obtained from shallow investigations are useful because they provide rapidly a picture of the underlayers. Seismic refraction and resistivity methods offer rapid, inexpensive, and accurate methods of sub-surface exploration. Their application to site investigation should be routine rather than the exception. When seismic refraction and resistivity methods are used widely, and particularly when allied with the exploratory drill, it will invariably speed the recovery of sub-surface information and reduce site investigation costs.

Tables and Figures without credit lines, included in this chapter, have been compiled by the author from comparative sources for this Handbook.

11.2 SEISMIC REFRACTION METHOD

11.2.1 Uses of Seismic Refraction

Fundamentally the seismic method relies on the fact that earth materials are commonly sub-horizontally layered and that strength normally increases with depth. The most common applications for seismic engineering surveys are:

- depth of bedrock,
- shape of bedrock surface,
- depth of water table,
- fault location,
- rippability assessment,
- blasting assessment,
- sand and gravel assessment,
- cavity detection, and
- determination of dynamic elastic constants,

11.2.2 Definitions

Elastic Constants

The elastic properties of substances are characterized by elastic moduli that specify the relation between 'stress' and 'strain'. The two moduli of immediate interest for the study of elastic waves are:

$$\begin{array}{lll} K & = & \text{bulk modulus} = \text{incompressibility, and} \\ \mu & = & \text{shear modulus} = \text{rigidity} \end{array}$$

Elastic Waves

In an elastic isotropic medium two kinds of elastic waves propagate:

P. Waves: primary waves, compressional waves, and longitudinal waves. The motion of the medium is in the same direction as the direction of wave propagation (Fig. 11.1). Their velocity is given by

$$V_p = \sqrt{\frac{K + 4/3\mu}{d}}$$

Where,

d is the density of the medium.



Fig. 11.1 P Waves

S. Waves: Secondary waves, shear waves, and transverse waves. The particles of the medium move at right angles to the direction of wave propagation (Fig. 11.2). Their velocity is given by:

$$V_s = \sqrt{\frac{\mu}{d}} .$$

Shear waves do not propagate through liquids and gases. V_p is greater than V_s .

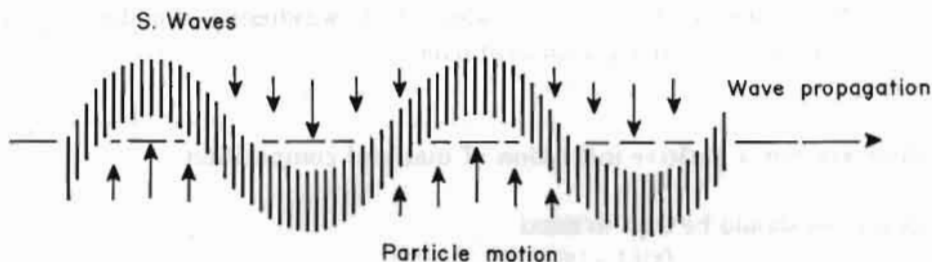


Fig. 11.2 S. waves

Velocities in Rocks

Generally only P waves are of importance as an exploration tool. Typical values for the velocity of P waves in some rocks are given in Table 11.1.

Effect of Porosity and Saturation

The velocities generally increase as porosity decreases. This is expressed by the law:

$$\frac{1}{V_r} = \frac{\phi_p}{V_f} + \frac{[1-\phi_p]}{V_{ma}}$$

where,

V_r	= rock velocity,
V_f	= fluid velocity, and
V_{ma}	= matrix velocity.

The velocities also increase, for a given porosity, as saturation increases. ($V_{air} = 330$ m/s, $V_{water} = 1500$ m/s). Table 11.2 provides velocities of propagation of seismic waves in some sub-surface materials.

Effect of Depth and Age

The velocities increase with depth of burial and geologic ages. Faust (1951), finds that for shale and sand:

$$\begin{aligned}V_r &= 46.5 Z^{1/6} T^{1/6} \text{ m/s,} \\Z &= \text{depth in metres, and} \\T &= \text{age in years.}\end{aligned}$$

Before attempting to estimate the composition from the computed velocities, the seismic analyst should familiarize himself with the general nature of the terrain under study. He should know :

- where the water table is,
- whether the overburden is a product of the weathering of underlying bedrock, and
- whether it is mostly glacial drift over.

Velocities alone are not a positive indication of material composition

Several general rules should be kept in mind

- I - velocity is roughly proportional to the degree of consolidation of rock or soil.
- II - in unconsolidated materials, velocity increases with water content.
- III - weathering of a rock will greatly reduce its velocity.
- IV - a particular rock type will include a range of velocities and these ranges **may overlap for different rock types**.
- V - correlation of velocity with the type of earth material, to a great extent, will depend upon the overall geological characteristics of the area under study.
- VI - velocity measurements are very sensitive to the dip of the interface. If high precision measurement velocities are required, always assume that a dip exists and follow the procedure for dipping discontinuity.

Seismic refraction techniques are generally used for site investigation for civil engineering purposes and reflection is a powerful tool in petroleum exploration.

11.2.3 Data Acquisition

The aim of seismic exploration is to determine the depth and characteristics of the near surface layers. There are two methods of seismic exploration; **reflection** and **refraction**. The two methods basically involve the production of **energy** that is transmitted into the ground. After a time interval this energy, having been **reflected** and **refracted** from one or more sub-surface physical discontinuities, returns to **detectors** spread on the surface of the ground.

Seismic Sources

The standard method of producing seismic waves on land is to explode a dynamic charge. Individual explosions from the energy source are called **shots** and their locations are called **shot points**. A hammer striking a steep plate is generally used for shallow refraction measurements. Seismographs actually

contain special circuitry that allows successive sets of waves from successive impacts to be added together. The purpose of summing is to strengthen weak signals and to increase the signal-to-noise ratio through cancelling random, background seismic noise. This process is called **stacking** because successive waves are stacked or added together.

The Detectors

The sensing devices used are called **geophones**. A geophone is a type of microphone (transducer) that converts seismic vibrations, or motions of the earth, to electric impulses (Fig. 11.3).

Table 11.1 Velocities of propagation of seismic waves in some subsurface materials

Materials	feet/sec.	metre/sec.
TOP SOILS:		
light and dry	600 - 900	200 - 300
moist	1000 - 1300	200 - 420
clayed	1300 - 2000	420 - 640
semi-consolidated sandy clay	1250 - 2150	400 - 700
wet loam	2500	800
Rubble or gravel (dry)	1970 - 2600	650 - 850
Cemented sand	2800 - 3200	900 - 1050
Cemented sandy clay	3800 - 4200	1200 - 1400
Water-saturated sand	4600	1500 -
Glacial till	5600 - 7400	1800 - 2400
Glacial moraine dry	2500 - 5000	800 - 1600
Glacial moraine saturated	5000 - 7000	1600 - 2250
Loose rock talus	1250 - 2500	400 - 800
WEATHERED AND FRACTURED ROCKS		
GRANITE		
- friable and highly decomposed	1540	500
- badly fractured and partly decomposed	2200	700
- softened and partly decomposed	10500	3300
- solid, monolithic	18500	6000
- badly broken and weathered	3000 - 8000	1000 - 2600
- little sign of weathering	10000 - 13000	3200 - 4200
- entirely unweathered	16000 - 20000	5100 - 6400

Geophones used in land surveys are electromagnetic geophones. A coil is placed between the poles of a magnet. The coil acts as an internal element while the magnet moves with the earth. The relative motion of the coil and the magnet produces an electric impulse proportional to the velocity of the motion of the earth.

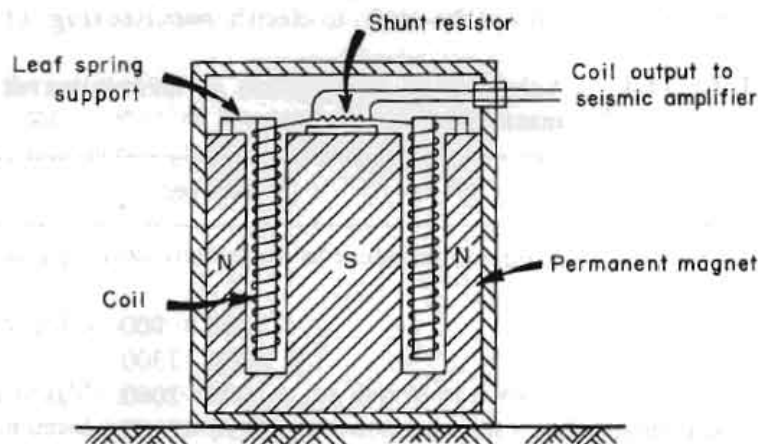


Fig. 11.3 Geophone

In most of the work, the geophones are placed along a straight line. The geophones are connected to the recording equipment by long cables.

Seismic Amplifier and Recorder

The geophone signals are transmitted by this cable to the **seismograph** where they are amplified and recorded by special equipment designed for this purpose. The record of the arriving pulse is called a **seismogram**. In addition to the simultaneous recording of the output signals, the recorder also marks the **zero time** instant of the explosion and a series of timing lines. Determining the time interval between the explosion and the arrival of the energy at the geophones, the raw data are transformed into a **graph** also called **dromochronique** (Figure 11.4). Generally, a large proportion of refraction surveys for engineering purposes are concerned with depths in the order of 10 to 30 metres. It is apparent that arrival times must be picked up with reasonable accuracy. This means that :

- the source energy,
- the amplifier gains, and
- the placement of the geophones,

are all important factors in obtaining the sharp breaks required for accurate timing of the first arrivals.

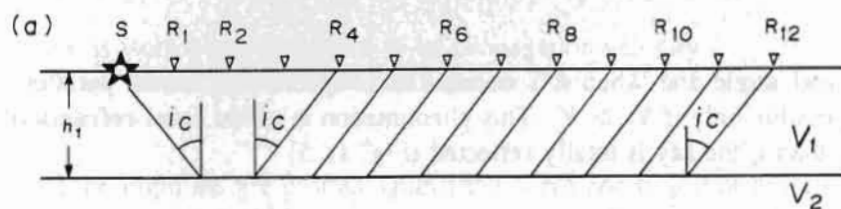
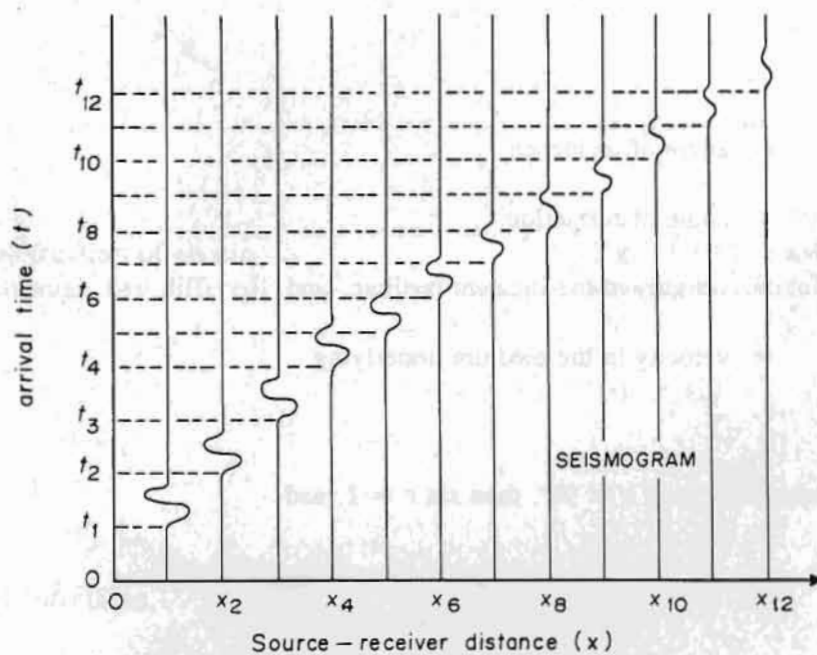
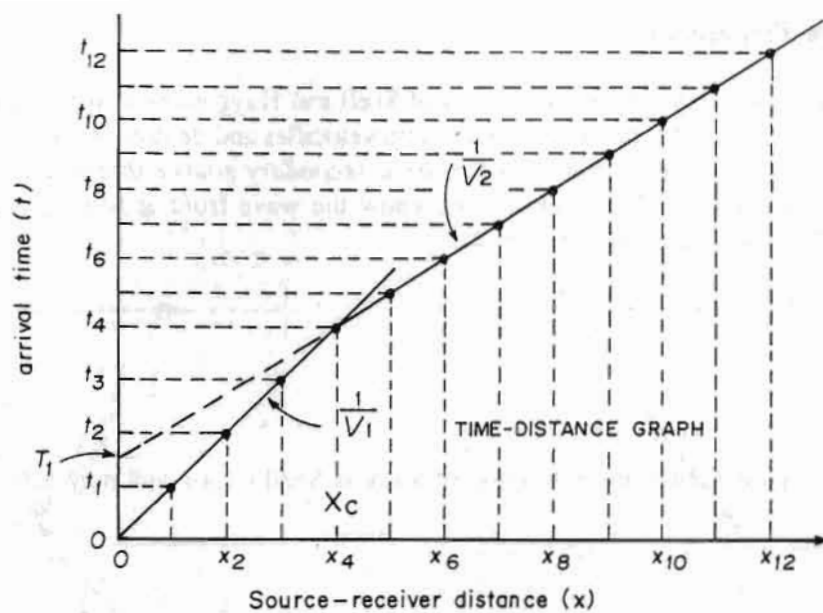


Fig. 11.4 Time-distance graph and seismogram

11.2.4 Seismic Wave Propagation

Light and seismic waves are very similar. The Laws of Snell and Huygens both apply making it possible to mathematically interpret travel times and distances into velocities and depths. Huygen's principle says: *Every point on a wave front may be considered to be a secondary source that emits waves travelling radially outward from the point*". This means if we know the wave front at time t , we can define the position of the wavefront at a later instant $t + \Delta t$.

Snell's Law

The fundamental law that describes the refraction of a ray is Snell's Law and may be expressed by the equation:

$$\frac{\sin i}{\sin r} = \frac{V_1}{V_2}$$

where,

i = angle of incidence,

r = angle of refraction,

V_1 = velocity in the incident medium, and

V_2 = velocity in the medium underlying,

when i increases, r increases, until $r = 90^\circ$, then $\sin r = 1$, and

$$\sin i_c = \frac{V_1}{V_2}$$

i_c is called the **critical angle** and when this occurs the refracted rays travel parallel to the interface. Obviously, this is possible only if $V_2 > V_1$. This phenomenon is called **total refraction**. If the angle of incidence is greater than i_c the ray is totally reflected (Fig. 11.5)

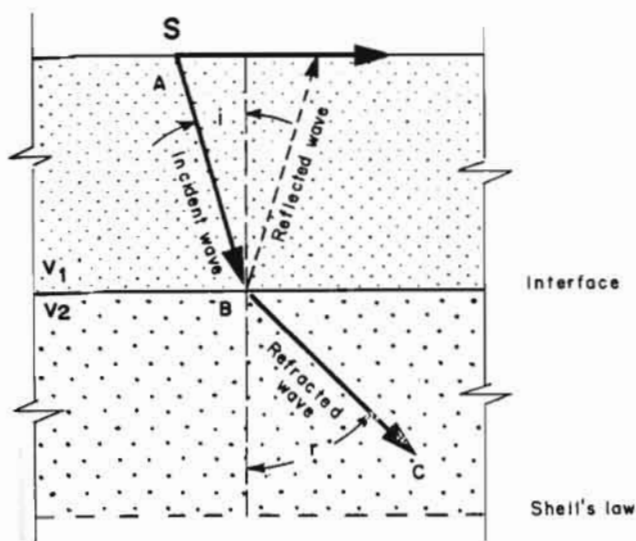


Fig. 11.5 (a) Refraction of elastic wave passing through two different velocity media

$$\frac{\sin i}{V_1} = \frac{\sin r}{V_2}$$

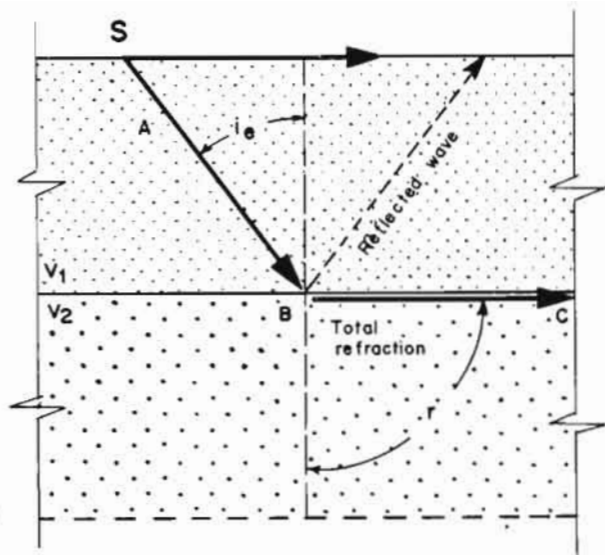


Fig. 11.5(b) Elastic wave striking at critical angle, i_c

$$\sin r = 1$$

$$\sin i_c = \frac{V_1}{V_2}$$

11.2.5 Parallel Interfaces

Let us begin with a simple case : two layers V_1 and V_2 with $V_2 > V_1$ and with plane and parallel boundary. Let us we assume that the sub-surface layers possess certain characteristics :

- each layer is isotropic with regard to its propagation velocity
- ray paths are made up of straight line segments, and
- $V_2 > V_1$.

The arrival times of the impulses are plotted against the corresponding shot to detector distances :

- the first arrival times are those of direct arrivals through the first layer, and
- if we draw a line through these points its slope will be $1/V_1$.

At some distance from the shot, a distance called **critical distance**, it takes less time for the energy to travel down to the top of the second layer, refract along the interface at the higher velocity V_2 , and travel back to the surface, than it does for the energy to travel directly through the top layer. The energy that arrives at the detectors beyond the critical distance will plot along a line with a slope $1/V_2$ (Fig. 11.6).

Critical Distance, X_c

The critical distance is the distance from the shot to the point at which the refracted energy arrives at the same time as the direct one. Beyond this critical distance the refracted wave arrives first to the detector.

Intercept Time

The line through these refracted arrivals, $1/V_2$, will not pass through the origin but will intersect the time axis at a time called the **intercept time**. Because both the intercept time and the critical distance are directly dependent upon the velocities V_1 and V_2 and the thickness of the top layer, they can be used to determine the depth to the top of the second layer.

11.2.6 Analysis of Time-distance Graphs

a. Parallel Interfaces

i) Two Layers

Velocities V_1 and V_2 may be read directly. They are given by the slopes of two straight lines. Numerical values of V_1 and V_2 may be used to identify the material.

Depths:- if we wish to determine the depth to the single discontinuity that separates the top layer from the underlaying material, this may be computed from the critical distance X_b , using the formula:

$$D_1 = h_1 = \frac{X_b}{2} \cdot \sqrt{\frac{V_2 - V_1}{V_2 + V_1}}$$

This may be computed also from the intercept time T_i using the formula :

$$D_1 = h_1 = \frac{T_i}{2} \cdot \frac{V_1 \cdot V_2}{\sqrt{V_2^2 - V_1^2}}$$

ii) Three Layers

The time distance graph will have three straight lines.

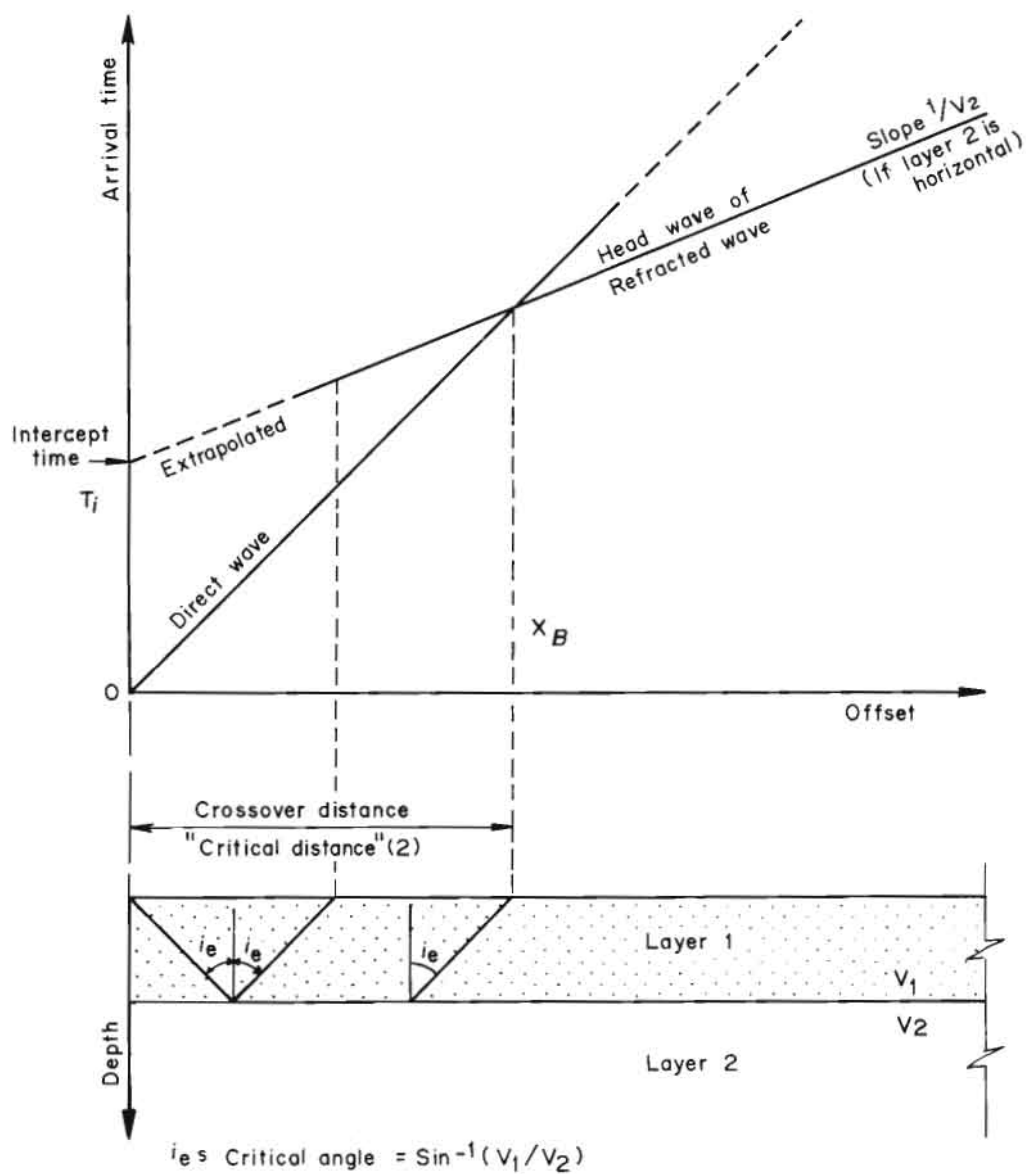


Fig. 11.6 Critical distance and intercept time for parallel interfaces

Velocities:- three straight lines on the seismic graph indicate three types of material. The top layer has a velocity V_1 , the middle V_2 , and the underlayer a velocity represented by slope V_3 .

Depths:- the depth of the bottom of the first layer may be computed by the two expressions:

$$D_1 = h_1 = \frac{Xb_1}{2} \cdot \sqrt{\frac{V_2 - V_1}{V_2 + V_1}} = \frac{T_{i1}}{2} \cdot \frac{V_1 \cdot V_2}{\sqrt{V_2^2 - V_1^2}}$$

The depth of the bottom of the second layer, which has the velocity V_2 , may be computed using:

$$D_2 = h_1 + h_2 = 0.8D_1 + \frac{Xb_2}{2} \cdot \sqrt{\frac{V_3 - V_2}{V_3 + V_2}}$$

or

$$D_2 = h_1 + h_2 = \frac{T_{i2}}{2} \cdot \frac{V_3 \cdot V_2}{\sqrt{V_3^2 - V_2^2}} - 2D_1$$

Non-Parallel Interfaces (Fig. 11.7)

In this case a single traverse, in one direction only, cannot determine whether or not the rock surface is horizontal. An additional traverse must be run in the reverse direction.

By inspection of the time - distance graphs **direct** and **reverse**, we may draw the following conclusions:

$T_{AB} = T_{BA}$ - these times must be equal, if this is not the case, there is something wrong with the data.

X_b down is < than X_b up, a large difference means a large dip.

T_i down is < than T_i up.

V'_2 apparent down is < than V_2 .

V'_2 apparent up is > than V_2 .

For an approximate interpretation we compute:

$$V_2 = 2 \cdot \frac{V'_2 \text{ down} \cdot V'_2 \text{ up}}{V'_2 \text{ down} + V'_2 \text{ up}}$$

V_1 down and V_1 up must be the same:

$$D_{\text{down}} = \frac{X_b \text{ down}}{2} \cdot \frac{\sqrt{V_2 - V_1}}{V_2 + V_1}$$

$$D_{\text{up}} = \frac{X_b \text{ up}}{2} \cdot \frac{\sqrt{V_2 - V_1}}{V_2 + V_1}$$

The approximate interpretation is usually sufficiently accurate, the error is less than 5 to 10 per cent.

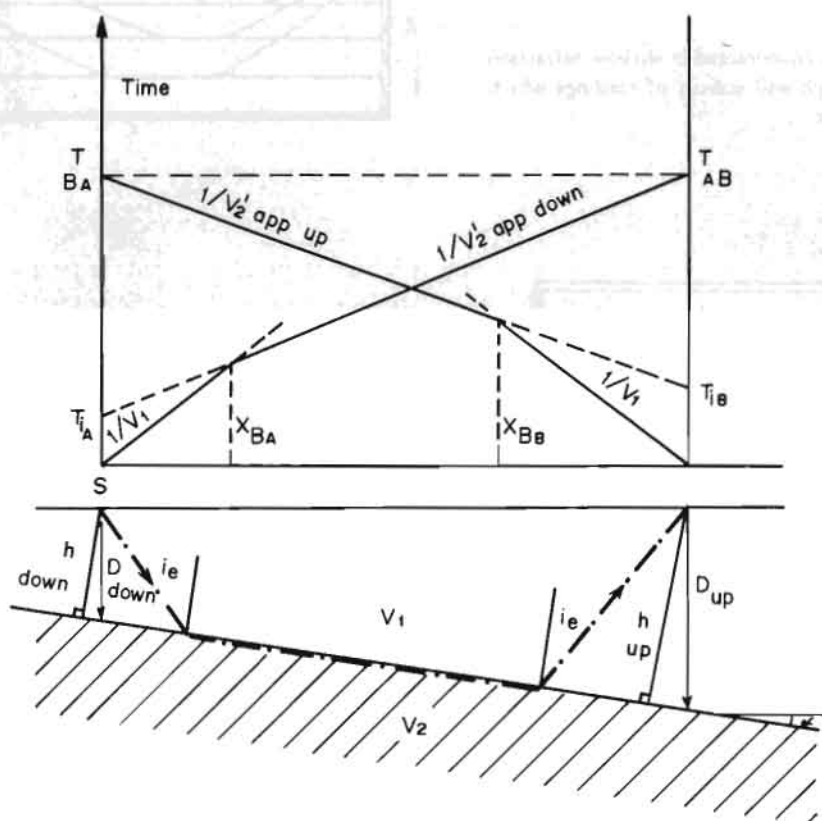


Fig. 11.7 Time-distance for non-parallel interfaces

11.2.7 Examples of Geological Models Inferred from Seismic Refraction (Fig. 11.8)

The topographic and layering conditions, in reality, are generally quite different from the idealized ones considered above.

Fig. 11.8(a) Multi-layered model

This model is very rarely encountered in shallow refraction survey. The seismic graph will consist of readings which lie on many straight lines.

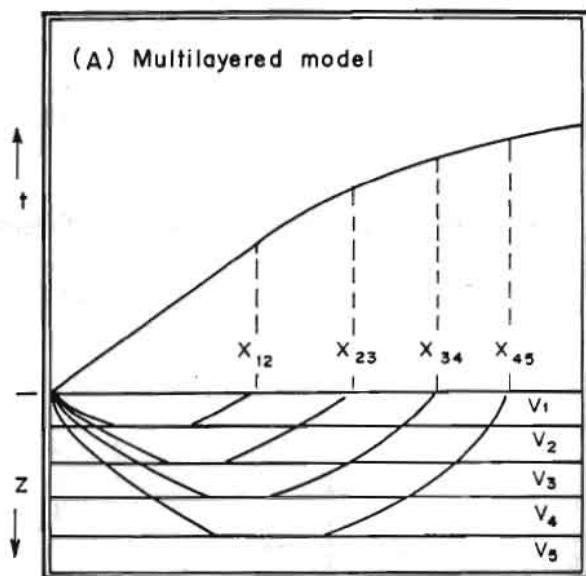


Fig.11.8(b) Continuous velocity increase

Probable interpretation is that the near-surface material is not completely uniform but becomes gradually harder with increasing depth. If the curvature is not great, draw an average straight line through it and treat it as uniform.

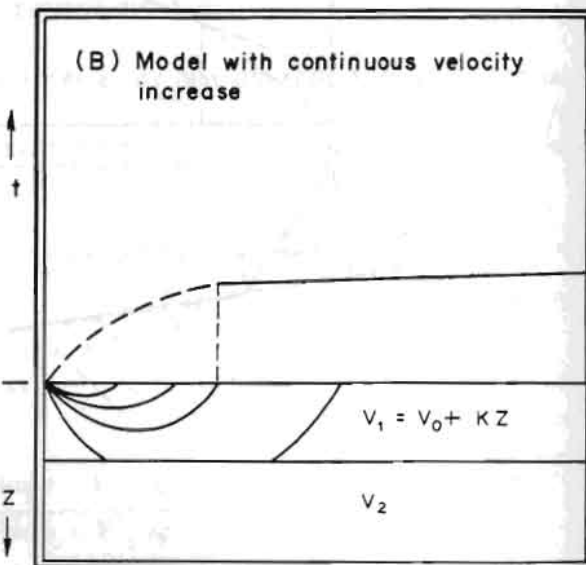


Fig. 11.8(c) Multi dipping layer model

The formulae needed for an exact interpretation are quite complicated because there are many unknown quantities to be determined.

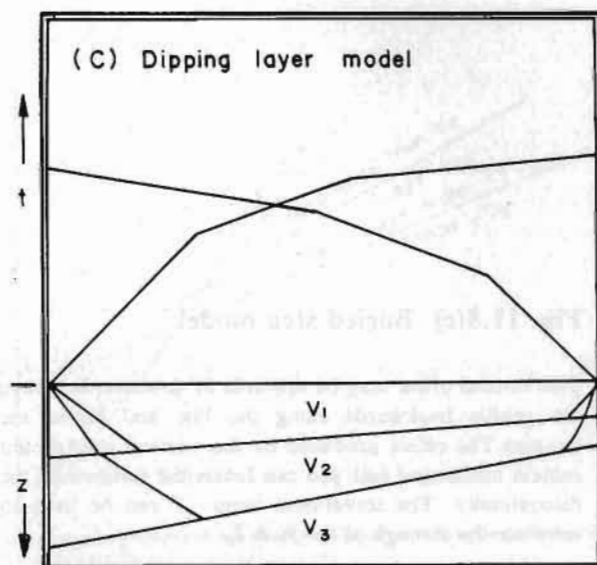


Fig. 11.8(d) Sloping surface model

If the lines run up or down the side of a hill, then the computed depths and dip will be in reference to the ground surface rather than the horizontal. Since the dip of the ground surface is easily measured, the correction can be applied after the interpretation has been completed.

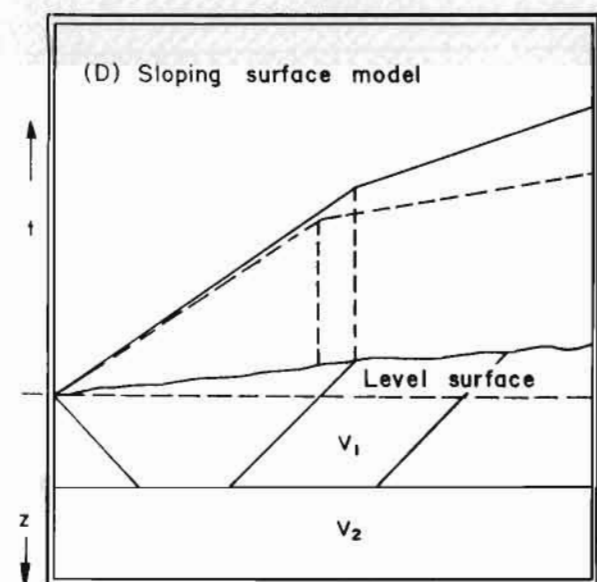


Fig. 11.8(e) Buried step model

The vertical offset may be upwards or downwards. Move the profile backwards along the line and repeat the traverse. The effect produced by the vertical step should remain unchanged and you can locate the position of the discontinuity. The travel-time jump T can be used to calculate the through of the fault Z_f .

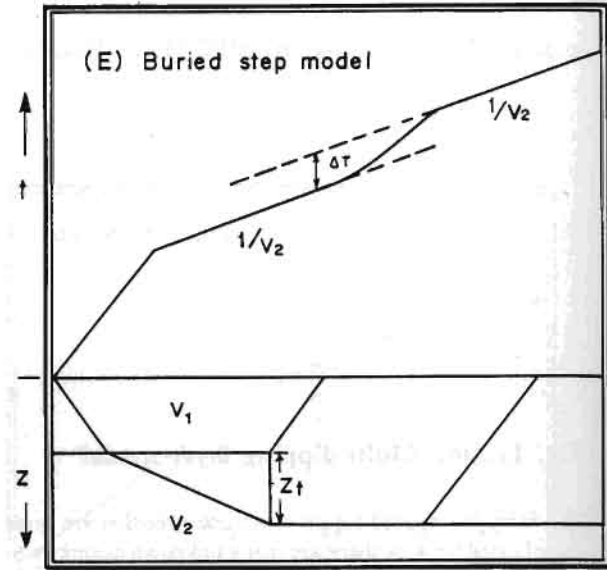


Fig. 11.8(f) Discordant body model

Generally the discordant body has a velocity, V_4 , greater than the others, so the seismic rays that cross it arrive sooner.

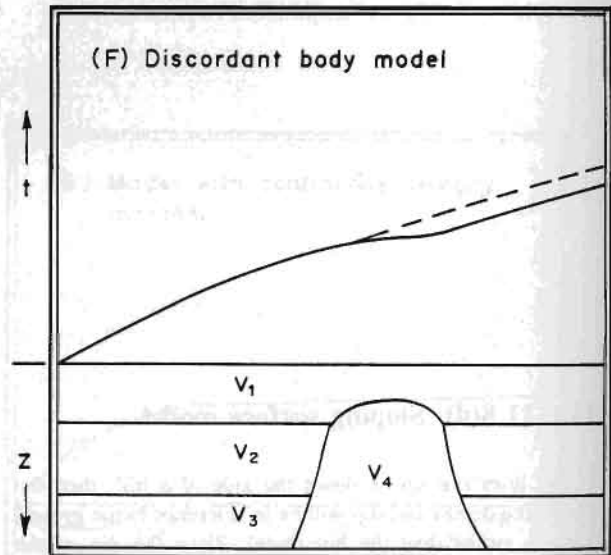
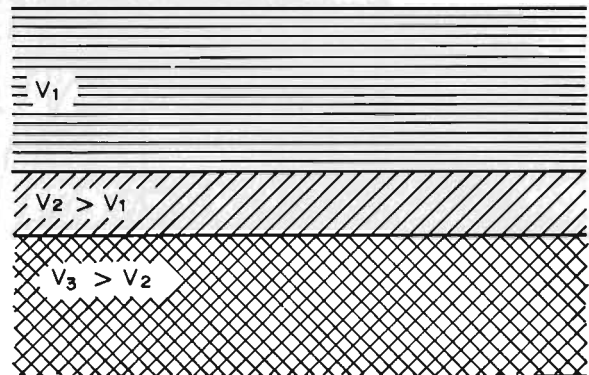
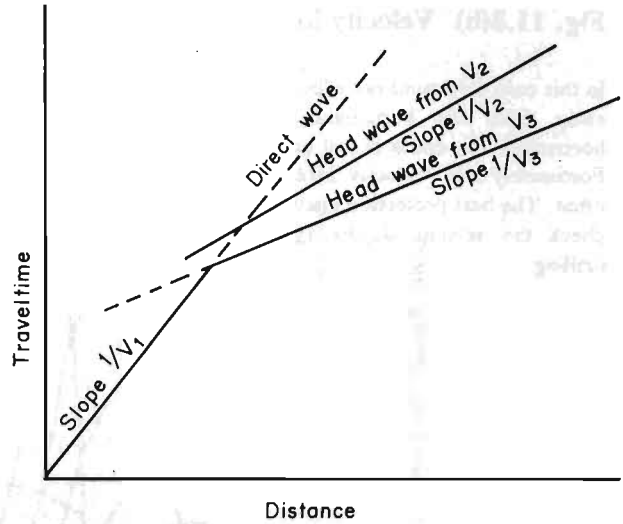


Fig. 11.8(g) Blind zone

The blind zone is one of the major problems in refraction studies. The blind zone refers to the portion of the underground that lies between the surface layer and a layer, V_3 , and is not represented in the graph of the 'first break'.

The existence of this blind zone leads to errors in the interpretation of the measurements. This volume of material is not suggested by the first breaks because of the **relative thickness** of the layers. The speed of the seismic wave in the blind zone is generally intermediate in value between that of the surface layer and the layer V_3 (Fig. 11.9).

In ordinary practice it is often represented by the zone of the water table above a high speed bedrock surface.



V_2 does not show as first arrival

Fig. 11.8(h) Velocity inversion

In this case the sound ray which enters is bent downwards, away from the horizontal, rather than towards the horizontal. The result is that no ray returns to the surface. Fortunately this 'velocity inversion' does not occur very often. The best protection against it, when suspected, is to check the seismic depths against known depths from drilling.

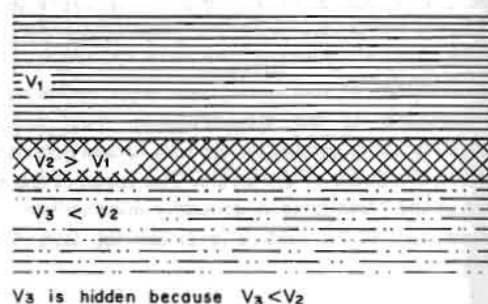
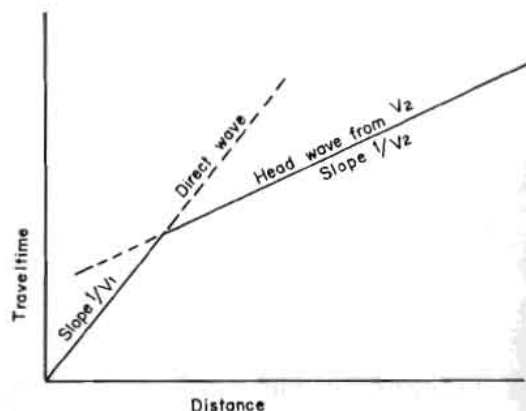
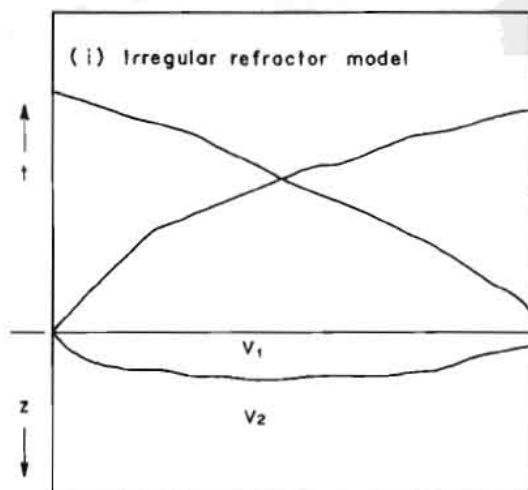


Fig. 11.8(i) Irregular refractor model

The readings will scatter about a straight line. We can interpret the straight line portion, this will give us the average depth along the line. Or we can use a more complicated method for mapping the bedrock surface by finding the depth under each geophone.



In every case, one should keep in mind that for a given graph there is a most probable interpretation but alternative interpretations are usually possible.

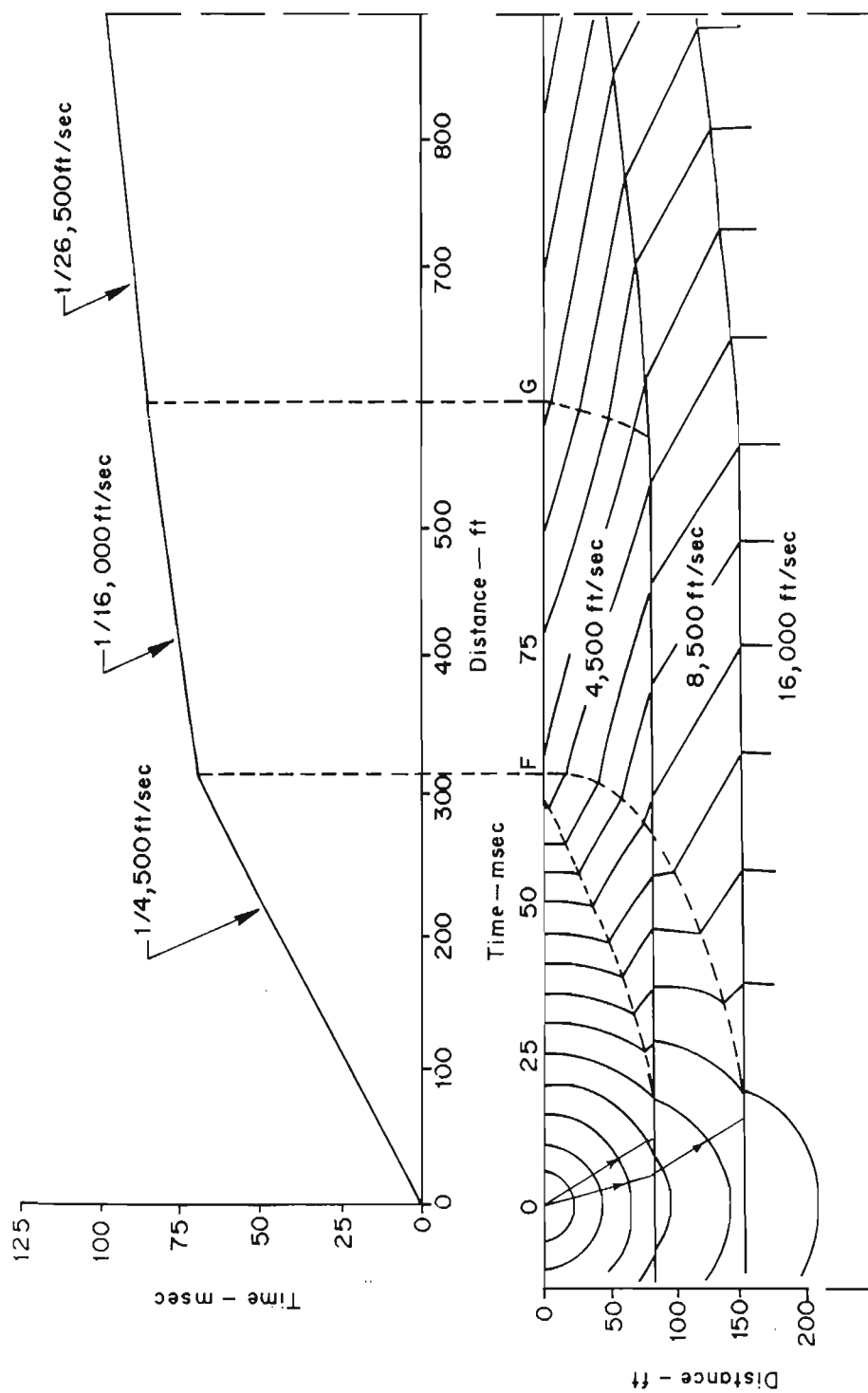


Fig. 11.9 Wave-front diagram and maximum 'undetectable' thickness of "blind zone"

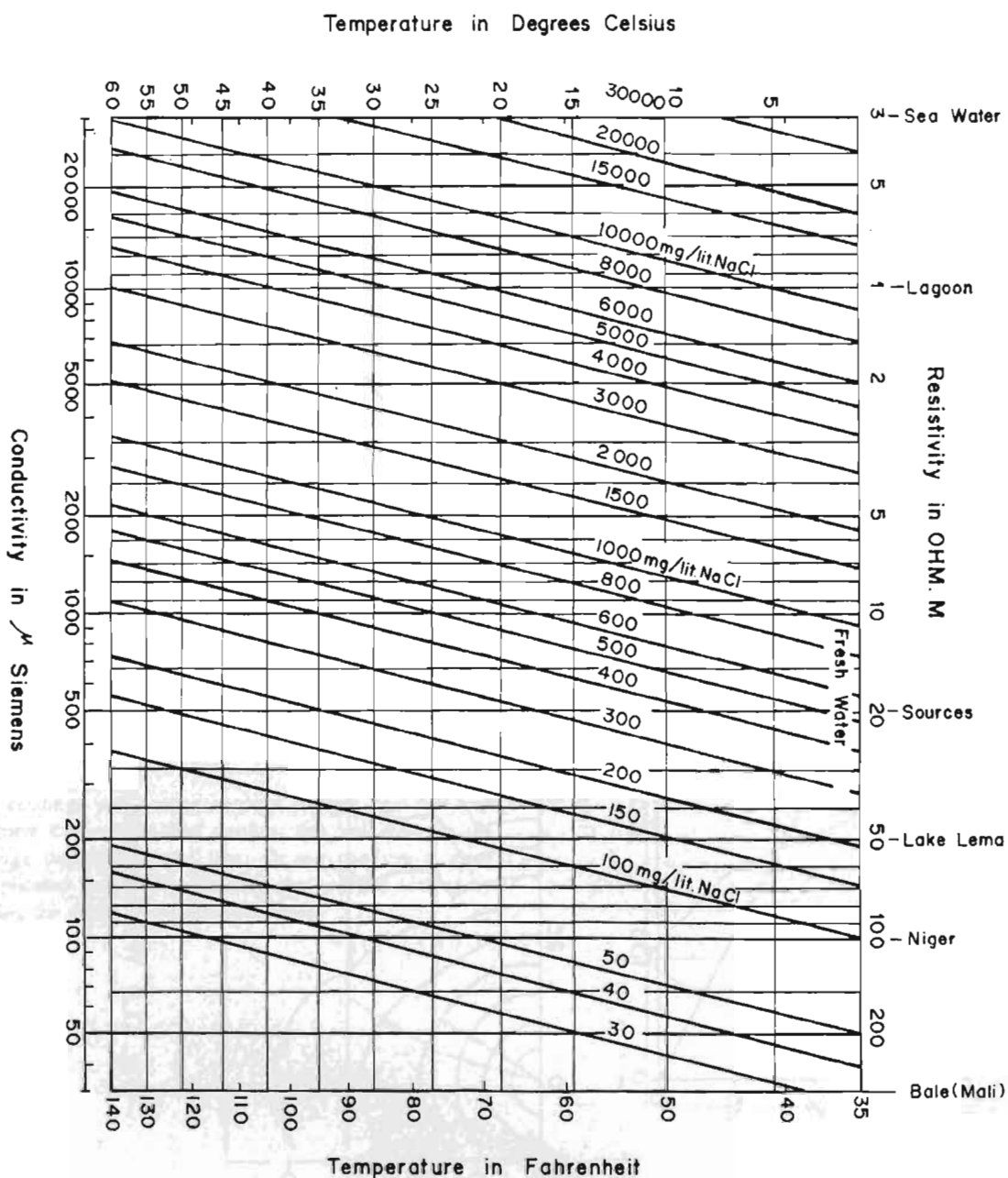


Fig. 11.10 Resistivity vs temperature and salinity

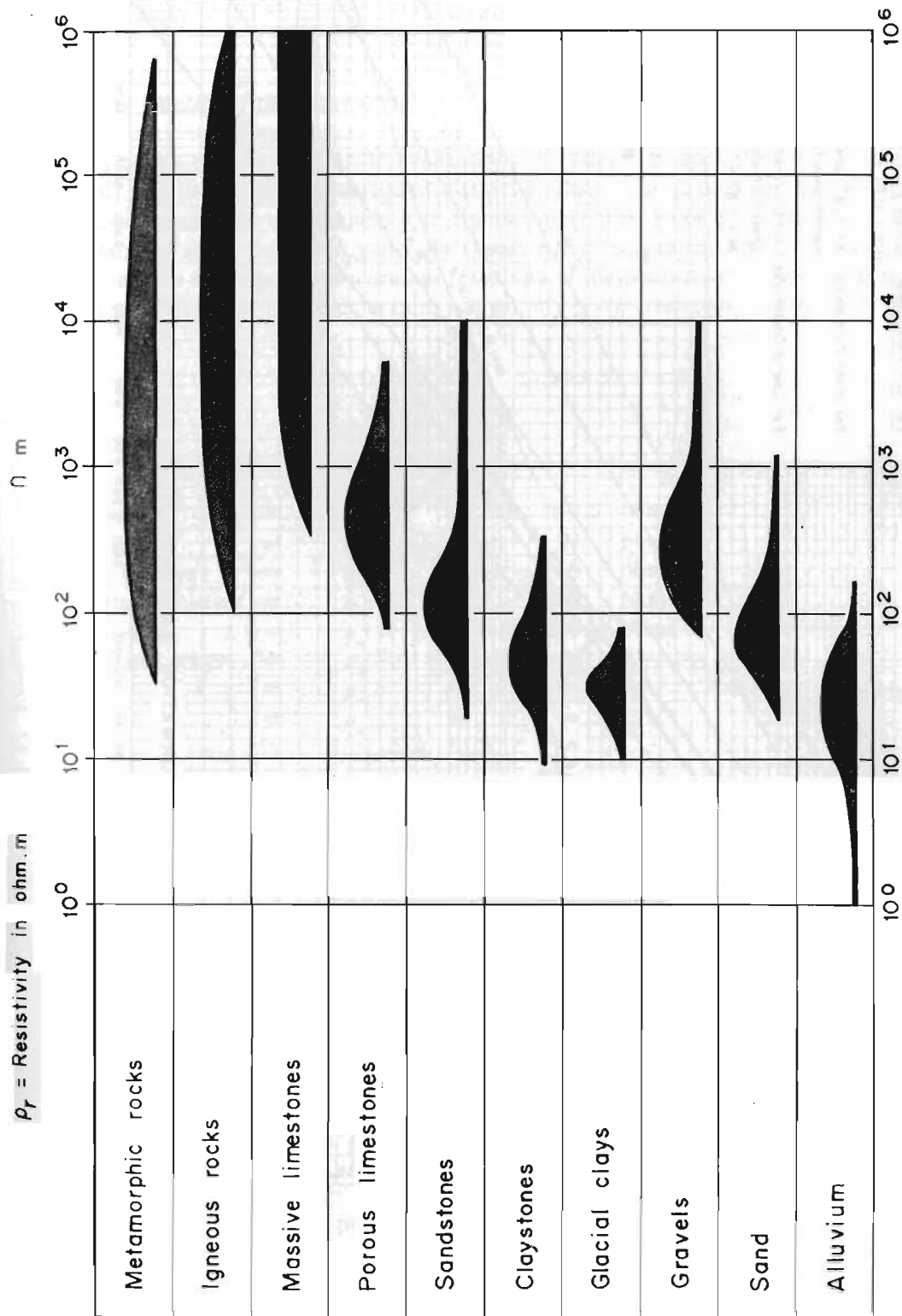


Fig. 11.11 Resistivity for different rock types

FORMATION FACTOR VERSUS POROSITY

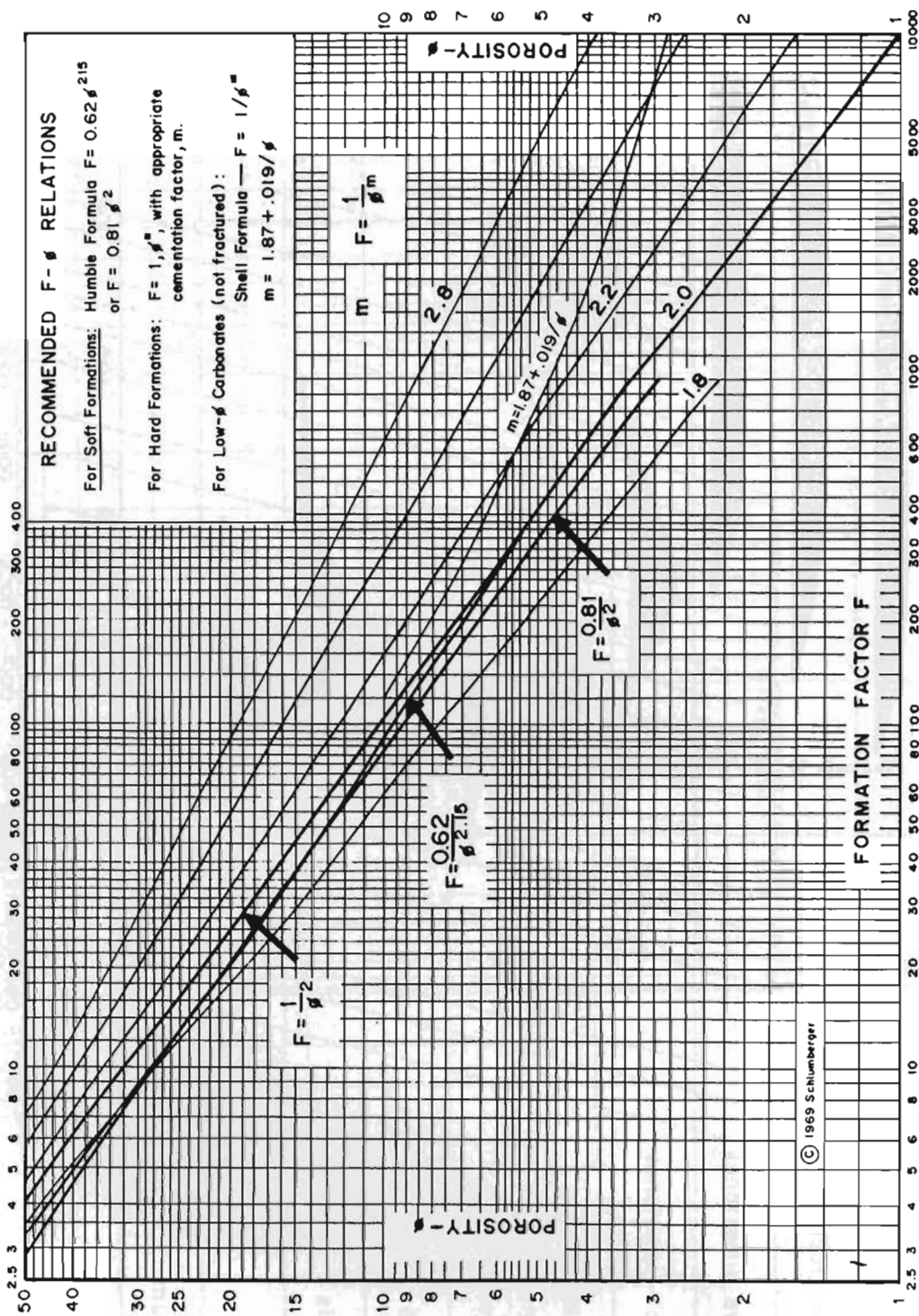


Fig. 11.12 Formation factor versus porosity

11.3 ELECTRICITY RESISTIVITY METHOD

11.3 Resistivity of Rocks

Electrical resistivity is a physical property that characterizes a material almost as definitely as its density. For most rocks the resistivity depends upon the quality and the quantity of the water filling the open spaces in the rock.

11.3.1a *The Quality of the Electrolyte*

The quality of the electrolyte, i.e., its resistivity, ρ_w , depends upon the salinity and the temperature (Fig. 11.10). Salinity is the percentage of dissolved salts, it is expressed in ppm, 1 mg/litre = 1 ppm. Water is considered to be undrinkable if it contains more than 8,000 ppm but it also depends upon the kind of dissolved salts. Salinity is generally expressed in "equivalent NaCl". Temperature also has an influence, because as temperature increases resistivity of the electrolyte decreases. Figure 11.10 (Chart 1) shows the influence of both temperature and salinity on the resistivity of the electrolyte.

Example:

Sea water	=	ρ_w	=	90.3	ohms.m
The Rhone	=	ρ_w	=	80	ohms.m
Lake Geneva	=	ρ_w	=	50	ohms.m
Charnawati River	=	ρ_w	=	200	ohms.m
Rainwater	=	ρ_w	=	30-1000	ohms.m
distillated water	=	ρ_w	=	∞	
oil	=	ρ_w	=	∞	
air	=	ρ_w	=	∞	

11.3.1b *The Quantity of Electrolyte*

Rocks are insulators in the dry state and their resistivities depend upon the water content. Water content in rocks is related to porosity ϕ and saturation S_w .

$$\text{porosity } \phi \text{ is defined as } = \frac{\text{Void volume}}{\text{Total volume}}$$

Porosity is expressed often as a percentage although it is used as a decimal $0 \leq \phi \leq 1$.

Table 11.2 Porosity of different materials

Materials	Grain Diameter	Porosity
Gravel	2.5 mm	45 %
Sand	0.125	40 %
Silty sand	0.005	32 %
Silt	0.003	36 %
Clayed silt	0.001	38 %
Clay	0.0002	47 %

It can be seen that porosity does not depend upon the grain size but it depends strongly upon the grain distribution. A well-graded, non-uniform soil will have a low porosity, a soil consisting of one or two grain sizes, i.e., a poorly-graded or uniform soil will have a high porosity of up to 50 per cent (Table 11.2).

The degree of saturation, S_w , is defined as

$$S_w = \frac{V_w}{V_v} \cdot 100 \quad 0 < S_w < 1$$

This equation expresses the ratio of water present in the soil pores to the total amount which could be present if all the pores were full of water. It is the percentage of total void volume that contains water.

11.3.2 Darcy's Law

The resistivity of porous, water-bearing rocks follows Darcy's Law.

In saturated rocks:

$$\rho_r = a \cdot \phi_p^{-m} \cdot \rho_w$$

where,

- ρ_r = resistivity of rock,
- ρ_w = resistivity of interstitial water,
- ϕ_p = porosity, and
- a, m = certain parameters.

In unsaturated rocks:

in this case saturation must be taken into account, and Darcy's Law becomes

$$\rho_r = F \cdot \rho_w \cdot S_w^{-n}.$$

The value of n is usually close to 2 if more than about 30 per cent pore space is water filled but can be much greater for lesser water content. Fig 11.11 provides the general resistivity values for different rock types:

F is called **formation factor**, $F = a \cdot \phi^{-m}$ (Fig. 11.12).

11.3.3 Point Current Electrode on Homogeneous Earth

Consider a point electrode on the surface of a homogeneous isotropic earth, extending to infinity in the downward direction, and having a resistivity. The current flowing into the earth spreads out radially and hemispherical equipotential develops (Fig. 11.13). The potential at a distance r from the point current source is:

$$V_r = \frac{\rho \cdot I}{2\Pi} \cdot \left(\frac{1}{r}\right).$$

In practice there are two electrodes, one positive A+, sending current into the ground, and, the other negative B- collecting the returning current.

The total potential at any point P in the ground will be :

$$V_p = \frac{\rho \cdot I}{2\Pi} \cdot \left(\frac{1}{r} - \frac{1}{r'}\right)$$

r and r' are the distances of P from the two electrodes.

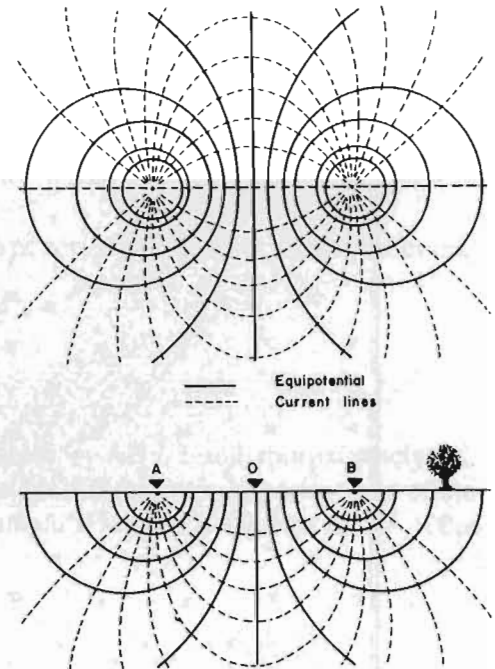


Fig. 11.13 Current flow through point electrodes

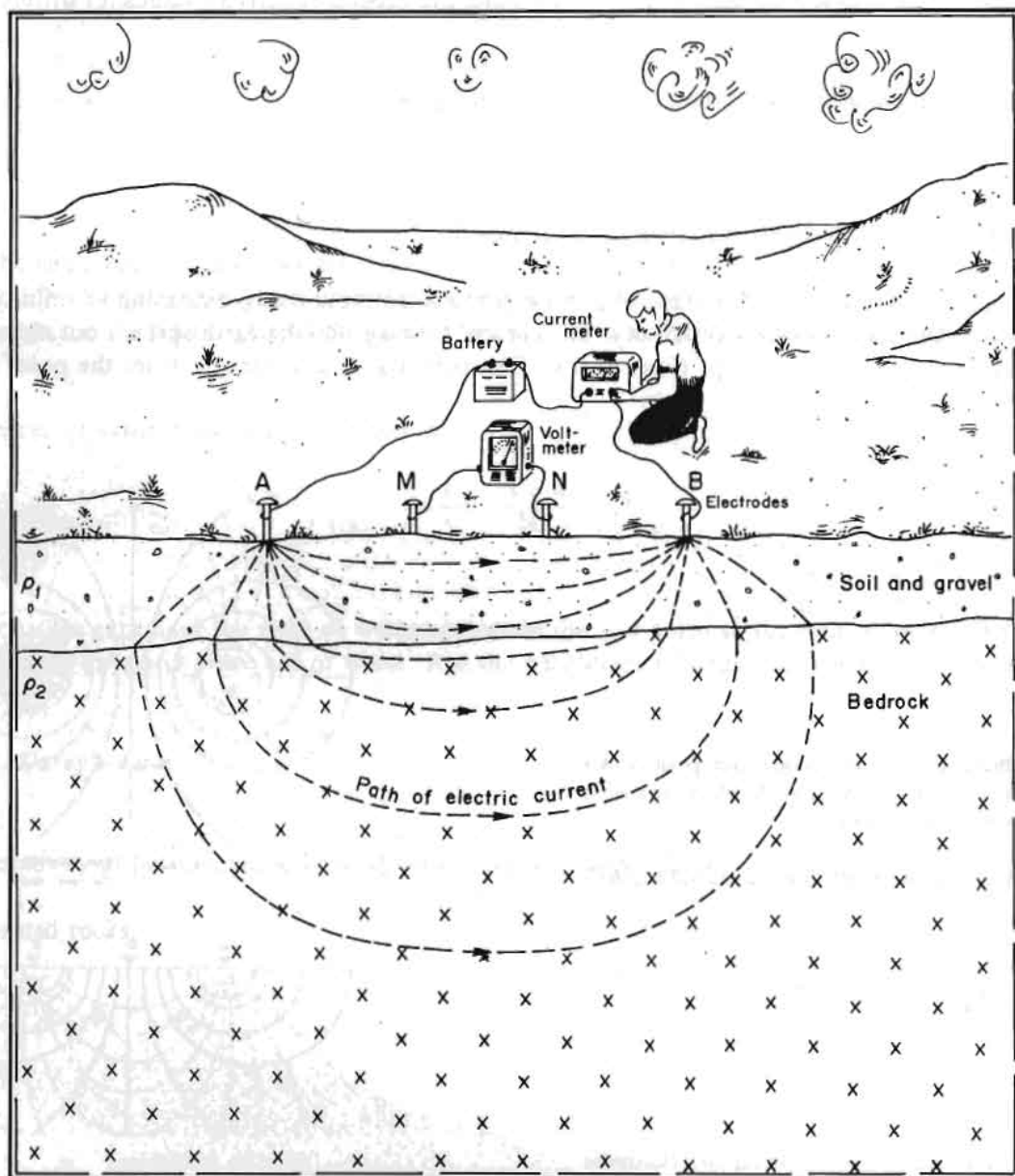


Fig. 11.14 Electrical resistivity survey

11.3.4 Apparent Resistivity

Let A +, B - be the current electrodes placed on the ground surface, and M, N two potential probes.

$$VM = \frac{\rho \cdot I}{2\Pi} \left(\frac{1}{AM} - \frac{1}{BM} \right)$$

$$VN = \frac{\rho \cdot I}{2\Pi} \left(\frac{1}{AN} - \frac{1}{BN} \right)$$

so,

$$\Delta V = VM - VN = \frac{\rho \cdot I}{2\Pi} \left(\frac{1}{AM} - \frac{1}{BM} - \frac{1}{AN} + \frac{1}{BN} \right)$$

and

$$\rho = \frac{2\Pi \cdot \Delta V}{I} \cdot \left(\frac{1}{\frac{1}{AM} - \frac{1}{BM} - \frac{1}{AN} + \frac{1}{BN}} \right)$$

$$\rho = \Delta V \cdot K$$

ρ is called the apparent resistivity, K is a **geometric constant**, so called because it depends only upon the geometric configuration.

This is the fundamental equation of the **resistivity method**. It gives resistivity in terms of quantities that can be measured ΔV , I and the electrode separation distance.

11.3.5 Current Penetration

The distribution of current lines shows that 1/3 penetrate to a depth = $AB / 2$ and approximately 1/2 penetrate to a depth equal to the distance AB. In fact we can consider that the most important part of the current lays down a parallel piped $AB/4$, $AB/2$, $3AB/2$. For example if we use a distance $AB = 100m$ more than 200'000 m³ will be taken into account.

11.3.6 Depth of Investigation

The **depth of investigation** is a function of the spacing between the two outer electrodes A and B. We can assume that the depth of investigation varies from 1/10 to 1/4 AB, but the heterogeneity of the ground can influence the depth of investigation.

11.3.7 *Heterogeneous Medium*

For a uniform sub-surface the apparent resistivity is equal to the true resistivity. If the earth is non-homogeneous, the current distribution will be affected and so is the potential and this produces a change in the resistivity measured. The measured **apparent resistivity** depends upon the resistivity of the various materials through which the current passes; it is an average of all those resistivities.

11.3.8 *Electrical Profiling or Mapping*

There are two basic field procedures used in the fields; **electrical profiling** in which the electrode separation remains constant during the survey, and **electrical sounding** in which the centre of the **electrode spread** is maintained at a fixed location and the electrode spacing AB is increased.

This method is normally employed in the rapid survey of an area. The object of mapping is to determine the lateral variations in the conductivity of the ground. Profiling or mapping is primarily useful for detecting local non-homogeneities and is employed typically in delineating geological boundaries, fracture zones, or steeply dipping contacts between different types of earth material. Figure 11.14 shows the lay-out of the electrical survey method.

Mapping Procedures

A number of different configurations of current and potential electrodes exists. In all arrangements, the electrodes are laid out along a line with the current electrodes generally placed on the outside of the potential electrodes. The opposite is theoretically equivalent. In the engineering world, three arrays have found wide usage (Fig. 11.15).

a. The Schlumberger Configuration

The Schlumberger Configuration is symmetric and colinear. The two potential electrodes MN are closely placed midway between the two current electrodes so that: $MN < AB / 5$.

b. The Wenner Array

The Wenner Configuration uses four electrodes, equally spaced along a straight line $AM = MN = NB$.

c. Dipole-Dipole Array

In this arrangement the current electrodes are on one side of the array and the potential electrodes on the other side. There is the same distance between the two current electrodes and between the two potential electrodes. The usual routine in this procedure is to move the chosen array with a fixed separation, as a whole, in suitable steps along the line of the array itself. When one traverse is finished the array is moved to the next parallel line and so on until the area of investigation is covered. Usually the array is moved so that each of the four electrodes advances through a distance equal to array separation AB, but it is also possible to advance through any other distance.

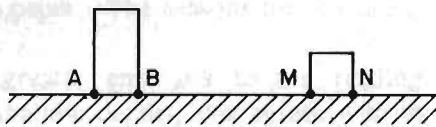
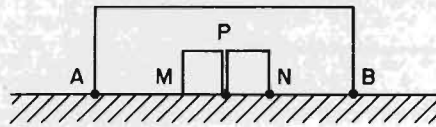
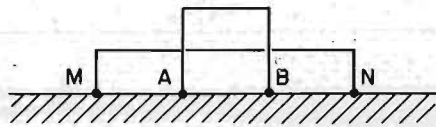
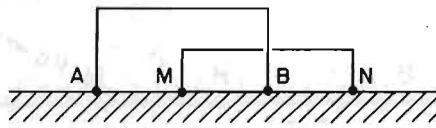
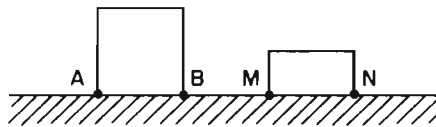
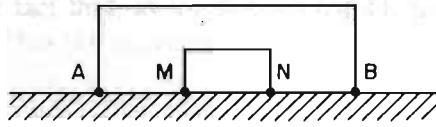
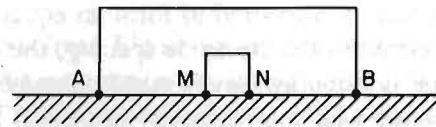


Fig. 11.15 Different configurations of current and potential electrodes

The apparent resistivity values calculated at each station are plotted on a map at positions corresponding to the centre of the array, and the map is contoured to form an equal resistivity contour map. Since the depth of investigation is roughly related to the electrode spacing, the depth of investigation, essentially, will be constant for all the readings. A mapping survey may be thought of as an **electrical trench**. The geologic boundaries can be correlated with the resistivity contours. A resistivity map must always be related to the spacing AB used. This type of procedure has proved helpful in delineating fault zones, contacts, and lateral variations (Fig. 11.16).

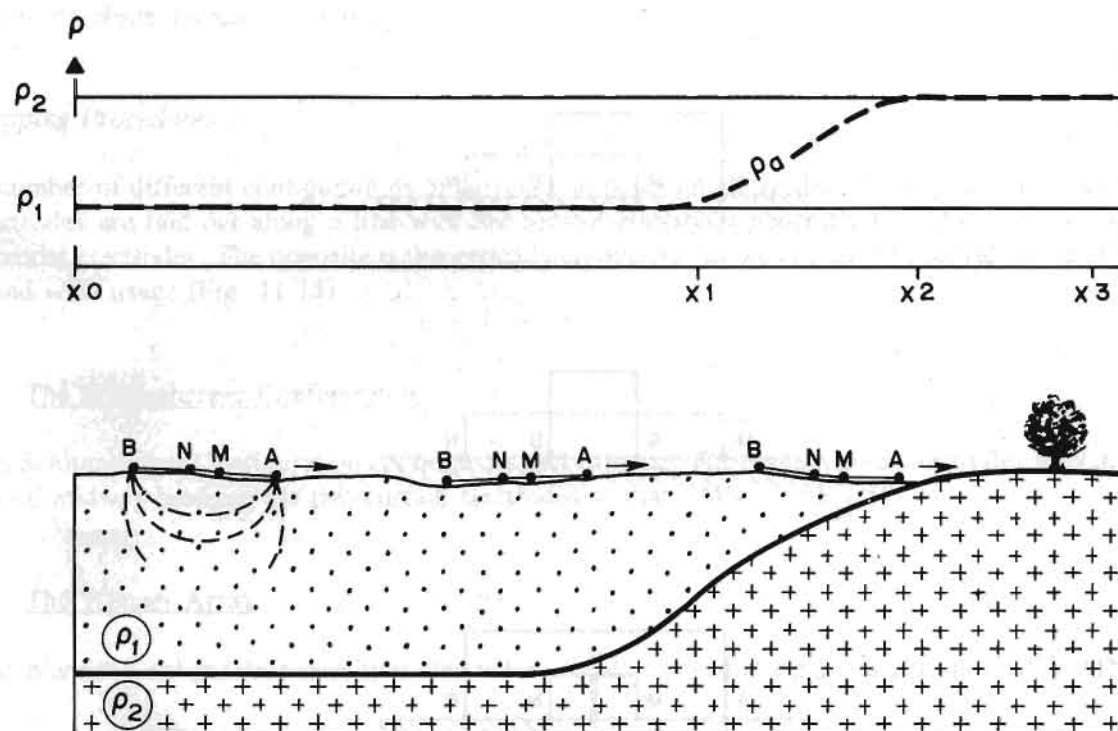


Fig. 11.16 Electrical profiling

11.4 ELECTRICAL SOUNDING

Electrical sounding, also called **Vertical Electrical Sounding (VES)**, is the second basic procedure designed to provide information on the variation in earth conditions **with depth**. Among the applications are : estimation of the variation of resistivity with depth, estimation of depth to water-bearing layer, and estimation of thickness of a layer. The essential idea behind electrical sounding, assuming resistivity variations with depth only, is the fact that, as the distance between AB is increased, the current lines reach increasingly deeper levels. Thus the apparent resistivity will be more and more influenced by the resistivity at deeper levels.

11.4.1 Field Procedure

The MN electrodes are kept fixed and AB moved outward symmetrically about the centre position O. At some stage the MN voltage V will in general fall below the reading accuracy of the voltmeter in which case the distance MN is increased maintaining of course the condition $MN < AB$ (Fig. 11.17).

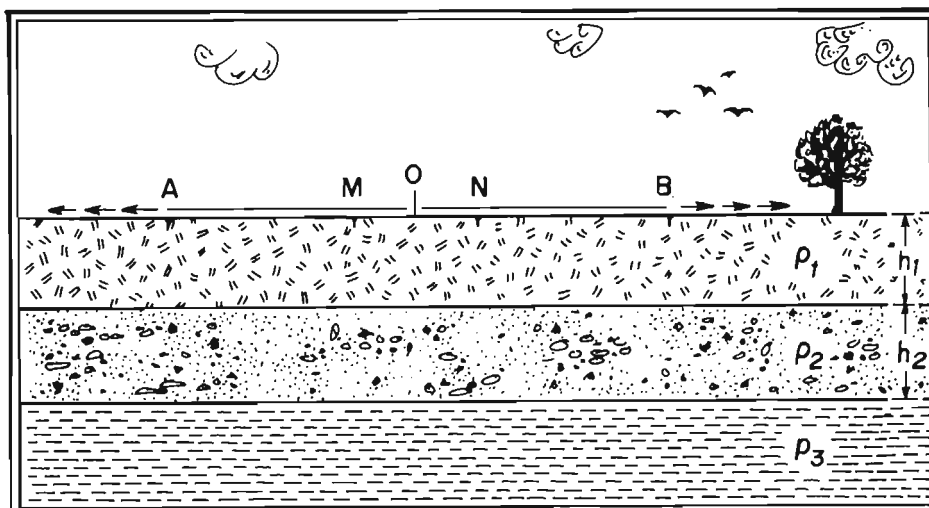


Fig. 11.17 Electrical sounding

11.4.2 Plotting

The data are plotted with $OA = AB/2$ on the x axis and the apparent resistivity on the Y axis (Fig. 11.18). **Logarithmic scale** is used along both axes. It is preferable to use double-logarithmic graph paper rather than ordinary cross-section paper. The reasons for this are given below.

1. The logarithmic plot gives greater emphasis to the readings at small electrode separations, corresponding to material at shallow depths, this agrees with the fact that the measured quantities (apparent resistivities) represent a weighted average of all the true resistivities in a fairly large volume and that the material close to the surface is always weighted more heavily than the material at depth.

2. The quantitative methods of interpretation require that the data be plotted on double logarithmic paper.
3. Use of logarithmic scales makes the shape and size of the curve independent of units of measurements so that comparison becomes easier.
4. The precision required, 10 per cent minimum, is relative to 10 or 11 ohms.m, 100 or 110, 1000 or 1100 and so on for the resistivities, the same for the depths.

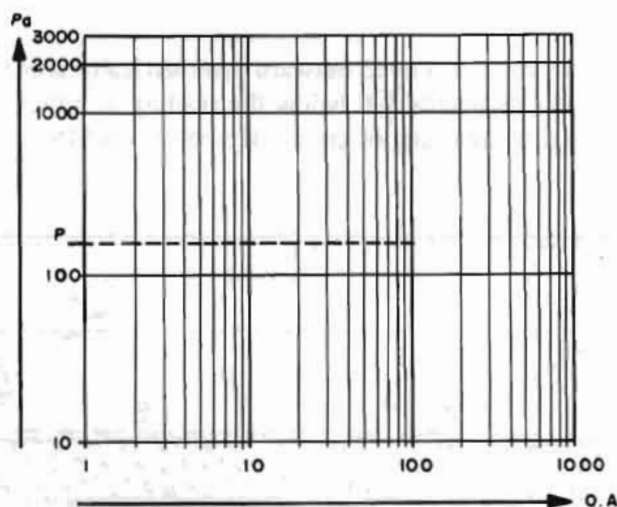


Fig. 11.18 Distance versus resistivity plot in a double logarithmic graph

11.4.3 Quantitative Interpretation

Homogeneous Earth

In this case, the apparent resistivity measured is in fact the true resistivity, no matter the distance AB. The sounding curve in this case will be a straight line crossing the Y axis at the value of the true resistivity.

Two Layer Structures

As a first example, consider a low resistivity layer, such as a wet soil, overlying a thick high resistivity layer such as a dense rock. The true resistivity of the surface material is not changed by the presence of the rock, since the rock does not extend to the surface (Fig. 11.19).

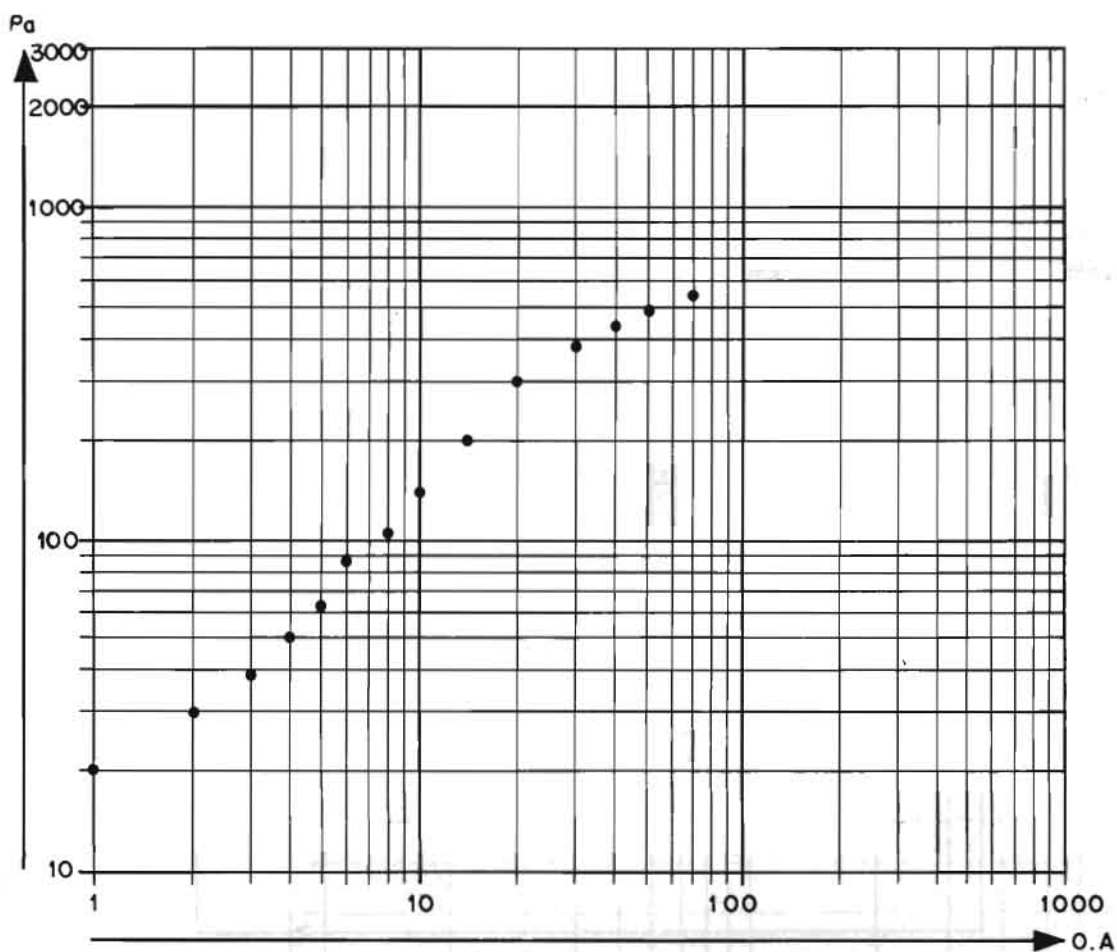
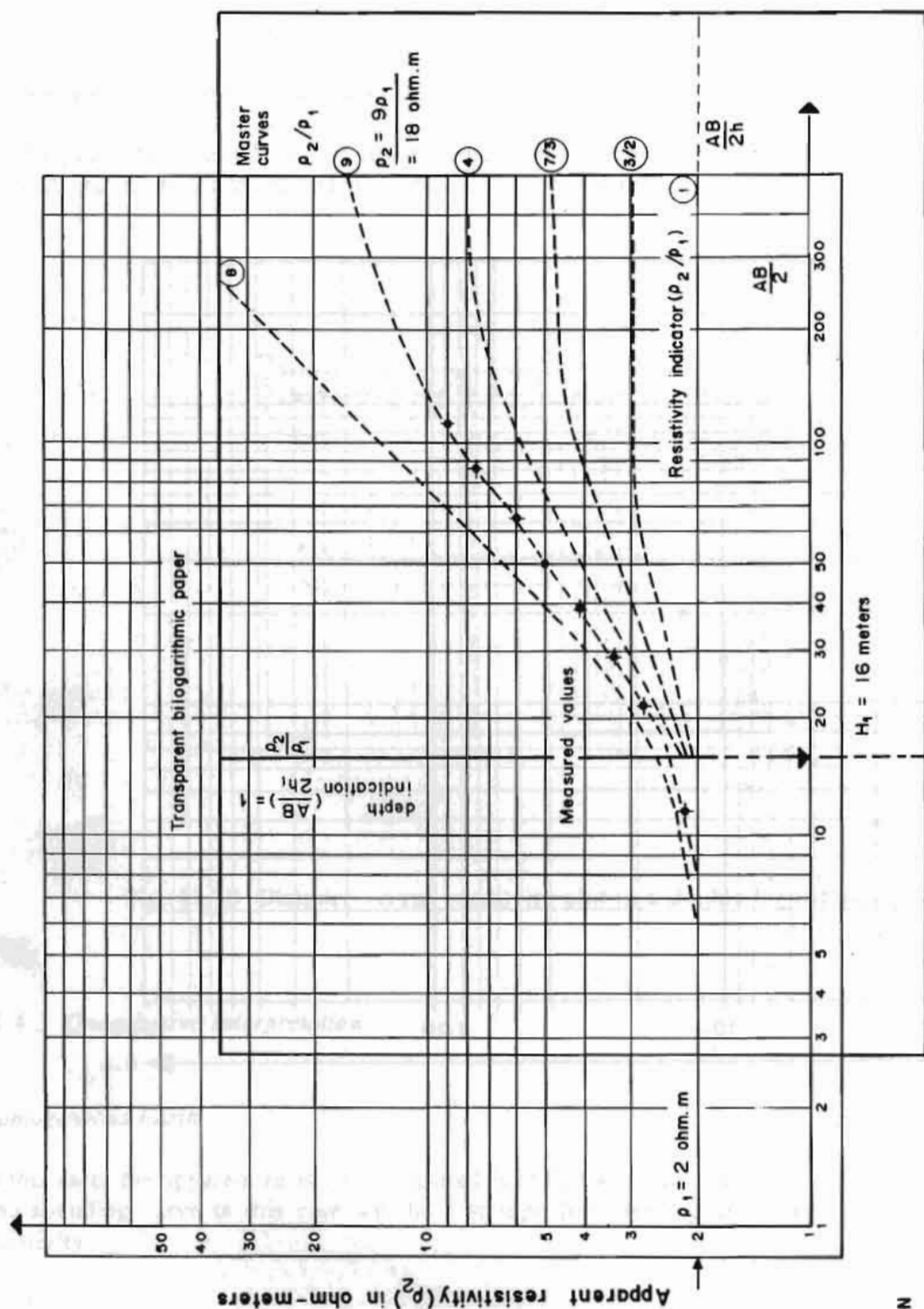


Fig. 11.19 Distance - resistivity plot



INTERPRETATION

Depth = 16 meters

Overburden Resistivity = 2 ohm-meters

Bedrock Resistivity = 18 ohm-meters

Fig. 11.20 Using curve matching to interpret a curve graphed in ohm-meters

The bedrock effect upon the distribution of current will depend more precisely upon the ratio of the electrode spacing to the depth of the bedrock; so when the electrode is small compared to the depth, the current density will be largely unaffected by the rock. As the electrode spacing is increased, the effect of the lower-lying high resistivity stratum increases. Hence, the apparent resistivity curve will rise smoothly to gradually approach the **true resistivity** of the bedrock layer as the electrode spacing becomes very large relative to the depth of the rock. The true resistivity of the near surface soil layer can be easily determined. It is simply the left hand limit of the sounding curve. If the sounding curve is extrapolated back to the limit of zero electrode separation, this apparent resistivity will be equal to the true resistivity of the surface layer.

11.4.4 *Interpretation by Curve Matching*

The first step is to plot ρ apparent against OA on transparent double logarithmic paper. The method involves a comparison of the measured curve with a set of theoretically calculated master curves (with the same double logarithmic modulus). Keeping the respective axes parallel, the paper is slid on various master curves in succession until a satisfactory match is obtained with some curve; if necessary an interpolated one (see Fig. 11.20). The value of OA, coinciding with the point 1 on the X axis of the matching curve, gives H1 and the measured value of ρ apparent coinciding with the point 1 on the axis gives ρ_1 . The value of ρ is obtained from the appropriate parameter belonging to the matching master curve.

MASS WASTING

12.1 INTRODUCTION

Mass wasting is a general term for a variety of processes by which large masses of earth materials are moved under gravity, either slowly or quickly, from one place to another. The term landslide is commonly used to denote the downward and outward movements of slope-forming materials along surfaces of separation by falling, sliding, and flowing at a faster rate. Although landslides are primarily associated with mountainous regions they can also occur in areas of low relief, especially in surface excavations for highways, buildings and open-pit mines. The geological history and human activities often cause unstable conditions that lead to slope failures.

12.2 TYPES OF MASS MOVEMENT

Table 12.1 shows the classification of slope movements (Varnes 1978) on the basis of the nature of the movement and the type of material involved in the process. Tables 12.2, 12.3, and 12.4 show the nature of hill slope processes in mountainous terrain along with geotechnical aspects, surveys, and remedial works.

12.2.1a *Falls*

Falls are abrupt movements of slope materials that become detached from steep slopes or cliffs. Movements occur by free fall or a series of leaps and bounds down the steep slope. The relatively free character and lack of a slide plane differentiates the rockfall and rockslide. Depending upon the type of slope materials involved, it may be a rockfall, soil fall, debris fall, earthfall, boulder fall and so on (Table 12.2).

12.2.1b *Topples*

A topple is a block of rock that tilts or rotates forward on a pivot or hinge and then separates from the main mass falling on the slope and subsequently bouncing or rolling down the slope.

12.2.1c *Slides*

The term slides refers to the mass movements with a distinct surface of rupture or zone of weakness separating the slide material from the more stable underlying materials (Table 12.2 and 12.3). The two major types of slides are **rotational** and **translational** slides.

Rotational Slides

Rotational slides occur on slopes of homogeneous clay or shale and soil slopes. The slide movement is more or less rotational about an axis that is parallel to the contour of the slope. The scarp at the head may be almost vertical, while the toe bulges upwards and sometimes flows out.

Translational Slides

Translational slides are mass movements on a more or less planar surface. The movement of translational slides is controlled by surfaces of weakness such as bedding planes, joints, and faults. Slide materials may range from loose unconsolidated soils to slabs of rock.

Block Slides

Block slides are translational slides in which the moving mass consists of a single unit of rock block that moves down slope.

12.2.1d *Spreads*

The failure in this case is caused by liquefaction, the process whereby saturated, loose, cohesionless sediments are transformed into a liquefied state. Rapid ground motions such as earthquakes usually trigger the failure.

12.2.1e *Flows*

Creep

A creep is an imperceptibly slow, steady, downward movement of slope forming soil or rock. The movement is essentially viscous enough to produce permanent deformation but too small to produce failures as in landslides. A creep is indicated by curved tree trunks, bent fences or retaining walls, tilted poles, and small soil ripples or ridges.

Debris Flow

Debris flow is a form of rapid mass movement involving loose soil, rocks, and organic materials along with entrained air and water to form a slurry that flows downslope. In general, five conditions are important for the debris flow to occur. They are :

- i) steep slopes
- ii) loose rock and soil materials,
- iii) clay minerals,
- iv) saturated soils, and
- v) rainfall or snowmelt generated runoff of sufficient intensity and duration to initiate slope movements. For more details, refer to Section 13.3.3 in Chapter 13.

Debris Avalanche

A debris avalanche is a type of very rapid to extremely rapid debris flow.

Earth Flows

Earth flows have a characteristic bowl-like depression at the head where the slope material becomes liquefied and flows out. The flow is usually channelised on the slope and spreads out at the toe. The flow generally occurs in fine-grained materials or clayey rocks under saturated conditions.

Mudflows

Mud flows are a type of earth flow consisting of material containing about 50 per cent of sand, silt, and, clay-sized particles that are well saturated and flow rapidly.

12.2.1f Complex Movements

Slope movements involving two or more principal types of movement are called complex movements. For example rolling rock blocks from higher elevations due to rockfalls may cause debris slides at lower elevations. Often landslide dams are formed because of a combination of movements of some of the following types - rock and earth slides, debris and mudflows, and rock and debris avalanches.

Table 12.1 Abbreviated version of Varnes' classification of slope movements

TYPE OF MOVEMENT			TYPE OF MATERIAL		
			BEDROCK	DEBRIS	SOILS
				Predominantly coarse	Predominantly fine
FALLS			Rock fall	Debris fall	Earthfall
TOPPLES			Rock topple	Debris topple	Earth topple
SLIDES	ROTATIONAL	FEW UNITS	-	Debris slump	Earth slump
			Rock block slide	Debris block slide	Earth block slide
	TRANSLATIONAL	MANY UNITS	Rockslide	Debris slide	Earth slide
SPREADS			Rock spread	Debris spread	Earth spread
FLOWS			Rock flow (deep creep)	Debris flow (soil creep)	Earthflow
COMPLEX			Combination of two or more principal types of movement		

Source: Modified from Varnes 1978

12.3 CAUSES OF LANDSLIDES

The various causative factors of landslides are listed below.

12.3.1 *Natural Factors*

- a. High relief or steep slopes.
- b. Undercutting of the banks by deeply incised rivers and streams.
- c. Extensive development of weak rocks such as phyllites, slates, and schists; presence of calcareous interlayers in these rocks which leads to high porosity and void formation due to leaching and dissolution.
- d. Heavily fractured rocks because of intense folding and faulting. As many as four systematic sets of fracture plus other random and stress relief joints are very common in mountainous countries.
- e. High weathering of the rocks.
- f. Concentrated precipitation.
- g. Seismic activity. The Himalayan Range lies in a high seismicity belt. Several active faults have been mapped. Landslides due to seismic loading are very common.

12.3.2 *Anthropogenic Factors*

a. *Deforestation*

Intensive deforestation has taken place in most parts of the *Himalaya*, excepting the *Higher Himalaya*, in the last decades.

b. *Improper Land Use*

This includes:

- agricultural practices on steep slopes,
- irrigation on steep and vulnerable slopes,
- overgrazing, and
- quarrying for construction material without considering the conditions of the terrain.

c. *Construction Activities*

Improper or total lack of terrain capability evaluation before placement of infrastructure on hill roads and canals, located in areas with high slope instability, with the result that hazards are common. An unlined

canal across a potential or active landslide or road cut in the tow of ancient landslide deposits are seen in many places. Maintenance of other infrastructures is either non-existent or very poor.

12.4 MAIN TRIGGERS OF MAJOR LANDSLIDES AND THEIR CONTROL

Landslides are the result of the interaction of geological and geographical environment. Earthquakes and rainstorms constitute two of the most important landslide-inducing agents.

12.4.1 *Earthquake-induced Landslides*

Earthquakes usually cause many large-scale landslides, some of which block rivers forming lakes. China is a country that has had many earthquakes. From 780 B.C to 1976 A.D., there have been as many as 656 earthquakes of $M > 6.0$. Earthquake-induced landslides were caused by 33.5 per cent of the total shocks in China, excluding earthquakes in marine areas, in Xizang and Taiwan (Feng and Guo 1985). Apart from the earthquakes themselves (i.e., seismic accelerations, duration of shock, focal depths, and angle and direction of the approach of seismic waves), the environmental factors, such as geology and landform, play a important part in the formation of landslides induced by earthquakes. This is why some smaller earthquakes induced far more landslides than other large earthquakes. Geological structure and the lithological character of rocks influence the landslides. Landslides are commonly seen on the slopes and spurs of mountains cut by faults. On slopes consisting of loosened limestone and igneous rocks, falls occur readily, but on slopes consisting of claystone, shale, and phyllite, falls are few in number.

The type of slope and the slope angle have a great influence upon landslides and falls. Straight slopes seldom have landslides and falls, but they are, however, common on the convex, concave, and complex slopes. The places where the landslides or falls occur are mostly steeper areas of slopes. The statistical data gathered from the earthquake areas of China from 1973 to 1976 give us part of the story: landslides were not found on slopes with a slope angle of less than 25° . Ninety per cent of the landslides occurred on slopes with a slope angle ranging from 30° to 50° . In most cases, falls happened on slopes with a slope angle of $67^\circ - 75^\circ$. Such figures would be of great help in selecting a relative safety zone in an earthquake prone area. The relative safety zone should be in a region with a slope angle of less than 25° in the mountains.

Earthquakes have acted as triggers to many landslides and ground failures in some parts of Nepal. The landslides in Bhajang can be cited as examples. The mountainous parts show seismically triggered slumps, debris slides, and rockfalls, whereas the Terai Region suffers from spreads, liquefaction, quicksand conditions, and sandboils. Moreover, there is evidence of landslides taking place during the following monsoon from colluvium loosened by the previous year's earthquake. Apart from these, the critical stage of toe undercutting of marginally stable slopes, especially with the older slide deposits, by floods and debris torrents as well as breaching of landslide dams, can be taken as secondary landslide triggers.

12.4.2 *Rainfall-induced Landslides*

Rainfall is another important landslide trigger. There is a direct correlation between the amount of rainfall and the incidence of landslides, as indicated below.

- a. If cumulative precipitation of the area amounts to about 50 mm to 100 mm in one day, and daily precipitation is more than 50 mm, somewhat small-scale and shallow debris landslides will occur.
- b. When the cumulative precipitation over 2 days amounts to about 150 mm, and daily precipitation is about 100 mm, the number of landslides has a tendency to increase with precipitation.
- c. When cumulative precipitation exceeds 250 mm over two days and has an average intensity of more than 8 mm per hour in one day, the number of large and vast landslides increase sharply.

12.5 PREVENTION AND CONTROL OF LANDSLIDES

The prevention and control works actually carried out in the landslide areas are based on the following concepts: Firstly, a great deal of importance is placed on human life, secondly, on public structures and buildings, road traffic, and prevention of river flooding if a landslide dams a river. For the sake of convenience, landslides can be arbitrarily divided into two groups; those occurring on artificial slopes and those occurring on natural slopes. The term artificial slope implies not only man-made or constructed slopes but also those that have been partly excavated or formed by human activities. It, therefore, includes levée, dam, reservoir bank, road slope, and mining spoils. Due to their locations, landslides occurring on natural slopes in wildland or forested watersheds receive less attention from the public. These landslides are not usually subject to treatment unless they endanger railways, roads, buildings, reservoirs, or other important installations. The control works for these two kinds of landslide are therefore somewhat different. Of course, some control works can certainly be carried out on both types, but, in general, artificial slopes receive more intense treatment than natural slopes. Measures of landslide control are summarised below.

A. For artificial slopes

- a. Avoidance:
Relocation, bridging, tunnelling (or open-cut and cover tunnel).
- b. Surface Drainage:
Drainage channels or ditches, prevention of leakages, cleaning natural ditches.
- c. Sub-surface drainage:
Drainage tunnels, counterfort trenches, deep-seated counterfort drains, vertical drill holes, horizontal boreholes, slope seepage ditches, drainage wells of ferro-concrete, drainage wells of liner plates.
- d. Supporters:
Retaining wall, anchor retaining wall, cribworks, gabions, piling works.
- e. Excavation:
Removal, flattening, and benching.

- f. River structural work:
Check dams, revetment, spur dikes.
- g. Other methods:
Vegetation, blasting, and hardening.

B. For natural slopes

- a. River structural work:
Check dams, revetment, groin, dikes.
- b. Benching and diversion.
- c. Revegetation, grass seeding, afforestation.

12.6 LANDSLIDE-DAMS

The natural damming of rivers by landslides is a significant hazard in many areas. Landslide-damming is particularly common in the high rugged mountains of the Hindu Kush-Himalayan Region. Many landslide-dams have failed catastrophically, causing major downstream flooding and loss of life in this area.

12.6.1 *Causes of Landslide-Dams*

Landslide-dams are common in the steep, narrow valleys of high rugged mountains because these valleys require relatively small amounts of material to form blockages. Landslide-dams can be caused by a broad range of mass movements in different physiographical settings. Most landslide-dams are formed by rock and earth slumps and slides, debris and mudflow, and rock and debris avalanches. A very few have been caused by rock and soil falls or by slope failure (liquefaction) in sensitive clays.

Schuster and Costa (1986) found that the two most important causes behind the initiation of landslide-dams are excessive precipitation (rainfall and snowmelt) and earthquakes. Volcanic eruptions constitute a minor landslide-dam forming process. Other mechanisms, including ice-dam failure, devegetation, and stream undercutting and entrenchment, account for very small percentages of triggering processes. Large landslide-dams are formed by large earth and rockslide/slumps and debris avalanches which commonly occur on steep slopes and attain high velocities that allow stream blockage before the material can be sluiced away by river action. Complex landslides that start as slumps or slides and break up into debris avalanches can also create large dams. The size of landslide-dams ranges in height from only a few metres to hundreds of metres. The size is controlled primarily by the volume of the mass failed down to the valley and the geometry of the valley. Two very large landslide-dams have blocked tributaries of the Yangtze River in Southwest China in this century: (1) the 255 m high Dixie Landslide-Dam, which failed in 1933, causing a catastrophic flood on the Min River that killed at least 2,423 people in three downstream counties, and (2) the 175 m high Tanggudong Landslide-Dam that blocked the Yalong River in 1967 and, upon failure by overtopping, causing a huge flood that travelled 1,000 km downstream (Li 1990).

12.6.2 *Failure of Landslide-Dams*

Landslide-dammed lakes may last for several minutes or several thousand years, depending upon many factors, including volume, texture, sorting of the dam material, rates of seepage through the dam, and rates of the sediment and water flow into the newly formed lake. A study of 73 cases of landslide-dam failure, for which the times of failure are known, indicates that 27 per cent of the dams failed within 1 day of formation; 41 per cent failed within 6 months; and 85 per cent failed within 1 year of formation.

Because of the lack of a protected spillway, landslide-dams commonly fail by over-topping followed by breaching from erosion by the overflowing stream. A very small percentage of landslide-dam failures contributes to seepage and piping or slope failure of the dam.

12.6.3 *Floods from Landslide-Dam Failure*

Landslide-dams create the potential for two very different types of flooding: (1) upstream flooding as the dam-lake fills and (2) downstream flooding as a result of the failure of the dam. The threat to life from upstream flooding is minimal because the water-rise behind the dam is relatively slow, but the property damage can be substantial as the basin of the natural impoundment is filled. Downstream floods resulting from the failure of landslide-dams are usually much larger than floods originating directly from snowmelt or rainfall and constitute a significant threat.

In 1841, hundreds of villages and towns were swept away by a large flood resulting from the failure of a landslide-dam at Lichan Gan, on the upper Indus River, North Pakistan. A Sikh army camp, close to the river, about 420 km downstream, was overwhelmed by the flood and about 500 soldiers were killed (Mason 1929).

It is usually possible to estimate accurately the extent and rate of upstream flooding from landslide-dams. Such estimates require knowledge concerning the height of the dam, crest rates of streamflow into the dam-lake, rates of seepage through or beneath the dam, and information on topography upstream from the dam. For the rapid assessment of downstream flood potential, the peak discharge of downstream flooding can be estimated by the regression equation given by Costa and Schuster (1987), namely:

$$Q = 0.063 PE^{0.42}$$

where,

Q is peak discharge in cubic metres per second and PE is potential energy in joules.

The potential energy is the specific energy of the lake water behind the dam prior to failure and can be computed as the product of dam height (metres), volume (cubic metres), and specific weight of water (9,800 newtons/cubic metre).

12.6.4 *Methods of Preventing Landslide-Dam Failure*

In recent years, construction of control measures has been attempted on many landslide-dams, as soon as possible after formation, to prevent dam failure and subsequent flooding. Spillways are the most simple and most common method. A well-known example of a successful spillway across a landslide-dam

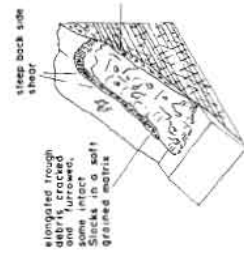
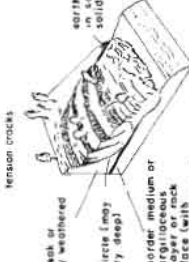
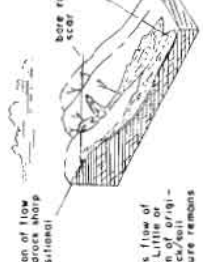
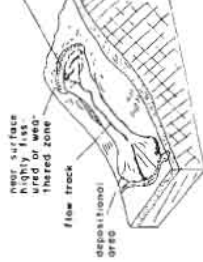
is the spillway constructed in 1959 by the U.S. Army Corps of Engineers on the Madison Canyon landslides, Montana (Harrison 1974). Pipes, tunnel outlets, and diversions have also been used to prevent dam failure and control discharge from the landslide-dam lake in many countries. A famous example is the 2,590m long, 3.4-4m diameter gravity-flow outlet tunnel through Tertiary tuffaceous and volcanic flow rocks composing the ridge immediately west of Spirit Lake in the U.S.A. (Sager and Chambers 1986). Excavation of this tunnel was done by TMB (tunnel boring machine) technique. This outlet tunnel permitted the lake level to be drawn down permanently to an elevation of 1,048m resulting in a safe lake volume of approximately 259 million m³.

In a few cases, large-scale blasting is used to excavate new river channels through landslide dams. In 1984, this technique was used to excavate a channel through the Zhougu Dam on the Bailong River in Gansu Province, China (Li 1990).

12.7 GLACIAL LAKE OUTBURST FLOODS

Glacial lake outburst floods (GLOF) are debris torrents resulting from a sudden and catastrophic release of water from a lake of glacial origin. The lakes are usually impounded by glacial ice or moraine. GLOF are generated either by the overtopping of lake water by ice or moraine, or by seepage and piping under these dams, resulting in their ultimate collapse. GLOF are common in glaciated mountain ranges, including the Himalayan Range. There are numerous lakes of glacial origin in the *Higher Himalaya* and all have different morphology, size, and type.

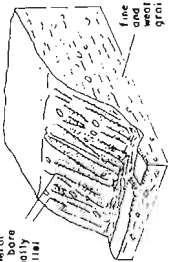
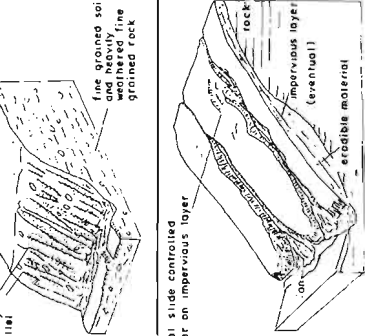
TABLE 12.3 Slides and Flows

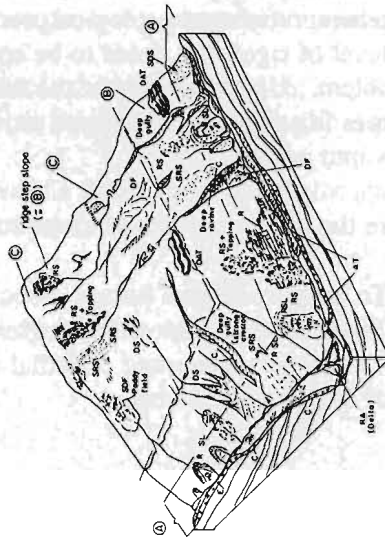
CHARACTERISTIC FORM	MATERIAL	MOUNTAIN ZONES	COMMON FACTORS CONTRIBUTING TO INSTABILITY OR EROSION	TYPICAL SLOPE ANGLE	COMMON RATE OF MOVEMENT	SURVEY TOPICS	CONSTRUCTION AND REMEDIAL WORKS
<p>C. Slideside (locally slide) (back side shear) often promoted by freeze/thaw cycle (frost, clay soil)</p> 	<p>fine to medium S fine to coarse S weakened by intense weathering in water Fine colluvial and soil (local debris) Parameters: C > 0 < 10 & other low</p>	<p>②③</p>	<p>1 W 2 P 3 L and by other movement 4 U 5 Upslope runoff/groundwater, debris in unsat-urable zone</p>	<p>10°-30°</p>	<p>Very slow (usually) to rapid</p>	<p>1 Soil study with estimate 2 Brief hydrogeology 3 Rock face position and water table position in potential failure zone 4 Seismicity through seismic R and resistivity</p>	<p>- Drainage through french drain and underground pipes - Erosion protection of eroding channels within slide and at toe - Erosion protection of toe - Revegetation</p>
<p>Rotational (slump) slump (slump) slump (slump) slump (slump)</p> 	<p>Thick accumulation of soft rock, transported soil, homogeneous fine S highly to completely weathered M and L interbedded coarse and fine silt-clay soils. Parameters: C > 0 to >> 10 & medium to low</p>	<p>②③ 1. P 2. U 3. U 4. EO and blasting</p>		<p>15°-40°</p>	<p>Very slow to rapid</p>	<p>1 Soil for rock study with estimate 2 Brief hydrogeology 3 Position of the perched water table and its continuity through resistivity and seismic-R</p>	<p>- Excavation of slope head - Loading of slope toe - Drainage of perched water by vertical gravity drains or - Erosion protection of toe - Erosion protection of toe - Erosion protection for large active slide</p>
<p>C- FLOW 1 Debris flow includes dry debris flow, mudflow, debris transport events</p> 	<p>Mainly medium-coarse highly-weathered S (no rock) or (no rock) with abundant surface face/ear surface groundwater Medium-coarse R and (no rock) (but not S) Parameters: C or rather small medium to high</p>	<p>②③</p>	<p>1 P and to raise water contents for viscous flow 2 U 3 Upslope runoff of groundwater and water and sediment supply, adding to debris flow in existing channels 4 E Q Debris heavily loaded flood may cause extensive undercut and debris flow</p>	<p>20°-45° as initial but may run on flatter slopes</p>	<p>Rapid to extremely rapid</p>	<p>In potential failure zones: estimate of thickness and position of the perched water table through resistivity surveys, at/and seismicity and resistivity surveys</p>	<p>- Drainage in failure zone - Clearing and road maintenance and erosion channels within flow</p>
<p>2. Mudflow variant: volcanic mud (Andes) mudflow (Andes) mudflow (Andes) mudflow (Andes) mudflow (Andes)</p> 	<p>Mainly fine S (no rock) M intensely weathered in presence of groundwater Fine C and R Parameters: C or rather high & 10</p>	<p>②③</p>	<p>1 P and to raise water contents for viscous flow 2 W 3 Upslope runoff of debris for debris flow (flow) 4 E Q</p>	<p>10°-30°</p>	<p>Slow to rapid</p>	<p>In potential failure zones: estimate of thickness and position of the perched water table through resistivity surveys, at/and seismicity and resistivity surveys</p>	<p>- Drainage in failure zone - Clearing and road maintenance - Erosion protection for eroding channels within flow - Consider realignment for large active flow</p>

Source: Varnes 1978, Fookes et al. 1984 and A. Wagner 1984 and 1988

Table 12.4

TABLE 12.4 Wash Erosion

A - WASH EROSION 1. Riits	CHARACTERISTIC FORM 	MATERIAL Highly-complexity weathered fine rocks or all types of materials in fine sand/silt range. Homogeneous silt-clay C soils. Parameters: 1. color 2. high 3. rather low	MOUNTAIN ZONES ①②③④	COMMON FACTORS CONTRIBUTING TO INSTABILITY OR EROSION 1. P through direct effect of surface runoff 2. Overgrazing, vegetation removal and soil disposal producing bare ground 3. W of fine S.M.I	TYPICAL SLOPE ANGLE 20-50°	COMMON RATE OF MOVEMENT	SURVEY TOPICS	CONSTRUCTION AND REMEDIAL WORKS - Erosion protection and revegetation - Excavation trimming and regrading
2. Guilles	rotational slide controlled by aquifer on impervious layer 	R, T and C soils soft or and compact of all types of rocks and clays and carbonates. Parameters: 1. color 2. high 3. rather low	②③④	1. P through direct effect of surface. 2. Afforestation 3. Alteration to side slope by fills, slips or excavation 4. Silt and clay in main stream/river 5. Mass movements up-slope concentrated gullies.			General geological survey of the potentially critical area or of the failed zone	- Erosion protection and measures for channels (as: check dams) - Erosion protection and revegetation of side slopes - Drainage of rotational slides if any.



STABILITY ANALYSIS OF SLOPES AND PROBABILITY OF SLOPE FAILURE

13.1 PURPOSE OF SLOPE STABILITY ANALYSIS

Slope stability analysis is the most important aspect relating to any infrastructure in the mountain areas. Engineering a structure in the hilly or mountainous areas involves analysis of slopes, both failed and unfailed, so that the level of risk and the associated mitigatory measures can be decided. Recently major landslides in the *Himalaya* have started causing panic to the public. Hence the importance of the subject.

A thorough slope stability analysis is a complex and involved task requiring theoretical understanding and experienced judgement relating to geological processes, soil and rock mechanics, and practicable remedial measures. The level of rigor that needs to be applied to the slope in question depends upon the size and nature of the problem. Understanding of the basic principles and techniques of the stability analysis of soil and rock slopes is a must for every one or, at least, for the engineer who wishes to work by taking natural processes into account.

The following are the main purposes of slope stability analysis.

- o To assess potential hazard associated with natural slopes.
- o To determine stable slope angles for proposed cut slopes.
- o To decide appropriate remedial measures for improvement of the stability of cut slopes or existing landslides.

A package of computer programmes makes analysis and design interesting and time-saving, but it pays to understand the mechanisms of landslides.

13.2 LEVELS OF SLOPE STABILITY ANALYSIS

Projects such as roads and canals cover a large area. The stability assessment for various stages of a project cycle should be different.

13.2.1 *Network Level Planning*

Screening of several alternatives for the purpose of investment planning needs rapid methods of stability assessment. Different instability criteria are grouped, weighted, and rated for different sections of the various alternatives.

Figures and Tables without credit lines in this Chapter are compiled by the author.

13.2.2 Project Level Planning

Once the alternatives are compared and reduced to one or two, detailed hazard mapping is necessary to develop tentative designs and cost estimates after matching the specified project to the natural processes. Hazard maps and their supporting maps provide a complete picture of geological structures, material types, geo-dynamical processes, and terrain slopes. Identification of areas requiring various levels of rigor for slope stability analysis is possible from these maps.

13.2.3 Implementation Level

The implementation level here implies the stages wherein detailed design and subsequent construction are carried out. Stability assessment during detailed design involves:

- o minimal investigations and quick methods to determine stable slope angles in low height cuts and in low hazard areas. Chart solutions are generally adequate for such areas;
- o intensive investigations and standard solutions to determine stable cut slope angles and minor remedial measures for areas involving medium height of cuts and medium hazard levels; and
- o rigorous investigations and analysis to determine stable cut slope angles and major remedial measures for areas in high cuts and in high hazard levels.

Stability assessment during the construction stage is just a repetition of the above steps for differing site conditions.

13.3 STABILITY ANALYSIS OF SOIL SLOPES

In mountain areas, it is rarely possible to find slopes with soils of an infinite depth. Solid or jointed bedrocks are mostly encountered within a few metres of residual or colluvial soils. Colluvial soil, in excess of 30 metres in depth, is also encountered in some hill areas of the *Lesser Himalaya*.

For the purpose of slope stability analysis, all slopes whose stability is governed by failure of the soil mass overlying the rockbed should be treated with soil slope stability analysis.

Slopes, irrespective of the thickness of overlying soil, that are failing primarily from the failure of underlying rocks should be dealt with under rock slope stability.

Two basic approaches to soil slope stability analysis with respect to mode of failure are 1) limit equilibrium analysis and 2) deformation analysis. Most of the methods so far available fall into the former category.

The limit equilibrium method of analysis is based on an assumed failure plane and the assumption that Coulomb's Failure Criterion is satisfied along the failure surface. Stress-strain relationship and *in situ* stresses are not considered and the deformation cannot be predicted by this method. The two-dimensional computer methods of analysis described in this chapter are limited to this method only in view of the

simplicity and adequacy for most infrastructural problems of infrastructures in developing countries. The shear strength parameters such as cohesion (c) and angle of friction (ϕ) used in most soil slope analyses are based on either total stress or effective stress. It is essential to understand the relevance of these parameters to design requirements.

13.3.1 *Total Stress and Effective Stress*

The shear strength parameters, such as c and ϕ , to be used in the stability analysis are obtained from laboratory tests or *in situ* direct shear test or back analysis of failed slope or standard tables. These parameters must represent the actual field conditions which have soil mass in either drained or undrained conditions.

When a saturated soil is sheared to failure without permitting drainage, the soil behaves as though it is purely cohesive, i.e., $\phi = 0$ and the shearing strength is the shear strength from undrained shear test in the laboratory. This condition may be representative of field conditions where pore pressures are governed by total stress changes and little time has elapsed so that no significant dissipation has occurred. This is also called an end-of-construction class of problem, e.g., stability of road embankments just after construction or landslide by liquefaction.

The usual conditions for most natural slopes of soil and rock are governed by steady seepage configurations, and stability analysis for such cases should be performed in terms of effective stresses. This is a case of long-term conditions which applies to most permanent cuts and fills and road embankments.

In total stress analysis it is implied that the pore-water pressures are those for failure conditions. In effective stress analysis, the pore-water pressures used are those predicted for existing (non-failure) conditions.

An effective stress analysis is relevant for all conditions where values of pore-water pressure are obtained from the static water table level or the appropriate flow net. Pore-water pressure may thus be an independent variable, determined from the static water table or from the flow net for steady seepage conditions. There is some misconception that seepage lubricates soil and rock and causes landslides. Actually effective stress (and not friction) is reduced.

The method adopted for the slope stability analysis of practical problems should be based on identification of the most dangerous conditions during the service life of the designed slope. Shear strength parameters for use in design are those representing the most dangerous conditions. Experience and judgements are necessary to predict probable changes in conditions between site investigation and the worst time during the design life of the slope.

13.3.2 *Analysis of Infinite Slope and Plane Translational Failures* (Fig. 13.1)

This is a very common mode of failure of talus along roads.

A) Factor of Safety

Consider a prism, in Figure 13.1 of inclined length $1 \times \sec \beta$, unit width and height H :

Factor of safety,

$$F.S. = \frac{\text{Shearing Resistance}}{\text{Shearing Force}} = \frac{\tau}{T}$$

Shearing Force,

$$T = (W + q_o) \sin \beta$$

Weight,

$$W = [\gamma (H - H_w) + \gamma_{sat} \times H_w]$$

$$\therefore T = \sin \beta [(q_o + \gamma H) + H_w (\gamma_{sat} - \gamma)]$$

Shearing resistance using Coloumb's equation,

$$\begin{aligned} \tau &= (c' + \sigma' \tan \phi') \sec \beta + q_o \cos \beta \tan \phi' \\ &= \frac{[(c' + \sigma' \tan \phi') + q_o \cos^2 \beta \tan \phi']}{\cos \beta} \\ &= \frac{[c' + (\sigma - u) \tan \phi' + q_o \cos^2 \beta \tan \phi']}{\cos \beta} \end{aligned}$$

Normal Stress,

$$\begin{aligned} \sigma &= \gamma(H - H_w) \cos^2 \beta + \gamma_{sat} \times H_w \cos^2 \beta \\ &= \cos^2 \beta [\gamma H - \gamma H_w + \gamma_{sat} H_w] \\ &= \cos^2 \beta [\gamma H + H_w (\gamma_{sat} - \gamma)] \end{aligned}$$

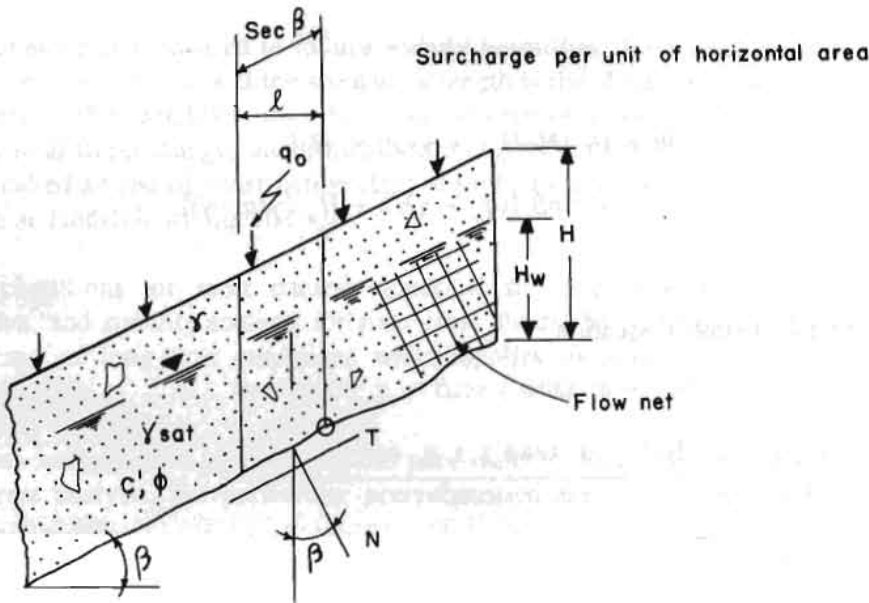
Pore Pressure,

$$\begin{aligned} u &= \gamma_w H_w \cos^2 \beta \\ \gamma_w &= \text{unit weight of pore fluid} \end{aligned}$$

Effective Stress,

$$\sigma' = \sigma - u = \cos^2 \beta [\gamma H + H_w (\gamma_{sat} - \gamma_w - \gamma)]$$

$$\begin{aligned} \therefore \tau &= \frac{[c' + \tan \phi' \cos^2 \beta \{q_o + \gamma H + H_w (\gamma_{sat} - \gamma_w - \gamma)\}]}{\cos \beta} \\ &= \tan \phi' \cos \beta \left[\frac{c'}{\cos^2 \beta \tan \phi'} + (q_o + \gamma H) + H_w (\gamma_{sat} - \gamma_w - \gamma) \right] \end{aligned}$$



Source: Gray and Leiser 1982

Fig. 13.1 Idealized infinite slope

Factor of safety,

$$F. S. = \frac{\tan \phi' \cos \beta \left[\frac{c'}{\cos^2 \beta \tan \phi'} + (q_o + \gamma H) + H_w (\gamma_{sat} - \gamma_w - \gamma) \right]}{\sin \beta [(q_o + \gamma H) + H_w (\gamma_{sat} - \gamma)]}$$

$$F. S. = \frac{\frac{\tan \phi'}{\tan \beta} \left[\frac{c'}{\cos^2 \beta \tan \phi'} + (q_o + \gamma H) + H_w (\gamma_{sat} - \gamma_w - \gamma) \right]}{[(q_o + \gamma H) + H_w (\gamma_{sat} - \gamma)]}$$

(13.1)

The above equation may be generalised easily for seismic conditions (Ranjan et al. 1984). It may be noted that surcharge K (e.g., trees) increases the factor of safety if $C < \gamma_w H_w \tan \phi \cos^2 \beta$. One may further note that H represents the average depth of the debris on rock in case of a slightly non-uniform slope surface.

For cohesionless soil with surcharge and water level at ground surface:

$$F.S. = \frac{\tan \phi'}{\tan \beta} \left[\frac{(q_o + \gamma H) + H_w (\gamma_{sat} - \gamma_w - \gamma)}{(q_o + \gamma H) + H_w (\gamma_{sat} - \gamma)} \right] .$$

For cohesionless soil and water level at ground surface but no surcharge:

$$F.S. = \frac{\tan \phi'}{\tan \beta} \left[\frac{(\gamma_{sat} - \gamma_w)}{\gamma_{sat}} \right] \quad (13.2)$$

and in seismic cases (Ranjan et al. 1984)

$$F.S. \approx \frac{\tan \phi}{\tan (\beta + \lambda)} \left[\frac{\gamma_{sat} - \gamma_w}{\gamma_{sat}} \right] ;$$

$\tan \lambda =$ horizontal component of earthquake acceleration.

For cohesionless dry soil and no surcharge

$$F.S. = \frac{\tan \phi'}{\tan (\beta + \lambda)} .$$

Thus, it may be noticed that saturated slopes in cohesionless soil, having a saturated unit weight of 2.0g/cc result in a factor of safety which is half of that for a cohesionless dry soil. This is the cause of talus failures/debris slides in rainy season due to temporary rise in the perched water table. (It may be noted that the drag force on boulders, caused by high seepage velocity, has been neglected in Eq. 13.2.)

It may also be noted that a dry slope underlain by sand is stable, regardless of the height and surcharge, provided the angle β between the slope and horizontal is equal to or less than the angle of internal friction ϕ for the sand in a loose state (and $\phi - \lambda$ in seismic cases).

The computer programme Stability Analysis of Slope with Talus Deposit (SAST) may be used to compute factors of safety with and without earthquake forces. It also gives remedial measures. The programme Back Analysis of Slope with Talus Deposit (BAST) performs analysis of failed talus slopes.

B) *Stability Number for Soil with Cohesion and Friction: Case of Infinite Slope*

Rewriting equation (13.1) for a factor of safety of 1.0, and for water table at surface and no surcharge:

$$c' + [(q_o + \gamma H) + H_w (\gamma_{sat} - \gamma_w)] \tan \phi' \cos^2 \beta = \cos \beta \sin \beta [(q_o + \gamma H) + H_w (\gamma_{sat} - \gamma)]$$

or,

$$\begin{aligned} c' &= H \gamma_{sat} \sin \beta \cos \beta - H(\gamma_{sat} - \gamma_w) \tan \phi' \cos^2 \beta \\ &= H [\gamma_{sat} \sin \beta \cos \beta - \gamma_b \tan \phi' \cos^2 \beta] \\ \gamma_b &= \text{buoyant unit weight} \\ &= H \gamma_{sat} \cos^2 \beta \left(\tan \beta - \frac{\gamma_b}{\gamma_{sat}} \tan \phi' \right) \end{aligned}$$

or,

$$\frac{c'}{H \gamma_{sat}} = \cos^2 \beta \left(\tan \beta - \frac{\gamma_b}{\gamma_{sat}} \tan \phi' \right)$$

Substituting $1/N_s$ (stability number) for right hand side of the eqn., we get:

$$\frac{c'}{H \gamma_{sat}} = \frac{1}{N_s}$$

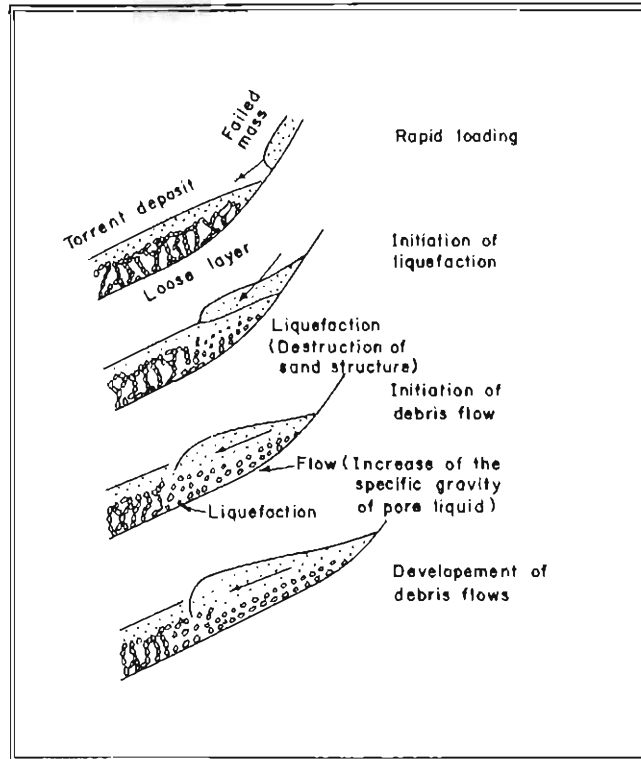
Treating this height when the factor of safety becomes 1.0 as the critical H_c ,

$$\frac{c'}{H_c \gamma_{sat}} = \frac{1}{N_s}$$

$$\therefore H_c = N_s \frac{c'}{\gamma_{sat}}$$

13.3.3 Debris Flow

Figure 13.2. illustrates the mechanism of debris flows along gullies. First of all, rainstorm causes landslides on the top, steep parts of gullies. The debris slide/boulder jumping on steep reaches triggers the debris flow of colluvium or torrent deposit along the flatter and main reaches of gullies or channels. Then two together flow like a viscous liquid with high velocities of 1-10 m/sec causing erosion *d/s*. Finally debris flow takes the shape of a fan deposit on very flat ground. The debris flow is arrested on slopes of 5° to 10° dip or by a river where landslide dams may be created if the valley is narrow.



Source: Sassa 1985

Fig. 13.2 Illustration of the Mechanism of Debris Flows

Sassa (1985) has shown experimentally that fine particles become suspended in water (mud) because of eddy currents of rapid debris flow. Consequently, the unit weight of pore fluid (mud) rises from 1 to 1.6 gm/cc depending upon flow velocity and clay content.

Substituting in Equation 13.2, $\gamma_{sat} = 1.75 \text{ gm/cc}$ for loose debris, $\gamma_w = 1.40 \text{ gm/cc}$, the factor of safety drops to one-fifth value in dry conditions. The angle ϕ is now the kinetic angle of friction which is much less than the static angle of internal friction. It is because of this sudden loss of strength, which is called liquefaction, that debris flows like liquid. The fluid dynamics of debris flow are complex.

The maximum size of boulders (d) that will be transported by an abnormal drag force, such as sediment, is in the order of $d \approx 0.2 v^2 \text{ (m)}$, where v is the mean velocity of debris flow in m/sec. So at $v=3\text{m/sec}$, huge boulders of 1.8m in size would be carried like sediment.

The debris flow will be arrested at an angle of β , according to Equation 13.2, in the shape of a debris fan (kinetic $\phi' = 25^\circ$):

$$\tan\beta = \tan 25^\circ \left[\frac{1.75-1.40}{1.75} \right]$$

$$\beta = 5^\circ \text{ (} 5^\circ - 10^\circ \text{ observed) .}$$

The rapid debris flow can be checked by Reinforced Cement Concrete (RCC) check dams. Narrow gullies can be crossed by well-raised bridges.

13.3.4 Finite Slope Failure on Curved Surface

Many slope failures occur on curved surfaces. There are several methods of analysing such failures. These may broadly be categorized as:

- o the friction-circle method and
- o the method of slices

The Friction Circle Method (FCM) considers the total forces acting on the whole mass lying above the assumed circular surface of failure.

The Method of Slices (MS) involves division of the mass above an assumed failure surface into vertical slices. The slices are then analyzed statically for stability employing assumptions for avoiding indeterminate situations. The presentation is based on the work of Terzaghi and Peck which can be found in 'Slopes: Analysis and Stabilization', Transportation Research Board, 1980.

Both of these methods require determination of the critical circular slip surface. This is possible by analysing several trial surfaces and finding the slope surface which gives the least factor of safety. The critical slip surface may sometimes be determined without trial, i.e., by analytical methods.

Chart Solution

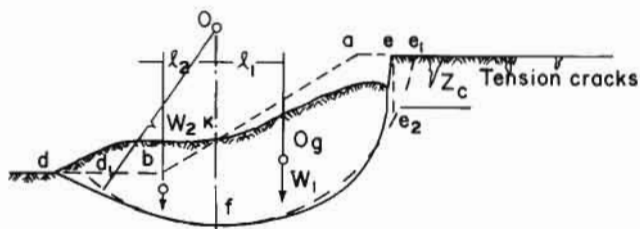
Hoek and Bray have prepared chart solutions based on trial slopes, circles, and methods of slices which are presented under the heading Hoek and Bray Charts for Circular Types of Failure (Fig. 13.10 to Fig. 13.14). These charts give only the static factor of safety where there are no earthquakes and no submergence of slopes.

Computer Solution

Package computer programmes are available to facilitate the rapid solution of stability problems involving complex and repetitive calculations. The programmes, **SARC** and **ASC**, are based on Bishop's Simple Method of slices. The Programme SARC is for the Stability Analysis of Reservoir Slopes with circular wedge mode of failure. The Programme Analysis of Slope with Circular Failure (ASC) is for determining cut slope angle. These programmes take into account earthquake forces and irregular slope surfaces also. ASC also analyses the radius of curvature of cut slope in the plan.

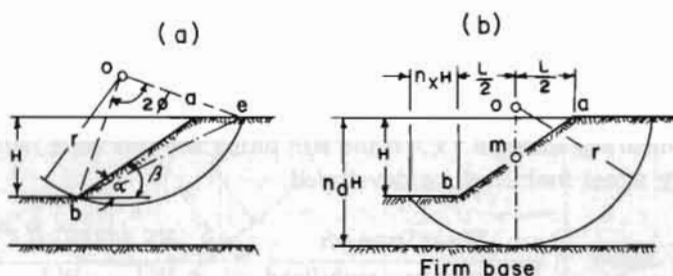
General Character of Slides in Homogeneous Cohesive Soil

A cohesive material having a shearing resistance $s = c + p \tan \phi$ can stand with a vertical slope, at least for a short time, provided the height of the slope is somewhat less than H_c . If the height of a slope is greater than H_c , the slope is not stable unless the slope angle β is less than 90° . The greater the height of the slope, the smaller must be the angle β . If the height is very great compared to H_c , the slope will fail unless the slope angle β is equal to or less than $\phi - \lambda$ ($\tan \lambda$ = coefficient of the horizontal component of earthquake acceleration).



Source: Adapted from Terzaghi and Peck 1980

Fig. 13.3 Deformation associated with slope failure



Source: Adapted from Terzaghi and Peck 1980

Fig. 13.4 Position of critical circle for (a) Slope failure (W.Fellenius 1927) (b) Base failure

The failure of a slope in a cohesive material is commonly preceded by the formation of a row of tension cracks behind the upper edge of the slope, as shown in Figure 13.3. Sooner or later, the opening of the cracks is followed by sliding along a curved surface, indicated by the full line in Figure 13.3. Usually, the radius of curvature of the surface of sliding is least at the upper end, greatest in the middle, and intermediate at the lower end. The curve, therefore, resembles the arc of an ellipse. If the failure occurs along a surface of sliding that intersects the slope at or above its toe (Fig. 13.4a), the slide is known as a **slope failure**. On the other hand, if the soil beneath the level of the toe of the slope is unable to sustain the weight of the overlying material, the failure occurs along a surface that passes at some depth below the toe of the slope. A failure of this type, shown in Figure 13.4b, is known as a **base failure**.

Factor of Safety

The Factor of Safety (F.S.) in slope analysis is generally expressed in terms of shearing strength:

$$F.S. = \frac{\text{Shearing strength of soil } (S_r)}{\text{Shear stress developed along failure surface}}$$

Failed Slopes

Failed slopes or slopes at the point of failure have a factor of safety equal to 1.0. For such slopes, we can find the shearing strength (S_r) of the soil along the failure surface from the geometry of the slope and the failure plane. In practice, the failure surface is located by test borings, slope borings, or deep pits.

Referring to Figure 13.3, the shearing strength of failed slope (S_r) is determined by:

$$W_1 l_1 = W_2 l_2 + S_r \times \text{arc length } d_1 e_2$$

therefore,

shear stress developed = shearing resistance

$$S_r = \frac{W_1 l_1 - W_2 l_2}{\text{arc length } d_1 e_2}$$

Unfailed Slopes

It is essential to know the shearing strength, S_r , of the soil along the probable failure plane in order to compare it with the shearing stress mobilized or developed.

$$\text{Factor of Safety} = \frac{\text{Shear Strength}}{\text{Shear stress mobilized}} = \frac{S_r \text{ arc length } d_1 e_2}{W_1 l_1 - W_2 l_2}$$

S_r for cohesive and frictionless soil may be determined from unconfined compressive strength (q_u) from laboratory tests. Shearing strength (S_r) which is referred to as the cohesion (c) for frictionless soil is roughly equal to half of the unconfined compressive strength. That is:

$$S_r = \frac{1}{2} q_u = c$$

For cohesive soil with friction, shearing strength may be determined by:

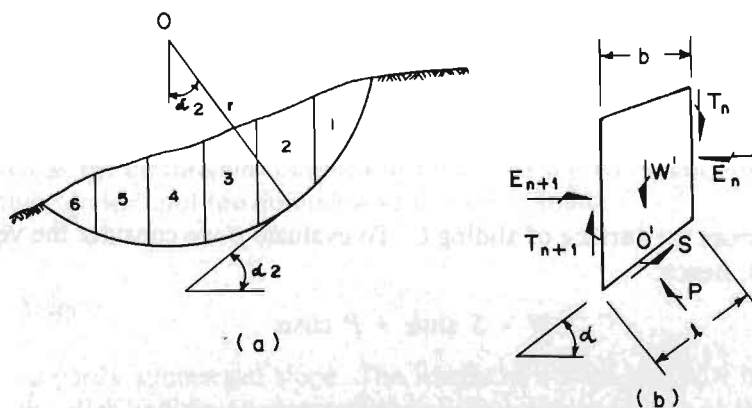
$$S_r = c + p \tan \phi$$

13.3.5 Soil Slope Analysis by Method of Slices

The following discussion, extracted from Terzaghi's 'Soil Mechanics in Engineering Practice'(1980), is intended to provide a basic concept of theory behind stability analysis by the Method of Slices. Readers interested in other methods or in knowing more about slope stability may refer to any standard book on soil mechanics.

Irregular Slopes on Non-uniform Soils (Bishop's Simple Method)

If a slope has an irregular surface that cannot be represented by a straight line, or if the surface of sliding is likely to pass through several materials with different values of c and ϕ , the stability can be investigated conveniently by the **method of slices**. According to this procedure, a trial circle is selected (Fig. 13.5a) and the sliding mass sub-divided into a number of vertical slices 1,2,3, etc. Each slice, such as slice 2 shown in Figure 13.5b, is acted upon by its weight W , by shear forces T and normal forces E on its sides, and by a set of forces on its base. These include the shearing force S and the normal force P . The forces on each slice, as well as those acting on the sliding mass as a whole, must satisfy the conditions of equilibrium. However, the forces T and E depend on the deformation and the stress-strain characteristics of the slide material and cannot be evaluated rigorously. They can be approximated with sufficient accuracy for practical purposes.



Source: adapted from Terzaghi and Peck 1980

Figure 13.5 Method of Slices for investigating the equilibrium of a slope located above a water table

(a) Geometry pertaining to one circular surface of sliding (b) Forces on typical slice such as slice 2 in (a)

The simplest approximation consists of setting these forces equal to zero. Under these circumstances, if the entire trial circle is located above the water table and there are no excess pore pressures, equilibrium of the entire sliding mass requires that:

$$r \sum W \sin \alpha = r \sum S \quad (13.3)$$

If s is the shearing strength of the soil along l , then:

$$S = \frac{s}{F} l = \frac{s}{F} \frac{b}{\cos \alpha} \quad (13.4)$$

and

$$r \sum W \sin \alpha = \frac{r}{F} \sum \frac{sb}{\cos \alpha} \quad (13.5)$$

hence

$$F = \frac{\sum \left(\frac{sb}{\cos \alpha} \right)}{\sum W \sin \alpha} \quad (13.6)$$

The shearing strength s , however, is determined by:

$$s = c + p \tan \phi$$

where,

p is the normal stress across the surface of sliding l . To evaluate p we consider the vertical equilibrium of the slice (Fig. 13.4b), hence:

$$W = S \sin \alpha + P \cos \alpha$$

and

$$p = \frac{P}{l} = \frac{P \cos \alpha}{b} = \frac{W}{b} - \frac{S}{b} \sin \alpha \quad (13.7)$$

Therefore,

$$s = c + \left(\frac{W}{b} - \frac{S}{b} \sin \alpha \right) \tan \phi = c + \left(\frac{W}{b} - \frac{s}{F} \tan \alpha \right) \tan \phi$$

and

$$s = \frac{c + \left(\frac{W}{b}\right) \tan \phi}{\left(1 + \frac{(\tan \alpha \tan \phi)}{F}\right)} \quad (13.8)$$

Let

$$m_\alpha = \left(1 + \frac{\tan \alpha \tan \phi}{F}\right) \cos \alpha \quad (13.9)$$

then

$$F = \frac{\sum \frac{[c + \left(\frac{W}{b}\right) \tan \phi] b}{M_\alpha}}{\sum W \sin \alpha} \quad (13.10)$$

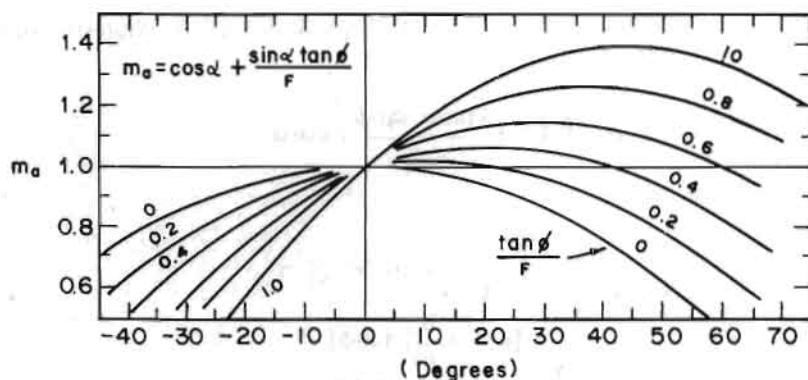
Equation 13.10, which gives the factor of safety F for the trial circle under investigation, contains on the right-hand side the quantity m_α (Eq. 13.9) which is itself a function of F . Therefore, Equation 13.10 must be solved by successive approximations in which a value of $F = F_1$ is assumed and used for calculation of m_α , whereupon F is then computed. If the value of F differs significantly from F_1 , the calculation is repeated. Convergence is very rapid. The calculations are facilitated by the chart (Figure 13.6a) from which values of m_α can be taken (Janbu 1954) and by a tabular arrangement of the computations (Fig. 13.6b). In as much as the calculations outlined in Figure 13.6 refer to only one trial circle, they must be repeated for other circles until the minimum value of F is found.

Partly Submerged Slope

Figure 13.7 shows a partly submerged slope. The weight of a slice will now be the sum of the weight of the dry part of the slice and the buoyant weight of the submerged part of this slice. It is reasonable to assume that groundwater table AA or the phreatic surface is the same as the reservoir level, at least up to the failure surface. Then there is no need to account for water pressures above and below the slices.

It is evident now that submergence reduces the toe support. Therefore, the factor of safety is reduced after submergence. In a seismic case of a partly submerged slope, the factor of safety is reduced significantly. This is because the seismic force acts upon the saturated weight of a slice and strength is mobilized by the submerged weight of the slice.

It has also been found that the factor of safety is not minimum at full reservoir level but at some critical level. Slope failure may cause turbidity currents in the reservoir eroding the valley for long distances.



(a)

Values from cross section

	1	2	3	4	5	6	7	8
Slice No.	α	$\sin \alpha$	W	$W \sin \alpha$	$c + W/b \tan \phi$	(5).b	$m\alpha$ $Fa =$	(6)/(7)
								$\Sigma(8)$

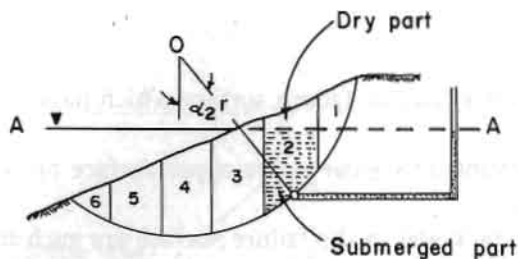
$$\text{For first trial, } F_a = \frac{\Sigma(6)}{\Sigma(4)} \quad F = \frac{\Sigma(8)}{\Sigma(4)}$$

(b)

Source: adapted from Terzaghi and Peck 1980

Fig. 13.6 Calculation of factor of safety for slope if surface of sliding is circular and forces between slices are neglected

(a) Chart for evaluating factor m_α (b) Tabular form for computation



Source: adapted from Terzaghi and Peck 1980

Fig. 13.7 Partly Submerged Slope

Hoek and Bray Chart for Circular Types of Failure on Slopes in Soils, Highly Jointed Rocks, and Rockfills

These charts enable the user to carry out a rapid check on the factor of safety of a slope or upon the sensitivity of the factor of safety to changes in groundwater conditions or slope profile. The following are some considerations relating to the chart.

- Failure generally takes place in the form of a circle in the case of soils. Soils do not have strongly defined structural patterns such as unfavourably oriented seams or discontinuities in the rocks and the failure surface is free to find the line of least resistance.
- Conditions of circular failure will arise when the individual particles in a soil or rock mass are very small, compared to the size of the slope, and when these particles are interlocked as a result of their shape: hence, broken rock in a large fill tends to behave as a 'soil' and large failures will occur in a circular mode.
- Soil consisting of sand, silt, and smaller particle sizes will exhibit circular failure surfaces, even on slopes a few metres in height. It is proper to design soil slopes on the crest of highly altered and jointed rocks, on the assumption that failure would be by a circular failure process.
- The charts differ from those published by Taylor in 1948 in that they include the influence of a critical tension crack and groundwater in the slope.
- Charts may also be used for analysing rock slopes with several joint sets that are favourably oriented so that rock mass behaves like soil mass.

Derivation of Circular Failure Chart (Extracted from Hoek and Bray 1981, p. 228)

The following assumptions are made in deriving the stability charts presented in this Chapter :

- a. the material forming the slope is assumed to be homogeneous, i.e., its mechanical properties do not vary with direction of loading;
- b. the shear strength of the material is characterized by a cohesion c and a friction angle ϕ which are related by the equation $\tau = c + \sigma \tan \phi$;

- c. failure is assumed to occur on a circular failure surface which passes through the toe of the slope**
- d. a vertical tension crack is assumed to occur in the upper surface or on the face of the slope;
- e. the locations of the tension crack and of the failure surface are such that the factor of safety of the slope is a minimum for the slope geometry and groundwater conditions considered;
- f. a range of groundwater conditions, varying from a dry slope to a fully saturated slope under heavy recharge, are considered in the analysis; and
- g. there is no progressive failure of the slope due to stress concentration from the toe towards the crest.

Groundwater Flow Assumptions

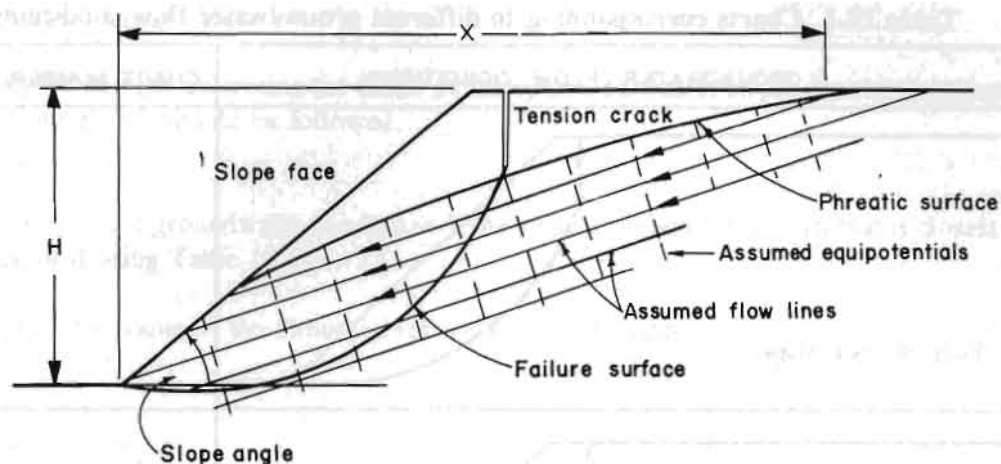
In order to calculate the uplift force due to water pressure acting on the failure surface and the force caused by water in the tension crack, it is necessary to assume a set of groundwater flow patterns that coincide as closely as possible with those conditions that are believed to exist in the field.

In the analysis of rock slope failures, it is normally assumed that most of the water flow takes place in discontinuities in the rock and that the rock itself is practically impermeable. In the case of slopes on soil or waste rock, the permeability of the mass material is generally several orders of magnitude higher than that of intact rock, and, hence, a general flow pattern will develop in the material behind the slope.

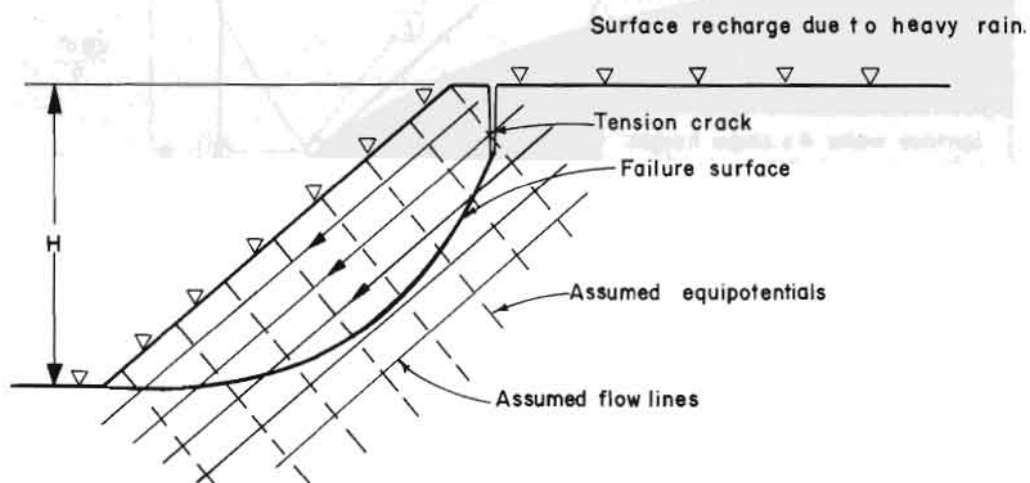
Within a soil mass, the equipotentials are approximately perpendicular to the phreatic surface. Consequently, the flow lines will be approximately parallel to the phreatic surface for the condition of **steady state drawdown**. Figure 13.8 shows that this approximation has been used for the analysis of the water pressure distribution on a slope under conditions of normal drawdown. Note that the phreatic surface is assumed to coincide with ground surface at a distance, measured in multiples of the slope height, behind the toe of the slope. This may correspond to the position of a surface water source such as a river or dam or it may simply be the point where the phreatic surface is judged to intersect the ground surface.

The phreatic surface itself has been obtained, for the range of slope angles and values of x in Figure 13.8 considered, by a computer solution of the equations proposed by Casagrande (1934), discussed in the text book by Taylor (1948). In the case of a saturated slope subjected to heavy surface recharge, the equipotentials and the associated flow lines used in the stability analysis are based upon the work of Han (1972) who used an electrical resistance analogue method for the study of groundwater flow through isotropic slopes. The charts are numbered 1 to 5 (Figure 13.10 to 13.14) to correspond with the groundwater conditions defined in Table 13.1. These charts were prepared using Bishop's Simple Method (Eq. 13.10).

** Terzaghi (1943) shows that the toe failure assumed for this analysis gives the lowest factor of safety provided that $\phi > 5^\circ$. The $\phi = 0$ analysis, involving failure below the toe of the slope through the base material, has been discussed by Skempton (1948) and by Bishop (1960) and Bjerrum and is applicable to failures that occur during or after the rapid construction of an embankment slope.



- a) Groundwater flow pattern under steady state drawdown conditions where the phreatic surface coincides with the ground surface at a distance x behind the toe of the slope. The distance x is measured in multiples of the slope height H .

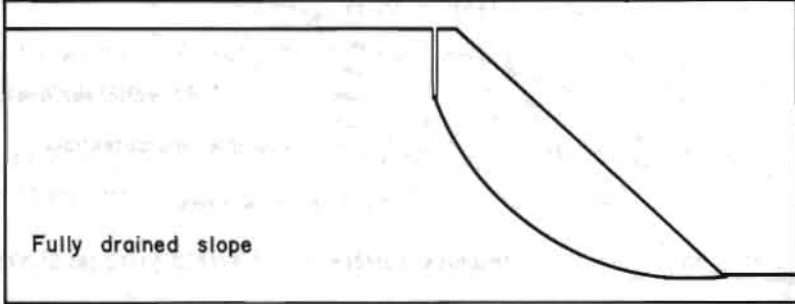
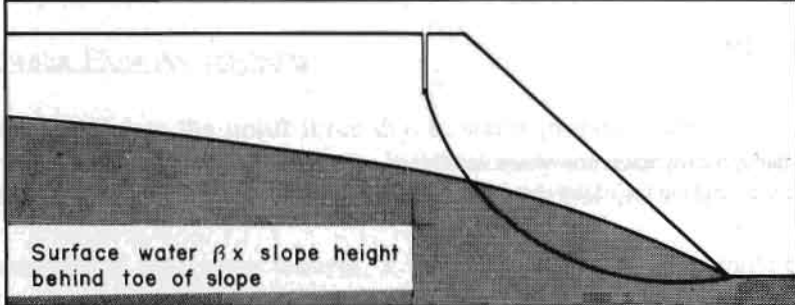
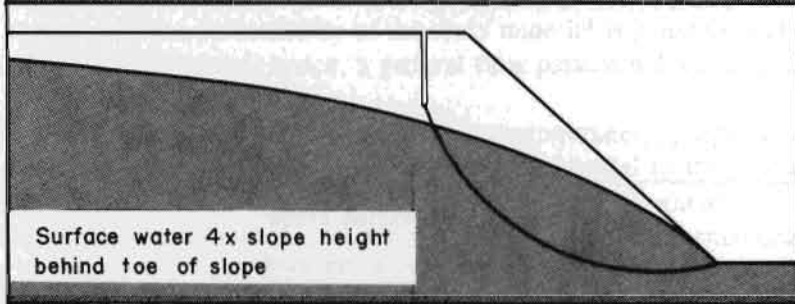
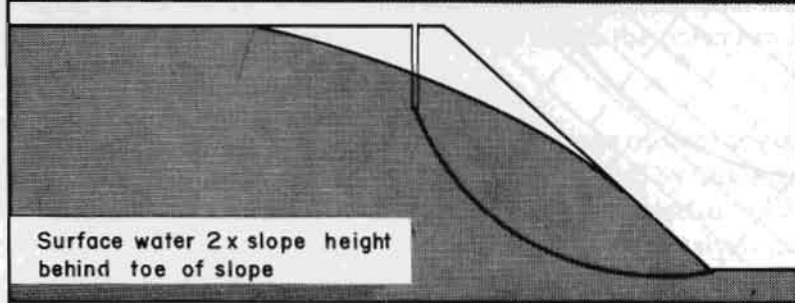
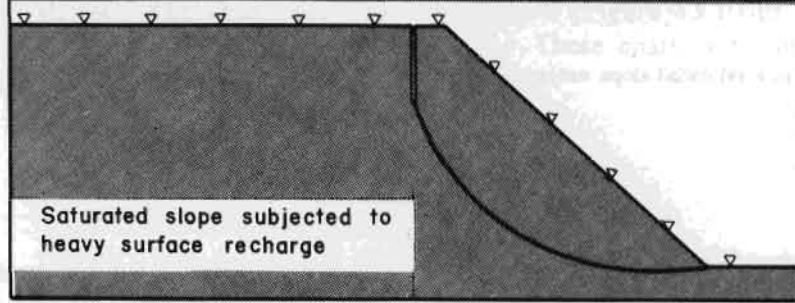


- b) Groundwater flow pattern in a saturated slope subjected to heavy surface recharge by heavy rain.

Source: USDT 1981

Fig. 13.8 Definition of groundwater flow patterns used in circular failure analysis of soil and waste rock slopes

Table 13.1 Charts corresponding to different groundwater flow conditions

GROUNDWATER FLOW CONDITIONS	CHART NUMBER
 <p>Fully drained slope</p>	1
 <p>Surface water β x slope height behind toe of slope</p>	2
 <p>Surface water 4 x slope height behind toe of slope</p>	3
 <p>Surface water 2 x slope height behind toe of slope</p>	4
 <p>Saturated slope subjected to heavy surface recharge</p>	5

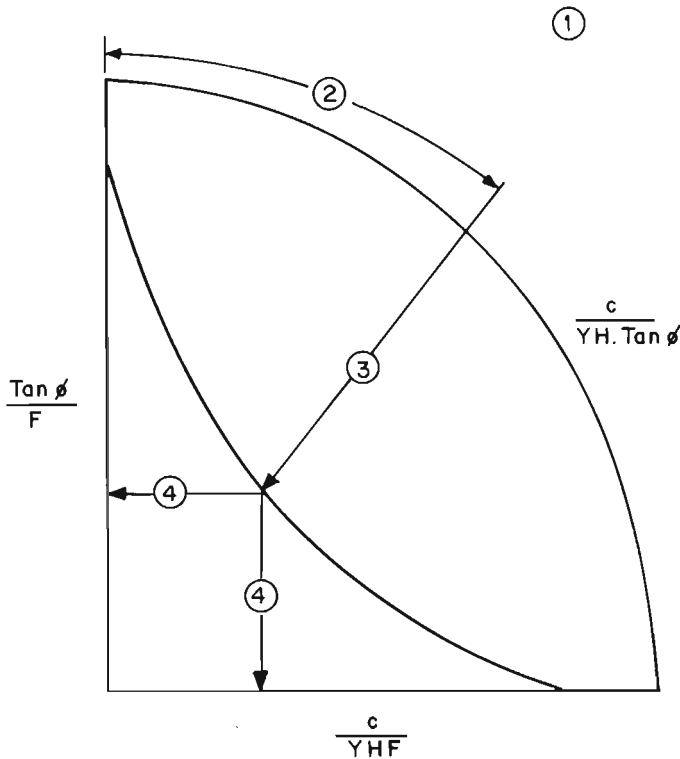
Source: USDT 1981

Use of the Circular Failure Charts

In order to use the charts to determine the factor of safety of a particular slope, the steps outlined below and shown in Figure 13.9 should be followed.

Step 1 : Assess upon the groundwater conditions of the slope and choose the chart that is closest to these conditions, using Table 13.1.

Step 2 : Calculate the value of the dimensionless ratio $c/\gamma H \tan \phi$.



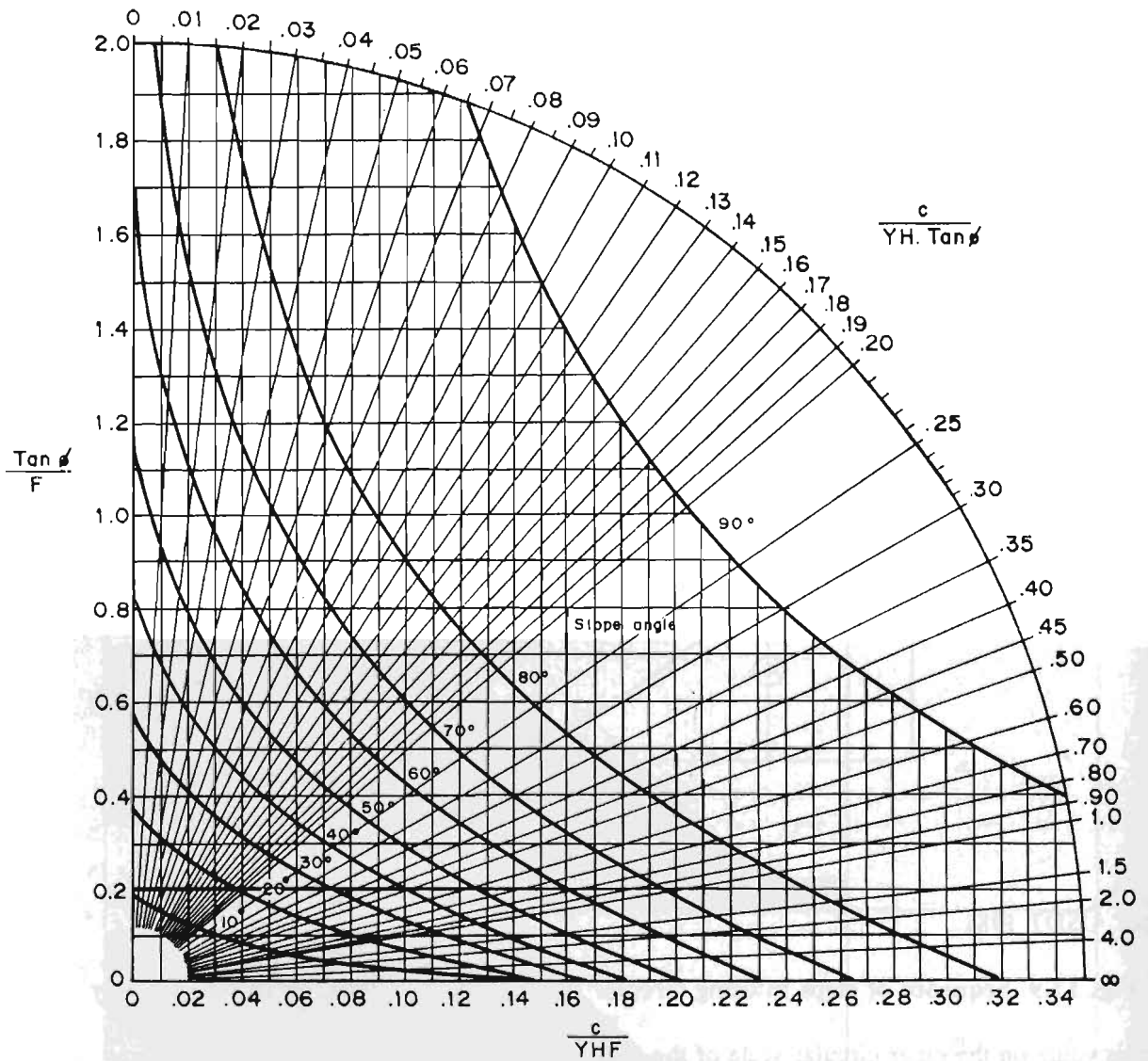
Source: USDT 1981

Fig. 13.9 Sequence of steps in using circular failure charts to find the factor of safety

Find this value on the outer circular scale of the chart.

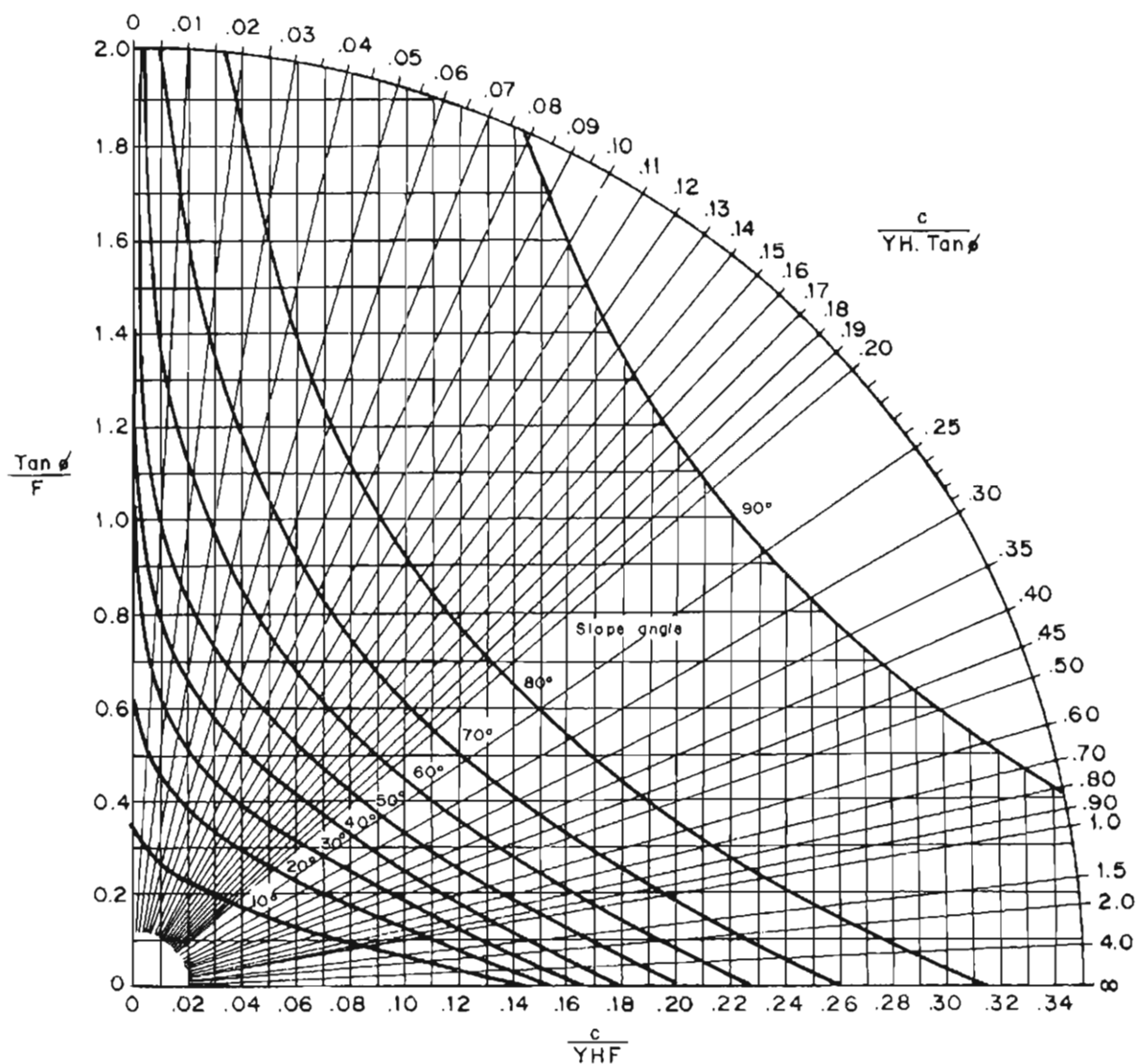
Step 3 : Follow the radial line from the value found in Step 2 to its intersection with the curve that corresponds to the slope angle under consideration.

Step 4: Find the corresponding value of $\tan \phi / F$ and calculate the factor of safety.



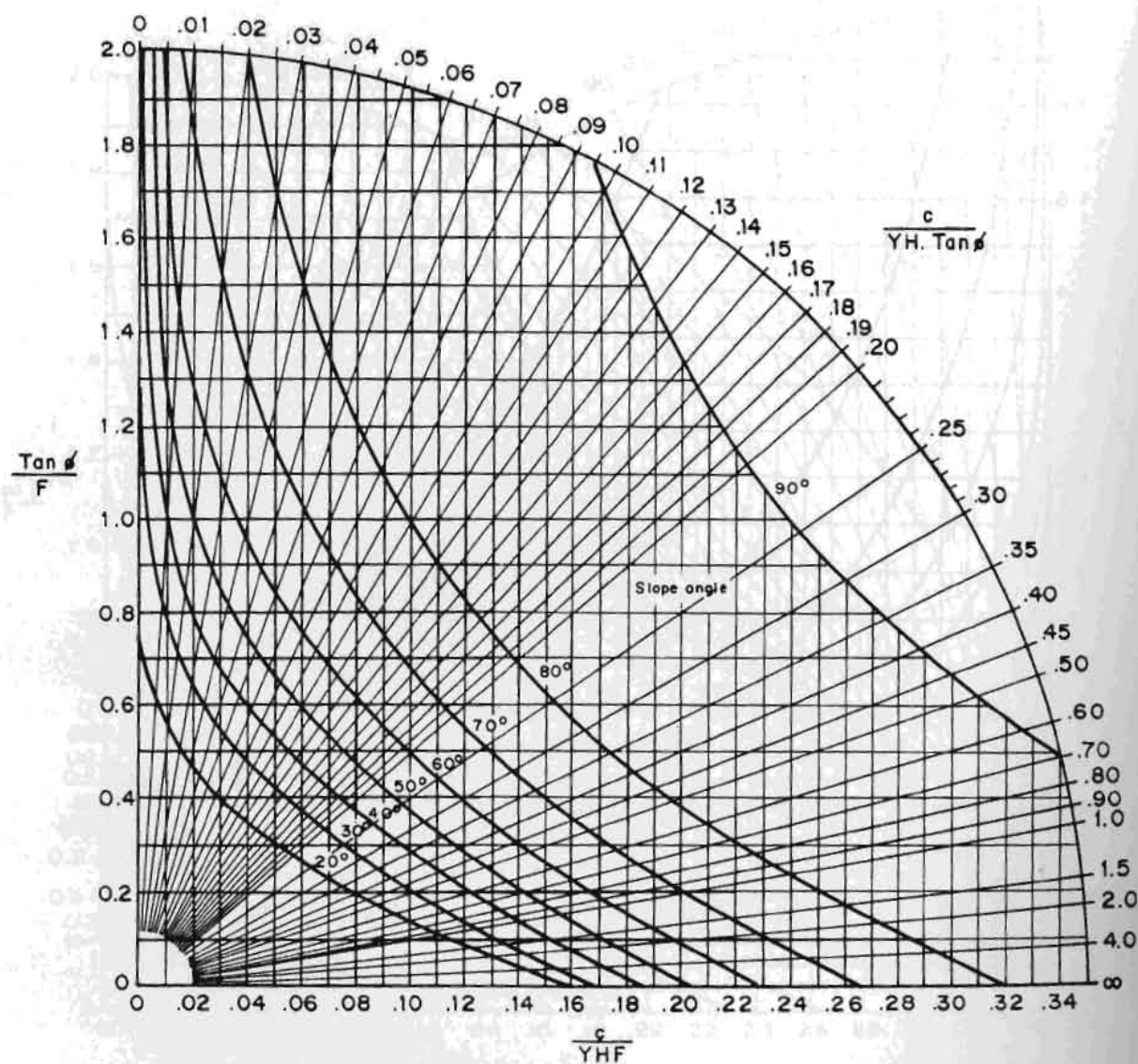
Source: USDT 1981

Fig. 13.10 Circular failure chart number 1



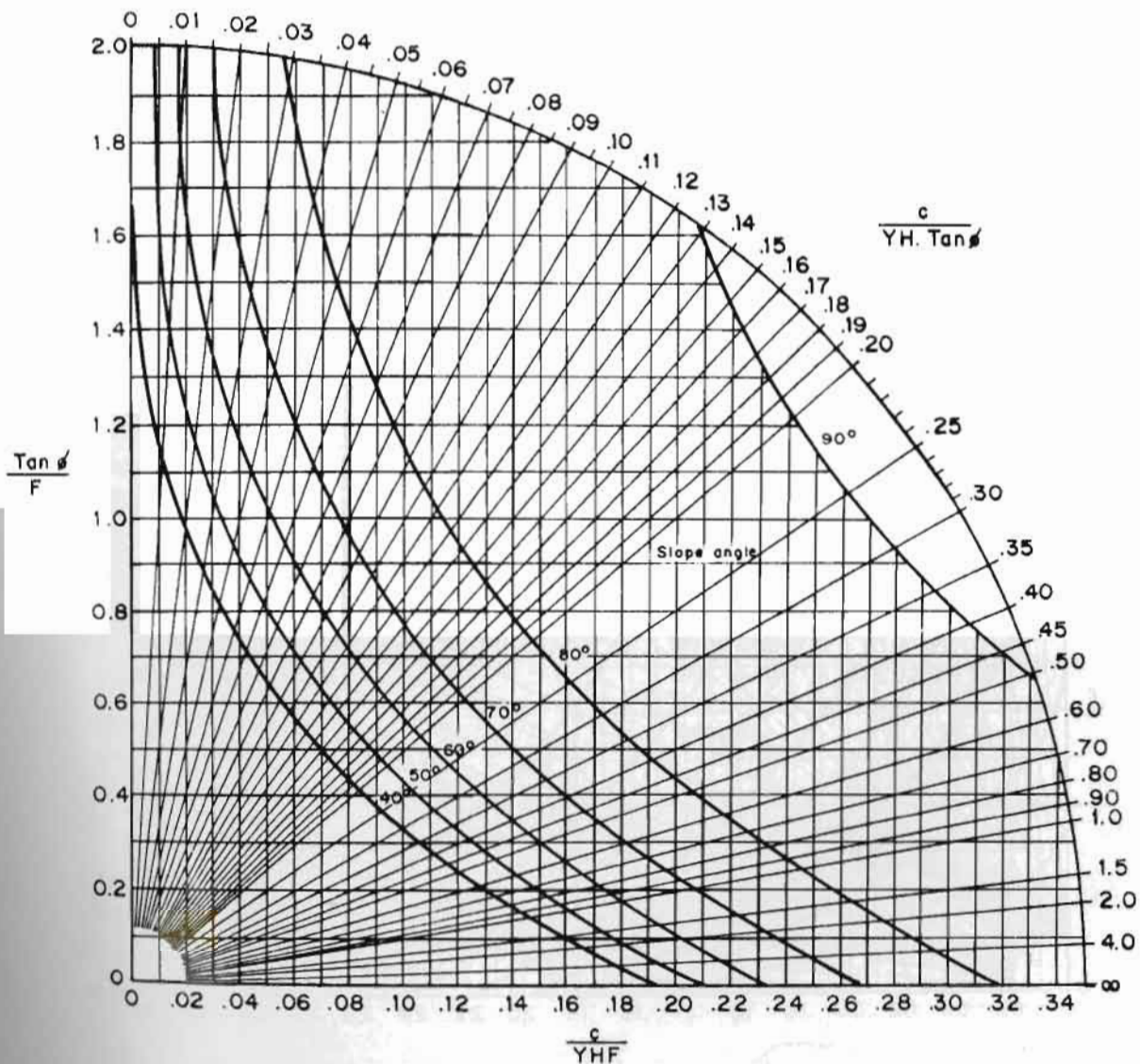
Source: USDT 1981

Fig. 13.11 Circular failure chart number 2



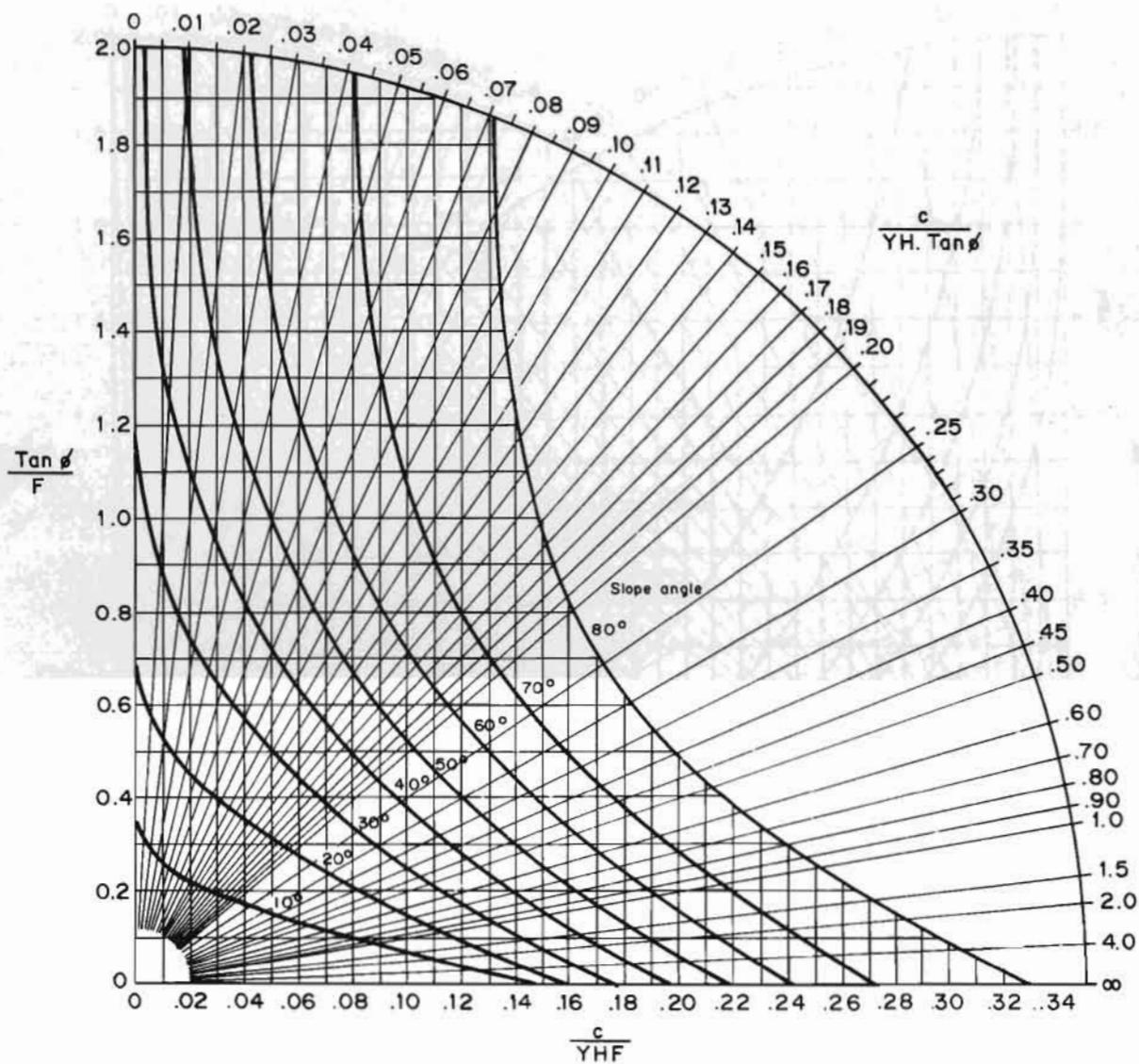
Source: USDT 1981

Fig. 13.12 Circular failure chart number 3



Source: USDT 1981

Fig. 13.13 Circular failure chart number 4



Source: USDT 1981

Fig. 13.14 Circular failure chart number 5

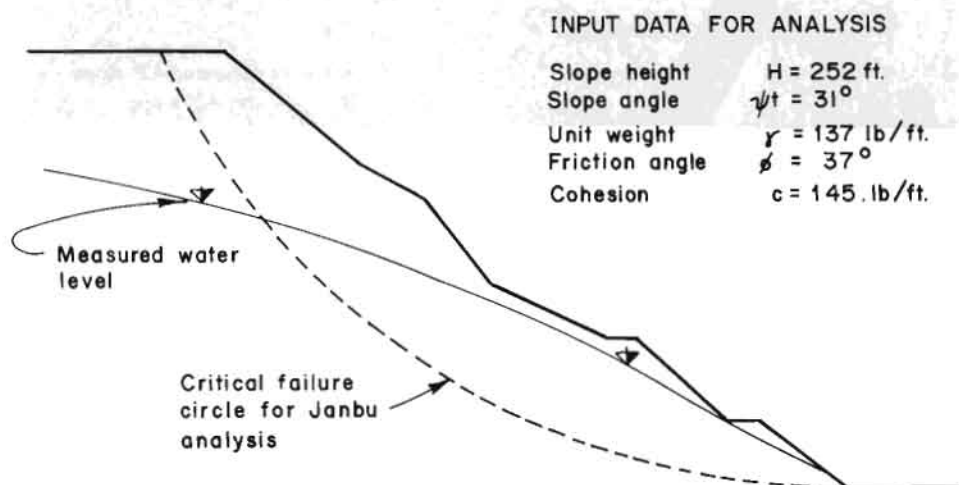
Examples

- 1) A 15 m high slope with a face angle of 40° is to be excavated in overburdened soil with a density $= 1.6 \text{ t/m}^3$, a cohesive strength of 3.9 t/m^2 and a friction angle of 30° . Find the factor of safety of the slope, assuming that there is a surface water source 60 m behind the toe of the slope.

The groundwater conditions indicate the use of Chart No. 3. The value of $c/(\gamma H \tan \phi) = 0.28$ and the corresponding value of $\tan \phi/F$, for a 40° slope, is 0.32. Hence, the factor of safety of the slope is 1.80.

- 2) China Clay Pit Slope.*** Ley (1972) has investigated the stability of a China clay pit slope which was considered to be potentially unstable. The slope profile is illustrated in Figure 13.15 and the input data used for the analysis is included in this figure. The material, a heavily kaolinized granite, was carefully tested by Ley and the friction angle and cohesive strength are considered reliable for this particular slope.

Two piezometers on the slope, and a known water source some distance behind the slope, enabled Ley to postulate the phreatic surface shown in Figure 13.15. The chart that corresponds most closely to these groundwater conditions is considered to be Chart Number 2. From the information given in Figure 13.15 the value of the ratio $c/(\gamma H \tan \phi) = 0.0056$ and the corresponding value of $\tan \phi/F$, from Chart Number 2, is 0.76. Hence, the factor of safety of the slope is 1.01. Ley also carried out a number of trial calculations using Janbu's Method (1954) and, for the critical slip circle shown in Figure 13.15, found a factor of safety of 1.03. These factors of safety indicate that the stability of the slope was inadequate under the assumed conditions and steps were taken to deal with the problem.



Source: USDT 1981

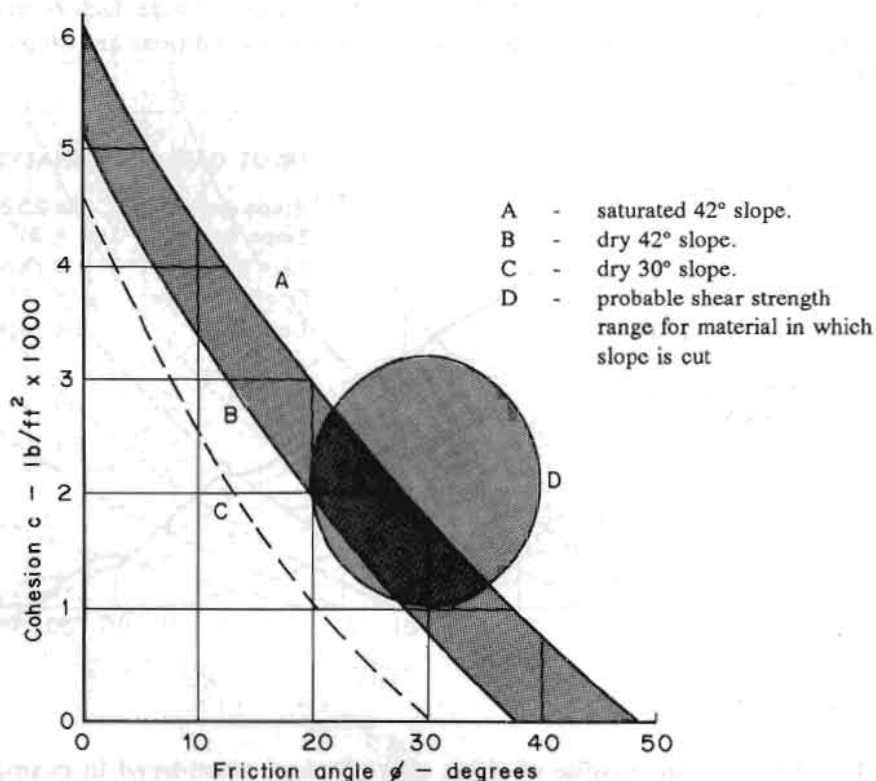
Fig. 13.15 Slope profile of china clay pit slope considered in example number 2

This section is extracted from Hoek and Bray 1981, p. 242.

- 3) **Projected Highway Slope.** A highway plan calls for a slope on one side of the highway having an angle of 42° . The total height of the slope will be 200ft when completed and it is required to check whether the slope will be stable. A site visit enables the slope engineer to assess whether the slope consists of weathered and altered material and whether failure, if it occurs, will be of a circular type. Insufficient time is available for groundwater levels to be accurately established or for shear tests to be carried out. The stability analysis is carried out as follows.

For the condition of limiting equilibrium, $F=1$ and $\tan\phi/F = \tan\phi$. For a range of friction angles, the values of $\tan\phi$ are used to find the values of $c/(\gamma H \tan\phi)$, for 42° , by reversing the procedure outlined in Figure 13.9. The value of the cohesion c , which is mobilized at failure, for a given friction angle, can then be calculated. These analyses are carried out for dry slopes, using Chart 1, and for saturated slopes, using Chart 5. The resulting range of friction angles and cohesive strengths that would be mobilized at failure are plotted in Figure 13.16 (back analysis of a slope with circular wedge failure is easily performed with the computer programme BASC).

The shaded circle included in Figure 13.16 indicates the range of shear strengths to be considered probable for the material under consideration. It is clear from this figure that the available shear strength may not be adequate to maintain stability on this slope, particularly when the slope is saturated. Consequently, the slope engineer would have to recommend that either the slope should be flattened or that investigations into the groundwater conditions and material properties should be undertaken in order to establish whether the analysis presented in Figure 13.16 is too pessimistic.



Source: USDT 1981

Fig. 13.16 Comparison between shear strength mobilized and shear strength available for the slope considered in example number 3

The effect of flattening the slope can be checked very quickly by finding the value of $c/(\gamma H \tan \phi)$ for a flatter slope, say 30° , using the same method as for the 42° slope. The dashed line in Figure 13.16 indicates the shear strength that would be mobilized in a dry slope with a face angle of 30° .

Composite Surface Sliding

In many instances, the geometric or geologic conditions of the slope are such that the surface of sliding may not be even approximately circular. For these conditions, the Method of Slices can be extended (Janbu 1954 and Nouveiller 1965).

If the subsoil contains one or more thin exceptionally weak seams, the sliding surface is likely to consist of three or more sections that do not merge smoothly one into another. In stability computations such a surface cannot be replaced by a continuous curve without the introduction of an error on the unsafe side.

Figure 13.17 represents a slope underlain by a thin layer of very soft clay with cohesion C . If such a slope fails, the slip occurs along any composite surface $abcd$. In the right-hand part of the sliding mass, represented by the area abf , active failure must be expected because the earth stretches horizontally under the influence of its own weight. The central part, $bcef$, moves to the left under the influence of the active pressure on bf . The left-hand part of the sliding mass, cde , experiences passive failure due to the thrust of the advancing central part, $bcef$.

Analysis of the failure is quite complicated. Hence experts in geotechnical engineering should be consulted for computing factors of safety. The computer programme SANC is also available for Stability Analysis of Slopes with Non-vertical Slices and Non-circular Slip Surfaces. Unlike the programme developed by Hoek, SANC converges rapidly into a realistic value of factors of safety and inter-slice forces.

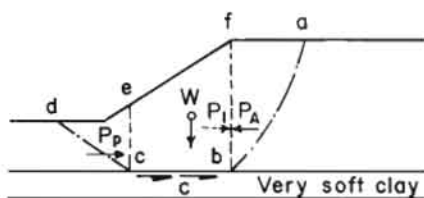


Fig. 13.17 Failure of slope underlain by thin layer of very soft clay

13.4 ROCK SLOPE STABILITY

As already discussed, failure in the soil may occur along a plane surface or curved surface. The plane failure, also called translational failure, may be in the form of debris flow or debris slide while failure along a curved surface is in the form of slumping. A major slide may be complex involving all the three conditions of flow, debris slide, and slumping.

Failures on rock slopes are in the form of planar slides, wedge slides, and topples or rockfalls. Almost all these failures are associated with existing discontinuities or joints resulting from weathering, gravitational, and tectonic forces: in many instances they are facilitated by surface and sub-surface water.

For most problems of rock slopes, the simple approach discussed in the following sections may be adequate. Analysis of a large area with several discontinuities requires the use of stereo plots. The computer programmes, Stability Analysis of Rock Slope with Plane Wedge Failure (SASP) and to determine the Factor of Safety of a Tetrahedral Wedge with Horizontal Slope Crest and with No Tension crack (SASW), based on Hoek and Bray (1981), for plane and wedge analysis may be used. The SASW Programme is for Stability Analysis of Slopes with Wedge Failure. The SASP Programme is for determining cut slope angle. These programmes take into account earthquake forces, water pressure, and submergence. The following sections aim to provide the fundamental concepts of plane and wedge slide analysis. These are based on Hoek and Bray and are extracted from "Rock Slopes" - a manual published by the United States Department of Transportation (USDT), Federal Highway Association (FHA), 1981.

13.4.1 *Plane Failure*

Introduction

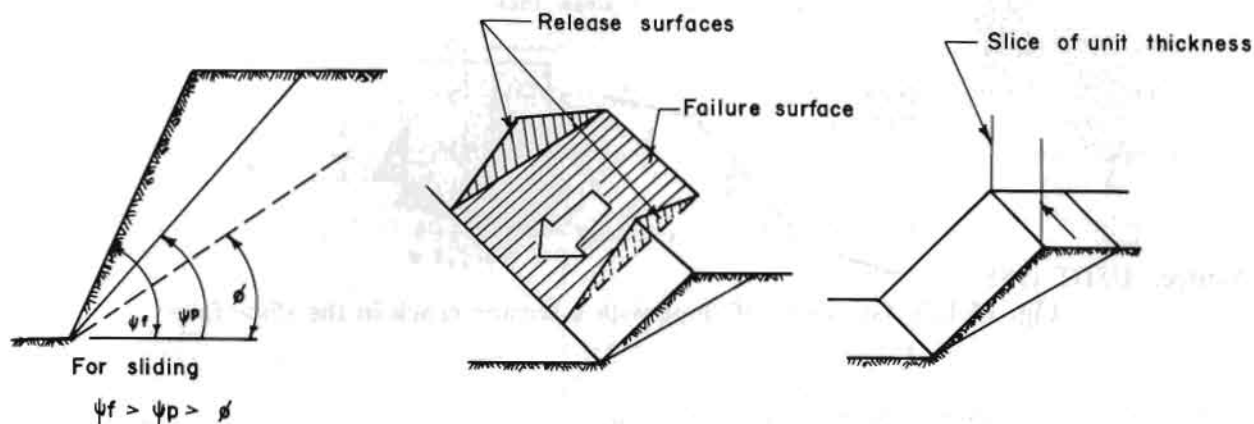
A plane failure is a comparatively rare phenomenon in rock slopes because it is only occasionally that all the geometrical conditions required to produce such a failure occur in an actual slope. The wedge type of failure is a much more general case and many rock slope engineers treat the plane failure as a special case of the more general wedge failure analysis.

While this is probably the correct approach for the experienced slope designer, who has a wide range of design tools at his disposal, it would not be right to ignore the two-dimensional case in this general discussion on slope failure. There are many valuable lessons to be learned from a consideration of the mechanics of this simple failure mode and it is particularly useful for demonstrating the sensitivity of the slope to changes in shear strength and groundwater conditions - changes that are less obvious when dealing with the more complex mechanics of a three-dimensional slope failure.

General Conditions for Plane Failure

For sliding to occur on a single plane, the following geometrical conditions must be present (Fig. 13.18).

- The plane on which sliding occurs must strike parallel or nearly parallel (within approximately 20°) to the slope face.
- The failure plane must 'daylight' on the slope face. This means that its dip must be smaller than the dip of the slope face, i.e., $\psi_f > \psi_p$.
- Release surfaces that provide negligible resistance to sliding must be present in the rock mass to define lateral boundaries of the slide. Alternatively, failure can occur on a failure plane passing through the convex 'nose' of a slope.



Source: USDT 1981

Figure 13.18 Plane failure

In analyzing two-dimensional slope problems, it is usual to consider a slice of unit thickness taken at right angles to the slope face. This means that the area of the sliding surface can be represented by the length of the surface visible on a vertical section, although the slope and the volume of the sliding block are represented by the area of the figure representing this block on the vertical section.

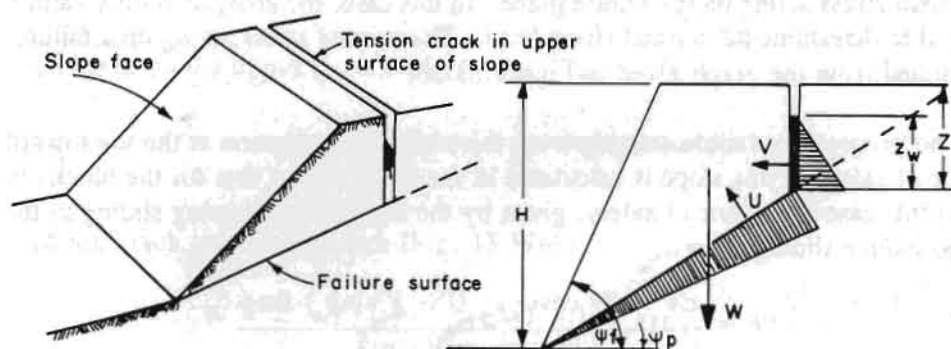
Plane Failure Analysis

The geometry of the slope considered in this analysis is defined in Figure 13.19. Note that two cases must be considered.

- A. A slope having a tension crack on its upper surface.
- B. A slope with a tension crack in its face.

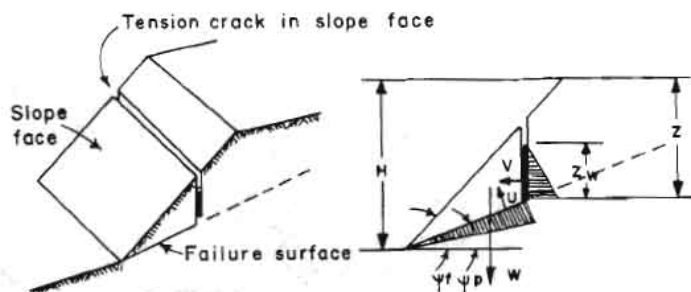
The transition from one case to another occurs when the tension crack coincides with the slope crest, i.e., when:

$$Z/H = (1 - \cot \psi_f \cdot \tan \psi_p) \quad (13.11)$$



Source: USDT 1981

Fig. 13.19a Geometry of a slope with a tension crack on the upper slope surface



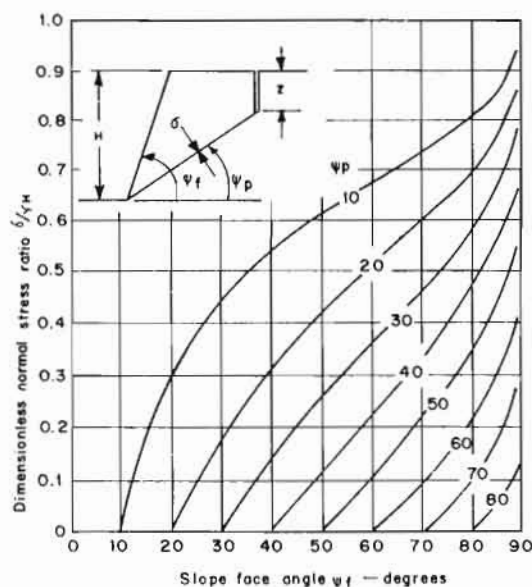
Source: USDT 1981

Fig. 13.19b Geometry of slope with a tension crack in the slope face

The following assumptions are made in this analysis:

- Both sliding surface and tension crack strike parallel to the slope surface.
- The tension crack is vertical and is filled with water to a depth z_w .
- Water enters the sliding surface along the base of the tension crack and seeps along the sliding surface, escaping at atmospheric pressure where the sliding surface daylights on the slope face. The pressure distribution induced by the presence of water in the tension crack and along the sliding surface is illustrated in Figure 13.19. It is assumed that the slope is not covered by snow or clay.
- The forces W (the weight of the sliding block), U (uplift force caused by water pressure on the sliding surface), and V (force caused by water pressure in the tension crack) all act through the centroid of the sliding mass. In other words, it is assumed that there are no moments that would tend to cause rotation of the block and hence failure is by sliding only. While this assumption may not be strictly true for actual slopes, the errors introduced by ignoring moments are small enough to neglect. However, on steep slopes with steeply dipping discontinuities, the possibility that toppling failure may occur should be kept in mind.
- The shear strength of the sliding surface is defined by cohesion c and a friction angle ϕ which are related by the equation $\tau = c + \sigma \tan \phi$. In the case of a rough surface having a curvilinear shear strength curve, the apparent cohesion and apparent friction angle, defined by a tangent to the curve, are used. This tangent should touch the curve at a normal stress value which corresponds to the normal stress acting on the failure plane. In this case, the analysis is only valid for the slope height used to determine the normal stress level. The normal stress acting on a failure surface can be determined from the graph given in Figure 13.20.
- There is no progressive failure starting from the stress concentration at the toe towards the crest. The factor of safety of this slope is calculated in the same way as that for the block on an inclined plane. In this case the factor of safety, given by the total force resisting sliding to the total force tending to induce sliding, is:

$$F = \frac{cA + (W \cos \psi_p - U - V \sin \psi_p) \tan \phi}{W \sin \psi_p + V \cos \psi_p} \quad (13.12)$$



$$\frac{\sigma}{\gamma H} = \frac{\{(1 - (z/H)^2) \cot \psi_p - \cot \psi_f\} \sin \psi_p}{2(1 - z/H)}$$

$$\text{Where } z/H = 1 - \sqrt{\cot \psi_f \tan \psi_p}$$

Source: USDT 1981

Fig. 13.20 Normal stress acting on the failure plane on a rock slope

where, from Figure 13.19:

$$A = (H - Z) \cdot \operatorname{cosec} \psi_p \quad (13.13)$$

$$U = \frac{1}{2} \gamma_w Z_w (H - Z) \cdot \operatorname{cosec} \psi_p \quad (13.14)$$

$$V = \frac{1}{2} \gamma_w Z^2 W \quad (13.15)$$

For the tension crack on the upper slope surface (Fig. 13.19a)

$$W = \frac{1}{2} \gamma H^2 \left[\left(1 - \frac{Z}{H}\right)^2 \cot \psi_p - \cot \psi_f \right] \quad (13.16)$$

and for the tension crack in the slope face (Fig. 13.19b)

$$W = \frac{1}{2} \gamma H^2 \left[\left(1 - \frac{Z}{H}\right)^2 \cot \psi_p (\cot \psi_p \tan \psi_f - 1) \right] \quad (13.17)$$

In the preceding discussion it has been assumed that it is only the water present in the tension crack and the water along the failure surface that influence the stability of the slope. This is equivalent to assuming that the rest of the rock mass is impermeable, an assumption that is certainly not always justified. Consideration must, therefore, be given to water pressure distribution; other than that upon which the analysis so far presented has been based.

The current state of knowledge in rock engineering does not permit a precise definition of the groundwater flow patterns in a rock mass. Consequently, the only possibility open to the slope designer is to consider a number of realistic extremes in an attempt to bracket the range of possible factors of safety and to assess the sensitivity of the slope to variations in groundwater conditions.

a. Dry Slopes

The simplest case which can be considered is that in which the slope is assumed to be completely drained. In practical terms, this means that there is no water pressure in the tension crack or along the sliding surface. Note that there may be moisture in the slope but, as long as no pressure is generated, it will not influence the stability of the slope. Under these conditions, the forces V and U are both zero and equation 13.12 reduces to:

$$F = \frac{c.A}{W.\sin\psi_p} + \cot\psi_p.\tan\phi \quad (13.18)$$

b. Water in Tension Crack and on Sliding Surface

These are the conditions that were assumed in deriving the general solution presented on the preceding pages. The pressure distribution along the sliding surface has been assumed to decrease linearly from the base of the tension crack to the intersection of the failure surface and the slope face. This water pressure distribution is probably very much simpler than that which occurs on an actual slope but, since the actual pressure distribution is unknown, this assumed distribution is as reasonable as any other that can be made.

It is possible that a more dangerous water pressure distribution could exist if the face of the slope became frozen in winter so that, instead of the zero pressure condition which has been assumed at the face, the water pressure at the face would be that caused by the full head of water in the slope. Such extreme water pressure conditions may occur from time to time and the slope designer should keep this possibility in mind. However, for general slope design, the use of this water pressure distribution would result in an excessively conservative slope and hence the triangular pressure distribution used in the general analysis is presented as the basis for normal slope design.

In the case of partly submerged rock slopes, it is found that the factor of safety is slightly increased as the effective weight of the plane wedge is reduced. However in seismic cases, the factor of safety is likely to decrease.

c. Saturated Slope with Heavy Recharge

If the rock mass is heavily fractured, so that it becomes relatively permeable, a groundwater flow pattern similar to that which would develop in a porous system could occur. The most dangerous conditions that would develop in this case would be those created by prolonged heavy rainfall.

Flow nets for saturated slopes with heavy surface recharge have been constructed and the water pressure distributions obtained from these flow nets have been used to calculate the factors of safety of a variety of slopes. The process involved is too lengthy to include in this chapter, but the results can be summarized in a general form. It has been found that the factor of safety for a permeable slope, saturated by heavy rain and subjected to surface recharge by continued rain, can be approximated by Equation 13.12 assuming that the tension crack is water-filled, i.e., $Z_w = Z$.

In view of the uncertainties associated with the actual water pressure distributions, which could occur in rock slopes subjected to these conditions, this analysis has not been further refined here.

Critical Tension Crack Depth

In the analysis that has been presented, it has been assumed that the position of the tension crack is known from its visible trace on the upper surface or on the face of the slope and that its depth can be established by constructing an accurate cross-section of the slope. When the tension crack position is unknown, because, for example, of the presence of soil on the top of the slope, it becomes necessary to consider the most probable position of a tension crack.

The influence of tension crack depth, and of the depth of water in the tension crack, upon the factor of safety of a typical slope is illustrated in Figure 13.21.

When the slope is dry or nearly dry, the factor of safety reaches a minimum value that, in the case of the example considered, corresponds to a tension crack depth of $0.42H$. This critical tension crack depth for a dry slope can be found by minimizing the right-hand side of Equation 13.18 with respect to Z/H .

This gives the critical tension crack depth as:

$$\frac{Z_c}{H} = 1 - \sqrt{\cot \psi_f \tan \psi_p} \quad (13.19)$$

From the geometry of the slope (Fig. 13.19) the corresponding position of the tension crack is:

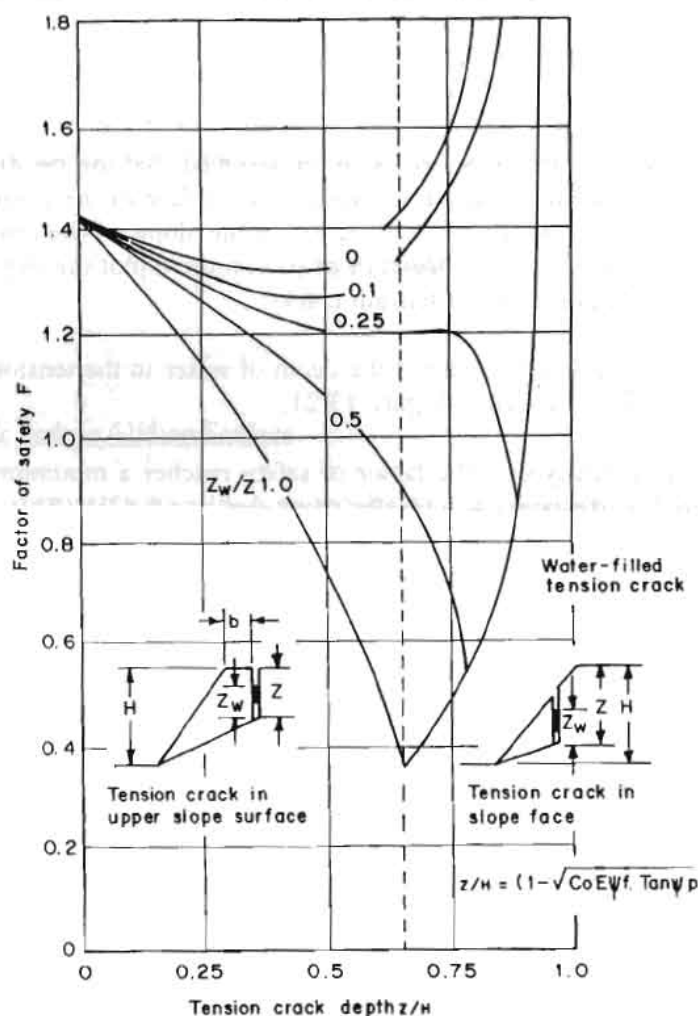
$$\frac{b_c}{H} = \sqrt{\cot \psi_f \cot \psi_p} - \cot \psi_f \quad (13.20)$$

Figure 13.21 shows that, once the water level Z_w exceeds about one quarter of the tension crack depth, the factor of safety of the slope does not reach a minimum until the tension crack is water-filled. In this case, the minimum factor of safety is given by a water-filled tension crack which is coincident with the crest of the slope ($b=0$).

It is most important, when considering the influence of water in a tension crack, to consider the sequence of tension crack formation and water filling. Field observations suggest that tension cracks usually occur

behind the crest of a slope and, from Figure 13.21, it must be concluded that these tension cracks occur as a result of movement in a dry or nearly dry slope. If this tension crack becomes water-filled, as the result of a subsequent rainstorm, the influence of the water pressure will be in accordance with the rules laid down earlier in this chapter. The depth and location of the tension crack are, however, independent of the groundwater conditions and are defined by Equations 13.19 and 13.20.

If the tension crack forms during heavy rain, or if it is located on a pre-existing geological feature such as a vertical joint, Equations 13.19 and 13.20 no longer apply. In these circumstances, when the tension crack position and depth are unknown, the only reasonable procedure is to assume that the tension crack is coincident with the slope crest and that it is water-filled. It may be noted that Equation 13.19 predicts the ratio of depth of tension crack and slope height to be unity for vertical slopes or cuts. In fact, this ratio is seldom more than 0.5.



Source: USDT 1981

Fig. 13.21 Influence of tension crack depth and of depth of water in the tension crack upon the factor of safety of a slope

The Tension Crack as An Indicator of Instability

Anyone who has examined excavated rock slopes cannot have failed to notice the frequent occurrence of tension cracks on the upper surfaces of these slopes. Some of these cracks have been visible for a number of years and, in many cases, do not appear to have had any adverse influence upon the stability of the slope. It is, therefore, interesting to consider how such cracks are formed and whether they can give any indication of slope instability.

In a series of very detailed model studies on the failure of slopes in jointed rocks, Barton (Barton and Chaubey 1977) found that the tension crack was generated as a result of small shear movements within the rock mass. Although these individual movements were very small, their cumulative effect was a significant displacement of the slope surfaces - sufficient to cause separation of vertical joints behind the slope crest and to form 'tension' cracks. The fact that the tension crack is caused by shear movements in the slope is important because it suggests that it must be assumed that shear failure initiated within the rock mass.

It is impossible to quantify the seriousness of this failure since it is only the start of a very complex progressive failure process about which very little is known. It is quite probable that, in some cases, the improved drainage resulting from the opening up of the rock structure, and the interlocking of individual blocks within the rock mass, could give rise to an increase in stability. In other cases, the initiation of failure could be followed by a very rapid decrease in stability with consequent failure of the slope.

In summary, Hoek and Bray 1981 recommend that the presence of a tension crack should be taken as an indication of potential instability and that, in the case of an important slope, this should signal the need for detailed investigation into the stability of that particular slope.

Critical Failure Plane Inclination

When a through-going discontinuity, such as a bedding plane, exists in a slope and the inclination of this discontinuity is such that it satisfies the conditions for plane failure, the failure of the slope will be controlled by this feature. However, when no such feature exists and when a failure surface, if it were to occur, would follow minor geological features and, in some places, would pass through intact material, how could the inclination of such a failure path be determined?

The first assumption that must be made concerns the shape of the failure surface. On a soft rock slope, or a soil slope with a relatively flat slope face ($\psi_f < 45^\circ$), the failure surface would have a circular shape. The analysis of such failure surfaces will be dealt with as for soils.

In steep rock slopes, the failure surface is almost planar and the inclination of such a plane can be found by partial differentiation of Equation 13.12 with respect to ψ_p and by equating the resulting differential to zero. For dry slopes this gives the critical failure plane inclination ψ_{pc} as:

$$\psi_{pc} = \frac{1}{2} (\psi_f + \phi) \quad (13.21)$$

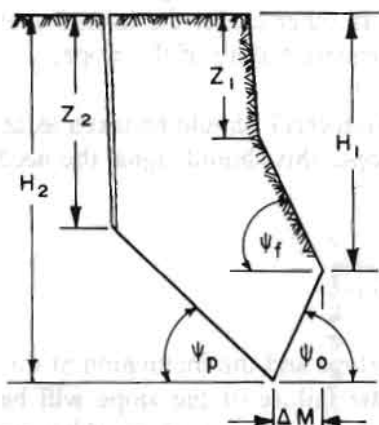
The presence of water in the tension crack will cause the failure plane inclination to be reduced by up to 10 per cent and, in view of the uncertainties associated with this failure surface, the added complication

of including the influence of groundwater is not considered justified. Consequently, Equation 13.21 can be used to obtain an estimate of the critical failure plane inclination on steep slopes which do not contain through-going discontinuity surfaces.

Influence of Undercutting of the Toe of a Slope

It is not unusual for the toe of a slope to be undercut, either intentionally by excavation or by natural agencies such as the weathering of underlying soft strata or, in the case of sea cliffs, by the action of waves. The influence of such undercutting on the stability of a slope is important in many practical situations and an analysis of this stability is presented here.

In order to generalise the solution, it is assumed that the geometry of the slope is that illustrated in Figure 13.22. A previous failure is assumed to have left a face inclined at ψ_f and a vertical tension crack depth Z_1 . As a result of an undercut of ΔM , inclined at an angle ψ_o , a new failure occurs on a plane inclined at ψ_p and involves the formation of a new tension crack of depth Z_2 .



Source: USDT 1981

Fig. 13.22a Geometry of undercut slope

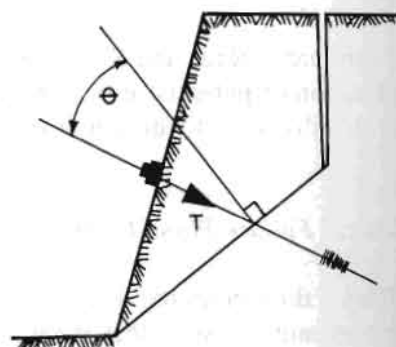


Fig. 13.22b Reinforcement of a slope

The factor of safety of this slope is given by Equation 13.12 but it is necessary to modify the expression for the weight terms as follows:

$$W = \frac{1}{2} \gamma [(H_2^2 - Z_2^2) \cot \psi_p - (H_1^2 - Z_1^2) \cot \psi_f + (H_1 + H_2) \Delta M] \quad .$$

(13.22)

Note that, for $\psi_o > 0$,

$$\Delta M = (H_2 - H_1) \cot \psi_o \quad .$$

(13.23)

The critical tension crack depth for a dry undercut slope is:

$$Z_2 = \frac{c \cdot \cos \phi}{\gamma \cos \psi_p \cdot \sin (\psi_p - \phi)} \quad (3.24)$$

Reinforcement of a Slope

When it has been established that a particular slope is unstable, it becomes necessary to consider whether it is possible to stabilize the slope by drainage or by the application of external loads. Such external loads may be applied by the installation of rock bolts or cables anchored into the rock mass behind the failure surface or by the construction of waste rock berm to support the toe of the slope.

The factor of safety of a slope, with external loading of magnitude T , inclined at an angle θ to the failure plane as shown in the Figure 13.22b is approximated by:

$$F = \frac{cA + (W \cdot \cos \psi_p - U - V \cdot \sin \psi_p + T \cdot \cos \theta) \tan \phi}{W \cdot \sin \psi_p + V \cdot \cos \psi_p - T \cdot \sin \theta} \quad (13.25)$$

This equation is correct for the condition of limiting equilibrium ($F=1$) but there are certain theoretical problems in using it for other values of F .

Computer Programmes

The following programmes are available for rapid computation of factors of safety and design of remedial measures:

- (i) SASP is for the stability analysis of slopes with plane wedge failure. It also gives designs of drainage systems and/or rock anchor systems as the situation demands.
- (ii) SARP is for the stability analysis of reservoir slopes with plane wedge failure.
- (iii) ASP is for determining cut slope angle of slope with plane wedge failure. It accounts for the radius of slope curvature in the plan.
- (iv) BASP is for the back analysis of slopes with plane wedge failure.

All programmes take earthquake forces and the non-linear strength criteria of Barton into account.

13.4.2 Wedge Failure

Introduction

The previous section was concerned with slope failure resulting from sliding on a single planar surface

dipping into the excavation and striking parallel, or nearly parallel, to the slope face. It was stated that the plane failure analysis is valid provided that the strike of the failure plane is within 20° of the strike of the slope face. This section is concerned with the failure of slopes in which there are structural features upon which sliding can occur and strike across the slope crest and where sliding takes place along the line of intersection of two such planes.

In this section, the basic mechanics of failure, involving the sliding of a wedge along the line of intersection of two planar discontinuities, are presented in a form that the non-specialist reader should find easy to follow. Unfortunately the very simple equations which are presented to illustrate the mechanics are of limited practical value because the variables used to define the wedge geometry cannot easily be measured in the field.

Consequently, the second part of this section deals with stability analysis in terms of the dips and dip directions of the planes and the slope face. In the transformation of the equations, which is necessary in order to accommodate this information, the basic mechanics become obscure but it is hoped that the reader will be able to follow the logic involved in the development of these equations.

In this section, discussion is limited to the case of the sliding of a simple wedge acted upon by friction, cohesion, and water pressure. The influence of a tension crack and of external forces because of bolts, cables, or seismic accelerations result in a significant increase in the complexity of the equations and, since it would only be necessary to consider these influences on the fairly rare occasions when the critical slopes are being examined, the complex solution to the problem is not included and the interested reader may refer to "Rock Slope Engineering", by Hoek and Bray, 1981, or other relevant books.

Definition of Wedge Geometry

The geometry of the wedge, for the purpose of analyzing the basic mechanics of sliding, is defined in Figure 13.23. Note that, throughout this section, the flatter of the two planes is called Plane A while the steeper plane is called Plane B.

As in the case of plane failure, a condition of sliding is defined by $\psi_f > \psi_i > \phi$, where ψ_f is the inclination of the slope face, measured in the view at right angles to the line of intersection, and ψ_i is the dip of the line of intersection. Note that ψ_f would only be the same as the true dip of the slope face if the dip direction of the line of intersection was the same as the dip direction of the slope face.

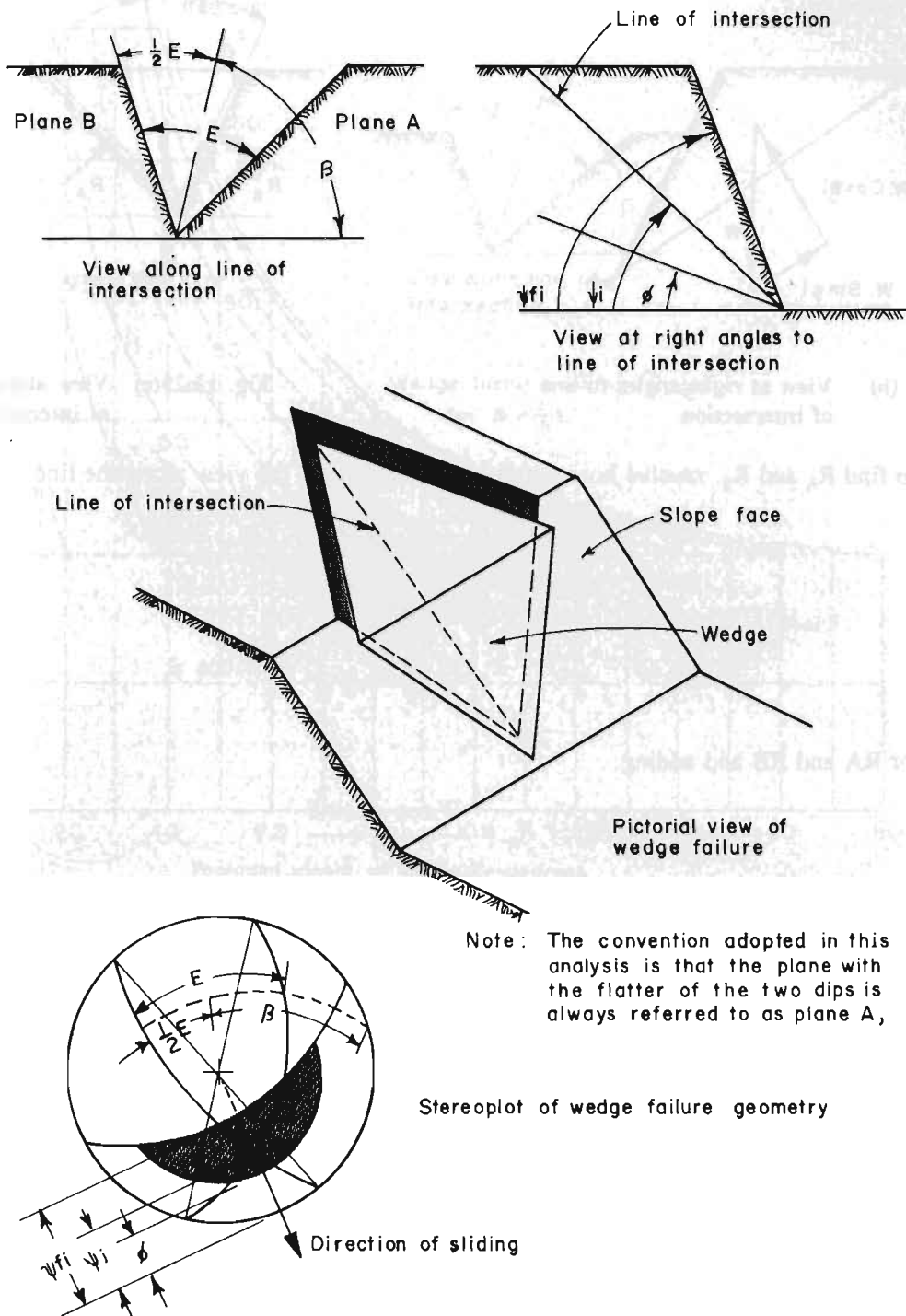
Analysis of Wedge Failure

The factor of safety of the wedge defined in Figure 13.23b and c assuming that sliding is resisted by friction only and that the friction angle ϕ is the same for both planes, is given by:

$$F = \frac{(R_A + R_B) \tan \phi}{W \sin \psi_i} \quad (13.26)$$

where,

R_A and R_B are the normal reactions provided by planes A and B as illustrated in the sketch below.



Source: USDT 1981

Fig. 13.23a Wedge failure geometry

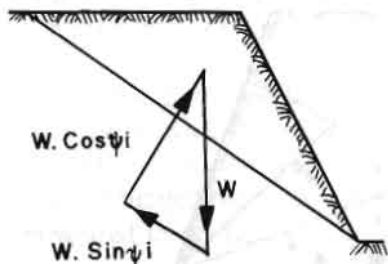


Fig. 13.23 (b) View at right angles to line of intersection

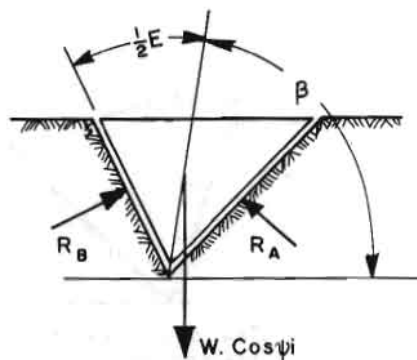


Fig. 13.23(c) View along line of intersection

In order to find R_A and R_B , resolve horizontally and vertically in the view along the line of intersection:

$$R_A \cdot \sin \left(\beta - \frac{1}{2} \xi \right) = R_B \cdot \sin \left(\beta + \frac{1}{2} \xi \right) \quad (13.27)$$

$$R_A \cdot \cos \left(\beta - \frac{1}{2} \xi \right) - R_B \cdot \cos \left(\beta + \frac{1}{2} \xi \right) = W \cdot \cos \psi_i \quad (13.28)$$

Solving for R_A and R_B and adding:

$$R_A + R_B = \frac{W \cdot \cos \psi_i \cdot \sin \beta}{\sin \frac{1}{2} \xi} \quad (13.29)$$

Hence,

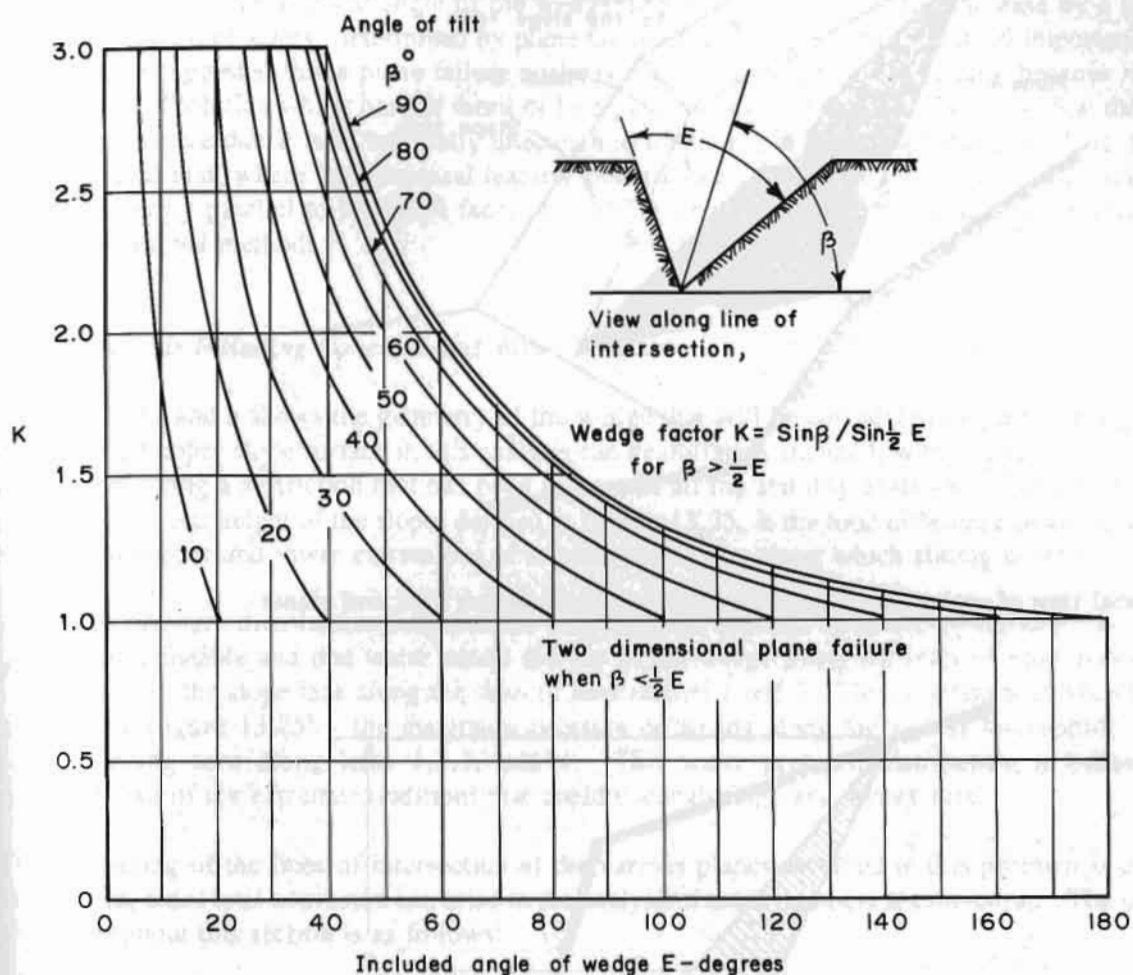
$$F = \frac{\sin \beta}{\sin \frac{1}{2} \xi} \cdot \frac{\tan \phi}{\tan \psi_i} \quad (13.30)$$

In other words:

$$F_w = K \cdot F_p \quad (13.31)$$

Where F_w is the factor of safety of a wedge supported by friction only, F_p is the factor of safety of plane failure in which the slope face is inclined at ψ_f and the failure plane is inclined at ψ_i .

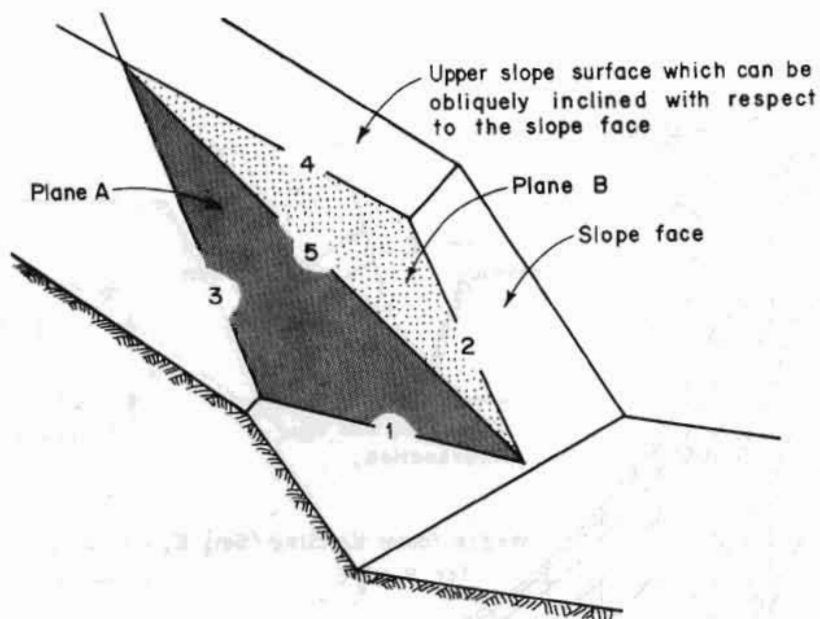
K is the wedge factor which, as shown by Equation 13.30 depends upon the included angle of the wedge and upon the angle of tilt of the wedge. Values for the wedge factor, K , for a range of values of β and ξ , are plotted in Figure 13.24.



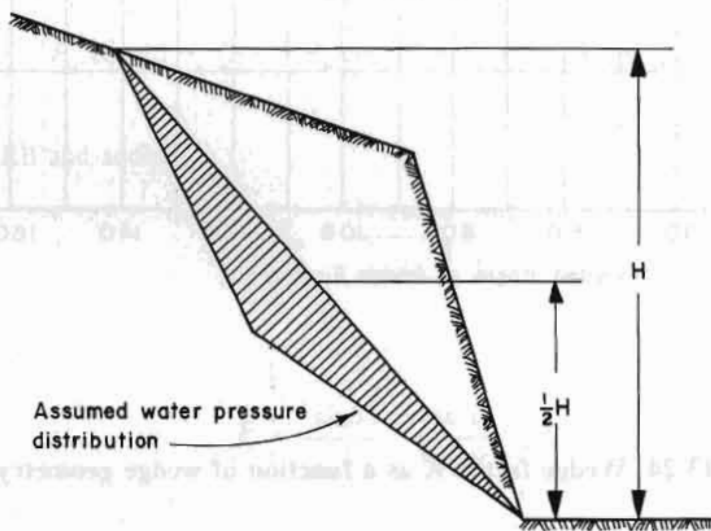
Source: USDT 1981

Fig. 13.24 Wedge factor K as a function of wedge geometry

As shown in the stereoplot given in Figure 13.23a, measurement of the angles β and ξ can be carried out on the great circle, the pole of which is the point representing the line of intersection of the two planes. Hence, a stereoplot of the features that define the slope and the wedge geometry can provide all the information required for the determination of the factor of safety. It should, however, be remembered that the case that has been dealt with is very simple and that, when different friction angles and the influence of cohesion and water pressure are allowed for, the equations become more complex. Rather than develop these equations in terms of the angles β and ξ , which cannot be measured directly in the field, the more complete analysis is presented in terms of directly measurable dips and dip directions.



a) Pictorial view of wedge showing the numbering of intersection lines and planes



b) View normal to the line of intersection 5 showing the total wedge height and the water pressure distribution

Source: USDT 1981

Fig. 13.25 Geometry of wedge used for stability analysis including the influence of cohesion and of water pressure on the failure surfaces

Before leaving this simple analysis, the reader's attention is drawn to the important influence of the wedging action as the included angle of the wedge decreases below 90°. The increase by a factor of 2 or 3 on the factor of safety, determined by plane failure analysis, is of great practical importance. Some experts have suggested that a plane failure analysis is acceptable for all rock slopes because it provides a lower bound solution which has the merit of being conservative. Figure 13.24 shows that this solution is so conservative that it is to be totally uneconomic for most practical slope designs. It is, therefore, recommended that, where the structural features that are likely to control the stability of a rock slope do not strike nearly parallel to the slope face, the stability analysis should be carried out by means of the three-dimensional method.

Wedge Analysis Including Cohesion and Water Pressure

Figure 13.25a and b shows the geometry of the wedge that will be considered in the following analysis. Note that the upper slope surface in this analysis can be obliquely inclined, with respect to the slope face, thereby removing a restriction that has been present in all the stability analyses discussed so far in this section. The total height of the slope, defined in Figure 13.25, is the total difference in vertical elevation between the upper and lower extremities of line of intersection along which sliding is assumed to occur.

The water pressure distribution, assumed for this analysis, is based upon the hypothesis that the wedge itself is impermeable and that water enters the top of the wedge along the lines of Intersection 3 and 4 and leaks from the slope face along the lines of Intersection 1 and 2. The resulting pressure distribution is shown in Figure 13.25b - the maximum pressure occurring along the line of Intersection 5 and the pressure being zero along lines 1,2,3, and 4. This water pressure distribution is believed to be representative of the extreme conditions that could occur during very heavy rain.

The numbering of the lines of intersection of the various planes involved in this problem is of extreme importance, since total confusion can arise in the analysis if these numbers are mixed-up. The numbering used throughout this section is as follows:

- 1 - intersection of plane A with the slope face,
- 2 - intersection of plane B with the slope face,
- 3 - intersection of plane A with the upper slope surface,
- 4 - intersection of plane B with the upper slope surface, and
- 5 - intersection of planes A and B.

It is assumed that sliding of the wedge always takes place along the line of the intersection numbered 5.

The factor of safety of this slope is derived from the detailed analysis of this problem published by Hoek and Bray (1981).

$$F = \frac{3}{\gamma H} (c_A \cdot X + c_B \cdot Y) + (A - \frac{\gamma_w}{2\gamma} \cdot X) \tan \phi_A + (B - \frac{\gamma_w}{2\gamma} \cdot Y) \tan \phi_B \quad (13.32)$$

where,

c_A and c_B are the cohesive strengths of planes A and B,

ϕ_A and ϕ_B are the angles of friction on planes A and B,

γ is the unit weight of the rock,

γ_w is the unit weight of water, and

H is the total height of the wedge (Fig. 13.25b).

X, Y, A, and B are dimensionless factors that depend upon the geometry of the wedge.

$$X = \frac{\sin \theta_{24}}{\sin \theta_{45} \cdot \cos \theta_{2na}} \quad (13.33)$$

$$Y = \frac{\sin \theta_{13}}{\sin \theta_{35} \cdot \cos \theta_{1nb}} \quad (13.34)$$

$$A = \frac{\cos \psi_a - \cos \psi_b \cdot \cos \theta_{na.nb}}{\sin \psi_5 \cdot \sin^2 \theta_{na.nb}} \quad (13.35)$$

$$B = \frac{\cos \psi_b - \cos \psi_a \cdot \cos \theta_{na.nb}}{\sin \psi_5 \cdot \sin^2 \theta_{na.nb}} \quad (13.36)$$

where ψ_a and ψ_b are the dips of planes A and B respectively and ψ_5 is the dip of the line of Intersection 5.

The angles required for the solution of these equations can most conveniently be measured on a stereoplot of the data that defines the geometry of the wedge and the slope.

Consider the following example:

Plane	Dip°	Dip direction°	Properties
A	45	105	$\phi_A = 20^\circ$, $C_A = 500$ lb/ft ²
B	70	235	$\phi_B = 30^\circ$, $C_B = 1000$ lb/ft ²
Slope face	65	185	$\gamma = 160$ lb/ft ³
Upper surface	12	195	$\gamma_w = 62.5$ lb/ft ³

The total height of the wedge H = 130 ft.

The stereoplot of the great circles representing the four planes, involved in this problem, is presented in Figure 13.26 and all the angles required for the solution of Equations 13.33 to 13.36 are marked in this figure.

Determination of the factor of safety is most conveniently carried out on a calculation sheet such as that presented in Table 13.2. Setting the calculations out in this manner not only enables the user to check all the data but it also shows how each variable contributes to the overall factor of safety. Hence, if it is necessary to check the influence of the cohesion on both planes falling to zero, this can be done by setting the two groups containing the cohesion values c_A and c_B to zero, giving a factor of safety of 0.62. Alternatively, the effect of drainage can be checked by putting the two water pressure terms (i.e., those containing γ_w) to zero, giving $F = 1.98$. As has been emphasized in previous sections, this ability to check the sensitivity of the factor of safety to changes in material properties or in slope loading is probably as important as the ability to calculate the factor of safety itself.

Wedge Stability Charts for Friction Only

If the cohesive strength of the planes A and B is zero and the slope is fully drained, Equation 13.32 reduces to:

$$F = A \tan \phi_A + B \tan \phi_B \quad (13.37)$$

The dimensionless factors A and B are found to depend upon the dips and dip directions of the two planes; values of these two factors have been computed for a range of wedge geometries and the results are presented as a series of charts on the following pages (Fig. 13.27).

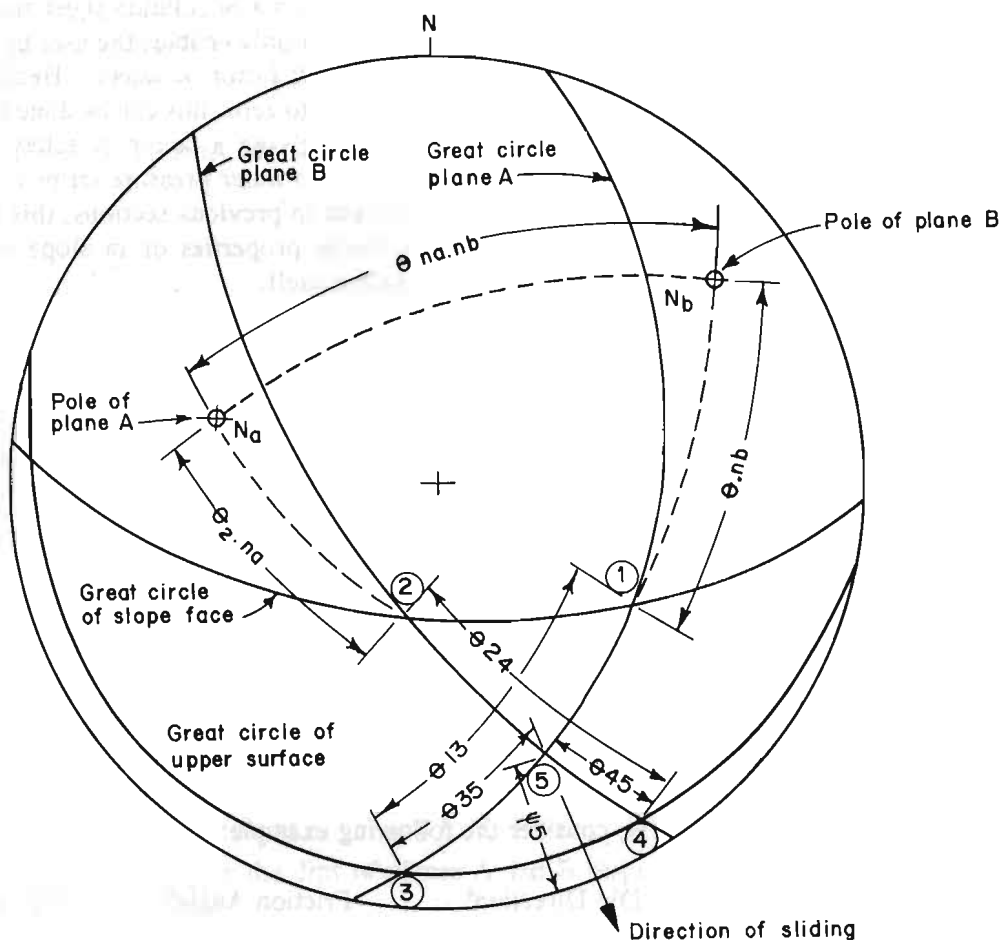
In order to illustrate the use of these charts, consider the following example:

	Dip°	Dip Direction°	Friction Angle°
Plane A	40	165	35
Plane B	70	285	20
---	---	---	---
Differences	30	120	

Hence, turning to the charts headed "Dip difference 30°", and reading off the values of A and B for a difference in dip direction of 120°, one finds that $A = 1.5$ and $B = 0.7$.

Substitution in Equation 13.37 gives the factor of safety as $F = 1.30$. The values of A and B give a direct indication of the contribution that each of the planes makes to the total factor of safety.

Note that the factor of safety calculated from Equation 13.37 is independent of the slope height, the angle of the slope face, and the inclination of the upper slope surface. This rather surprising result arises because the weight of the wedge occurs in both the numerator and denominator of the factor of safety equation and for the friction only case. This term cancels out, leaving a dimensionless ratio that defines the factor of safety (see Equation 13.30).



Source: USDT 1981

Fig. 13.26 Stereoplot of data required for wedge stability analysis

This simplification is very useful in that it enables the user of these charts to carry out a very quick check on the stability of a slope on the basis of the dips and dip directions of the discontinuities in the rock mass into which the slope has been cut. An example of such an analysis is presented later in this chapter.

Many trial calculations have shown that a wedge, having a factor of safety in excess of 2.0, as obtained from the friction only stability charts, is unlikely to fail under even the most severe combination of conditions to which the slope is likely to be subjected. Consider the example discussed earlier in which the factor of safety for the worst conditions (zero cohesion and maximum water pressure) is 0.62.

WEDGE STABILITY CALCULATION SHEET

INPUT DATA	FUNCTION VALUE	CALCULATED ANSWER
$\psi_a = 45^\circ$ $\psi_b = 70^\circ$ $\psi_5 = 31.2^\circ$ $\theta_{na.nb} = 101^\circ$	$\cos \psi_a = 0.7071$ $\cos \psi_b = 0.3420$ $\sin \psi_5 = 0.5180$ $\cos \theta_{na.nb} = -0.191$ $\sin \theta_{na.nb} = 0.982$	$A = \frac{\cos \psi_a - \cos \psi_b \cdot \cos \theta_{na.nb}}{\sin \psi_5 \cdot \sin^2 \theta_{na.nb}} = \frac{0.7071 + 0.342 \times 0.191}{0.5180 \times 0.9636} = 1.5475$ $B = \frac{\cos \psi_b - \cos \psi_a \cdot \cos \theta_{na.nb}}{\sin \psi_5 \cdot \sin^2 \theta_{na.nb}} = \frac{0.3420 + 0.7071 \times 0.191}{0.5180 \times 0.9636} = 0.9557$
$\theta_{24} = 65^\circ$ $\theta_{45} = 25^\circ$ $\theta_{2,na} = 50^\circ$	$\sin \theta_{24} = 0.9063$ $\sin \theta_{45} = 0.4226$ $\cos \theta_{2,na} = 0.6428$	$X = \frac{\sin \theta_{24}}{\sin \theta_{45} \cdot \cos \theta_{2,na}} = \frac{0.9063}{0.4226 \times 0.6428} = 3.3363$
$\theta_{13} = 62^\circ$ $\theta_{35} = 31^\circ$ $\theta_{1,nb} = 60^\circ$	$\sin \theta_{13} = 0.8829$ $\sin \theta_{35} = 0.5150$ $\cos \theta_{1,nb} = 0.5000$	$Y = \frac{\sin \theta_{13}}{\sin \theta_{35} \cdot \cos \theta_{1,nb}} = \frac{0.8829}{0.5150 \times 0.500} = 3.4287$
$\phi_A = 30^\circ$ $\phi_B = 20^\circ$ $\gamma = 160 \text{ lb/ft}^3$ $\gamma_w = 62.5 \text{ lb/ft}^3$ $c_A = 500 \text{ lb/ft}^2$ $c_B = 1000 \text{ lb/ft}^2$ $H = 130 \text{ ft}$	$\tan \phi_A = 0.5773$ $\tan \phi_B = 0.3640$ $\gamma_w/2\gamma = 0.1953$ $3c_A/\gamma H = 0.0721$ $3c_B/\gamma H = 0.1442$	$F = \frac{3c_A}{\gamma H} \cdot X + \frac{3c_B \cdot Y}{\gamma H} + \left(A - \frac{\gamma_w}{2\gamma} \cdot X\right) \tan \phi_A + \left(B - \frac{\gamma_w}{2\gamma} \cdot Y\right) \tan \phi_B$ $F = 0.2405 + 0.4944 + 0.8934 - 0.3762 + 0.3478 - 0.2437 = 1.3562$

Table 13. 2 Wedge Stability Table

This is 50 per cent of the factor of safety of 1.24 for the friction only case. Hence, had the factor of safety for the friction only case been 2.0, the factor of safety for the worst conditions would have been 1.0, assuming that the ratio of the factors of safety for the two cases remains constant.

On the basis of such trial calculations, Hoek and Bray (1981) suggested that the friction only stability charts can be used to define those slopes that are adequately stable and that can be ignored in subsequent analyses. Such slopes, having a factor of safety in excess of 2.0, pass into the stable category. Slopes with a factor of safety, based upon friction only, of less than 2.0 must be regarded as being in the potentially unstable category, i.e., these slopes require further detailed examination. In many cases, there are a number of wedges that may slide in chain reaction, one after another, as support provided by adjoining wedges is lost. This possibility should be studied in detail (Wagner et al. 1988).

In many practical problems involving the design of the cut slopes for a highway, it will be found that these friction only stability charts provide all the information that is required. It is frequently possible, having identified a potentially dangerous slope, to eliminate the problem by a slight realignment of the benches or of the road alignment. Such a solution is clearly only feasible if the potential danger is recognized before excavation of the slope is started, and the main use of the charts is during the site investigation and preliminary planning stage of a slope project.

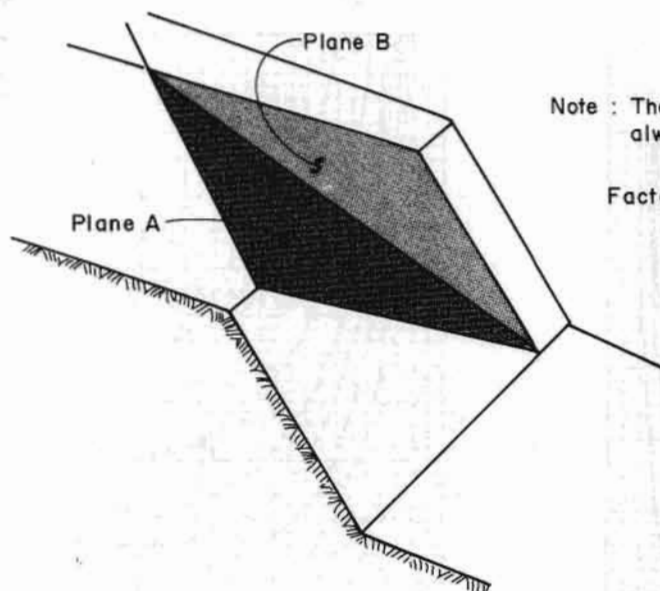
Once a slope has been excavated, these charts will be of limited use since it will be fairly obvious if the slope is unstable. Under these conditions, a more detailed study of the slope will be required and use would then have to be made of the analytical solution. In Hoek and Bray's experience (1981) relatively few slopes require this detailed analysis and the reader should beware of wasting time on such an analysis when the simpler methods presented in this chapter would be adequate. A full stability analysis may look very impressive in a report but, unless it has enabled the slope engineer to take positive remedial measures, it may have served no useful purpose.

Computer Programmes SASP and SASW for wedge failure are available for rapid computation of static and dynamic factors of safety for any number of joint sets. The programmes also account for submergence of rock slopes. Programme SASP gives cut slope angle for a given factor of safety. For rigorous analysis of wedges with tension cracks, inclined top terraces, and rock bolts, the programme known as WEDGE may be used.

13.5 LANDSLIDES

Any attempt to predict landslides and to stabilize existing landslides requires a thorough understanding of the causes of landslides and the mechanics of stability. The discussions in the preceding chapters help to understand the mechanics of stability.

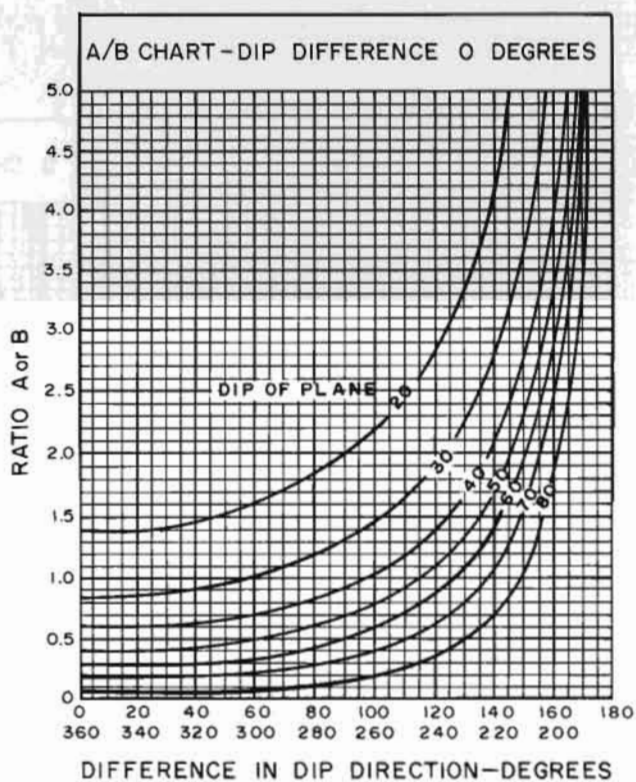
It may be recalled that almost all slope failures primarily fall into one of the three categories: planar, rotational, and toppling. However, a large landslide may contain several types of failure through its width, height, and depth due to the heterogeneity and anisotropy of the material. Once a large landslide has occurred and the landslide mass is momentarily remaining stable, it is vulnerable to smaller slides within the mass and to reactivation of the entire slide mass, depending upon the extent of causative factors over time. Landslides are, in many instances, themselves the cause of new landslides in adjoining areas which were otherwise stable. This is so because the adjoining areas are then exposed and subject to surface erosion, gullyng, toe erosion, weathering, and freedom of movement.



Note : The flatter of the two planes is always called plane A.

Factor of safety

$$F = A \cdot \tan \phi_A + B \cdot \tan \phi_B$$



Source: USDT 1981

Fig. 13.27 Wedge stability charts for friction only

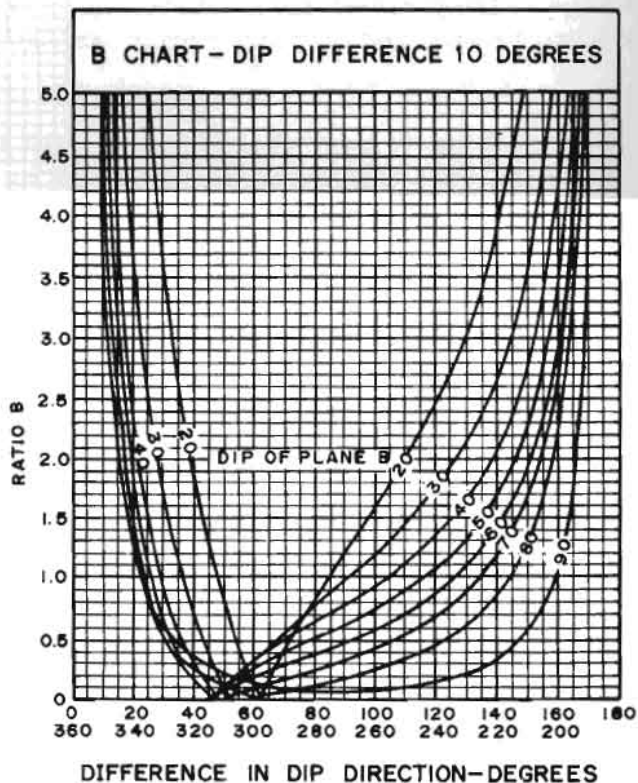
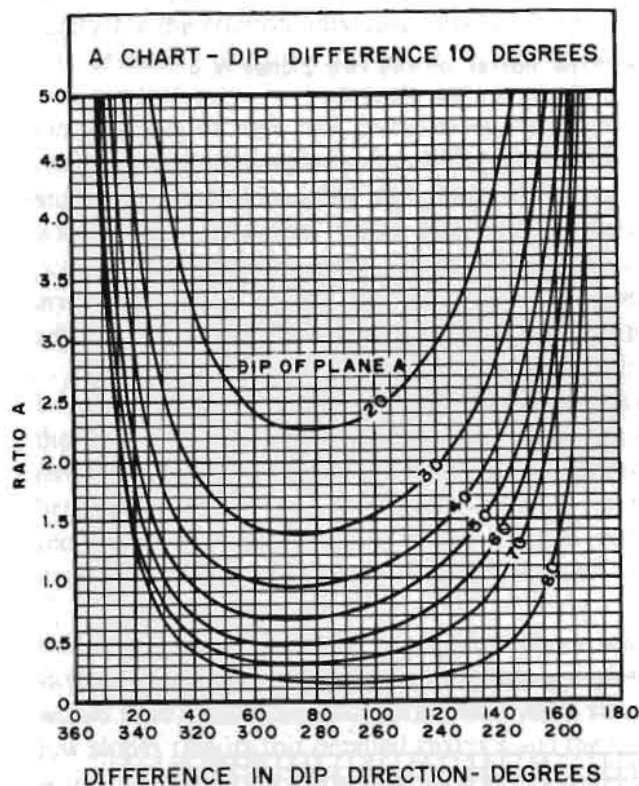


Fig. 13.27 Wedge stability charts for friction only (contd.)

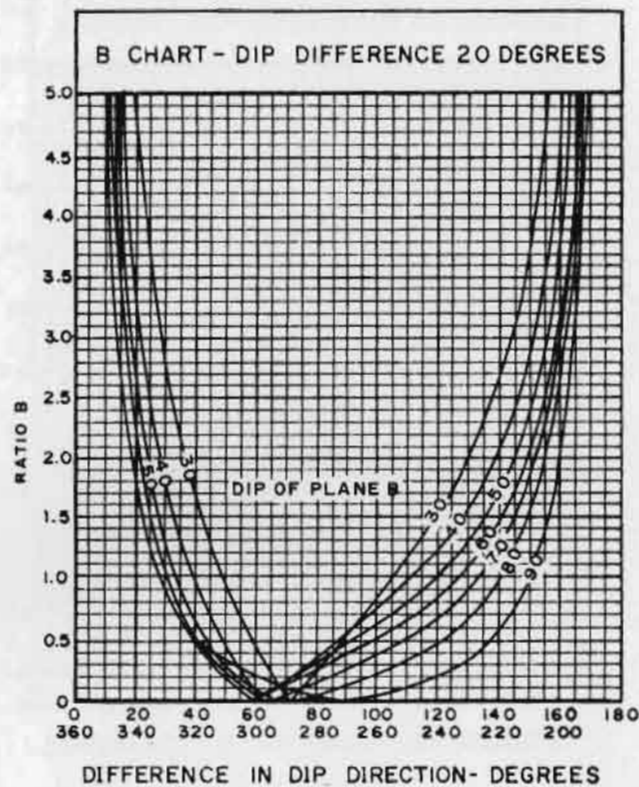
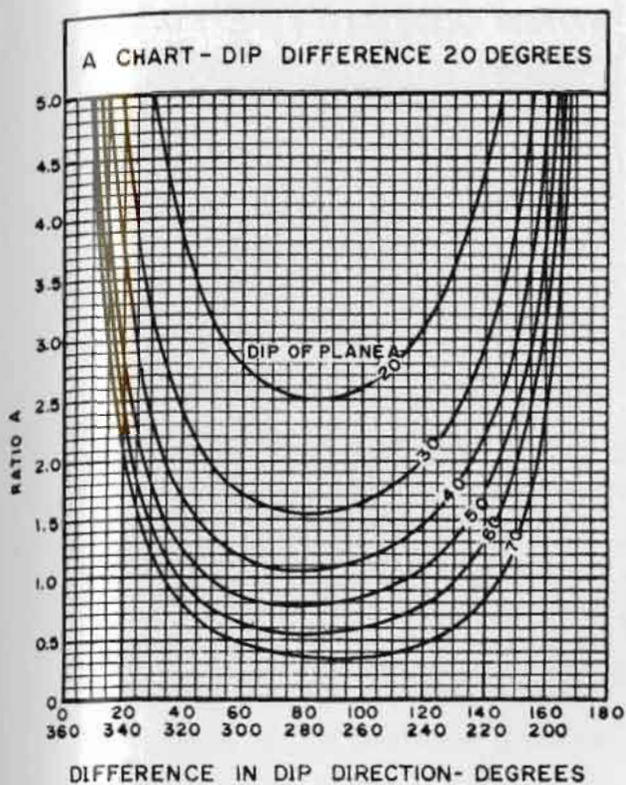


Fig. 13.27 Wedge stability charts for friction only (contd.)

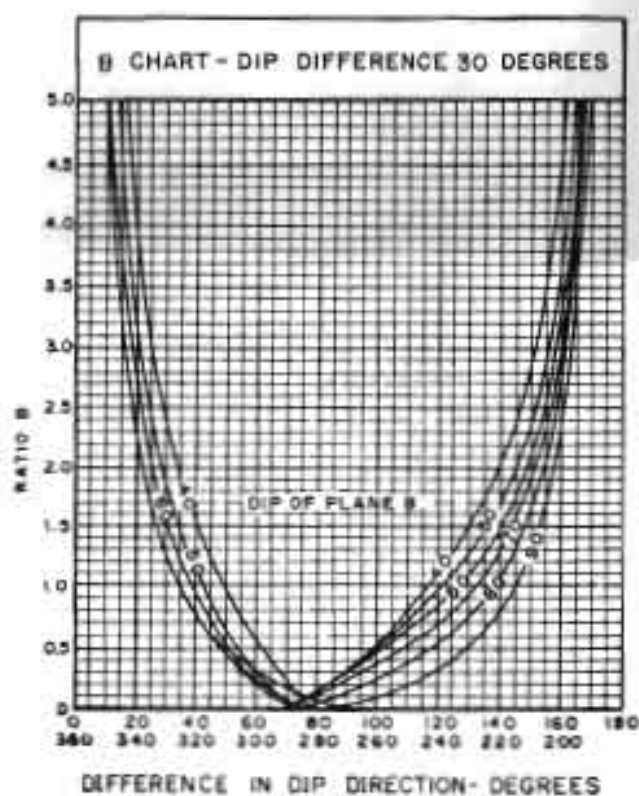
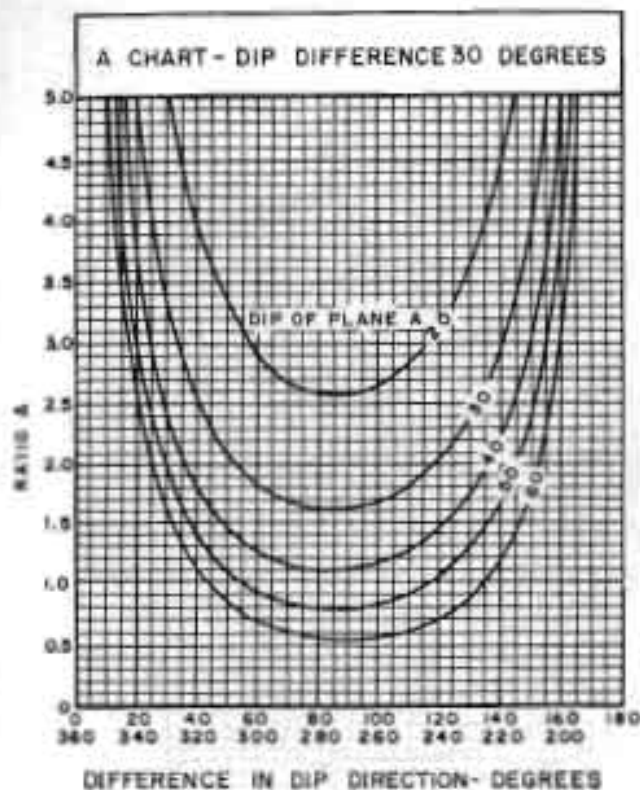


Fig. 13.27 Wedge stability charts for friction only (contd.)

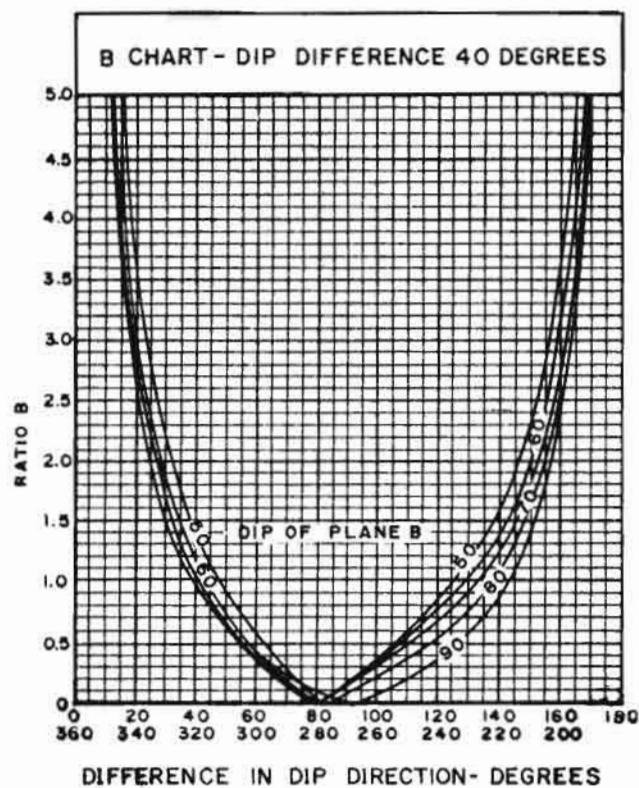
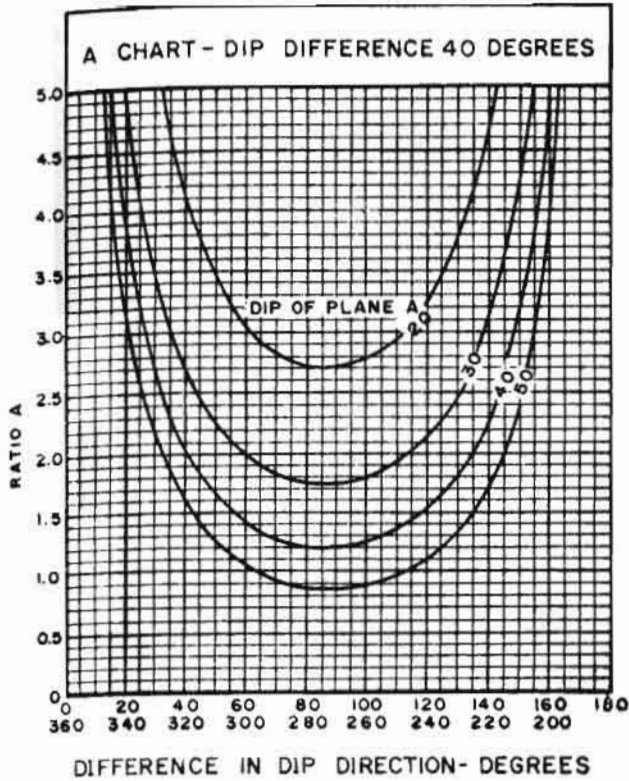


Fig. 13.27 Wedge stability charts for friction only (contd.)

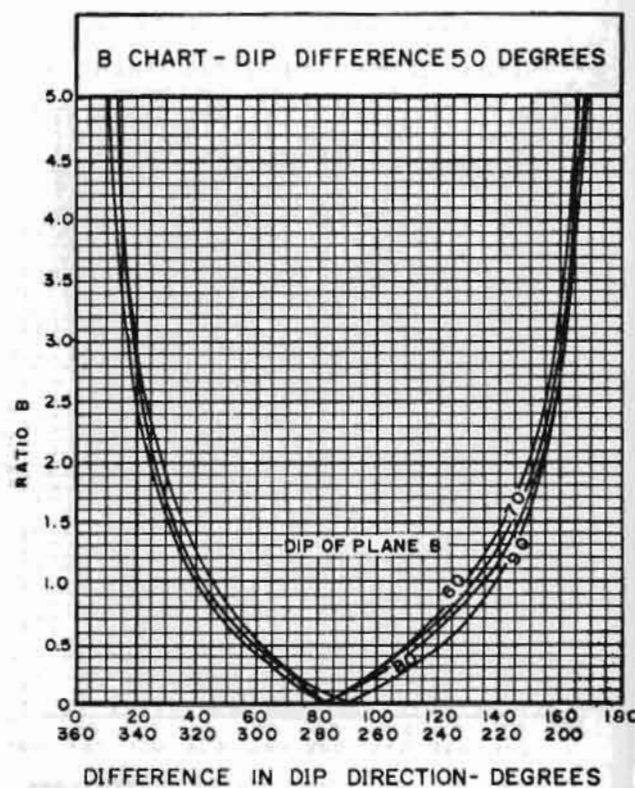
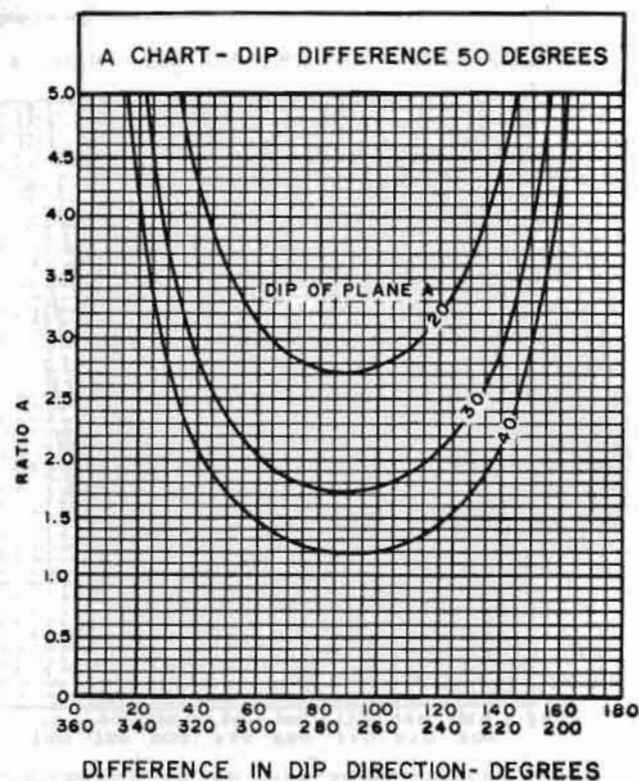


Fig. 13.27 Wedge stability charts for friction only (contd.)

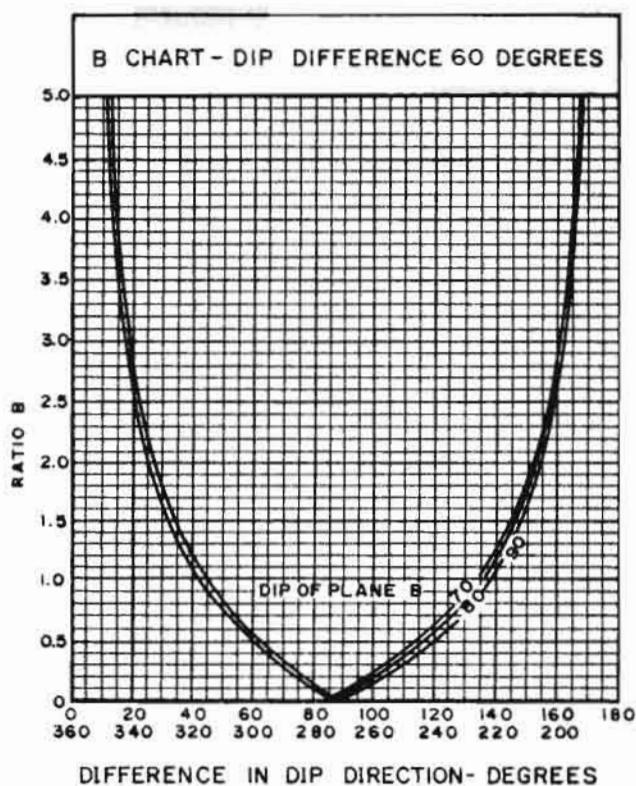
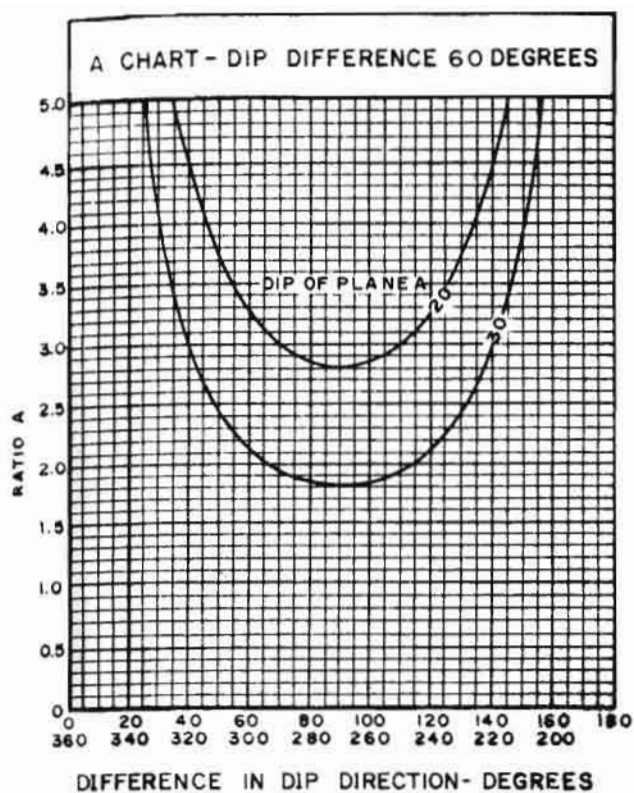


Fig. 13.27 Wedge stability charts for friction only (contd.)

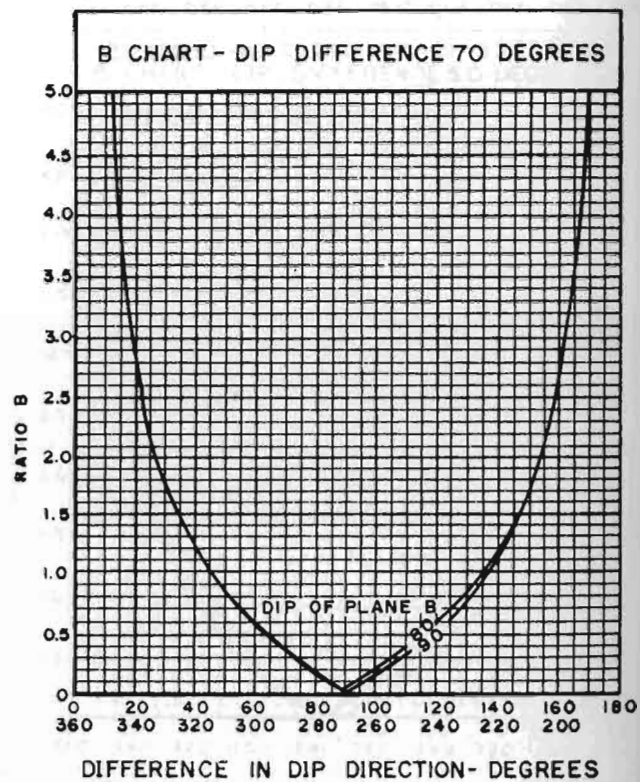
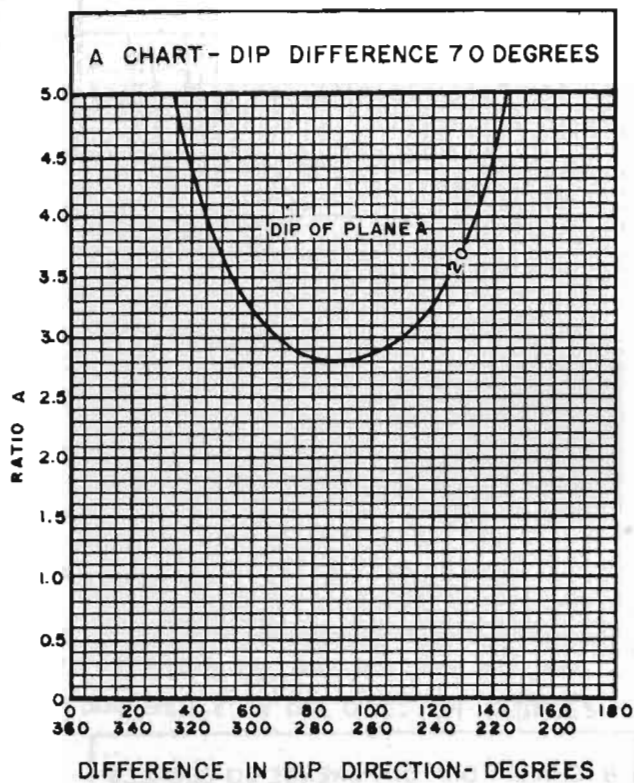


Fig. 13.27 Wedge stability charts for friction only (contd.)

The following discussion is aimed at an understanding of landslides in order to plan and design appropriate stabilization measures.

13.5.1 Causes of Landslides

The major causes of landslides are not the same as the causes of triggering of slides. It is useful to understand both of them.

Landslide Trigger

- (i) Cloud burst (200-1000 mm per day)
- (ii) Uncontrolled flow of water on slope surface from overflowed steep gullies.
- (iii) Toe cutting may activate failure by overtoppling of rock blocks or slides in colluvium.
- (iv) Earthquake vibrations.
- (v) Blasting vibrations.
- (vi) Flash flood due to glacier lake outburst/failure of landslide dam/cloudburst, etc.

Major Causes of Landslide

Man-made causes

- (i) Large-scale indiscriminate deforestation.
- (ii) Large-scale indiscriminate blasting and quarrying.
- (iii) Excessive hill cutting, daylighting planes of weakness followed by toe erosion.
- (iv) Intense agricultural operations, such as irrigation of paddy fields and water storage ponds, above the hill slope.
- (v) Mass-scale construction of houses, sewerage systems, and heavy structures on the entire hill.
- (vi) Submergence by lakes, dam reservoirs, and canals.
- (vii) Side-casting or throwing excavated material downhill (throwing of landslide material on to the road triggers the slide again because of loss of toe support).
- (viii) Vibrations of heavy vehicles on the hill road.
- (ix) Undermining caused by mining and tunnelling.

Erosion Process

- (x) Blocking of natural drainage systems and narrow culverts by logs, boulders, and gully bank slides.
- (xi) High flow velocities in steep gullies move very large boulders that will destroy roads, culverts, and the ecosystem.
- (xii) Large-scale slide of banks along steep gullies or *nalas* can even block the river after very long spells of continuous rain and form a landslide-dam.
- (xiii) Uncontrolled flow of rainwater on slope surface washes out soil and boulders.

- (xiv) Wind erosion leads to the formation of heaps of loose soil or slope material (thin chips of rocks) on the road; it is not, however, a major problem in the Himalayan Region.

Pore-water Pressure due to Adverse Hydrogeological Conditions

- (xv) Groundwater table rises up temporarily in the monsoon. It washes out the cementing material from soil and rock masses.
- (xvi) Perched water table builds up very fast in the monsoon on impervious surfaces, e.g., clay seams, clay layers, bedrocks, etc.
- (xvii) Water pressure in tension cracks not only pushes the slope forward but it also generates pore-water pressure along joints or bedding planes. As the slide starts, the opening of the rough joints increases due to dilatation. Thus the plane of sliding acts as a natural channel for the flow of water.
- (xviii) Seepage from choked catch drains may raise pore-water pressure along the slip surface.
- (xix) Inadequate size and choking of roadside drains may also lead to the same problem.
- (xx) Pressure of aquifers, such as sand layers or sandstone layers (in between impervious beds) can cause very high pore-water pressure on overlying layers in slopes in sedimentary deposits.
- (xxi) Saturation destroys capillary tension in soils and reduces its cohesion because of the increase in moisture content. Earthquake may liquefy loose, fine soil and seams in the rock mass.

Adverse Geological Conditions

- (xxii) Dips of bedding planes, clay seams, or weak rock layers are nearly the same as those of the slope causing planar sliding. (Thin beds may buckle due to self-weight on very high slopes.)
- (xxiii) Dip direction of joint set is nearly the same as that of the slope ($\pm 20^\circ$).
- (xxiv) Greater number of unfavourably-oriented joint sets with many wedges.
- (xxv) Weathering of rock mass.
- (xxvi) Slope material is loose, cohesionless material, e.g., colluvium, soil, etc.
- (xxvii) Huge boulders are sitting on the hill surface and are likely to topple or slide down.
- (xxviii) Steeply dipping joints or bedding planes may lead to slope failure by overtoppling of rock blocks.
- (xxix) Talus or debris contains fines and clay friction.
- (xxx) Clay seams, etc. have low coefficient of friction and so sliding takes place easily.

- (xxxix) Pre-existing slip surface in old landslide areas can be reactivated because of adverse hydrogeological conditions.
- (xxxixii) Swelling clay/sensitive clay/fissured over consolidated clay is present and loses strength because of water absorption/disturbance/release of stress during cutting.
- (xxxixiii) Soluble rocks with solution cavities.
- (xxxixiii) High tectonic stress will lead to heaving and buckling of layers at the bottom of the pit after removal of the overburden. High tectonic stresses will also result in excessive deformation on the cut slope until locked-up strain energy is released.

Progressive Failure

Theoretically cut slopes should fail in the first intense monsoon wherever conditions for sliding exist. However, in reality, slopes may fail progressively for several years. If corrective measures are not taken in time, failure may progress slowly upwards to several hundred metres. Eventually it may reach the top of the mountain.

Another interesting observation is that some rock slopes fail violently releasing a vast amount of stored strain energy in the form of rock blocks moving with great speed. However, such failures are rare. Violent failure is possible along pre-existing, non-circular surfaces of weakness only because movement is locked in until brittle failure of the hard rock occurs.

Intensive field research is needed in order to know more about landslides in the *Himalaya*. Natural landslides may be more difficult to understand and control. These are defined as landslides caused by natural causes. Man-made landslides are defined as those caused by man-made causes (as discussed above).

13.5.2 Mechanics of Landslides

Once the landslide has taken place, it is easier to know the mechanics of the landslide. It may be recalled that the mode of sliding may be idealized for simple and common landslides as given below.

Rock Slope

- (i) Planar Sliding.
- (ii) Wedge sliding along two joint planes.
- (iii) Circular wedge sliding.
- (iv) Dip sliding/sliding of regolith (Crozier 1986).

Soil/Talus Slope

- (v) Talus or debris slide along bedrock/clay seam (just like dip sliding) in case of dip slopes in talus.
- (vi) Circular wedge sliding in homogeneous soil mass or colluvium.

Gullies

- (vii) Circular/plane wedge sliding along banks
- (viii) Landslide debris flow like a viscous fluid (Sassa 1985) depending upon clay fraction, kinetic friction, etc.

Rock Fall Jumping

- (ix) Smaller rock blocks will come down, bouncing along the rock slope or steep gully with rocky beds upto distances of several kilometres even if the slope is very gentle.

There are many landslides in which slope movement is frightening and complex, but the mechanics of the initial slide are simple as discussed above. For example, slope movement in the case of debris flow on dip slopes consists of a series of tension cracks, followed by slumps and slides, and finally appearing as a mudflow. It may be idealized as in the case of a high perched water table. Further complex rockfalls may be the result of dip sliding far above the road.

The real challenge is to analyse the huge complex landslides where different modes of failure are occurring at the top, middle, and bottom of the landslide. Each slide is unique and its corrective measures are also unique. In such difficult situations the advice of a team of experts and a geologist should be taken; for which detailed investigations would be necessary.

13.5.3 Back Analysis of Landslides

Before suggesting corrective measures, it would be better to back-analyse failed slopes to find out the shear strength parameters of the natural slope material. The method of back analysis is now easy using computer programmes.

- i) The BASC Programme for the Back Analysis of (soil/rock) Slopes with Circular Wedge Failures (Singh and Ramasamy 1979).
- ii) The BAST Programme for Back Analysis of Talus/Debris/Regolith/Dip Slope Failures.
- iii) The BASP Programme for Back Analysis of Rock Slope with Plane Wedge Failure.

The shear strength parameters should then be used to study the stability of slopes with suitable corrective measures.

13.5.4 Design Factors of Safety

The design factors of safety for stable or stabilized slopes in the worst conditions should be as follows:

Soil Slopes

Static factor of safety 1.50

Dynamic factor of safety 1.0

or

Dynamic displacement < 1 m or 1 per cent of slope height

Rock Slopes

Static factor of safety 1.20

Dynamic factor of safety 1.0

or

Dynamic displacement < 1 m or 1 per cent of slope height

HAZARDS AND RISKS

14.1 INTRODUCTION

Road engineering on hill slopes involves analysis and design within the context of uncertain knowledge of slope stability. In particular, uncertainty regarding slope stability arises from three inter-related sources.

14.1.1 *Natural Variability*

The geologically active Himalayan slopes are constantly under the influence of uplift, weathering, and erosion. The variations in the tectonic movements, parent material, altitude, and climate result in variations in the extent of slope instability in time and space.

14.1.2a *Measurement Errors*

Spatial and temporal averages of various physical parameters, relating to soil and rock behaviour, result in measurement errors of true values. Such errors result in the uncertainty of true values.

14.1.2b *Simplification Errors*

Analytical models often involve a simplification of the physical world. Simplification is responsible for a certain degree of variation in properties defined by such models. Examples of such properties include the effective stress in soil, soil classifications, and rock joint strength parameters.

This chapter is addressed to the conceptual structures and techniques for dealing with the uncertainty of slope stability for road engineering in hilly areas.

14.2 HAZARDS

Hazard is a source of risk that may cause damage to, or loss of, life and property. Hazard can also be defined as the probability of occurrence of a particularly damaging phenomenon, within a specified period of time and within a given area, because of a set of existing or predicted conditions in the given time and space. The damaging phenomenon becomes a matter of concern only when it entails a certain degree of damage or loss to the population or the resources within its influence.**

Hazards may be classified as relative hazard, absolute hazard, and monitored hazard (Harten and Viberg 1988). Relative hazard is assessed by assigning ratings to different factors contributing to hazard. Absolute hazard is expressed deterministically, e.g., factor of safety, or probabilistically. Monitored hazard is assessed by actual measurements of the effects, e.g. deformations.

* Tables without credit lines in this Chapter are compiled by the author.

** Einstein (1988) has also defined hazard as: Hazard = probability that a particular danger will occur within a given period of time.

14.3 RISKS

Risk is a potential loss of life and property and may be defined as *"the combined effect of the probability of occurrence of an undesirable event and the magnitude of the event"*. Thus, there is always an element of uncertainty associated with risk. Varnes (1984) proposed the following definitions of risk in a UNESCO study:

"Natural hazard (H) means the probability of occurrence within a specified period of time and within a given area of a potentially damaging phenomenon.

Vulnerability (V) means the degree of loss to a given element or set of elements at risk (see below) resulting from the occurrence of a natural phenomenon of a given magnitude. It is expressed on a scale from 0 (no damage) to 1 (total loss).

Specific risk (R_s) means the expected degree of loss due to a particular natural phenomenon. It may be expressed by the product of H times V.

Element at risk (E) means the population, properties, economic activities, including public services, etc., at risk in a given area.

Total risk (R_t) means the expected number of lives lost, persons injured, damage to property, or disruption of economic activity due to a particular natural phenomenon, and is therefore the product of specific risk (R_s) and elements at risk (E). thus:

$$R_t = (E) (R_s) = (E) (H \times V). "$$

Varnes points out that the French word *risque* should be regarded as equivalent to the English word hazard. Einstein (1988) has defined risk as *"probability of an event times the consequences if the event occurs"*. It may be expressed as:

$$\text{RISK} = \text{hazard} \times \text{potential worth of loss.}$$

14.4 USE OF HAZARDS AND RISKS IN DECISION-MAKING ON HILL ROADS

14.4.1 Prefeasibility and Feasibility Assessments

The prefeasibility and feasibility stages of the decision-making process, relating to linear structures such as roads, involve the choice of a route from several alternative routes and the choice of alternative technologies for a given route.

The comparison of technological alternatives will become necessary only for major investments, that is major roads and major structures, such as tunnels, high-tech retaining walls, stabilisation of major landslides, and major river training works.

Risk analysis involves analysis of physical risks, i.e., risks of failure of structure and analysis of economic risks, i.e., certainty of the return on investments. Economic risk analysis involves identification of all variables that account for costs and benefits, assessment of probability, distribution of each variable, and the use of simulation technologies to obtain a distribution of probability and rate of return. Pouliquen (1975) gives a detailed account of these procedures.

For most purposes relating to linear hill infrastructure, physical risk analysis is adequate. The information from physical risks alone could be used for a choice of route. The value of physical risks may be incorporated into the traditional cash flow analysis for a choice of route based on economic feasibility.

The steps involved in prefeasibility and feasibility risk assessments based on physical risks are:

- assessment of hazard by subjective probability distributions based on engineering-geologic information,
- assessment of loss caused by the hazard based on subjective judgements from past experience,
- assessment of expressed value of risk by multiplying the hazard by the loss, and
- selection of the route based on either the total risk (total length of route likely to be lost) or the economic return given this loss as additional costs.

It should be noted that the assessment of probability of damage at a particular time or a series of damages at various points in time in the design life is a question of rigor, depending upon the scale of work. Direct use of binomial or other mathematical distributions are less likely to represent the distribution of probability that would actually happen with landslide occurrences in real life. Distributions obtained by step rectangular distributions through subjective assessments of likelihood, based on the experiences of relevant experts, would probably lead to the most representative curve fit. The simplest approach, that of using a single probability for a time immediately after the completion of the structure, is believed to serve the purpose for most cases of feasibility decisions.

The subjective assessment of the extent of damage, should the hazard occur, is again dependent upon the technological level, i.e., the extent of mitigation at the design perceived during feasibility assessment. It is thus suggested that, for simplicity, the design and mitigation selected during the assessment should be such that no significant modification of hazard is occurring as a result of the selected standards. The use of hazard-based standards and mitigation suggested in the Application Guide of this handbook is believed to ensure that such an assumption is reasonable and applicable to most situations of hill roads in a primarily rural economy.

14.4.2 Detailed Design Stage Assessments

Decisions on alternative designs, involving major investments and sophisticated technology for risk mitigatory actions, require more rigorous analysis of risks and decision-making techniques.

Decision-making concerning choice of standards for road cut designs, design of retaining walls and breast walls, design of drainage and erosion controls, and design of stabilizations for minor slides for most of the road sections can be based on the hazard levels, or rapid assessments of water table conditions and geotechnical properties of the soil and risk without rigorous investigations and analysis, but with experienced judgements and empirical designs. However, major structures and major stabilizations require

detailed geotechnical investigations and rigorous analysis of slope stability. Decision-making on the design type, under the uncertainties of variation in the material properties and site conditions over time, requires characterisation of uncertainty, rigorous assessment of probabilities, and use of a decision tree. A brief discussion on these is therefore presented in the following sectors.

a) *Uncertainty Characterization*

The characterization of uncertainty involves methods to estimate such probabilities. This section will outline approaches to the characterization of uncertainties.

Two approaches are possible for estimating probabilities or, more generally, probability distribution functions. The first is the classical frequentist approach that is based on a definition of the probability of realizing an event A , $P(A) = PB$, as being the per cent of times event A would be observed in an experiment that can be repeated an infinite number of times under constant conditions. The second approach is based on probability as a subjective degree of belief of the likelihood of realizing the event of concern. Standard books, such as the one by Guttman et al. (1982), provide statistical estimation methods to follow the first approach and the same book discusses the second approach using Bayesian Updating.

The choice of approach regarding estimation of probabilities is largely determined by the resource constraints of the investigation. While the subjective approach is more readily done, the frequentist approach has the advantage of scientific rigor, i.e., it will be more reliable. In terms of road projects, the subjective approach is suited to preliminary investigations and the frequentist approach will serve the needs of detailed phases best.

In addition to estimation, probability models and forecasting methods are useful in risk assessment. Readers are referred to Ross (1985) for probability modelling and to Guttman et al. (1982) for forecasting.

b) *Examples of Risk Mitigation Calculations*

Let us take the case of a 0.65 probability that wedge failure will occur on a given section of a hill road in the year of rock-bolting and it is proposed to rock-bolt to minimise the possibility of wedge failure. To calculate the effectiveness of rock-bolting as an active countermeasure against wedge failure, reductions in the probability of realizing the danger, given rock-bolting,^{***} as well as reductions in possible damage, given rock-bolting, must be estimated. The probability of wedge failure $p(wf)$, given rock-bolting (rb), can be calculated, using Bayesian updating as:

$$P(wf/rb) = \frac{p(rb/wf) p(wf)}{p(rb/wf) p(wf) + p(rb/\overline{wf}) + p(\overline{wf})} \quad (1)$$

^{***} The notation to indicate a probability of realizing an event A given the occurrence of another event B is $p(A/B)$.

where,

$p(rb/wf)$ = a likelihood function (posterior probability) that indicated the probability of rock-bolting failure against wedge failure or the true negative rate,

$p(wf)$ = the prior probability of a wedge failure, i.e, the hazard is 0.65,

$p(rb/\overline{wf})$ = another likelihood function that indicates the probability of rock-bolting success against wedge failure or the false positive rate, and

$p(\overline{wf})$ = the prior probability of no wedge failure, i.e., the complement of $p(wf)$:0.35.

The values of $p(rb/wf)$ and $p(rb/\overline{wf})$ may be estimated subjectively or objectively as follows: to estimate $p(rb/\overline{wf})$ ask the following question: "In what percentage of wedge failure cases is rock-bolting a success?" The question implies that the success of rock-bolting means that there was no failure and that rock-bolting was used. The estimation of $p(rb/wf)$ may be calculated as the complement of $p(rb/\overline{wf})$.

In our case, $p(wf) = 0.65$ and $p(\overline{wf}) = 1-0.65 = 0.35$. Suppose past experience is used to estimate $p(rb/\overline{wf}) = 0.90$ and so $p(rb/wf) = 1-p(rb/\overline{wf}) = 0.10$. Using equation (1), $p(wf/rb) = 0.17$. This means that the application of rock-bolting as an active countermeasure will reduce the probability of a wedge failure from the original value of 0.65 to 0.17.

If one kilometre of road is completely damaged, in the event of wedge failure occurring, then the expected loss in the year immediately after rock-bolting will be:

$$E_L = 0.17 \times 1 = 0.17 \text{ Km.}$$

This probability of 0.17 can be treated as a probability for the successive year and then the re-rock-bolting, if done, will result in a probability of:

$$\begin{aligned} P_2(wf/rb) &= \frac{0.17 \times 0.10}{0.17 \times 0.10 + 0.9 \times 0.83} \\ &= 0.02 \end{aligned}$$

The expected loss in year 2:

$$E_2 = 0.02 \times 1 = 0.02 \text{ Km.}$$

This process can be continued until $P_n(wf/rb) = \leq 0.01$. The total loss is then the sum of all the expected values.

A decision tree is a network of nodes connected by arcs that represent decisions, possible outcomes, or consequences (Fig. 14.1). The nodes can either be event nodes (Nodes 2,3, and 4 in Fig. 14.1) or decision nodes (Node 1 in Fig. 14.1), depending upon whether the arcs originating from the node represent possible events or decision alternatives respectively. The arcs originating from an event node are assigned probabilities, based on the relative likelihood or the occurrence of the event realization that the arc represents. A decision problem involving uncertainty can be represented on a decision tree by configuring arcs and nodes to model the decision problem and the uncertainties.

Each possible path through the tree, that originates at the source node, can be assigned a numerical value whose magnitude is an expression of the relative merit (or dismerit) of the sequence of decisions and outcomes that the path represents. The numerical value is frequently expressed in monetary terms in engineering applications of decision trees. Numerical values of losses are shown in Figure 14.1.

Expected values (which represent the most probable values) of utility functions, u , are used to choose between alternative decisions. The expected value criterion is a practical method of choosing between alternative actions if a function, $u(\text{path}_i)$, is such that $u(\text{path}_i)$ represents the relative preference for path i . In the case of individuals, who are usually risk averse, the utility function might be non-linear in the measure of relative merit (rupees, for example) so that each path's relative merit measure would have to be transformed into a utility based on a non-linear utility function. On the other hand, large firms and political bodies usually have utility functions that are linear in the measure of relative merit, since the amount of money involved in any one decision is small compared to the volume of monetary activity these organisations are involved in. When utility is linear with relative merit, the relative merit itself is a valid criterion for choosing among alternative decisions, since a linear transformation will not affect the preference ranking. Road projects may be assumed to have a utility function that is linear in monetary measure.

Once a tree has been configured to model a decision problem facing uncertainty, and the end utilities have been assigned, the backward roll procedure can be used to determine the best path, i.e., the path that maximizes utility. The procedure begins at the end of the tree, with the utilities for sets of arcs leading back to the same event node. The expected value of each set of arcs is assigned to the predecessor nodes of those sets of arcs. Next, the procedure examines the sets of event nodes leading back to the same decision nodes. The procedure assigns the greatest utility, from among the event nodes, to the predecessor decision node, for all sets of event nodes leading back to the same node. In doing so, it selects the best decision arc for that particular decision node. This procedure of taking expected values at event nodes and maximizing utility at decision nodes is repeated until the associated expected value for the best strategy will have been identified. An example of the application of this procedure is given below.

Suppose a cut slope is made as a marginal equilibrium slope. The options available are 1) to leave the slope as is in the hope that it will not fail, 2) to construct breast walls to ensure that no failure occurs, and 3) to apply cheap vegetative stabilizations that will improve the slope's stability but not ensure it. Figure 14.1 illustrates a decision tree model of the situation. Assume that the probabilities of failure in the three cases are 0.60, 0.05, and 0.30, respectively, and that failure results in a loss of pavement worth Rs. 250,000 plus any cost incurred in implementing the decision (let the cost of the breast wall be Rs. 100,000 and the cost of vegetative stabilizations be Rs. 50,000).

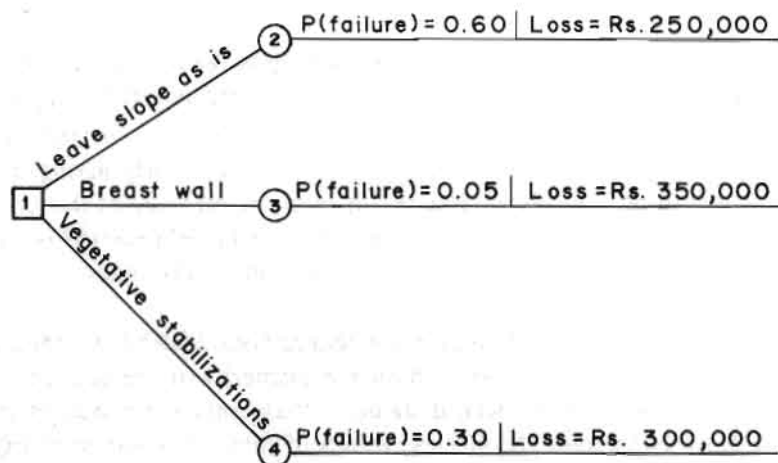


Fig. 14.1 Decision tree for cut slope

Using the backward roll procedure discussed earlier, Nodes 2,3, and 4 are assigned the expected values of the utility, their events have:

$$\begin{aligned}
 \text{Utility}_{\text{node 2}} &= 0.60 (250,000) = \text{Rs. } 150,000 \\
 \text{Utility}_{\text{node 3}} &= 0.05 (350,000) = \text{Rs. } 17,500 \\
 \text{Utility}_{\text{node 4}} &= 0.30 (300,000) = \text{Rs. } 90,000
 \end{aligned}$$

14.5 ASSESSMENT OF HAZARDS AND RISKS

The Mountain Risk Engineering (MRE) approach is concerned with hazards and risks relating to decision-making on the choice of alignment or design type for linear infrastructures such as roads or canals in mountainous areas. The concept of hazards and risks and the techniques of their assessment in this chapter are based on the mapping framework by Einstein (1988). The formal risk assessment procedure described by Einstein involves 5 levels, and these are given below.

1. State of Nature Mapping
2. Danger Mapping
3. Hazard Mapping
4. Risk Determination
5. Actions

For linear infrastructures, e.g., hill roads in developing countries, it is not always possible to adopt rigorous investigation, data collection, procedures, or mapping techniques. Table 14.1 is therefore suggested for the extent of rigor in hazard and risk assessments for various types of road at various stages of the project cycle. Table 14.2 presents a simplified chart for hazard and risk assessment. Please read the footnotes to Table 14.2 carefully.

Table 14.1 Approach to Hazard and Risk Assessment and Utilization

Project Cycle	* Minor Roads	* Medium Roads	* Major Roads and High Volume Roads
Prefeasibility Stage	Record of dangers by walk-over survey. No further work.	No detailed mapping of state of nature and danger. Assess hazards and risks as per 22.2.3 in Chapter 22. Summarize hazards and risks as per Table 14.2. Comparison of alignments based on risk.	Same as for medium roads. Helicopter should be used for overview of the terrain along proposed routes.
Feasibility Stage	No extra work.	Detailed mapping of state of nature, danger and hazards. Assess hazards (Section 23.2). Design to be based on hazard levels. Assess risks using Tables 22.4 to 22.11 in Chapter 22. Incorporate risk in economic analysis.	Detailed mapping state of nature, danger, and hazard Risks to be assessed to compare alternative alignments and alternative technologies. Tables 22.4 to 22.11 can be used for risk assessment.
Detailed Survey and Design Stage	Avoidance, and mitigation by direct observation in the field.	Detailed mapping only in areas that are changed/ different from the feasibility assessments. Further detailed mapping in critical areas, employing geophysical investigations. Geotechnical parameters also to be investigated and tested for critical areas Optimize design on the basis of information from hazard parameters and geotechnical information and analysis. Choice of design to be based upon risk analysis using decision tree for major structures.	Rigorous investigation of geotechnical parameters in the critical areas identified from hazard maps, and design optimization employing rigorous analysis of slope stability, uncertainty, characterization, and decision trees for critical structures.

See Chapter 22 for definitions

Table 14.2 Hazards and Risk

Chainage	Length L	Hazard (probability of occurrence)								Per cent of road likely to be damaged*								Risk to (only the high cost value of p-x) p-x/100
		MSS p	MRS p2	MDF p3	MUC p4	MJSS p5	MJRS p6	MJDS p7	MJUC p8	MSS x1	MRS x2	MDS x3	MUC x4	MJSS x5	MJRS x6	MJDS x7	MJUC x8	

* X_1, X_2, X_3, X_4 - Based upon past experience, may be 20 to 30 per cent.
 X_5, X_6, X_7, X_8 - Based upon past experience, may be 80 to 100 per cent.

Notes

- 1) L = length of road section with uniform characteristics, e.g. soil/rock type, slope, water table/seepage conditions, dip slope of rock, influence of faults, rainfall, and existing instabilities such as landslides, under cutting and land use.
 MSS = Minor Soil Slide;
 MRS = Minor rockslide;
 MDF = Minor debris flow; and
 MUC = Minor under cutting
 MJSS = Major soil slide;
 MJRS = Major rockslide;
 MJDF = Major debris flow; and
 MJUC = Major undercutting
- 2) Probability of occurrence is suggested for only one time occurrence immediately after the completion of the road. Even though there could be several occurrences during the design life of the road, the probabilities differ for each depending upon the state of nature, counter measures, and danger events at the time of other failures. The prediction of these probabilities, although possible, is quite complicated and is not recommended for decision making at the feasibility stage and for normal design of road elements. However, rigorous treatment and prediction is justifiable for decisions relating to large-scale structures on major roads.
- 3) Risks at the later periods of the design life of the road do not significantly affect the feasibility decisions based on economic analysis because of the discounting to present value.
- 4) The hazard prediction without the road could be different from that with the road depending upon the design type, standard, and mitigatory measures for the proposed road. A low cost and double-lane road in the mountains may significantly increase the hazards. However, it is found that roads planned, designed, and constructed based on MRE approaches are the ones which do not significantly alter the hazard level ascertained for "without the road" cases.
- 5) Hazard levels can be subjectively ascertained either by using information from rigorous field data collection and the subsequent state-of-nature maps, and danger maps or by direct inspection and observations in the field, depending upon the level of likely investment, size, and importance of the proposed infrastructure.
- 6) Prediction of the extent of road failure at 100 per cent probability because of the various events is again a subjective judgement based on prior experience. Statistical data, if available, may be used depending on the importance of the road and the structures under consideration.
- 7) Damage to the environment because of road failure is also not considered, since MRE-based roads are not expected to significantly alter the hazard that already exists without the road.
- 8) See Chapters 22 and 23 for further details on hazard and risk assessment techniques suggested for roads.

CONSTRUCTION MATERIALS

15.1 PURPOSE AND USES OF AGGREGATES

15.1.1 *Aggregates Used without the Addition of a Cementing Material*

Aggregates are used by themselves, that is, without the addition of a cementing material, in such applications as bases or sub-bases for flexible and rigid pavements. In the case of a base for a rigid pavement, the purpose of the layer may be to prevent **pumping**, to cover a frost-susceptible material, or to improve the general drainage characteristics of the section. Load-carrying capacity of the base layer is not a primary consideration in the choice of a material. Rather, gradation is the primary consideration. In the case of bases and sub-bases for flexible pavements, however, load-carrying capacity is a primary factor in the selection of materials. Here, too, gradation plays an important role, but, in addition, the material used in any particular layer of the flexible pavement system must reinforce those layers beneath it and must be capable of withstanding and transmitting the load to which it will be subjected. Strength tests such as the triaxial compression test and the California Bearing Ratio Test (CBR) are commonly used to evaluate such materials.

Aggregates by themselves frequently make up the entire pavement structure. This type of pavement, sometimes referred to as the low-cost road, is one *"in which a layer of predominantly granular material is placed on the natural soil to serve as a wearing course or a base course for a relatively thin flexible surface"*. Again, the requirements for these materials are mainly gradational requirements, with perhaps a restriction placed on the plasticity of the material passing the No. 2000 sieve. The emphasis here is on the maximum use of local materials.

Aggregates are also used without the addition of cement for shoulder material. The main requirements in this application are again gradation and stability. Naturally, all shoulders are not composed of uncemented graded aggregates. The trend towards paved shoulders has progressed rapidly.

15.1.2 *Aggregates for Bituminous Pavement Layers*

There are many types of bituminous pavement layers used by various highway agencies. The situation with regard to bituminous mixtures is not so simple as it may appear with Portland Cement Concrete (PCC) mixtures. In the latter case there is one basic type of mixture for slab construction, whereas there is a multiplicity of types of mixtures in the former. In spite of the many types of bituminous layers that

All the tests, figures, quotations, and tables in this chapter are adapted from lecture notes by D. Janssen, CETS 464, 1985, University of Washington. Figures and Tables without credit lines have all been compiled from these notes.

are used, the ideal aggregate for bituminous construction, regardless of class or type, would have the following characteristics :

1. strength and toughness,
2. ability to crush into chunky particles, free from flakes, slivers, and pieces that are unduly thin and elongated,
3. low porosity (however, it should not be completely lacking in porosity),
4. hydrophobic characteristics, and
5. particle size and gradation appropriate to the type of construction.

15.1.3 *Aggregate in Fresh, Plastic Concrete*

When concrete is freshly mixed, the aggregates really are suspended in the cement-water-air bubble paste. Behavior of this suspension (i.e., the fresh, plastic concrete), for instance, ease of placement without segregation causing rock packets or sand streaks, is crucially influenced by selection of the amount, type, and size gradation of the aggregate. Depending upon the nature of the aggregates employed, a fairly precise balance between the amount of fine and coarse-sized fractions may have to be maintained to achieve the desired mobility, plasticity, and freedom from segregation, all lumped under the general term 'workability'. Selection of mixture proportions should aim to achieve optimum behavior of the fresh concrete consistent with developing desired properties in the hardened product.

15.1.4 *Aggregates in Hardened Concrete*

The aggregates contribute many qualities to the hardened concrete. The strength-giving, binding material holding concrete together results from the chemical union of the mixing water and cement and is, of course, the basic ingredient. This hardened cement-water-air bubble paste would, by itself, be a very unsatisfactory building material, not to speak of its high cost. Indicative of the cost is the observation that if such a paste were used alone with the water contents of average concrete, it would contain from about 10 to 13 tons of cement per cubic yard. The paste, subsequent to initial hardening, unless restrained by contained aggregates, undergoes an intolerable amount of shrinkage upon drying. The exposed portions of such pastes dry out first, and differential shrinkage between the outside and inside portions often results in cracking. The presence of aggregates provides an enormous contact area for intimate bonding between the paste and aggregate surfaces. Rigidity of the aggregates greatly restrains volume change of the whole mass. Shrinkage of concrete is only about one-tenth that of paste. Thus, the aggregate is not only cost-conserving but is really essential.

In some cases, cement grouts containing little or no aggregate are employed successfully for underground work where severe drying is not expected. Expanding agents are also used to compensate for shrinkage, where drying is anticipated such as in grouting tendons in post-tensioned, pre-stressed members.

It is an inescapable conclusion that aggregates are not simply fillers used to dilute the expensive water-cement paste and thus make a cheaper product. Economics are important, but significant improvements in the workability of the fresh concrete are contributed by proper choice of aggregates. Such a choice influences the highly important properties of the hardened concrete such as volume stability, unit weight, resistance to the destructive environment, strength, thermal properties, and pavement slipperiness.

A major use of aggregates in the highway industry is, of course, in Portland Cement Concrete for rigid-pavements, slabs, bridges, and other structures. Aggregates for concrete should be physically and chemically stable. It was earlier stated that the properties of an aggregate were primarily dependent upon its mineralogic composition, internal texture, and internal structure. These factors then influence the concrete-making quality of an aggregate to a major degree. The general requirements of aggregates for Portland Cement Concrete are as follows : size, distribution and interconnections of voids; surface character and texture; gradation; internal texture and structure; mineral composition; and particle shape.

Probably no other physical characteristic of an aggregate has such an important effect on the water requirements and workability of fresh concrete mixtures as the gradation or particle size distribution. These factors profoundly influence a large number of other important concrete properties. Particle shape also affects concrete workability, segregation, and bleeding.

15.2 AGGREGATE QUALITIES OF CONCERN

- | | |
|-----------------------|--------------------------------------|
| 1. Gradation | 6. "D" cracking potential |
| 2. Maximum size | 7. Alkali reaction potential |
| 3. Surface properties | 8. Deleterious substance |
| 4. Particle shape | 9. Resistance to wear |
| 5. Soundness | 10. Affinity to bituminous materials |

15.2.1 *Test for the Evaluation of the Quality of Aggregates*

Not only do aggregates from different sources differ widely in their composition and properties, but samples from the same source may also show considerable variation. For determining the suitability of aggregates, the following acceptance tests are commonly in use :

Sieve Analysis

The grading required in a road aggregate varies according to the purpose for which it is to be used. The results of sieve analysis are normally required for comparison with the specification of the American Society for Testing Materials ([ASTM] C-136).

Soundness Test

The soundness of an aggregate is commonly evaluated by accelerated soundness tests using either (1) sodium sulfate or magnesium sulfate (ASTM C-88) or (2) the freezing and thawing method of the

American Association of State Highway and Transportation Officials ([AASHTO] T-130). Aggregates that stand up well in these tests can be expected to give satisfactory performance.

Flotation Test

Coal, lignite, and other deleterious material can be separated from an aggregate on the basis of low specific gravity. Natural aggregates are separated into two groups : those which float in liquid, and those which sink in liquid. The lighter aggregates are undesirable (ASTM C-123).

Friable particle Test

This test is used to determine the amount of soft particles, such as clay lumps, in the aggregate (ASTM C-127 and C-128).

Alkali Reaction

The mortar bar test (ASTM C-227), measuring expansion and the amount of silica dissolved in a standard NaOH solution (ASTM C-289) is used to determine the alkali reaction potential of aggregates.

Abrasion Test

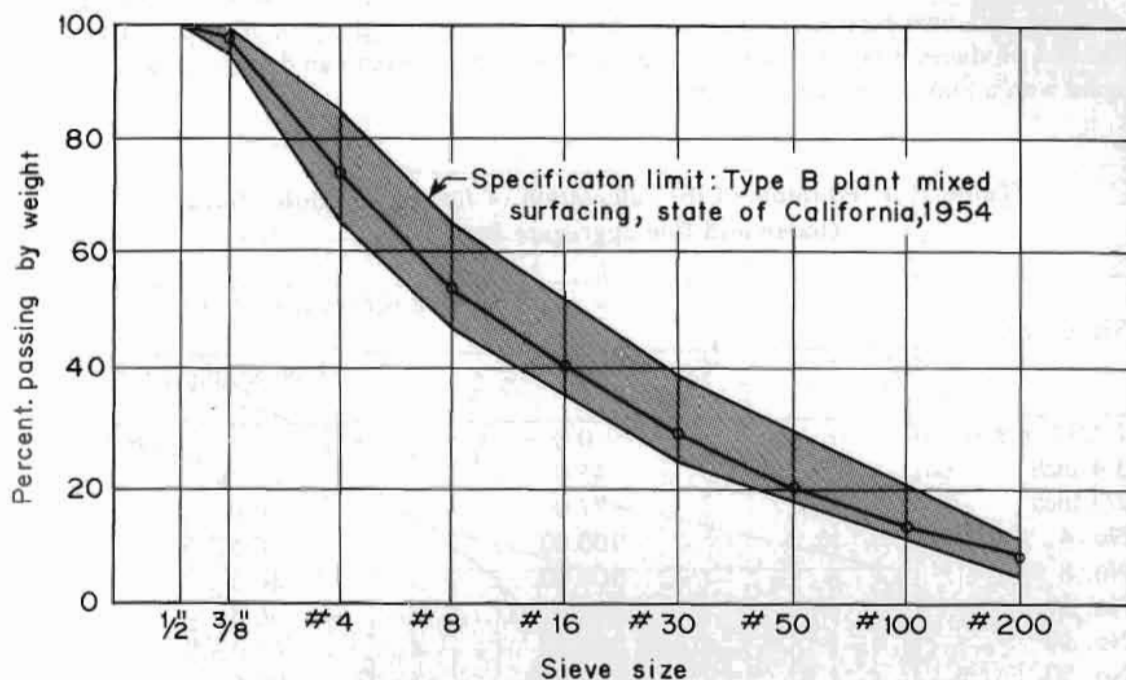
The most commonly used abrasion test is the Los Angeles Abrasion Test (ASTM C-535).

Aggregate-Bitumen Affinity Test

These tests include the Stripping Test and the Immersion-Compression test (ASTM D-1075).

One of the important classifications of aggregates is that based on size. Size classification is invariably controlled by specifications that will dictate the distribution of particle sizes to be used for a particular mixture. Figure 15.1 illustrates a typical specification controlling the size distribution or gradation of an aggregate for an asphalt concrete mix. For convenience, the ordinate is plotted as per cent by weight passing a given size on an arithmetic scale; the abscissa is the particle size plotted to a logarithmic scale. Generally, the size distribution is determined by dry sieve analysis.

Various terminologies have been used to describe the size distribution of aggregates. Typical gradations, together with their descriptive nomenclature, are illustrated in Figure 15.2. In addition to the descriptive nomenclature shown in this figure, aggregate quite often is referred to as coarse aggregate, fine aggregate, and filler. In this discussion, coarse aggregate will be referred to as material retained on the No. 4 sieve; fine aggregate will be referred to as that material passing the No. 4 sieve. While not referred to in these notes, filler is usually the material passing the No. 200 sieve. Also related to the size distribution of an aggregate are several other concepts which are described in the following passages.



Source: University of Washington 1985

Fig. 15.1 Typical gradation specifications

Fineness Modulus

The fineness modulus (FM) of an aggregate grading is a useful, descriptive number from which an idea of the relative coarseness or fineness of the aggregate grading may be obtained. The fineness modulus is computed by adding the cumulative percentages retained on each sieve of the logarithmic sieve series (6 inches, 3 inches, 1 1/2 inches, 3/4 inch, 3/8 inch Nos. 4, 8, 16, 30, 50, 100) and dividing the result by 100. It is a term most commonly associated with aggregates for PCC. An example of the calculation of the fineness modulus for a coarse aggregate and a fine aggregate (FA) is shown in Table 15.1.

Maximum Density

The size distribution of an aggregate may be specified by the formula:

$$p = 100 (d/D)^n$$

where,

- p = percentage of material by weight that passes a given sieve having openings of width d,
- D = the maximum particle size of a given aggregate, and
- n = an exponent upon whose value coarseness or fineness of gradation depends.

From this formula one can calculate the percentage of material of any given fraction for an aggregate of a given top size for some particular value of n . Studies have shown that, for $n = 0.5$, a gradation is determined that produces maximum density. Figure 15.3 shows a maximum density gradation curve for an aggregate with a maximum size of 1.5 inches.

Table 15.1 Example of the calculation of fineness modulus for a coarse and fine aggregate for concrete

Sieve size	Cumulative percentage retained	
	Coarse aggregate	Fine aggregate
1 1/2 inches	0.0	
3/4 inch	45.0	
2/3 inch	77.0	0.0
No. 4	100.00	0.5
No. 8	100.00	10.5
No. 16	100.00	36.3
No. 30	100.00	68.3
No. 50	100.00	91.6
No. 100	100.00	98.4
	$Z = 722.0$	$Z = 305.6$

Source: University of Washington 1985

Fineness Modulus (Coarse aggregate) $FM_{CA} = 722.0/100 = 7.22$

Fineness Modulus (Fine aggregate) $FM_{FA} = 305.6/100 = 3.06$

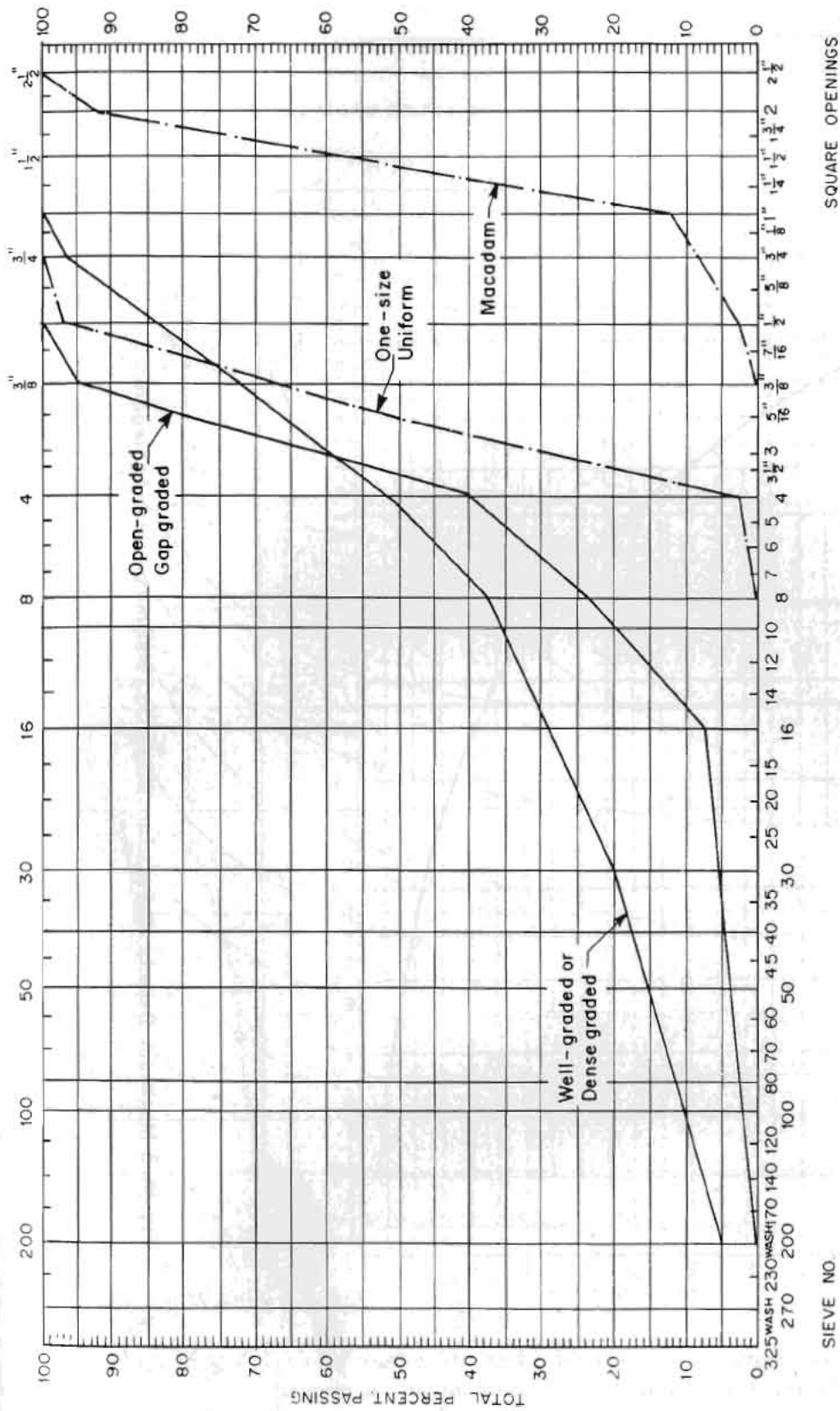
Aggregate Voids

Many references to "voids in aggregates" are made in literature dealing with the use of these materials. Confusion sometimes results because of a lack of understanding of terminology. One must distinguish here between **voids** (more properly, **pores**) in a piece of aggregate and the void system in a loose or compacted aggregate mass that makes up the space between aggregate pieces. The former is a characteristic that influences such things as specific gravity and absorption of a material (see ASTM Designations C 127 and 128), while the latter may influence the design of a PCC mixture or bituminous concrete mixture using the material (see ASTM Designation C 30).

15.2.2 Maximum Size Aggregate in Concrete

Figures 15.4 to 15.6 are data from a research report showing the effect of varying the maximum size of aggregate (dense graded mixes) with the cement content. The net result is that, as strength increases with age or cement content, the optimum size of aggregate decreases. Therefore, various economies may result if available aggregate sources are limited in size.

Fig. 15.2 Typical aggregate gradations



Source: University of Washington 1985

AGGREGATE GRADING CHART

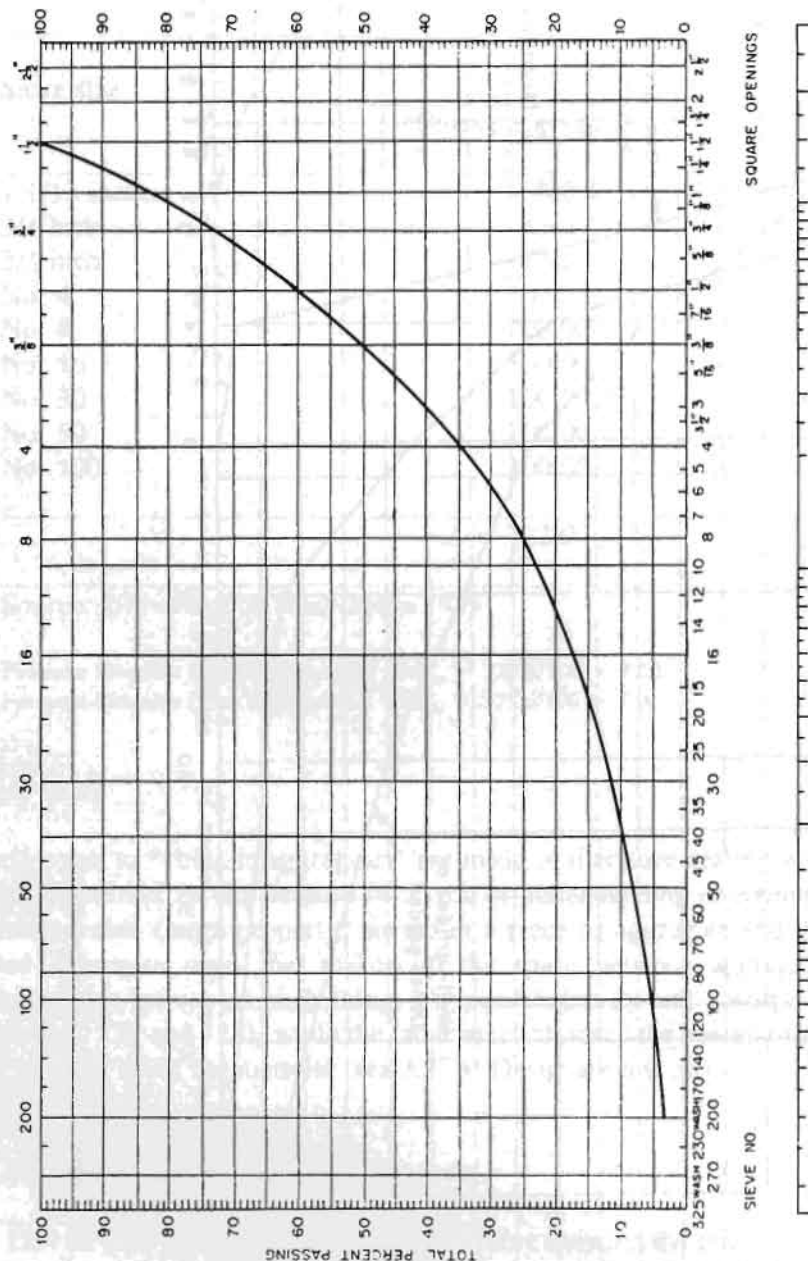
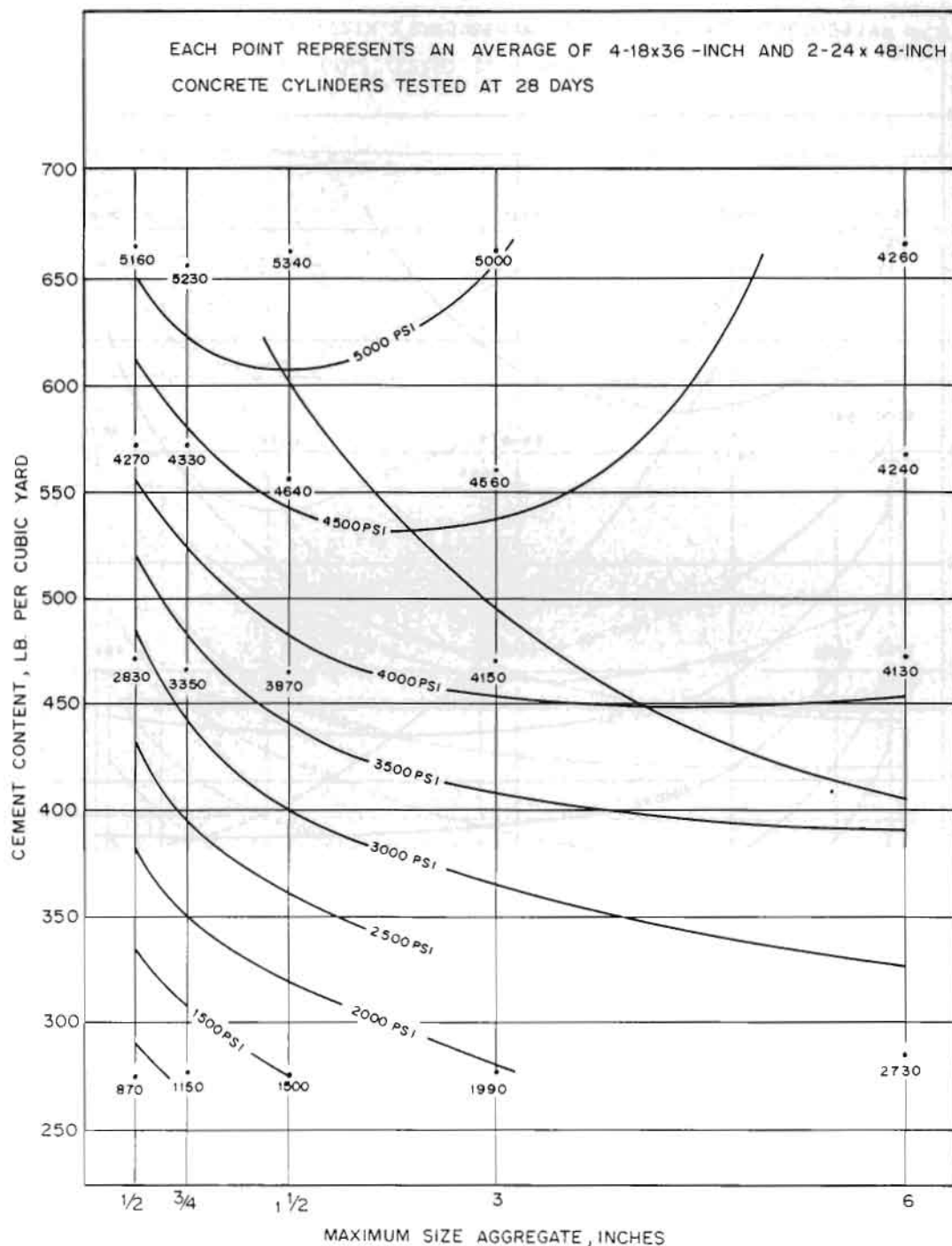


Fig. 15.3 Maximum Density Curve for 1 1/2 in. Maximum-size Aggregate

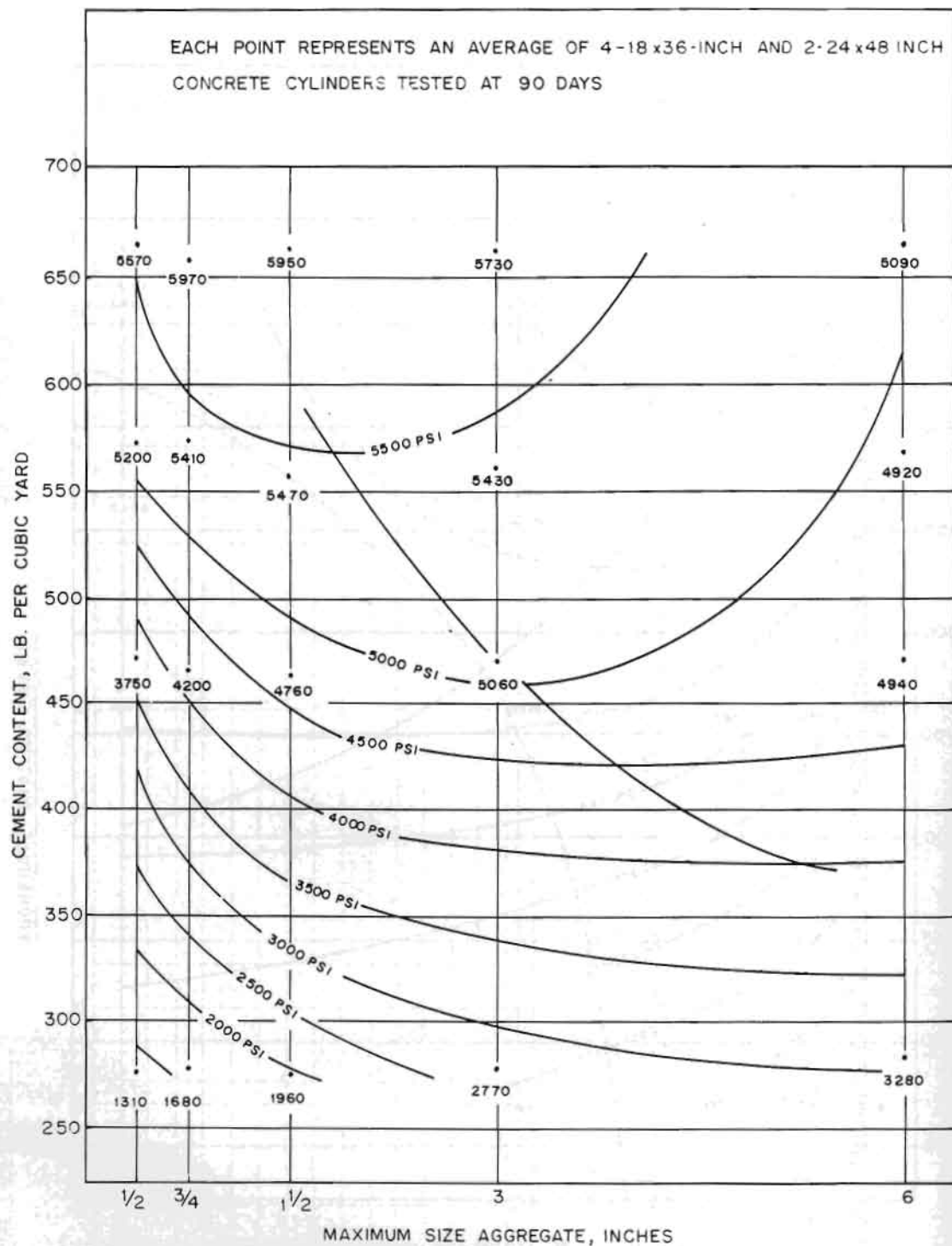
Source: University of Washington 1985

Fig. 15.3 Maximum density curve for 1.5 in maximum-size aggregate



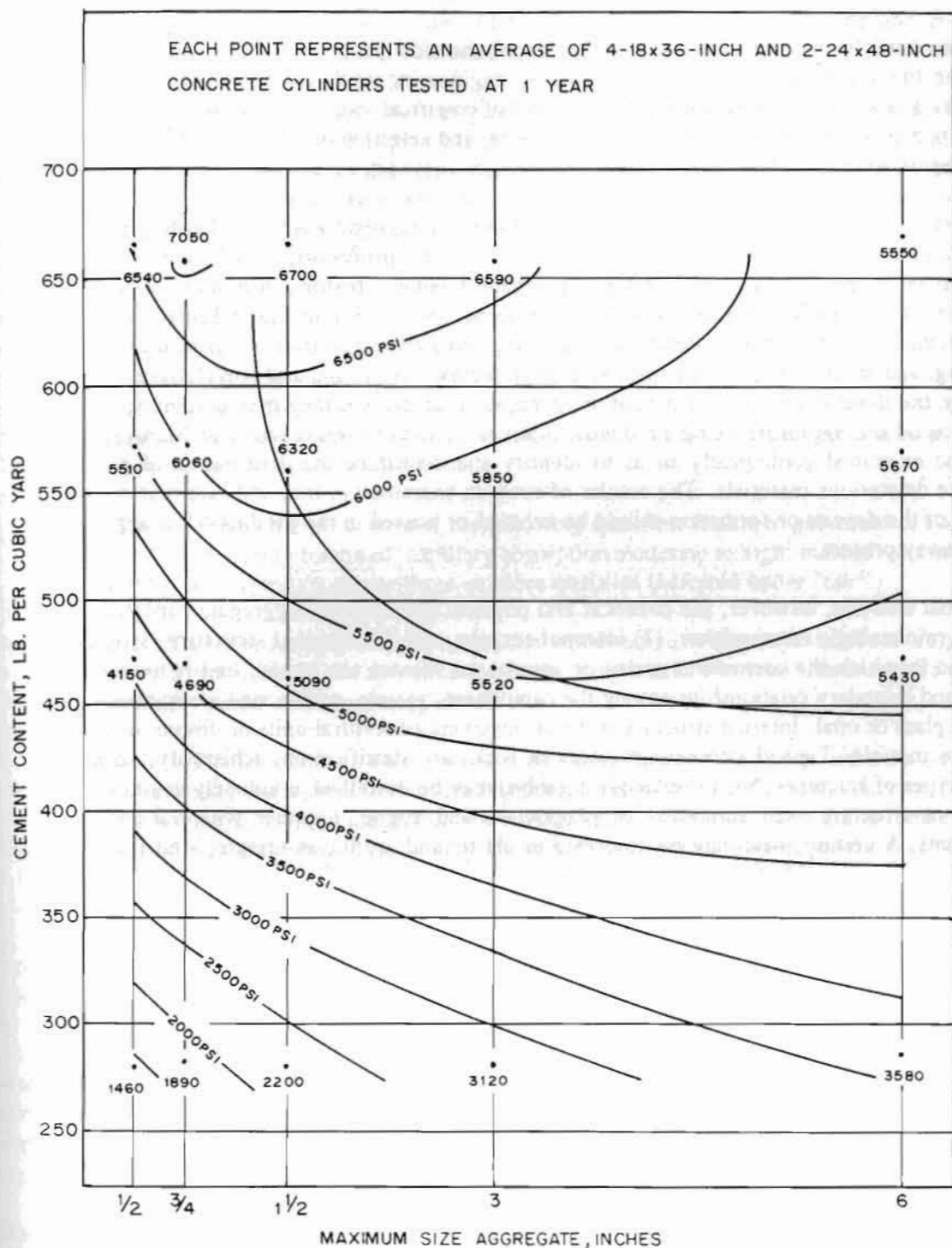
Source: University of Washington 1985

Fig. 15.4 Compressive strength decreases with increasing maximum size aggregate for minimum cement content (28 day-old specimens)



Source: University of Washington 1985

Fig. 15.5 Compressive strength decreases with increasing maximum size aggregate for minimum cement content (90 day-old specimens)



Source: University of Washington 1985

Fig. 15.6 Compressive strength decreases with increasing maximum size aggregate for minimum cement content (one year-old specimens)

15.3 PROPERTIES OF AGGREGATES

Aggregate particles possess a series of physical and chemical properties which, together with grading, determine the suitability of the aggregate for an engineering application. An understanding of these properties is essential as a basis for the development of empirical tests, for establishing specification limits based upon such tests and, in general, for evaluation and selection of aggregates for use under specific conditions of service.

The physical and chemical properties of particles of mineral aggregates arise in (1) **the geological history of the sand or gravel** or of the rock formation and (2) **the processing to which the materials were subjected** in the production of the finished aggregate. **Geologic history** includes the origin or mode of formation of the rock types as well as subsequent processes such as folding, faulting, jointing, recrystallization, hydrothermal alteration, weathering, erosion, deposition of secondary substances, such as coating, and so on. The geologic features of rock formations or sand and gravel deposits are important factors in the development and operation of aggregate sources, and they may determine the quality and limitations of the aggregate being produced. Sources of mineral aggregates for highway construction should be examined geologically so as to identify and determine the distribution of any unsound or otherwise deleterious materials. The results of such an examination may indicate that certain zones or portions of the deposit or formation should be avoided or wasted in the production of aggregates for use in a highway project.

In the final analysis, however, the chemical and physical properties of aggregate particles depend upon their (1) **mineralogic composition**, (2) **internal texture**, and (3) **internal structure**. Internal texture is the fabric in which the constituent grains or amorphous masses are joined, that is to say, the mutual, spatial, and boundary relationships among the component crystals, grains, and amorphous phases, e.g., volcanic glass or opal. Internal structure is the arrangement of textural units or discontinuities within the aggregate particle. Typical internal structures of rocks are stratification, schistosity, vesicularity, and various types of fractures. So, for example a gabbro may be described as coarsely crystalline in texture, massive in structure, and composed of plagioclase and augite, together with various other minor constituents. A certain shale may be described as clastic and argillic in texture, stratified and fissile in structure, and composed of an illite-type (hydromica) clay and specific proportions of silt and sand of a certain petrographic identity.

Mineralogic composition, internal texture, and internal structure of rocks (or earth materials in general) relate specifically to the geologic conditions of origin and to subsequent geologic history. Because of this relationship, the petrographer almost always can determine the origin and geologic history of a rock from an examination of representative particles. Igneous rocks are formed by solidification of molten siliceous materials intruded into the crust of the earth or extruded upon its surface. If the melt cools very slowly, the igneous rock will be wholly crystalline and a coarse crystalline texture like that of granite may result. If the melt cools rapidly a portion or the entirety of the material may solidify as glass before crystallization can be completed.

Sedimentary rocks develop by grain-by-grain accumulation of particles. The particles are joined together during geologic time by secondary processes of cementation, consolidation, or crystallization so that a coherent rock is produced. Metamorphic rocks form by crushing, fragmentation, and recrystallization of previously existing rocks as a result of geologic processes at elevated temperature, pressure, or shearing stress. The texture and internal structures that result reflect the nature of the original rock and the environmental conditions under which the metamorphism is consummated.

Aggregates vary widely in lithologic and mineralogic composition, both because of the nature and distribution of geologic formations and because of the selective action of weathering and erosion in destroying certain rocks and minerals and concentrating others.

Within each petrographic classification, such as granite, basalt, sandstone, or schists, a wide variation of composition, texture, and structure is possible. Hence any rock types produce particles that may be either sound or unsound physically, or deleteriously reactive or innocuous chemically as a constituent of concrete aggregate. The terms descriptive of the degrees of physical and chemical quality of the aggregate particles may be defined as follows :

1. Satisfactory : Particles are hard to firm, relatively free from fractures, and not chiplike; capillary absorption is very small or absent; and the surface texture is relatively rough.
2. Fair : Particles exhibit one or two of the following qualities : firm to friable; moderately fractured; capillary absorption small to moderate; flat or chiplike; surface relatively smooth and impermeable; very low compressibility; coefficient of thermal expansion approaching zero, or being negative in one or more directions.
3. Poor : Particles exhibit one or more of the following qualities: friable to pulverulent, slake when wetted and dried; highly fractured; capillary absorption moderate to high; marked volume change with wetting and drying; combine three or more qualities indicated under 'fair'.
4. Innocuous : Particles contain no constituents that will dissolve or react chemically to a significant extent with constituents of the atmosphere, water, or hydrating Portland Cement while enclosed in concrete or mortar under ordinary conditions.
5. Deleterious : Particles contain one or more constituents in significant proportion that are known to react chemically under conditions ordinarily prevailing in Portland Cement, concrete, or mortar in such a manner as to produce significant volume change, interfere with the normal course of hydration of portland cement, or supply substances that might produce harmful effects upon concrete or mortar.

As a consequence of its mineralogic composition, texture, and internal structure, each rock or mineral particle in aggregate is characterized by a suite of physical and chemical properties that determines the response of the particle to environmental conditions and thus its performance in engineering service.

15.3.1 *Physical Properties*

The physical properties of aggregates have important engineering significance. Included are such properties as porosity, permeability, surface texture, thermal, volume change, and others.

Porosity, Permeability, and Absorption

The internal pore characteristics are the most important properties of aggregates. The size, abundance, and continuity of pores influence or control such qualities as strength, elasticity, abrasion resistance, surface texture, specific gravity, bond with cementitious binder, resistance to freezing and thawing action, and the rate and magnitude of various cement-aggregate reactions.

Surface Texture

Surface texture of an aggregate particle is the fabric or pattern and the relative roughness or smoothness of the periphery. Surface texture encompasses all of the physical features of the rim and their dimensions, both areally and radially, and details of the form of the surface, such as the relative planeness, curvature, and rugosity. Clearly, surface texture depends upon the internal texture, structure, abrasion, and leaching to which the particle has been subjected.

Surface texture influences the bond developed between an aggregate particle and the cementing material in concrete. Table 15.2 shows the results of bond tests to indicate the effect of the surface texture of aggregate on bond strength in tension. The surface texture of aggregate also influences the water requirement of Portland Cement for a given consistency.

Volume Change with Wetting and Drying

The volume change of PCC with wetting and drying is influenced by aggregate in three general ways. First, in particles containing clay minerals of the expanding lattice type, such as the montmorillonites and some illites, wetting and drying leads to progressive increase in volume of the particle at any selected level of moisture content. Second, particles of high compressibility, such as certain weak sandstones, fail to resist drying shrinkage of Portland Cement paste and so permit inordinate shrinkage of concrete. Third, certain aggregates, because of their particle shape and surface texture, increase the water requirement for a given consistency and thus increase drying shrinkage. In areas where aggregates contributing to drying shrinkage of concrete are likely to be proposed for use, a wetting-and-drying test should be included in the standard specifications of the highway department.

Table 15.2 Effect of surface texture on bond strength
(aggregate embedded in cement briquets)

Surface texture of aggregate	Bond Strength in Tension, psi		
	28 days in water	28 days in water, then 28 days in air	28 days in water, then 28 cycles of wetting and drying
Rough, porous	350	260	235
Rough	240	275	230
Rough	215	300	245
Fairly rough	250	185	160
Smooth	120	45	
Smooth, conchoidal	285	170	45
Very smooth	195	40	25

Source: University of Washington 1985

Thermal Properties

The thermal properties of aggregates that are of significance to the performance of PCC are 1) coefficient of expansion, 2) specific heat, and 3) conductivity. These properties are not significant in bituminous pavement or for aggregates used as sub-base materials.

In mass concrete construction, specific heat, conductivity, and diffusivity must be considered in the design of cooling systems, and these properties of the proposed aggregates may influence the selection of the Portland Cement for the project. In pavement concrete these properties are not of significance.

The thermal coefficients of expansion for aggregates as a whole, and for those of individual particles, may be of importance in concrete highway structures. Of primary concern is the difference in (1) expansivity of the aggregate particle and of the concrete and (2) in the expansivity of the coarse aggregate and of the mortar or cement paste. A difference of 3.0×10^{-6} per degree Fahrenheit in the thermal coefficient of expansion of the coarse aggregate and that of the mortar can reduce freezing and thawing resistance considerably. Difference in the thermal coefficient of expansion between the aggregate and cement paste, low compressibility of the aggregate particles, and an inferior cement-aggregate bond are thought to contribute to the expansion and deterioration of concrete highway pavements and other structures containing the so-called sand-gravel aggregates in Kansas, Nebraska, Iowa, and Missouri, USA.

In general, however, the thermal properties of aggregates are of minimal importance as a factor in aggregate selection for concrete construction on highway projects.

Data on thermal coefficients of expansion of rocks, concrete, and Portland Cement Paste are summarized in Table 15.3. Note that serious difference in expansivity of the cement paste and that of the aggregate is to be expected only with rocks of very low expansivity. Rocks characterized by a linear thermal coefficient of expansion of 1.0×10^{-6} per degree Fahrenheit or less include granites, limestones, and marble.

Strength and Elasticity

High strength and elasticity of the particles are desirable for road metal and ballast because the rate of disintegration is minimized and the stability of the compacted course is maximum. However, for PCC, optimum results may be obtained by a compromise between strength and elasticity - so low that the strength of the concrete suffers and drying shrinkage is excessive - and level of strength and elasticity - so high that the adjustment of volume change of the concrete takes place primarily in the cement paste and along cement-aggregate boundaries, rather than moving uniformly throughout the concrete. Near-surface portions of pebbles and sand grains may be seriously weakened by weathering even though the interior of the grains is not modified significantly. The strength and elasticity of aggregate are not reflected proportionately in the strength and elasticity of the concrete.

A factor in the strength and elasticity of aggregate particles is the degree to which the particles are fractured either internally or because of the process of crushing by which the aggregate is manufactured. Fractures contribute to a breakdown of particles during handling and processing and to fragmentation in ballast or road metal and in the surface of bituminous pavements. Internal fracturing of aggregate particles makes a final screening operation, just prior to use of the aggregate, especially necessary in order that the desired grading can be maintained.

Table 15.3 Thermal coefficient of expansion of some rocks,* concretes, and Portland Cements (expansion per degree Fahrenheit, in a range of from -4° to 212°F)

Materials	No. of specimens	Range in mean linear thermal coefficient
Granites	27	1.0 to 6.6
Diorites and andesites	17	2.3 to 5.7
Gabbros, basalts, diabases	15	2.0 to 5.4
Sandstones	24	2.4 to 7.7
Quartzites	20	3.9 to 7.3
Dolomites	7	3.7 to 4.8
Limestones	65	0.5 to 6.8
Siliceous limestones	6	2.0 to 5.5
Cherts	9	4.1 to 7.3
Marbles	29	0.6 to 8.9
Slates and argillites	5	4.5 to 4.8
Portland Cements, neat	10	5.9 to 9.0
Concretes	27	3.6 to 6.8

Source: University of Washington 1985

* All coefficients of rocks were obtained on dry specimens

Density

The density of an aggregate particle is dependent upon the true density of its mineral constituents and upon the porosity. The density of a porous material may be defined to include in its volume all, some, or none of the volume of the pore space. Thus, there are such terms as bulk, apparent, and true specific gravity. The bulk density (dry basis) of common rocks ranges from about 1.6 to 3.2.

Bulk density or bulk specific gravity of specific rock types can be correlated with approximate ranges of porosity and, commonly, also with degrees of soundness, such as resistance to freezing and thawing breakdown. Such correlations are empirical but, with proper control and evaluation, are of great value in aggregate selection in specific areas.

Hardness

The resistance of an aggregate to abrasion and degradation is controlled by the hardness of the mineral constituents, by the firmness with which the individual grains are cemented or interlocked together, and the frequency of fracturing (see above). Particles composed of minerals of a low degree of hardness may be designated as 'soft'; those which are easily disintegrated because of poor cementation or intensity of fracturing may be designated as 'weak'. Weak and soft particles are objectionable in aggregate because

they break down during processing, changing the gradation of the aggregate from that contemplated, and are susceptible to continuing disintegration during services as a result of impact, abrasion, and weathering.

Particle Shape

The shape of aggregate particles may significantly affect the engineering performance of the aggregate. The workability of concrete, the strength, asphalt demand, and workability of asphaltic mixtures, as well as the frictional characteristics of graded aggregate mixtures, are but a few examples of the influence of particle shape on the quality of aggregate.

The size and shape of rock and mineral particles in aggregate depend to a considerable extent upon the presence and spacing of natural partings and cleavage in the parent formation. It is for this reason that certain formations characteristically produce more or less equidimensional, slabby, or elongated forms in certain size fractions and why it is not possible to obtain substantial production of large-sized aggregate from certain sources. The shape of particles depends also upon the relative strength, elasticity, and abrasion resistance of the rock or mineral and upon the natural or artificial processes whereby the aggregate is produced. It is common to find certain rock and mineral types in an aggregate represented by subangular or even well-rounded particles, whereas other rock and mineral particles in the same sample are angular.

Two relatively independent properties, sphericity and roundness, control particle shape. Sphericity describes the relation of the surface area of the particle to its volume or the relative volume of the particle and that of the circumscribing sphere. Roundness measures the relative sharpness or angularity of the edges and corners of the particle.

Coatings

A coating is a layer of substance covering a part of the entirety of the surface of an aggregate particle. The coating may be of natural origin, such as mineral deposits formed in sand and gravel by groundwater, or artificial; such as stone dust resulting from crushing and handling. Natural coatings usually do not cover the entire surface of pebbles and sand grains; rather, they tend to concentrate at the bottom of the particles as they lie in the deposit. Coatings usually are composed of silt, clay, and calcium carbonates; carbonate, organic matter, iron oxides, opal, manganese oxides, alkali and alkali-earth sulfates, and soluble phosphates have been identified.

The coating materials may be essentially inert chemically, or they may be potentially deleterious. Many coatings are physically weak, porous, absorptive, and poorly bonded to the aggregate particles. In such instances they may seriously impair the quality of the aggregate for the intended use.

15.3.2 Chemical Properties

The chemical properties of aggregates are frequently of great engineering significance.

Solubility

Few rocks, gravels, or sand that would be considered seriously for use as aggregate contain a sufficient proportion of water-soluble substances to affect the quality of the aggregate in service. Nevertheless, occasional formations and deposits of sand and gravel contain concentrations of water-soluble substances, such as gypsum, in the form of coatings or seam fillings, sufficient to cause difficulty in PCC. Such substances can be detected by petrographic examination or by qualitative chemical tests; they may be revealed by efflorescence at natural exposures of the formation or deposit.

Oxidation, Hydration, and Carbonation

Various unstable minerals are susceptible to oxidation, hydration, or carbonation if exposed to the atmosphere. These effects are insignificant for road metal, ballast, or bituminous construction, if ordinary caution is used in selection of the materials. However, PCC may become unsightly or distressed by these actions. Susceptible substances include from sulfides (marcasite, pyrite, and phrrhotite), ferric and ferrous oxides in clay-ironstone particles, free lime (C_3O), free magnesia (M_2O) in industrial products and wastes, and certain zeolites.

15.4 SPECIFICATIONS AND PROPERTIES

A specification may be defined as a concise description, preferably in measurable terms, of the significant characteristics of a material. The determination of such needs, in terms of characteristics that can be set up easily in a specification, requires logical thought based on sound chemical and engineering principles.

Requirements should be set forth in a clear, detailed but concise manner and should be quantitative rather than qualitative to reduce to a minimum decisions based on personal opinion.

There are five important requisites of a specification :

- | | |
|----------------------------|---------------------|
| 1. accuracy and precision, | 4. flexibility, and |
| 2. workability, | 5. acceptability. |
| 3. suitability, | |

A specification should never be considered as final or complete. Frequently an outmoded specification will prove a greater deterrent to progress than no specification at all. Any specification should be examined periodically, in view of technical advances in manufacture, testing, and use requirements.

Specifications for any material represent the purchaser's or user's conception of those characteristics of the material which are necessary for the successful use of the product in his application. Preparing a specification for a material is not a simple matter. It is frequently very difficult to put into specific quantitative terms the properties that the material should and should not possess. There is an ever present danger of specifying too rigidly and the consequences of that are higher prices. In addition, one may know well what specific characteristics of an end product are desirable but, in preparing specifications for components of that end product, may not know with the same certainty the properties of the components that determine the ultimate success of the end product.

This is sometimes the case with mineral aggregates. Take, for example, aggregates for portland cement concrete for a highway pavement. A desirable aggregate for this application is one that will make workable, then strong, durable concrete. However, present-day methods are not always adequate to perform this evaluation. The relatively recent discovery of concrete failures caused by the presence of certain forms of silica support the contention that there may still be present in aggregates certain very important characteristics hitherto ignored and unknown.

This should not imply, however, that specifications for aggregates are at the level of guesswork. There are many, perhaps most, aggregate properties that can be specified on a firm scientific basis. Aggregate specifications are dynamic. They are constantly being refined and improved as new research takes place and further experience is gained.

15.4.1 Local Specifications and Their Importance

Many of the examples of specifications for aggregates are those of national rather than local character. Such specifications must necessarily be broad. Hence, they should be regarded primarily as guides rather than as absolute standards. There are many mistakes that may be made by using or imposing a general specification in all areas of the country. First of all, the aggregates differ. Secondly, the climate may differ, so a material which may be extremely deleterious in one area may be completely innocuous in another.

15.4.2 Quality Requirements for Aggregates

Under "quality requirements" one can list all usual specification provisions other than those dealing with gradation. Quality requirements can be divided into five distinct groups.

1. General quality requirements
2. Abrasion resistance
3. Soundness
4. Restrictions on 'deleterious' constituents
5. Special requirements

It is the purpose of this section to discuss each of these five types of quality requirements, giving reasons for each.

General

Most specifications for aggregates for use in PCC, bituminous mixtures, or in similar classes of use begin with a paragraph heading such as "Description", "General Characteristics", "General Requirements", or something similar. It is the purpose of the paragraph, first, to describe in general terms the type of material considered to be acceptable and, second to collect in one place those rather nebulous requirements that undoubtedly influence the acceptability of the material but for which a good quantitative testing method test does not exist.

For example, the following is an extract from the first paragraph of a specification dealing with coarse aggregates called 'Description' :

"Coarse aggregates.... shall be composed of clean, tough, durable fragments of crushed limestone or dolomite, crushed or uncrushed gravel, or slag, free from an excess of flat, elongated, thinly laminated, soft or disintegrated pieces and free from fragments coated with dirt or other objectionable matter" (ASTM Designation [33-49]).

Similarly, ASTM Designation C 33-49 presents the general characteristics of coarse aggregate for concrete as follows :

"Coarse aggregate shall consist of crushed stone, gravel, blast-furnace slag, or other approved inert materials of similar characteristics, of combinations thereof, having hard, strong, durable pieces, free from adherent coatings and conforming to the requirements of these specifications" (ASTM Designation [33-49]).

Currently, however, ASTM Designation C 33-55T does not contain such indefinite requirements as "hard, strong, durable pieces," etc. This later revision of the specifications for concrete aggregates attempts to put all desirable qualities into definite terms and, as such, is a more practical type of specification. This is a desirable trend, and, no doubt, as technology progresses, aggregate specifications will continue to be refined to produce better definitions in all areas.

Abrasion Resistance

The qualities of material known as **hardness** and **toughness** have historically been regarded as essential to good aggregate. The properties of hardness and toughness are very closely related. Hardness is made up, in part, by abrasion resistance and toughness is generally understood to mean the power possessed by a material to resist fracture under impact.

At present, practically all (if not all) highway agencies specify a limit on abrasion resistance of aggregate which is based on the Los Angeles' test. The actual maximum loss specified may vary from place to place and, of course, will also vary depending upon the use to which the coarse aggregate will be put. For example, ASTM Designation C 33-55T cites a maximum loss of 50 per cent whereas ASTM Designation D 692-54 specifies that coarse aggregate for bituminous-concrete surface courses will have a maximum loss of 40 per cent. It is significant to note that ASTM Designation C 33-55T also states that:

"Coarse aggregate having an abrasion loss greater than 50 per cent may be used, provided the aggregate produced satisfactory strengths in concrete of the proportions selected for the work".

There is recognition of a current trend, on the part of some people, away from rigid abrasion-resistance specifications for coarse aggregate for PCC.

Soundness

The soundness of aggregates or their resistance to the forces of weathering is undoubtedly one of the most important considerations in the selection of a material for highway construction. The primary exposure

that one is concerned with is alternate freezing and thawing. Somewhat less frequently one may be concerned with the resistance of materials to alternate heating and cooling, wetting and drying, or the action of aggressive waters. Most specifications for aggregates in cold climate areas should include a provision for soundness that is designed to ensure the selection of a material that is durable in freezing and thawing.

The most common soundness requirement for aggregates (both coarse and fine) is based on the sodium or magnesium sulfate soundness test (ASTM Designation C 88-55T). This method may be used for acceptance of material but rejection should be based on other determinations such as freezing and thawing tests.

Freezing and thawing tests of the aggregate are also commonly used as the basis for a soundness specification. No ASTM test method exists for this, although there is an AASHTO standard method in existence (T 103-42).

In the particular case of aggregates for PCC, soundness in freezing and thawing is sometimes specified on the basis of results of tests in which concrete, made with the aggregate, is exposed to alternate freezing and thawing and the deterioration of the concrete is noted (ASTM Designations C 290, 291, 292, and 310). Specifications based on this type of test appear to be better founded than those based on a sulfate soundness test.

Restrictions on Deleterious Constituents

It is generally recognized that the presence of certain substances in aggregates for PCC is undesirable. These substances, if present, would tend to decrease the durability of the concrete and make it less abrasion-resistant than would otherwise be the case, cause pop-outs, or inhibit strength gain. Specifications for such aggregates, therefore, normally contain a section in which the deleterious materials are named and a limit placed on the amount of each that is allowable.

Obviously, the same deleterious substances do not occur in all locations and even materials that are called by the same name may differ in their effect on concrete from one area of the country to another. Hence one cannot list all deleterious materials with fixed allowable percentages of each. The most commonly recognized deleterious materials are clay lumps, coal and lignite, soft organic impurities, lightweight particles, and material finer than the No. 200 sieve. Some specifications list in detail each type of substance with a corresponding limiting percentage. Others may set up a general category based on a physical property rather than on specific names. For example, ASTM Designation C 33-55T contains the following Table (15.4).

In this case, instead of a detailed list of such items as shale, shells, and other light and soft materials, the specification lists the general categories of soft particles and lightweight particles. In any case the specification should recognize, by class or by name, those substances which may be harmful and limit the amount of each to a level consistent with the quality of concrete which is sought. For other uses of aggregates on highways, the restrictions on deleterious constituents are frequently not as rigid as they are for aggregate of PCC. For example, ASTM Designation D 692-54, the Standard Specification for Crushed Stone, Crushed Slag, and Gravel for Bituminous Base and Surface Course of pavements, does not include a section on deleterious substances but contains only a statement under the heading "General Characteristics", that the course aggregate *"shall consist of hard, strong durable pieces, free from*

adherent coatings...." This recognizes that small amounts of materials such as shell, chert, etc., are not as harmful to bituminous concrete as they are to PCC. It is assumed, then, that other specification provisions, such as those for soundness and abrasion, will eliminate aggregates containing harmful quantities of objectionable substances.

Table 15.4 Limits for deleterious substances in coarse aggregates for concrete

Item	Maximum Per Cent by Weight of Total Sample
Clay lumps	0.25
Soft particle	5.0
Chert that will readily disintegrate (soundness test, 5 cycles)	1.0
Material finer than No.200 sieve	1.0*
Oven-dry material floating on a liquid having a specific gravity of 2.0	1.0**

Source: ASTM Designation C33-55T

* In the case of crushed aggregate, if the material finer than the No. 200 sieve consists of the dust of fracture, essentially free from clay or shale, this percentage may be increased to 1.5.

** This requirement does not apply to blast-furnace-slag coarse aggregate.

It should be stated, however, that some agencies specify aggregates on the basis of class rather than on the basis of use and may employ the same class of aggregate for PCC and some high type of bituminous construction. In this case, specification provisions that are primarily intended for the control of quality of concrete aggregates may be imposed upon aggregates for bituminous construction, and vice versa.

Special Requirements

Under this heading may be listed a number of items that are sometimes included in specifications, often simply a general statement, but sometimes with quantitative limits attached. Some of the most common of these are :

- a Statement limiting the presence of flat and elongated pieces in coarse aggregate;
- a "service requirement" provision that may say, in effect, that even if the aggregate conforms to all other requirements of the specification, if it has been shown to give poor field performance it can be rejected: on the other hand, it may be acceptable if it has had a satisfactory service record in the past,

- c. aggregates for use in bituminous mixtures may be required to pass a stripping test;
- d. aggregates for use in bituminous mixtures may have to meet a specification requirement on minimum percentage of crushed pieces, and
- e. blast-furnace slag may have to meet a requirement for minimum unit weight.

15.5 AGGREGATE CALCULATIONS

15.5.1 *Sieve Analysis Data*

In the presentation of data for the results of sieve analyses, the aggregate gradation is generally expressed as a percentage of the total weight of the material passing a given sieve size. To obtain this information, material is passed through a number of sieves and the weight of material retained on each sieve is determined. The method for calculating the aggregate gradation, based on the results of a sieve analysis, is shown in the example in Table 15.5.

15.5.2 *Combining Aggregate Gradings*

In the majority of situations, the gradation of an aggregate from a particular source does not conform to the limits defined by a given grading specification. In the production of hot asphalt concrete, aggregate, after being dried and heated, is separated into 3 or 4 size fractions. In this case it is also necessary to combine the materials from each of the storage bins to meet the specifications for the particular job. The simplest means by which the proper combination can be obtained is by a trial-and-error procedure and is illustrated in Tables 15.6 and 15.7. This particular situation might be linked to a hot-mix plant with a two-bin separation of aggregate, plus a bin for mineral filler. In deciding the proper proportions of the aggregates to use by the trial-and-error procedure, one can quickly obtain at least approximate percentages of the various materials by studying the various sieves to ascertain which aggregate will control the quantity of material passing a particular sieve.

As an example, assuming 5 per cent of aggregate C is to be used (200 mesh sieve controlling), then aggregate B would contribute the majority of material passing the No. 8 sieve. Approximately 35 per cent of material B would be required.

Thus, as a first trial, try 5 per cent of C, 35 per cent of B, and 60 per cent of A and determine whether this combination will produce the desired grading.

Checking the column for the combination against the specification limits it can be seen that the assumed proportions are satisfactory since the combination in all cases lies within the grading limits. If the combination was outside the limits for a particular size, it would then be necessary to modify the percentages somewhat and proceed as before.

Table 15.5 Example illustrating aggregate gradation determination based on sieve analysis data

Sieve Size	Weight Retained on Sieve (gm)	Cumulative Wt. Retained (gm)	% Retained	% Passing
3/4 "	0	0	0	100
3/8 "	80	80	8	92
No 4	120	200	20	80
8	100	300	30	70
16	150	450	45	55
30	90	540	54	46
50	90	630	63	37
100	170	800	80	20
200	110	910	91	9
pan	90	1000	100	-

Table 15.6 Example of three aggregates to be combined to meet specification limits

Sieve Size	% Passing By Weight			
	Specification Limits	Aggregate A	Aggregate B	Aggregate C
1"	100	100	100	100
3/4"	95-100	95	100	100
3/8"	65-80	45	100	100
No4	45-60	12	100	100
8	30-45	3	85	100
30	15-25	0	48	100
200	3-7	0	7	80

Table 15.7 Example of trial-and error procedure for combining aggregate

Sieve Size	Aggregate A	Aggregate B	Aggregate	Combined (A) + (B) + (C)
1"	100 x .60 = 60	100 x .35 = 35	100 x .05 = 5	100
3/4"	95 x .60 = 57	100 x .35 = 35	100 x .05 = 5	97
3/8"	45 x .60 = 27	100 x .35 = 35	100 x .05 = 5	67
No.4	12 x .60 = 7	100 x .35 = 35	100 x .05 = 5	47
8	3 x .60 = 2	85 x .35 = 30	100 x .05 = 5	37
30	0 x .60 = 0	48 x .35 = 17	100 x .05 = 5	22
200	0 x .60 = 0	7 x .35 = 2	80 x .05 = 4	6
	60 % (A) +	35 % (B) +	5 % (C) =	Comb.

15.5.3 Two Graphical Methods for Blending Aggregates

i) Straight-Line Method

This method, which is recommended by both the Road Research Laboratory, Great Britain, and the Asphalt Institute, U.S.A., is widely used. The method is illustrated in Figure 15.7 showing a diagram with vertical percentage scales for the two aggregates and horizontal scales for the proportion of the aggregates in the final mix. Points on the vertical scales, corresponding to the percentages passing the various sieves, are connected by straight lines in respect of the same sieve sizes. To exemplify the method, aggregates A and B, as described in Table 15.8 and Figure 15.8, have been represented on the diagram.

According to the method described by the Road Research Laboratory, a vertical line is drawn through the point where the sloping line representing a certain sieve intersects the horizontal line representing the percentage of material required in the specification to pass this sieve. The intersection of the vertical line with the horizontal axes defines the proportion. This method takes into account only one point on the grading curve which the aggregate is required to approximate. By repeating the procedure for other sieve sizes, however, the mix representing the closest approximation can be estimated.

A better procedure, when grading limits are specified, is to draw the percentage ranges allowed for each sieve on a scale corresponding to the vertical scale of the diagram. By sliding this scale over the sloping line of the diagram, the proportion of the two aggregates can be determined where possibly all the sloping lines fall within the respective ranges specified. In Figure 15.8 the specification limits are shown with solid lines, while the material outside of the specification is dashed. In terms of the envelope specified in Table 15.8 and reproduced in Figure 15.8, this condition is fulfilled for a proportion of 0.45 A + 0.55 B with the exception of the percentage passing sieve No. 200. Addition of fines is required to comply with the requirements of sieve No.200. This method can be used to great advantage when more than one grading specification may be considered. A vertical, sliding scale can then be made for each specification, and the one chosen to which a combination of the two materials at hand can be closest approximated.

When, on the other hand, a large number of controls to approximate one given specification are made, another procedure is advantageous : points on the vertical scales, corresponding to the percentages passing the various sieves, are marked with pins and corresponding sieve sizes on the two axes are joined by strings. The sliding specification scale is placed under the threads and moved to a position where the greatest number of threads crosses within the specified limits. Again, the proportion of A and B are read off on the horizontal scales.

The straight-line method, as described by the Asphalt Institute, involves mixing three aggregates. In this procedure, two straight-line charts are joined together. The best combination of two aggregates is found on the one chart and this combination is then combined with the third aggregate on the second chart. This way of combining may not necessarily lead to the best combination of the three aggregates, and the method so employed is more cumbersome than certain other methods.

ii) Rothfuchs' Method

The method development by Rothfuchs is, no doubt, one of the most useful graphical procedures, as it is reasonably quick and simple and can be applied to mixtures of any number of components. Rothfuchs' Method will be briefly described by considering the four materials A, B, C, and D, the sieve analysis for which is given in Table 15.9 and the grading in Figure 15.9.

1. The cumulative curve of the required aggregate grading (median of envelope) is plotted, using linear ordinates for the percentage passing but by choosing a scale of sieve aperture size so that the grading plots are a straight line. This is readily done by drawing an inclined straight line and marking on it the sizes corresponding to the various percentages passing (line M in Fig. 15.10). It may be noted that, if the grading of the median complies with the formula, the horizontal scale will be exponential. More specifically, if $n = 0.45$, the diagram obtained will be the Bureau of Public Roads' Chart. If $n = 0.5$, the horizontal scale will be divided according to the square root of the sieve (a way of presentation often used and which complies with the Fuller Curve). Refer to Figure 15.10.
2. The gradings of the aggregates to be mixed are plotted on this scale. It will generally be found that they are not straight lines (curves marked A, B, C, and D).
3. The straight lines that most nearly approximate to the grading curves of the single aggregates are drawn. This is done by selecting for each curve a straight line, so that the areas enclosed between it and the curve are a minimum and are balanced about the straight line (curves marked A', B', C' and D').
4. The opposite ends of these straight lines are joined together (large dashed lines) and the proportions for mixing can be read off from the points where these joining lines cross the straight line representing the required grading. From Figure 15.10, it is seen that this method yields the proportions:

$$0.25 A + 0.25 B + 0.43 C + 0.07 D.$$

The grading for this combination is calculated in Table 15.9 and plotted in Figure 15.9. Had Material B been omitted, we would have had :

$$0.44 A + 0.49 C + 0.07 D, \text{ and}$$

finally, had only materials A and C been used, we would have had:

$$0.44 A + 0.56 C.$$

Considering for a moment the theoretical basis for Rothfuchs' Method, by approximating the individual sieve grading curves to straight lines, these lines are aligned with the specification median through multiplication with the factor representing the proportion of each aggregate in the mixture.

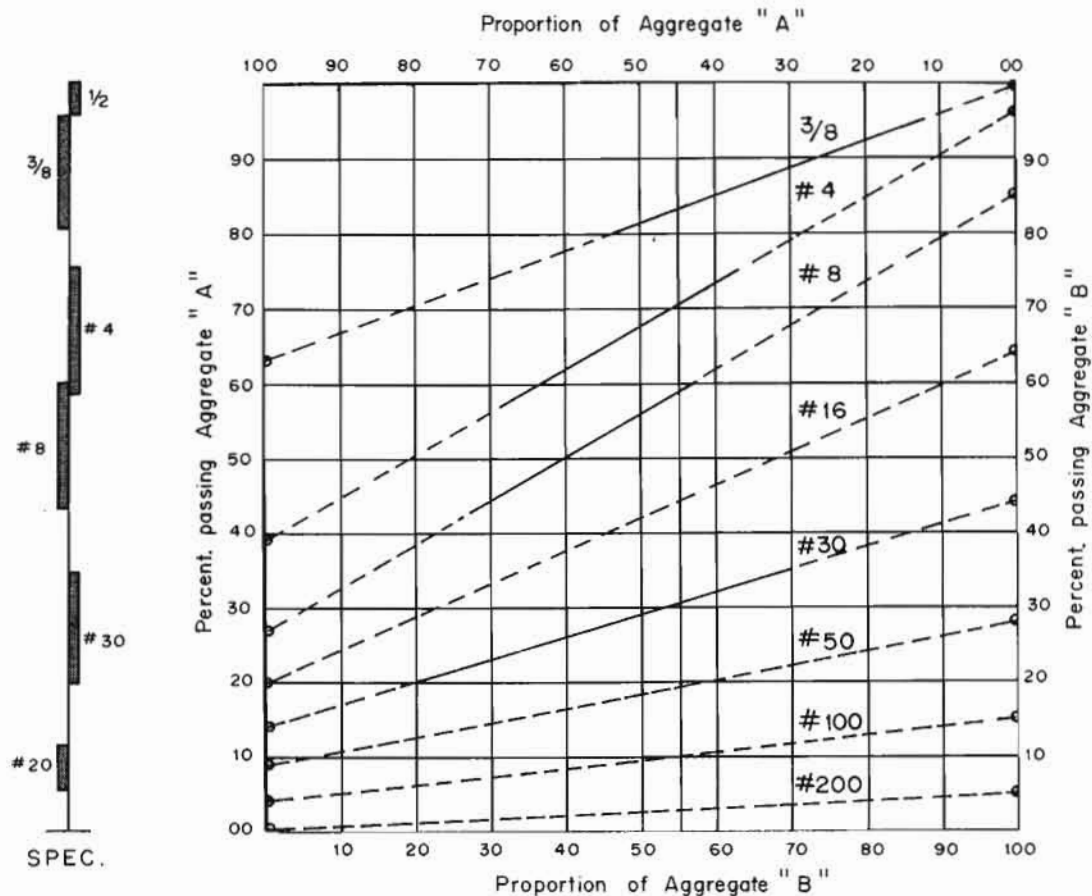


Fig. 15.7 Example of the straight-line method

Table 15.8 Aggregate gradations for graphical straight-line blending

Sieve Size	Aggregate A	Aggregate B	0.45 A + 0.55 B	Spec
3/4"	100	-	100	100
1/2"	91	-	96	95 - 100
3/8"	63	100	83	80 - 95
No. 4	39	96	70	58 - 75
8	27	85	59	43 - 60
16	20	64	44	-
30	14	44	30	20 - 35
50	9	28	19	-
100	4	15	10	-
200	0	5	3	6 - 12

Fig. 15.8 Results of graphical blending, two aggregates

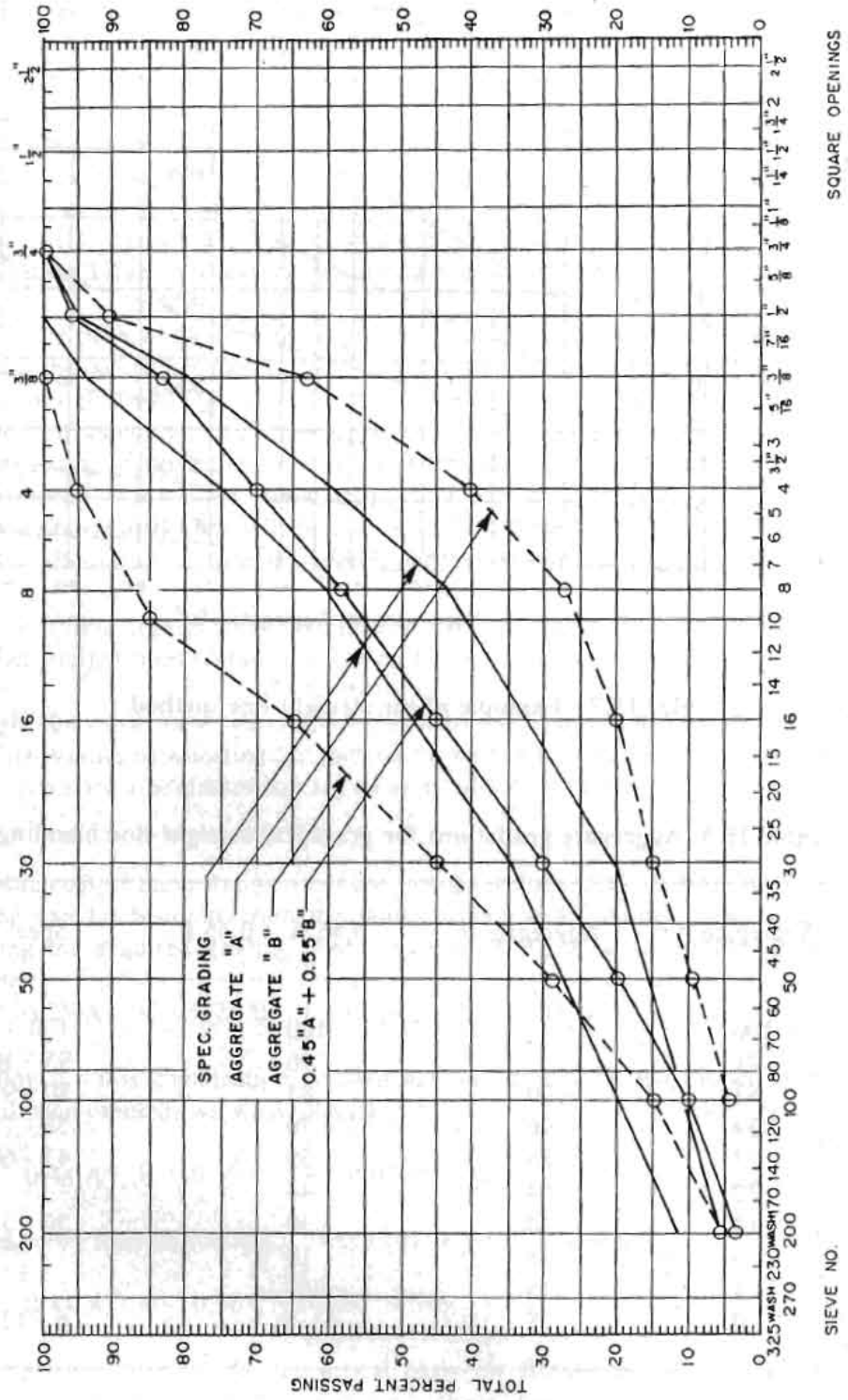


Table 15.9 Aggregate gradation for Rothfuchs' Method of blending

Sieve Size	Spec. Grading	Required Grading	Materials				Rothfuchs' Method $0.025 A + 0.25 B$ $+ 0.43C + 0.07 D$
			A	B	C	D	
1/2 "	95 - 100	98	100				100
3/8 "	80 - 99	88	79	100			95
No. 4	58 - 75	67	18	68	100		72
8	43 - 60	52	6	11	95		52
16			2	3	60	100	34
30	20 - 35	28	1	2	41	95	25
50			1	2	31	66	19
100			1	1	22	39	13
200	6 - 12	9	1	1	20	30	11

15.6 AGGREGATE PROPERTIES AND BEHAVIOUR PECULIAR TO BITUMINOUS MIXTURES

Particle surface texture is even more important when considering the resistance to deformation of asphalt-coated aggregate particles. The point is illustrated schematically in Figure 15.11 which suggests why, for two mixtures with the same film thickness of asphalt, irregular surfaced aggregate should be expected to develop the greater frictional resistance for a given contact pressure.

Angularity of particles may influence, to a lesser degree, the interparticle friction. Test results indicate that angular material exhibits higher strength in comparison to a rounded aggregate of the same source at the same constant void ratio. Unfortunately, in these comparisons, the angular material is usually produced from rounded material by crushing. Hence, the effect of angularity is to a certain extent masked by the change in particle surface texture produced by crushing.

Particle angularity influences the compaction of asphalt mixtures; that is, a mix containing an angular aggregate will compact under a given compactive effort to a lesser degree than will a mix containing a rounded aggregate. It is possible, however, that an angular aggregate may permit a greater degree of compaction, particularly when heavy rollers are used. The mix made with the rounded material may actually shove and push excessively under the roller and decompact.

Angularity, however, may be beneficial when the pavement is subjected to traffic, since all available evidence indicates that the mix containing the more angular materials are less susceptible to densification under heavy traffic and subsequent reduction in load-carrying ability. However, this may be also influenced by particle surface texture rather than by angularity.

Fig. 15.9 Gradations of four aggregates to be blended

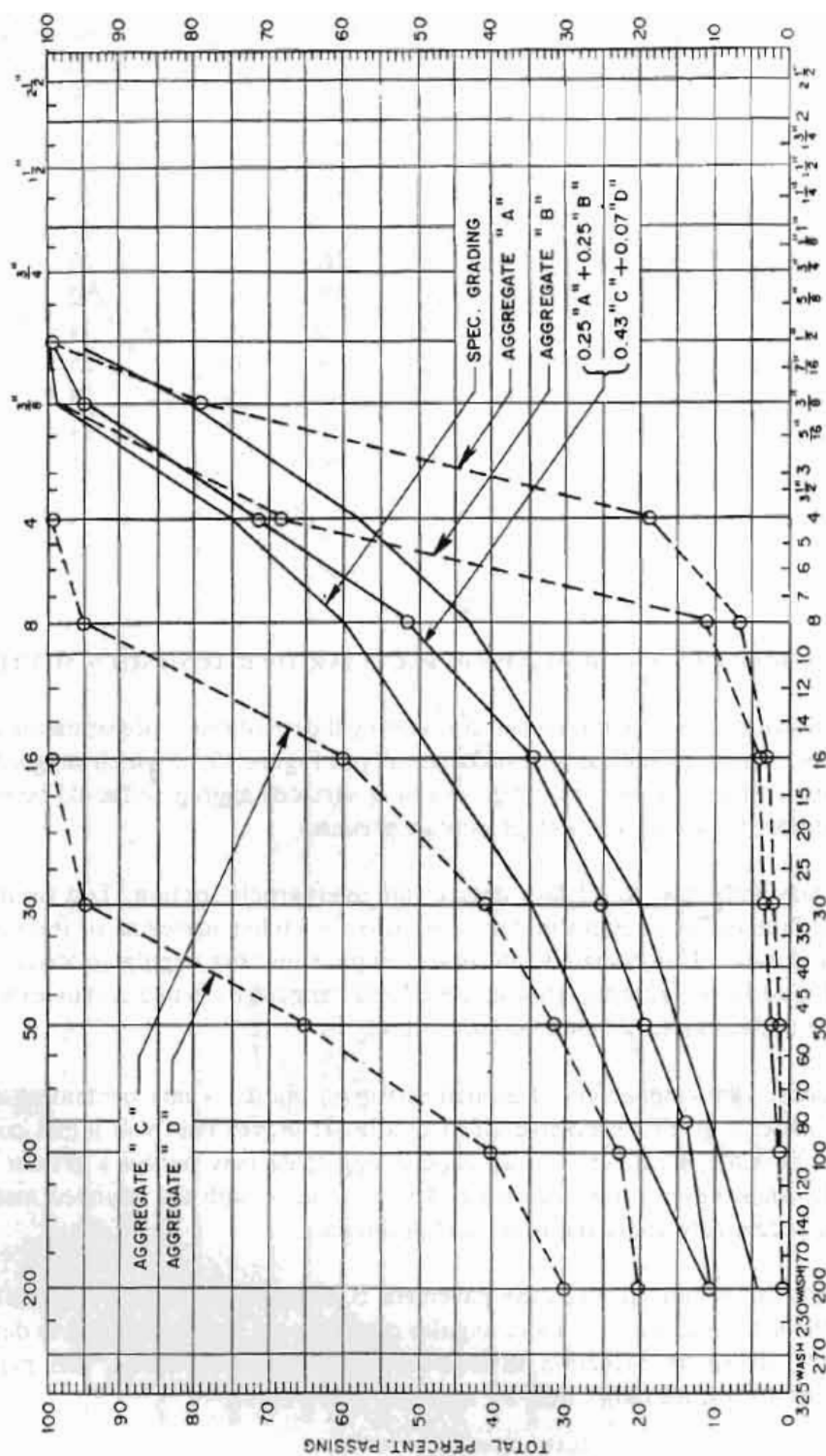
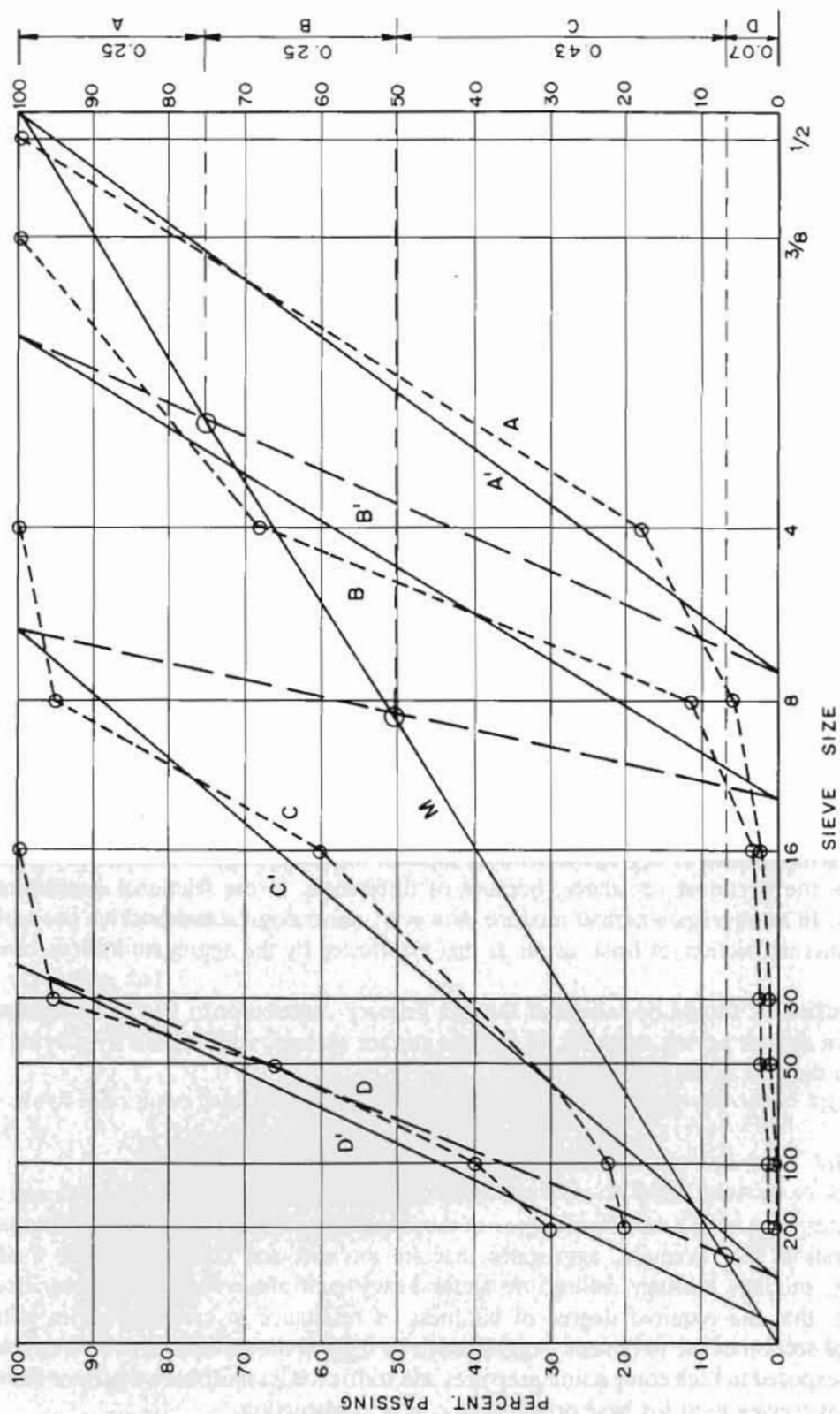


Fig. 15.9 Gradations of four aggregates to be blended

SIEVE NO.

SQUARE OPENINGS

Fig. 15.10 Example of blending using Rothfuchs' Method



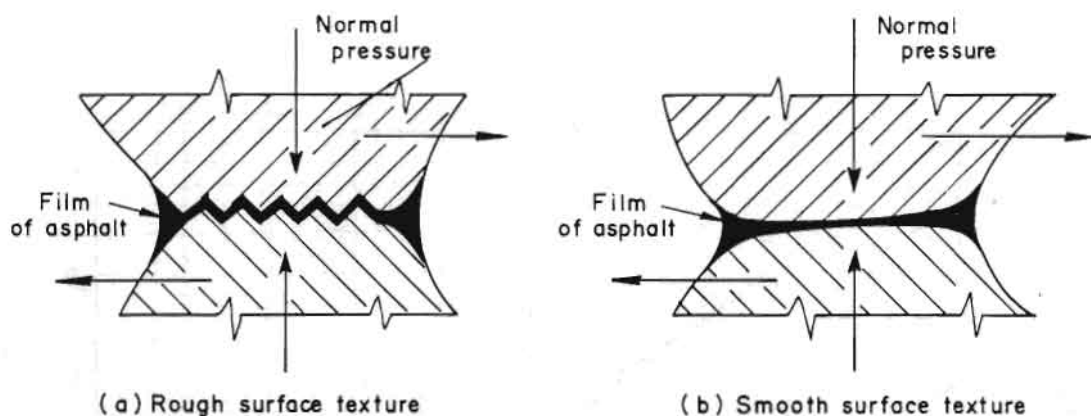


Fig. 15.11 Comparison of contact surface of aggregates with different texture

Particle size appears to have little effect on interparticle friction, at least in laboratory investigations. In actual pavements, however, due to limited thickness, structural effects may cause particle size to have an influence on the interparticle friction of the composed aggregate asphalt mixture. Particle gradation will influence internal friction to a certain extent. The denser the gradation of aggregate, the more contact areas in the compacted aggregate mass; hence, the greater the frictional resistance.

Void ratio, or degree of packing (compaction), will influence internal friction in the same manner as gradation; that is, the lower the void ratio, or the greater the degree of packing, for a given aggregate gradation, the greater will be the frictional resistance of the aggregate mass. The presence of asphalt will modify this relationship.

In compacted masses of aggregates without asphalt, the mineralogical composition of the aggregate may influence the frictional resistance, because of differences in the frictional coefficients of the various minerals. In an aggregate asphalt mixture, however, mineralogical composition probably has little effect on the internal friction, at least, as far as that manifested by the aggregate itself is concerned.

In conclusion, it should be reiterated that the primary contributor to frictional resistance of aggregate, for use in asphalt paving mixtures, is particle surface texture, with angularity playing a lesser role than has been thought in the past.

Durability

Aggregates must have a sufficient degree of those qualities necessary to resist crushing, degradation, and disintegration. For example, aggregates that are too soft and crush under the loads applied during handling, mixing, placing, rolling, or under heavy traffic may be undesirable. It should be noted, however, that the required degree of hardness or resistance to crushing varies with location in the structural section of the pavement. Aggregate to be used in the asphalt concrete surfacing, which will be directly exposed to high compaction pressures and traffic loads, must have a greater resistance to crushing than an aggregate used for base or sub-base course construction.

Aggregates for asphalt-paving mixtures must also exhibit resistance to degradation. By degradation we mean the production of fine material (usually material passing the # 100 and # 200 mesh screens) by mechanical action such as that produced by repeated application of traffic loads or by excessive handling prior to mixing. Hardness of aggregate is not necessarily related to degradation, since hard particles may wear excessively. Excessive abrasion of aggregate in an asphalt pavement produces fine material which may be either uncoated or insufficiently coated with asphalt and, in turn, can lead to disintegration of the surface.

Disintegration is the breaking down of aggregate particles due to chemical action and usually requires the presence of water to accelerate this action. Fortunately, however, when aggregate is coated with asphalt, disintegration is either minimized or eliminated entirely. Hence, in a well-designed asphalt concrete, disintegration of the aggregate is not as important as in the case of untreated aggregates for base course construction.

Disintegration is related to the mineralogical composition of the aggregate. For example, it is possible that the aggregate may contain minerals that, due to the action of water, will break down into clayey materials. In untreated base courses, this will result in loss in frictional resistance and increased resilient deformations under the action of traffic which, in turn, can lead to cracking of the pavement.

Wettability

Exposure to water is a condition to which all road-building aggregates are subjected. For good performance, any aggregate selected should be reasonably free from any detrimental effects on strength, durability, or flexibility caused by the presence of water. In the case of asphalt-coated aggregates, it is desirable that the aggregate will be of such a nature that water will not displace the asphalt from the aggregate surface. Hence, proper adhesion between the aggregate and the asphalt must be obtained, particularly in the presence of water. Properties of aggregates considered to affect adhesion are:

- surface, texture,
- surface coatings,
- particle size and surface area,
- porosity and absorption,
- chemical reactivity, and
- surface energy.

At present, there are at least three theories regarding the water resistance of asphalt-coated aggregates. These theories are :

- i. chemical reaction concept: acidic components of asphalt react with basic minerals of aggregate to form water insoluble compounds;
- ii. mechanical concept: emphasizes the role of surface roughness and porosity; and
- iii. surface energy concept: adhesion resulting from interfacial energy relationships at the aggregate, asphalt, water, and air interfaces.

Considering first the chemical reaction concept, when a solid is wetted by a liquid, absorption occurs at the surface and is followed by a chemical reaction between absorbed material and constituents of the solid phase. For an asphalt to show good adhesion to a solid, the asphalt must contain certain acid or polar compounds and must produce a water insoluble reaction compound. An acidic stone (e.g., quartz) cannot react with an acid oil. Basic oxides (limestones), however, can react with acid oils.

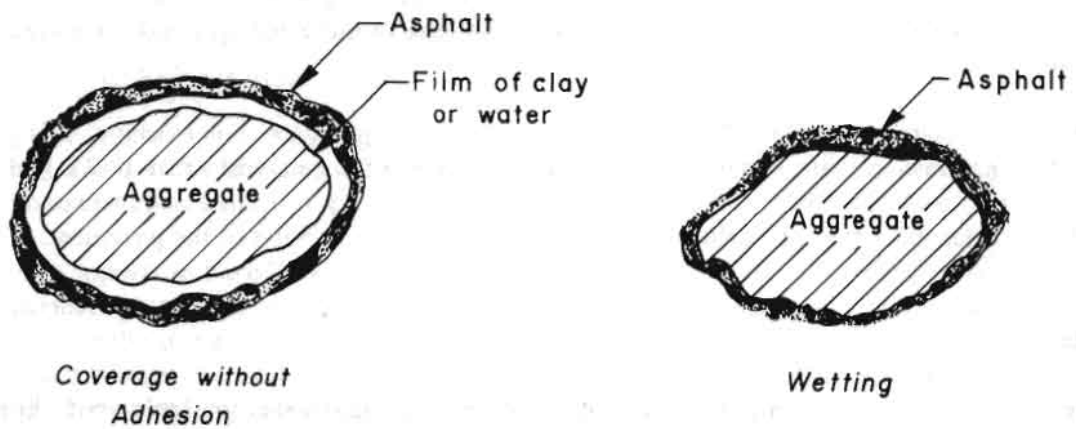


Fig. 15.12 Effect of surface film on aggregate coverage

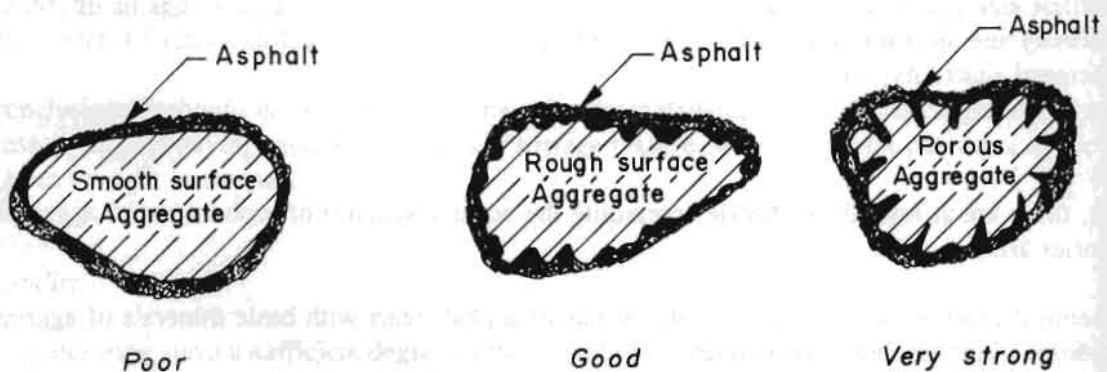


Fig. 15.13 Effect of aggregate surface texture on adhesion

According to the mechanical theory, the composition of the rock is important only to the extent that it affects surface texture. It is thought that the rougher the surface texture, the better the adhesion. Porous aggregates usually show better adhesion to asphalt, due also in part to mechanical interlock. In the case of porous materials, however, it is difficult at times to remove the water from the pores during the drying process. This may be a detriment with respect to adhesion.

Surface coatings also affect adhesion and fall into the mechanical interlock concept. If a layer of clay surrounds the aggregate particle, it is possible to develop coating of the aggregate, but the asphalt will not actually contact the aggregate particle. A film of water surrounding the aggregate particle will also produce a similar result.

Various aspects of the mechanical theory are illustrated in Figures 15.12 and 15.13. The surface energy concept, in part, makes use of the classical theory of wetting to explain adhesion. In the presence of water, the chemical theory states that :

$$r_{sw} = r_{sb} + r_{wb} \cos \theta$$

where,

- r_{sw} = aggregate-water interfacial tension,
- r_{sb} = aggregate-asphalt interfacial tension, and
- r_{wb} = asphalt-water interfacial tension.

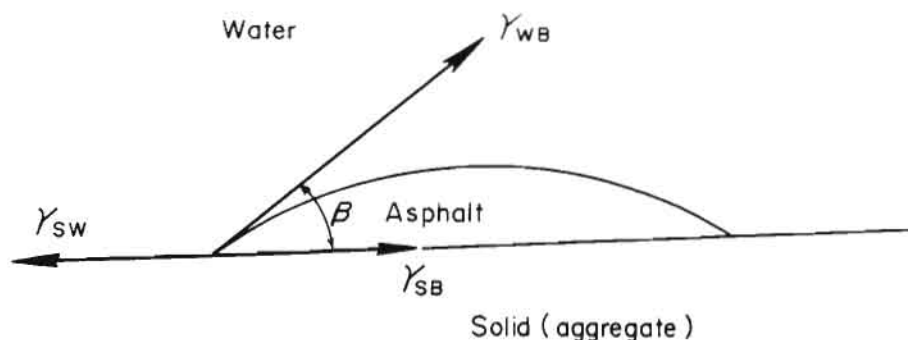


Fig 15.14 Contact angle in an aggregate, asphalt, and water system

From Figure 15.14 it can be seen that the smaller the contact angle, Θ , the greater is the possibility that the asphalt will flow over the surface of the aggregate and form the desired bond.

This formula is presented primarily to emphasize the importance of interfacial analysis in the study of the effects of water in asphalt mixtures. It should be noted, however, that such a strictly physical approach to adhesion is open to considerable criticism.

The values involved are difficult to measure and their application should be tempered with reservation. Nevertheless, as an attempt to explain the relative abilities of asphalt and water to coat aggregate particles, such a formula provides a valuable foundation for further discussion.

A somewhat more practical approach to an explanation of the adhesion phenomenon is found through use of the principle of polarity. Here one may find basic reasons for the terms commonly used in connection with mineral aggregates, 'hydrophilic' (water loving) and 'hydrophobic' (water hating).

Mineral aggregates, in particular those formed from freshly broken stone, ordinarily exhibit some degree of polarity. This tendency depends upon the chemical and crystalline structure of the material, upon its surface condition, and upon other factors of its physical condition. Figure 15.15 presents a graphical generalization of the possible effects of polarity upon adhesion.

Asphalts are generally rather weakly polarized. In other words, they tend to be weak dipoles. Since water molecules are all dipoles and are thus very active electrically, it is easy to see why water presents such a problem to the paving technologists with respect to stripping failures.

Actually, two conclusions might be drawn in this situation : (1) if an aggregate particle is already coated with water (or some other active dipole), it is impossible for the normal asphalt cement to displace the water and bond to the stone; and (2) if the particle should be coated with an asphalt, it is still possible for the water to later strip the bitumen from the aggregate. Fortunately, these generalizations do not always apply.

In some cases an aggregate-asphalt combination may exhibit polar tendencies which are considerably stronger than the polar action of the same aggregate with water. In such a case, the asphalt would displace water on the surface of the stone and a little stripping action might be expected. Also, the polar tendencies of some bituminous materials tend to increase with age, because of the orientation of polar materials within the main body of the asphalt. Consequently, a certain mixture might happen to be weakly water-resistant shortly after its preparation, but it would later have satisfactory adhesion as polar orientation proceeded (Fig 15.16). Particle size is important when considering the surface energy concept, because the surface areas and surface energy effects for the very fine sizes are large in relation to particle mass.

In general, it would appear that all three concepts are necessary to explain the behavior of asphalt and aggregate in the presence of water because chemical reactions may take place, mechanical interlock occurs, and surface energy relationships influence adhesion.

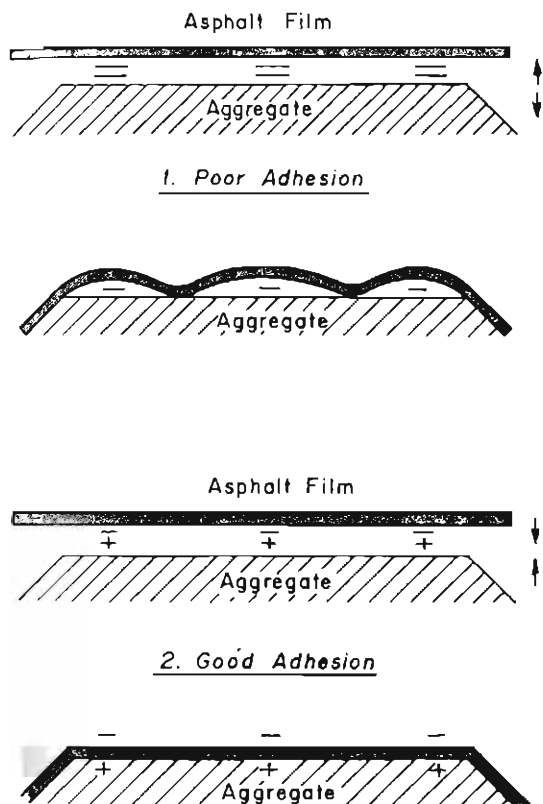


Fig. 15.15 Effect of polarity on adhesion

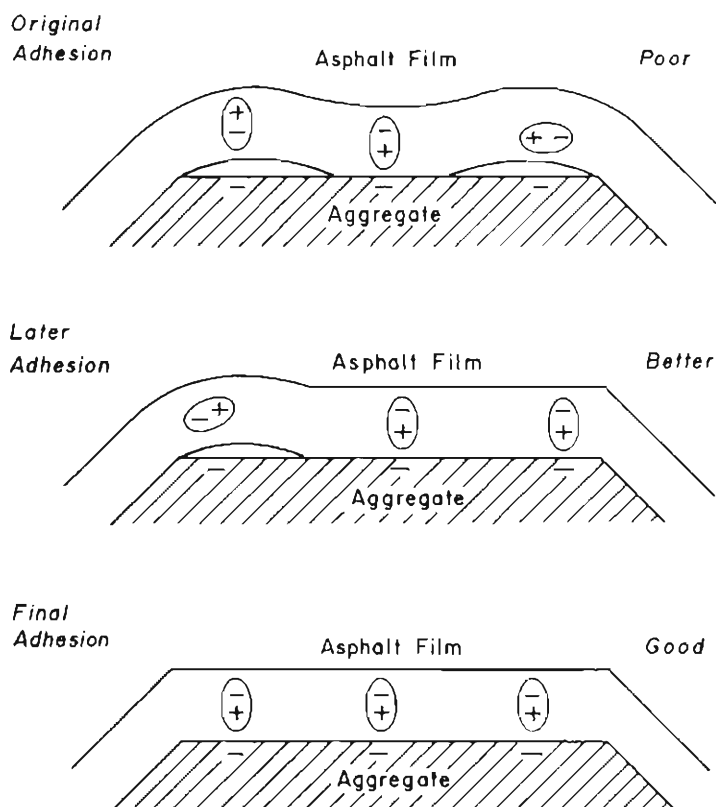


Fig. 15.16 Molecular orientation

15.7 SUMMARY OF PHYSICAL PROPERTIES, ENGINEERING PROPERTIES, AND MINERAL COMPOSITION OF ROCKS (See Tables 15.10, 15.11, and 15.12)

Table 15.10 Average values for physical properties of the principal types of rocks

Types of rock	Bulk	Absorption specific gravity*	Loss of abrasion %	
			Deval	Los Angeles
			% **	***
Igneous :				
Granite.....	2.65	0.3	4.3	38
Syenite.....	2.74	0.4	4.1	24
Diorite.....	2.92	0.3	3.1	
Gabbro.....	2.96	0.3	3.0	18
Peridotite.....	3.31	0.3	4.1	
Felsite.....	2.66	0.8	3.8	18
Basalt.....	2.86	0.5	3.1	14
Diabase.....	2.96	0.3	2.6	18
Sedimentary :				
Limestone.....	2.66	0.9	5.7	26
Dolomite.....	2.70	1.1	5.5	25
Shale.....	1.8-2.5			
Sandstone.....	2.54	2.8	7.0	38
Chert.....	2.50	1.6	8.5	26
Conglomerate.....	2.68	1.2	10.0	
Breccia.....	2.57	1.8	6.4	
Metamorphic :				
Gneiss.....	2.74	0.3	5.9	45
Schist.....	2.85	0.4	5.5	38
Amphibolite.....	3.02	0.4	3.9	35
Slate.....	2.74	0.5	4.7	20
Quartzite.....	2.69	0.3	0.3	28
Marble.....	2.63	0.2	6.3	47
Serpentine.....	2.62	0.9	6.3	19

* After immersion in water at atmospheric temperature and pressure

** American Association of State Highway Officials (AASHO) Method T3

*** AASHO Method T96.

Table 15.11 Summary of engineering properties of rocks

Types of rock	Mechanical strength	Durability	Chemical stability	Surface characteristics	Presence of undesirable impurities	Crushed Shape
Igneous :						
Granite, syenite						
Diorite.....	Good	Good	Good	Good	Possible	Good
Felsite.....	Good	Good	Questionable	Fair	Possible	Fair
Basalt, diabase						
Gabbro	Good	Fair	Questionable	Good	Seldom	Fair
Peridotite.....	Good	Fair	Questionable	Good	Possible	Good
Sedimentary :						
Limestone						
Dolomite.....	Good	Fair	Good	Good	Possible	Good
Sandstone.....	Fair	Fair	Good	Good	Seldom	Good
Chert.....	Good	Poor	Poor	Fair	Likely	Poor
Conglomerate						
Breccia.....	Fair	Fair	Good	Good	Seldom	Fair
Shale.....	Poor	Poor	Good	Possible	Fair to poor
Metamorphic :						
Gneiss, schists..	Good	Good	Good	Good	Seldom	Good to poor
Quartzite.....	Good	Good	Good	Good	Seldom	Fair
Marble.....	Fair	Good	Good	Good	Possible	Good
Serpentine.....	Fair	Fair	Good	Fair to poor	Possible	Good
Amphibolite.....	Good	Good	Good	Good	Seldom	Fair
Slate.....	Good	Good	Good	Poor	Seldom	Poor

Table 15.12 Mineral composition of rocks

Name of Rock	No. of samples tested	Essential mineral composition										Iron Ore	Remainder
		Quartz	Ortho-class. microcline	Plagioclase	Augite	Hornblende	Mica	Calcite	Chlorite	Kaolin	Epidote		
Igneous rocks													
Granite.....	165	30	45	(8)	6	(6)	5
Biotite granite...	51	27	41	9	11	(7)	5
Hornblende granite....	20	23	34	12	...	13	4	(10)	4
Augite syenite.....	23	(4)	52	7	8	...	4	...	(3)	(11)	(3)	(4)	4
Diorite.....	75	8	7	30	...	27	(4)	...	(3)	(8)	(5)	(3)	5
Gabbro.....	50	44	28	9	(3)	(6)	10
Rhyolite.....	43	32	45	(3)	(5)	...	(4)	(3)	...	(4)	4
Trachyte.....	6	(3)	42	6	...	(3)	(3)	(14)	(8)	(7)	5
Andesite.....	67	48	14	3	(6)	...	(3)	(8)	6
Basalt.....	70	36	35	(3)	5
Altered basalt.....	196	32	31	(9)	(4)	...	(4)	3
Diabase.....	29	44	46	(4)	6
Altered diabase.....	231	35	26	(15)	(9)	...	(4)	11
Sedimentary rocks:													
Limestone.....	875	(6)	83	3
Dolomite.....	331	(5)	11	...	(4)	...	(9)	2
Sandstone.....	109	79	(5)	3
Feldspathic Sandstone.....	191	35	26	(3)	(3)	(22)	...	(4)	7
Calcareous Sandstone.....	53	46	(3)	42	(3)	6
Chart.....	62	93	7
Metamorphic rocks:													
Granite gneiss.....	169	34	35	(4)	20	7
Hornblende gneiss ..	18	10	16	15	(3)	45	(4)	7
Mica schist.....	59	36	14	(1)	40	9
Chlorite schist.....	23	11	...	10	...	(5)	39	...	28	(4)	3
Hornblende schist ..	68	10	(3)	12	...	61	(7)	...	7
Amphibolite.....	22	(3)	...	8	...	70	12	(5)	7
Slate.....	71	29	(4)	55	7
Quartzite.....	61	34	(3)	(4)	9
Feldspathic Quartzite.....	22	46	27	(7)	...	(3)	(10)	7
Pyroxene quartzite...	11	29	10	15	24	(5)	8
Marble.....	61	(3)	96	1

Source:

b Values shown in parentheses indicate minerals other than those essential

for the classification of the rock.

c Includes 10 to 20 % rock glass.

d Limestone contains 8 % of the mineral dolomite : the rock dolomite contains

82 % of this mineral.

e Includes 3 % opal.

f Includes 3 % garnet.

15.8 SOME COMMONLY USED GEOLOGICAL AND MINERALOGICAL TERMS

Acidic :	Term applied to igneous rocks containing more than 65 per cent silica (SiO_2).
Calcareous:	Term applied to rocks containing calcium carbonate.
Calcite:	The mineral calcium carbonate, CaCO_3 .
Chert:	Very fine-grained, siliceous rock containing cryptocrystalline quartz, chalcedony, opal, or a combination thereof. Porous varieties are usually light coloured and have splintery fractures. Dense varieties are hard, have conchoidal fracture, greasy lustre, and occur in many colors including white, yellow, brownish stained, or green. The coloured varieties are sometimes called 'jasper' and dense, gray variety called 'flint'. All varieties will scratch glass and cannot be scratched by a knife blade. Some of its constituents may be reactive with cement alkalis, and it should also be considered suspect as concrete aggregate for exposed concrete in cold climates.
Clay:	Very fine particles consisting of hydrosilicates of aluminum or magnesium or both. In concrete aggregates, the term frequently refers to these materials occurring as coatings finer than the No. 200 (75 μm) sieve which may be removed by washing. Clay may also occur well dispersed in rocks between laminations so as to weaken the structure or cause the particle to be susceptible to freeze-thaw attack.
Claystone:	An indurated clay, having the texture and composition of shale but lacking its fine lamination of fissility, a massive mudstone in which clay predominates over silt, a non-fissile clay shale.
Conglomerate:	(1) Rock consisting of rounded pebbles cemented together with finer material. (2) A coarse-grained, clastic sedimentary rock, composed of rounded to sub-angular fragments larger than 2 mm in diameter (granules, pebbles, cobbles, and boulders), set in a fine-grained matrix of sand or silt and commonly cemented by calcium carbonate, iron oxide, silica, or hardened clay, the consolidated equivalent of gravel both in size range and in the essential roundness of gravel and sorting of its constituent particles.
Coral:	A general name for any of the large groups of bottom-dwelling sessile, marine invertebrate organisms that belong to the class <i>Anthozoa</i> .
Detritus:	Fragmental material such as sand, silt, and clay moved from its place of origin.
Diorite:	Medium to coarse-grained rock composed essentially of plagioclase feldspar and ferromagnesium minerals.
Dolerite:	A basic intrusive rock composed of labradorite and pyroxene and which is characterized by ophitic texture.
Dolomite:	The mineral calcium-magnesium carbonate $\text{CaMg}(\text{CO}_3)_2$. A common rock-forming rhombohedral mineral.

Foliated:	More or less parallelism of mineral grains in metamorphic rocks as distinct from the stratified structure of some sedimentary rocks.
Glass:	Component of some volcanic rocks resulting from such a rapid cooling from the molten state that no crystal structure is present. Obsidian is a natural glass.
Garnet:	A group of minerals, brittle and transparent to sub-transparent mineral, having vitreous lusture, no cleavage, and a variety of colors, dark red being the most common.
Gneiss:	A banded or foliated rock (e.g., granite gneiss, diorite gneiss) formed by regional metamorphism in which bands or lenticles of granular minerals alternate with bands or lenticles in which minerals having flaky or elongated prismatic habits predominate. Generally less than 50 per cent of the minerals show preferred parallel orientation and are rich in feldspar and quartz.
Granite:	A plutonic rock in which quartz constitutes 10 to 50 per cent of the felsic components and in which the alkali feldspar to total feldspar ratio generally ranges from 65 to 90 per cent. Rock has large grains easily visible to the eye and consisting predominantly of quartz and alkali feldspar.
Hematite:	Ferric oxide, Fe_2O_3 .
Kaolinite:	One of the clay minerals consisting of a hydrous aluminum silicate.
Laterite:	A term used for highly-weathered, red subsoil or material rich in secondary oxides of iron, aluminum, or both, nearly devoid of bases and primary silicates and commonly with quartz and kaolinite.
Limestone:	A sedimentary rock consisting chiefly of calcium carbonate, primarily in the form of the mineral calcite and with or without magnesium carbonate. Common minor constituents include silica, feldspar, clays, pyrite, and siderite.
Loess deposits:	A widespread, homogeneous, commonly non-stratified, porous, friable, slightly coherent, usually highly calcareous, fine-grained, blanket deposit, consisting predominantly of silt with subordinate grain sizes ranging from clay to fine sand.
Magma:	Naturally occurring mobile rock material, generalized within the earth and capable of intrusion and extrusion, from which igneous rocks are thought to have been derived through solidification and related processes.
Marble:	A metamorphic rock consisting predominantly of fine to coarse-grained, re-crystallised calcite and/or dolomite, usually with a granoblastic saccharoidal texture.
Mudstone:	An indurated mud having the texture and composition of shale, but lacking its fine lamination or fissility. A blocky or massive, fine-grained, sedimentary rock in which the proportion of clay and silt are approximately equal.

Peat:	An unconsolidated deposit of semi-carbonized plant occurring in a water-saturated environment, such as a bog or pan, and of persistently high moisture content.
Phyllite:	A metamorphosed rock, intermediate in grade between slate and mica schists. Minute crystals of sericite and chlorite impart a silky sheen to the surfaces of cleavage.
Quartz:	Most abundant form of the mineral silica (SiO_2). Very hard, will scratch glass but cannot be scratched by a knife. Colourless when pure, glassy lusture, with conchoidal fracture.
Quartzite:	There are two types of quartzite (1) A granoblastic metamorphic rock consisting mainly of quartz and formed by re-crystallization of sandstone or chert by either regional or thermal metamorphism. (2) Extremely hard, tough, and stable sandstone. Sand grains have been cemented together with secondary quartz. Excellent concrete aggregate but may crush to thin or elongated pieces.
Sandstone:	A medium-range, clastic sedimentary rock composed of abundant rounded or angular fragments of sand size, set in a fine-grained matrix and more or less firmly united by a cementing material.
Schists:	A strongly-foliated, crystalline rock formed by dynamic metamorphism. It can be readily split into thin flakes or slabs because of the well-developed parallelism of more than 50 per cent of the minerals present, particularly those of lamellar or elongate prismatic habit, e.g., mica and hornblende. It originates from a number of igneous or sedimentary rocks. It is characterized by thin, platy, flat fragments.
Shale:	A fine-grained detrital sedimentary rock, formed by the consolidation of clay, silt, or mud. It is characterized by a thinly laminated structure and a fissility approximately parallel to the bedding. The rock breaks readily into thin layers and is commonly most conspicuous on weathered surfaces. The rock is a poor candidate as a concrete aggregate unless proved otherwise.
Slate:	A fine-grained, low-grade metamorphic rock which breaks easily, not necessarily parallel to laminations. Less suspect as a concrete aggregate than shale.
Colluvium:	Rock fragments of any size or shape derived from, and lying at the base of, a cliff or very steep rocky slope. Talus cones are constituted of colluvium.

ECOLOGY AND BIOTECHNICAL STABILIZATIONS

16.1 ECOLOGICAL CONCERNS OF ROADSIDE PLANTATIONS

16.1.1 Introduction

Roadside plantation is a form of land use system which is assuming increasing significance. The new roles being ascribed to this activity are partly the outcome of knowledge development, e.g., bioengineering techniques for the stabilization of slopes alongside roads. The other factors contributing to the significance of the roadside land have emanated from increasing pressure on land use and its resources. It is being realised that to meet the needs of the growing human population every bit of land has to be brought under proper land use with as much benefit as possible. In this respect, in recent times, roadside plantations have been seen to complement forestry in most developing countries. Therefore, roadside plantation is helping to provide an economic benefit in addition to the benefits of solving the ecological problems of the restoration and maintenance of ecosystems.

Under mountain conditions, the **plantations on roadsides** have different objectives. So far most efforts have been concentrated on using vegetation to stabilize slopes made vulnerable to erosion as a result of road construction. This objective focuses on plantations only in vulnerable areas and the rest of the roadside land has been rarely used for populations. In most cases, a second priority in roadside plantations was given to the aesthetic aspect, i.e., planting flowering trees and other species on land not covered under the first objective. Even in the case of the first objective, use of vegetation is a recent phenomenon. It is assumed, therefore, that most of the roadside land falling under different categories of roads is yet to be brought under proper land use planning. Also, the focus of plantations may vary with the available width of land on the sides of roads, and this varies with road type. On a particular mountain road, the vegetation variation is a function of varying climatic regimes, farming systems, and ecosystems. As such, it depends on the characteristics of locations through which the road passes, e.g., **forest ecosystems**, pastures or range lands, and horticulture or crop-dominated farming systems' areas; or **detritus ecosystems**, i.e., industrial dominated areas, pure habitations like urban areas, valleys, low, and high mountain areas.

This chapter discusses roadside plantations under an ecosystemic framework. The overall objective is to develop concepts whereby roadside vegetation makes a meaningful contribution to the ecosystem's health and stability.

The possible contributions of plantation practice fall within three broad categories:

- a. contributions to restoration, conservation, and maintenance of ecosystems,
- b. contributions supporting sustainability of agro-ecosystems, and
- c. contributions to maintain the quality of physical health of ecosystems.

* Tables and Figures in this Chapter that have not been credited to any source have been compiled by the author.

The degree of contribution under each of these categories depends upon two factors. One, how much land width is available on the roadside? and two, what efforts are made to realise full use of all the available land for plantations, taking all aspects into consideration? Land availability for plantations on roadsides depends upon the amount of land acquired along different categories of roads. Regulations in this regard may differ among regions and countries. For example, in India there are three main categories of road; national highways, state highways, and district/village roads. Under the first category, the usable combined width of roadside area is 45m in the plains and 24m in the mountains; for State highways it is 45m for the plains and 24 m for the hills; and for district level roads it is 25m for the plains and 15-18m for the mountains (Table 16.1) Village link roads are generally 9 m wide with 9-12m of combined open area on the sides.

Whenever a road passes through an agricultural area, there may be situations where the planned width of the roadside land strip is not available or where it has been encroached upon by farmers. It may permit only one row of plantation and even the choice of species may be decided upon by the person whose agricultural fields were acquired for construction of the road. Such instances arise where roads have been built under special programmes without paying compensation to the people whose lands were acquired. There is yet another situation where land available for roadside plantations is much more than the acquired width. Such situations are commonly met on mountain roads passing through slopy areas. These areas generally come under wasteland, grassland, forests, etc. and many of them are either already well vegetated or they may be degrading due to climatic harshness or excessive use.

Table 16.1 Available widths of roadside land along different categories of mountain roads: case of India as an example

Category of roads	Width of total land recommended to be acquired for constructing road				Main road width	Land normally available for roadside plantations ¹	
	Mountainous areas, slopy lands		Valley plains, least slopy plains			Mountainous areas	Valley plains
	Normal (m)	Range (m)	Normal (m)	Range (m)		(m)	(m)
National highways	30	30-60	45	30-60	12.0	18	33
State highways ²	30	30-60	45	30-60	12.0	18	33
District roads	20	15-25	25	30-60	9.0	11	16
Village roads	10	15-20	12	15-20	7.5	3	4.5

Source: Information developed through personal communications with road engineers and the Secretariat of the Indian Roads' Congress, 1988.

Note:

1. The actual available area differs because of the range. It may increase or decrease because of the range of acquired land, common encroachment problems, and steep slopes in rocky mountain areas.
2. In practice State highways are less wide than national highways.

16.1.2 Contributions for Restoration, Maintenance, and Conservation of Ecosystems

The micro-ecosystems of mountain areas along the alignment of roads will be affected in terms of vegetation disturbances because of the clearing of the area for construction and also because of the uncontrolled throwing of debris. After a road is built there are always general accusations that the road accelerates deforestation in an area. Moreover, with increasing accessibility several valuable plant species are overexploited to the extent that fears of their becoming extinct become imminent. Efforts have been made here to conceptualize an approach to make use of plantations to repair the damage to the best possible extent.

i) *Plantations as Part of Restoration Ecology*

Areas exposed because of road construction activity or made vulnerable by it can be partly or fully restored to the original condition of vegetation cover if it existed previously. This will mean restoring the ecological system back to normal. In using plantations for restoration and maintenance, the aim is to alter conditions on **failed slope surfaces** to induce stability through a variety of functions, catching material moving downslope, armouring the slope and protecting the surface, draining the slope, and supporting the slope by reinforcement.

Incorporating plantations, for the restoration and maintenance of roadside areas, is a relatively recent endeavor. It was first attempted on a considerable scale during the 1960s (Greenway 1987). This endeavor has grown steadily in the last 20 years and the influence that grass, shrubs, and trees may have on **slope stability** is now emerging as a successful experience.

Although the technique is discussed in detail in Section 16.2 of this chapter, the point emphasized here is its value as an approach to **restoration ecology**. If by restoration we imply that the components affected, i.e., the kinds of plant species, are to be restored then it does mean that species used as tools of restoration should necessarily be among the flora of the local ecosystem. The point advocates giving preference to local plant species, rather than using introductions, as far as possible. Introductions may help restore the physical environment but they also bring changes in the phytosociological structure of plant communities which might sometimes lead to unaccountable transformations in ecosystemic structure and function. In such cases they help restoration only partially.

ii) *Contributions to the Conservation of Plant Resources*

The present day accusations against road development are that it is a cause of accelerating deforestation and erosion of plant resources. Wherever road development takes place a similar scenario develops. There are instances within the Hindu Kush-Himalayan Region where, within a short time of road development, the areas have been subjected to complete loss of their tree cover. Roads by themselves are not the agents of destruction. Destruction is also a result of population pressure, scarce land resources, and lack of alternatives to sustenance. Both forest resources and forest land for agriculture become economically very important with access.

Under such circumstances, threat of the extinction of vegetation becomes imminent. In the first instance, economically important plant resources are overexploited and their conservation becomes a necessity. They cannot survive in their natural habitat due to its loss or management control limitations. Roadside

land provides an excellent, unconventional **alternative habitat** for **conservation plantations** of such plant species. The management of the conservation plantations on roadside sites is relatively easy and more effective in control. Representatives of all threatened life forms, i.e., trees, shrubs, and herbs, can be conserved this way. In a way such efforts can turn these sites into replicas of botanical gardens. Nevertheless, the conservation effort herein means that it could be one of the criteria used for choice of species for maintaining roadside stabilization and using unmanaged land areas. The concept is an ideal example of combining development with conservation and conservation with development.

On priorities regarding the conservation of species, the World Conservation Strategy (IUCN 1980) has outlined the following criteria which might prove helpful in species' selection for plantations in the present context. It outlines that priorities should be given to these categories:

- i. species that are endangered throughout their range, and
- ii. species that are the sole representatives of their family or genus.

The formulation is illustrated in Table 16.2.

Table 16.2: Formulation for determining conservation priority of threatened species

Size of loss	Imminence of loss		
	<i>Rare</i>	<i>Vulnerable</i>	<i>Endangered</i>
Family	4	2	1
Genus	7	5	3
Species	9	8	6

Source: IUCN 1980

Note:

1 - 9	= suggested order of priority
1,2,3	= highest priority
4,5,6	= intermediate priority
7,8,9	= Lower priority

Further priority should be given to those plant species that are most threatened and most needed. As pointed out, such a conservation effort assumes that there is institutional and public concern for conservation but the felt constraint is habitat, because of the ongoing expansion of land use transformation in the original habitat or because there is a lack of infrastructural facilities to preserve distant plantations *in situ*. The advantages of using roadsides for plant conservation efforts lie in better management through accessibility and through the status of land, i.e., protected under more strict regulations and the convenience of forcing regulations.

Such a conservation strategy, however, calls for the multidisciplinary efforts of several institutional agencies, such as the department of roads, to make land available, and the department of forests and environment, for the resources and research institutions to prepare priority lists of threatened species for an area. Given the national awareness and international concerns and funding assistance for the conservation of natural resources (World Bank 1986), the execution of this unconventional method of plant resources' conservation seems possible for some areas.

iii) *Plantations to Maintain Natural Ecological Systems*

Natural ecological systems or ecosystems consist of several components or **trophic levels** that provide channels for energy flow. Groups of components performing a similar function make one trophic level. For example, rats eating grain crops form one trophic level of herbivores. Snakes, cats, and birds together form another trophic level. They form a web of **food chains** through which ecosystemic energy flows. The sustainability of an ecosystem depends upon the diversity of components within trophic levels as well as the diversity of trophic levels within an ecosystem. The more diverse a system the more stable and self sustaining will it be.

Existence of these trophic levels, however, depends heavily upon the amount of available plant resources within an area. In the absence of diverse plant forms these components will be eliminated for want of a suitable habitat or 'niche'. Take, for instance, the case of agricultural land spread over a vast area without much natural vegetation, trees, or shrubs. The crops in this area will have more chances of insect infestations, and additional efforts will be needed for the control of insect pests to minimize crop losses. For effective **biological control**, creating a suitable habitat for insect predators, birds may provide an answer. In addition, because the birds eat insects at a particular time of year, they contribute to biological control and should be provided with resting places, nesting places, and food for lean periods by providing wild fruits from trees and shrubs. This would further add to their comfortable stay in the area.

Plantations on roads passing through such crop-land dominated valleys can play a very special role in restoring ecological systems or the natural ecosystemic functioning impaired by over-simplification of the agro-ecosystems. The choice of species in this respect can be further linked to other development efforts; for example, noting the slack period for bee flora in the area and choosing species that compensate for it.

16.1.3 *Contributions Supporting the Sustainability of Agroecosystems*

i) *Increasing Role of Roadside Land as Common Property Resources for the Local Populations*

Common property resources are still an important form of natural resource endowment in the rural mountain areas of the developing countries. Broadly defined, **common property resources** (CPR) are those used by an entire community without any exclusive individual ownership or access rights (Jodha 1985). CPRs have been the backbone of subsistence mountain farming and have fulfilled various kinds of subsistence needs: green and dry fodder, fuel, grazing land, etc. The land is categorized as community lands, waste lands, degraded forests, shelter belts, panchayat land, etc.

In the absence of regulatory institutions and because of rapid population growth, exerting tremendous pressure on land for cultivation, the trend is towards the gradual depletion of common property resources. The profitability of, rather than the upkeep of, CPRs has become the guiding force behind the choice of enterprises and usage patterns of CPRs. Privatization of these resources through legal processes, illegal seizure, and overexploitation are contributing in a major way to their depletion. This process of change deprives a region of its comparative advantage in a key subsistence or economic activity (Jodha 1985).

The future of CPRs should be considered according to their several advantages, for example, such as promoting the economic activity best suited to the natural resource base of a region, sustaining the rural poor, and assuring the use of land according to its capability.

Apart from several measures suggested for saving CPR lands (Jodha 1985) to ensure sustainable benefits, there is yet another alternative. This lies in strengthening the role of roadside land as CPRs. Although legally they are government lands, used for raising revenues, *de facto* they have been increasingly used as CPRs. Under mountain conditions, several roads, both highways and feeder roads, pass through subsistence mountain farming areas where people depend upon plant resources from the non-agricultural land of CPRs. Curiously, while traditional forms of CPR are depleting with the increasing road network, the new version of CPRs in roadside land is increasing. In several areas it can be seen to be taking over the role of CPRs almost completely.

To derive maximum benefits, an institutional strategy on the following lines might help : recognize the significance of roadside land for CPR use, establish effective regulations to create and maintain it, and ensure the cooperation of the local people for the systematic management of its productive resources, for example, social forestry systems and technological support for selecting productive, environmentally suitable plant species and managing a healthy plant community on this land resource.

ii) *Farming Needs of Communities Living along the Road and the Contribution of Roadside Plantations*

Probably the most serious deforestation and conservation problems faced by mountain areas are caused by the lack of rural development. In their struggle for food and fuel, growing numbers of desperately poor people find themselves with little choice but to strip available vegetation, resulting in harmful consequences such as soil erosion.

This is also the general scenario encountered near roadside habitations in several mountain areas. Often the rural mountain communities responsible for this destruction do not need to be told that it is a mistake. What such communities need is to be equipped to win their livelihoods in sustainable ways. Therefore, there is a need to develop the means to help these rural communities to conserve plant resources as an essential basis for the development they so sorely need.

Plants growing on the roadside could be important and renewable resources, particularly for rural mountain communities. The food and nutritional importance of these plants or their products, *per se*, for the local people, are generally underestimated and ignored.

One recalls a situation in which village school children were picking wild fruits (*Zizyphus*, *Rubus*, Currants, Indian gooseberry, peaches, apricots, pears, and *Hyppophae* from roadside plantations while going to school and on returning home in the afternoon. One can visualize roadside plantations becoming a source of fruits for cowherds and shepherds. It is useful to know that *Aesculus*, a tree recommended

for roadside plantations (Tiwari and Singh 1984) in high altitude areas, is a source of food during hunger gaps. Families in several areas of the Himalayan Region, whose grains are exhausted early before the next crop is harvested, process the kernels of the bitter fruits of *Aesculus* to yield a kind of flour. As the fruit production per tree is in quintals, it is a viable proposition. *Aesculus* fruits also provide nutritious fodder for cattle and this is generally saved for the snowy, winter period. *Hyppophae*, a roadside plant of the high mountain *Trans-Himalaya* yields juicy berries, a rich source of Vitamin C, even if taken in small quantities. More important, this rich Vitamin C source is available to those who can otherwise not afford to purchase Vitamin C to contain deficiency. Plantations of *Hyppophae* managed on roadsides may help improve the nutritional status of the remote high mountain people on a sustainable basis rather than conducting crash programmes of child nutrition improvement over a short period. Besides, large-scale plantations of this species will also help improve soil fertility and provide cash benefits from the sale of berries or their products.

The Indian gooseberry (*Phyllanthus amblica*) is another rich source of Vitamin C and it is a plant of the lower hills. In Himachal Pradesh, a Himalayan State of the Indian Union, the Roads' Department raises *Phyllanthus* plantations on several roads. Both the department and the local public make good use of its fruits; the former to raise revenue and the latter to use as food.

Prinsepia, a thorny shrub, is a good plant for slope stabilization and relatively less palatable for livestock. Its fruits have been in use as a source of edible oil by subsistence farming communities in the mountains. Dried twigs are used for fuel. Planted on roadsides, it may serve as a multipurpose species.

Sapindus is a tree whose fruit wall is a source of natural soap. Subsistence communities use it for washing clothes. A farming family's needs are met by a tree or two. The excess is always sold in local markets. In Himachal Pradesh, this species has been planted on roadsides in the lower hills. *De jure* the property belongs to the Government but *de facto* nearby farming families collect the produce from these trees.

Likewise, there are an unaccountable number of economic plant species for roadside plantations.

iii) *Role of Roadside Plantations in Off-farm Income and Employment Generation: The Case of Apiculture*

Roadside plantations, established as bee forage, particularly for forage scarcity periods, enhance the scope of beekeeping which, in turn, increases the possibility for farmers to earn additional income from honey. This also increases crop yields through the pollination services of bees. Recent experiences gained from using roadside plantations for large-scale apiculture, as a form of off-farm activity, have been described in Pakistan. The United Nations' High Commission for Refugees and the Government of Pakistan have provided bee colonies to Afghan refugees, who move them along the road lengths for the whole year. Hundreds of tents and bee colonies can be seen on the sides of all the roads in the Northwest Frontier Province (NWFP). This activity has provided subsistence to several hundred people.

But why do we need roadside plantations for apiculture? Populations of most pollinating insects are declining because of the vast clearance of waste lands for cultivation. The extensive practise of agriculture and monoculture is reducing their hibernating and nesting places. Indiscriminate pesticidal/insecticidal sprays are killing them continuously. Under the present state of affairs we have to depend upon domesticated honey bees for the pollination of crops. To sustain bees and encourage apiculture, varieties of bee

flora are required which provide subsistence rewards during some parts of the year and surplus during the others. Some agricultural and horticultural crops serve as useful and plentiful forage but the availability is restricted to short durations only. This means that agricultural and horticultural crops provide honeybees with nectar and pollen for a short period in the year only, restricting the scope of beekeeping. Therefore, apart from crops, other kinds of plantation that flower for long periods in a year, or a combination of several tree species that blossom during different months, so that nectar and pollen are almost continuously available to honey bees, are needed. The exercise carried out along the roadsides would involve the whole mountain road length, passing through different climatic regions, and this would provide the advantage of diversity in terms of species and their blossom calendars. To ensure variations in the efficient use of roadside flora throughout the year, the bee colonies need constant movement along the road length, for example, summer in the high mountains, winter in the foothills, and spring in the mid-hills. Table 16.3 lists species which are important as honey plants, in addition to other uses. Plant species can be selected out of the whole list for roadside plantation, keeping other needs in mind.

iv) *Aesthetics, Comfort, and the Role of Plantations*

Historically, the role of roadside plantations was perceived as a means of comfort for travellers. Although much has changed with time, the concept of the provision of comfort to travellers is still followed. In most parts of the sub-tropical hill terrain, the provision of shade during hot summer months assumes the highest importance. In the present age of automobiles, planting tree groves to provide shade and a good environment at some selected places, where travellers may stop and rest, is considered necessary. While the avenue may provide shade to the travellers, it should not be so dense as to obstruct the view of the landscape. Also it should not trap exhaust gases and mist under the canopy to adversely affect visibility. The aim of comfort for travellers should be integrated with other imperatives of roadside plantations. Wherever species are planted to serve the aforementioned imperatives, but the plantations clash with the above interests of the travellers, the solution lies in creating rows of plantations. The first row should provide the traveller with comfort and rest and the rows behind it should contain some species of choice to serve other imperatives.

16.1.4 *Contributions to Maintain the Quality of Physical Health of Ecosystems*

Although roads add to the well-being of human beings, and the intentions in road development are always for overall improvements in quality and sustainability of ecosystems, the physical environment of an area is adversely affected by road development in the following ways:

- (a) erosion of soil due to exposure of bare surface and debris;
- (b) atmospheric pollution created by emissions from vehicles plying on the road, as well as from material used to construct the road; and
- (c) noise pollution created by vehicles.

i) *Erosion*

Much of the soil surface becomes exposed during road construction. In mountain areas, this is further compounded by the downward dumping of debris and the destruction of vegetation cover for a considerable distance. This adversely affects the habitat quality of the surrounding area. In the high mountains, where vegetation cover takes a long time to develop because of harsh climatic conditions, such an exercise proves disastrous. Restoration efforts mostly prove ineffective because they are inadequate. Long-term impacts include further enlargement in erosion areas and effects on local water quality.

Plantations can create an effective vegetation cover on the exposed parts and save the area from erosion. More discussion on the topic is given under biotechnical stabilization in Section 16.2.

ii) *Atmospheric Pollution*

Dust stirred up from the road surface, especially during dry weather, carbon smoke from automobiles, and other activities such as crushers on roadsides, all add to atmospheric pollution around roadsides. Large-scale use of the road by heavy vehicles helps to increase the ground temperature and lower atmospheric humidity locally. This, in turn, interferes with plant establishment (in the initial stages), soil, micro-flora, and fauna.

The sulphur and nitrogen compounds from burning fossil fuel are causes of acid rain. The bitumen used as the wearing coat in all roads is hydrocarbon and starts melting at 38°C and is converted into molecular form through the traction of moving vehicles. From all these sources the atmosphere in and around roads contains the following pollutants:

- a. carbon dioxide (CO_2)
- b. carbon monoxide (CO)
- c. lead and other metal compounds, and
- d. unburnt petrol and oils.

Among the heavy metals, lead, copper, cadmium, and asbestos dust are released by vehicles along with smoke.

Therefore, the sides of roads polluted by the presence of solid, gaseous, and liquid substances in the atmosphere are injurious to human beings, agriculture, and animals. Clinically, several disorders and diseases are ascribed to this kind of air pollution. Sulphur dioxide affects the respiratory tract and causes chronic nasal pharyngitis and nitrous oxides are injurious to eyes and nose. Lead poisoning causes abdominal pain, headaches, weakness, and several other diseases and discomforts. Carbon monoxide impairs oxygen intake by the blood and has disastrous effects on human beings. A study on lead, cadmium, and copper contamination, due to vehicular emission, has established that the effect is noticeable in the biological chains and results in the toxicity of some of the foods eaten by man (Panda 1988).

All these factors contribute to the disastrous effect on the health of road users as well as those living near roads. Sometimes the impacts of excess pollution are even visible on plants. It induces mortality in some species or impairs their growth. Pollution of water along the roadside by these agents kills one form of plant species and helps the growth of plants such as Parthenium and Water Haycinth. While Parthenium

causes allergies, Water Hyacinth chokes waterways, helps spread malaria, and kills other useful aquatic flora and fauna by shutting out oxygen.

Systematic roadside plantations with combinations of herbs, green shrub barriers, and trees with appropriate architecture, wherein all this vegetation makes a green belt, can effectively control atmospheric pollution. The poisonous elements are taken up by plants on the roadsides; they partly absorb the gases and partly help in raising them high into the atmosphere for possible dilution. This saves roadside habitations from harmful concentrated exposures to a large extent.

iii) *Noise Pollution*

Excessive noise from vehicular traffic is a form of environmental pollution. Vehicular traffic on a busy road generates a sound intensity which becomes irritable. The sound of horns is harmful to the health of those living near the roads. Sound levels above 50 decibels are irritable and those in excess of 150 decibels become harmful to human beings (Odum 1971). Trees and shrubs planted on roadsides are an effective noise-reducing medium. Each 30m width of trees can absorb 6 to 8 decibels of sound intensity (Tiwari and Singh 1984). However, the effectiveness of a belt of trees and shrubs as a noise-reducing medium depends upon the height of the tree, width, and overall density of planting and foliage distribution. The width of the belt of trees being limited by the space available for the purpose, the trees and shrubs producing denser belts will prove more effective in noise abatement. To reduce the noise generated by high speed traffic on highways to tolerable limits, belts of trees and shrubs are necessary. The reports reveal that, to reduce the noise generated by a moderately speeding car, a 7 to 15m wide green belt works as an effective measure of noise control (Tiwari and Singh 1984). Evergreen trees are better for noise abatement than deciduous trees which do not afford a barrier to sound when leafless. In the hills, trees planted uphill from a road provide maximum sound control (Tiwari and Singh 1984). Detailed criteria for the choice of species for noise pollution control are described by Cook and Haverbecke (1971).

16.1.5 *Pattern of Changes in Roadside Plantation Approaches*

Trees were planted along the roads, as a first concept, mainly to provide shade and shelter to the traveller (Malik 1973). Avenue planting was carried out for travellers' comfort rather than slope stabilization, economic returns, or social benefits. Later, the emphasis shifted to economic returns (Singh 1973; Ladwa 1976) particularly in areas where the area under forest declined or where it was already very small. In such circumstances, the acute shortage of forest products provided support to the view point that the strip plantations along roads should be managed primarily to meet the requirements of local people and that the considerations of comfort to travellers and aesthetics should receive only secondary consideration (Gandhi 1976). For example, in India, the National Commission on Agriculture (NCA 1976) recommended the proper planning of roadside land use for planting beneficial plant species. It stressed that the activity of raising roadside plantations should be treated as a commercial investment. It brought a change in the objectives of the management of roadside plantations. Roadside land thus came to be recognized as a potential site for the production of various forest species. The institutional management systems became busy planning for maximum revenue realization from these plantations. The maximization of social benefits from these plantations is a developing approach. This new concept is developing with a view to meeting the growing shortage of fuelwood and small timber from roadside plantations that have better locations and site conditions.

16.1.6 *Engineering Angles on the Orientation of Plantation*

Because of the past focus, primarily on traveller and economic benefits, only trees and shrubs have been so far considered in planting designs. The planting systems usually followed are of the following types: viz. balanced line, unbalanced continuous line, unbalanced discontinuous line, sporadic system, and parkway system. Of these, the first two are widely practised wherever possible. The **balanced line system** produces a continuous green wall of trees that are uniform in size, as in the case of long stretches of eucalyptus avenues, and is not always considered to be aesthetically desirable. An **unbalanced continuous line**, produced as a result of alternating avenues of different species, interspersed by different kinds of trees, is preferred to the former option. A plantation is expected to be such that it does not shut out the view of landscape, scenic beauty, places of interest, and beautiful hill and country features.

The position of the first row of trees and the number of rows to be planted, on either side of the road, will depend upon the category of the road, the recommended width of the land acquired, and the width of the roadway for different categories of roads.

Single row planting is normally possible along village roads and other district roads, while more than one row can be planted in the case of the remaining three categories of road. In the case of **multiple row planting**, the first row is generally for shade and ornamental value and the remaining rows may be planted with plant species to meet the farming and other needs of local people. The spacing between the trees in the first row of shade or ornamental trees will have to be wider than that between the trees in the remaining rows. The crown spread of the species to be planted determines the spacing. While too wide spacing may defeat the very objective, too close spacing may increase costs and impair visibility. Excessively dense avenues may also cause clouds of dust and smoke to linger. It is also desirable to keep the initial planting closer in order to provide for mortality and to keep a selection of better plants for final retention. Too close spacing on hill roads, particularly on the curves, is dangerous. It may be desirable to miss a tree or two in such places. The trees should also not obstruct the view in places where the pedestrians or domestic animals might be crossing the road near the villages.

The general practice followed is to plant the first row 7.5 - 9m away from the centre, according to the type of road. The remaining could be spaced, keeping the landscape in mind. In India spacing between trees in the first row is 7.5m and in the remaining rows it is kept at 3m (Tiwari and Singh 1984). The spacing, however, should not be a fixed criteria and needs to be adjusted according to species and objectives. The above criteria are developed keeping in mind the trees alone. What about shrubs and herbaceous vegetation? Similarly, criteria need to be developed for each location in the case of slope stabilization and social plantations. The spacing between species should differ depending upon the species being planted. It could be 10m for shade trees, 5m for commercial species, and 2m for fuelwood and fodder species. Spacing for slope stabilization on mountains needs entirely different considerations, however.

The choice of species is broadly determined by the climate, site conditions, and object of planting. The mountain areas have several major and micro-climatic zones through which the roads cross. On the basis of temperature alone, the following major climatic zones are classified in the Hindu Kush-Himalayan Region, viz., subtropical low hills and a mid-hill temperate zone, representing the high hills, and a cold arid zone comprising the trans-Himalayan high mountain areas. Besides temperature, the annual rainfall varies widely in geographic terms. Equally variable could be the site conditions, depending upon soil and other modifications brought about in the course of road construction. Removal of top soil during road

construction, or the dumping of debris creating a new soil profile, will add to the transformation in soil structure and the creation of specific micro-habitat conditions.

Choice of species, therefore, has to be made, keeping in mind the suitability of the available micro-climatic and edaphic environment to species that are to be planted.

Other considerations, in the selection of species, include species with small, thin leaves which, after falling on the ground, will soon decay and be converted into humus to help the growth of ground grass cover on slopes. This will help prevent the cutting action of rain down the slopes. Thicker leaves take a longer time to decay and also become fire hazards on roads. The needle-type leaves of conifers make the road slippery, enhancing chances of accidents. The rooting of trees planted because of other considerations should have deeper roots to avoid damage to either the roads or to the pavements. Plants having leaves with hair follicles on them, and a large foliage volume ratio, are especially recommended for areas prone to noise pollution.

16.1.7 *Choice of Species for Planting*

The selection of appropriate plant species for each locality depends upon the purpose for which the plants in that locality are required and the physical and climatic characteristics of the site. In the roadside plantations of mountain areas, stabilization of mountain slopes to maintain road worthiness all the year round is the primary aim. However, on sites where stabilization is not a problem of primary concern, plantations aimed at location-specific purposes, described earlier in the text, can be kept in mind. As no single species will meet all requirements, it becomes necessary to select a combination of species that will meet all or almost all the requirements.

The great diversity in physical and climatic conditions within the Hindu Kush-Himalayan Region is represented on one extreme by the hot and humid foothill regions, which can sustain a luxuriant growth of vegetation, and on the other by the rugged tracts of the high Himalayan windy cold deserts which nurse the hardiest plants only with difficulty. This poses both enormous opportunities and problems to plantation choice. Unless care is taken to select suitable species, efforts are likely to go to waste.

In the cold deserts of the high Trans-Himalayan Region only trees with moisture conservation mechanisms will grow. In water-logged areas only those species that allow copious water transpiration will stay and on steep slopes and windy areas only plants with special adaptations for firm rooting will survive. There are species with wide ecological amplitudes which can be successfully planted over a wide range of climatic conditions (Table 16.4). However, species also exist that have narrow ecological amplitude and can be grown only in specific micro-climates of their preference.

Shrubs, although generally neglected when laying plantations, have great value for slope stabilization and for other purposes. Several shrub species are capable of fixing nitrogen, are good soil binders, provide good surface cover, and could be significant as fodder, food, and fuel plants. They are important noise abettors in green belt plantations (Cook and Haverbecke 1971). The role of grasses is secondary to other forms. The list of species in Tables 16.3 and 16.4, recommended for plantations, contains mostly trees with broad ecological amplitude. The listing is incomplete, however, in the sense that it leaves scope for shrubs and herbs to be included.

Table 16.3: List of honey plants of the Hindu Kush-Himalayan Region for roadside plantations from the apicultural perspective

Botanical Name	Blooming Period*	Honey Potentiality		Economic and other uses ²	Distribution and Remarks
		Nector Rating	Pollen Rating		
<i>Acacia auricul-aeformis</i> A. Cunn. Ex. Benth.	VI - VII	N ₃	P ₃	Timber, fire-wood, shade, other uses - gums, medical	Subtropical to sub-temperate
<i>A. catechu</i> (Linn.) Wild.	VI - VII	N ₃	P ₃	Medicinal, fuel, fodder for goats & sheep	Subtropical
<i>A. senegal</i> (Linn.) Wild.	VII - VIII	N ₃	P ₃	Food-pods, fodder-pods and leaves; timber, fuel, land use-hedges, shade; other uses -gum and tannin	Grows in poor soil/sandy area, survives hot dry winds
<i>Aesculus indica</i> Colebr.	IV - V	N ₂	P ₂	Fodder-mashed seeds for cattle, fuel, timber, other uses-shade amenity and medicinal	Temperate climate concentration 29% to 69 %
<i>Albizia lebbek</i> (Linn.) Benth	IV - V	N ₂	P ₂	Fodder, timber, and fuel; nitrogen fixer	Subtropical climate
<i>A. chinensis</i> (Osborne) Merr.	IV - V	N ₂	P ₂	Fuel and timber	- do -
<i>Azadirachta indica</i> A. Juss. climate	III - IV	N ₁	P ₁	Fodder-leaves, timber, fuel, medicinal-leaves, extract oil	Tropical to sub-fertilizer, tropical grows quickly, starts flowering in 2 years, recommended for planting to increase honey
<i>Bauhinia variegata</i> Linn.	III - IV	N ₂	P ₂	Fodder, food (floral buds), fuel	Tropical to sub-tropical climate
<i>B. vahlii</i> W. and A.	IV - VI	N ₂	P ₂	Fodder and fuel	- do -

Botanical Name	Blooming Period*	Honey Potentiality		Economic and other uses ²	Distribution and Remarks
		Nectar Rating	Pollen Rating		
<i>Bombax ceiba</i> Linn.	II - III	N ₁	P	Food-flowers, fodder-seeds for livestock feed, other uses cotton for stuffing & seeds for oil/soap, and used for timber	Subtropical, nectar sugar concentration approx. 6%
<i>Butea monosperma</i> (Lam.) Taub. (<i>B. frondosa</i>) Koenig	- II	N ₁	P	Timber, fuel & other uses-food for lac insect, red dye from flowers and bark as medicinal	Subtropical
<i>Cassia fistula</i> Linn.	IV - V	N ₂	P ₁	Fuel and medicinal	Tropical to subtropical climate, recommended for planting to increase honey production
<i>Delonix regia</i> (Boj.) Rafin	VI - VIII	N ₂	P ₂	Fuel, shade, ornamental tree	Subtropical, quick growing plant with profuse flowering
<i>Emblica officinalis</i> Gtn.	III - VI	N ₂	P	Food-fruits, fuel, medicinal	Lowhills with subtropical climate
<i>Eriobotrya japonica</i> (thumb) Lindl.	XI - I	N ₂	P	Food-fruits, land use amenity, liquor from fruits	Tropical to sub-tropical climate; nectar sugar concentration 30.5% to 65.0% %
<i>Eucalyptus</i> spp.	XII - IV	N ₁	P ₁	Paper and pulp, timber, oil from leaves	Wide ecological amplitude, nectar sugar concentration up to 30 %
<i>Grevillea robusta</i> A. Cunn.	XI - VII (in some areas during III - IV)	N ₁	P	Timber, fuel, land use-shade, amenity and windbreak	Wide ecological amplitude, nectar secretes from flower for 3 days, nectar sugar concentration 15% to 79%, recommended to increase honey production

Botanical Name	Blooming Period*	Honey Potentiality		Economic and other uses ²	Distribution and Remarks
		Nectar Rating	Pollen Rating		
<i>Grewia oppositifolia</i> <i>Buch-Ham ex Roxb</i>	IV-VI	N ₁	P	Fodder, fibre, and fuel	Subtropical climate Good source of nectar if allowed to flower
<i>Lagerstroemia indica</i> Linn.	VI - VIII	-	P	Ornamental	Fairly wide ecological amplitude
<i>Leucaena leucocephala</i> (Lam.) de Wit	IV - V	N ₁	P ₁	Fodder, fuel, and timber	low to mid-hills with subtropical climate
<i>Litchi chinensis</i> (Gaert.) Sonner	IV - V	N ₁ N	P	Food-fruits and timber	Nectar sugar concentration up to 76.2 %
<i>Mangifera indica</i> Linn.	III - IV	N ₂	P	Food-fruits, fuel, timber, land use	Subtropical, nectar secretion amenity
<i>Melia azadirachta</i> Linn.	III - IV	N ₁	P ₁	Medicinal leaves, seeds with insecticidal use	Tropical climate, foothills
<i>Moringa oleifera</i> Lamk.	I - III	N ₁	P ₁	Food-leaves, roots, flowers, and pods, land use - hedges, amenity; other uses - medicinal oil from seeds for perfumery and lubrication	Visited by bees in swarming number
<i>Pongamia pinnata</i> (Linn.) Pierre	III - IV	N ₁	P ₁	Fodder-leaves, pressed cake for poultry feed, fuel, land use-afforestation, amenity, soil benefit erosion control, green manure, other uses-roots & medicinal-oil, twig & bark	Fairly wide ecological amplitude, subtropical

Botanical Name	Blooming Period*	Honey Potentiality		Economic and other uses ²	Distribution and Remarks
		Nector Rating	Pollen Rating		
<i>Prunus pudu</i> , Roxb.	IX - XII	N ₁	P	Fuel	Wide ecological amplitude. Nectar sugar concentration from 12 to 18 %. Good source of nectar in hills during autumn
<i>Punica granatum</i> Linn.	IV - V	-	P	Food-seeds, fuel, and medicinal seeds	Wide ecological amplitudes. Subtropical to sub-temperate
<i>Robinia pseudacacia</i> Linn.	IV - V	N ₁	-	Timber, fuel, land use-soil conservation	Nectar sugar concentration varies from 30% to 62 %, wide ecological amplitude
<i>Salix spp.</i>	III - IV	N ₂	P ₂	Wood for cricket bats, land use-soil conservation	Fairly widespread, nectar sugar concentration varies from 15% to 79 %
<i>Sapindus emarginatus</i> Vahl	X - XII	N ₁	P ₁	Land use-shade amenity, fruits use as substitute for soap	Subtropical, recommended for plantation to increase honey production
<i>S. mukorissi</i> Gaertn.	V - VI	N ₁	P	- do -	- do -
<i>Sapium sebiferum</i> Roxb.	VI - VIII	N ₁	-	- do -	Nectar sugar concentration from 23 to 31 %.
<i>Syzgium cuminii</i> Skeels	II - IV	N ₁	P ₁	Food-fruits; vinegar, vine, & fruit juice, fodder-leaves, timber, fuel, land use-shade, windbreak, amenity, other uses-tannin from bark, seeds, kernel of the fruit is specific for diabetes	Nectar secretion erratic, nectar sugar concentration varies from 9-72 %, flowers within 3-5 years

Botanical Name	Blooming Period*	Honey Potentiality		Economic and other uses ²	Distribution and Remarks
		Nectar Rating	Pollen Rating		
<i>S. heyneanum</i> L.	II - III	N ₁	P ₂	Fodder, timber, fuel, land use-shade and wind-break	Subtropical and sub-temperate
<i>Terminalia arjuna</i> (Roxb.) W. & A	IV - V	N ₁	P	Timber, fuel land use, medicinal fruits	Foothills and low hill areas with subtropical climate
Herbs <i>Artemisia</i> spp (21 spp)	V - VII	N ₂	P ₃	Good for slope stabilization and soil erosion control	Sub-temperate
<i>Impatiens</i> spp (20 spp)	VII - IX	N ₂	P ₃	Pioneer plant species for roadside soil debris	Temperate
<i>Iris</i> spp	III - VI	N ₂	P ₂	Due to extensive rhizome spread a good soil kinder for slopy areas, pioneer plant	Sub-temperate to temperate
<i>Plectranthus</i> spp	VIII - XI	N ₁	P ₂	A plant suitable for bare surface cover, pioneer for new, disturbed areas	Tropical to temperate
<i>Medicago</i>	VII - XI	N ₂	P ₂	A plant suitable for bare surface cover, pioneer for new, disturbed areas	Tropical to temperate
<i>Trifolium</i> spp (18 spp)	IV - VIII	N ₁	P ₁	Pioneer for surface cover of bare lands	widespread distribution
<i>Fragaria</i> spp	IV - VI	N ₂	P ₂	Provides surface cover through horizontal spread	Temperate

Botanical Name	Blooming Period*	Honey Potentiality Nector Rating	Pollen Rating	Economic and other uses ²	Distribution and Remarks
Shrubs					
<i>Adhatoda vesca</i>	IV - V	N ₁	P ₂	Good for slope stabilization and soil conservation	Subtropical to temperate
<i>Berberis lycium</i>	III - V	N ₂	P ₁	Thorny shrubs-fuel, fencing medicinal/ commercial value and good for growing on slopy sites	- do -
<i>Prinsepia utilis</i>	IX - X	N ₁	R ₁	Fuel, fodder, fruit, oil seed, suitable for slope stabilization	Temperate to sub-temperate
<i>Rosa brunonii</i> <i>R. macrophylla</i>	IV - XI	N ₁	P ₁	Fodder, fuel, suitable for slopes	Sub-temperate to temperate

Source: Verma 1988 unpublished.

1. January - December months indicated as I - XII

2. Information developed by author.

N₁ - Major honey source
 N₂ - Medium honey source
 N₃ - Minor honey source
 N - Importance unrated

P₁ - Major pollen source
 P₂ - Medium pollen source
 P₃ - Minor pollen source
 P - Importance unrated

Table 16.4: Some common plant species of different climatic regimes of the Hindu Kush-Himalayan Region to facilitate selection of appropriate roadside plantations

Species	Uses	Remarks
(1)	(2)	(3)
A. TEMPERATE REGION COMPRISING MOSTLY OF HIGH MOUNTAIN AREAS		
1. <i>Alnus nepalensis</i> (piak, newn, kunis, utis)	Timber, fuel, nitrogen fixing	Large trees suitable for growing on river banks, ravines, and newly-formed soils, useful for soil conservation in landslide areas, more common in Eastern Himalayan Region grown by direct sowing or by transplanting, entirely good for slope stabilization
2. <i>Alnus nitida</i> (kunsh, hunis, utis)	Timber, fuel, nitrogen fixing	Similar to above; more common in Western Himalayan Region on riversides and ravines, good for slope stabilization
3. <i>Betula alnoides</i> (kath bhuj)	Plywood, furniture, and tool handles	A medium-sized tree, suitable for broken marginal lands, can be grown by transplanting entirely and also by direct sowing, can be used for slope stabilization
4. <i>Buxus sempervirens</i> (papri)	Carving, mathematical instruments	Slow growing small tree, suitable for shady, rocky, ravinous areas, can be grown by transplanting entirely, rare tree, much valued
5. <i>Carpinus viminea</i> (chamkharik)	Timber for shuttle making, fuel, fodder	Middle-sized tree, wood used, grown by transplanting entirely
6. <i>Corylus colurna</i> (bhotia badam)	Fruits, timber, fuel	Middle-sized tree edible fruit is much relished, can be grown by transplanting entirely as well as by direct sowing, can be planted on gentle slopy roadsides, middle-sized tree, grown by transplanting entirely
7. <i>Eucalyptus saligna</i>	Timber, fuel	
8. <i>Exbucklandia populnea</i> (pipli)	Timber, furniture, plywood	Large tree of Eastern Himalayan Region; useful for soil conservation, grown by transplanting entirely

Species	Uses	Remarks
(1)	(2)	(3)
9. <i>Fraxinus excelsa</i> (angu)	Furniture, axe, handles, sports' goods	Large tree, grown by transplanting entirely
10. <i>Juglans regia</i> (akhrot)	Timber, furniture and carving, gun-stock, fruits	Large tree, grown by transplanting entirely and also by direct sowing
11. <i>Morus serrata</i> (kimu)	Fodder, sports' goods, furniture, toys	Large tree, suitable for growing on marginal slopy lands and on roadsides passing through farmlands, can be grown by branch cuttings and direct sowing
12. <i>Olea ferruginea</i> (kahu)	Tool handles, walking sticks, toys, agricultural implements, fodder fatty oil	Small tree, suitable for growing on bouldery marginal lands; can be grown by direct sowing, transplanting entirely or by branch cuttings, good for slope stabilization
13. <i>Populus nigra</i>	Light timber, matchwood, pulpwood, fuel, ornamental	Large tree, suitable for dry valleys, grown by branch cuttings, important plant for roadside slope, stabilization
14. <i>Prunus cerasoides</i> (padam)	Timber, fuel, fodder, wood used in religious ceremonies	Medium tree, suitable for marginal lands and around villages, grown by transplanting entirely, also by branch cuttings, good for beekeeping
15. <i>Prunus persica</i> (aru)	Fruits, timber, fuel	Small tree, suitable for near habitation, gentle, stable slopes, and plain valley areas, grown by transplanting entirely
16. <i>Pyrus malus</i> (sew)	Fruits	Small trees, suitable for growing near habitations, farming areas in valleys and marginal lands, grown by transplanting entirely
17. <i>Quercus incana</i> (banj)	Timber for agricultural imple-mentations, medicinal, tussah silk rearing	Large tree of Eastern Himalayan Region, suitable for marginal lands, grown by direct sowing, good for slope stabilization in high mountain areas
18. <i>Quercus lamellosa</i> (shaishi)	Timber for agricultural imple-ments, fuel, fodder tussah silk rearing	Large tree of Western Himalayan Region, suitable for deep soil, moist localities on marginal lands and roads passing through commons, grown by rearing transplanting and also by direct sowing, can be used on slopes

Species	Uses	Remarks
(1)	(2)	(3)
19. <i>Robinia pseudoacacia</i>	Fuel, fodder, soil conservation	Medium tree, suitable for marginal lands and for stabilizing ravinous land, grown by transplanting, commonly planted on roadsides in lower hills; can be planted on slopes of any degree
20. <i>Salix alba</i>	Cricket bats, matchwood, tool handles, fuel, fodder	Large tree, grown by branch cuttings
21. <i>Salix babylonica</i> (manju)	Fodder, fuel, ornamental	Large tree, suitable for growing around water, grown by branch cuttings
22. <i>Salix daphnoides</i> (Bhashli, bashroi)	Basket-making, fuel, tools and implements	Small tree, suitable for inner arid tracts of the Himalaya, grown by branch cuttings, the dominant roadside tree of trans-Himalayan roads in India

B. SUB-TROPICAL REGION COMPRISING FOOTHILLS OF WESTERN HIMALAYAN REGION AND CENTRAL HIMALAYAN MOUNTAINS

1. <i>Albizia-lebbeck</i> (siris)	Timber, fuel, fodder, medicinal	Large tree, suitable for open roadside lands and along narrow pathways, grown by transplanting entirely, direct sowing and cuttings
2. <i>Azadirachta indica</i> (neem)	Timber, bark and seed medicinal, insecticidal, fertilizer, fodder	Large tree, suitable for open valley lands, roadside near and along roads and paths, grown by entire transplanting and direct sowing
3. <i>Bauhinia purpurea</i> (khairwal, guiral)	Gum, fuel, fodder	Medium tree, suitable for roads passing through farm, grown by transplanting entirely and direct sowing
4. <i>Bauhinia variegata</i> (kachnar)	Gum, fodder, flower buds eaten, bark yields dye and medicine	Medium tree, suitable for road passing through farm grown by entire transplanting and direct sowing
5. <i>Celtis australis</i> (kharik)	Timber, fuel, fodder, sports goods, utensils	Medium tree suitable for certain sites and fodder and fuel demanding farming areas, grown by transplanting entirely, direct sowing, and branch cuttings
6. <i>Dalbergia sissoo</i> (shisham)	Timber, furniture, plywood, fuel, fodder	Large or medium tree, suitable for growing in lower to mid-hill plantations, on village roads, grown by transplanting entirely, root and shoot cuttings and direct sowing suitable on slopy sites

Species	Uses	Remarks
(1)	(2)	(3)
7. <i>Dendrocalamus strictus</i> (bans)	Paper pulp, constructional, tent poles, basket-making	Large bamboo, suitable for growing on open marginal land road sites and near homesteads, grown by transplanting entirely and from rhizomes
8. <i>Embllica officinalis</i> (sonia)	Fruits, tannin, timber, fuel, fodder	Medium tree, suitable for roadsides near homesteads and farms, grown by transplanting entirely or direct sowing, Himachal Pradesh already using it for roadside plantations for socioeconomic value
9. <i>Eucalyptus camaldulensis</i>	Timber, fuel, charcoal, gum, medicinal	Large tree, suitable for both dry and swampy areas, grown by transplanting entirely
10. <i>Eucalyptus grandis</i>	Timber, paper, pulp, fuel, essential oil	Large tree, suitable for marginal land road sites, grown by transplanting entirely
11. <i>Exbucklandia populnea</i> (pipli)	See (a) (i) (8)	
12. <i>Ficus religiosa</i> (pipal)	Timber for packing cases, trees on roadsides	Suitable for growing as single tree or as avenues, grown by branch cuttings, significant as shade
13. <i>Grevillea robusta</i>	Ornamental, timber	Large tree, suitable for shade or as avenues, (cabinet making, toys, grown by direct sowing, fuel, panelling), shade tree in tea gardens
14. <i>Grewia optiva</i> (bhimal)	Timber-cot frames, fibre, fodder	Medium tree, suitable for farming need areas. good as fodder, fiber and fuel, grown by transplanting entirely
15. <i>Melia azadirachta</i> (bakain,dek)	Box planks, fuelwood, paper pulp, fodder medicinal	Medium tree, suitable for roads going around fields and on marginal lands, grown by transplanting entirely or direct sowing
16. <i>Moringa oleifera</i> (sahjan)	Fruits and flowers edible, medicinal, fodder, wood for pulp	Small tree, fast growing, suitable on slopy edges and on hedges near habitations, grown by branch cuttings and direct sowing
17. <i>Morus alba</i> (tut)	Fruits - edible, timber, sports goods, fodder, leaves for silkworm feeding	Medium tree, suitable for marginal lands, grown by transplanting entirely, direct sowing, or branch cuttings
18. <i>Morus laevigata</i> (shahtut)	Fruits - edible, timber, sports goods, fodder	Large tree, suitable for gardens, homesteads, and marginal lands

Species	Uses	Remarks
(1)	(2)	(3)
19. <i>Populus deltoides</i>	Matchwood, pulpwood, light timber, fuel	Large tree, suitable for field edges and marginal lands in the Himalayan foothill areas, grown by branch cuttings
20. <i>Prunus armeniaca</i> (zardalu)	Fruits, timber, fuel	Small tree near habitation, farmland roadsides, grown by branch cuttings.
21. <i>Prunus persica</i> (aru)	See (A) (i) (15)	In valleys and on stable land near habitation road sites
22. <i>Pyrus communis</i> (ritha)	Fruits, fuel	Small tree, suitable for homesteads and field edges, grown by grafting
23. <i>Sapindus mukorossi</i> (ritha)	Fruits, soapnut, fodder	Medium tree, suitable for growing near houses and on field edges, grown by transplanting entirely or by direct sowing, provides traditional soapy material from fruits, a source of income for poor people
24. <i>Toona ciliata</i> (tun)	Timber, fuel	Large tree, suitable for growing on roadsides passing through lands and village commons, grown by transplanting entirely

C. SUB-TROPICAL CLIMATE OF CENTRAL AND EASTERN HIMALAYAS:

1. <i>Acrocarpus fraxinifolius</i>	Fuel, boxwood, boards, planks	Large tree, suitable for roadsides and marginal lands and village commons, grown by transplanting entirely or direct sowing
2. <i>Ailanthus grandis</i> (gogal)	Plywood, ornamental	Large tree, suitable for growing on village commons and roadsides, grown by transplanting entirely or direct sowing
3. <i>Albizia lebbeck</i> (siris)	See (b) (1)	
4. <i>Albizia procera</i> (safed siris, kinni)	Timber, fuel, fodder	Large tree, suitable for growing on village commons, marginal lands, and roadsides, grown by transplanting entirely and direct sowing, good for areas requiring fuel and fodder
5. <i>Bauhinia purpurea</i> (khairwal, guiral)	See (b) (3)	
6. <i>Betula cylindrostachys</i>	Essential oil, fuel, charcoal, timber	Large tree, suitable for cut up marginal lands, grown by transplanting entirely, economic value, income generation to people

Species	Uses	Remarks
(1)	(2)	(3)
7. <i>Grevillea robusta</i>	See (b) (3)	
8. <i>Grewia elastica</i> (dhaman)	Ornamental, timber, toy-making, fuel, fodder	Medium tree, suitable for slopy and plain roadsides, grown by transplanting entirely
9. <i>Michelia</i> <i>champaca</i> (champ)	Decorative timber, fuel, ornamental	Large tree, suitable for valley roads - marginal lands, and village commons
10. <i>Melia</i> <i>azadirachta</i> (bakain, dek)	See (b) (15)	
11. <i>Morus serrata</i> (kimu)	See (a) (11)	

D. TROPICAL REGION

(i) HIGH RAINFALL AREAS OF NEPAL & NORTH EASTERN PARTS OF INDIA

1. <i>Ailanthus</i> <i>grandis</i> (gogal)	See (c) (2)	
2. <i>Albizia lebbeck</i> (siris)	See (b) (1)	
3. <i>Albizia procera</i> (safed siris)	See (c) (4)	
4. <i>Artocarpus</i> <i>integrifolia</i> (kathal)	Timber, fruits, fodder	Large tree, suitable for growing along roads passing through habitations, aesthetic value, grown by transplanting entirely and by direct sowing
5. <i>Azadirachta</i> <i>indica</i> (neem)	See (b) (2)	
6. <i>Bambusa</i> <i>balcooa</i>	Constructional purposes, paper pulp, cottage industry	Medium bamboo, suitable for growing on marginal lands, grown from rhizomes
7. <i>Casuarina</i> <i>equisetifolia</i> (saru)	Timber, fuel, ornamental	Tall tree, fast growing, suitable for warm sandy areas of some foothills; ideal for fuelwood lots, grown by transplanting entirely

Species	Uses	Remarks
(1)	(2)	(3)
8. <i>Chukrasia tabularis</i> (chikrasi)	Timber, furniture, decorative plywood, fuel	Large tree, suitable for growing around village roads, grown by transplanting entirely
9. <i>Cinnamomum zeylanicum</i> (dalchini, lavang)	Cinnamon, essential oil, medicinal	Medium tree, suitable for growing on village roads and near rural habitations, grown by transplanting entirely and direct sowing
10. <i>Cocos nucifera</i> (nariyal)	Fruits, copra, oil coir, toddy, jaggery	Roads of foothill valleys near habitations grown by transplanting entirely, good examples seen in Sri Lanka, Dharan, Nepal, and in parts of India
11. <i>Dendrocalamus hamiltonii</i> (kagshi bans)	Paper pulp, vegetables - young shoots, constructional purposes	Tall bamboo, suitable for marginal lands, grown by direct sowing and by rhizomes, meets local requirements of rural people
12. <i>Dalbergia latifolia</i> (shisham, biti, jitengi, iti) rosewood	Timber, furniture, cabinet	Large tree, suitable for growing in village, on State and national highways, grown by transplanting entirely
13. <i>Emblica officinalis</i> (aonla)	See (b) (8)	
14. <i>Ficus elastica</i> (bor attab), India rubber tree	Ornamental, rubber, fodder	Large tree, suitable for growing on all kinds of roads, grown by transplanting entirely or by branch cuttings
15. <i>Gmelina arborea</i> (gamhar)	Timber, printing block, musical instruments, cart axles, fuel, medicinal	Large tree, suitable for village roads, grown by transplanting entirely and direct sowing
16. <i>Lagerstroemia speciosa</i> (jarul)	Timber - constructional purposes, furniture, agricultural implements, telegraph poles, fodder, medicinal	Large tree, suitable along pathways, grown by transplanting entirely

Species	Uses	Remarks
(1)	(2)	(3)
17. <i>Melia azadirachta</i>		See (b) (15)
18. <i>Melocanna baccifera</i>	House construction, mats, baskets, paper pulp	Medium bamboo, suitable for growing in 3rd row onwards, grown by transplanting entirely
19. <i>Mangifera indica</i> (am), Mango tree	Edible fruits, fatty oil, plywood, shoe heels, furniture, fuel	Large tree, suitable for growing on roadsides of all kinds of roads, more preferable for village roads, good only for valleys and stable areas. grown by transplanting entirely (grafted)
20. <i>Michelia champaca</i> (champ)		See (c) (9)
21. <i>Parkia roxburghii</i> (supota)	Fruits, fuel, ornamental, medicinal	Medium tree of Eastern parts, suitable for roadsides, grown by transplanting entirely
22. <i>Sesbania graniflora</i> (agast, banas)	Light timber, fodder, medicinal, flower edible.	Small tree, suitable for near habitation roads and road hedges, grown by direct sowing or transplanting entirely
23. <i>Syzgium cuminal</i> (jamun)	Fruit edible and medicinal timber, tools & implements, fuel, fodder	Large tree, suitable for growing along relatively less slopy areas or valleys

(ii) **MEDIUM RAINFALL AREAS OF LOW TO MID HILLS**

1. <i>Acacia auriculiformis</i> (Akashmuni)	Timber, fuel, ornamental	Medium trees, suitable for slopy lands, grown by transplanting entirely and direct sowing
2. <i>Acacia nilotica</i> (babu, kikar)	Timber, fuel, fodder, tannin, gum	Medium tree, suitable for sites of slopy lands, marginal lands and village commons, grown by direct sowing
3. <i>Aegle marmelos</i> (bel, vilva)	Fuel, gum, bark, and fruit, medicinal	Small tree, suitable for roadsides near rural habitations and houses, grown by transplanting entirely
4. <i>Ailanthus excelsa</i> (arru)	Timber, packing cases, fishing floats, and boards, bark, medicinal, fodder	Large tree, suitable for growing on roads on marginal lands and village commons, grown by transplanting entirely and by direct sowing

Species	Uses	Remarks
(1)	(2)	(3)
5. <i>Schleichera trijuga</i> (kusum)	Timber, tools and implements, fuel, lac cultivation	Large tree, suitable for open land around village, boundaries and village commons, grown by transplanting entirely
6. <i>Tectona grandis</i> (sagaun)	Timber - railway carriages and wagons, cabinet, furniture	Large tree, suitable for field edges, marginal lands, and village commons.
7. <i>Terminalia arjuna</i> (arjun)	Timber, mine-props, plywood, bark, tannin, medicinal, fodder, leaves for tussah silkworm	Large tree, suitable for growing along water courses and in water-logged areas, grown by transplanting entirely

E. TRANS-HIMALAYAN, HIGH MOUNTAIN COLD ARID ZONE

1. <i>Salix spp.</i>		A popular tree of the <i>Trans-Himalaya</i>
2. <i>Populus spp.</i>	See (b) 20.	Also commonly grown by mountain communities for fuel and fodder
3. <i>Prunus armeniaca</i> (Apricot)	See (A) (1) (15)	A popular oil seed and fruit tree-wild as well as domesticated
4. <i>Alnus spp.</i>	Nitrogen fixing See (a) (1 & 2)	Wild forms for roadside plantations
5. <i>Betula utilis</i> (Bhoj Patra)	See (A) (3)	
6. <i>Hyppophae spp.</i>	Fruits, fuel, timber, nitrogen fixation, soil fertilization.	Shrub and tree both suitable for dry sandy or rocky locations, riversides, moist areas, good for roadsides passing through farmlands
7. <i>Prunus Persica</i>	Fruits, fuel	Wild forms for roadside plantations

Source: Author's compilation.

16.2 BIOTECHNICAL STABILIZATION

16.2.1 Introduction

The design of biotechnical stabilizations requires an appreciation of the mechanics that link plants and slope stability parameters (referred to as **plant mechanics** here), as well as an understanding of plant biology. Plant mechanics is essential for defining the slope stability problem vis-a-vis vegetation and evaluating a solution to that problem, while **plant biology** is needed to generate solutions to the vegetative slope stability problem.

Plant biology can readily supply information regarding the selection of species whose characteristics suit the natural conditions that sustain the plant but is often pressed to provide information regarding plant characteristics that relate to slope stability parameters.

This chapter is divided into three sections. The sections deal with three stability problems that plants can help to solve; the three problems are common in attempts to stabilize cut slopes, the influence area of a road, and a failure zone. The three problems are: (1) surface erosion, (2) increase in soil shear strength, and (3) groundwater table or moisture content reduction. The first two problems are treated with both plant mechanics and plant biology while the third problem is treated with plant biology and drainage measures.

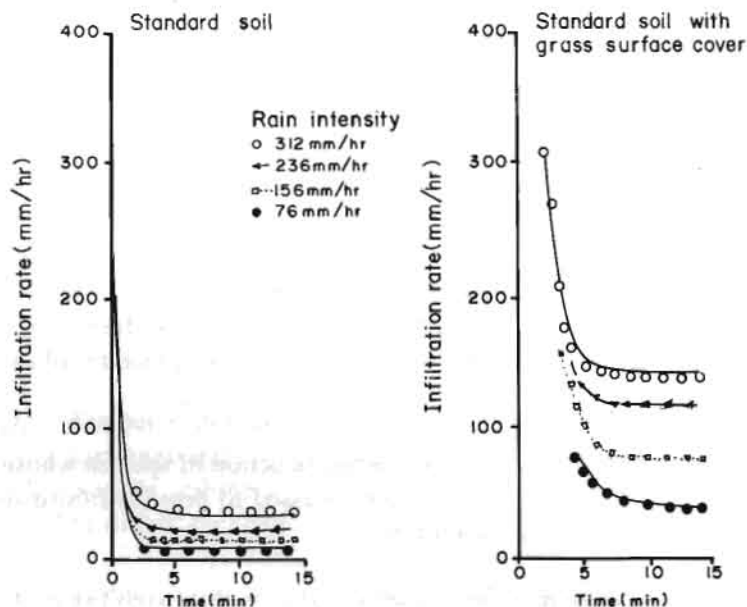
16.2.2 Surface Erosion

Soil loss on a given slope is determined by the interaction that erosive rainfall has with erodible soil. The interactions involve processes that are governed by characteristics of the rainfall and soil as well as by several other slope attributes. Vegetation cover is one such slope attribute. Vegetation cover reduces the erosivity of rainfall through (1) interception which armours soil and reduces the water available for infiltration or runoff (see Table 16.5), (2) an increase in infiltration caused by roots, vacant root channels, and increased surface roughness (Fig. 16.1), and, finally, (3) root binding which reduces the susceptibility of soil particles to be dislodged by splash or sheet erosion.

Table 16.5 Approximate average rainfall interception, evergreen rainforest of Brazil

Penetrating to rain gauge at 1.5a		33.0 %	
Evaporated directly from tree crowns		20.0 %	
Running down trunks 46 %	evaporated from surface	9.2 %	
	absorbed by roots	9.2 %	
	reaching by barks	27.6 %	absorbed by roots 20.7 %
			reaching water table 6.9 %

Source: Greenway 1987



Source: Nasif and Wilson

Fig 16.1 Comparative infiltration capacities from a 9° slope

The Universal Soil Loss Equation (USLE) (Wishmier and Smith 1978) provides a means to predict soil loss from sheet and rill erosion: it is a widely used method and provides the best approximation of soil loss. Its relevance here is as a vegetative cover design equation. As explained below, application of the USLE requires work to adjust input values to suit conditions in Nepal. While the USLE has been accepted as the best approximation of soil loss in other parts of the world, its validity in Nepal remains to be tested. Tests may, or may not, show that the USLE requires modification for application in Nepal. Regardless of whether the USLE is proved to require modification or not, it is the starting point in analyzing soil erosion for the design of preventive measures.

The Universal Soil Loss Equation

The USLE is defined as:

$$A = RKLSCP \quad (1)$$

where,

- A = soil loss in metric tons per hectare per period P,
- R = rainfall erosivity,
- = EI_{30} ,
- E = kinetic energy of a storm in metric ton-metres per hectare,
- I_{30} = maximum 30 minute storm intensity in cm per hour,
- K = soil erodibility in metric tons per hectare per metric EI unit,
- L = slope length factor (dimensionless),
- S = slope gradient factor (dimensionless),
- C = vegetative cover factor (dimensionless), and
- P = soil erosion control practice factor (dimensionless).

a) Rainfall Erosivity, R

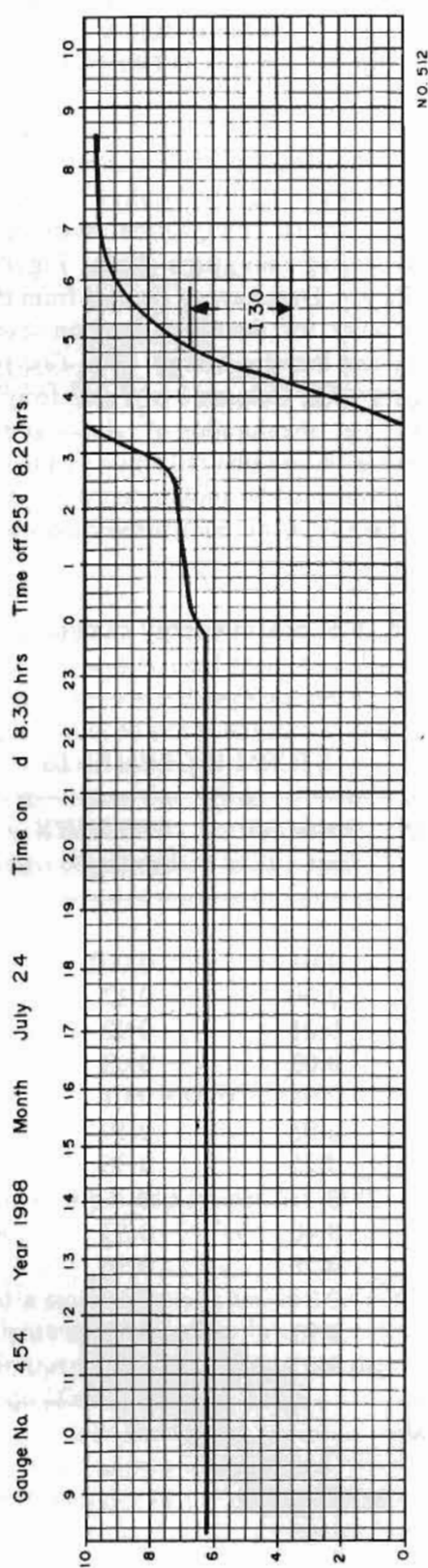
Tests have shown that the erosive power of rainfall is best measured by the product of the total energy of a storm (E) and the maximum intensity of a storm for 30 consecutive minutes (I_{30}). EI_{30} must be calculated for each storm for the period the soil loss is being calculated for (a year or 3 months, for example).

Unlike countries where past work with the USLE permits a quick calculation of R based on **isoerodent maps** (that show contours of equal R values geographically) or empirical equations that relate R to rainfall parameters, such as the average annual precipitation, work in Nepal must begin from primary data. Data must be collected from recording rain-gauge charts; Figure 16.2 shows such a chart from Kathmandu Airport Meteorological Station. Data have to be read from the chart as millimeters of rainfall in minutes of time at each inflection point for the entire duration of each storm. Every inflection point signifies a change in rainfall intensity and thereby energy. The first two columns of Table 16.6 show readings taken from the chart in Figure 16.2; Column 3 of Table 16.6 is the difference in time readings at each inflection point of Figure 16.2, i.e., the duration of rainfall at different intensities. Column 4 of Table 16.6, is the difference in amount at those same inflection points. Column 6 is the intensity during the different periods of the storm, obtained by looking up the energy for the intensities of Column 5 of Table 16.6 and in Table 16.7. Finally, Column 7 is the total energy for every intensity; it is the product of Columns 4 and 6.

Table 16.6 Storm energy calculation

CHART READINGS		STORM INCREMENTS			ENERGY	
TIME	DEPTH (mm)	DURATION (min)	AMOUNT (cm)	INTENSITY (cm/hr)	PER CM	FOR INCREMENT
18:15	6.15					
23:45	6.25	330	0.01	0.002	0	0
00:15	6.80	30	0.06	0.12	121	7
00:45	6.85	30	0.01	0.02	0	0
01:45	7.15	60	0.03	0.03	0	0
02:30	7.20	45	0.01	0.01	0	0
02:48	7.50	18	0.03	0.10	121	4
03:30	10.00	42	0.25	0.36	175	44
03:30	0.00	0	0	0	0	0
04:15	4.00	45	0.40	0.53	184	74
04:45	6.75	30	0.28	0.56	191	54
06:00	9.10	75	0.24	0.19	148	36
07:00	9.40	60	0.03	0.03	0	0
08:20	9.50	80	0.01	0.01	0	0

I_{30} = 0.33 cm/hr
 Total Energy = 2.19
 EI_{30} = 0.72



Source: Dept. of Meteorology, HMG, Nepal, 1988.

Fig 16.2 Recording rain gauge chart, KTM Airport, July 24, 1988

The sum of all rows, divided by 100 (a scaling convention), is E, the total kinetic energy of the storm. I_{30} is obtained by reading the maximum amount of rain falling in any consecutive 30 minutes and multiplying it by two. When the duration of a storm itself is less than 30 minutes, I_{30} is twice the amount of rain. The product EI_{30} is thus calculated for each storm over period P. The sum of EI_{30} over P is R for that period. Table 16.8, below, gives values of EI_{30} for Kathmandu Airport in 1988 and Figure 16.3 gives the cumulative frequency of EI_{30m} at Kathmandu Airport in 1988.

Table 16.7 Kinetic energy of rainfall: expressed in metric ton-metres per hectare per centimetre of rain¹

Intensity cm/h	.0	0.1	0.2	0.3	0.4	0.5	0.6	0.7	0.8	0.9
0	0	121	148	163	175	184	191	197	202	206
1	210	214	217	220	223	226	228	231	233	235
2	237	239	241	242	244	246	247	249	250	251
3	253	254	255	256	258	259	260	261	263	264
4	264	265	266	267	268	268	269	270	271	272
5	273	273	274	275	275	276	277	278	278	279
6	280	280	281	281	282	283	283	284	284	285
7	286	286	287	287	288	288	289 ²			

¹ Computed by the equation $E = 210 + 89 \log_{10} I$

where,

E = kinetic energy in metric-ton metres per hectare per centimetre of rain and

I = rainfall intensity in centimetre per hour.

² The 289 value also applies for all intensities greater than 7.6 cm/h.

Table 16.8 EI_{30} at Kathmandu Airport in 1988

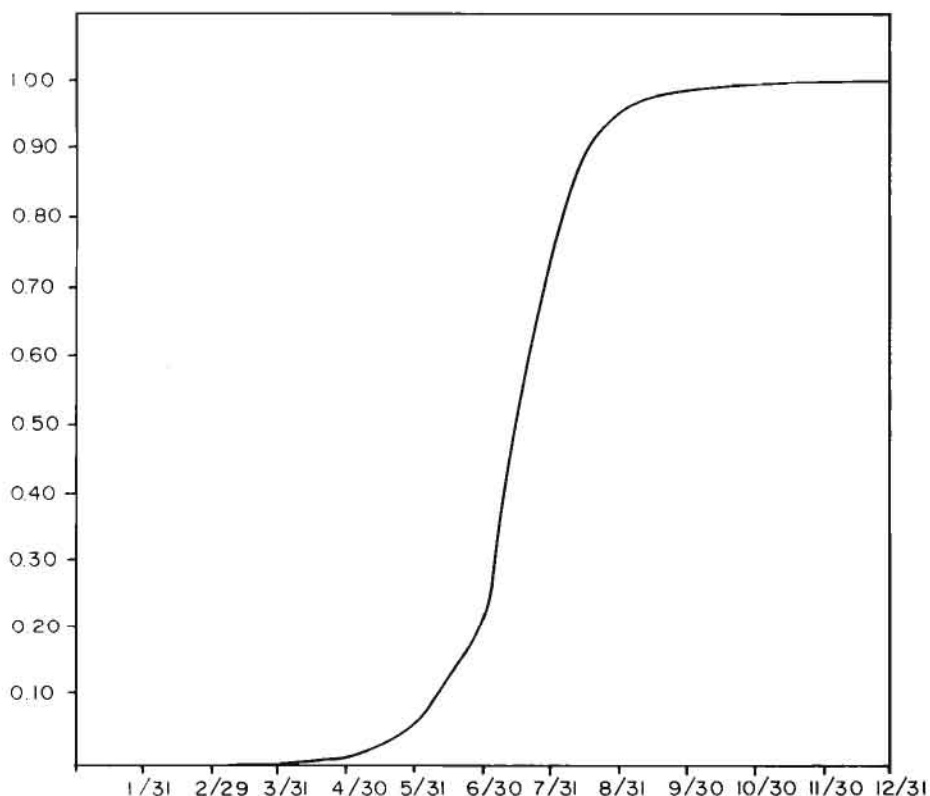
<i>Date</i>		EI_{30}^*
January	1-15	0.01
January	16-31	0.00
February	1-15	0.04
February	16-29	1.68
March	1-15	2.90
March	16-31	0.14
April	1-15	0.28
April	16-30	0.22
May	1-15	4.06
May	16-31	14.68
June	1-15	27.88
June	16-30	38.03
July	1-15	196.62
July	16-31	36.04
August	1-15	65.36
August	16-31	16.08
September	1-15	11.24
September	16-30	5.11
October	1-15	1.61
October	1-15	0.00
November	1-15	0.66
November	16-30	0.00
December	1-15	0.00
December	16-31	0.07
		$EI_{30} = 423$

Source: Department of Meterology, HMG, Nepal, 1988.

- * Missing storms in recording rain gauge charts have not been included. Although the mean EI_{30} for a given month is a bad proxy of EI_{30} for missing storms, the inclusion of those values for all missing storms results in an annual EI_{30} of 502.

The Department of Meteorology, HMG, has 8 operating recording rain-gauge stations in the country. Their names and the years for which data exist are as follows:

Surkhet:	May 1988 onwards,	Dhankuta:	1986 onwards,
Bhairawa:	1986 onwards,	Biratnagar:	1986 onwards,
Pokhara:	March 1988 onwards,	Taplejung:	1986, and
Okhaldunga:	1986 onwards,	Kathmandu:	1986 onwards.



Source: Dept. of Meteorology, HMG, Nepal, 1988

Fig. 16.3 Cumulative frequency of EI_{30m} at Kathmandu Airport, 1988

b) Soil Erodibility, K

The soil erodibility, factor K, is the rate of soil loss for a given soil type as experimentally determined on a standard unit plot. K represents the inherent susceptibility of a given soil to erode.

Direct measurements of K require experiments that need to cover not only the range of soil property combinations that are relevant but also need to account for all possible storm sizes and antecedent soil conditions. Such experiments will clearly be costly and time consuming; fortunately they are not necessary. Nomographs have been developed from empirical relationships derived from experiments of soil erodibility. Figure 16.4 shows a nomograph (Wischmeier and Smith 1978) that requires only five properties of the soil for use. These properties are: (1) per cent silt and very fine sand (0.002 - 0.10 mm), (2) per cent sand (0.10 - 2.0 mm), (3) per cent organic matter, (4) structure, and (5) permeability. Furthermore, only the first three properties are needed to make a first approximation of K_E . To use the chart, enter the per cent of silt and very fine sand in the left chart. Proceed to the curve that matches

the per cent of sand of the slope soil. Turn upwards to intersect the appropriate curve for the per cent of organic matter. Continue along the ordinate axis to obtain a first approximation of K_E . Then continue with the right chart as indicated by the dotted line. Linear interpolations are to be used between curves on the nomograph. Figure 16.4 gives K_E in units of tons per acre per unit R. Since (1) is in metric units, the reading from Figure 16.4, K_E , has to be converted to its metric equivalent, K as $K = 1.292 K_E$.

c) Topographic Factor, LS

The topographic factor, LS, is the ratio of expected soil loss per unit area to soil loss on a standard plot, for different values of the slope length, L , and the slope steepness, S . The LS factor will be substantially over unity, therefore particular attention is required in choosing an appropriate LS value.

As in the case of K , experimentally derived values of LS exist. However, these were developed for use in the plains' area and do not extend beyond slope angles of 45° . Table 16.9 shows experimentally verified LS factors for slopes up to a length of 305 m and 100 per cent (the equation at the bottom can be used to estimate LS for slopes steeper than 100 per cent but it should be borne in mind that the resulting LS factors have not been experimentally verified). Verified estimates of LS for slopes steeper than 100 per cent can only be obtained by experimentally verifying the validity of LS calculated from the equation in Table 16.9.

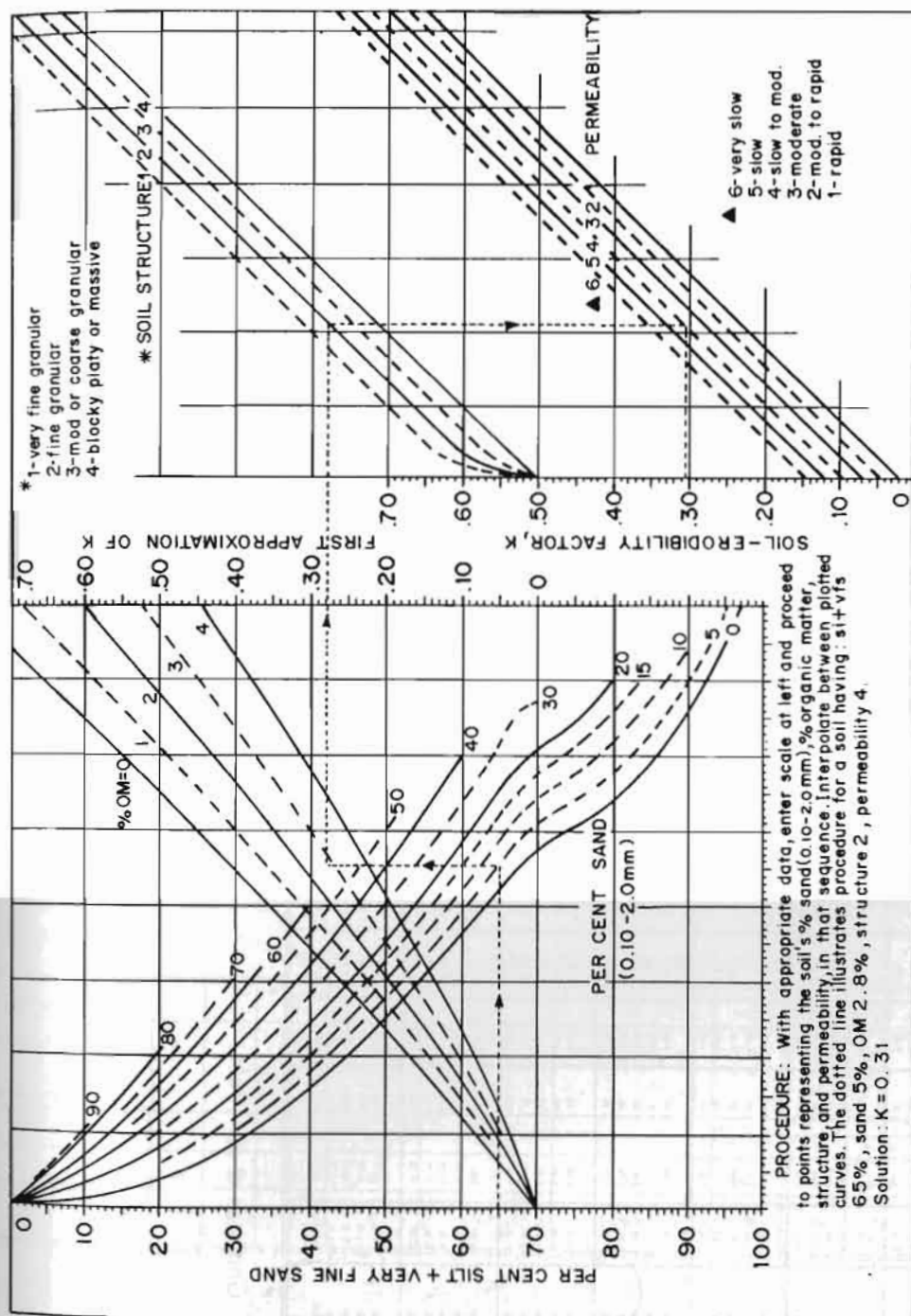
In a case where the gradient of the slope changes along its length without causing soil deposition, the following equation is used to calculate LS:

$$LS = \{[(L_{\lambda_1} S_{s_1}) \lambda_1 - (L_{\lambda_2} S_{s_1}) \lambda_0] + [(L_{\lambda_2} S_{s_2}) \lambda_2 - (L_{\lambda_1} S_{s_2}) \lambda_1] + [(L_{\lambda_3} S_{s_3}) \lambda_3 - (L_{\lambda_2} S_{s_3}) \lambda_2] + \dots [(L_{\lambda_n} S_{s_n}) \lambda_n - (L_{\lambda_{n-1}} S_{s_n}) \lambda_{n-1}]\} / (l_1 + l_2 + l_3 + \dots + l_n)$$

in which,

$$\begin{aligned} L_n &= \text{length factor for slope segment } \left(\frac{l_n}{72.5}\right)^m, \\ l_n &= \text{length of slope segment } n, \\ &\quad 0.2 \text{ for slope gradient of 0 to 1 per cent,} \\ &\quad 0.3 \text{ for slope gradient of 1 to 3 per cent,} \\ m &= 0.4 \text{ for slope gradient of 3.5 to 4.5 per cent,} \\ &\quad 0.5 \text{ for slope gradients greater than 5 per cent,} \\ S_n &= \text{slope factor for slope segment } n, \\ &= \frac{65.41 S_n^2}{S_n^2 + 10,000} + \frac{4.56 S_n}{\sqrt{S_n^2 + 10,000}} + 0.65, \\ s_n &= \text{slope gradient in per cent of segment } n, \text{ and} \\ \lambda_n &= \text{the sum of the slope segment lengths from the top of the slope to the} \\ &\quad \text{bottom of slope segment } n. \end{aligned}$$

The LS factors of Table 16.9 can be used to obtain LS values. A convenient tabular calculation format is illustrated for the case shown by Figure 16.5 in Table 16.10. In Table 16.10, Column 13 shows the cumulative LS values, the total being 2.21. So the equation to compute soil loss would be $A = RK$ (33.22) CP.



Source: Wischmeier and Smith 1978

Fig. 16.4 The soil-erodibility nomograph

Where the silt fraction does not exceed 70 per cent, the equation is $100 K = 2.1 M^{1.4} (10^{-4}) (12-a) + 3.25 (b-2) + 2.5 (c-3)$
 Where $M = (\text{per cent si} + \text{vfs}) (100 - \text{per cent c})$, $a = \text{per cent organic matter}$, $b = \text{structure code}$, and $c = \text{profile permeability class}$.

Table 16.9 LS Values* (10)

Slope ratio	Slope gradient A, %	LS values for following slope lengths, L, ft (m)										LS values for following slope lengths, L, ft (m)												
		10	20	30	40	50	60	70	80	90	100	150	200	250	300	350	400	450	500	600	700	800	900	1000
100:1	0.5	0.06	0.07	0.07	0.08	0.08	0.09	0.09	0.09	0.09	0.10	0.10	0.11	0.11	0.12	0.12	0.13	0.13	0.13	0.14	0.14	0.14	0.15	0.15
1	0.06	0.09	0.10	0.10	0.11	0.11	0.12	0.12	0.12	0.12	0.13	0.13	0.14	0.14	0.15	0.15	0.16	0.16	0.17	0.17	0.18	0.18	0.19	0.20
2	0.10	0.12	0.14	0.15	0.16	0.17	0.18	0.19	0.19	0.20	0.20	0.21	0.22	0.22	0.23	0.23	0.24	0.25	0.26	0.26	0.27	0.28	0.29	0.30
3	0.14	0.18	0.20	0.22	0.23	0.25	0.26	0.27	0.28	0.29	0.30	0.32	0.33	0.34	0.35	0.36	0.37	0.38	0.39	0.40	0.41	0.42	0.43	0.44
4	0.16	0.21	0.25	0.28	0.30	0.33	0.35	0.37	0.38	0.40	0.42	0.44	0.46	0.48	0.50	0.52	0.54	0.56	0.58	0.60	0.62	0.64	0.66	0.68
5	0.17	0.24	0.29	0.34	0.38	0.41	0.45	0.48	0.51	0.53	0.56	0.59	0.62	0.65	0.68	0.71	0.74	0.77	0.80	0.83	0.86	0.89	0.92	0.95
6	0.21	0.30	0.37	0.43	0.48	0.52	0.56	0.60	0.64	0.67	0.71	0.75	0.79	0.83	0.87	0.91	0.95	0.99	1.03	1.07	1.11	1.15	1.19	1.23
7	0.26	0.37	0.45	0.52	0.58	0.64	0.69	0.74	0.79	0.83	0.88	0.93	0.98	1.03	1.08	1.13	1.18	1.23	1.28	1.33	1.38	1.43	1.48	1.53
8	0.31	0.44	0.54	0.63	0.70	0.77	0.83	0.89	0.94	0.99	1.04	1.09	1.14	1.19	1.24	1.29	1.34	1.39	1.44	1.49	1.54	1.59	1.64	1.69
9	0.37	0.52	0.64	0.74	0.83	0.91	0.98	1.06	1.11	1.17	1.23	1.29	1.35	1.41	1.47	1.53	1.59	1.65	1.71	1.77	1.83	1.89	1.95	2.01
10:1	0.43	0.61	0.75	0.87	0.97	1.06	1.15	1.22	1.30	1.37	1.44	1.51	1.58	1.65	1.72	1.79	1.86	1.93	2.00	2.07	2.14	2.21	2.28	2.35
11	0.50	0.71	0.86	1.00	1.12	1.22	1.32	1.41	1.50	1.58	1.66	1.74	1.82	1.90	1.98	2.06	2.14	2.22	2.30	2.38	2.46	2.54	2.62	2.70
12.5	0.61	0.86	1.03	1.20	1.36	1.49	1.61	1.72	1.82	1.90	2.00	2.08	2.16	2.25	2.33	2.42	2.50	2.58	2.66	2.74	2.82	2.90	2.98	3.06
15	0.81	1.14	1.40	1.60	1.81	2.03	2.14	2.29	2.43	2.56	2.69	2.81	2.93	3.05	3.17	3.29	3.41	3.53	3.64	3.75	3.86	3.97	4.08	4.19
16.7	0.96	1.36	1.67	1.97	2.15	2.38	2.54	2.72	2.88	3.06	3.24	3.43	3.62	3.81	3.99	4.17	4.36	4.54	4.72	4.90	5.08	5.26	5.44	5.62
20	1.29	1.82	2.22	2.58	2.88	3.16	3.41	3.65	3.87	4.08	4.28	4.46	4.64	4.82	5.00	5.17	5.35	5.52	5.69	5.86	6.03	6.20	6.37	6.54
22	1.51	2.13	2.61	3.02	3.37	3.69	3.99	4.27	4.53	4.77	5.00	5.22	5.43	5.64	5.84	6.04	6.24	6.43	6.62	6.81	7.00	7.18	7.36	7.54
25	1.86	2.60	3.25	3.75	4.16	4.56	4.90	5.27	5.59	5.89	6.18	6.46	6.73	7.00	7.27	7.54	7.80	8.06	8.32	8.57	8.82	9.07	9.32	9.57
30	2.31	3.56	4.36	5.09	5.62	6.16	6.65	7.11	7.54	7.95	8.34	8.71	9.07	9.43	9.78	10.13	10.47	10.81	11.14	11.47	11.80	12.12	12.44	12.76
33.3	2.98	4.72	5.17	5.96	6.67	7.30	7.88	8.43	8.96	9.49	10.02	10.54	11.06	11.58	12.09	12.60	13.11	13.61	14.11	14.61	15.11	15.61	16.11	16.61
35	3.20	5.37	5.60	6.48	7.23	7.92	8.56	9.14	9.70	10.22	10.72	11.22	11.72	12.22	12.72	13.22	13.72	14.22	14.72	15.22	15.72	16.22	16.72	17.22
40	4.00	6.80	7.30	8.40	9.40	10.30	11.10	11.90	12.60	13.30	14.00	14.70	15.40	16.10	16.80	17.50	18.20	18.90	19.60	20.30	21.00	21.70	22.40	23.10
45	4.81	8.00	8.30	9.60	10.70	11.70	12.70	13.60	14.40	15.20	16.00	16.80	17.60	18.40	19.20	20.00	20.80	21.60	22.40	23.20	24.00	24.80	25.60	26.40
50	5.64	9.70	9.90	11.40	12.70	13.80	14.90	15.90	16.90	17.80	18.70	19.60	20.50	21.40	22.30	23.20	24.10	25.00	25.90	26.80	27.70	28.60	29.50	30.40
55	6.48	11.10	11.20	13.00	14.40	15.60	16.80	17.90	18.90	19.90	20.90	21.90	22.90	23.90	24.90	25.90	26.90	27.90	28.90	29.90	30.90	31.90	32.90	33.90
60	7.32	12.50	12.60	14.60	16.20	17.50	18.80	19.90	21.00	22.10	23.20	24.30	25.40	26.50	27.60	28.70	29.80	30.90	32.00	33.10	34.20	35.30	36.40	37.50
66.7	8.44	14.00	14.10	16.30	18.10	19.60	21.10	22.40	23.70	25.00	26.30	27.60	28.90	30.20	31.50	32.80	34.10	35.40	36.70	38.00	39.30	40.60	41.90	43.20
70	8.98	14.70	14.80	17.10	19.00	20.60	22.20	23.60	25.00	26.40	27.80	29.20	30.60	32.00	33.40	34.80	36.20	37.60	39.00	40.40	41.80	43.20	44.60	46.00
75	9.78	15.80	15.90	18.30	20.30	21.90	23.70	25.30	26.90	28.50	30.10	31.70	33.30	34.90	36.50	38.10	39.70	41.30	42.90	44.50	46.10	47.70	49.30	50.90
80	10.55	16.90	17.00	19.50	21.60	23.30	25.30	27.00	28.70	30.40	32.10	33.80	35.50	37.20	38.90	40.60	42.30	44.00	45.70	47.40	49.10	50.80	52.50	54.20
85	11.30	18.10	18.20	20.70	22.90	24.60	26.80	28.60	30.40	32.20	34.00	35.80	37.60	39.40	41.20	43.00	44.80	46.60	48.40	50.20	52.00	53.80	55.60	57.40
90	12.02	19.40	19.50	22.00	24.30	26.10	28.40	30.30	32.20	34.10	36.00	37.90	39.80	41.70	43.60	45.50	47.40	49.30	51.20	53.10	55.00	56.90	58.80	60.70
95	12.71	20.70	20.80	23.30	25.70	27.60	29.90	31.90	33.90	35.90	37.90	39.90	41.90	43.90	45.90	47.90	49.90	51.90	53.90	55.90	57.90	59.90	61.90	63.90
100	13.34	21.80	21.90	24.50	26.90	28.90	31.30	33.50	35.70	37.90	40.10	42.30	44.50	46.70	48.90	51.10	53.30	55.50	57.70	59.90	62.10	64.30	66.50	68.70

Source: Goldman et al. 1986

$$LS = \left(\frac{65.41 \times s^2}{s^2 + 10,000} \right) + \frac{45.6 \times s}{\sqrt{s^2 + 10,000}} + 0.065 \left(\frac{l}{72.5} \right)^m$$

where,

LS = topographic factor

l = slope length, ft (m x 0.3048)

s = slope steepness,

m = exponent dependent upon slope steepness

(0.2 for slopes < 1%, 0.3 for slopes 1 to 3%

0.4 for slopes 3.5 to 4.5%, and 0.5 for slopes > 5%)

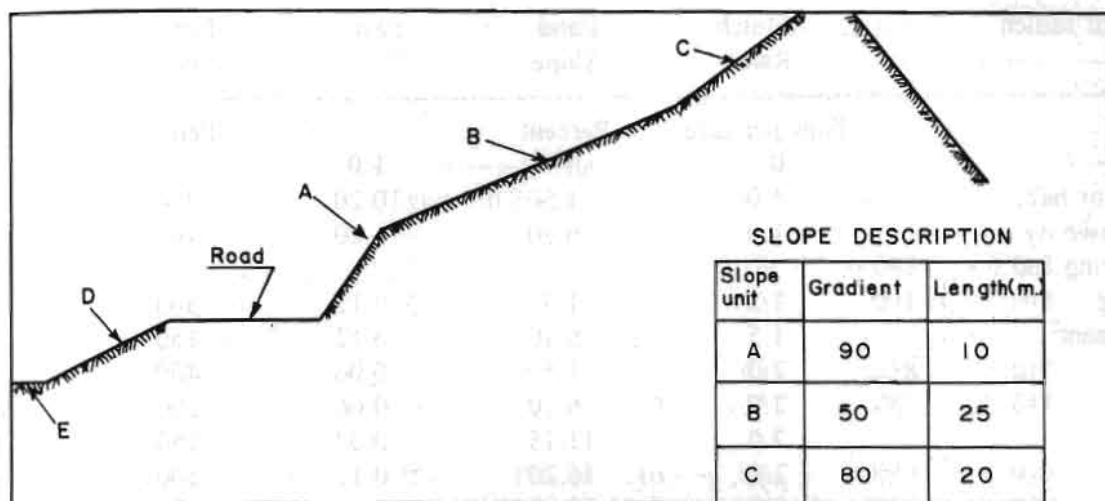


Fig 16.5 Multiple slope situation

d) Vegetative Cover Factor, C (Tables 16.11a, 16.11b, and 16.11c)

The vegetative cover factor, C, is the ratio of soil loss from a certain slope under specified cover conditions to the soil loss from a standard slope. Many factors influence C for given conditions and the estimated value of C combines all these factors.

Estimates of C vary by land use. As Nepal-specific C values are yet to be experimentally derived, approximations using C values from other areas have to be used. Judgement is crucial to choosing C values from the tables given below and it is advisable to consult a biologist in doing so; especially for C values during different periods in the year (an example problem illustrates this later on).

Table 16.11a gives C values for land use other than agricultural land. Derivation of C values for Nepalese agricultural conditions requires substantial experimental work that has not been done to date. It is recommended that Table 16.11b be used to estimate C values for agricultural land as well.

Table 16.10 LS calculation for multiple slopes

COLUMNS	C1	C2	C3	C4	C5	C6	C7	C8	C9	C10	C11	C12	C13
CALCULATION	n	r_n	L_n	λ_n	λ_{n-1}	$L\lambda_n S_{s_n}$	$L\lambda_{n-1} S_{s_n}$	(C.4) (C.6)	(C.5) (C.7)	(C.8) (C.9)	(C.10) (C.3)	E C.10	(C.12)/ (C.4)
SLOPE UNIT													
C	1	80	20	20	0	27.03	0	414.60	0	414.60	20.73	414.60	20.73
B	2	50	25	45	20	21.57	14.43	970.65	286	684.65	27.93	1099	24.42
A	3	90	10	55	45	50.88	46.00	2798	2070	728	72.80	1827	33.22

Table 16.11a Mulch factors and length limits for construction slopes

Type of Mulch	Mulch Rate	Land Slope	Factor C	Length limit ¹
	Tons per acre	Percent		Feet
None	0	all	1.0	-
Straw or hay,	1.0	1.5	0.20	200
tied down by	1.0	6.10	.20	100
anchoring and				
tacking	1.5	1.5	0.12	300
equipment ²	1.5	6.10	0.12	150
	2.0	1.5	0.06	400
	2.0	6.10	0.06	200
"	2.0	11.15	0.07	150
	2.0	16.20	0.11	100
	2.0	21-25	0.14	75
	2.0	26-33	0.17	50
	2.0	34-50	0.20	35
Crushed stone,	135	< 16	0.05	200
1/4 to 1in	135	16-20	0.05	150
	135	21-33	0.05	100
	135	34-50	0.05	75
"	240	< 21	0.02	300
	240	21-33	0.02	200
	240	34-50	0.02	150
Wood chips	7	< 16	0.08	50
	7	16-20	0.08	50
"	12	< 16	0.05	150
	12	16-20	0.05	150
	12	21-33	0.05	75
"	25	< 16	0.02	150
	25	16-20	0.02	150
	25	21-33	0.02	100
	25	34-50	0.02	75

Source: Wischmeier and Smith 1978

- 1 Maximum slope length for which the specified mulch rate is considered effective. When this limit is exceeded, either a higher application rate or mechanical shortening of the effective slope length is required.
- 2 When the straw or hay mulch is not anchored to the soil, C values on moderate or steep slopes of soils, having K values greater than 0.30, should be taken at double the values given in this table.

Table 16.11b Factor C for permanent pasture, range, and idle landslide

Vegetative canopy		Cover that contacts the soil surface						
Type and height ²	Per cent cover ³		Per cent ground cover					
		Type	0 20	40	60	80	95+	
No appreciable canopy		G	0.45	0.20	0.10	0.042	0.013	0.003
		W	.45	.24	.15	.091	.043	.001
Tall weeds or short brush with average drop fall height of 20in	25	G	.36	.17	.09	.038	.013	.003
		W	.36	.20	.13	.083	.041	.011
	50	G	.17	.10	.06	.032	.011	.003
		W	.17	.12	.09	.068	.038	.011
	75	G	.17	.10	.06	.032	.011	.003
		W	.17	.12	.09	.068	.038	.011
Appreciable brush or bushes, with average drop fall height of 6 ft	25	G	.40	.18	.09	.040	.013	.003
		W	.40	.22	.14	.087	.042	.003
	50	G	.34	.16	.08	.038	.012	.003
		W	.34	.19	.13	.082	.041	.011
	75	G	.28	.14	.08	.036	.012	.003
		W	.28	.17	.12	.078	.040	.001
Trees, but no appreciable low brush. Average drop fall height of 13 ft.	25	G	.42	.19	.10	.041	.013	.003
		W	.42	.23	.14	.089	.042	.001
	50	G	.39	.18	.09	.040	.013	.003
		W	.39	.21	.14	.087	.042	.011
	75	G	.36	.17	.09	.039	.012	.003
		W	.36	.20	.13	.084	.041	.011

Source: Wischmeier and Smith 1978

- ¹ The listed C values assume that the vegetation and mulch are randomly distributed over the entire area.
- ² Canopy height is measured as the average fall height of water drops falling from the canopy to the ground. Canopy effect is inversely proportional to drop fall height and is negligible if fall height exceeds 33 ft.
- ³ Portion of total-area surface that would be hidden from view by canopy in a vertical projection (a bird's-eye view).
- ⁴ G: Cover at surface is grass, grasslike plants, decaying compacted duff, or litter at least 2in deep.
W: Cover at surface is composed mostly of broad-leaved herbaceous plants (as weeds with little lateral-root network near the surface) or undecayed residue or both.

Table 16.11c Factor C for undisturbed forest land¹

Percentage of area covered by canopy of trees and undergrowth	Percentage of area covered by duff at least 2in deep	Factor C ²
100-75	100-90	.0001 - .001
70-45	85-75	.002 - .004
40-20	70-40	.003 - .009

Source: Wischmeier and Smith 1978

¹ Where effective litter cover is less than 40 per cent or canopy cover is less than 20 per cent, use Table 16.11b. Also use Table 16.11b where woodlands are being grazed, harvested, or burned.

² The ranges in listed C values are caused by the ranges in the specified forest litter and canopy covers and by variations in effective canopy heights.

Table 16.12 has been derived from knowledge of typical Nepalese land use patterns and from Table 16.11b. It covers most cases likely to be encountered and provides an example of deriving C values for Nepalese land use conditions.

(e) Practice Support Factor, P

The P factor is the soil loss ratio of a specific practice such as terracing to a standard experimental culture condition. Effectiveness of a given practice in reducing erosion would be reflected by a small P value and vice versa. P values for cut slopes will be close to 1.0 as shown in Table 16.13a. The information on P values suitable to Nepalese land use conditions has to be derived from information for other areas. P values for agricultural practices relevant in Nepal are given in Table 16.13b.

Sample Problem

The case shown in Figure 16.5 has been considered in the example below in Table 16.14 that calculates soil loss for each month of the year. The rainfall erosivity used is from Table 16.8. The agro-ecological zone that the area lies within is a subtropical location in the middle mountains of the Nepalese hills. Slope units B and C are range/pastureland with very good grass cover. It is assumed that the site is protected from overgrazing and that the grass is systematically harvested in the month of October/November and dried as winter fodder. Table 16.15 summarizes the results.

Table 16.12 C values for Nepalese land use patterns

CASE MONTH	1	2	3	4	5	6
JAN	0.20	0.20	0.20	0.032	0.003	0.032
FEB	0.16	0.20	0.20	0.003	0.003	0.003
MAR	0.16	0.20	0.165	0.003	0.14	0.003
APR	0.16	0.20	0.13	0.10	0.14	0.10
MAY	0.09	0.20	0.107	0.10	0.10	0.10
JUN	0.076	0.13	0.107	0.09	0.09	0.09
JUL	0.076	0.13	0.107	0.038	0.038	0.038
AUG	0.076	0.13	0.107	0.011	0.011	0.011
SEPT	0.076	0.13	0.13	0.068	0.011	0.011
OCT	0.067	0.107	0.165	0.145	0.17	0.011
NOV	0.093	0.041	0.20	0.12	0.06	0.12
DEC	0.135	0.041	0.20	0.12	0.06	0.12

Case Descriptions

1. An area with shrubs, tall weeds, and grass; ecologically indicating partial degradation in terms of vegetation frequency.
2. Forest with broad-leaved trees, shrubs, and grasses; not much undergrowth.
3. Pure stands of pine forest in the temperate zone of the *Himalaya*.
4. Pure cropping in which the winter crop of wheat is followed by maize as the dominant summer crop.
5. Pure-mixed cropping in which mustard in the winter is followed by corn and beans simultaneously.
6. Pure-relay cropping in which wheat is followed by corn relay with finger millet.

Table 16.13a P Factors for construction sites

Surface condition	P Value
Compacted and smooth	1.3
Trackwalked along contour*	1.2
Trackwalked up and down slope+	0.9
Punched straw	0.9
Rough, irregular cut	0.9
Loose to 12in (30cm) depth	0.8

Goldman et al. 1986.

* Tread marks oriented up and down slope.

+ Tread marks oriented parallel to contours.

Table 16.13b P Values for contour-framed terraced fields¹

Land slope (%)	Farm planning		Computing sediment yield ³	
	Contour factor ²	Strip crop factor	Graded channels sod outlets	Steep backslope underground outlets
1 to 2	0.60	0.30	0.12	0.05
3 to 8	.50	.25	.10	.05
9 to 12	.60	.30	.12	.05
13 to 16	.70	.35	.14	.05
17 to 20	.80	.40	.16	.06
21 to 25	.90	.45	.18	.06

Source: Wischmeier and Smith 1978

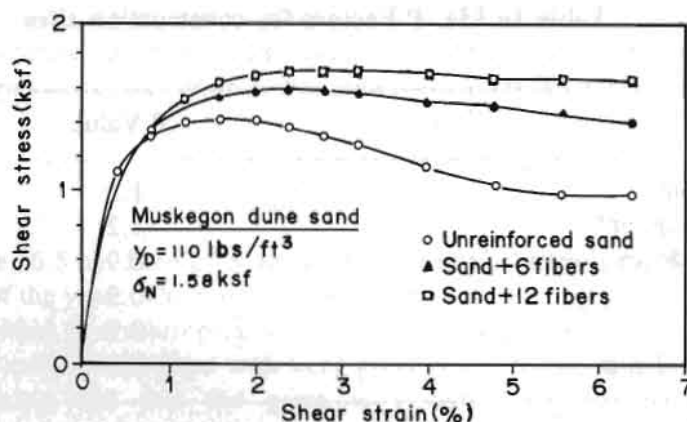
¹ Slope length is the horizontal terrace interval. The listed values are for contour farming. No additional contouring factor is used in the computation.

² Use these values for control of inter-terrace erosion within specified soil loss tolerance.

³ These values include entrapment efficiency and are used to control off-site sediment within limits and for estimating the field's contribution to watershed sediment yield.

16.2.3 Increase in Shearing Strength

The presence of roots in a soil matrix influences the shearing strength of the soil. Specifically, the frictional anchoring of roots embedded in soil causes the roots to develop tensile resistance to shearing. Thus roots increase the shearing resistance of soil. Figure 16.6 shows the results of direct shear tests in sand with and without reinforcing fibre reeds. In Figure 16.6, notice that fibre reeds lower the loss of residual strength in addition to increasing the shearing strength.



Source: Gray and Leiser 1982

Fig. 16.6 Results of direct shear test on sand with weeds

Table 16.14 Range and pasture land - Middle Himalayan Range of Nepal

COLUMNS		C1	C2	C3	C4	C5	C6	C7	C8
TIME PERIOD	SLOPE SEGMENT	R	K	LS λ From c.10 Table 6	RKLS λ [(c.1)(c.2)(c.3)] 10 ⁶ in metric tons per month per metre slope width	C	P	RKLS λ_{CP} [(c.4)(c.5)(c.6)] 10 ⁶ in metric tons per month per slope width	NOTES
OCT	C	1.61	0.55	414.60	0.04	0.613	1.0	0.0005	Land use: C and B are pasture grazing land while A is a cut slope that has just been made and left bare. Grass is dominant & growth is at its peak
	B	1.61	0.50	684.65	0.06	0.013	1.0	0.0008	
	A	1.61	0.52	728	0.08	1.00	1.0	0.06	
					-----			-----	
Total					0.16			0.06	
NOV	C	0.66	0.55	414.60	0.02	0.042	1.00	0.0008	Grass withers at this time
	B	0.66	0.50	684.65	0.02	0.042	1.00	0.0008	
	A	0.66	0.52	728	0.02	1.00	1.00	0.02	
					-----			-----	
Total					0.06			0.02	
DEC	C	0.07	0.55	414.60	0.002	0.10	1.00	0.0002	Grass withers further
	B	0.07	0.50	684.65	0.002	0.10	1.00	0.0002	
	A	0.07	0.52	728	0.003	1.00	1.00	0.003	
					-----			-----	
Total					0.01			0.0003	
JAN	C	0.01	0.55	414.60	0.0002	0.33	1.00	0.00007	The grass vegetation is at its max. stage of withering; mostly litter covers the soil (10% ground contact cover)
	B	0.01	0.50	684.65	0.0003	0.33	1.00	0.00007	
	A	0.01	0.52	728	0.0004	1.00	1.00	0.00004	
					-----			-----	
Total					0.0009			0.0003	
FEB	C	1.72	0.55	414.60	0.04	0.33	1.00	0.01	Vegetation dormant. Only litter covers soil.
	B	1.72	0.50	684.65	0.06	0.33	1.00	0.02	
	A	1.72	0.52	728	0.07	1.00	1.00	0.07	
					-----			-----	
Total					0.17			0.10	
MAR	C	3.04	0.55	414.60	0.07	0.26	1.00	0.02	Minor percentage of vegetation emergence (15% ground contact cover)
	B	3.04	0.50	684.65	0.10	0.26	1.00	0.03	
	A	3.04	0.52	728	0.12	1.00	1.00	0.12	
					-----			-----	
Total					0.29			0.17	
APR	C	0.50	0.55	414.60	0.01	0.20	1.00	0.002	Little increase in green vegetation cover due to new emergence and further growth.
	B	0.50	0.50	684.65	0.02	0.20	1.00	0.004	
	A	0.50	0.52	728	0.02	1.00	1.00	0.02	
					-----			-----	
Total					0.05			0.03	
MAY	C	18.74	0.55	414.60	0.43	0.10	1.00	0.04	Large-scale emergence in new vegetation; seed germination and new growth from stolons
	B	18.74	0.50	684.65	0.64	0.10	1.00	0.06	
	A	18.74	0.52	728	0.71	1.00	1.00	0.71	
					-----			-----	
Total					1.78			0.81	
JUN	C	65.91	0.55	414.60	1.50	0.042	1.00	0.06	All green cover, vegetative stage
	B	65.91	0.50	684.65	2.26	0.042	1.00	0.09	
	A	65.91	0.52	728	2.50	1.00	1.00	2.50	
					-----			-----	
Total					6.26			2.65	
JUL	C	232.66	0.55	414.60	5.31	0.028	1.00	0.15	Further increase in the density of green cover. Flowering period initiation (70% ground contact cover)
	B	232.66	0.50	684.65	7.96	0.028	1.00	0.22	
	A	232.66	0.52	728	8.81	1.00	1.00	3.81	
					-----			-----	
Total					22.08			3.13	
AUG	C	81.44	0.55	414.60	1.86	(90%)	1.00	0.01	Full bloom. Maximum green cover (90% ground contact cover)
	B	84.44	0.50	684.65	2.79	0.006	1.00	0.02	
	A	81.44	0.52	728	3.08	0.006	1.00	3.08	
					-----	1.007		-----	
Total					7.73			3.11	
SEPT	C	16.35	0.55	414.60	0.37	0.006	1.00	0.00	Maximum green cover. Vegetation entering into fruiting stage.
	B	16.35	0.50	684.65	0.56	0.006	1.00	0.003	
	A	16.35	0.52	728	0.62	1.00	1.00	0.62	
					-----			-----	
					1.55			0.63	

Table 16.15: Efficiency of vegetative cover

<i>Month</i>	<i>Percentage Reduction of Erosion by Vegetation in Table 16.14</i>
OCT	63
NOV	67
DEC	70
JAN	44
FEB	41
MAR	41
APR	40
MAY	54
JUN	58
JUL	58
AUG	60
SEP	59

Note: per cent reductions would be much higher had the cut slope also been grassed

i) *Root Reinforcement Model*

Root reinforcement calculations make it possible to evaluate the increment in shearing strength caused by the presence of roots. The increase in shear strength, s , can be included in the numerator of the equation to calculate the factor of safety against planar sliding in an infinite slope model (see Chapter 13). Various types of vegetation can be evaluated to identify the species that adds the most to shear strength.

Figure 16.7 shows a model where a flexible elastic root passes through a shear zone of depth z . The intact root is assumed to be perpendicular to the shear zone plane. The intact root is shown to have deformed at the angle of shear distortion in Figure 16.7. The shear distortion angle can be calculated as:

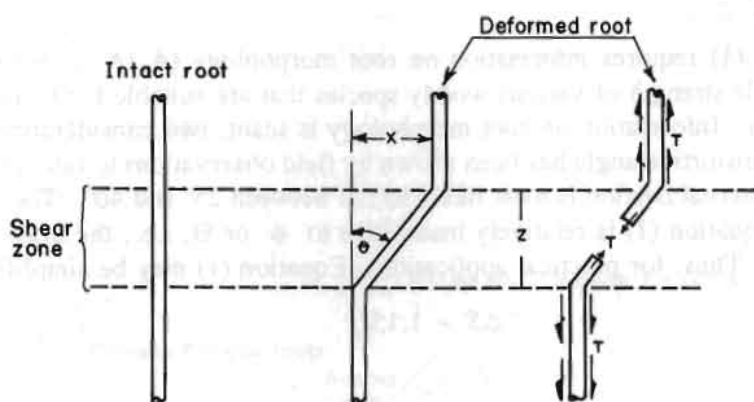
$$\theta = \tan^{-1} \left(\frac{x}{z} \right) .$$

The increase in shear strength, ΔS , can be calculated by resolving the forces due to the tension in the root as:

$$\Delta S = t_R (\sin\theta + \cos\theta + \tan\phi)$$

where,

- t_R = tensile strength of roots per unit area,
- A_R = total cross-sectional area of all the roots in a given cross-section of the soil,
- A = area of the soil cross-section under study,
- ϕ = angle of internal friction, and
- θ = angle of shear distortion.



Source: Gray and Leiser 1982

Fig 16.7 Root reinforcement model

The tensile strength of roots per unit area can be calculated as:

$$t_R = T_R \left(\frac{A_R}{A} \right) \quad (1)$$

where,

- T_R = mean tensile strength of roots,
- A_R = total cross-sectional area of all the roots in a given cross-section of the soil, and
- A = area of the soil cross-section under study.

The root area ratio, A_R/A , can be calculated as:

$$\frac{A_R}{A} = \sum \frac{n_i a_i}{A}$$

where,

- n_i = number of roots in size class i , and
- a_i = mean cross-sectional area of roots in class i .

Also, if root tensile strength varies with size, the mean tensile strength of the root can be computed as:

$$T_R = \frac{\sum T_i n_i a_i}{\sum n_i a_i}$$

where,

- T_i = tensile strength of roots in size class i .

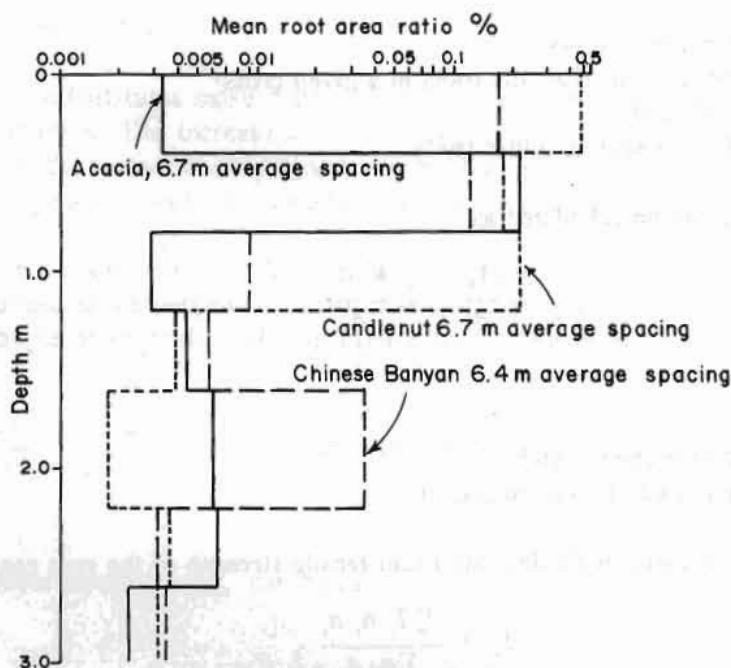
Application of Equation (1) requires information on root morphology (A_R/A) as well as data on root strength (T_R). The tensile strength of various woody species that are suitable for Himalayan conditions are given in Table 16.16. Information on root morphology is scant; two considerations are relevant in this regard: i) the shear distortion angle has been shown by field observations to fall between 40° and 70° . Similarly, the angle of internal friction is most likely to fall between 25° and 40° . These facts mean that the braceleted term in Equation (1) is relatively insensitive to ϕ or Θ , i.e., the braceleted term varies between 1.0 to 1.3 only. Thus, for practical applications, Equation (1) may be simplified as:

$$\Delta S = 1.15 t_R \quad (2)$$

where,

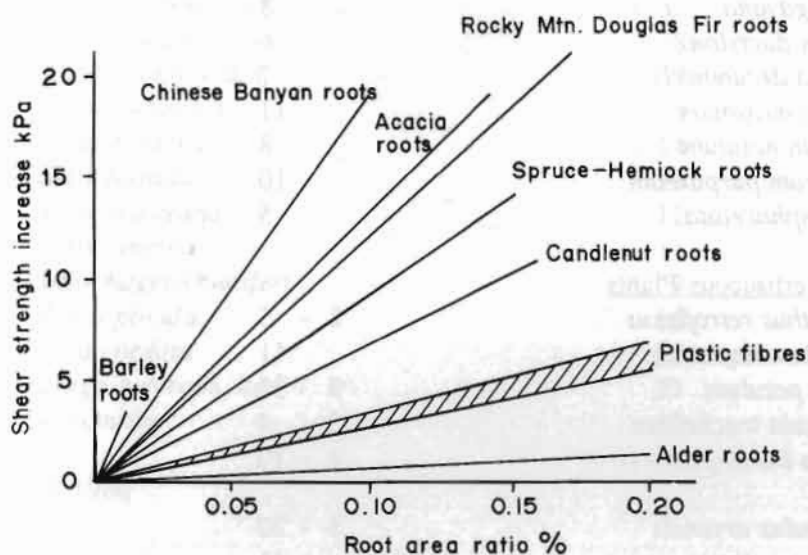
1.15 is an average value of the braceleted term in Equation (1).

The second consideration pertains to the root area ratio. The data required is the variation of root area ratio with depth for various species, as shown in Fig. 16.8. Trial pits have to be dug and measurements made to develop an inventory of species having the needed root area ratio data. Educated guesswork can be very misleading, i.e., about 2-3 orders of magnitude difference in Figure 16.9 shows the effects of root reinforcement for some species.



Source: Greenway 1987

Fig 16.8 Root area ratio distributions



Source: Gray and Leiser, 1982

Fig 16.9 Potential shear strength increase due to roots

Figure 16.9 provides a potential or upper bound estimate of shear strength increase based on a simple force-equilibrium model of fibre reinforcement. It also entails the following critical assumptions:

1. the shear distribution angle (Θ) falls between 40 and 70 degrees
2. the roots are sufficiently long or kinky to avoid pullout (slipping), and
3. there is full mobilisation of the tensile strength of the root fibres.

Research carried out by Gray and Leiser 1982 has shown that assumption No. 3 is rarely achieved.

Shear strength increase from root reinforcement in sandy soils can be estimated from the results of both laboratory and field tests (Gray and Ohashi 1983 and Ziemer 1981). Both studies showed a linear increase between ΔS_R and the root or fibre biomass per unit volume of soil (see Table 16.17). The coefficient of proportionality was very similar in both studies and can be used to estimate ΔS_R based on a simple measure of root biomass per unit volume of soil or root area ratio versus depths.

Table 16.16 Tensile strength of plant roots

Plant Species	Tensile Strength (MPa)
<u>Grasses</u>	
<i>Agropyron repens</i>	7 - 25
<i>Chloris gayana</i>	8
<i>Cynodon dactylon</i>	6
<i>Digitaria decumberis</i>	7
<i>Panicum maximum</i>	11
<i>Paspalum notatum</i>	8
<i>Pennisetum purpuream</i>	10
<i>Setaria sphaceolata</i>	5
<u>Other Herbaceous Plants</u>	
<i>Amaranthus retroflexus</i>	2 - 5
<i>Artemisia compestris</i>	11
<i>Atriplex patulum</i>	9 - 30
<i>Campanula trachelium</i>	0 - 4
<i>Caspella bursa-pastoris</i>	4 - 10
<i>Convolvulus arvensis</i>	5 - 20
<i>Medicago sativa</i>	41
<i>Plantago lanceolate</i>	4 - 8
<i>Plantago major</i>	3 - 6
<i>Rumx conglomeratus</i>	2 - 6
<i>Solanum nigrum</i>	16 - 38
<i>Taraxacum officinalis</i>	0 - 4
<i>Trifolium pratense</i>	11 - 18
<u>Woody plants (trees and Shrubs)</u>	
<i>confusa</i>	11
<i>Alnus firma</i> var <i>yasha</i>	4 - 74
<i>Alnus firma</i> var <i>multinervis</i>	51
<i>Alnus incana</i>	32
<i>Alnus japonica</i>	41
<i>Betula pendulai</i>	37
<i>Ficus microcarpa</i>	16
<i>Picea abies</i>	27
<i>Picea sitchensis</i>	23
<i>Pinus desiflora</i>	32
<i>Pinus radiata</i>	18
<i>Populus nigra</i>	5 - 12
<i>Populus deltoides</i> (USSR)	38
<i>Populus deltoides</i> (New Zealand)	36
<i>Populus euramericana</i> (1-78)	46
<i>Populus euramericana</i> (1-488)	32

Plant Species

Tensile Strength (MPa)

<i>Populus yunnanensis</i>	38
<i>Quercus robur</i>	32
<i>Robinia pseudoacacia</i>	68
<i>Salix purpurea</i> (Booth)	36
<i>Salix matsundana</i>	36
<i>Salix fragilis</i>	18
<i>Y Salix dasyclados</i>	17
<i>Salix elaeagnos</i>	15
<i>Salix helvetica</i>	14
<i>Salix hastata</i>	13
<i>Salix starkeana</i>	12
<i>Salix cinerea</i>	11
<i>Salix hagetschweileri</i>	9
<i>Thuja plicata</i>	56
<i>Tilia cordata</i>	26
<i>Tsuga heterophylla</i>	27
<i>Vaccinium</i>	16

Source: Schiechl 1980

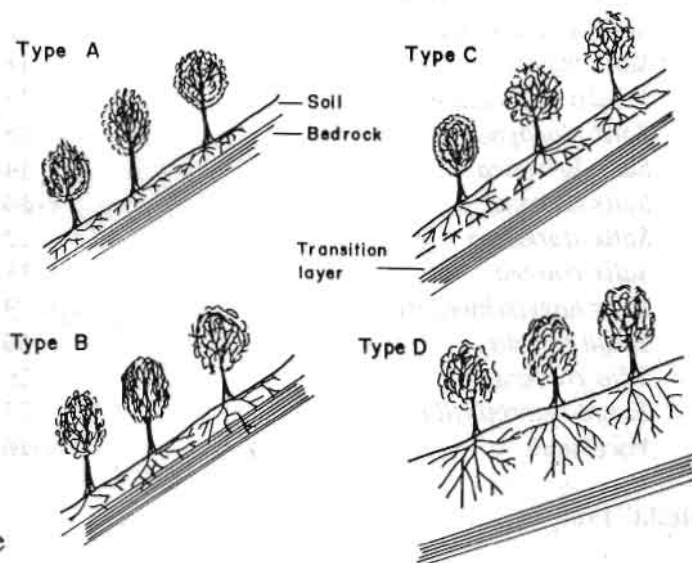
Table 16.17 Summary of root fibre contributions to soil shear strength

FIBRE OR ROOT SYSTEM	MAXIMUM FIBRE OR ROOT BIOMASS CONC.		SHEAR STRENGTH INCR. PER UNIT FIBRE CONC.		MAX SHEAR STR. INCR. MEAS. IN TESTS (PSI)
	AREA RATIO (%)	WT. CONC. lbs root of soil	PSI lb/cf	kPa kg/cu m	
VERTICAL SURFACE, LATERAL ROOTS Tree roots (<i>pinus contorta</i>) Vertical shear surface, coastal sand Live roots < 17 mm diameter <i>in situ</i> direct shear test	0.78	0.31	7.4	3.2	2.3
LAB TESTS ON FIBRE-PERMEATED SANDS Reed fibres (<i>phragmites communis</i>) Natural fibre: diameter = 2.0 mm Uniform sand Direct shear test	1.70	0.68	8.7	3.7	5.9
AVERAGES	1.24	0.50	8.1	3.5	4.1

Source: Received from Gray personally in 1990

ii) Root Anchoring

Figure 16.10 shows conditions where frictional anchoring can or cannot develop to make roots capable of providing tensile resistance.



Source: Tsukamoto and Kusakabe

Fig 16.10 Slope classification based on root reinforcement and anchoring

Type A shows a case where a shallow topsoil layer is resting on a bedrock with little or no fractures. The roots cannot find anchor inside the rock but will attach themselves to the rocks provided there is some anchoring. Also, the roots will develop functional resistance along their lengths in the soil layer. A minimum root length, L_{\min} , is needed to make the frictional anchoring sufficient to present pullout before the tensile strength of the root, T_R , is attained:

$$L_{\min} = \frac{\tau_r d}{L_1 \tau_b}$$

where,

d = root diameter, and

τ_b = limiting bond stress between root and soil.

While the root will increase the shear strength of the soil if L_{\min} is attained, root reinforcement may not be relevant for case A where the plane of failure can be the soil-rock interface. The root system will not help against sliding on that interface.

Type B is identical to Type A in all respects, except for the fact that the underlying rock is fractured. The root system will penetrate the rock and find sound anchoring. This case is one where the roots can make a full contribution to shear strength by tensile resistance. Roots will weaken fractured rock,

however, and it is important to ensure that the fracture pattern is not going to be disturbed so that a wedge is destabilized.

Type C shows a case with thicker soil layers. Soil density and shear strength increase with depth in Type C. Roots will find firmer anchoring as they penetrate the transition layer provided L_{min} is attained. This case is suitable for root reinforcement as well.

Type D shows a case where the soil layer is thick. The failure plane is likely to be below the root system. Although the root system will increase shear strength in the rooted zone (as L_{min} will probably be attained), the root system cannot help stabilize a deep-seated slide. Root reinforcement is unsuitable for such cases where a potential for deep-seated slides exist.

iii) Surcharge Effect

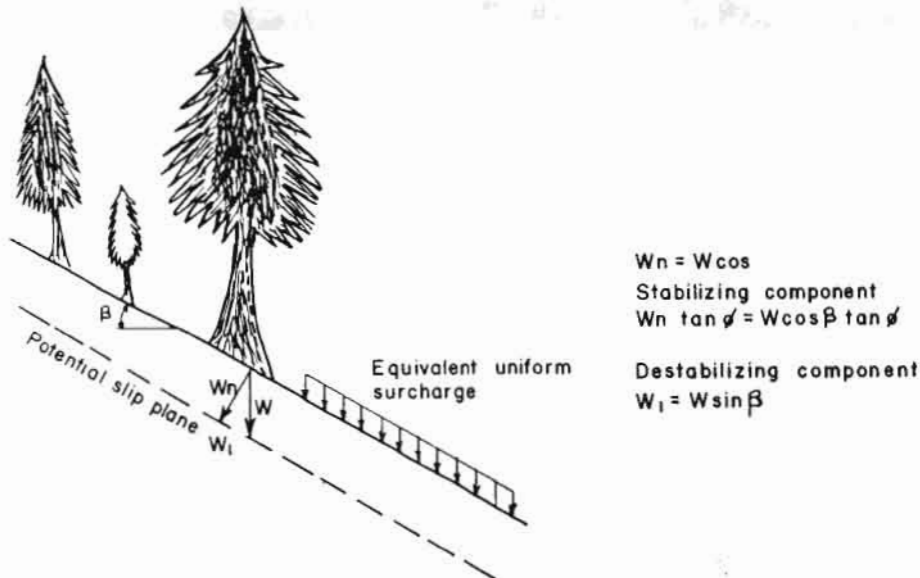
The surcharge that a tree creates on a slope is depicted in Figure 16.11.

In terms of an infinite slope model (Chapter 13) surcharge will have a beneficial effect on stability if:

$$C < \gamma_w H_w \tan \phi \cos^2 \beta \quad (3)$$

where,

- H_w = piezometric height above sliding surface,
- ϕ = angle of internal friction of the soil,
- c = cohesion of soil,
- β = slope angle, and
- γ_w = density of water.



Source: Greenway 1987

Fig. 16.11 Surcharge effect of tree weight

Using Equation 3, if the effect of surcharge is seen to be beneficial to stability, a conservative estimate of surcharge should be used in the infinite slope model, i.e., the gross weight of trees on the slope divided by the gross slope area. If surcharge is evaluated to be adverse to slope stability, the estimate of surcharge should be biased conservatively again; in this case surcharge may be estimated as the weight of an average tree divided by its stem area.

iv) *Example Problem - Sandy Soil on Fractured Bedrock (Fig. 16.12)*

For the infinite slope model of sandy soil overlying fractured bedrock,

- find the F.S. of the slope against planar failure along the bedrock, and
- evaluate woody plants to ensure a F.S. of 1.2.

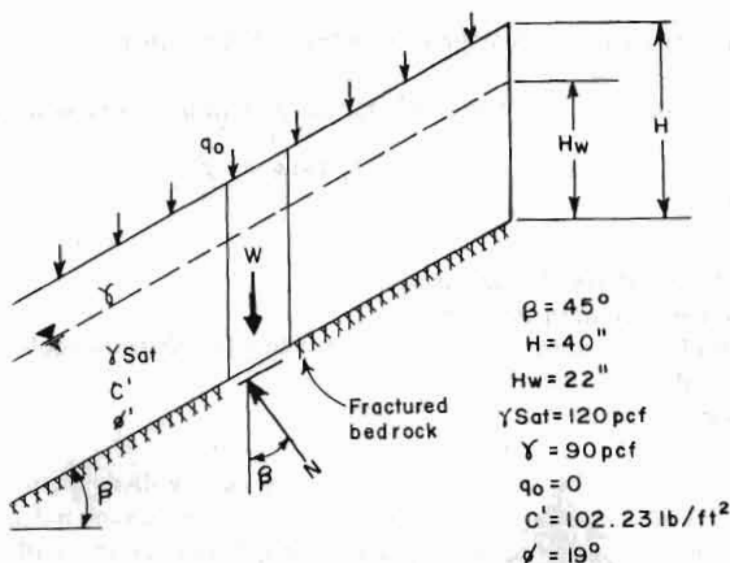


Fig 16.12 Sandy soil on fractured bedrock

Solution

$$\begin{aligned}
 \text{a) } F.S. &= \frac{\left[\frac{c'}{\cos^2 \beta \tan \phi'} + (q_0 + \gamma H) + (\gamma_{\text{BUOY}} - \gamma) H_w \right] \frac{\tan \phi'}{\tan \beta} + \Delta S}{[(q_0 + \gamma H) + (\gamma_{\text{SAT}} - \gamma) H_w]} \\
 &= \frac{\left[\frac{102.23}{\cos^2 45^\circ \tan 19^\circ} + 90(3.33') - 32.43(1.83) \right] \frac{\tan 19^\circ}{\tan 45^\circ}}{[90(3.33) + (120 - 90) 1.83]} \\
 &= \frac{(594 + 299.70 - 59.35) 0.34}{299.70 + 54.90} \\
 &= \frac{283.68}{354.6} = 0.80
 \end{aligned}$$

b) *Surcharge Effect:*

$$\begin{aligned} & \gamma_w H_w \tan\phi \cos^2\beta \\ &= (62.43 \frac{\text{lb}}{\text{ft}^3}) (1.83\text{ft}) (\tan 19^\circ) (\cos^2 45^\circ) \\ &= 1.67 \text{lb/ft}^2 \end{aligned}$$

Surcharge is beneficial to the stability of infinite soil slope, when $c < \gamma_w H_w \tan\phi \cos^2\beta$ (Gray 1982). As $c = 102.23 \text{ lb/ft}^2 > 19.67 \text{ lb/ft}^2$ the effect of surcharge on the slope will be adverse. The surcharge can be estimated as the weight of an average tree divided by its stem area.

Suppose the species *Acacia* were to be evaluated for its effectiveness in increasing the shear strength. Furthermore, assume *Acacia* has a surcharge of 104.43 lb/ft^2 directly beneath itself. Then:

$$\begin{aligned} F.S. &= \frac{[\frac{102.33}{\cos^2 45^\circ \tan 19^\circ} + 104.43 + 90(3.33) - 32.43(1.83)] \frac{\tan 19^\circ}{\tan 45^\circ} + \Delta S}{[(104.43 + 90)(3.33) + (120 - 90)(1.83)]} \\ &= \frac{594 + 404.13 - 59.35 + 0.34 + \Delta S}{404.13 + 54.90} \\ &= \frac{319.19 + \Delta S}{459.03} \end{aligned}$$

or,

$$\Delta S = 231.84 \text{ lb/ft}^2$$

Using Equation (2),

$$\Delta S = 231.84 \text{ lb/ft}^2 = 1.15 t_R$$

$$\therefore t_R = 201.60 \text{ lb/ft}^2$$

For *Acacia*, at a depth of 1m, $A_R/A = 0.003 \times 10^{-2}$. Similarly, Table 16.17 gives $T_R = 11 \text{ MPa}$ for *Acacia*. Thus $t_R = (2.32 \times 10^5 \text{ lb/ft}^2) (3 \times 10^{-5}) = 6.96 \text{ lb/ft}^2$. Since 6.96 lb/ft^2 is much less than the required additional strength of 201.60 lb/ft^2 , *Acacia* will not be suitable.

Suppose Chinese Banyon also had $q_o = 104.43 \text{ lb/ft}^2$. For Chinese Banyon, $A^R/A = 0.009 \times 10^{-2}$ and $T_R = 6 \text{ MPa}$. Thus $t_R = (3.37 \times 10^5 \text{ lb/ft}^2) (9 \times 10^{-5}) = 30.30 \text{ lb/ft}^2$ which is also inadequate. It can be concluded that neither *Acacia* nor Chinese Banyon are suitable for stabilizing the slope.

16.2.4 Moisture Content and Groundwater Table Reduction

The principal mechanisms responsible for the effects plants have on soil moisture content are i) rainfall interception, ii) increase in surface roughness leading to higher infiltration, and iii) transpiration. This section only cites evidence that plants affect soil moisture content and groundwater table. Neither analysis of the plant-soil mechanisms nor predictions of the extent of soil moisture content reduction are addressed here. Readers are referred to the work of Tien H. Wu, Professor of Civil Engineering, Ohio State University, Columbus, for an analytical framework to predict pore-water pressure changes caused by evapotranspiration.

i) *Interception Losses*

Interception losses, caused by vegetative foliage, vary by vegetative cover characteristics and rainfall intensity. Table 16.5 shows an observation of interception losses from an evergreen rainforest in Brazil. Other observations have shown that interception losses of rainfall can vary between 10 per cent and 100 per cent with decreasing rainfall intensity.

ii) *Infiltration*

Roots, vacant root channels, and increased surface roughness in the rooted area cause higher infiltration rates. The angle of the slope affects the degree to which infiltration is increased. Figure 16.1 shows the effect of grass on infiltration rates.

iii) *Transpiration*

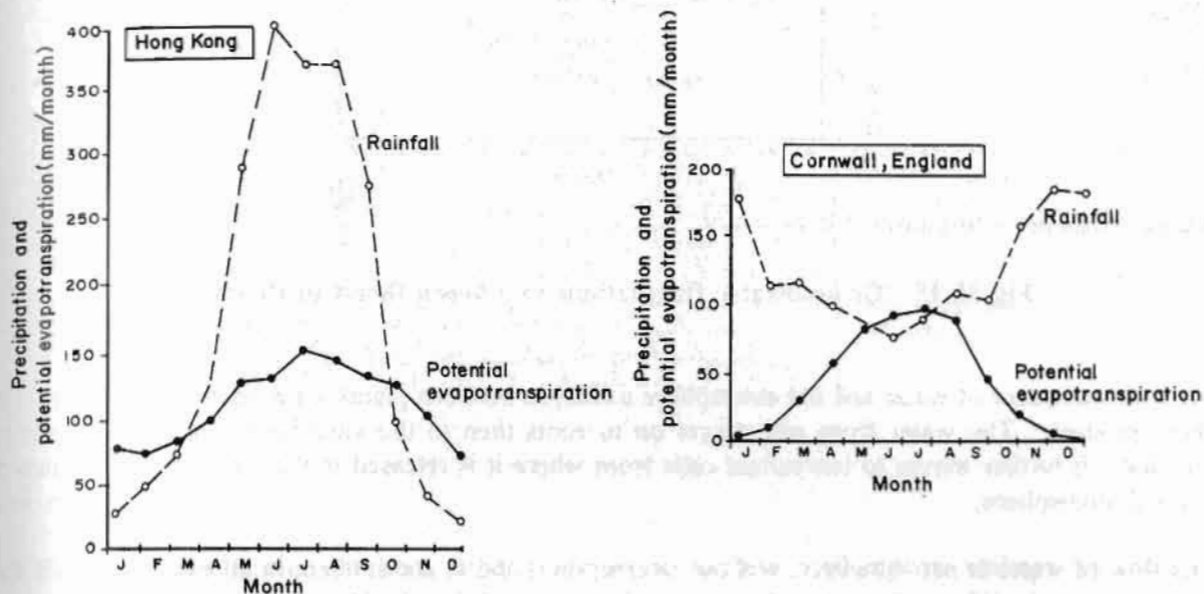
Plants that transpire most are called **phreatophytes**. Aside from the characteristics of the plant, that make it a phreatophyte, the weather, climatic, and seasonal factors, as well as slope attributes (aspect, moisture, and soil type), influence the transpiration of a plant. Thus, the transpiration rate is a plant and site-specific parameter. Only data from identical areas reflect what the transpiration rate may be for a given slope. Moreover, transpiration rates change over the year so the effect of transpiration on critical groundwater levels must be studied as a function of time. An illustration of the site-specificity (seasonal and climatic) of transpiration is provided by the examples shown in Figures 16.13 and 16.14.

Just as transpiration reduces the groundwater level, a sudden removal of plants increases the groundwater level. Thus clearfelling for road construction may create instability. An illustration of this phenomenon from a clearfelling in Denmark is given below in Figure 16.15.

Exploiting Transpiration Phenomenon

Transpiration has been, so far, considered as a necessary evil of water loss by plants. About two thirds of the water, falling as precipitation in temperate lands, is returned to the atmosphere by transpiration. This example explains the magnitude of the phenomenon and it is for this reason that plant physiological research on transpiration, especially in the field of agriculture, has been heavily involved in understanding the process in order to devise ways to control it. In the present context, using the transpiration phenomenon positively, as a method to drain out more water from the soil to help stabilize roadside slopes, is unique. The discussion, therefore, concentrates on aspects that are of interest in exploiting this

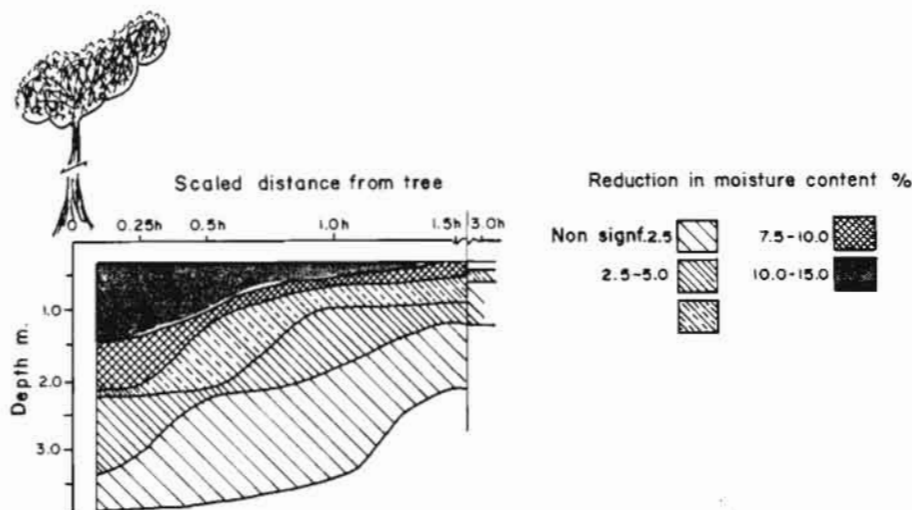
phenomenon in the context of reducing the moisture content. The focus will be to know what the key organs of plants involved in transpiration are and how their function is regulated. Are transpiration rates of species measurable to affect their selection for roadside slope stabilization?



Greenway 1987

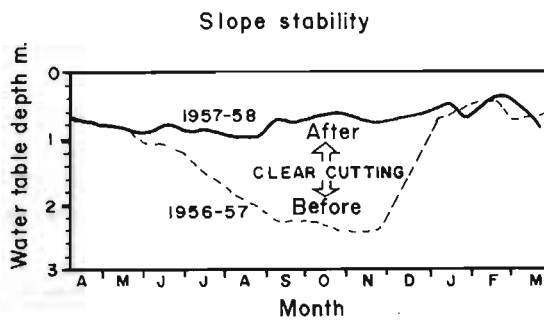
Fig 16.13 Comparative evapotranspiration rates

Moisture content, due to extraction of soil moisture by roots, affects the distribution of soil moisture (and pore-water pressures) around the root area. Again, the actual impact is site-specific, but the reduction of moisture decreases at increasing distances from the plant. Figure 16.14, illustrates the case.



Source: Biddle 1983

Fig 16.14 Soil suction response of a model slope



Source: Hostener - Jorgensen 1967

Fig 16.15 Groundwater fluctuations in a beech forest in Denmark

The soil is a source of water and the atmosphere a sink; in between plants act as factors operating on the whole process. The water from soil passes on to roots then to the vascular tissue of the stems and branches. It further moves to leaves/leaf cells from where it is released in the form of vapours into the external atmosphere.

This flow of water is not, however, without interruptions and is not uniform in all plants. It does vary from plant to plant depending upon the impact of the sum total of both internal and external resistance factors. In other words, it is also known as the mechanism regulating transpiration.

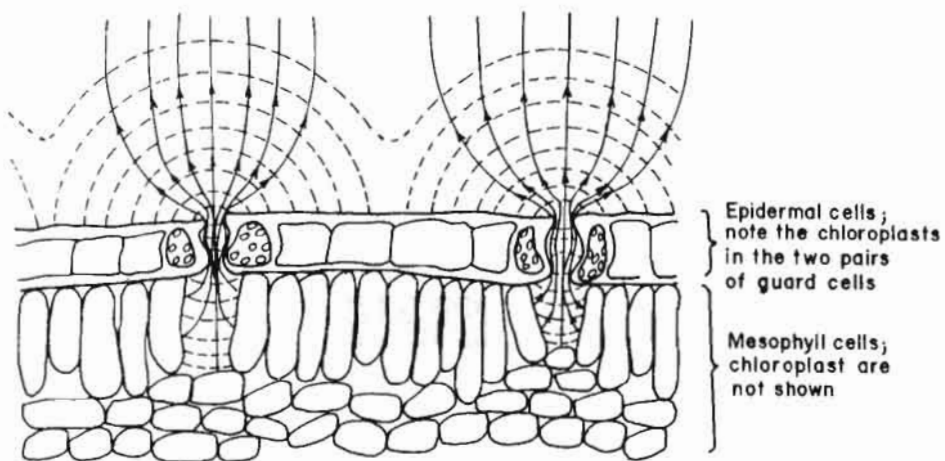
A. Internal Mechanism to Regulate Water Flow

There are two plant organs that regulate transpiration.

- i. Stomata in leaf epidermal tissue. Water loss occurs principally through stomatal pores on the leaf surfaces (Fig. 16.16).
- ii. Cuticle layer of waxy material on the leaf surface.

Cuticle transpiration is of academic interest only and there is, in fact, a very small amount of water passing through the cuticle. In mature plants it is thick and practically no water loss takes place through it in most species. The epidermis of a leaf can be considered a multiperforate system through the pores of which outward diffusion of water vapour occurs. It is useful to think of diffusion through this pathway as being analogous to the flow of an electric current through a circuit. The greater the resistance, the smaller the flow. By visualizing the process in this manner, the pathway of diffusion can be considered to be a system of resistances in series. These can be grouped in two categories 1) the internal resistance, and 2) the resistance external to the leaf.

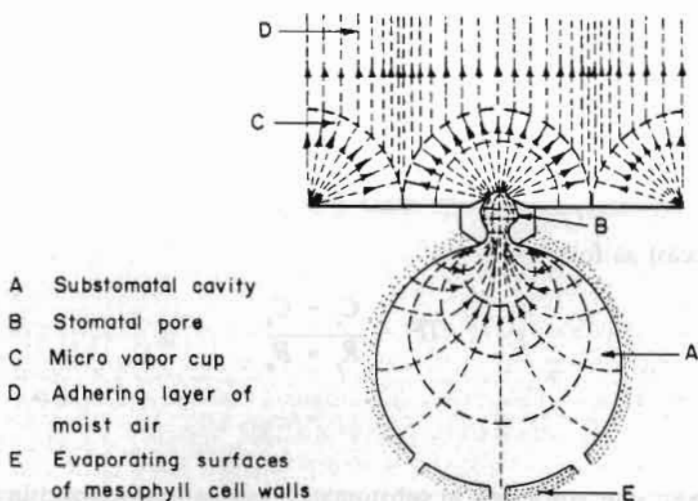
The internal resistance to outward diffusion of water is associated with stomata and depends on their shape, size, stomatal pore size, and opening (Fig. 16.17). Also the internal resistance to outward diffusion of water vapour depends upon the number of stomata per square centimetre of leaf surface, i.e., the stomatal frequency.



Source: Gates 1962

Fig 16.16 Schematic diagram of the diffusion pathway of water vapour in stomatal transpiration from a leaf

Path of diffusion of water vapour shown as solid (arrowed) lines. Surfaces of equal water vapour concentration are shown as dashed lines.



Source: Gates 1962

Fig 16.17 Idealized representation of the diffusion pathway of water vapour, from a stomata of *Sebrina pendula*, shown in median transverse section

Paths of diffusion of water vapour are shown as dotted (arrowed) lines. Surfaces of equal water vapour concentration are shown as dashed lines.

The greater the stomatal frequency, the smaller the internal resistance of the leaf. The external resistance is mainly in the form of a thin boundary layer of unstirred moisture through which water vapour molecules must diffuse. This boundary layer consists, in part, of microvapour cups that cover the ends of the stomatal pores and in part of a sheet of moist air that covers the entire surface of the leaf (Fig. 16.17).

Evidence shows that under natural conditions stomatal resistance is far more important than boundary layer existence in determining transpiration flux (Fig. 16.18). Figure 16.18 also shows that transpirational flux at any given stomatal aperture is always lower in still air than in moving air. In moving air, when wind blows over a leaf, even at low velocities, the boundary layer is swept away. Thus, the rate of transpiration depends primarily on stomatal apertures for regulating transpiration.

Estimation of Transpiration Rates

Rate of transpiration for individual plants is expressed in units such as grains of water vapour per second per plant. It is also approximate to use the term 'Transpiration Flux', meaning the quantity of water vapour transpired by a unit area of leaf surface in a unit of time. The units used most often are, $\text{gm.}^2\text{h.}^{-1}$ or $\text{g.cm.}^2\text{s.}^{-1}$. Under field conditions, such as the present roadside slope context, the transpiration rate is approximately expressed in terms of a unit land area, e.g., $\text{gal acre}^{-1} \text{ day}^{-1}$.

$$\text{Transpiration flux} = \frac{\text{Magnitude of the driving force}}{\text{Total resistance in the diffusion pathway}}$$

1. Driving force is the difference in concentration of water vapour between a leaf and bulk air beyond the leaf.
2. Total resistance is the sum total of the stomatal resistance and the boundary layer resistance.

Thus, the equation is recast as follows:

$$TF = \frac{C_i - C_a}{R_s + R_e}$$

where,

C_i and C_a are water vapour concentrations in substomatal cavities in a leaf and in the bulk air beyond the leaf respectively; R_s is the stomatal resistance and R_e is the resistance of the boundary layer of water vapour external to the leaf.

It can be used in field studies. In the usual field applications, relative humidity inside a leaf is assumed to be 100 per cent, making it easy to calculate c_l (water vapour concentration) if the leaf temperature is known. C_l can be calculated from the measured relative humidity of air and temperature of the air above the leaf. R_s is measured with a potometer. Since truly still conditions are rarely if ever realized in

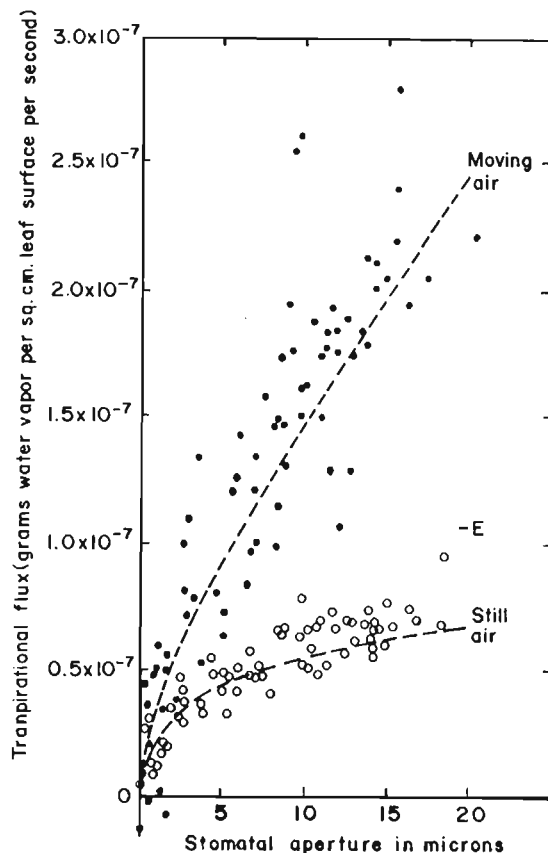
nature, R_e can be assumed to be zero in field studies. Knowing the values for C_l , C_a and R_s , TF can be calculated by modifying this equation:

$$TF = \frac{C_l - C_a}{R_s} .$$

Field Conditions

Figure 16.18 The relation between transpiration flux and stomatal aperture in still air and moving air

Experimental values in still air are indicated by open circles and those in moving air by block dots. The dashed lines represent theoretical values.



Source: Bange 1953

Measurement of Transpiration rates

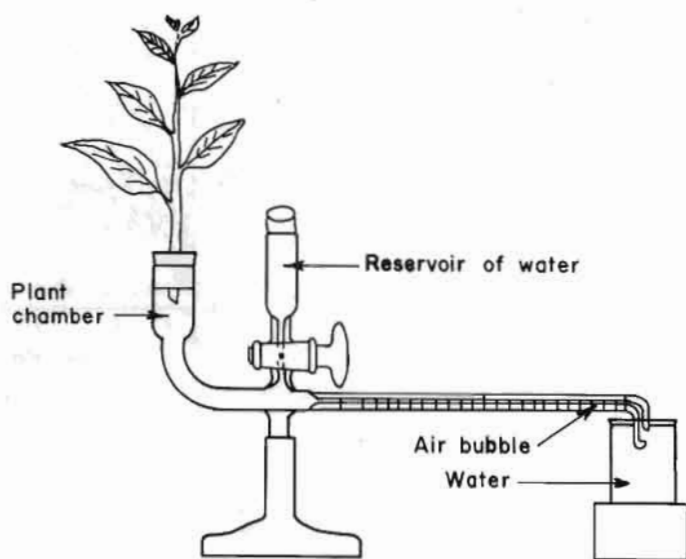
The techniques used to measure transpiration rates are both simple as well as complex with sophisticated measuring devices.

1. The Pysimeter method or gravimetric or pot method. A potted, intact plant is selected and the soil around the roots is watered thoroughly. Then the pot and the root system are sealed within a

container composed of material impervious to water (e.g., a sheet of polythene or a metal sheet) so that the loss of water is only through the plant. Now the entire assembly is weighed periodically, say at hourly intervals. The loss in weight represents the quantity of water transpired. Evaluation of the rate of transpiration in terms of a unit of evaporation area (e.g., $\text{gm cm}^{-1} \text{ hour}^{-1}$) requires that the total leaf area be estimated. Also to be recorded is whether the leaves of the experimental plant have stomata on one side only or on both sides.

In another version of this technique, air is passed over the transpiring tissue and then is conducted through an absorption vessel containing a water vapour absorbent (e.g., anhydrous calcium chloride or phosphorous pentoxide). At the same time, a stream of air is passed at the same rate directly through a separate water vapour absorption vessel, without passing over plant tissue. The difference in the gain in weight of the two absorption vessels represents the quantity of water vapour transpired during the experimental period. With this technique, even the transpiration rates of plant communities rooted in outdoor habitats have been estimated. In such cases large transparent plastic tents have been used.

Transpiration measurement by **potometer** is another way suitable for laboratory level experimentation. It is explained in Figure 16.19.



Source: Kramer 1959

Fig 16.19 The potometer method of measuring transpiration

The stem of a cut shoot is placed in a closed chamber of water. To prevent the formation of air bubbles in open xylem vessels, the stem should be cut under water. The chamber is attached to a graduated capillary tube into which an air bubble is introduced (by lifting the tube momentarily out of the water in the beaker). The rate of travel of the air bubble across the length of the graduated tube can be used to demonstrate the effects of environmental changes on the rate of transpiration. The air bubble can be returned when necessary to the right hand end of the capillary tube by admitting water through the stopcock. In another type of potometer, the plant chamber is large enough to admit the entire root system of a small plant.

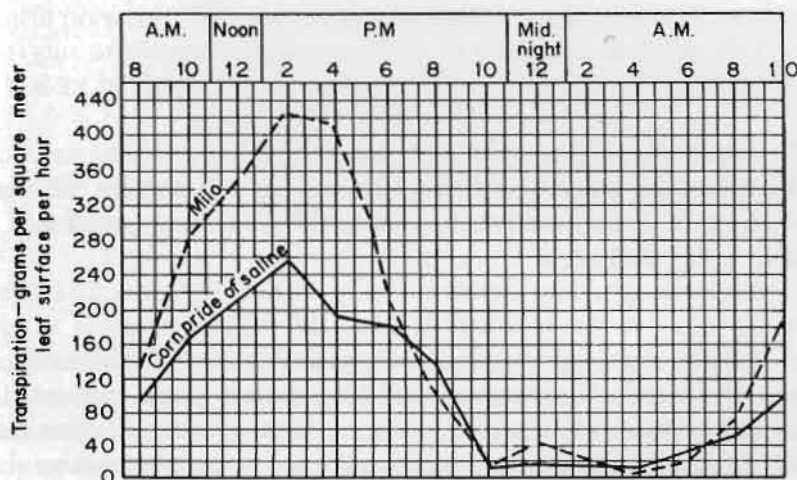
Factors Affecting Transpiration Mechanism of Plants

Loss of water through stomata depends on the opening and closure of their pores. Stomatal pores open and close in response to changes in one or another of the following environmental factors:

- the supply of water to the leaves,
- the temperature of the leaf environment,
- light availability, and
- concentration of carbondioxide in the leaf environment

Under general drought conditions, creating leaf water deficits, the stomata of a plant will remain closed, even overriding all other stimuli positive to stomatal opening. The effect of temperature is noticeable especially at the extreme ranges, i.e., either below 0°C or above $30\text{--}35^{\circ}\text{C}$.

Since transpiration is energized by solar radiation, the diurnal cycle of transpiration (Fig. 16.20) can be expected to parallel the radiation received at the surface of the earth.



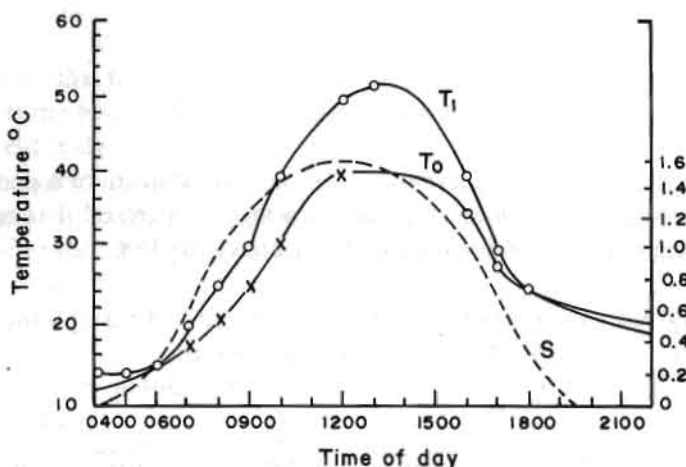
Source: Miller 1938

Fig 16.20 The transpiration rates of maize (Pride of Saline) and sorgu, (Milo) grown under the same conditions in Kansas

That this is so can be seen by comparing Figure 16.18 with the diurnal cycle of solar radiation shown in Figure 16.21.

Figure 16.21 also shows the temperatures of a fully sunlit, exposed leaf and the air around it during the day and night, under conditions assumed to be ideal. The night time leaf temperature is usually a few degrees below air temperature because leaves lose heat by thermal radiation to the sky and receive relatively little heat from the air around them. In the morning, after the sun rises, a sunlit leaf warms quickly, and its temperature rises above the temperature of the air. But, at the same time, the stomata, which were closed during the night, will be open. Thus the leaf will transpire and lose heat. As a result,

the temperature of a sunlit leaf is usually only slightly higher than the air temperature (see Fig. 16.21). The temperature of a shaded leaf also will follow a diurnal cycle similar to that shown in Figure 16.21, except that daytime temperature will probably not exceed the temperature of the air around it.



Source: Gates 1966

Fig 16.21 The variation in solar radiation received at the surface of the earth (S) air temperature (T_a), and temperature of a fully sunlit, exposed leaf (T_l) during the course of a day and night

Under both conditions stomatal openings remain closed even if other environmental conditions favour opening. If the supply of water is adequate and leaf temperature is not extreme, light induces the stomatal pores to open and darkness induces their closure. Thus stomata are open during the day and closed during the night. Stomatal movements in most higher plants are **photoactive**.

Moderate sunlight brings about maximum opening in most temperate plant species. However, the response time varies from species to species. Experimental evidence shows that **potassium ions** have a critical role in stomatal opening.

Concentration of carbon dioxide in the atmosphere external to a leaf is yet another factor that has been found to influence stomatal movement. If leaves are exposed to concentrations of CO_2 above the natural atmospheric level, i.e., approximately 300 ppm, they show a tendency to close, affecting transpiration adversely. In maize, for example, stomata can be closed by raising the concentration of the surrounding atmospheric carbon dioxide (CO_2) to about 1,000 ppm, keeping all other conditions normal. For soybeans this critical CO_2 level is 2,500 ppm.

This means that each species requires different CO_2 concentration levels to cause the closing of its stomata. It has important implications for roadside vegetation plantations in which plants are exposed to higher levels of CO_2 . Thus, for choice of species for roadside plantation, CO_2 concentration levels and the critical endurance values of plants could be important factors.

RETAINING WALLS

17.1 INTRODUCTION

Retaining walls are structures used to hold backfill and maintain a difference in the elevation of the ground surface. By the mechanics of performance, retaining walls may be classified as:

1. gravity,
2. tieback,
3. driven cantilever, and
4. reinforced earth.

Figure 17.1 illustrates the mechanics of how each type of wall develops the resistance to react against the imposed lateral earth pressure. The classification of walls, with respect to mechanics of the design and the probable behaviour of the construction medium, is presented in Table 17.1. Types 4, 5, and 6 are the ones most prevalent in Nepal.

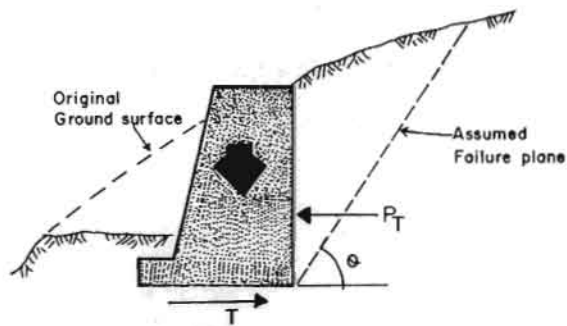
This chapter aims to provide basic concepts relating to the principles and design of some of the common types of retaining walls. Principles of design of gravity, earth reinforcement, and tieback walls with design examples of masonry gravity type have been presented.

The design of a retaining structure consists of two principal parts, the evaluation of loads and pressures that would act on the structure and the design of the structure to withstand those loads and pressures. The live loads on the structure are estimated, either by using specified codes or by estimation based on available data and experience, depending upon the situation and practices. The evaluation of pressures requires an understanding of earth pressure theories. The earth pressure can be estimated, either by empirical methods or by theoretical analysis, using one or several of the existing theories. Design structure, then, is a matter of analysis for external stability and internal stability based on the mechanics and material properties of the structure.

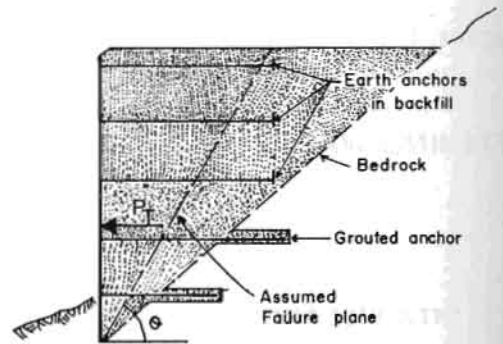
17.2 LATERAL EARTH PRESSURE

Earth pressure can be classified into **at rest**, **active**, and **passive**. The calculation of magnitude and distribution of lateral earth pressure, at rest between a soil mass and an adjoining structure, is simplified by assuming the condition of **plane strain**, i.e., strains in the longitudinal dimension are assumed to be zero. The rigorous analysis of earth pressure problems is rarely possible. However, it is the failure condition of the soil mass that is of primary interest and, in this context, provided a consideration of displacement is not required, it is possible to use the concept of plastic collapse. Earth pressure problems can thus be considered as problems in plasticity.

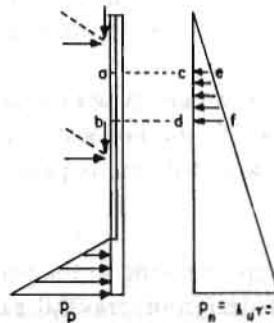
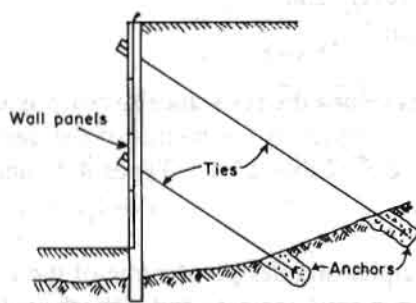
* Tables and Figures for which sources are not credited in this chapter are compilations of the author(s).



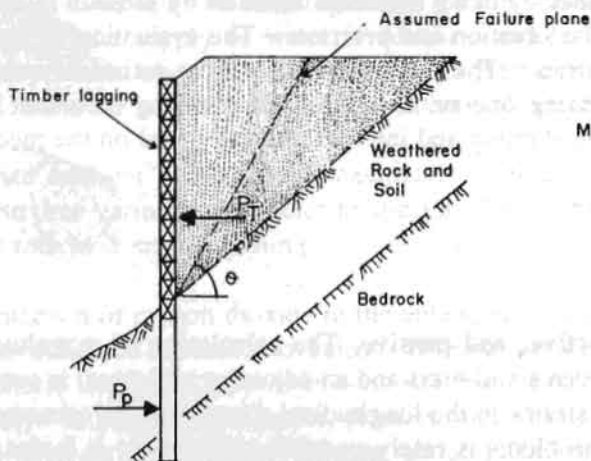
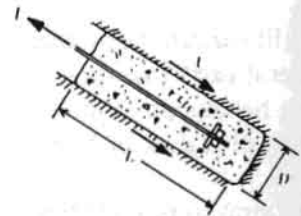
1. Gravity wall



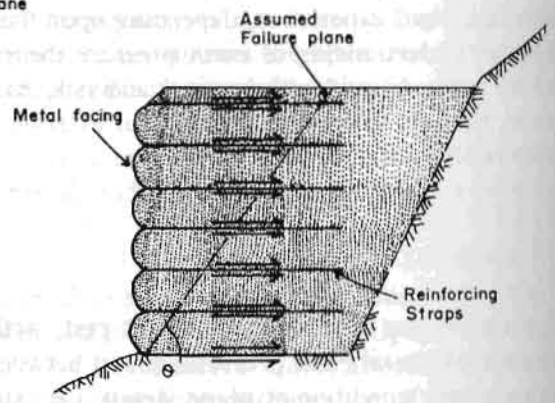
2 a. Tie back wall



2 b. Tieback wall



3. Driven cantilever wall



4. Reinforced Earth wall

Source: Adopted from Driscoll 1979 and Winterkorn and Fang 1975

Fig. 17.1 Mechanics of wall systems

Table 17.1 Wall classification

Gravity	Anchored
1. Bin Walls <ul style="list-style-type: none"> a. Rectangular b. Circular c. Cross Tied 	1. Vertical Culvert Pipe 2. Horizontal Sheet Pile 3. H-Pile, Timber Lagged 4. Vertical Sheet Pile 5. Stack Sack 6. All Gravity Structures 7. Ter-Voile Structure
2. Concrete Crib 3. Timber Crib 4. Gabions 5. Cement Masonry 5. Dry Stone Masonry 6. Concrete Cantilever 7. Drum Walls	R.C.C. Walls 1. Cantilever 2. L Type 3. Buttressed Wall (front or back) 4. Frame Retaining Wall
Reinforced Backfill 1. Reinforced Earth 2. Fabric 3. Stack Sack	Cantilever Piles 1. Vertical Sheet Piles 2. H-Pile, Timber Lagged

Plastic collapse occurs after the state of plastic equilibrium has been reached in part of a soil mass. Plastic equilibrium is said to be the state at which the shear stress, at every point within the soil mass, reaches the state of yield stress represented by point Y in Figure 17.2 which is an idealized stress-strain relationship in a soil mass. The use of this relationship implies that soil after yielding behaves as a perfectly plastic material, with unrestricted plastic flow taking place at constant stress, and that yielding and shear failure both occur at the same time.

The applied load system, including body forces, at plastic collapse is referred to as the **collapse load**. Determination of collapse load using the plasticity theory is complex. However, complex analysis can be avoided by using limit theorems of plasticity to determine lower and upper bounds to the true collapse load. The limit theorems can be stated as follows.

The Lowerbound Theorem states that if a state of stress can be found that at no point exceeds the failure criterion for the soil and which is in equilibrium with a system of external loads (which includes self weight of soil), then collapse cannot occur: the external load system thus constitutes a lower bound to the true collapse load.

The Upperbound Theorem states that if a mechanism of plastic collapse is postulated and if, in an increment of displacement, the rate of work done by a system of external loads is equal to the rate of dissipation of energy by the internal stresses, collapse must occur: the external load system thus constitutes an upper bound to the true collapse load.

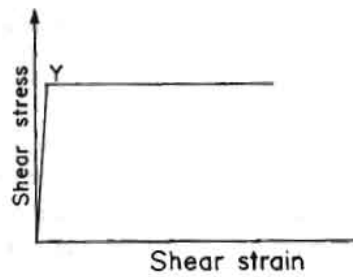
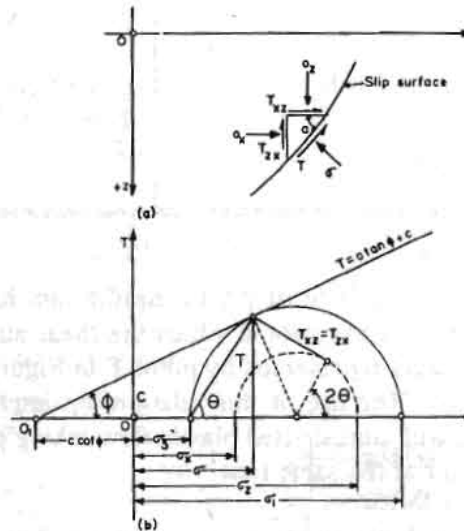


Fig. 17.2 Idealized stress-strain relationship

17.2.1 Equations for Static Conditions for Stresses in a Two-dimensional Case

The plastic state of stress distribution is characterized by a slip surface such as the one shown in Figure 17.3a. The Mohr's circle representing the state of stress at any point touches the failure envelope which is a Mohr-Coulomb straight line (Fig. 17.3b).



Source: Winterkorn and Fang 1975

Fig. 17.3 (a) Stresses acting on elements along the sliding surface
(b) Failure condition and Mohr's circle.

From Figure 17.3 we can write the following equations for static conditions:

$$\frac{\partial F}{\partial s} = 0 \quad (17.1)$$

where,

$$F = (\tau - \sigma \tan \phi) \quad (17.2)$$

must be valid on the surface of sliding.

The following are the three basic equations that express in mathematical form the static conditions for stresses in the two-dimensional case ($\sigma_x, \sigma_z, \tau_{xz} = \tau_{zx}$) :

$$\frac{\partial \sigma_x}{\partial x} + \frac{\partial \tau_{xz}}{\partial z} = 0$$

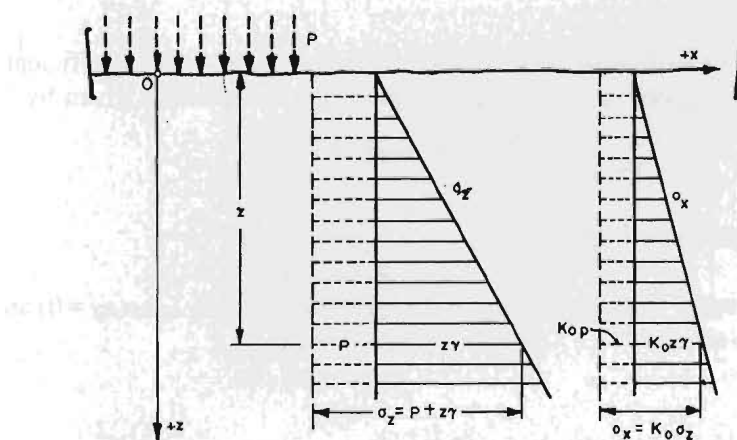
$$\frac{\partial \sigma_x}{\partial z} + \frac{\partial \tau_{xz}}{\partial x} = \gamma$$

$$\left[\frac{1}{2} (\sigma_z + \sigma_x) + c \cot \phi \right] \sin \phi - \left[\frac{1}{4} (\sigma_x - \sigma_z)^2 + \tau_{xz}^2 \right]^{\frac{1}{2}} = 0 \quad (17.3)$$

The material has been characterized by three different constants: the bulk density γ , the coefficient of friction $\tan \phi$, and the cohesion c . These can be either zero or greater than zero.

17.2.2 Lateral Earth Pressure for At-rest Condition

Figure 17.4 represents the cross section of a halfspace bounded by a horizontal surface. The halfspace is either unloaded or loaded with a uniformly distributed load. The stresses are independent of x ; the lines $z = \text{const}$ and $x = \text{const}$ are principal stress directions σ_z and σ_x are principal stresses, and $\tau_{xz} = 0$.



Source: Winterkorn and Fang 1975

Fig. 17.4 Semi-infinite half space: vertical and horizontal stresses in the at rest condition

Thus, from Equation 17.3

$$\frac{\partial \sigma_z}{\partial z} = \frac{d \sigma_x}{d z} = \gamma$$

and

$$\sigma_z = z\gamma$$

From Figure 17.4

$$\sigma_z = z\gamma + p \quad (17.4)$$

Experience and experiments show that in the state of complete rest (at rest condition):

$$\frac{\sigma_x}{\sigma_z} = \text{const} = K_o \quad (17.5)$$

and

$$\sigma_z = \gamma z + p$$

$$\sigma_x = K_o z \gamma + K_o p$$

for

$$p = 0, \sigma_x = K_o Z \gamma \quad (17.5 a)$$

The stress distribution is thus hydrostatic (Fig. 17.4). The quantity K_o is the coefficient of earth pressure at rest; numerical values are given in Table 17.2. A good approximation is given by:

$$K_o = 1 - \sin \phi \quad (17.6)$$

which fits most of the experimental data.

In this case the soil is prevented from expanding or compressing laterally ($\epsilon_x = \epsilon_y = 0$) and from the theory of elasticity we obtain the equation:

$$\sigma_x = \frac{\nu}{1 - \nu} \sigma_z \quad (17.7)$$

where ν is Poisson's Ratio.

Earth pressure acting on walls that do not yield laterally - e.g., stiff, heavy walls, caissons, rigid frames, etc. - can be computed from the following equation (Fig. 17.5):

$$E_o = K_o \frac{h^2 \gamma}{2} + K_o p h \quad (17.8)$$

$$E_o = K_o \frac{h^2 \gamma}{2} \quad \text{for } p=0.$$

For a slanting wall (Fig. 17.5b) with no surcharge:

$$E_o = \frac{h^2 \gamma}{2} \sqrt{K_o^2 + \tan^2 \beta} \quad (17.9)$$

and

$$\tan \delta = \frac{(1-K_o) \cot \beta}{1+K_o \cot^2 \beta} \quad (17.10)$$

Equation 17.5 is valid for effective stresses only. Therefore, if there is groundwater present, but no water movement occurs, the neutral stresses must be considered separately:

$$\sigma_z = \bar{\sigma}_z + u$$

and

$$\sigma_x = K_o \bar{\sigma}_z + \mu = K_o \sigma_z + (1-K_o) u$$

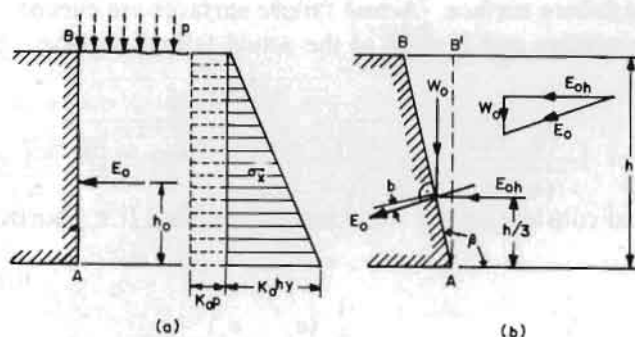


Fig. 17.5 Earth pressure at rest acting on (a) a vertical and (b) an oblique surface

Table 17.2 Coefficient of earth pressure at rest

Soil	W_1	I_p	K_a
Loose sand, saturated	-	-	0.46
Dense sand, saturated	-	-	0.36
Dense sand, dry ($e=0.6$)	-	-	0.49
Loose sand, dry ($e=0.8$)	-	-	0.64
Compacted, residual clay	-	9	0.42
Compacted, residual clay	-	31	0.66
Organic silty clay, undisturbed	74	45	0.57
Kaolin, undisturbed	61	23	0.64-0.70
Sea clay (Oslo), undisturbed	37	16	0.48
Quick clay	34	10	0.52

Source: Bishop 1957, 1958, Bernatzils 1947, and Simons 1958.

17.2.3 Active and Passive Earth Pressure

Active earth pressure is associated with the movement of the wall away from the backfill and passive pressure is associated with the wall moving into the backfill. In designs of earth pressure for retaining walls, with no external forces acting on the backfill, active pressure from the backfill is the only required lateral earth pressure. The passive resistance, due to earth filling or a small embedment in front of the wall, if any, is normally neglected since these cannot be relied upon unless it is certain that the soil in front of the wall will not be eroded.

Active earth pressure can be determined by using Rankine's Theory, Coulomb's Wedge Theory, or Log Spiral Theory. Rankine's Theory (1857) may also be interpreted as a lower bound case of plastic failure. It ignores friction between wall and backfill. Coulomb's Wedge Theory may also be interpreted as a lower bound case of plastic failure and accounts for wall friction as well. The Rankine and Coulomb theories both assume a plane failure surface. Actual failure surfaces are curved. The Log Spiral Method considers the curved failure surface and is close to the actual failure surface.

The Rankine Active State

Referring to Figure 17.3, and considering the Rankine Active State (i.e., horizontal stress equals active pressure):

$$\sin \phi = \frac{\frac{1}{2} (\sigma_1 - \sigma_3)}{\frac{1}{2} (\sigma_1 + \sigma_3 + 2 c \cot \phi)}$$

$$\begin{aligned}\sigma_3 &= \sigma_1 \left(\frac{1 - \sin\phi}{1 + \sin\phi} \right) - 2c \sqrt{\left(\frac{1 - \sin\phi}{1 + \sin\phi} \right)} \\ &= \sigma_1 \tan^2 \left(45^\circ - \frac{\phi}{2} \right) - 2c \tan \left(45^\circ - \frac{\phi}{2} \right) .\end{aligned}$$

For no surcharge, i.e., $p=0$:

$$\sigma_1 = \gamma z$$

and if,

$$\frac{1 - \sin\phi}{1 + \sin\phi} = K_a$$

$$\sigma_3 = K_a \gamma z - 2c \sqrt{K_a} . \quad (17.11)$$

For $c = 0$:

$$\sigma_3 = K_a \gamma z .$$

Now, referring to Figure 17.6:

$$P_a = \frac{1}{2} \gamma H^2 K_a - cH \sqrt{K_a} . \quad (17.12)$$

$$K_a = \frac{1 - \sin\phi}{1 + \sin\phi} \quad (17.13)$$

$$K_a = \cos\beta \left[\frac{\cos\beta - \sqrt{(\cos^2\beta - \cos^2\phi)}}{\cos\beta + \sqrt{(\cos^2\beta - \cos^2\phi)}} \right] . \quad (17.14)$$

For non-cohesive backfill:

$$P_a = \frac{1}{2} \gamma H^2 K_a .$$

The basic assumptions in Rankine's Active State Theory are that:

1. the soil is homogeneous and isotropic, possesses internal friction, and is in a state of plastic equilibrium,
2. the failure surface within the backfill is planar,
3. the shear strength is mobilized uniformly on all planes throughout the backfill,
4. the presence of the wall does not influence the state of stress in the backfill,
 - the failure is a two-dimensional problem, and
 - the resultant, P_a , is inclined at angle β to the wall.

Figure 17.6 shows soil structure system and force polygons for Rankine's Active State

Coulomb's Theory

Coulomb's Theory (1776) involves consideration of the stability, as a whole, of the wedge of cohesionless soil between a retaining wall and a trial failure plane. Friction between the wall and the adjacent soil is taken into account. This friction angle is denoted by σ and can be determined in the laboratory by means of a direct shear test. A number of trial failure planes would have to be selected to obtain the maximum value of P , corresponding to a particular value of Θ , and is given by:

$$\frac{\partial P}{\partial \theta} = 0$$

This leads to the following solution for P , (see Figure 17.7):

$$P_a = \frac{1}{2} K_A \gamma H^2 \quad \text{for } c = 0 \text{ and } Q = 0$$

where,

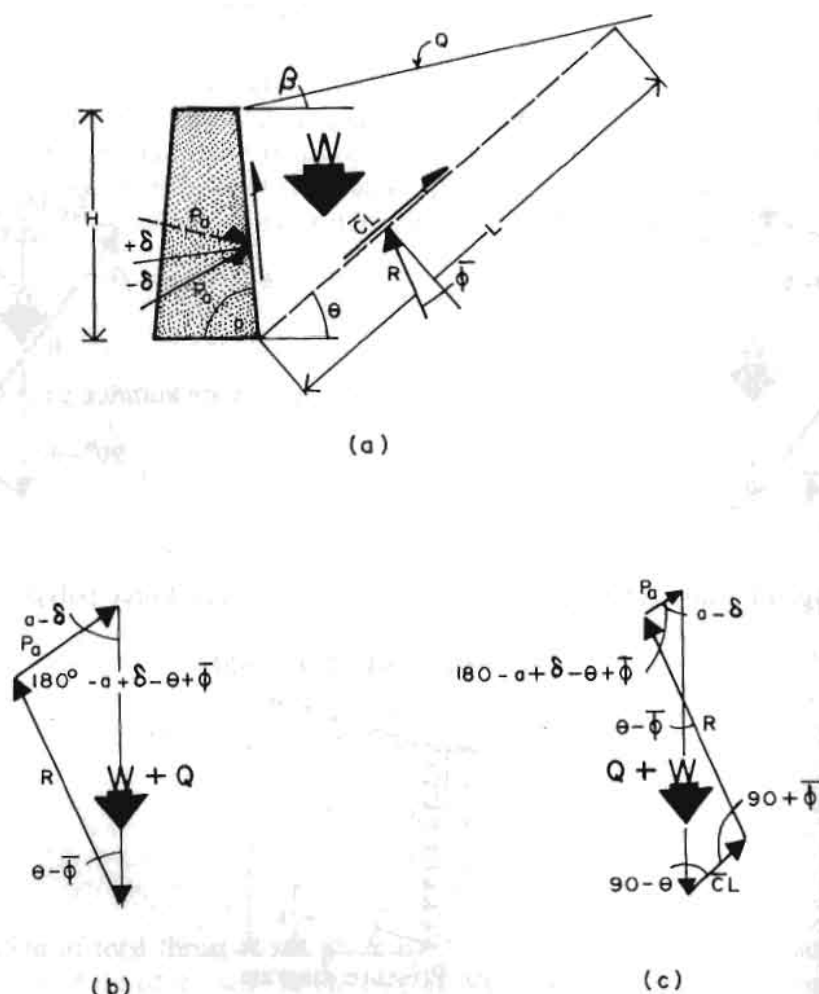
$$K_A = \left(\frac{\frac{\sin(\alpha+\phi)}{\sin\alpha}}{\sqrt{[\sin(\alpha-\sigma)]} + \sqrt{\left[\frac{\sin(\phi+\sigma) \sin(\phi-\beta)}{\sin(\alpha+\beta)} \right]}} \right)^2 \quad (17.15)$$

The point of application of total thrust is not given by Coulomb's Theory but is assumed to act at a distance of $H/3$ above the base of the wall in the case of dry backfill. In the case of partly submerged backfill, γ will be equal to submerged unit weight in the submerged part.

The basic assumptions in the Coulomb analysis are that:

1. the soil is homogeneous and isotropic, possesses internal friction and cohesion, and is in a state of plastic equilibrium,
2. the failure surface in the backfill is planar,
3. the shear strength, τ , is mobilized uniformly along the failure plane, and $\tau = \bar{c} + \bar{\sigma}_n \tan \phi'$,
4. the failure wedge is a rigid body.
5. there is wall friction; that is, as the failure wedge moves, the shear strength along the soil-wall interface is mobilized, and
6. the failure is a two-dimensional problem.

Figure 17.7(a) shows the soil-structure-surcharge system for Coulomb's Active Case. Figures 17.7f(b) and (c) show the resulting force polygons for cohesion equal to zero and a value greater than zero, respectively. Comparison of Figures 17.7(b) and (c) shows that the presence of cohesion decreases the value of P_a ; the total active thrust. Equation 17.12 has also been generalized for seismic condition and surcharge as in Equations 17.14 and 17.17.



Source: Driscoll 1979

Fig. 17.7 Coulomb's Active Case

17.3 RIGOROUS DESIGN OF RETAINING WALLS

Retaining walls and breast walls may be designed using semi-empirical methods or theoretical methods employing Rankine's Active State or Coulomb's Theory or the Log Spiral Theory for earth pressure calculations. Graphical methods are also available for determination of earth pressures by theoretical methods. The Log Spiral Theory is generally considered to be the most accurate of these three methods. However, the variation in active earth pressure from Coulomb's Theory is about 10 per cent on the conservative side, while Rankine's Active State results in about 10 per cent variation on the non-conservative side. For passive pressure the values from these three theories are widely divergent.

This section presents a design method for gravity walls employing Coulomb's Wedge Theory. Design examples by manual and computer methods have been presented. A computer programme is very helpful in developing various designs for the selection of the most economical option. Section 17.3.2 and 17.3.3 provide concepts of design for a Reinforced Cement Concrete (R.C.C.), Crib Wall and Tieback Wall. The empirical design of an Earth Reinforced Wall is presented in Section 17.3.4.

17.3.1 Design of Gravity Type Retaining Wall

All gravity walls (both retaining walls and breast walls) are designed as simple rigid walls. For purposes of analysis, equivalent sections of a gabion wall are considered as shown in Figure 17.8.

a) Design Criteria

- | | | |
|------|---|---|
| i) | Factor of safety against overturning (F_o) | > 2.0
(static loads) |
| | Factor of safety against overturning (f_o) | > 1.5
(earthquake forces) |
| ii) | Factor of safety against sliding (F_s) | > 1.5
(static forces) |
| | Factor of safety against sliding (f_s) | > 1.0
(earthquake forces) |
| iii) | Highest base pressure, f_{max} (static) | $< q_a$
(allowable bearing capacity) |
| | Lowest base pressure, f_{min} (static or dynamic) | > 0 |
| | Highest base pressure (dynamic), f_{max} (dynamic) | $< 1.25 q_a$ |
| iv) | If the hill slope itself is not stable, the wall cannot be stable, as the cylindrical slip surface may pass below the toe and heel of the wall. So stability of the slope should also be checked (Fig. 17.8). Indirectly the criteria in (iii) account for an unstable slope as the allowable bearing pressure will be very low in that case. | |

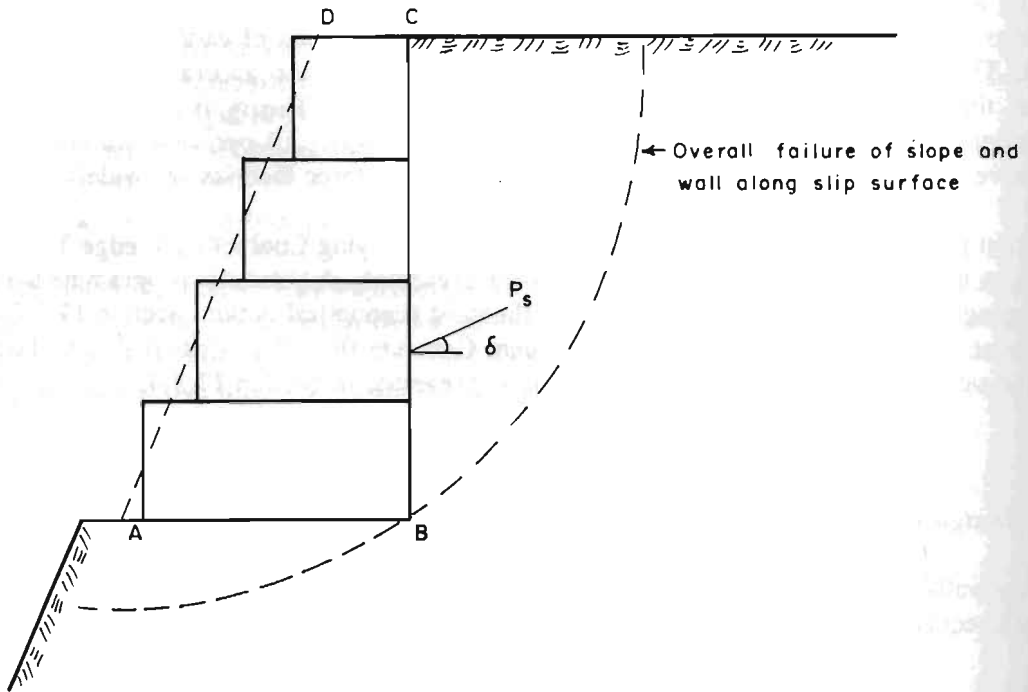


Fig.17.8 Assumed trapezoidal section of gabion wall (ABCD)

For low volume roads, it is suggested that walls may not be designed for earthquake forces. Otherwise, wall sections will become too thick and uneconomical. It would be more economical to repair failed walls after earthquakes. It may also be mentioned here that the significant tilt of the base of the wall towards the hillside will ensure its dynamic stability against earthquake forces.

b) Assumptions

- i) The gravity wall is a rigid body and behaves as one integral body.
- ii) Backfill is isotropic and homogeneous material.
- iii) Backfill obeys Coulomb's Law of Shear Strength.

$$\tau = c + (\sigma - u) \tan \phi$$

where,

- σ = normal stress across failure plane,
 u = pore-water pressure,
 c = cohesion, and
 ϕ = angle of internal friction.

- iv) Pore-water pressure u is,

$$u = (B) \sigma$$

B = pore pressure coefficient
0 for dry backfill, and
0.1 to 0.4 for moderate to heavy seepage pressures.

- v) Earth pressure (both static and dynamic) acts at an angle of σ with normal to the back face of the wall (Fig. 17.9). The angle of wall friction(s) is generally assumed as to be:

$$\delta = \frac{2\phi}{3}$$

Adhesion is neglected on the back face of the wall.

- vi) Static earth pressure (P_s) acts at one third the height of the wall. Whereas the dynamic increment of earth pressure (P_{di}) acts at half the height of the wall (Fig. 17.9).
- vii) The shearing resistance (τ) at the interface of the base of the wall and the foundation is given by:

$$\tau = Ca + \mu (\sigma - u)$$

where,

Ca = adhesion, and

μ = coefficient of friction ($= \tan \sigma$)

- viii) The slip surface in backfill is plane and inclined at an angle of Θ with the horizontal. It is assumed that the wall will move towards the valley and the wedge of the backfill will tend to slide on the critical slip surface. A critical slip surface is that slip surface which gives maximum earth pressure. Critical slip surfaces are different for static and dynamic conditions. This results in conservative estimates of earth pressures.
- ix) There is no progressive failure of backfill and strength is uniformly mobilized along the slip surface.

Actually if a displacement analysis of wall-backfill interaction is made, earth pressure will not be found to vary linearly with height. In actual practice, a theoretical slip surface may not develop at all due to the steep excavation of the hill profile. The present design method, based on the above assumption, is a little conservative.

c) Design Parameters

Values of backfill parameters, and properties of structural materials and foundation may be obtained from Chapter 9 of the manual or from any standard text or handbook. A laboratory check is sometimes justified when the size of structure and economies from design are considerable.

d) Forces on Retaining Wall

Forces on retaining wall (a, b, c, d) and the wedge (b, d, e) are shown in Figure 17.9. Details are given below.

Forces on Wedge

i) Weight of Wedge	=	W_w
ii) Weight due to vertical earthquake acceleration	=	$\alpha_v W_w$
iii) Force due to horizontal earthquake acceleration	=	$\alpha_h W_w$
iv) Reaction at an angle of the normal on slip surface	=	R
v) Surcharge on backfill	=	Q_s
vi) Surcharge due to vertical component of earthquake	=	$\alpha_v Q_s$
vii) Force due to horizontal earthquake acceleration on surcharge	=	$\alpha_h Q_s$
viii) Uplift due to pore pressure on slip surface	=	U
ix) Static earth pressure	=	P_s
x) Dynamic increment of earth pressure	=	P_{di}
xi) Cohesion along slip surface = $c \times d_e$	=	C

Forces on Wall

i) Weight of retaining wall	=	W_R
ii) Weight due to vertical earthquake acceleration	=	$\alpha_v W_R$
iii) Force due to horizontal earthquake acceleration	=	$\alpha_h W_R$
iv) Base friction	=	F
v) Adhesion at base = $C \times$ base width	=	Cab_2
vi) Normal reaction at base	=	V_f
vii) Uplift on base of wall	=	V

It may be seen that a_3 in Figure 17.9 will be a negative quantity for breast walls or retaining walls with negative batter.

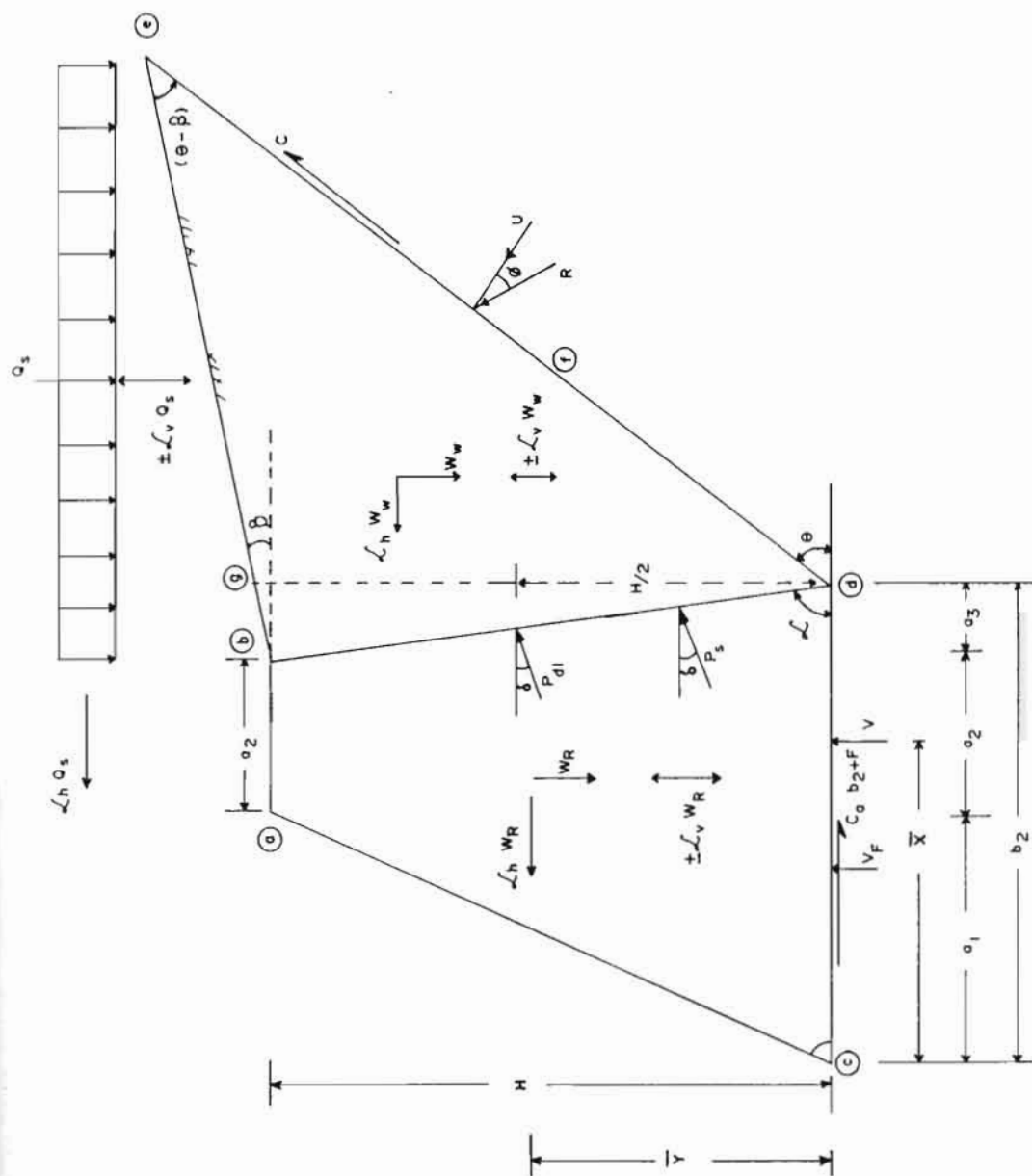


Fig. 17.9 Forces on retaining walls

e) Earth Pressure on Wall

The total pressure $P_d (= P_s + P_{di})$ is obtained by the following expression after considering the equilibrium of the wedge (Viladkar et al. 1985):

$$P_d = \frac{(W_w + Q_s) [\alpha_h \cot(\theta - \phi) + 1 \pm \alpha_v] - U [\cos\theta - \cot(\theta - \phi) \sin\theta] - c [\sin\theta + \cot(\theta - \phi) \cos\theta]}{\cos(\alpha - \delta) [1 + \tan(\alpha - \delta) \cot(\theta - \phi)]} \quad (17.13)$$

$$= \frac{1}{2} \gamma_s H^2 K_A + H K_A \sin\alpha \operatorname{cosec}(\alpha + \beta) Q_s \quad (17.14)$$

For

$$\alpha_h, \alpha_v = 0$$

$$P_d = P_s + P_{di} = P_s + 0 = P_s \quad (17.16)$$

where,

$$U = 0.5 B \gamma_s [H (\operatorname{cosec}\alpha \sin(\alpha + \beta))]^2 \sec\beta \operatorname{cosec}(\theta - \beta) \quad (17.17)$$

$$C = cH \operatorname{cosec}\alpha \sin(\alpha + \beta) \operatorname{cosec}(\theta - \beta) \quad (17.18)$$

where,

- γ_s = unit weight of backfill or soil,
- α = angle between back face of wall and its base,
- θ = dip of slip surface,
- β = slope of backfill, and
- H = height of wall above heel.

For cohesionless backfill, the earth pressure coefficient K_A is given by:

$$K_A = (1 \pm \alpha_v) \sin^2(\alpha - \lambda + \phi) [\cos\lambda \sin^2(\alpha - \lambda) \sin(\alpha - \lambda - \delta) (1 + \frac{1}{\sqrt{m}})^2] \quad (17.19)$$

where,

$$m = \frac{\sin(\phi+\delta) \sin(\phi-\beta-\lambda)}{[\sin(\alpha+\beta) \sin(\alpha-\lambda-\delta)]} \quad (17.20)$$

$$\lambda = \tan^{-1} \left[\frac{\alpha_h}{1 \pm \alpha_v} \right] \quad (17.21)$$

f) Factors of Safety

The dynamic factor of safety against sliding is:

$$F_s = \frac{\mu [-v + W_R (1 \pm \alpha_v) + Pd \cos(\alpha-\delta)] + Cab_2}{[\alpha_h W_R + Pd \sin(\alpha-\delta)]} \quad (17.22)$$

$$= F_s \text{ (static)}, \alpha_v = \alpha_h = 0$$

where,

$$u = 0.5 \gamma_s BH \operatorname{cosec} \alpha \sec \beta \sin(\alpha+\beta) b_2 \quad (17.23)$$

The factor of safety against overturning is:

$$F_o = \frac{(1 \pm \alpha_v) W_R \bar{x} + \cos(\alpha-\delta) [P_s (\alpha_1 + \alpha_2) + (\alpha_3 - \frac{H \cot \alpha}{3}) + Pdi \{ \alpha_1 + \alpha_2 + \alpha_3 - \frac{H \cot \alpha}{2} \}]}{\alpha_h W_R \bar{y} + H \sin(\alpha-\delta) [\frac{P_s}{3} + \frac{Pdi}{2}] + 2b_2 \frac{V}{3}} \quad (17.24)$$

$$= F_o \text{ (static)}, \alpha_h = \alpha_v = 0$$

where,

\bar{x}, \bar{y} = coordinate of centre of gravity of wall
with respect to its toe (Fig. 17.9).

g) Base Pressures

The resultant of the line of action of all forces will strike the base of the wall at a distance of \bar{x}_1 , from the toe as follows:

$$\bar{x}_1 = \frac{W_R (1 \pm \alpha_v) \bar{x} - \alpha_h W_R \bar{y} + P_s [\cos(\alpha - \delta) (b_2 - \frac{H \cot \alpha}{3}) - H \frac{\sin(\alpha - \delta)}{3} + M_d]}{W_R (1 \pm \alpha_v) + P_d \cos(\alpha - \delta)} \quad (17.25)$$

where,

$$M_d = P_d i [\cos(\alpha - \delta) (b_2 - \frac{H \cot \alpha}{2}) - \frac{H \sin(\alpha - \delta)}{2}]$$

Thus the eccentricity (e) of the resultant force is given by:

$$e = \frac{b_2}{2} - \bar{x} \quad (17.26)$$

The dynamic base pressures are:

at toe

$$f_1 = \frac{V_F}{b_2} (1 + \frac{6e}{b_2}) \quad (17.27)$$

at heel

$$f_2 = \frac{V_F}{b_2} (1 - \frac{6e}{b_2}) - 2 \frac{v}{b_2} \quad (17.28)$$

The static analysis is obtained by substituting α_h and α_v equal to zero in the above equations. The analysis is solved for different wall dimensions until design criteria are satisfied. Thus the final wall section is arrived at. A typical example is solved for cohesionless backfill and for a drystone masonry wall and is presented in the following pages.

h) Computer Aided Design of Retaining Walls

To save time from calculations and iterations, a computer programme RETAIN has been developed. Using Equation 17.16, the programme first computes the critical wedge angle Θ , following an iterative procedure for which the static earth pressure P_s is maximum. The static factors of safety for sliding and

overturning are calculated from Equations 17.22 and 17.24 for initially assumed wall dimensions. Static base pressures are also checked from Equations 17.27 and 17.28. If all the design criteria are not satisfied, wall dimensions are changed and all of the above calculations are repeated. Iterations are made until the desired wall dimensions are obtained. Similarly calculations are repeated for earthquake forces. The programme thus gives wall dimensions for a dynamic case also after satisfying all the design criteria for the dynamic case.

The RETAIN programme has been used for the last 15 years to design many retaining walls. Realistic and economical wall sections are easily obtained for static conditions. For dynamic conditions, the programme gives too large a section for a low volume hill road if the base of the wall is not tilted. Figure 17.10 gives some computer results. The design parameters are:

$$c = 0; \phi = 30^\circ, \beta = 0, Y_{wall} = 1.9 \text{ t/m}^2,$$

$$Y_{soil} = 2.0 \text{ t/m}^2, \beta = 0, Ca = 0, q_a = 20 \text{ t/m}^2, q_s = 2 \text{ t/m}^2$$

$$\alpha_h = 0, \alpha_v = 0, H = 6 \text{ m}.$$

Figure 17.10 clearly shows that a negative batter of as small as 5:1 can result in substantial savings in the cost of a wall. In the case of a wall with a negative batter of 3:1, the saving is even more. This concept became clear only after using the above programme.

i) Example of Retaining Wall Design by Manual Calculations

Typical Design Example

Given $H = 8 \text{ m}$, $\phi = 40^\circ$, $\delta = 22.5^\circ$, $\mu = 0.6$, $\alpha_h = 0.08$, $\gamma_s = 1.8 \text{ t/m}^3$, and $\gamma_m = 2.0 \text{ t/m}^3$, design a masonry retaining wall section when the bearing capacity of the rock under normal loads is 15 t/m^2 . Forces acting on the wall are shown in Figure 17.11

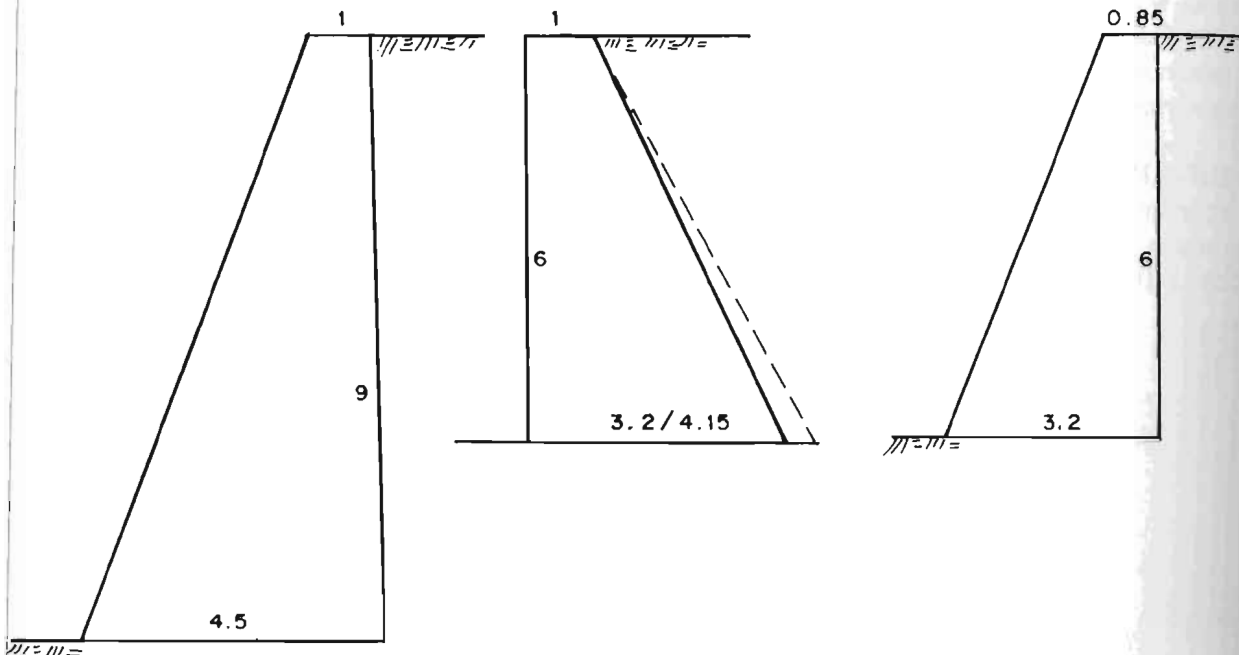
The retaining wall section is adopted, as having a top width b equal to 0.6 m , face slope 1 horizontal to 3 vertical, base slope 6H:1V and the toe projection as 0.45 m wide and 0.675 m high as shown in Figure 17.12.

For $\phi = 40^\circ$, $\sigma = 22.5^\circ$, and $\alpha_h = 0.08$, $\alpha = 90^\circ$, $\beta = 0$; from Equation 17.19,

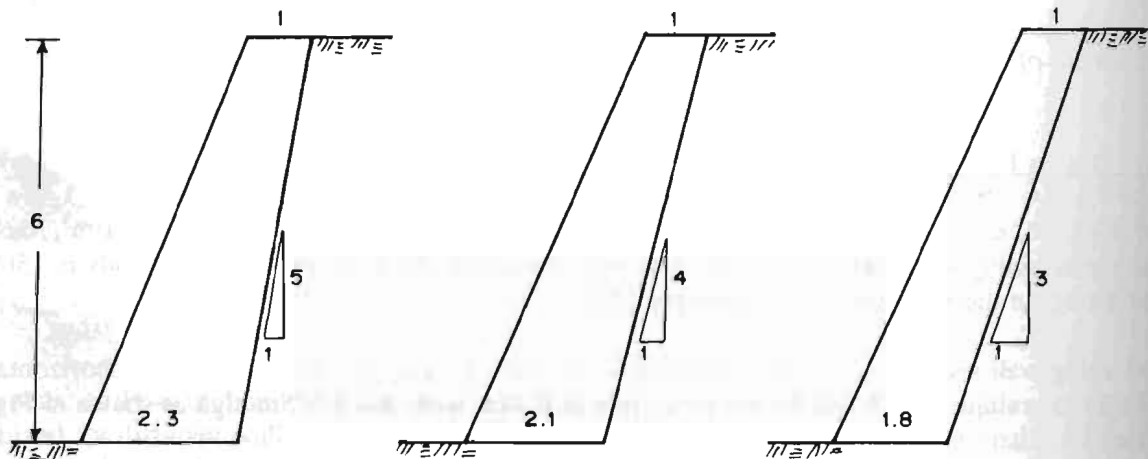
$$K_a = 0.1992, K_{ad} = 0.2485.$$

Static earth pressure:

$$\begin{aligned} P_s &= (1/2) \gamma_s K_a H^2 = 1/2 \times 1.8 \times 0.1992 \times 8^2 \\ &= 11.50 \text{ t acting at } (H/3) \text{ } 2.667 \text{ m above base.} \end{aligned}$$



(a) Positively battered walls



(b) Negatively battered walls

Fig. 17.10 Wall sections (metres) by computer programme-negative battered vs positively battered walls (solid and dotted lines for 40 and 20 t/m² bearing pressures, q_0)

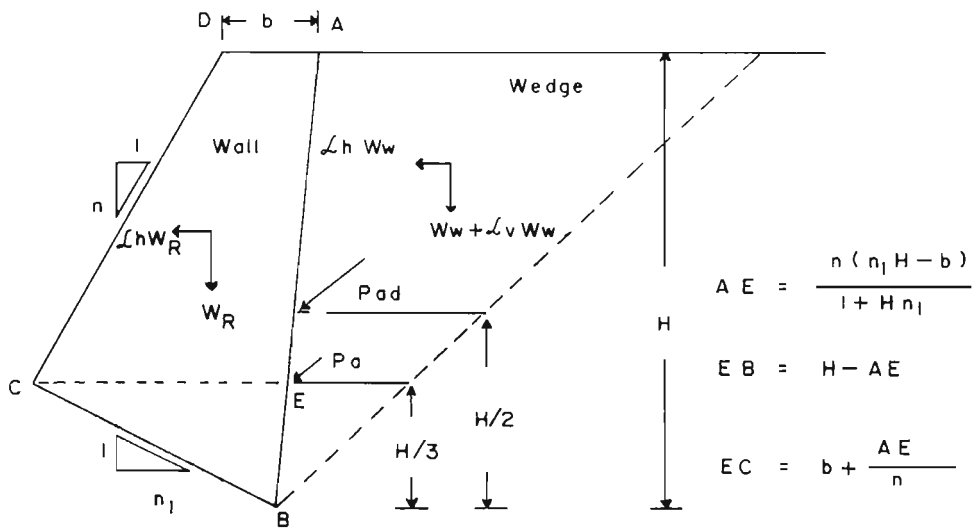


Fig. 17.11 Seismic forces on retaining wall

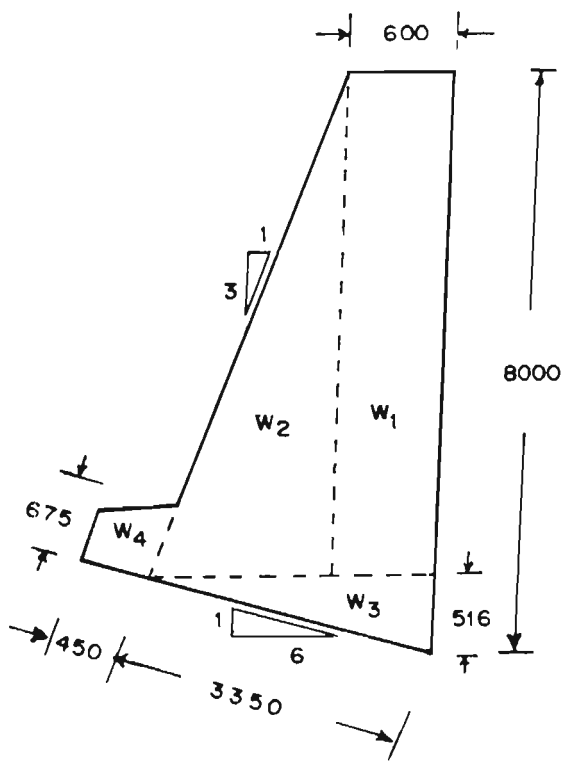


Fig. 17.12 Assumed section

Total dynamic earth pressure:

$$P_d = (1/2) \gamma_s K_a H^2 = 14.26 \text{ t.}$$

Dynamic increment:

$$\begin{aligned} P_{di} &= P_d - P_s = 14.26 - 11.50 \\ &= 2.76 \text{ t acting at } (H/2), 4.0\text{m above base.} \end{aligned}$$

Both the pressures P_s and P_{di} will be inclined at angle 22.5° to the horizontal, where $\cos 22.5^\circ$ and $\sin 22.5^\circ = 0.9239$ and $\sin 22.5^\circ = 0.3827$.

From the expressions shown in Figure 17.11 the various dimensions of the present retaining wall shown in Figure 17.12 will be as follows:

$$\begin{aligned} AE &= \frac{n (n_1 H - b)}{(1 + H n_1)} \\ &= \frac{3 (6 \times 8 - 0.6)}{(1 + 3 \times 6)} \\ &= 7.484 \text{ m} \end{aligned}$$

$$EB = H - AE = 8.0 - 7.484 = 0.516\text{m}$$

$$EC = b + AE/n = 0.60 + 7.484/3 = 3.095\text{m}$$

The components of forces and their moments about B are given in the next section.

Retaining Wall Calculations - Moments About Heel (B)
(Horizontal force to left + ve; Anticlockwise moment + ve)

Force	Calculation	Horizontal Component			Vertical Component		Force L.A.
Moment	Force	L.A.	Moment				
(1)	(2)	(3)	(4)	(5)	(6)	(7)	(8)
P_s	11.50×0.9239	10.60	2.667	28.27	-	-	-
	11.20×0.3827	-	-	-	4.40	0	0
W_1	$0.6 \times 7.484 \times 2.0$	-	-	-	8.98	0.30	2.69
W_2	$0.5 (3.095 - 0.6) \times 7.484 \times 2.0$	-	-	-	18.67	1.432	26.74
W_3	$0.5 \times 3.095 \times 0.516 \times 2.0$	-	-	-	1.60	1.032	1.65
W_4	$0.4 \times 0.675 \times 2.0$	-	-	-	0.61	3.320	2.02
Sub total		10.60	-	28.27	34.26	-	33.10

1	2	3	4	5	6	7	8
Pdi	2.76 x 0.9239	2.55	4.0	10.20	-	-	-
	2.76 x 0.3827	-	-	-	1.06	0	0
EQ1	0.08 x 8.98	0.72	4.258	3.06	-	-	-
EQ2	0.08 x 18.67	1.49	3.011	4.50	-	-	-
EQ3	0.08 x 1.60	0.13	0.322	0.04	-	-	-
EQ4	0.08 x 0.61	0.05	0.854	0.04	-	-	-
Total		15.54	-	46.11	35.32	-	33.10

Check for Sliding

Here the sliding movement will be up the slope, hence the force required to cause sliding is governed by the force resolved along the plane of sliding.

i) Actuating Force

$$\begin{aligned}\text{Static case} &= P_s \cos(\sigma + \text{angle ECB}) = P_s \cos(22.5 + 9.46^\circ) \\ &= 11.5 \cos(31.96^\circ) = 9.76 \text{ tons.}\end{aligned}$$

$$\text{With earthquake} = 14.26 \cos(31.96^\circ) = 12.10 \text{ tons.}$$

ii) Resisting Force

$$\begin{aligned}F &= \frac{\mu \cos \theta + \sin \theta}{\cos(\delta + \theta) - \mu \sin(\delta + \theta)} \times W \\ &= \frac{0.6 \cos 9.46^\circ + \sin 9.46^\circ}{\cos(31.36) - 0.6 \sin(31.96^\circ)} \times W \\ &= \frac{0.76}{0.53} \times W \\ &= 1.425 W.\end{aligned}$$

Here θ is the dip of the foundation towards the hillside.

$$\begin{array}{lll}\text{Static case} & F = 1.425 W = 1.425 \times 34.26 = 48.82 & > 9.76 \text{ tons } \underline{\text{ok.}} \\ \text{With earthquake} & F = 1.425 \times 35.32 = 50.33 \text{ tons} & > 12.10 \text{ tons } \underline{\text{ok.}}\end{array}$$

Stresses at Base

(a) Without Earthquake

$$\text{Total moment about B} = 28.27 + 33.10 = 61.37 \text{ tons.}$$

$$\begin{aligned}\text{Resultant load normal to base} &= 36.26 \cos 9.46^\circ + 10.6 \sin 9.46^\circ \\ &= 35.54 \text{ tons.}\end{aligned}$$

$$\text{Inclined base width} = 3.095 \sec 9.46^\circ + 0.45 = 3.800 \text{ m.}$$

$$\text{Distance of resultant from B} = 61.37 / 35.54 = 1.727 \text{ m,}$$

$$e = 1.727 - 3.80/2 = -0.173 \text{ m, that is towards B.}$$

$$\begin{aligned}p &= \frac{35.54}{3.8} \left[1 \pm \frac{6 \times 0.173}{3.8} \right] \\ &= 11.91, 6.79 \text{ t/m}^2 < 15 \text{ t/m}^2 \quad \text{O.K.}\end{aligned}$$

(b) With Earthquake

$$\begin{aligned}\text{Total moment about B} &= 46.11 + 33.10 \\ &= 79.21 \text{ t-m.}\end{aligned}$$

$$\begin{aligned}\text{Resultant load normal to base} &= 35.32 \cos 9.46^\circ + 15.54 \sin 9.46^\circ \\ &= 37.39.\end{aligned}$$

$$\text{Distance of resultant from B} = 79.21 / 37.39 = 2.118 \text{ m,}$$

$$e = 2.118 - 1.900 = 0.218 \text{ m,}$$

$$\begin{aligned}p &= \frac{37.39}{3.8} \left[1 \pm \frac{6 \times 0.218}{3.8} \right] \\ &= 13.23 \text{ t/m}^2\end{aligned}$$

Allowable bearing pressure in earthquake conditions will be 25 per cent more, i.e., $15 \times 1.25 = 18.75 \text{ t/m}^2$ - hence safe. It is seen that there is a possibility of slight reduction in the toe protection; 0.3m x 0.45m size could be used.

17.3.2 Crib Walls

Crib Walls (Fig. 17.13a) may be built of timber, precast concrete, or steel members. Many types of precast concrete and prefabricated steel cribs are available from manufacturers. The insides of the crib are filled with soil and the whole unit acts as a gravity wall.

In the design of crib walls, stringers are considered to act as simply supported beams that span the space between the ties. The stringers that make up the face are subjected to the pressure of the soil inside the crib, while those that make up the back must resist the difference between the earth pressure exerted by the backfill and that of the soil inside. The earth pressure exerted by the backfill on the wall may be computed in the same manner as the gravity wall. The soil inside the crib is usually placed in well-compacted layers and the inside pressure would be close to the at rest earth pressure given in Table 17.3.

The computation for safety, with respect to overturning and sliding, is the same as for the concrete gravity wall. However, not all the weight of the soil in the crib can be counted on to resist the overturning moment. If the wall tilts forward, the soil inside may not move as an integral part of the wall. Rather, it may move downwards with respect to the wall, and shear stresses would develop between the soil and the wall. These shear stresses act vertically downwards and contribute to the resistance against overturning. The stress may be computed by means of the **Arching Theory** (Terzaghi 1943). If the angle of friction between the soil and wall is σ , the average stress on the wall at depth y is:

$$\sigma = \frac{ab}{2(a+b)} \frac{\gamma K_o}{\tan \delta} \left\{ 1 - \exp \left[- \frac{2y K_o(a+b)}{ab} \tan \delta \right] \right\}. \quad (17.29)$$

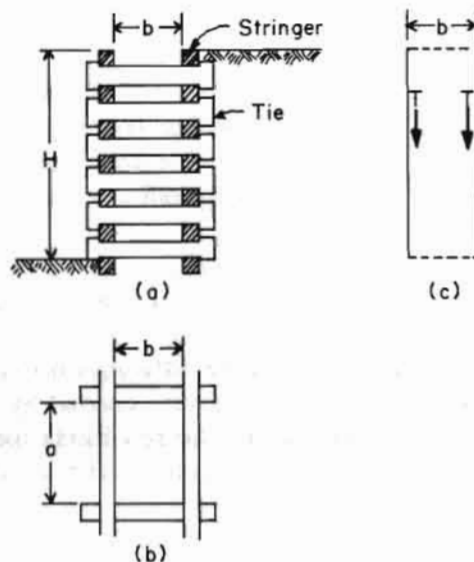
The shear stress between soil and wall is (Fig. 17.14c):

$$T = \sigma_x \tan \delta$$

and the total vertical force transmitted by friction is:

$$F = ab\gamma \left\{ H - \frac{ab}{2(a+b) \tan \delta K_o} \left[1 - \exp \left(- \frac{2(a+b)}{ab} H \tan \delta K_o \right) \right] \right\}. \quad (17.30)$$

The force F plus the weight of the crib constitutes the weight W to be used for the calculation of resisting forces and moments. The stringers should be designed to resist σ_x . Since stringers are usually of the same size in a given crib wall, the value of y in Equation 17.29 should be set equal to H .



Source: Winterkorn and Fang 1975

Fig. 17.13 Crib walls

Table 17.3 Coefficients of earth pressure at rest

Soil	K^0
All types, normally consolidated	1-Sin
Compacted clay, hand tamped	1.0 to 2.0
Compacted clay, machine tamped over entire backfill	2.0 to 6.0
Clay, overconsolidated	1.0 to 4.0
Sand, loosely dumped	0.5
Sand, compacted	1.0 to 1.5

Source: Winterkorn and Fang 1975

17.3.3 Tieback Wall

Retaining walls are sometimes supported by tiebacks anchored in firm material as shown in Figure 17.1(2b). Basement walls may be designed to support the sides of excavations during construction. Construction usually begins with the installation of columns, or soldier beams. These are supported by the anchor ties. The wall between the columns may consist of reinforced concrete, precast concrete panels, fabricated metal pieces, or wooden lagging. The ties are stressed to support the columns.

The wall deflection is naturally dependent upon the tension in the tie and may range from almost zero to 7.5cm at the top for walls 15m in height (Shannon and Strazer 1970). If the bottom of the column is not driven into stiff soils, considerable movement may take place at the bottom. Model tests of tieback

walls in sand (Hanna and Matallana 1970) have indicated that this may be as large as $0.05H$. With such movements, the earth pressure distribution would be close to that for braced excavations. If the bottom of the column is driven into soil and the ties are adequately tensioned, the earth pressure would be close to the at rest earth pressure and the values given in Table 17.3 may be used for design.

Table 17.4 Bond stresses for design of anchors

Soil Type	Bond Stress f
Stiff clay	$5t/m^2$ or 0.25 times unconfined compression strength
Dense sand	$10t/m^2$
Sound rock	$15t/m^2$

Source: Winterkorn and Fang 1975

The wall panels should be designed as beams (Figure 17.1 [2b]) supported by columns. Each panel, such as **ab** in Figure 17.1 (2b), should be designed to support a uniform load equal to the earth pressure in the shaded area **cdef**. If the ties are anchored in sound rock, the columns are designed as continuous beams supported by the ties; and at the bottom. However, a small yield in the anchor can significantly effect the bending moments in the column, in so far as it would reduce the negative moments at the tie and increase the positive moment. If the ties are anchored in soil, the maximum positive moments should be computed on the assumption that the column acts as a simply supported beam between ties (Mansur and Alizadeh 1970). The bottom end of the column is supported by passive earth pressure as shown in Figure 17.1 (2b).

The ties are anchored in rock or firm soil by high strength cement grout. The bond between the grout and the surrounding soil provides the anchor age and must resist the tension in the tie-rod. If T is the tie-rod tension and f if the bond Figure 17.1 (2b), then:

$$T = \pi DLf \quad (17.31)$$

where,

D is the diameter of the drilled hole.

In current design practice, the bond strength varies between $5t/m^2$ and $15t/m^2$ (Table 17.4); the lower value is for stiff clays and the higher value for sound rock. It is the recommended practice to proof-test the anchors to at least 1.5 times the design load. A linear load-displacement relationship up to this load may be used as an accepted criterion. Alternatively, the anchors may be required to hold the design load without appreciable relaxation.

17.3.4 Design of Reinforced Earth Walls-Empirical Method

Use of the reinforcement in the backfill results in substantial increase in its overall cohesive strength (c). As such reinforced earth may be treated as soil having a very high value of cohesion. The reinforced earth slope can, therefore, stand unsupported just like hard clay. The reinforcement element is generally geogrid made of plastic mesh or plastic fabric. The manufacturing companies provide all the details of strengths of reinforcement grids and design charts. Figure. 17.14 shows a typical earth-reinforced wall that is considered suitable for low volume hill roads. The principles of design are given below.

- i) The length of reinforcement (L) is generally taken to be 0.7-0.8 times the wall height and is kept at more than 4m. Figure 17.16 gives a ratio L/H for a different face or slope angle and an angle of internal friction for dry cohesionless backfill.
- ii) Slope angle β should be adopted as 70° or 3:1 for ease of construction. A too steep wall is difficult to construct without form work.
- iii) Provide a drainage layer of gravels to intercept seepage in the backfill. In dry backfill or free draining backfill, it is not required.
- iv) Spacing of reinforcement grids generally varies from 20 to 100 cm.
- v) Approximate depth (Z_i) of the reinforcement layer is obtained from Equation 17.34 (Fig.17.15). It is assumed that height of the wall is $H + 1^m$ to account for surcharge load due to traffic.

The coefficient of active earth pressure (K_A) may be determined from Figure 17.16 for dry cohesionless backfill. The unit weight and ϕ of the backfill or soil are taken from Table 9.3 of Chapter 9. The safe design tensile strength of reinforcement (f_t) is defined as:

$$f_t = \frac{f_k}{F_k F} \quad (17.32)$$

where,

- | | | |
|-------|---|--|
| f_k | = | characteristic tensile strength of reinforcement grid (layer) per unit length of wall, |
| F_k | = | 1.5 (overall factor of safety of wall), |
| F | = | partial factor of safety for geogrid depending upon backfill, |
| | = | 1.1-1.6 for fine-grained soil, and |
| | = | 1.6 for gravel. |

- vi) Place a couple of additional grids of reinforcement in the top part of the backfill and adjust the spacing of lower grids also such that their spacing is within limit (20-100cm) and is a multiple of a specified thickness of compacted layers (e.g., 15cm)
- vii) A backfill of silt or clay is not recommended for a reinforced wall. Plasticity index of fines in the backfill must be less than 6 in any case. Maximum boulder size should not be more than 125cm.

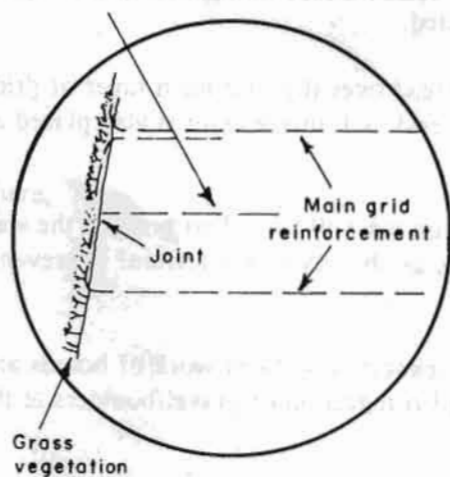
Construction of Reinforced Earth Retaining Wall

- i) The first layer of reinforcement grid is laid after cleaning the foundation area of loose soil/logs/boulders, etc. (Fig. 17.16). The direction of the grid should be as assumed in the design. Then inside the backfill use U-shaped clips to maintain positions.
- ii) The backfill should be compacted well in horizontal layers of 15 to 30cm. It is important to ensure that backfill is free of fines to keep it free draining. Do not use boulders longer than 125cm in size.
- iii) Place boulders or gravel (thickness 25 cm) at the front face where the grid is to be wrapped up. It would be better if jute fabric was wrapped up inside the grid to prevent soil from coming out of the grid.
- iv) Place the next layer of the secondary grid over the compacted backfill and tie it to the main reinforcement grid with the help of high strength plastic wires (called braid and shown in Fig. 17.14).
- v) Another layer of backfill is laid and compacted. Care should be taken to ensure that grid is not damaged and displaced during compaction. For Himalayan rural roads, manual compaction is suggested.
- vi) After the required thickness of backfill is laid, wrap up the first layer of the main grid as shown in Figure 17.14.
- vii) Repeat the above steps to lay the next main grid and then the secondary grid.
- viii) In this way the entire wall of reinforced earth is constructed.
- ix) In the case of seepage problems, the drainage layer is spread over the first main layer of grid, then the backfill is laid and compacted. At the end of the grid, a drainage layer is also placed as shown in Figure 17.14.
- x) Seeds are planted inside the face of the wall to grow grass on the wall face. This protects the wall from erosion, theft, rodents, and fire. Grass also restores the beauty of the terrain. It prevents local bulging of the grid.
- xi) The tolerances in the position of the grids are half the thickness. Use form work of boards and logs to retain a steep wall face during construction. Good compaction of gravel/boulders at the face is required to keep a steep face stable.

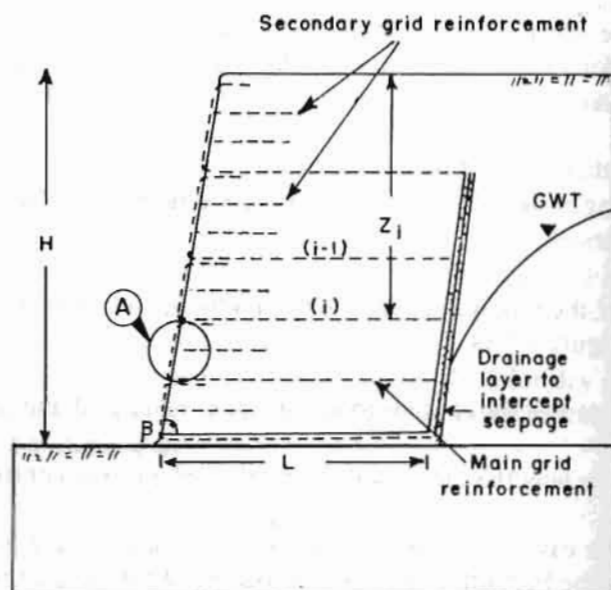
Advantages

- (i) It may take less time to construct the reinforced earth wall than gabions.
- (ii) Excavated material from the cut may be used as backfill material provided it is not silt or clay and does not have fines. This is a major advantage where boulders or rock blocks are not available for gabions and dry stone.

Secondary reinforcement joined to main reinforcement with braid



Detail - A



i $0.7 - 0.8H < L > 4\text{m}$ or as per Fig.17.15 (17.33)

ii $Z_i = [2\text{ft}/K_A \gamma_s]^{1/2} - 1 \text{ (m)}$ (17.34)

iii $Z_i = Z_{i-1} = 0.2 - 1.0 \text{ m}$ or multiple of layer thickness (17.35)

iv $\beta = 70^\circ$ or 3:1 face slope (17.36)

Fig. 17.14 Empirical design of reinforced earth retaining wall ($9H < 15\text{m}$)

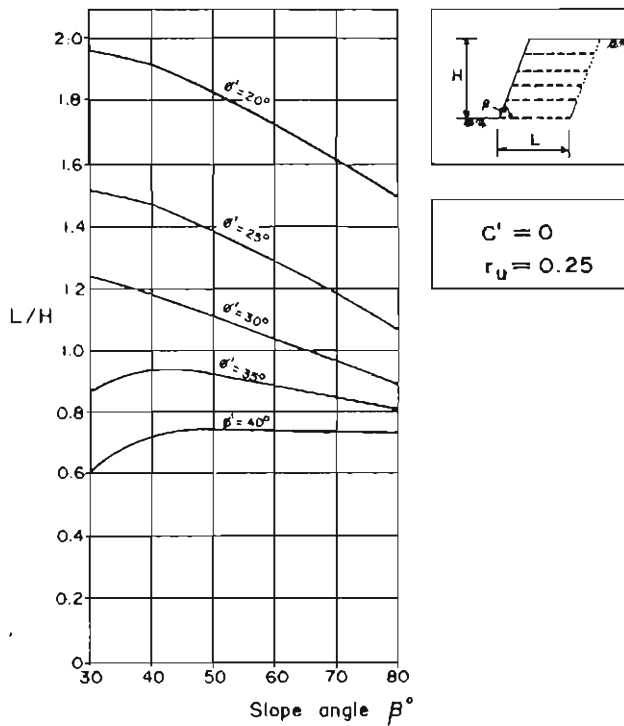
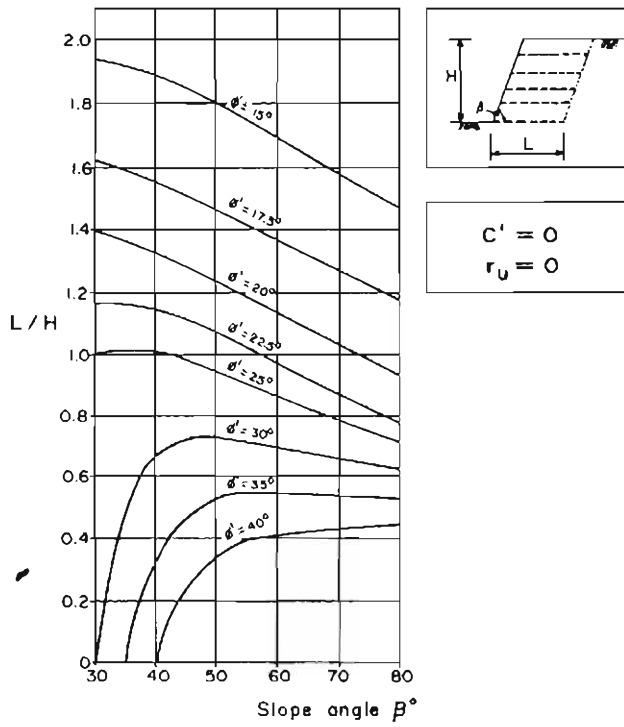
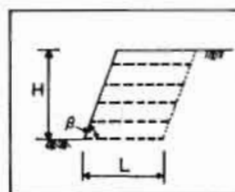
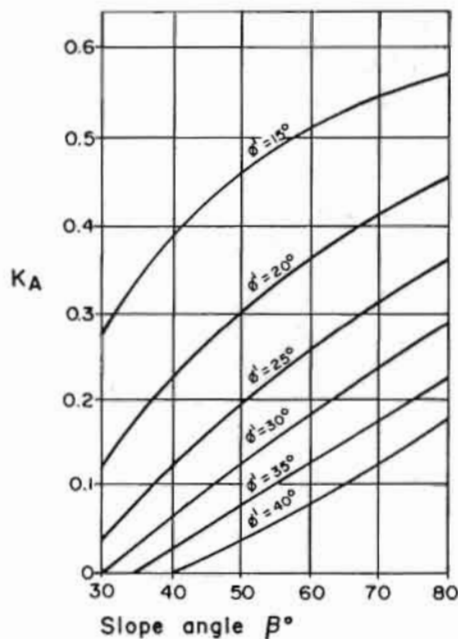
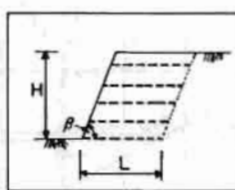
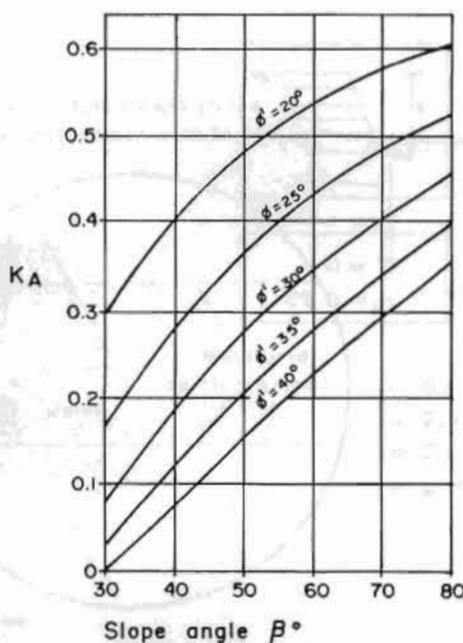


Fig. 17.15 Ratio of length of reinforcement L to wall height H



$$C' = 0$$

$$r_u = 0$$



$$C' = 0$$

$$r_u = 0.25$$

C' = Cohesion

r_u = Pore water pressure coefficient

$$K_A \text{ Values} = \frac{\text{Pore water pressure at depth } z}{\text{Vertical Pressure at depth } z}$$

Fig. 17.16 k_A Values

PAVEMENT DESIGN

18.1 TRAFFIC CONVERSION TO EQUIVALENT SINGLE AXLE LOAD

Empirical designs are based on commercial vehicles or on equivalent 8.16 ton single axle (ESA) or on equivalent 18 kips single axle load (EAL). Most of the recent empirical design tables are based on equivalent axle load, either ESA or EAL (see Table 18.1).

It is, therefore, necessary to convert the traffic to equivalent single axle loads. Vehicles of different axle loads can be converted to equivalent single axle loads by using empirical relationships established by the American Association of State Highway Officials (AASHO) Road Test. The equivalency factor, sometimes also called damaging power, depends upon the number of axles of the vehicle, structural number of the pavement, and current serviceability of the pavement. The following equation has been derived from the AASHO Road Test for:

$$F_j = \frac{W_{18}}{W_x} = \left[\frac{L_x + L_2}{18 + 1} \right]^{4.79} \left[\frac{10 G/\beta_{18}}{10 G/\beta_x} \right] = \frac{1}{L_2^{4.33}}$$

where,

F_j	$=$	$\frac{W_{18}}{W_x}$	$=$	axle load equivalency,
W_{18}	$=$	axle load in terms of a single axle of 18,000 pounds,		
L_x	$=$	axle load of a given vehicle W_x ,		
L_2	$=$	code for axle configuration, 1 for a single axle and 2 for a tandem axle,		
G	$=$	$\log \left[\frac{4.2 - P_t}{4.2 - 1.5} \right]$	$=$	a function of the ratio of loss in serviceability at time t to the potential loss taken to a point where $P_t = 1.5$,
P_t	$=$	terminal serviceability index,		
B	$=$	$0.4 + \frac{0.081 (L_x + L_2)^{3.23}}{(SN + 1)^{5.19} L^{3.23}}$, and		
SN	$=$	structural number.		

An axle load study should be carried out to determine the axle loads of the different traffic on existing roads.

Table 18.1 AASHTO equivalent factors - flexible pavement

Axle Load (kips)	Structural Number, SN					
	1	2	3	4	5	6
2	0.0002	0.0002	0.0002	0.0002	0.0002	0.0002
4	0.002	0.003	0.002	0.002	0.002	0.002
6	0.01	0.01	0.01	0.01	0.01	0.01
8	0.03	0.04	0.04	0.03	0.03	0.03
10	0.08	0.08	0.09	0.08	0.08	0.08
12	0.16	0.18	0.19	0.18	1.17	0.17
14	0.32	0.34	0.35	0.35	0.34	0.33
16	0.59	0.60	0.61	0.61	0.60	0.60
18	1.00	1.00	1.00	1.00	1.00	1.00
20	1.61	1.59	1.56	1.55	1.57	1.60
22	2.49	2.44	2.35	2.31	2.35	2.41
24	3.71	3.62	3.43	3.33	3.40	3.51
26	5.36	5.21	4.88	4.68	4.77	4.96
28	7.54	7.31	6.78	6.42	6.52	6.83
30	10.38	10.03	9.24	8.65	8.73	9.17
32	14.00	13.51	12.37	11.46	11.48	12.17
34	18.55	17.87	16.30	14.97	14.87	15.63
36	24.20	23.30	21.16	19.28	19.02	19.93
38	31.14	29.95	27.12	24.55	24.03	25.10
40	39.57	38.02	34.34	30.92	30.40	31.25

Single Axles, Pt = 2.0

Tandem axles, Pt = 2.0

Axle Load (kips)	Structural Number, SN					
	1	2	3	4	5	6
10	0.01	0.01	0.01	0.01	0.01	0.01
12	0.01	0.02	0.02	0.01	0.01	0.01
14	0.02	0.03	0.03	0.03	0.02	0.02
16	0.04	0.05	0.05	0.05	0.04	0.04
18	0.07	0.08	0.08	0.08	0.07	0.07
20	0.10	0.12	0.12	0.12	0.11	0.10
22	0.16	0.17	0.18	0.17	0.16	0.16
24	0.23	0.24	0.26	0.25	0.24	0.23
26	0.32	0.34	0.36	0.35	0.34	0.33
28	0.45	0.46	0.49	0.48	0.47	0.46
30	0.61	0.62	0.65	0.64	0.63	0.62
32	0.81	0.82	0.84	0.84	0.83	0.82
34	1.06	1.07	1.08	1.08	1.08	1.07
36	1.38	1.38	1.38	1.38	1.38	1.38
38	1.76	1.75	1.73	1.72	1.73	1.74
40	2.22	2.19	2.15	2.13	2.16	2.18
42	2.77	2.73	2.64	2.62	2.66	2.70
44	3.42	3.36	3.23	3.18	3.24	3.31
46	4.20	4.11	3.92	3.83	3.91	4.02
48	5.10	4.98	4.72	4.58	4.68	4.83

Table 18.1 (continued)

Axle Load (kips)	Structural Number, SN					
	1	2	3	4	5	6
2	0.0004	0.0004	0.0003	0.0002	0.0002	0.0002
4	0.003	0.004	0.004	0.004	0.003	0.002
6	0.01	0.02	0.02	0.01	0.01	0.01
8	0.03	0.05	0.05	0.04	0.03	0.03
10	0.08	0.10	0.12	0.10	0.09	0.08
12	0.17	0.20	0.23	0.21	0.19	0.18
14	0.33	0.36	0.40	0.39	0.36	0.34
16	0.59	0.61	0.65	0.65	0.62	0.61
18	1.00	1.00	1.00	1.00	1.00	1.00
20	2.61	1.57	1.49	1.47	1.51	1.55
22	2.48	2.38	2.17	2.09	2.18	2.30
24	3.69	3.49	3.09	2.89	3.03	3.27
26	5.33	4.99	4.31	3.91	4.09	4.48
28	7.49	6.98	5.90	5.21	5.39	5.98
30	10.31	9.55	7.94	6.83	6.97	7.79
32	13.90	12.82	10.52	8.85	8.88	9.95
34	18.41	16.94	13.74	11.34	11.18	12.51
36	24.02	22.04	17.73	14.38	13.93	15.50
38	30.90	28.30	22.61	18.06	17.20	18.98
40	39.26	35.89	28.51	22.50	21.08	23.04

 Single axles, $P_t = 2.5$

 Tandem axles, $P_t = 2.5$

Axle Load (kips)	Structural Number, SN					
	1	2	3	4	5	6
10	0.01	0.01	0.01	0.01	0.01	0.01
12	0.02	0.02	0.02	0.02	0.01	0.01
14	0.03	0.04	0.04	0.03	0.03	0.02
16	0.04	0.07	0.07	0.06	0.05	0.04
18	0.07	0.10	0.11	0.09	0.08	0.07
20	0.11	0.14	0.16	0.14	0.12	0.11
22	0.16	0.20	0.23	0.21	0.18	0.17
24	0.23	0.27	0.31	0.29	0.26	0.24
26	0.33	0.37	0.42	0.40	0.36	0.34
28	0.45	0.49	0.55	0.53	0.50	0.47
30	0.61	0.65	0.70	0.70	0.66	0.63
32	0.81	0.84	0.89	0.89	0.86	0.83
34	1.06	1.08	1.11	1.11	1.09	1.08
36	1.38	1.38	1.38	1.38	1.38	1.38
38	1.75	1.73	1.69	1.68	1.70	1.73
40	2.21	2.16	2.06	2.03	2.08	2.14
42	2.76	2.67	2.49	2.43	2.51	2.61
44	3.41	3.27	2.99	2.88	3.00	3.16
46	4.18	3.98	3.58	3.40	3.55	3.79
48	5.08	4.80	4.25	3.98	4.17	4.49

Source: AASHTO Pavement Design Guide 1985

Private cars do not contribute significantly to the structural damage caused to road pavements by traffic. Therefore, for the purpose of structural design, cars can be ignored and only the total number and axle loading of commercial vehicles, that will use the road during its design life need be considered. A commercial vehicle is defined as any goods or public service vehicle that has an unladen weight of 1.5 tons or more.

18.2 LANE DISTRIBUTION OF TRAFFIC

The design traffic load for pavement design is obtained by determination of the actual traffic in the design lane. This can be done either by actual studies of traffic in each lane or by an empirical method of distribution of the total traffic in both directions. The traffic distribution by direction varies from 0.3 to 0.7 of the total of two direction traffic. Normally the directional distribution is taken as 0.5.

Once the traffic in each direction is known, this is again distributed by lane, if there is more than one lane for the traffic in a particular direction. For single lane, one-directional traffic the distribution is taken as 1.0 of the directional traffic. This lane distribution is reduced by 0.2 for each additional lane.

The following distribution may be followed for design of traffic in developing countries by using empirical design nomographs, most of which are developed for roads with two or more lanes.

- i) Single-lane (3.5 - 3.75 width) :
design traffic = 2 x traffic in both directions, to account for channelization of wheel loads.
- ii) Single-lane (4 to 4.5m width) :
design traffic = 1.5 x traffic in both directions.
- iii) Single-lane (4.5 to 5.5m width) :
design traffic = 1 x traffic in both directions.
- iv) Two-lane, single carriageway road (5.5 to 6.5m width) :
design traffic = 0.75 x traffic in both directions.
- v) Two-lane, single carriageway roads (6.5 to 7.5m width) :
design traffic = 0.5 x traffic in both directions.

The traffic need not be increased for load concentration effect as in cases i) and ii) above when design is carried out using a Structural Number (SN) or mechanistic empirical methods.

18.3 DESIGN LOAD

The design traffic is considered in terms of the cumulative number of standard axles (in the lane carrying maximum traffic) to be carried during the design life of the road.

The following equation may be used to calculate the total design traffic load:

$$N_D = \frac{365 \times N [(1 + r)^n - 1]}{r}$$

where,

N_D	=	total design traffic in ESA,
N	=	initial average daily traffic in the design lane in ESA,
r	=	growth rate, and
n	=	design life in years.

18.4 DESIGN METHODS

Some of the methods based on material characterization for pavement design are:

- CBR method**,
- R - value method**,
- Structural number method**, and
- Mechanistic design method.***

These methods are commonly known by agency, examples of which are given below.

1. National Crushed Stone Association
2. California
3. AASHTO, 1985
4. Transport and Road Research Laboratory
5. Asphalt Institute

The following discussion is an introduction to a few of the several methods of pavement design. The reader is, however, advised to refer to appropriate literature for further details.

18.4.1 CBR Method

In this method the California Bearing Ratio (CBR) used is for material characterization. The thickness of different layers of a pavement can be obtained by using CBR values of the materials to be used in different layers. Standard design charts, or nomographs, prepared by several agencies are available which allow determination of thickness against the input of traffic load and CBR. Most agencies have developed design charts relating axle load to the thickness of surface and sub-base of a given material type for various sub-grade CBR values. This requires adaptation of the base and sub-base materials having the same properties as specified in the development of design charts. Adjustment for variability in the properties of base, sub-base, and surface materials available is therefore not possible in using such design charts.

** empirical methods

*** Analytical and empirical method

18.4.2 *U.S. Corps of Engineers' Method*

Section 18.5.1 is an example of design using this method.

18.4.3 *The TRRL Method*

The Transport and Road Research Laboratory's (TRRL) Road Note 31 and Road Note 29 describe empirical methods based on performance tests for the design of pavements for traffic loads of up to 2.5 million ESA and greater than 2.5 million ESA respectively. TRRL Road Note 31 is especially developed for the tropical and subtropical conditions of developing countries. Traffic load and sub-grade CBR are basic inputs. The surface, base, and sub-base materials have to conform to those adopted in the design for application of this method. Sections 18.5.2 and 18.5.3 present design example by this method.

18.4.4 *R-value Method*

This method uses R-value, which is a stabilometer value to characterize the property of each layer as against CBR value in the CBR method. This method is based on California methods.

18.4.5 *Structural Number (AASHTO 1985) Method*

The Structural Number (SN) is defined as an index number derived from an analysis of traffic, roadbed, soil conditions, and regional factors that may be converted to the thickness of various flexible-pavement layers through the use of suitable layer coefficients related to the type of material being used in each layer of the pavement structure. The layer coefficients (designated by a_1 , a_2 , and a_3 , for surface, bases, and sub-base respectively) give the empirical relationship between SN for a pavement structure and layer thickness and express the relative ability of a material to function as a structural component of the pavement.

Analytically, the SN is given by:

$$\begin{aligned} \text{SN} &= a_1 D_1 + a_2 D_2 m_2 + a_3 D_3 m_3, \\ D_1, D_2, D_3 &= \text{actual thickness of surface, base, and sub-base, and} \\ m_2, m_3 &= \text{drainage coefficients for base and sub-base respectively.} \end{aligned}$$

The Structural Number Design Method is based the on the 1950-1960 American Association of State Highway Officials (AASHTO) Road Test. The advantages of the SN method of design are:

- provision for drainage conditions,
- flexibility to design for variable material properties for different layers, and
- use or reliability.

Section 18.5.4 presents an example of design by this method.

18.4.6 *Mechanistic Empirical Method*

This method, also known as the layered elastic design method, is an analytical method that calculates stresses and strains at different depths of the pavement layer. Fatigue of asphalt surface and rutting of sub-grade, under the designed load, are used as failure criteria for the design of different layers of the pavement. This method tries to characterize the problems of all materials in terms of the dynamic modulus of elasticity. The dynamic modulus of elasticity, sometimes called resilient modulus, is a dynamic test response defined as the ratio of repeated axial deviator stress to the recoverable axial strain, E_a :

$$M_R = \frac{\sigma_1}{\epsilon_a}$$

18.4.7 *Criteria for Failure*

Rutting Criteria for Failure

Rutting is the permanent deformation resulting from traffic-associated distress. It is the phenomenon of longitudinal depressions in the wheel paths, resulting from compaction or lateral migration of one or more pavement layer materials under the action of traffic and environment. The equation developed by Finn et al. for failure by deformation of sub-grade is given by the Equation in Section 18.5.6.

Fatigue Criteria for Failure

Fatigue is defined as the phenomenon of load-induced cracking due to repeated stress at strain levels below the ultimate strength of the material. The strain at the bottom of the asphalt layer is the measure of cracking. The allowable strain is different for different quality surface layers. Several equations have been developed by various agencies to equate the failure to a given level of allowable strain. The fatigue model is given by the Equations in Section 18.5.7.

18.4.8 *Advantages and Disadvantages of Mechanistic Design*

Advantages of Mechanistic Design

With mechanistic design, it is possible to try several combinations of material and thickness for the various layers in order to come up with the most economical solution for the same strength.

Disadvantages of Mechanistic Design

The following are some problems associated with mechanistic design:

the assumption that pavement layers are homogeneous, isotropic, and elastic is not completely true,

- computer use is essential,
- the dynamic modulus of elasticity of *in situ* materials cannot be easily determined, and
- the dynamic modulus of elasticity for layers of granular material is dependent on the stress conditions of the layer and stress sensitivity relationships are needed to adjust the lab modulus to the actual conditions.

Several agencies have developed design charts based on mechanistic analysis and performance tests for their own conditions. Section 18.5.5 and 18.5.6 present examples of design by these methods. Section 18.5.7 is based on The CHEVPC computer programme.

Each user agency may develop their own failure equations and use them with the stresses or strains calculated by computer analysis in order to design pavement layers. The following discussions present the background of existing computer programmes for layered-elastic analysis. Section 18.5.7 presents examples of designs using computer analysis and given failure equations.

18.4.9 Existing Computer Programmes for Layered-Elastic Analysis

The following discussion presents an overview of existing computer programmes for multi-layered elastic analysis based on background material after NewComb, University of Washington, 1985.

Background

Much of what is currently used in the structural analysis of pavements is based on technology that has evolved over the last 60 years. The first use of the layered-elastic theory in pavement design occurred in 1926 when Westergaard applied these principles to Portland Cement Concrete (PCC) pavements. Burmister later used the theory of elasticity as an approach to the solution of multi-layered, elastic pavement structures. In the development of his solution, Burmister assumed that each layer could be represented as a homogeneous, isotropic, and linear elastic material. Each layer was assumed to extend infinitely in the horizontal direction, and the bottom layer was assumed to extend infinitely downwards. The other layers were assumed to have finite thickness.

In pavement systems, loads generally occur over an elliptical area. The resulting vertical stresses are distributed in a bell-shaped fashion on the horizontal surfaces. The maximum stress is located on a vertical line to the midpoint of the load. Several influence charts and tables have been developed to determine the stresses, strains, and deflections in a one-layer system for any value of Poisson's Ratio.

Typical pavements are composed of different layers and material stiffness decreases with depth. The end result is the reduction of stresses, strains, and deflections in the sub-grade compared to the one layer case.

In two-layer systems, materials within a specific layer are assumed to be homogeneous, isotropic, and elastic. Furthermore, the layers are assumed to extend an infinite distance horizontally. The surface layer has a finite depth and the underlying layer is assumed to be semi-infinite in the vertical. For boundary and continuity considerations, there are no shearing and normal stresses outside the loaded area for the surface layer and the layers are assumed to be in continuous contact.

For a three-layer pavement system, several charts and tables have been developed by Peattie, Jones, and Fox (1962) to determine the stresses, strains, and deflections. Peattie developed graphical solutions for vertical stress in three-layer systems. Jones presented solutions for horizontal stresses in a tabular form. Both these solutions were based upon Poisson's Ratio of 0.5 for all layers.

The logical extension of these solutions was the development of computer programmes in order to expedite analysis and allow greater flexibility in the accommodation of material properties and multiple loads. Even the most elementary of these allow for materials with Poisson's Ratio other than 0.5. Some are capable of ascertaining the effects of multiple gear configurations and/or non-linear material behavior. Recently, Bush developed a computer programme which essentially works layered-elastic analysis in reverse to determine material properties from non-destructible deflection measurements.

Finite element analysis has been recently proposed to evaluate the response of pavement structures to loading. This method defines the pavement in terms of elements that are connected at nodal points. The stiffness at each nodal point is calculated by means of assuming displacement variation within the element along with a knowledge of the stress-strain behavior of the element material. Equilibrium at each nodal point may be expressed by two equations which are used to solve the unknown displacements. Once the displacements at all the nodal points have been calculated, the stresses and strains for each element may be computed.

Computer Programme Descriptions and Operating Notes

This section provides the user with a general overview of some computer programmes for pavement designs in the U.S.A. It contains information on the principles of operation, the assumptions associated with each programme, the characteristics and limitations, and specific warnings on possible pitfalls the user may encounter. The information presented here is intended to be supplemented by the user's manuals and other references that contain more detailed descriptions of the programme.

The layered-elastic system computer programme was developed at the University of California, Berkeley, and can be used to analyze up to ten identical loads on a five-layer system. The programme computes various components of stresses, strains, and displacements along with principal values in a three-dimensional, ideal layered-elastic system.

The top surface of the pavement is assumed to have no shear. As with other layered-elastic systems, the layers are assumed to have uniform thicknesses and to be infinite in horizontal distance. Layered interfaces are assumed to be continuous. A finite thickness may be used for the bottom layer or it may be assumed semi-infinite. If a finite thickness is used, the programme assigns a rigid underlying layer to support it and a continuous or frictionless interlayer must be assumed.

Input data for ELSYM5 are any two of three load determinants (load in pounds, stress in pounds per square inch, radius of load in inches), load position, elastic modulus, Poisson's Ratio, location of analysis points, and thickness of each layer (except the lowest). Coordinates for load positions and analysis points are expressed in terms of x and y for horizontal locations and z for depth.

Loads are assumed to be uniform, static, and circular, and the principle of superposition is used for determining the effect of multiple loads. Hicks et al. (1978) identified the following programme characteristics:

- (a) one to five systems may be evaluated in a single run,
- (b) one to five layers may be used in the systems,
- (c) one to ten identical circular loads may be applied to the pavement,
- (d) one to 100 locations may be specified for pavement response results (stress, strain, deflection),
- (e) no depth may be specified for pavement response results if the point is below the top of the rigid underlying layer,
- (f) no negative data are allowed except for horizontal distances,
- (g) Poisson's Ratio can be any value except one; for a sub-grade on rigid support, Poisson's Ratio must not be within the range of 0.748 to 0.752, and
- (h) results are approximate at or near the pavement surface and at some horizontal distances from the load; this is due to a truncated series used in the integration process.

CHEVNL (CHEVPC)

This programme presents solutions for multi-layered elastic systems. The original version of this computer programme was developed by the Chevron Research Company (formerly California Research Corporation) in the early 1960s. It computes stresses, strains, and deflections as a result of a single, uniform, circular load applied vertically to the pavement. This system is capable of analyzing up to 15 layers. All layers are of finite thickness, except the bottom which is of semi-infinite thickness. The horizontal dimension is infinite for all layers. The surface of the pavement is assumed to have no shear forces acting upon it.

Radial and vertical distances are expressed in cylindrical coordinates as R and Z respectively. The z-axis at R=0 extends through the centre of the load.

The vertical load and contact pressure are used to describe the problem loading conditions. Using these parameters, the programme computes the load radius. Material properties of individual layers are expressed in terms of the modulus of elasticity (resilient modulus), Poisson's Ratio, and thickness.

At least 30 radial and 30 vertical points may be selected for analysis. In addition to typical strain values, the programme identifies and describes the maximum, principal tensile strain with respect to its angle from the radial axis. The following programme operating characteristics have been identified:

- (a) up to 15 layers may be incorporated in the programme,
- (b) the materials may be assigned any values of moduli,
- (c) Poisson's Ratio may be any value other than one,
- (d) the mathematics are relatively easy and self-contained, and
- (e) the effects of multiple gears must be computed outside of the programme, using superposition.

BISAR

This computer programme uses the layered-elastic theory to solve stresses, strains, and displacements in pavement systems with one or more uniform circular loads applied vertically on the surface. BISAR has the additional capability of considering surface loads to be combinations of vertical, normal, and unidirectional horizontal forces. The usual layered-elastic assumptions apply in this programme except for continuity. Layer interfaces are assumed to be either in full contact or frictionless.

Stresses, strains, and displacements, due to each load, are accumulated separately in a cylindrical coordinate system. In multiple load problems, the cylindrical coordinate system is transformed to Cartesian. The effects of multiple loads are computed by summing the effects of each individual load. Specific output parameters must be designated in the programme for locations and components.

Inputs for the layers include the modulus of elasticity, Poisson's Ratio, thickness, and boundary conditions (rough or frictionless). Particular care should be used in selecting the desired parameters for output. These must be consistent with the coordinate system established by the programmer.

Some of the characteristics of BISAR include:

- (a) a maximum of 10 layers may be used,
- (b) up to 99 systems may be evaluated in one run,
- (c) up to 99 points within a system may be specified for evaluation,
- (d) no negative data may be used as input except for horizontal distances, and
- (e) there are no provisions for non-linear behaviour in the materials.

PSAD2A

This program is a multi-layered elastic system which may be used to determine stresses and strains while allowing material moduli to vary with stress levels. It also automatically computes stresses and strains caused by dual wheel configurations. The major advantage of PSAD2A is the estimation of the sub-grade modulus from the modulus-deviator stress relationship which is used as input. This relationship may be described by the equation (see Figures 18.1 and 18.2):

$$M_R = K_1 \sigma_d^{k_2}$$

where,

M_R	=	resilient modulus (psi) of sub-grade
σ_d	=	deviator stress (psi), see Figure 18.3, and
K_1, k_2	=	material constants.

Base or sub-base course stress sensitive materials are characterized by modulus-bulk stress relationships as defined (see Figure 18.2).

$$M_R = K_1 \theta^{k_2}$$

where,

M_R	=	resilient modulus (psi),
θ	=	bulk stress (psi), see Figure 18.3, and
K_1, k_2	=	regression constants.

For non-stress dependent materials, a horizontal relationship is used as input. Another advantage of PSAD2A is that overburden pressures (stresses) may be incorporated into the solution by superimposing load-induced and overburden stress.

The iterative process of this programme compares the stress state in the material with the initially assumed modulus. This is repeated until the stress state and modulus value are reconciled to specified accuracy limits. It should be noted that the first set of stresses, displacements, and strains in the output are for a single load. The following output pages list stresses and strains due to dual loads.

Particular characteristics of this programme have been identified as follows:

- (a) five layers must be used in the analysis,
- (b) output values may be obtained for 48 to 121 points in the pavement,
- (c) no negative data may be used as input,
- (d) Poisson's Ratio may be any value except one, and
- (e) three to 20 modulus-deviator stress points may be used as input.

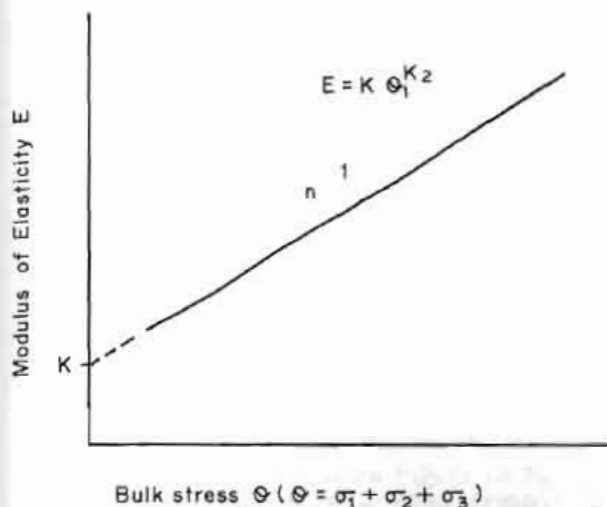
BISDEF

As mentioned earlier, this programme provides a means for predicting the moduli of up to four layers from non-destructive deflection data. It does this by iteratively matching deflection values with material properties using the BISAR layered-elastic programme. There may be a maximum of four deflection measurements and one load used for input. Deflection points are defined in terms of x and y coordinates as well as depth. The load is defined in terms of its centre x and y coordinates, vertical stress, and radius.

A certain amount of judgment must be used when considering input values for initial material properties. Since the programme iteratively matches deflection values with layer moduli, a tolerance must be specified for stopping the programme. Ten per cent is recommended for this value. Also, a maximum number of iterations (usually three) must be specified to stop the programme to prevent the use of an excessive amount of computer time.

A minimum and maximum allowable modulus must be specified for each material of unknown modulus. Boundary conditions must be set as either rough or frictionless. An initial estimate of the modulus, Poisson's Ratio, and the thickness of all layers except the sub-grade must be input to the programme. The closer the initial modulus estimate is to the actual value, the faster the programme will close and the less costly the run. Bush (1980) recommends that the modulus of asphalt concrete be determined by first estimating the temperature at mid-depth. Furthermore, he suggests a range between 600,000 and 1,500,000 psi as a modulus range for cement-stabilized materials.

BISDEF uses a free-format input. If the programme has not closed within the specified tolerance in the allotted number of iterations, the programme will notify the user. If this happens, the user is advised to adjust the modulus input values and rerun the programme.



Source: University of Washington 1986

Fig. 18.1 Modulus-deviator stress relationship for fine-grained materials

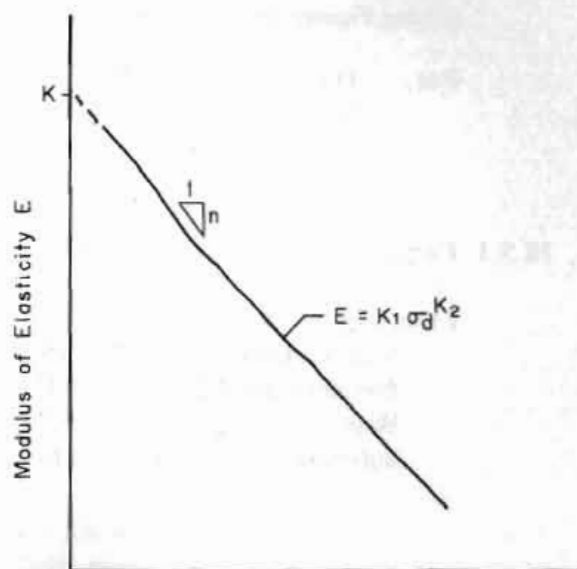
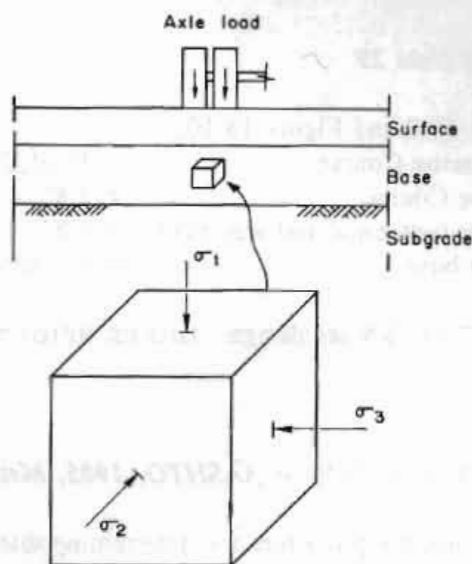


Fig. 18.2 Modulus-bulk stress relationship for coarse-grained materials



Bulk stress, $\Theta = \sigma_1 + \sigma_2 + \sigma_3$

Deviator stress, $\sigma_d = \sigma_1 - \frac{\sigma_2 + \sigma_3}{2}$

Source: University of Washington 1986

Figure 18.3 Principal stresses due to axle load

18.5 EXAMPLE OF NEW PAVEMENT DESIGN BY DIFFERENT METHODS
(Using Figures 18.4 to 18.24 and Tables 18.2 to 18.13a)

For, Traffic = 2×10^6 ESA
Sub-grade CBR = 7%

18.5.1 Corps of Engineers CBR Method

From Figure 18.4,
total thickness = 16"
therefore use AC = 3"
Base = 7"
Sub-base = 6"

18.5.2 TRRL Road Note 31

From Figure 18.5,
Bituminous Premix = 150 mm = 2"
Base = 150mm = 6"
Sub-base = 158mm = 6"

18.5.3 TRRL Road Note 29

From Table 18.3 and Figure 18.10,
Wearing Course = 1" of DBM
Base Course = 2.4" of DBM
Base (untreated and wet mix) = 6.8"
Sub-base = 6" (minimum thickness from Figure 18.6)

Figures 18.7 to 18.9 are design charts for different surfacing and bases.

18.5.4 Structural Number (SN) = AASHTO, 1985, Method

Figure 18.11 illustrates the procedure for determining thicknesses

(i) Full depth AC,

a) assume, E_{ac} = 500,000 psi, (E_{ac} = 500,00 psi at 82°F from Fig. 18.13)
reliability = 85%
standard deviation = 0.45, and
serviceability loss = 3.00.

from Figure 18.12,

$$SN_1 = 3.5$$

$$\text{therefore, } D_1 = SN_1/a_1 = 3.5/0.46 = 7.6". \text{ (} a_1 = 0.46 \text{ from Fig. 18.14)}$$

b) assume for emulsified AC Type II of Asphalt Institute,

$$\begin{aligned} E_{ac} &= 2,000,000 \text{ psi,} \\ a_1 &= 0.29, \text{ and} \\ D_1 &= SN_1/a_1 = 3.5/0.29 = 12". \end{aligned}$$

Assume for 4 layers,

$$\begin{aligned} E_{ac} &= 500,000 \text{ psi,} \\ E_{base} \text{ for CBR 70, from Figure 18.15} &= 28000 \text{ psi,} \\ E_{Sub-base} \text{ for CBR 20, from Figure 18.16} &= 127000 \text{ psi, and} \\ E_{sub-grade} \text{ for CBR 7, (} E = 1500 \times \text{CBR)} &= 10500 \text{ psi.} \end{aligned}$$

From Figure 18.12,

$$\begin{aligned} SN_1 &= 2.3, \\ SN_2 &= 3.2, \text{ and} \\ SN_3 &= 3.5. \end{aligned}$$

$$\begin{aligned} \text{From Figure 18.14, } a_1 &= 0.46, \\ \text{from Figure 18.15, } a_2 &= 0.13, \text{ and} \\ \text{from Figure 18.16, } a_3 &= 0.07, \end{aligned}$$

$$\begin{aligned} \text{therefore, } D_1 = SN_1 / a_1 &= 2.3/0.46 = 5", \\ D_2 = SN_2 - SN_1 / a_2 &= 3.2 - 2.3 / 0.13 = 6.92 = 7", \end{aligned}$$

$$\text{therefore, } SN_2 = 7 \times 0.13 = 0.91,$$

$$\begin{aligned} D_3 &= [SN_3 - (SN_1 + SN_2)]/a_3 \\ &= [3.5 - (2.3 + 0.9)]/0.07 = 4.14 = 4.2". \end{aligned}$$

$$\begin{aligned} \text{Adopt, } D_1 &= 5", \\ D_2 &= 7", \text{ and} \\ D_3 &= 4.2". \end{aligned}$$

Figure 18.17 illustrates the sub-grade modulus relationship for various pressures of sub-grade strength.

(iii) Assume for 4 layers using emulsified AC Type II,

$$E_{ac} = 200,000 \text{ psi},$$

$$E_B = 28,000 \text{ psi}, E_{ab} = 127,000 \text{ psi}, E_{sgr} = 10,500 \text{ psi},$$

$$SN_1 = 2.3,$$

$$SN_2 = 3.2,$$

$$SN_3 = 3.5,$$

$$a_1, \text{ from Figure 18.14} = 0.29,$$

$$a_2 = 0.13, \text{ and}$$

$$a_3 = 0.07.$$

$$D_1 = SN_1/a_1 = 2.3/0.29 = 7.93 = 8"$$

$$\text{therefore, } SN_1 = 8 \times 0.29 = 2.32.$$

$$D_2 = (SN_2 - SN_1)/a_2 = (3.2 - 2.32)/0.13 = 0.88/0.13 = 6.77 = 7"$$

$$\text{therefore, } SN_2 = 7 \times 0.13 = 0.91$$

$$\text{therefore, } D_3 = \{SN_3 - (SN_1 + SN_2)\}/a_3 = 4.14 = 4.2"$$

$$\text{therefore,}$$

$$D_1 = 8",$$

$$D_2 = 7", \text{ and}$$

$$D_3 = 4.2".$$

Table 18.4 gives values of coefficient m to account for drainage conditions in pavement layers. The equations in Figure 18.11 account for drainage in base by using the factor m_2 and in the sub-base by using factor m_3 . Tables 18.5 to 18.7 give suggested reliability levels, minimum thickness of pavement layers, and analysis period for different traffic levels.

18.5.5 Asphalt Institute Method

$$MR = 1500 \text{ CBR} = 1500 \times 7 = 10,500 \text{ psi}$$

- i) From Figure 18.18,
full depth AC = 9.63"
- ii) From Figure 18.19, full depth Type II emulsified AC = 11.81"
(emulsified asphalt mix made with semi-processed
crusher, pit run, or bank aggregates).
- iii) From Figure 18.20,
AC = 210 mm = 8.3", and
base (untreated) agg = 150 mm = 6"
(ASTM D 2940).

- iii) From Figure 18.20,
 $AC = 210 \text{ mm} = 8.3"$, and
 base (untreated) agg = $150 \text{ mm} = 6"$
 (ASTM D 2940).

18.5.6 TRRL Laboratory Report 1132

From Figure 18.21,

HRA = $115 \text{ mm} = 4.5"$ for sub-grade CBR of 5%,
 base = $222 \text{ mm} = 8.75"$, and
 sub-base = $225 \text{ mm} = 9"$.

18.5.7 Mechanistic - Empirical Design Using CHEVPC Computer Programme

In this method, the load capacity of the pavement is determined by fatigue and rutting criteria. The Finn et al. (1977) model for 10 per cent and 45 per cent cracking for fatigue and for 0.75 in deformation of sub-grade has been used in this example. The relationship is given by:

$$\begin{aligned} \log N_f \text{ 10\%} &= 15.947 - 3.291 \log \epsilon_t / 10^{-6} - 0.854 \log MR / 10^3, \\ \log N_f < 45\% &= 15.986 - 3.291 \log \epsilon_t / 10^{-6} - 0.854 \log MR / 10^3, \end{aligned}$$

N_f = $1.077 \times 10^{18} (1/106 \times \epsilon_{vs})^{4.4843}$,
 N_f = load in ESA to failure by fatigue of surface layer,
 N_r = load in ESA to failure by rutting of sub-grade,
 ϵ_t = tensile strain at the bottom of AC,
 ϵ_{vs} = vertical compressive strain at top of sub-grade, and
 MR = resilient modulus of AC.

The strains are calculated by using CHEVPC. The stress sensitivity of untreated aggregates is not accounted for here. Figure 18.22 and Table 18.8 give examples of calculation of stresses and strains using CHEVPC. The thickness for the desired load (traffic) is calculated by iterative process for trial runs for different layers. Table 18.2 compares load to failure for different combinations of thickness and materials.

18.5.8 R-value Method

Figure 18.23 is a design chart for design by the R-value method. Figure 18.24 and Tables 18.9 and 18.10 are examples of design guide for treated and untreated bases.

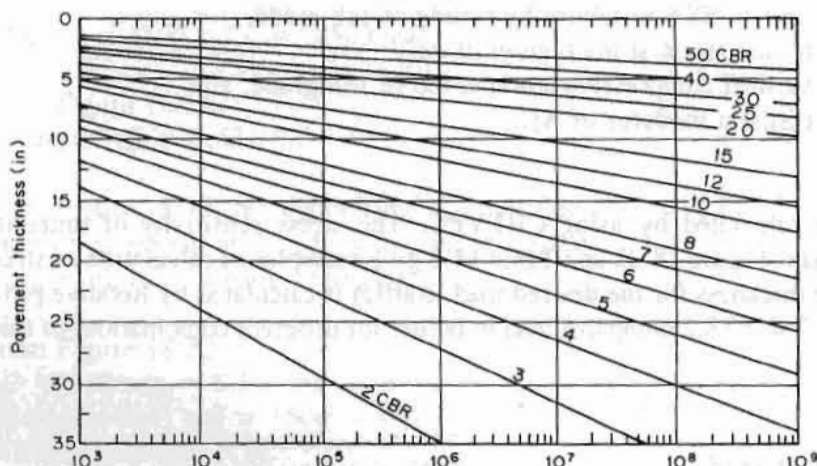
Table 18.2 Comparison of new pavement design by different methods

No. of layers	Properties of material in psi	Thickness of Layers			Mechanistic-Empirical Based Methods		
		U.S. Corps of Engrs	TRRL RN 29	TRRL RN 31	SN Method	Asphalt Institute	CHEVPC
2.	$E_{AC} = 5000,000$ $E_{sgr} = 10,000$	-----	-----	-----	AC = 9.6	AC = 9.6	AC=8
2.	$E_{ac} = 200,000$ $E_{sgr} = 10,500$	-----	-----	-----	AC = 12	AC = 11.8	AC=11.5
4.	$E_{ac} = 5000,000$ $E_b = 28,000$ $E_{sb} = 12,700$ $E_{sgr} = 10,500$	AC = 3" Base = 7" Sbase = 6"	DMB = 3.5" Base = 7" Sbase = 6"	"Premix" = 2" Base = 6" Sbase = 6" Sbase = 4.2"	AC = 5" Base = 6" Base = 7"	AC = 8.3" Base = 6" DBM = 4.5" Base = 8.8" Sbase = 9"	"Low fatigue life with untreated bases and sub-bases."

The design values from TRRL Lr 1132 are based on 5 per cent sub-grade CBR and may be lower for 7 per cent sub-grade CBR. The AASHTO Method uses the actual material properties as against standard materials adopted in other methods. The CHEVPC Method indicated that fatigue life is a problem with thinner surfacing or in pavements with untreated bases.

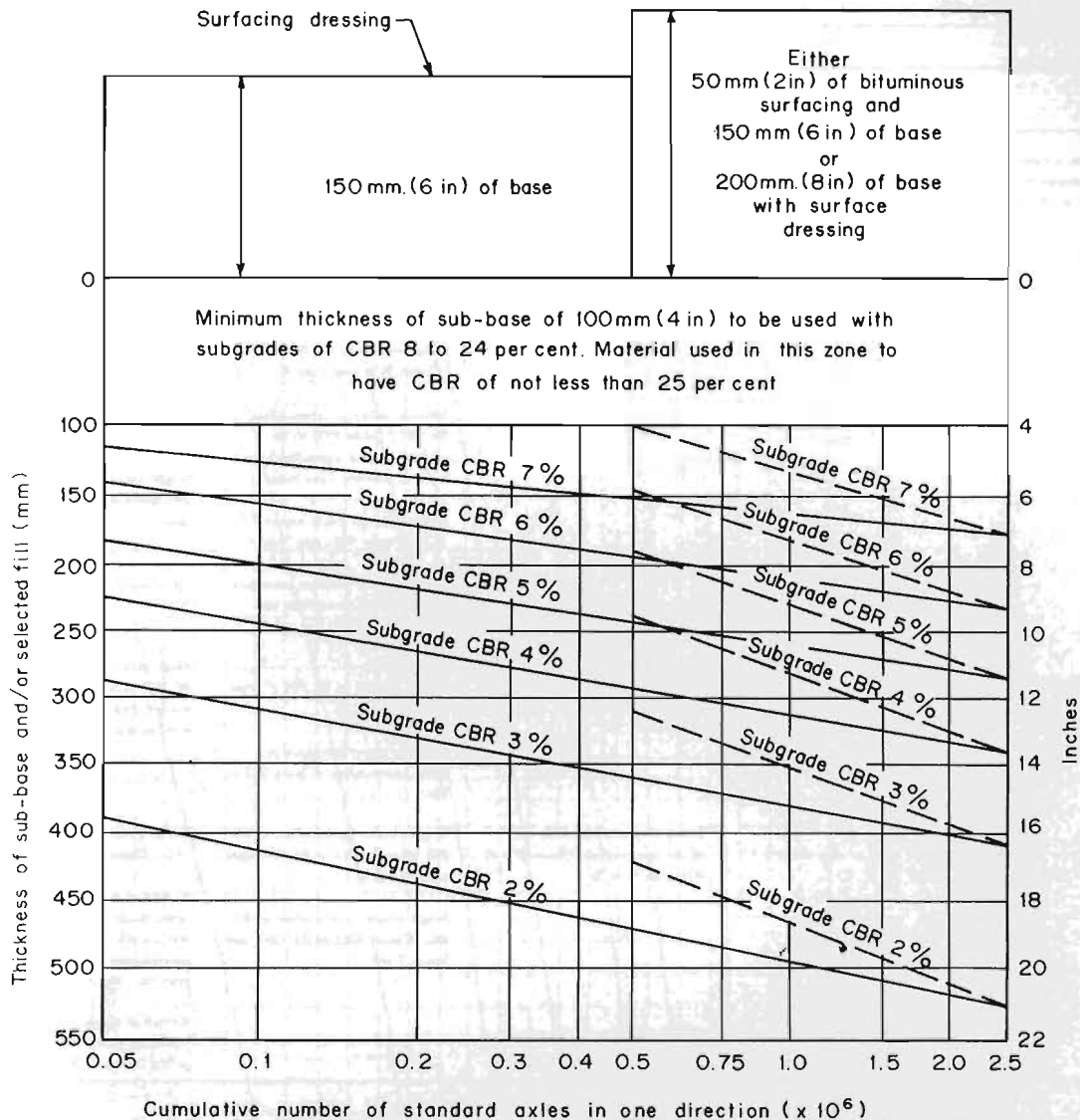
Thickness from variable methods may be converted to a desired combination of this surfacing and thicker based and sub-based by adopting equivalency factors, 1" AC = 3.0 of untreated crushed stone base, and 1 untreated crushed stone base = 2 untreated, gravel sub-base. Also dense, graded asphalt concrete may be treated equal to 1.43" of emulsified asphalt concrete. It may be noted that the fatigue life of thin surfacing over untreated base will be lower than the design life of base and sub-base layers and periodic (every 5 years) renewal of the thin surfacing is essential.

DESIGN OF FLEXIBLE HIGHWAY PAVEMENTS



Source: Yoder and Witczak 1975 18,000 LB Single-axle dual-wheel load operations

Figure 18.4 CBR design curves for 18,000 E.A.L.



Source: TRRL Road Note 31, 1971

If desired to provide at the time of construction a pavement capable of carrying more than 0.5 million standard axles, the designer may choose either a 150 mm (6 in) base with a 50 mm (2 in) bituminous surfacing or a 200 mm (8 in) base with a double surface dressing. For both of these alternatives, the recommended sub-base thickness is indicated by the broken line.

Alternatively, a base 150 mm (6 in) thick with a double surface dressing may be laid initially and the thickness increased when 0.5 million standard axles have been carried. The extra thickness may consist of 50 mm (2 in) of bituminous surfacing or at least 75 mm (3 in) of crushed stone with a double surface dressing. The largest aggregate size in the crushed stone must not exceed 19 mm (3/4 in) and the old surface must be prepared by scarifying to a depth of 50 mm (2 in). For this stage of the construction procedure, the recommended thickness of sub-base is indicated by the solid line.

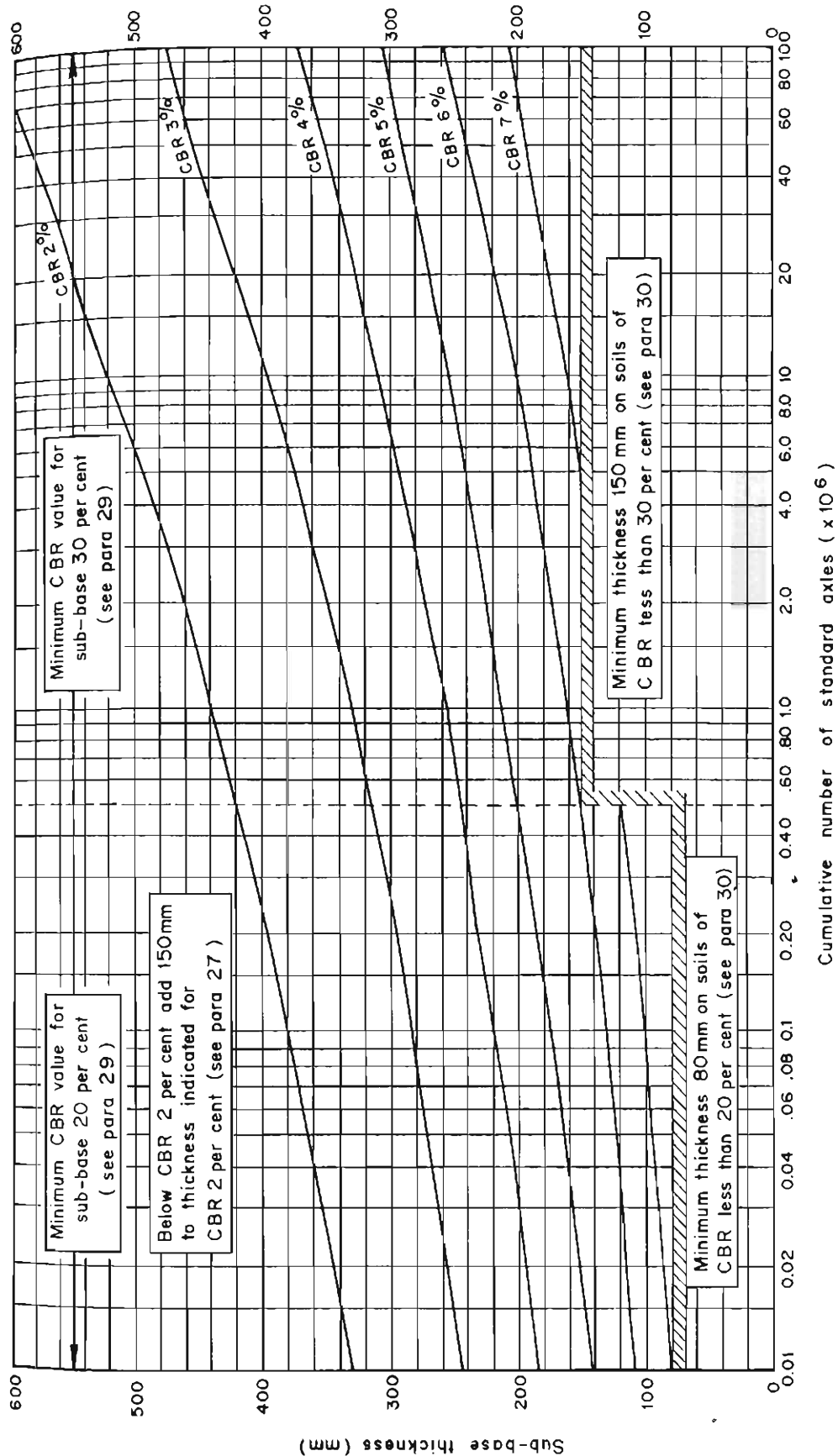
Fig. 18.5 Pavement design chart for flexible pavements

Table 18.3 Recommended bituminous surfacings for newly constructed flexible pavements

Traffic (cumulative number of standard axles)			
Over 11 million (1)	2.5-11 million (2)	0.5-2.5 million (3)	Less than 0.5 million (4)
<p>Wearing course (crushed rock, or slag, coarse aggregate only) Minimum thickness 40 mm Rolled asphalt to BS 594 Rolled asphalt to BS 594 (pitch bitumen) may be used (clause 907)</p>		<p>Wearing course Minimum thickness 20 mm Minimum thickness (pitch-bitumen binder may be used) (Clause 907)</p> <p>Dense tar surfacing to BTIA Specification (Clause 909)</p> <p>Coold asphalt to BS 1690 (Clause 910) (see Note 4)</p> <p>Medium-textured tarmacadam to BS 802 (Clause 913) to be surface-dressed immediately or as soon as possible - see Note 4)</p> <p>Dense bitumen macadam to BS 1621 (Clause 908) (see Note 4)</p> <p>Open-textured bitumen macadam to BS 1621 (Clause 912) (see Note 4)</p>	<p>Two course</p> <p>a) Wearing course -</p> <p>20 mm cold asphalt to BS 1690 (Clause 910) (see Note 4), coated macadam to BS 802 BS 1621, BS 1241 or BS 2040 (Clause 913, 912 or 908) (see Notes 2 and 4)</p> <p>b) Base course, coated macadam to BS 802, BS 1621, BS 1241, or BS 2040 (Clause 906 or 905) (see Note 2)</p> <p>Single course rolled asphalt to BS 594 (pitch-bitumen binder may be used)</p> <p>Dense tar surfacing to BTIA specification (Clause 908) (see Note 4)</p>
<p>Base course Minimum thickness 60 mm</p>	<p>Base course Rolled asphalt to BS 594 (Clause 902) (see Note 2)</p>	<p>Base course Rolled asphalt to BS 594 (Clause 902) (see Note 2)</p> <p>Dense bitumen macadam per dense tarmacadam (Clause 903 or 904)</p>	<p>Medium textured tarmacadam to BS 802 (Clause 913) (to be surface-dressed immediately or as soon as possible - see Note 4)</p>
<p>Dense bitumen macadam or dense tarmacadam (crushed rock or slag only) (Clause 903 or 901)</p>	<p>Dense bitumen macadam or dense tarmacadam (Clause 903 or 904) (see Note 3)</p>	<p>Single course tarmacadam to BS 802 (Clause 906) or BS 1241 (see notes 2 and 5)</p> <p>Single course tarmacadam to BS 802 (Clause 906) or BS 1241 (see Notes 2 and 5)</p>	<p>Dense bitumen macadam to BS 1621 (Clause 908) (see Note 4)</p> <p>60 mm of single coarse tarmacadam to BS 802 (Clause 906) or BS 1241 (to be surface-dressed immediately or as soon as possible - see Note 4)</p> <p>60 mm of single, coarse bitumen macadam to BS 1621 (Clause 905) or BS 2040 (see Note 4)</p>

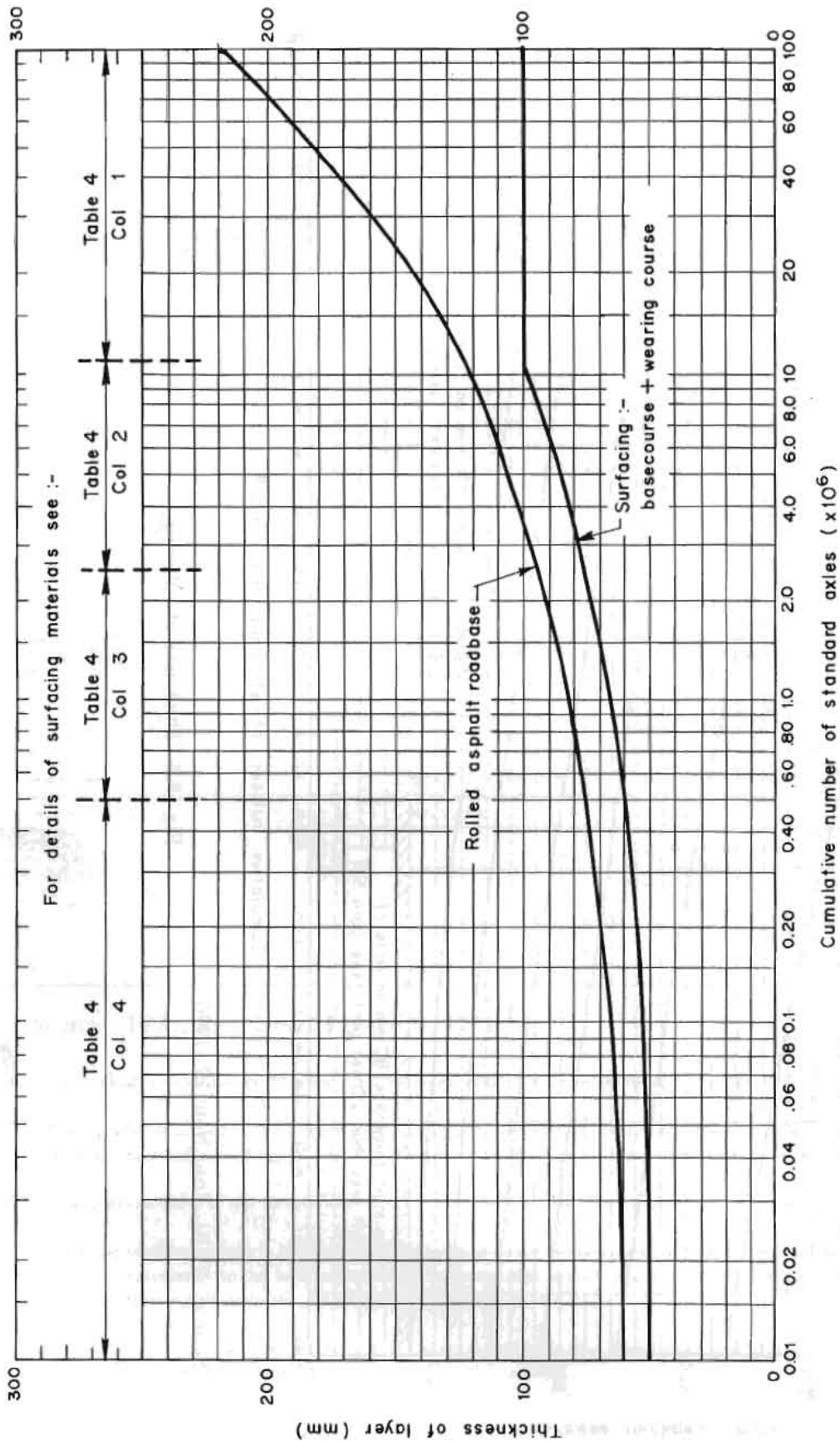
Source: TRRL Road Note 29 (Note 1), 1970

1. The thickness of all layers of bituminous surfacing should be consistent with appropriate British Specification.
2. When gravel other than limestone is used, 2 per cent of Portland should be added to the mix and the percentage of fine aggregate reduced accordingly.
3. Gravel tarmacadam is not recommended as base course for roads designed to carry more than 2.5 million standard axles.
4. When the wearing course is neither rolled asphalt nor dense tar surfacing, and where it is not intended to apply a surface dressing immediately to the wearing course, it is essential to seal the construction against the ingress of water by applying a surface dressing either to the road base or to the base course.
5. Under a wearing course of rolled asphalt or dense tar surfacing, the base course should consist of rolled asphalt to BS 594 (Clause 902) or of dense coated macadam (Clause 903 or 904).



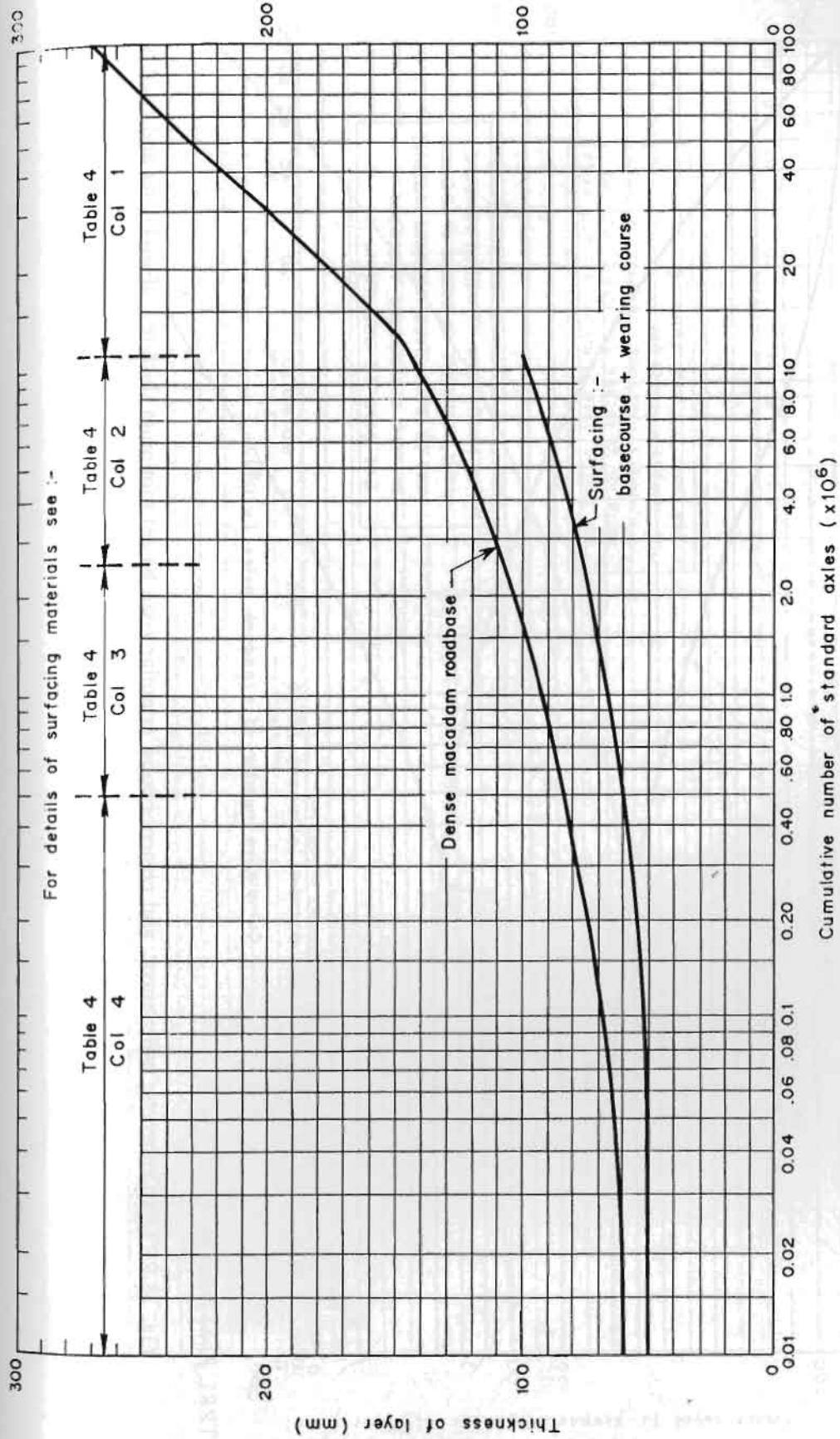
Source: TRRL Road Note 29, 1970

Fig 18.6 Thickness of sub-base



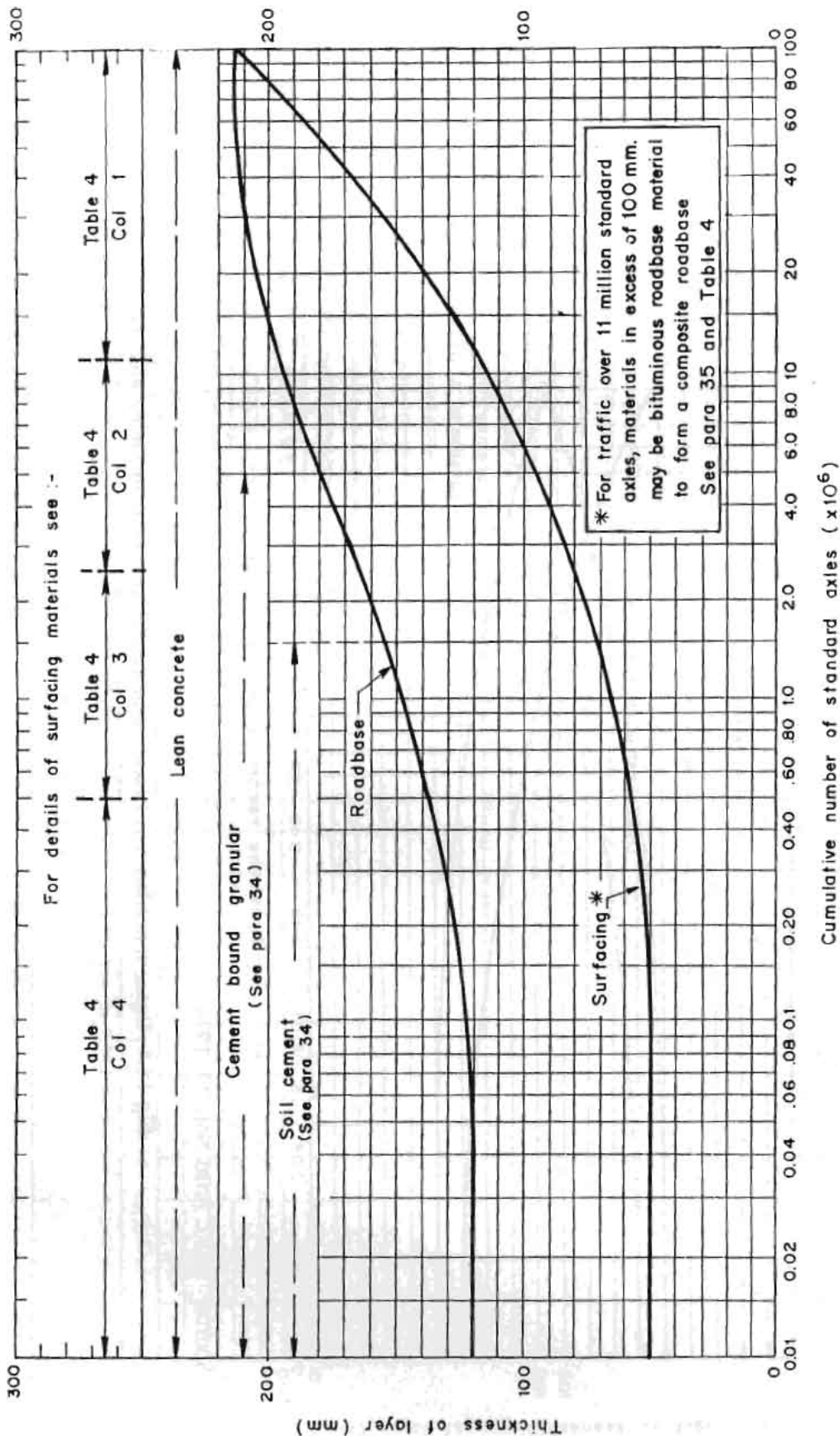
Source: TRRL Road Note 29, 1970

Fig 18.7 Rolled asphalt road base: minimum thickness of surfacing and road base



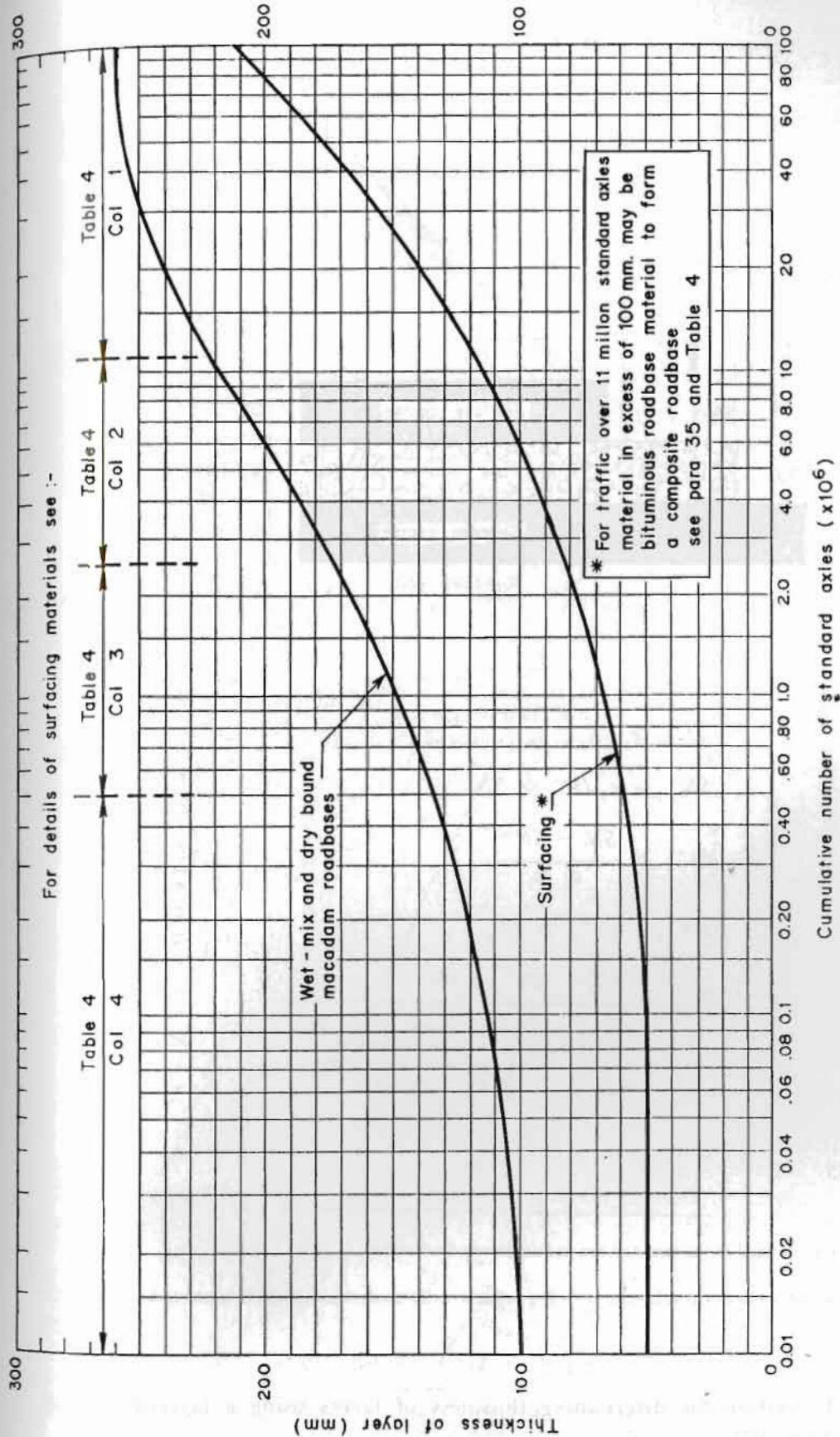
Source: TRRL Road Note 29, 1970

Fig 18.8 Dense macadam road base: minimum thickness of surfacing and road base



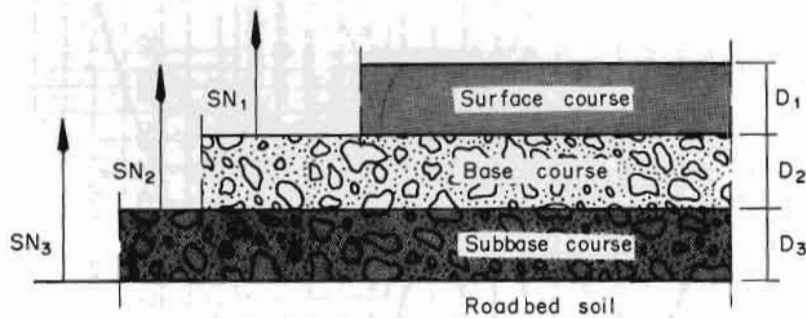
Source: TRRL Road Note 29, 1970

Fig. 18.9 Lean concrete, soil cement, and cement-bound granular road bases: minimum thickness of surfacing and road base



Source: TRRL Road Note 29, 1970

Fig. 18.10 Wet-mix and dry-bound macadam road base; minimum thickness of surfacing and road base



$$D^*_{\cdot 1} \geq SN_1 a_1$$

$$SN^*_{\cdot 1} = a_1 D^*_{\cdot 1} \geq SN_1$$

$$D^*_{\cdot 2} \geq \frac{SN_2 - SN^*_{\cdot 1}}{a_2 m_2}$$

$$SN^*_{\cdot 1} + SN^*_{\cdot 2} \geq SN_2$$

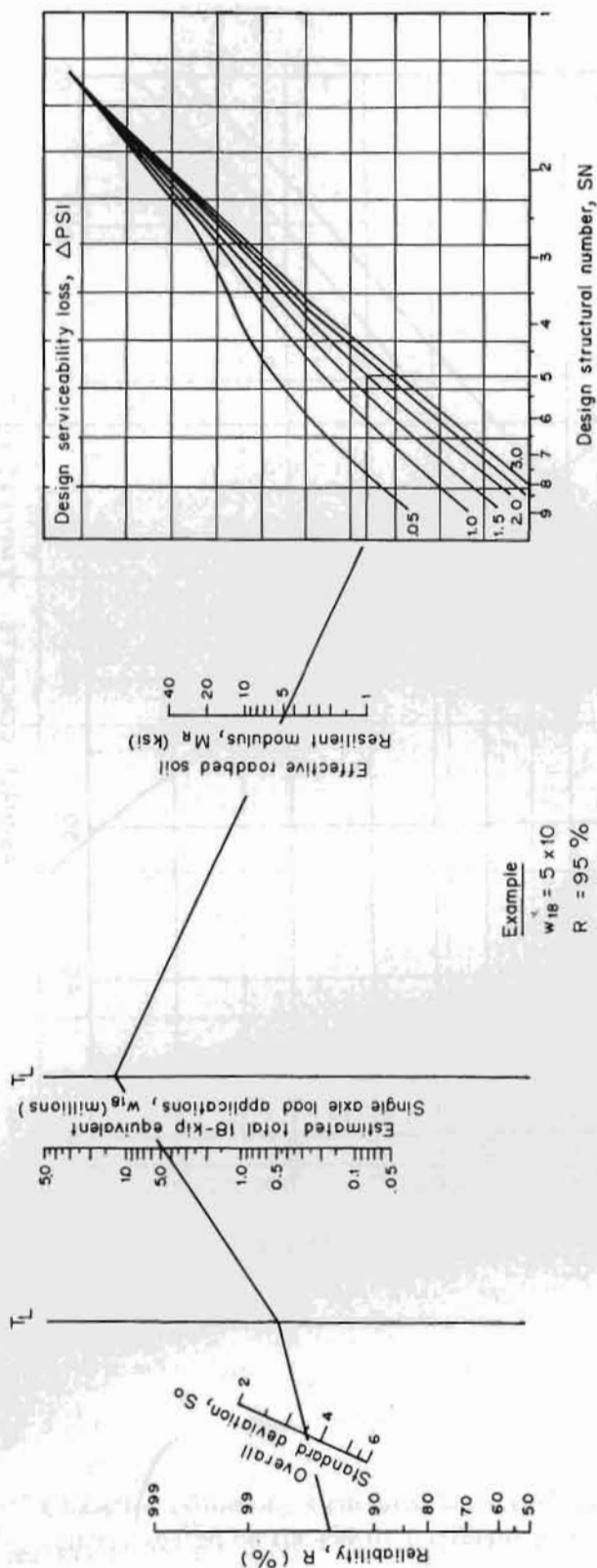
$$D^*_{\cdot 3} \geq \frac{SN_3 - (SN^*_{\cdot 1} + SN^*_{\cdot 2})}{a_3 m_3}$$

Source: AASHTO 1985

- 1) a , D , m and SN are as defined in the text and are minimum required values.
- 2) An asterisk with D or SN indicates that it represents the value actually used, which must be equal to or greater than the required value.

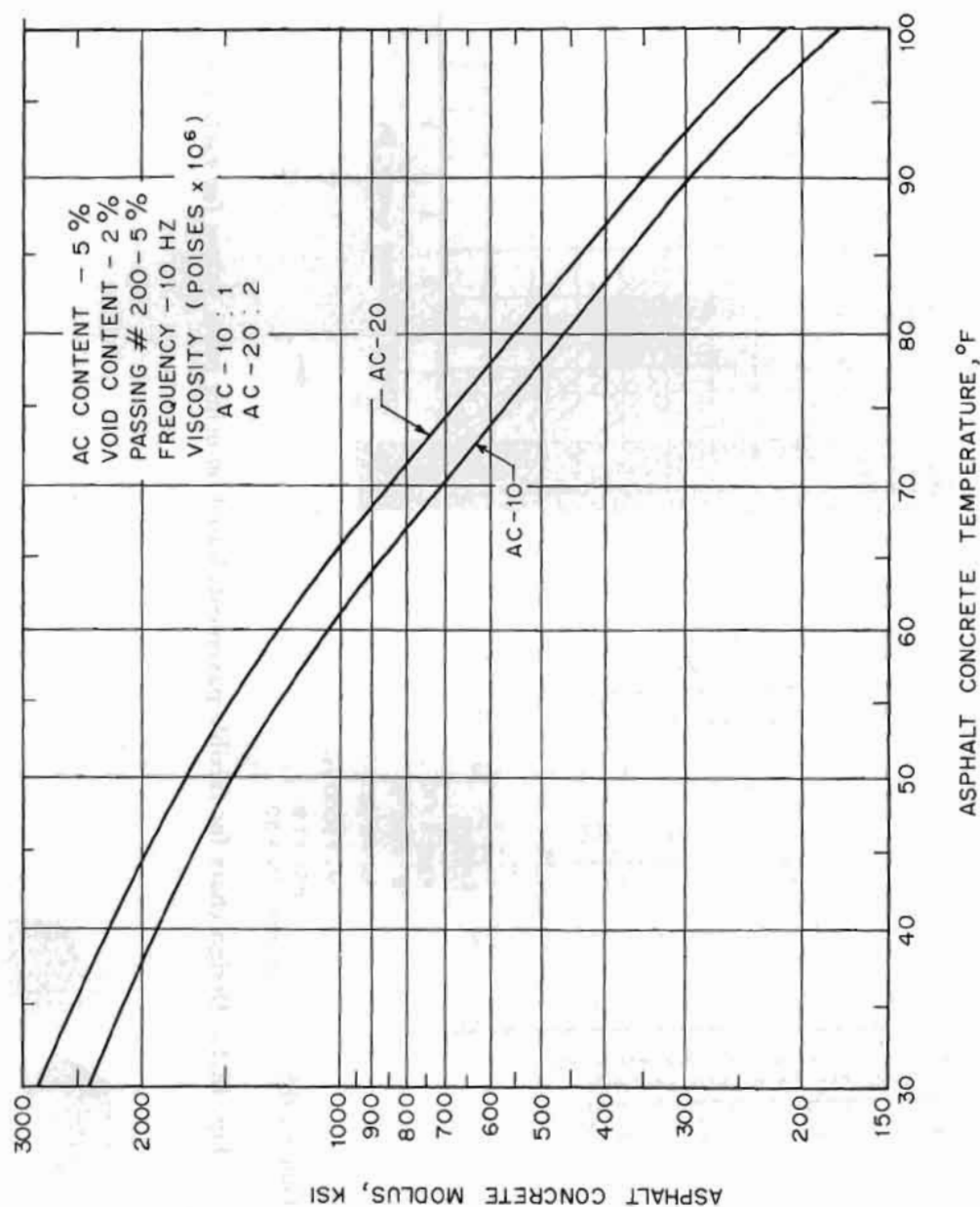
Fig. 18.11 Procedure for determining thickness of layers using a layered analysis approach

$$\log_{10} 18 = Z_R * S_o + 9.36 * \log_{10}(SN + 1) - 0.20 + \frac{\log_{10} \left[\frac{\Delta PSI}{4.2 - 1.5} \right] + 2.32 * \log_{10} M_R - 8.07}{0.40 + \frac{1094}{SN + 1^{5.19}}}$$



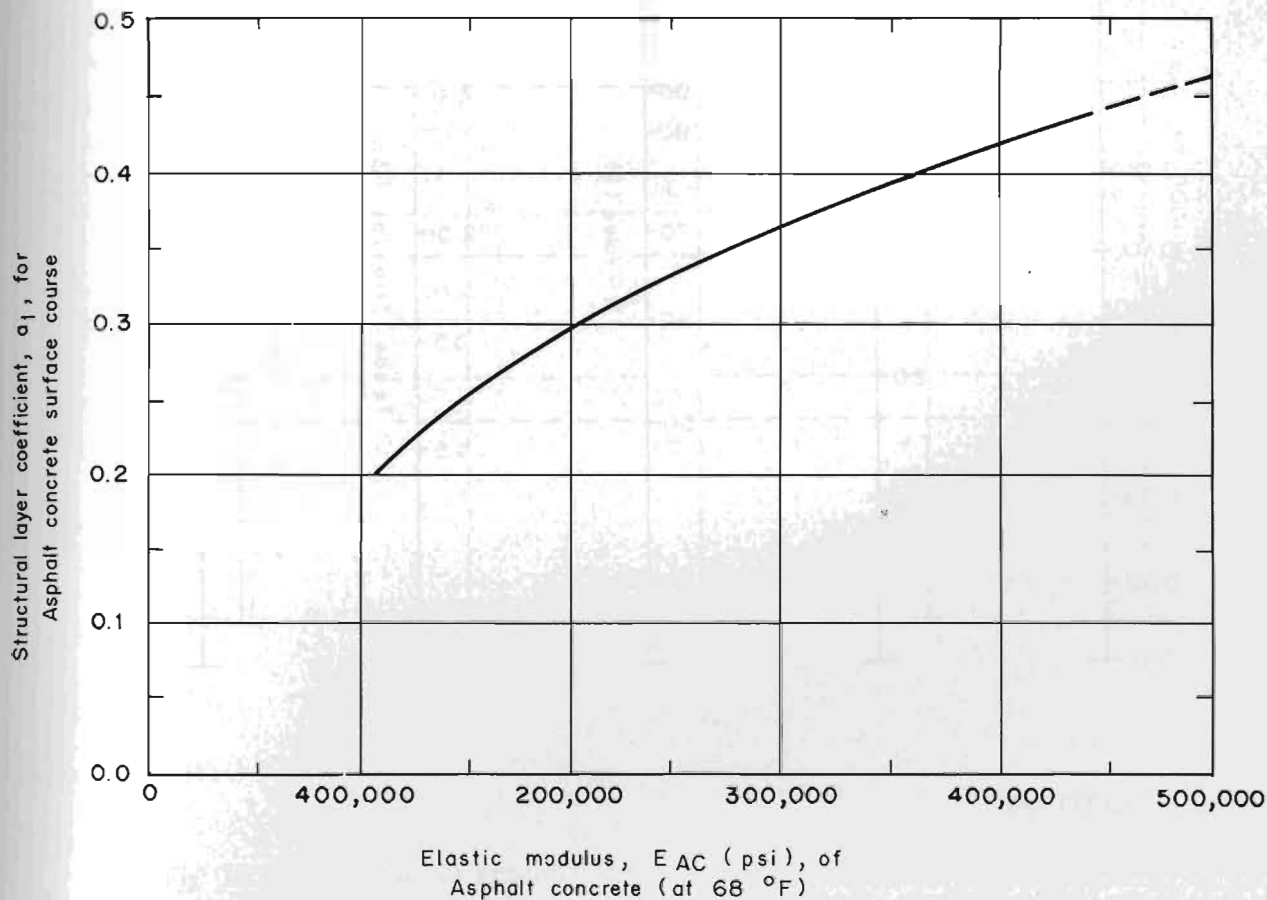
Source: AASHTO Design Guide 1985

Fig. 18.12 Design chart for flexible pavements based on using mean values for each input



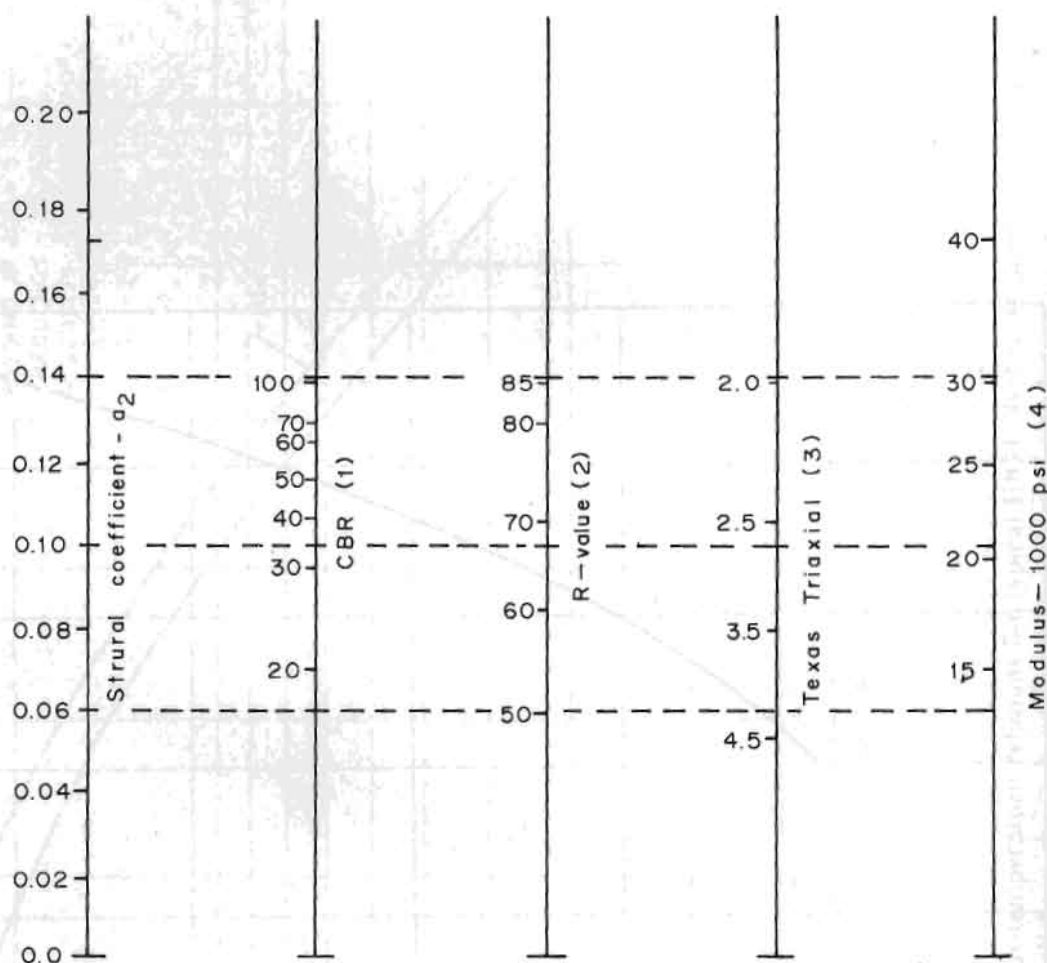
Source: Thompson and Cation 1986

Fig 18.13 Asphalt concrete modulus-temperature relations for typical IDOT (Illinois Department of Transportation) Class I



Source : AASHTO 1985

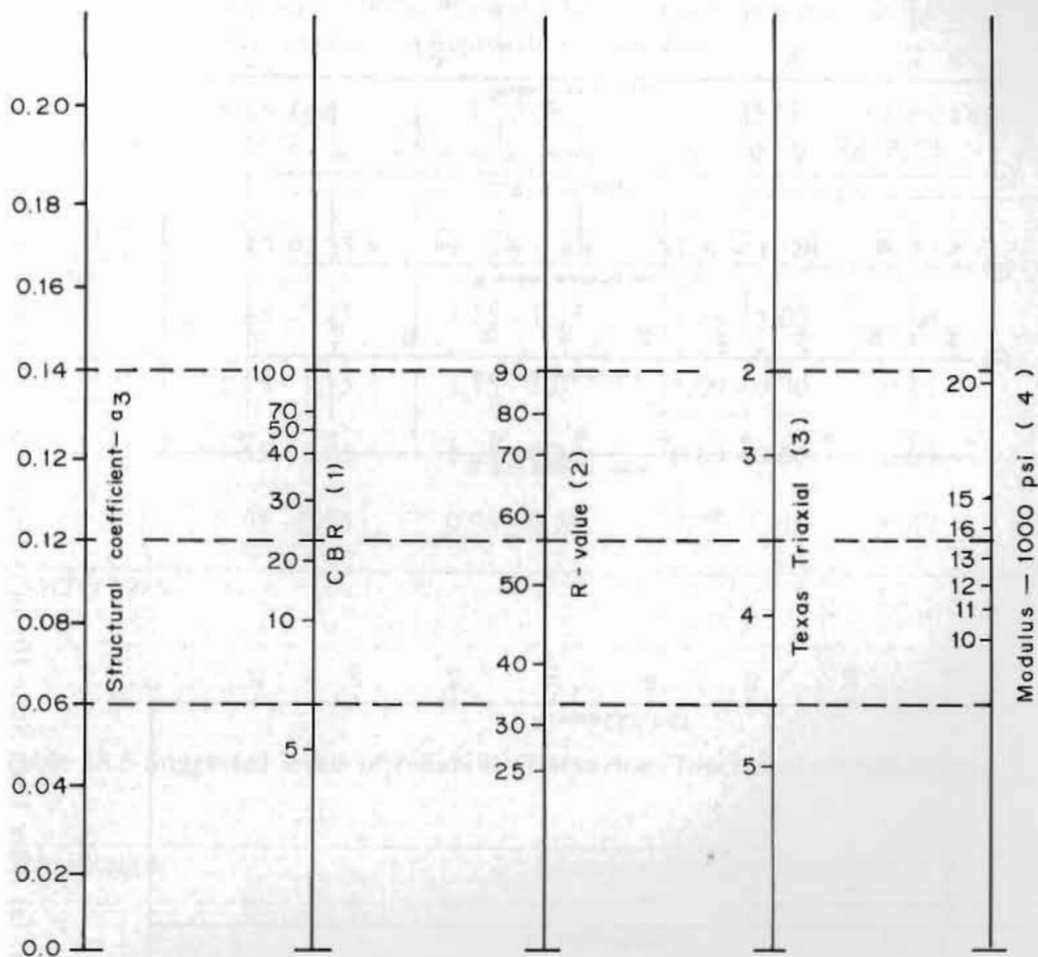
Fig. 18.14 Chart for estimating structural layer coefficient of dense-graded asphalt concrete based on the elastic (resilient) modulus



Source: AASHTO 1985

Fig. 18.15 Variation in granular base layer coefficient (a_2) with various base strength parameters

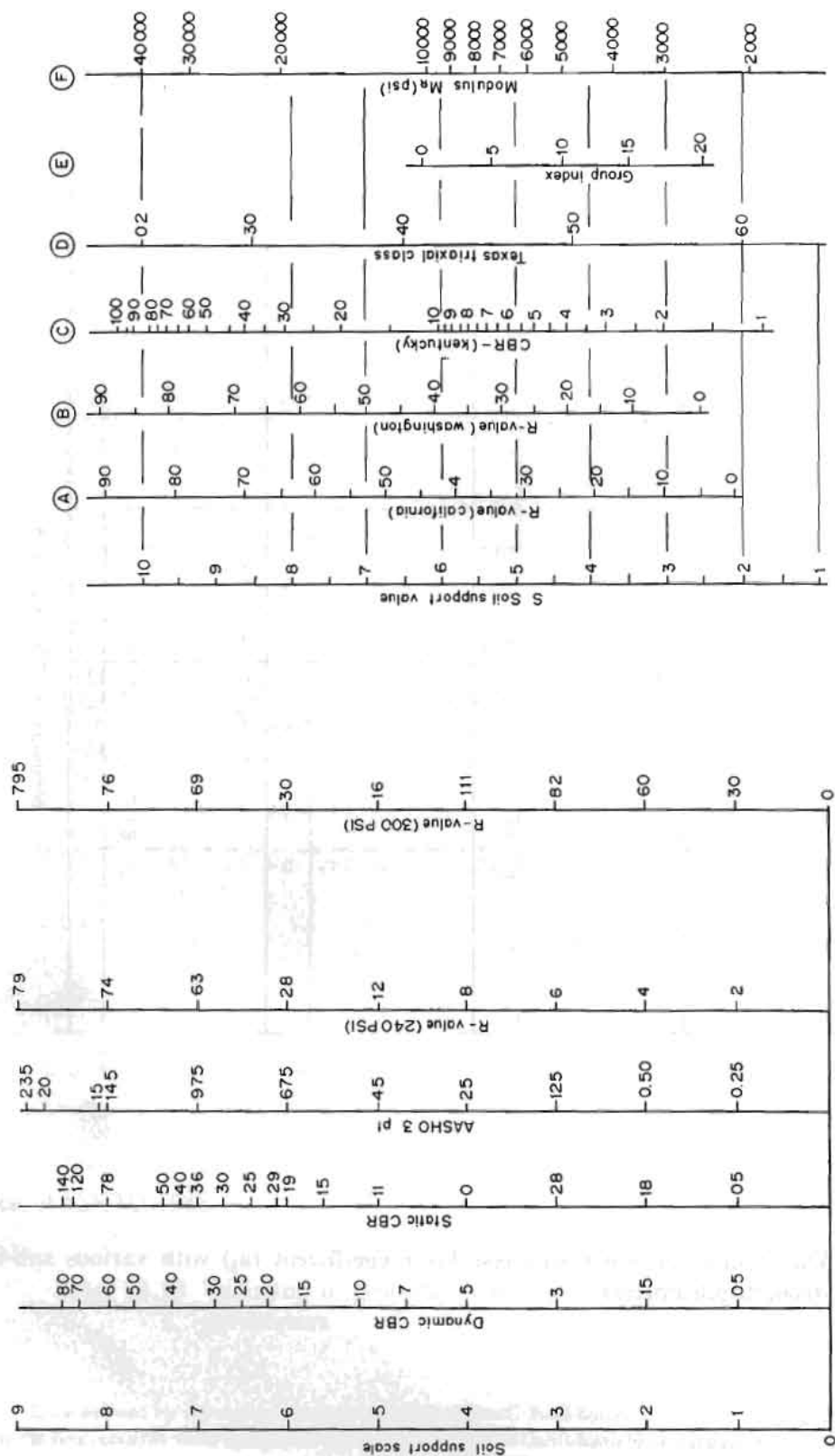
- (1) Scale derived by averaging correlations obtained from Illinois.
- (2) Scale derived by averaging correlations obtained from California, New Mexico, and Wyoming.
- (3) Scale derived by averaging correlations obtained from Texas.
- (4) Scale derived on National Cooperative Highway Research Programme (NCHRP) project (3)



Source: AASHTO 1985

Fig. 18.16 Variation in granular sub-base layer coefficient (a_2) with various sub-base strength parameters

- (1) Scale derived by averaging correlations obtained from Illinois.
- (2) Scale derived by averaging correlations obtained from The Asphalt Institute, California, New Mexico, and Wyoming.
- (3) Scale derived by averaging correlations obtained from Texas.
- (4) Scale derived by the NCHRP project (3)



Source: Yoder and Witczak 1975

Fig. 18.17 Soil support value correlations. (a) After Utah State Highway Department and (b) from Van et al. (NCHRP 128)

Table 18.4 Recommended m_1 values for modifying structural layer coefficient of untreated base and sub-base materials in flexible pavements

Quality of Drainage	Per cent of Time Pavement Structure is Exposed to Moisture Levels Approaching Saturation			
	Less Than 1 %	1 - 5 %	5 - 25 %	Greater Than 25 %
Excellent	1.40 - 1.35	1.35 - 1.30	1.30 - 1.20	1.20
Good	1.35 - 1.25	1.25 - 1.15	1.15 - 1.00	1.00
Fair	1.25 - 1.15	1.15 - 1.05	1.00 - 0.80	0.80
Poor	1.15 - 1.05	1.05 - 0.80	0.80 - 0.60	0.60
Very Poor	1.05 - 0.95	0.95 - 0.75	0.75 - 0.40	0.40

Source : AASHTO 1985

Table 18.5 Suggested levels of reliability for various functional classifications

Functional Classification	Recommended Level of Reliability	
	Urban	Rural
Interstate and other freeways	85 - 99.9	80 - 99.9
Principle arterials	80 - 99	75 - 95
Collectors	80 - 95	75 - 95
Local	50 - 80	50 - 80

Source: AASHTO 1985

Note: Results based on a survey of the AASHTO Pavement Design Task Force

Table 18.6 Minimum thickness (inches)

Traffic, ESAL'S		Asphalt Concrete	Aggregate Base
less than	50,000	1.0 (or surface treatment)	4
50,001 -	150,000	2.0	4
150,001 -	500,000	2.5	4
500,001 -	2,000,000	3.0	6
2,000,001 -	7,000,000	3.5	6
greater than	7,000,000	4.0	6

Source : AASHTO 1985

Table 18.7 Analysis periods for pavement design

Highway Conditions	Analysis Period (years)
High volume, urban	30 - 50
High volume, rural	20 - 50
Low volume, paved	15 - 25
Low volume, aggregate surface	10 - 20

Table 18.8 Design of pavement by mechanistic - empirical method using CHEVPC computer programme

Eac psi	Thickness of Layers inches	ϵ_1	ϵ_{v2}	Fatigue Life Finn model A.C.		Rutting Life Finn Model
				10% crack	45% crack	
				Nf	Nf	Nr
500000	8.50	157.36	343.6	2.58E+6	2.83E+6	4.57E+6
500000	7.50	187.80	405.80	1.45E+6	159E+6	2.17E+6
200000	11	1.87	439.40	2.15E+6	2.35E+6	1.52E+6
200000	12	184.70	389.08	3.33E+6	3.65E+6	2.62E+6
500000	5,7,10	326.60	276.80	2.34E+6	2.56E+5	1.20E+6
500000	5,10,10	226.89	274.50	7.76E+5	8.49E+5	1.25E+7
500000	5,15	221.40	315.04	8.40E+5	9.19E+5	4.15E+6
500000	5,15,10	219.40	208.56	8.65E+5	9.46E+6	4.29E+7
200000	8,7,10	237.70	271.80	1.45E+6	1.59E+6	1.31E+7
200000	8,10,10	228.70	230.10	1.65E+6	1.81E+6	2.76E+7
200000	8,15	222.80	292.58	1.80E+6	1.97E+6	9.39E+6
200000	8,15,10	220.78	177.50	1.85E+6	2.03E+6	8.83E+7

Failure Criteria:

Finn,
Fatigue:

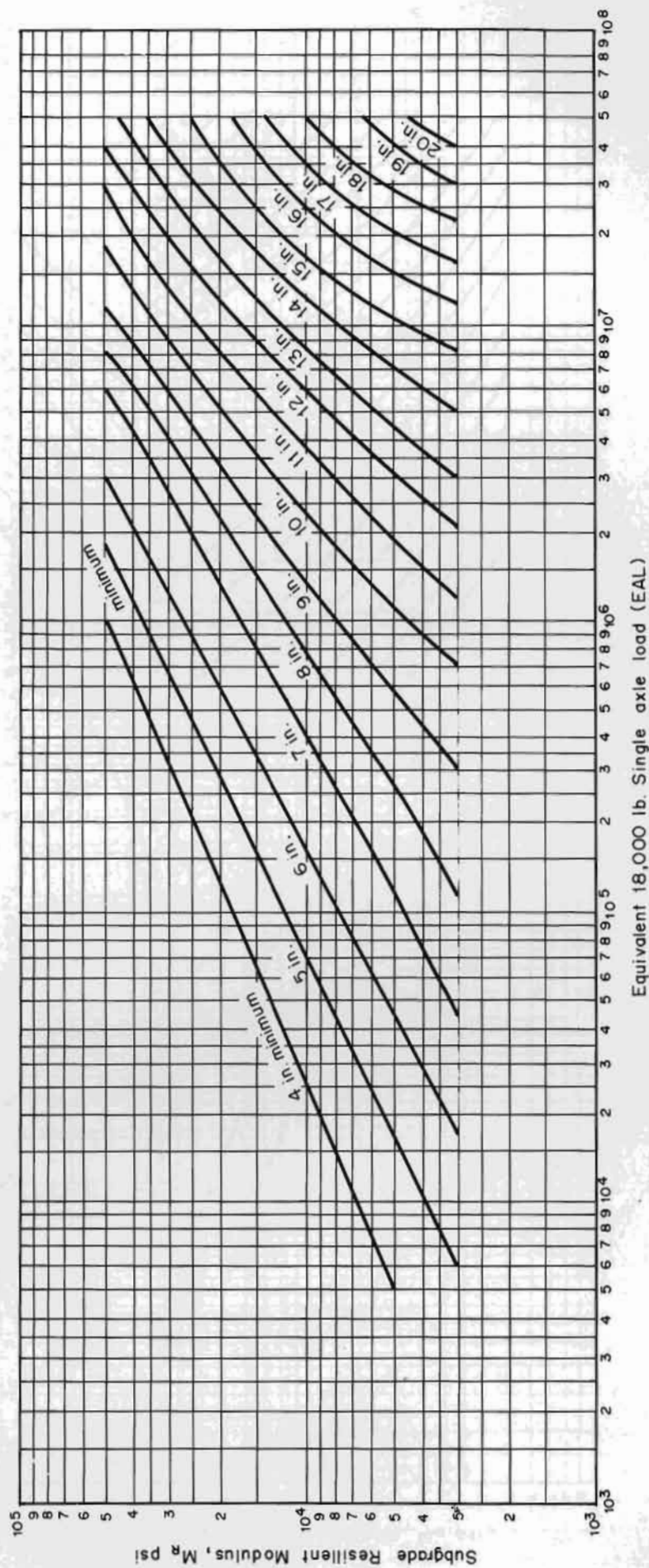
$$\leq 10\% \log Nf = 15.947 - 3.291 \times \log \epsilon_1 / 10^{-6} - .854 \times \log MR / 1000$$

$$\leq 45\% \log Nf = 15.986 - 3.291 \times \log \epsilon_1 / 10^{-6} - .854 \times \log MR / 1000$$

Rutting:

$$Nr = 1.07 \times 10^{18} \times (1/cv)^{4.483}$$

Full-depth asphalt concrete

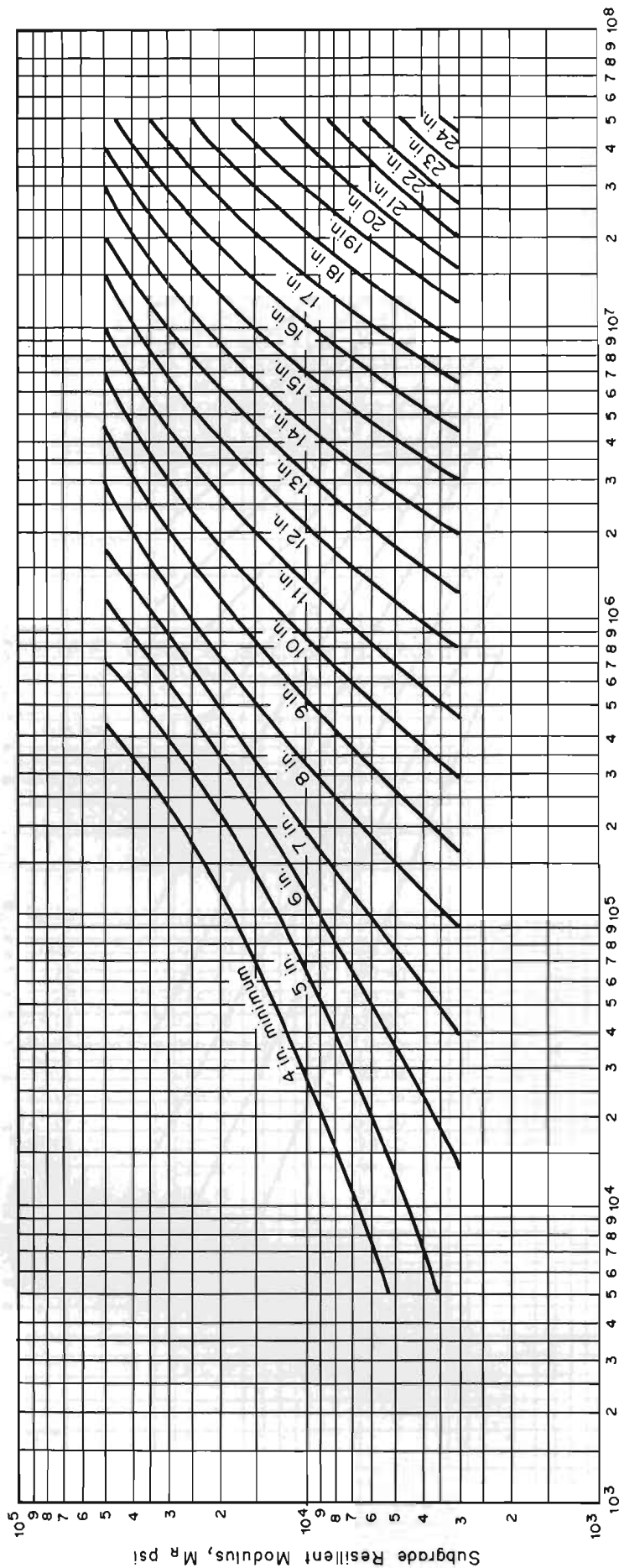


Source: Asphalt Institute 1981

Fig 18.18 Design chart

Emulsified asphalt mix type II

(Emulsified asphalt mixes made with semi processes, crusher run, pit-run, or bank run aggregates)

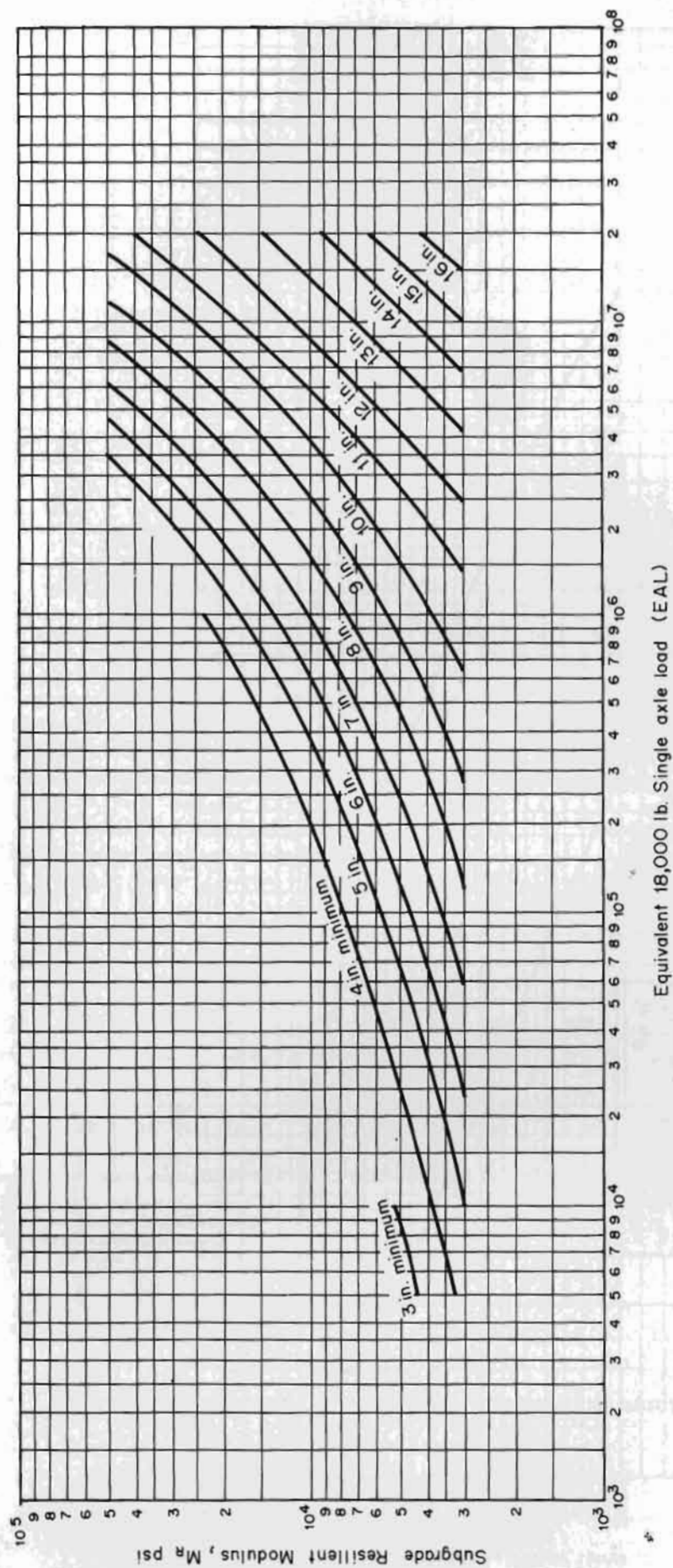


Equivalent 18,000 lb. Single-axle load (EAL)

Source: Asphalt Institute 1981

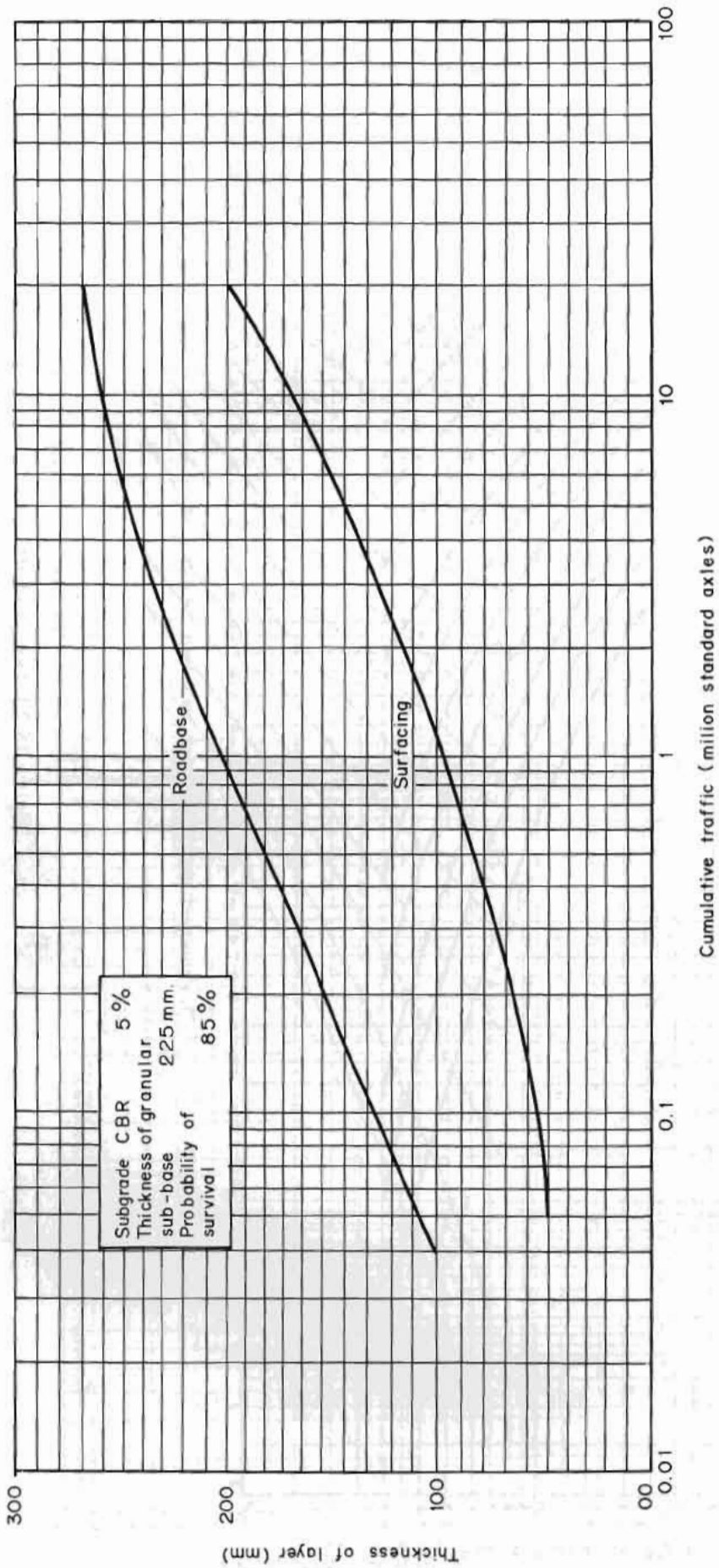
Fig 18.19 Design chart

Untreated aggregate base 6.0 in thickness



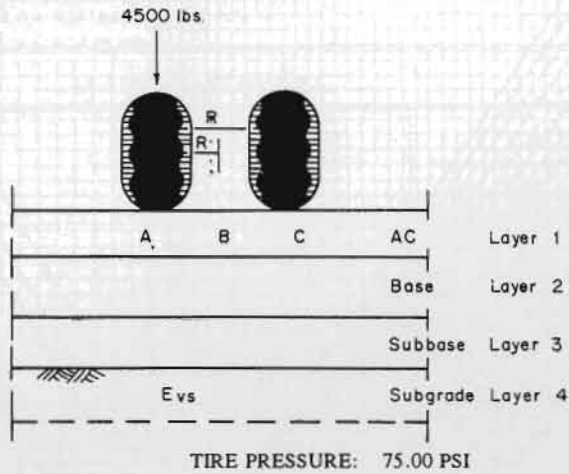
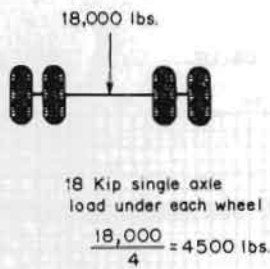
Source: Asphalt Institute 1981

Figure 18.20 Design chart



Source: TRRL Laboratory Report 1132, 1984

Figure 18.21 Design curves for roads with wet mix road base



THE PROBLEM PARAMETERS ARE

TOTAL LOAD: 4500.00 LBS
LOAD RADIUS: 4.37 IN.

LAYER 1 HAS MODULUS 5,00000
LAYER 2 HAS MODULUS 10500

POISSON'S RATIO 0.350
POISSON'S RATIO 0.450

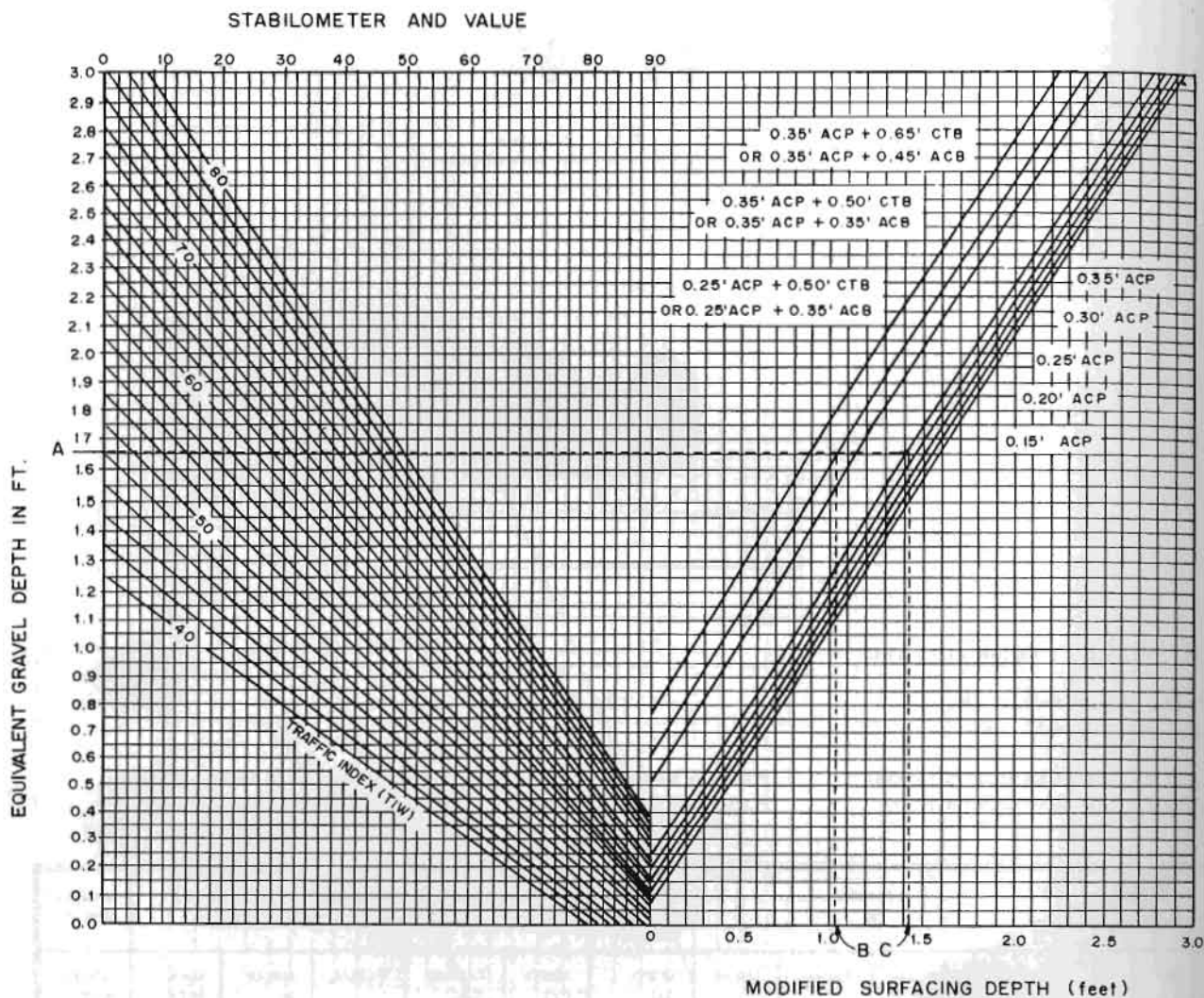
AND THICKNESS 8.50 IN.
AND IS SEMI-INFINITE

Location		STRESSES PSI				DEF- LECTION INCHES	STRAINS MICRO INCHES/INCH					ANGLE DEG
R	Z	VERTI- CAL	TANGEN- TIAL	RADIAL	SHEAR	VERTI- CAL	VERTI- CAL	TANGEN- TIAL	RADIAL	SHEAR IN MICRO RAD.	MAX. PRIN. IN TENS- ILE DIP	WITH P. AXIS
0.00	-8.50	-3.2648	71.7945	71.7545	0.0000	0.007855	-107.04	95.62	95.62	0.00	95.62	TR
0.00	8.50	-3.2648	-0.8458	-0.8458	0.0000	0.007855	-238.44	95.62	95.62	0.00	95.62	TR
5.50	-8.50	-2.6379	53.4541	42.5668	-0.5544	0.007474	-72.77	78.68	50.36	-2.99	78.68	T DIP
5.50	8.50	-2.6379	-0.8240	-1.0291	-0.5544	0.007474	-171.81	78.68	50.36	-153.13	78.68	T DIP
11.00	-8.50	-1.7787	30.2756	14.1699	-0.5118	0.006699	-34.67	51.88	8.39	-2.76	51.88	T DIR
11.00	8.50	-1.7787	-0.7226	-1.0375	-0.5118	0.006699	-98.97	51.88	8.39	-141.36	51.98	T DIR

Note: Maximum strain under dual wheel load
= [strain at B due to load under each wheel],
or [strain at A due to load at A and C],
whichever is greater.

Example,
et = 95.62 + 51.8 = 147.42, or 2 x 78.68 = 157.36
therefore adopt, et = 157.36

Figure 18.22 Example of stress, strain calculations using CHEVPC



Source: University of Washington 1986

Fig. 18.23 Structural design chart for flexible pavement

TRAFFIC INDEX, $T_1 = 6.7 (EWL/10^6)$, EWL = equivalent 5000 lb wheel load in one direction

EXAMPLE:

given an R Value of 25 and a traffic index of 6.0, cover thickness requirements can be determined as follows: an equivalent gravel depth of 1.65' (round to 1.7) at point A. A modified surfacing depth of 1.05 ft at point B for a pavement of 0.35 ft ACP + 0.50 ft CTB, or 0.35 ft ACP + 0.35 ft ACB. A modified surfacing depth of 1.43 ft (round to 1.45) for pavement of 0.35 ft ACP.

AC, D = 0.35

Untreated Base,

$D = 1.45 - 0.35 = 1.10$ ft

Table 18.9 Minimum pavement designs

MAIN ROADWAYS			
TRAFFIC INDEX	PAVEMENT	TREATED BASE	
		CTB	ACB
7.0 or more	0.35 Ft. ACP	0.65 Ft.	0.45 Ft.
6.5 to 6.9	0.35 Ft. ACP	0.50 Ft.	0.35 Ft.
6.4 or less	0.25 Ft.	0.50 Ft.	0.35 Ft.
RAMPS			
TRAFFIC INDEX	PAVEMENT	TREATED BASE	
7.0 or more	0.25 Ft. ACP	0.60 Ft. PCC	
6.5 to 6.9	0.35 Ft. ACP	0.35 Ft. ACP	
	0.25 Ft. ACP	0.50 Ft. PCC	
5.7 to 6.4	0.25 Ft. ACP	0.50 CTB or 0.35 Ft. ACB	
5.0 to 5.6	0.30 Ft. ACP	Untreated	
4.9 or less	0.15 Ft. ACP	Untreated	
In arid-areas BST may be used			
REST AREAS			
DESIGNATED AREA	PAVEMENT	TOP COURSE	
RAMPS, ACCESS ROADS, AND TRUCK PARKING	0.35 Ft. ACP	0.30 Ft. crushed surfacing	
CAR PARKING	0.25 Ft. ACP		

Source: University of Washington 1986

Table 18.10 Minimum depths of crushed surfacing for flexible pavements

UNDER BITUMINOUS PAVEMENT AND TREATED BASES		
TYPE OF PAVEMENT OR TREATED BASE	MINIMUM CRUSHED SURFACING DEPTH WHERE BASE IS:	
	GRAVEL BASE CLASS A OR BALLAST	GRAVEL BASE CLASS B OR SUB-GRADE
HIGH (a) (e)	0.20 ft	0.30 ft
INTERMEDIATE	0.20 ft	0.30 ft
LOW	0.25 ft	0.35 ft
ACB	0.15 ft (or 0.20 ft) (b)	0.20 ft (or 0.25 ft) (b)
CTB	None (c)	0.05 ft (d)
NOTES:		
a)	Applies when exceptions are allowed in arid areas and treated base is not required.	
b)	Use where traffic index is equal to or greater than 7.0.	
c)	Requires only sufficient fine material for keying and levelling. May be crushed or screened. Usually CTB aggregate.	
d)	0.10 ft minimum depth of crushed CTB aggregate may be used instead.	
e)	Includes Portland Cement Concrete pavement.	
ON SHOULDERS		
TYPE OF SHOULDER TREATMENT	MINIMUM CRUSHED SURFACING DEPTH WHERE BASE IS:	
	GRAVEL BASE CLASS A OR BALLAST	GRAVEL BASE CLASS B OR SUB-GRADE
0.15 Ft ACP BST	0.15 ft 0.20 ft	0.20 ft 0.25 ft
On ramps, frontage roads, and other miscellaneous lines these values may be reduced 0.05 ft		
Pavement types shown are divided into the following categories.		
High	Asphalt concrete pavement 0.25 ft minimum on treated base.	
Intermediate	Asphalt concrete pavement on untreated base.	
Low	Bituminous surface treatment.	
Exceptions are permitted in arid areas.		

Source : University of Washington 1986

Table 18.11 Flexible pavement design catalogue for low-volume roads

Tables 18.10 and 18.11 present a catalogue of flexible pavement SN-values (structural numbers) that may be used for the design of low-volume roads when the more detailed design approach is not possible. Table 18.10 is based on the 50 per cent reliability level and Table 18.11 is based on the 75 per cent level. The range of SN shown for each condition is based on a specific range of 18 kip ESAL applications at each traffic level :

High	:	700,000	to	1,000,000
Medium	:	400,000	to	600,000
Low	:	50,000	to	30,000

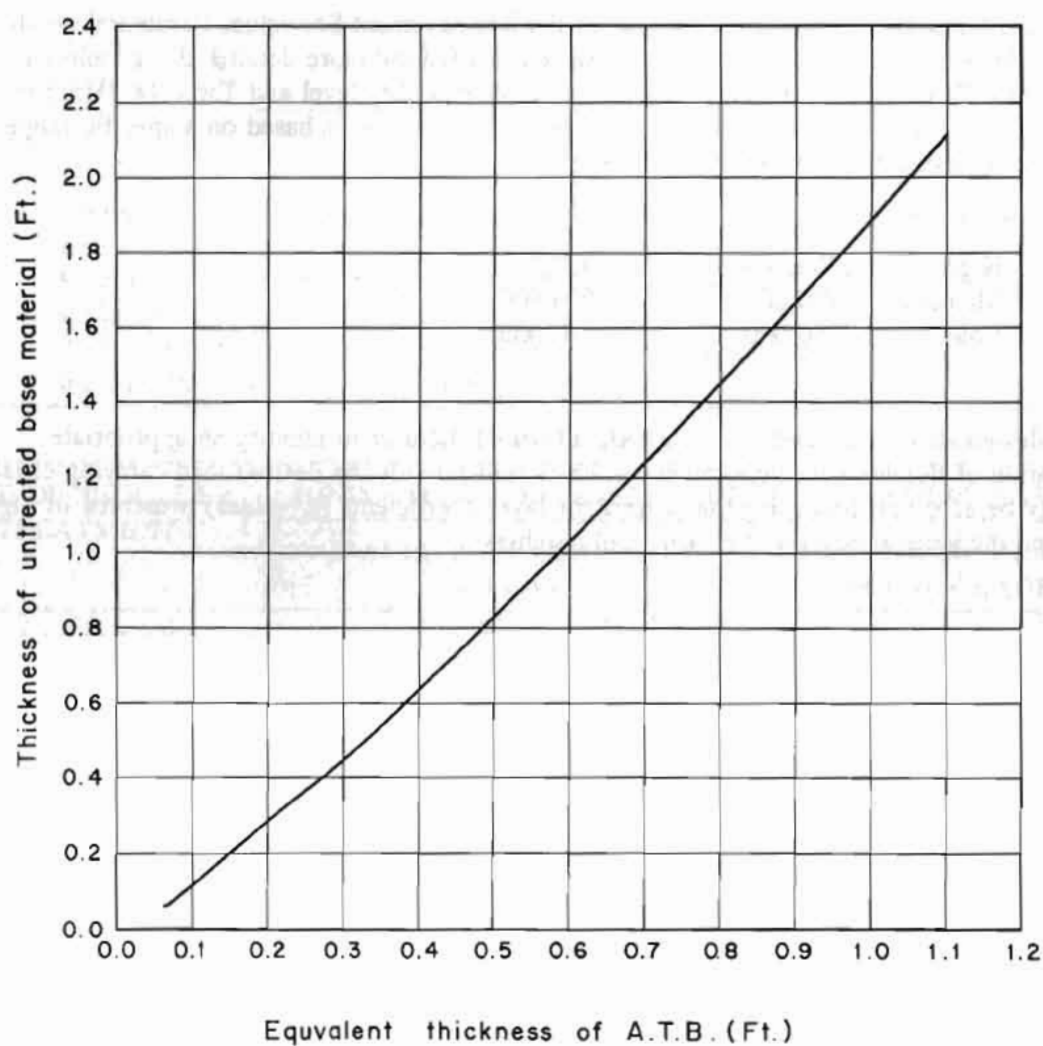
Once a design structural number is selected, it is up to the user to identify an appropriate combination of flexible pavement thickness which will provide the desired load-carrying capacity. This may be accomplished using the criteria for layer coefficients (a_i -values) presented in Figure 18.15 and the general equation for structural numbers :

$$SN = a_1D_1 + a_2D_2 + a_3D_3$$

a_1, a_2, a_3 = layer coefficient for surface, base, and sub-base course materials, respectively, and
 D_1, D_2, D_3 = thickness (in inches) of surface, base, and sub-base course, respectively.

Source: AASHTO 1985

A.T.B. DESIGN CHART



Source: University of Washington

Fig. 18.24 Design chart

Table 18.12 Flexible pavement design catalogue for low-volume roads: recommended ranges of structural number (SN) for six U.S. climate regions, three levels of axle load traffic, and five levels of roadbed soil quality: inherent reliability 50%

Relative Quality of Roadbed Soil	Traffic Level	U.S. Climatic Region					
		I	II	III	IV	V	VI
Very Good	High	2.3-2.5 ¹	2.5-2.7	2.8-3.0	2.1-2.3	2.4-2.6	2.8-3.0
	Medium	2.1-2.3	2.3-2.5	2.5-2.7	1.9-2.1	2.2-2.4	2.5-2.7
	Low	1.5-2.0	1.7-2.2	1.9-2.4	1.4-1.8	1.6-2.1	1.9-2.4
Good	High	2.6-2.8	2.8-3.0	3.0-3.2	2.5-2.7	2.7-2.9	3.0-3.2
	Medium	2.4-2.6	2.6-2.8	2.8-3.0	2.2-2.4	2.5-2.7	2.7-2.9
	Low	1.7-2.3	1.9-2.4	2.0-2.7	1.6-2.1	1.8-2.4	2.0-2.6
Fair	High	2.9-3.1	3.0-3.2	3.1-3.3	2.8-3.0	2.9-3.1	3.1-3.3
	Medium	2.6-2.8	2.8-3.0	2.9-3.1	2.5-2.7	2.6-2.8	2.8-3.0
	Low	2.0-2.6	2.0-2.6	2.1-2.8	1.9-2.4	1.9-2.5	2.1-2.7
Poor	High	3.2-3.4	3.3-3.5	3.4-3.6	3.1-3.3	3.2-3.4	3.4-3.6
	Medium	3.0-3.2	3.0-3.2	3.1-3.4	2.8-3.0	2.9-3.2	3.1-3.3
	Low	2.2-2.8	2.2-2.9	2.3-3.0	2.1-2.7	2.2-2.8	2.3-3.0
Very Poor	High	3.5-3.7	3.5-3.7	3.5-3.7	3.3-3.5	3.4-3.6	3.5-3.7
	Medium	3.2-3.4	3.3-3.5	3.3-3.5	3.1-3.3	3.1-3.3	3.2-3.4
	Low	2.4-3.1	2.4-3.1	2.4-3.1	2.3-3.0	2.3-3.0	2.4-3.1

Source: AASHTO 1985

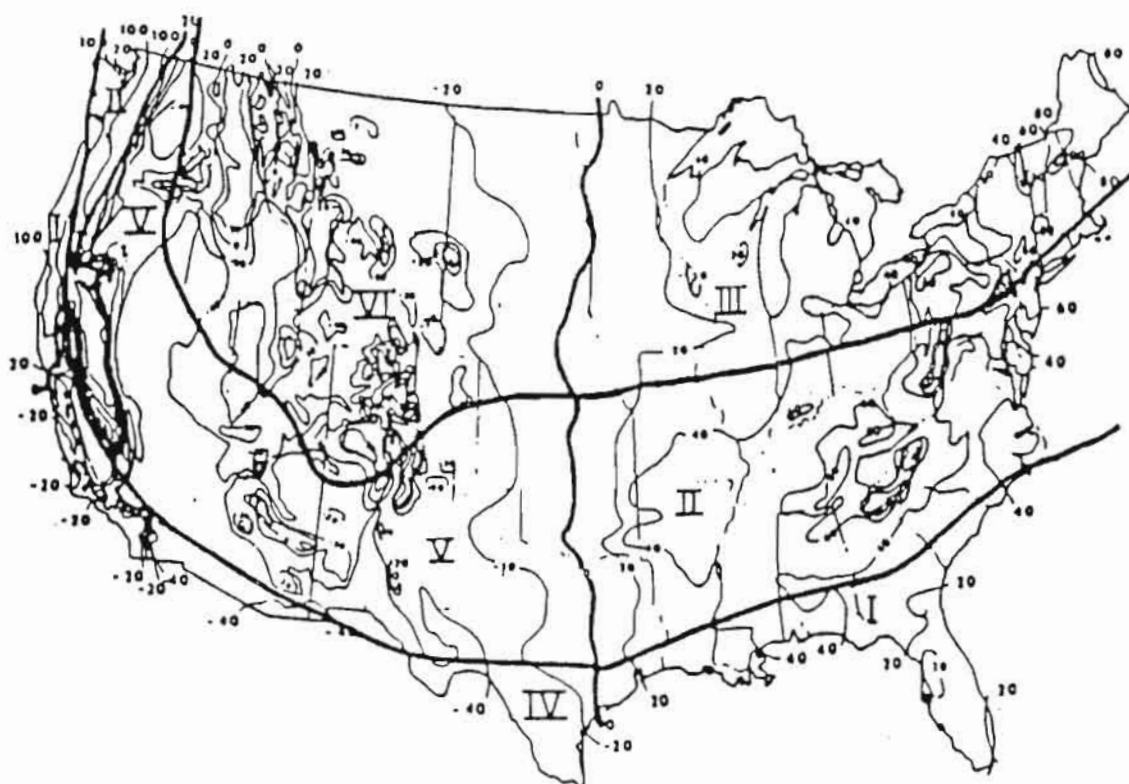
¹ Recommended range of structural number (SN).

Table 18.13 Flexible pavement design catalogue for low-volume roads: recommended ranges of structural number (SN) for six U.S. climate regions, three levels of axle load traffic and five levels of roadbed soil quality: inherent reliability, 75%

Relative Quality of Roadbed Soil	Traffic Level	U.S. Climatic Region					
		I	II	III	IV	V	VI
Very Good	High	2.6-2.7 ¹	2.8-2.9	2.8-3.0	2.1-2.3	2.4-2.6	2.8-3.0
	Medium	2.3-2.5	2.5-2.7	2.5-2.7	1.9-2.1	2.2-2.4	2.5-2.7
	Low	1.6-2.1	1.8-2.3	1.9-2.4	1.4-1.8	1.6-2.1	1.9-2.4
Good	High	2.9-3.0	3.0-3.2	3.0-3.2	2.5-2.7	2.7-2.9	3.0-3.2
	Medium	2.6-2.8	2.7-3.0	2.8-3.0	2.2-2.4	2.5-2.7	2.7-2.9
	Low	1.9-2.4	2.0-2.6	2.0-2.7	1.6-2.1	1.8-2.4	2.0-2.6
Fair	High	3.2-3.3	3.3-3.4	3.1-3.3	2.8-3.0	2.9-3.1	3.1-3.3
	Medium	2.8-3.1	2.9-3.2	2.9-3.1	2.5-2.7	2.6-2.8	2.8-3.0
	Low	2.1-2.7	2.2-2.8	2.1-2.8	1.9-2.4	1.9-2.5	2.1-2.7
Poor	High	3.5-3.6	3.6-3.7	3.4-3.6	3.1-3.3	3.2-3.4	3.4-3.6
	Medium	3.1-3.4	3.2-3.5	3.1-3.4	2.8-3.0	2.9-3.2	3.1-3.3
	Low	2.4-3.0	2.4-3.0	2.3-3.0	2.1-2.7	2.2-2.8	2.3-3.0
Very Poor	High	3.8-3.9	3.8-4.0	3.5-3.7	3.3-3.5	3.4-3.6	3.5-3.7
	Medium	3.4-3.7	3.3-3.5	3.3-3.5	3.1-3.3	3.1-3.3	3.2-3.4
	Low	2.6-3.2	2.4-3.1	2.4-3.1	2.3-3.0	2.3-3.0	2.4-3.1

Source: AASHTO 1985

¹ Recommended range of structural number (SN).



REGION	CHARACTERISTICS
I	Wet, no freeze
II	Wet, freeze - thaw cycling
III	Wet, hard-freeze, spring thaw
IV	Dry, no freeze
V	Dry, freeze - thaw cycling
VI	Dry, hard freeze, spring thaw

Source: AASHTO 1985

Table 18.13(a) The six climatic regions in the United States

REGION	CHARACTERISTICS
I	Wet, no freeze
II	Wet, freeze-thaw cycling
III	Wet, hard-freeze, spring thaw
IV	Dry, no freeze
V	Dry, freeze-thaw cycling
VI	Dry, hard freeze, spring thaw

18.6 OVERLAY DESIGN (Based on J.P. Mahoney, 1985)

Pavements constitute about 15-25 per cent of the total cost of hill roads. Once the road is constructed, most of the works during maintenance are related to the pavement. The maintenance of roads in developing countries incur annual expenditure as costs for maintenance agencies in the range of 1.5 to 3 per cent of the updated construction costs. In addition there are user costs such as vehicle operation, time, and accident costs, associated with the road construction.

The general trends in the maintenance of roads in developing countries are limited to i) repair of drains, potholes, shoulders, retaining walls, and culverts and ii) resealing the surface with sand seal, chip seal, or single or double bituminous surfacing at intervals of from 4 to 8 years.

Traffic growth, axle load increase, and design life, in terms of total load rather than the number of years, is seldom analyzed in deciding the periodic maintenance levels. There are instances in which the roads, that are mostly designed for a lifespan of 10 to 15 years, realize the designed load much earlier rendering the original pavement structurally inadequate. Under such circumstances, resealing or surface treatment do not contribute much since they do not enhance the structural capability of the pavement. Overlaying based on traffic and axle load study, then, is the proper answer to considerably improve the life of the pavements and cost effectiveness of the investments. Periodic maintenance decisions, after about 5 years of service, of any important road, must therefore be based on proper evaluation of pavement conditions and alternatives.

It must be remembered that pavements on weak sub-grades have a much smaller load capacity to withstand both fatigue and rutting failures, compared to pavements of a similar thickness but on stronger sub-grades. Double bituminous surface treatment (DBST) may last 4 to 6 years provided the sub-grade is strong enough to withstand failure against rutting (deformation of sub-grade) for at least that period. The purpose of DBST would then be to prevent the weakening of base, sub-base, and sub-grade by moisture seeping down from the top. Thus, if the existing pavement has 40 years of rutting life, then DBST could be good enough for periodic maintenance for seven, 5 year cycles of DBST. The purpose of periodic maintenance in this case would be to save the underlying layers from accelerated weakening. The seven, 5 year cycles of DBST could be replaced by designing the surface course for a fatigue life of 40 years at the outset. This, however, is not possible because i) asphalt pavements are subject to aging of bitumen after 12 to 15 years, ii) the initial investment would be excessively high, and iii) traffic growth is not predictable. The next choice would be to initially design for 12-15 years of fatigue life and overlay every 12-15 years.

The important thing is to assess the difference in the maintenance efforts in terms of costs, investment levels, practicability, and reliability in choosing among 4 to 6 year cycles of DBST, 12-15 year cycle overlays, or 40 year cycle rigid pavements. In the case of a pavement on weak sub-grades, having a shorter life in terms of failure from rutting, there is no choice other than overlaying or new construction. DBST on these pavements will have a much shorter life than the normal 4-6 years for DBST. This section aims to present an example of practical situations in dealing with periodic maintenance of road pavements through overlay design by various methods. The example of overlay design presented here is based on the data and investigations relating to a 30 kilometre section of a highway in Nepal. Traffic and axle load data (Table 18.14) have been taken from existing studies for similar roads in Nepal. Pavement tests (Table 18.15) were carried out for a representative test section of 500 metres for each 5 km road length.

The purposes of this example are i) to emphasize the need for a systematic design approach to the design of overlays, ii) to familiarize the readers with some of the existing design methods, iii) to illustrate the

need for engineering judgement and experience, along with the use of existing design charts and analysis, in the final selection of overlay design types and thickness appropriate to specific conditions. This example serves as a useful guide to the concepts and approaches for those pavement maintenance agencies where ad hoc decisions or experience-based judgement alone, rather than tests and analyses, are the practices in deciding pavement rehabilitation designs.

In this section, overlay design examples are presented using some of the several existing methods which are given below:

- o a component analysis based on the Asphalt Institute,
- o a component analysis based on the AASHTO Design Guide, and
- o deflection based designs using:
 - the Asphalt Institute Design charts,
 - the TRRL Design charts,
 - the Canadian Good Road Association (CGRA) Design charts, and
 - the Mechanistic Design.

18.6.1 *Overlaying Design by Component Analysis Based on the Asphalt Institute*

This component analysis approach to overlay design involves the development of a total pavement structure as a new design for the specified service conditions, and then a comparison of the existing pavement structure (taking into account pavement condition, type, and thickness of pavement layers). A review of current component design procedures quickly reveals that substantial judgement is required to use them effectively. This judgement is mainly associated with selection of 'weighting factors' to use in evaluating the structural adequacy of the existing pavement layers.

The Asphalt Institute Method of component analysis (called "effective thickness") uses the relationships of sub-grade strength, pavement structure, and traffic. The existing structural integrity of pavement is converted to an equivalent thickness of asphalt concrete which is then compared to that required for a new design.

The three essential parts of this overlay design procedure will be briefly described and will include:

1. sub-grade analysis,
2. pavement structure thickness analysis, and
3. traffic analysis.

Sub-grade Analysis

Testing of sub-grade materials is encouraged, even if original design records are available. Use of resilient modulus (M_r), soaked CBR or R-value tests appear to be the easiest to use with this procedure. For actual design, the design strength of the sub-grade must be characterized in terms of resilient modulus. Associated correlations for CBR and R-value are :

$$\begin{aligned} M_r \text{ (psi)} &= 1,500 \text{ (CBR)} \\ &= 1,155 + 555 \text{ (R-value)}. \end{aligned}$$

If test data in terms of M_r , CBR, or R-value are not available, sub-grades can be placed into one of the three classes for design purposes as given.

1. Poor soils. Soft and plastic when wet, generally composed of silts or clays. Typical properties : $M_r = 4,500$ psi, CBR = 3, R-value = 6.
2. Medium soils include soils such as loams, silty sands, and sand-gravels that contain moderate amounts of clay and silt. These soils can be expected to lose only a moderate amount of strength when wet. Typical properties: $M_r = 12,000$ psi, CBR = 8, R-value = 20.
3. Good soils. These soils can be expected to retain a substantial amount of their strength when wet and include clean sands and sand-gravels. Typical properties: $M_r = 25,000$ psi, CBR = 17, R-value = 43.

Pavement Structure Thickness Analysis

The goal of this portion of the design method is to determine the "Effective Thickness (T_e)" of the existing pavement structure. The Asphalt Institute has two approaches that can be used, only one will be illustrated in this section. First, the significant pavement layers are identified and their conditions determined. Second, "conversion factors" are selected for each layer (judgement by the designer is very important at this point). Third, the effective thickness for each layer is determined by multiplying the actual layer thickness by the appropriate conversion factor. The effective thickness of the complete pavement structure is the sum of the individual effective thickness. Typical layer thickness conversion factors are shown in Table 18.16.

Traffic Analysis

The Asphalt Institute treatment of traffic includes consideration of volume composition and axle weights with the goal being to develop the equivalent number of 18,000 to equivalent single axle loads (18-KEAL). Because of the trend of loading trucks heavily in the developing countries, the equivalency of trucks in terms of 18-KEAL or ESA tend to be much higher than in developed countries. It is, therefore, suggested that the equivalency factor for traffic load should be established based on axle load surveys of existing studies relevant to the situation concerned.

Table 18.17 is an example of overlay design based on the Asphalt Institute Component analysis. Conversion factors from Table 18.16 are used to convert the existing pavement to the effective thickness. The thickness of designed overlay is obtained for the given load and sub-grade strength from Figure 18.19.

It should be noted that the asphalt concrete to be used in overlays by this method should be the same as those assumed in the development of design charts which are for U.S. conditions (assuming an asphalt concrete modulus of 400,000 to 500,000 psi).

Table 18.14 Traffic data and ESA calculation

S. No.	Year	AADT				Traffic Growth % Per Year	Source	Equiv. Factor			ESA OR 18 KEAL	Cumulative ESA	Cumulative ESA in million.	Cumulative RSA x 106 one Lane	Remarks
		Buses	Trucks	Cars Light	Total AADT			Bus	Truck	Cars Light					
1	1978	71	213	72	356	7		.739	2.718	.002	230515	230680	.23	.12	
2	1979	76	224	75	371	7		.739	2.718	.002	242509	473023	.47	.24	
3	1980	80	240	80	400	7		.739	2.718	.002	259734	732757	.73	.37	
4	1981	86	257	85	428	7		.739	2.718	.002	278221	1010978	1.01	.51	
5	1982	92	275	91	458	7		.739	2.718	.002	297701	1308680	1.31	.65	
6	1983	98	294	98	490	7		.739	2.718	.002	318174	1626854	1.63	.81	
7	1984	105	315	105	525	7		.739	2.718	.002	340901	1967755	1.97	.98	
8	1985	112	337	112	561	7		.739	2.718	.002	364620	2332374	2.33	1.17	
9	1986	120	360	120	600	7		.739	2.718	.002	389601	2721975	2.72	1.36	
10	1987	129	385	128	642	7		.739	2.718	.002	416836	3138812	3.14	1.57	
11	1988	138	412	137	687	7		.739	2.718	.002	446056	3584868	3.58	1.79	
12	1989	148	444	147	735	7		.739	2.718	.002	577280	4062148	4.06	2.03	
13	1990	158	472	157	787	7		.739	2.718	.002	510690	4372838	4.37	2.29	
14	1991	169	505	168	842	7		.739	2.718	.002	546438	5119276	5.12	2.56	
15	1992	181	540	180	901	7		.739	2.718	.002	584689	5703965	5.70	2.85	
16	1993	194	578	192	964	7		.739	2.718	.002	623617	6329582	6.33	3.16	
17	1994	207	618	206	1031	7		.739	2.718	.002	669410	6998992	7.00	3.50	
18	1995	222	662	220	1103	7		.739	2.718	.002	716269	7715261	7.72	3.86	
19	1996	237	708	235	1180	7		.739	2.718	.002	766408	8481669	8.48	4.24	
20	1997	254	757	252	1263	7		.739	2.718	.002	820056	9301725	9.30	4.65	
21	1998	271	810	269	1351	7		.739	2.718	.002	877460	10179185	10.18	5.09	
22	1999	290	867	288	1446	7		.739	2.718	.002	938882	11118068	11.12	5.56	
23	2000	311	928	309	1547	7		.739	2.718	.002	1001604	12122672	12.12	6.06	

Source: University of Washington 1986

Note: 1. Equivalency factors for both the lanes are assumed to be same since deflection results do not show specific trend and this particular road carries loaded traffic in both directions.

2. Design traffic:

Case-1 = 10 years (end of 1988 to end of 1997) = $3.08:10^6$ ESA

Case-2 = 5 years (end of 1988 to end of 1992) = $1.28:10^6$ ESA

3. Base year traffic = 1986 = $3.14/2 = 1.57 \times 10^6$ ESA (for one lane)

Table 18.15 Test and design parameter

TEST DATA												ADOPTED FOR DESIGN			
TEST SECTION	KM	CR. DEFLN. (15k axle) = $\frac{x+2SD}{x10^3}$ in	AV. γ_d (In situ) pcf	AV.W (In situ) %	γ_d max pcf	Wopt % SOAKED	AV Field CBR (Dep) %	AV. Lab CBR Soaked %	PVT. TEMP °F	PVT. Thk in	SOIL TYPE	Design $\times 10^{-3}$ 15k axle	Defln. in 18k axle	CBR	MR ksi
Surface Base Sub-grade	0-5	11.42	111.39 113.45	24.2 3.15	133.19 139	7.4 7.8	36.0 44.5	64.00 7.5	84.2	2 13.71	Well-graded sandy gravel with little fines.	11.42	14.28	36 36	22 15.80
Surface Base Sub-grade	6-10	39.76	109.7 112.09	4.2 6.58	134.35 127.35	5.0 8.8	33.5 32.5	37.00 11.00	86	2.2 11.8		39.76	49.70	34 28	21 14.40
Surface Base Sub-grade	11-15	42.52	125.06 105.47	4.56 10.19	139.38 127.35	7.5 10.0	33.0 28.0	33.50 12.50	95	2.2 8.3	Well-graded sandy gravel with very little fines.	42.52	53.15	33 28	21 14.40
Surface Base Sub-grade	16-20	36.22	129.87 105.31	4.81 10.88	136.31 136.2	7.6 9.8	33.5 18.5	25.50 15.50	87.8	2 6.7	well-graded sandy gravel with little fines.	36.22	45.28	45 20	22.50 12.70
Surface Base Sub-grade	21-25	48.42	125.54 104.64	2.49 10.84	136.00 139.88	6.7 6.5	31.5 19.0	39.00 3.50	84.2	2 7.9	well graded sandy gravel with little fines.	48.42	60.53	32 19	20.50 12.70

a) Field CRR values are adopted without any adjustments since:

1. No seasonal factor is considered because the tests were carried out when the sub-grade conditions were wetter.
2. The results of soaked CRR are erratic and too unreliable to be accepted for design.
3. The material properties and classification do not have a definite trend.
4. Tests are carried out for the worst 500 m length for each 5 km road length, therefore involve conservatism.
5. Deflection under 18,000 pound axle dual wheels should be taken as 1.25 times the deflection under 14,000 pound axle dual wheels, wherever necessary. This is based on PSADZA computer analysis carried out by the University of Washington, Seattle, during a study for Washington State Department of Transportation on "Evaluation of Frost Related Effects on Pavements", May 1984.

Table 18.16 Example of Asphalt Institute conversion factors for estimating thickness of existing pavement components to effective thickness

Description of Layer Material	Conversion Factor ¹
1. Native sub-grade	0.0
2a. Improved sub-grade - predominantly granular materials	
b. Lime modified sub-grade of high PI soils	
3a. Granular sub-base or base-CBR not less than 20	0.1 - 0.3
b. Cement modified sub-bases and constructed from low PI soils	
4a. Cement or lime-fly ash bases with pattern cracking	0.3 - 0.5
b. Emulsified or cutback asphalt surfaces and bases with extensive cracking, rutting, etc	
c. PCC pavement broken into small pieces	
5a. Asphalt concrete surface and base that exhibit extensive cracking	0.5 - 0.7
6a. Asphalt concrete - generally uncracked	0.9 - 1.0
b. PCC pavement - stable undersealed and generally uncracked pavement	

Source: Asphalt Institute 1981

¹ Equivalent thickness of new asphalt concrete

Table 18.17 Overlay design by component analysis method - Asphalt Institute

- Design Traffic = 3.08×10^6 ESA, = (Case 1 = 1988-1997)
- Design Traffic = 1.28×10^6 ESA, = (Case 2 = 1988-1992)

Description	<u>Section 1</u> 0 - 5 km	<u>Section 2</u> 6 - 10 km	<u>Section 3</u> 11 - 16 km	<u>Section 4</u> 11 - 21 km	<u>Section 5</u> 22-26 km
Sub-grade, MR,					
ksi 15.8	14.4	14.4	12.7	12.7	
Total existing thickness	15.78in.	14.00in.	10.50in.	8.7in.	9.9in.
Effective AC thick. of existing pavt., in (from Table 18.16)	0.5 x 2 + 3x15.78" = 5.73	0.5 x 2 + 3x14 " = 5.20	0.5 x 2 + 3x10.5" = 4.15	0.5 x 2 + 3x8.1" = 3.61	0.5 x 2 + 3x9.9" = 3.97
Total thick. of AC reqd. for design ESA, in. (Fig 18.19)					
Case - 1	9.30	9.70	9.70	10	10
Case - 2	7.60	8	8	8.20	8.20
<u>Designed Overlay</u>					
Reqd. overlay (dense graded) thick., in.					
Case - 1	3.75	4.50	5.55	6.39	6.03
Case - 2	1.87	2.80	3.85	4.59	4.23

Source: Asphalt Institute Manual Series No. 1, 1981

The above AC may be converted to emulsified AC and a two layer overlay with a combination of AC and untreated aggregate by using the following conversions.

1" Ac = 1.43" type II emulsified AC. 1"AC = 3" gravel.

(Type II emulsified asphalt mixes made with semi-processed all crusher run, pit run, or bank run aggregates.)

18.6.2 *Overlay Design Based on AASHTO Design Guide*

This method of design requires the determination of the total thickness of pavement based on traffic, reliability, drainage factors, serviceability loss, and layer co-efficients. The existing pavement structure is then deducted from the total thickness required by the new design, with the difference being the required overlay thickness. One of the significant assumptions in this method is that each layer of the pavement structure is assigned a layer co-efficient on the basis of experience.

Figure 18.12 illustrates the new design concept and Figures 18.13 to 18.18 and Tables 18.13 and 18.14 are nomographs and design parameters. Table 18.18 is an example of design by this method. It may be noted that the existing thickness of pavement with bituminous surfacing (about 2") and base course of untreated aggregates have been converted to the equivalent thickness of 400,000 psi asphalt concrete by assuming that 1" of existing bituminous surfacing is equivalent to 2" of untreated base course and 3" of untreated base course is equivalent to 1" of 400,000 psi asphalt concrete. Similarly, the total design thickness, in terms of 400,000 psi asphalt concrete, is obtained by converting the untreated base to asphalt concrete by assuming an equivalency of 3:1. Thus the difference of the total equivalent thickness of existing and new designs gives the thickness of overlay expressed in terms of 400,000 psi asphalt concrete.

One should be very careful in comparing the results of design by various methods. It must be ensured that the conditions of materials and assumptions in the designs are similar. For example, the design for a reliability of 50 per cent would be quite different from the design for a reliability of 80 per cent. Similarly, the design for an asphalt concrete of stiffness 200,000 psi would give much greater thickness in comparison to a design for 400,00 psi AC.

18.6.3 *Overlay Based on Deflection Criteria*

The objective of deflection testing is to measure the structural properties of the pavement by non-destructive testing. This is done by imposing a known load on the pavement and measuring its response (i.e., surface deflection). Thus, an overall or effective strength is measured that combines all influencing factors such as material properties (including sub-grade), thickness of pavement layers, and environmental effects. The most commonly used, deflection-based, overlay design procedures do not attempt to isolate material properties of individual pavement layers.

The dominant type of measurement used for non-destructive, overlay design procedures is surface deflection (or deflection basins) obtained with known load conditions (i.e., contact pressure, force, and time-loading). Each of these factors can influence the pavement response to loading. Surface deflection measurements can be categorized into three types of non-destructive test: static deflections, steady-state deflections, and impact load response. Some examples of equipment associated with these tests are given below.

1. Static Deflections :

Benkelman Beam, travelling deflectometer, and plate-bearing test (ASTM D 1196).

Table 18.18 Overlay design based on AASHTO design guide

Past traffic = 1.575×10^6 ESA

Design Future traffic, Case 1 = 3.08×10^6 ESA

Case 2 = 1.28×10^6 ESA

Assuming three layers including sub-grade,

Structural Number, $SN = a_1 D_1 + a_2 D_2 m_2 + a_3 D_3 m_3$

$n_2 = 1.0$ for good drainage quality

$a_1 = 0.42$ assuming average annual pavement temperature of 90 F. (from Fig. 18.15)

$E_1 = 400,000$ psi at 84 F (Fig. 18.14)

$a_2 = 0.249 (\log E_{base}) - 0.977$.

Description	Section-1	Section-2	Section-3	Section-4	Section-5
CBRbase	36	34	33	45	32
Ebase, ksi (Table 18.15)22	21	21	22.50	20.50	
a_2 .104	.099	.099	.107	.097	
CBR _{sgr} (Table 18.15)	36	28	28	20	19
Es _{gr} , ksi (Fig 18.17)	15.80	14.40	14.40	12.70	12.70
From Fig. 18.13, for reliability 50% std. deviation of 0.45 SN1					
Case 1	1.9	1.9	1.9	1.8	2.0
Case 2	1.0	1.0	1.0	1.0	1.0
SN2					
Case 1	2.4	2.6	2.6	2.7	2.7
Case 2	1.5	1.6	1.6	1.7	1.7

Total thickness

$D_1 = SN_1/a_1 = sn_1/.275$ $D_2 = (SN_2-SN_1)/a_2$ 0.8 ; $m_2 = 0.8$ from Table 18.5 for Fair and > 25 % case.

Description	Section-1	Section-2	Section-3	Section-4	Section-5
Case 1					
D1, in	4.5	4.5	4.5	4.3	4.8
D2, in	4.8	7.1	7.1	8.4	7.2
Case 2					
D1, in	2.4	2.4	2.4	2.4	2.4
D2, in	4.8	6.1	6.1	6.5	7.2

Existing thickness, D2 in

In terms of untreated base material (assuming 1" existing surface = 2" base)	13.78+2x2 = 17.78	12+2x2 = 16	8.5+2x2 = 12.5	6.7+2x2 = 10.70	7.9+2x2 = 11.9
In terms of new A.C (assuming 1" AC 400 ksi = 3"base)	5.93	5.33	4.16	3.56	3.96

Overlay thickness, in

AC 400 ksi; DE - (D1 + D2/3)					
Case 1	0.2	1.5	2.7	3.6	4.7
Case 2				1.0	0.8

Source: AASHTO 1985

2. Steady-state Deflections :
Dynalect, Road Rater (several models), Waterways Experiment Station Plate Vibrators, and the Federal Highway Waterway Association (FHWA) Deflection Van (Cox 1981).
3. Impact Load Response :
Falling Weight Deflectometer.

Figure 18.25 outlines the general approach used in most of the overlay design procedures based on deflection measurements. The three basic elements of such design procedures are :

1. deflection measurement,
2. pavement conditions, and
3. traffic.

The minimum elements to be encompassed in mechanistic overlay design are given in Figure 18.26. A widely used deflection-based overlay design procedure is the Asphalt Institute Method. It will be described to illustrate the approach for asphalt concrete overlays placed on existing flexible pavements.

Asphalt Institute Overlay Design by Deflection Analysis

The basic approach of the overlay design procedure is to identify continuous pavement sections of uniform performance, obtain 'static' pavement, surface deflections with the Benkelman Beam and an 18,000lb single axle, and determine the expected traffic by user-equivalent axle loads.

The Asphalt Institute recommends that a minimum of 20 deflection measurements be taken each mile and randomly located in the outer wheelpath. From this data for each 'uniform' pavement section, a "representative rebound deflection" (RRD), is determined as follows :

$$RRD = (x + 2s) (f) (c)$$

where,

- | | | |
|-----|---|---|
| RRD | = | representative rebound deflection (in.), |
| x | = | mean of the individual deflections (in.), |
| s | = | standard deviation of the deflections (in.), |
| f | = | temperature adjustment factor, and |
| c | = | critical period adjustment factor (where c = 1 if deflection tests made during the most critical period). |

This calculation of RRD represents the upper bound of about 97 per cent of all deflections measured. The temperature adjustment factor used in the equation above adjusts the existing asphalt concrete surfacing to a standard temperature of 70° F (refer to Fig. 18.27).

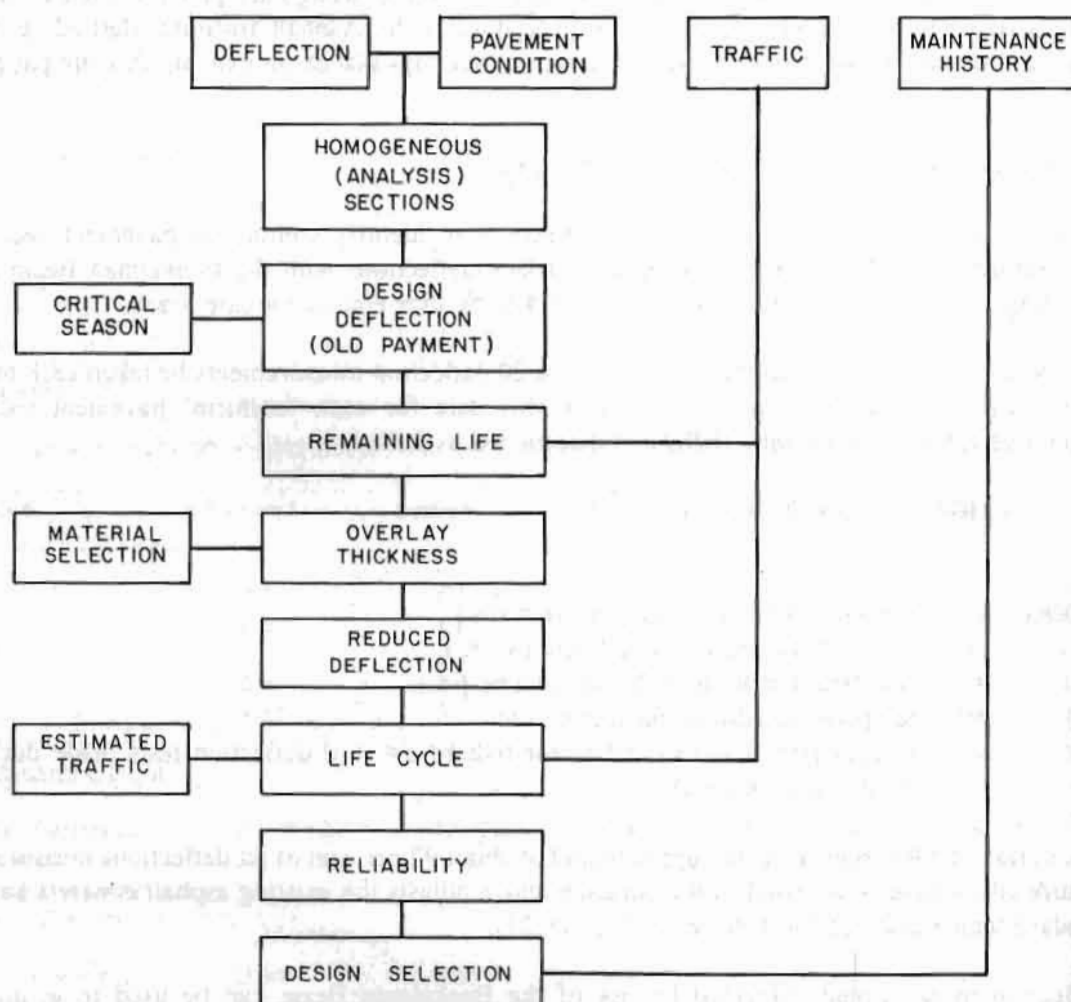
The deflection measurements obtained by use of the Benkelman Beam can be used to estimate the remaining life of the pavement or the needed thickness of asphalt concrete overlay. To determine the required overlay thickness, Figure 18.28 is used with the RRD and 18 KEAL as the required input.

Table 18.19 presents an example of overlay design by the Asphalt Institute Method.

Table 18.20 presents an example of overlay design based on allowable deflection criteria (Fig. 18.29 and Fig. 18.30) and GGRA design chart (Fig. 18.31).

The Transport and Road Research Laboratory (TRRL) Method

Table 18.21 presents an example of overlay design based on Transport and Road Research Laboratory Lab. Report No. 833 (1978). Figures 18.32, 18.33, and 18.34 are design charts for standard (allowable) deflection. This method involves determination of the remaining life of the existing pavement to ascertain whether overlay is required or not. The design charts for this method are applicable to sub-grade CBR up to 15 per cent only. However, these charts have been used here just to present an example only.



Source: University of Washington 1986

Figure 18.25 Overlay design with deflection measurements

18.6.4 Overlay Design by Mechanistic Analysis

Mechanistic Analysis

Significant interest has developed in the use of mechanistic overlay design procedures. The term 'mechanistic' as defined in most dictionaries (such as Webster's Seventh New Collegiate) is "mechanically determined" or "pertaining to the doctrine of mechanism". In turn, 'mechanism' is defined as the "fundamental physical processes involved in or responsible for an action, reaction, or other natural phenomenon". This roughly translates to pavement engineers as determining the fundamental **stresses**, **strains** and **deflections** caused by traffic and/or the environment in pavement structures. Knowledge of these stresses, strains, or deflections can in turn be used with limiting criteria to evaluate not only the need for an overlay but remaining pavement life as well.

The greatest advantage of mechanistic-based methods is the versatility provided in evaluating different materials under various environments and pavement conditions. The mechanistic procedures provide a basis for rationally modelled pavement systems. As these models improve, better correlations can be expected between design and performance parameters. It is anticipated that these procedures will replace limiting deflection, overlay methods since the latter do not account for sub-surface material properties. Mechanistic overlay design should, at a minimum, encompass the elements illustrated in Figure 18.26. Selected elements shown in this figure will be separately discussed.

Analysis Sections

A reasonable amount of uniformity should exist within a given pavement segment being considered for overlaying. These actions can be initially identified by use of condition surveys and, finally, deflection measurements. There exist numerous methods to determine the required number and location of such measurements. A minimum sample generally consists of deflection measurements every 250 to 500 ft. After collection of the deflection measurements, statistical measures can be used to delineate between analysis sections (along with the condition surveys).

Layer Characteristics

The mechanistic approach to overlay design can encompass both material characterization from the laboratory and non-destructive test data collected in the field. Total reliance on either laboratory or field data is generally felt to be inappropriate at the current stage of development. However, recent developments have provided estimates from field data of *in situ* moduli of the pavement layers. Illustrations of these approaches include :

1. FHWA - Resource International overlay design procedure,
2. BISDEF - computer programme developed by Bush (1980) at the Waterways Experiment Station (not an overlay design system),
3. ELMOD - computer programme by Ullidtz (1977), and
4. several other analysis procedures which use deflection basins from the Falling Weight Deflectometer, Dynaflect, or Road Rater.

Laboratory testing for mechanistic analysis generally implies the determination of resilient moduli (essentially a "modulus of elasticity" for pavement materials). Standard test methods such as the American Society for Testing and Materials (ASTM), D4123 - 82, are used for bituminous mixtures and triaxial procedures such as those recommended by Kalcheff and Hicks (1973) can be used for unbound granular materials. Laboratory determined moduli from unbound base, sub-base, and sub-grade materials are stress-sensitive and as such must be recognized.

The laboratory derived moduli are often adjusted by using layered-elastic analysis to calculate the resulting maximum deflection or deflection basin for a specified loading condition. In turn, field deflections are compared to the estimated deflections. If differences exist, the laboratory values are modified to reasonably match field measurements. More recently, computer programmes such as BISDEF have been used to estimate layer moduli for up to four pavement layers. Input data for this programme include the non-destructive test (NDT) load, measured deflection basin, layer thickness and limiting ranges, and expected values of moduli for each pavement layer. The programme then estimates the moduli for each layer which results in the best fit of the field deflection basin (within a user-specified error range).

Limiting Failure Criteria

Pavement sections deteriorate with time because of a progression of defects (because of traffic loads, environment, and other factors acting on the pavement structure). The pavement reaction to its total loading condition can be characterized by estimating the induced stress, strain, and deflections. When these pavement responses reach cumulative limiting value, distress results. The resulting serviceability loss can occur as a result of the accumulation of a single distress type (often fatigue), rutting, or a combination of several types.

Fatigue-related distress can be defined as the phenomenon of load-induced cracking caused by repeated stress or strain level below the ultimate strength of the material. The classical type of fatigue failure is commonly described as 'alligator' cracking, because of the pattern of cracks which appear on the pavement surface. These cracks appear to be best associated with tensile strains at the bottom of the asphalt concrete layers. A common expression used to relate the number of loads to fatigue failure as a function of tensile strain is:

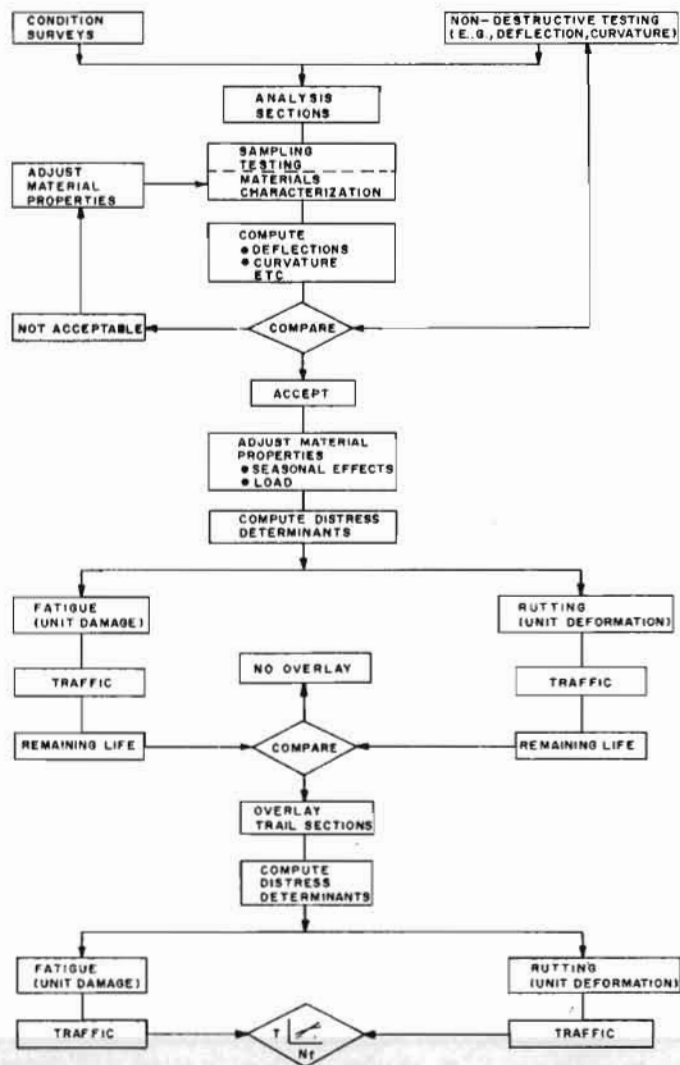
$$N_f = K_1 (1/E_t)^{K_2}$$

where,

$$\begin{aligned} N_f &= \text{load repetitions to failure,} \\ E_t &= \text{initial tensile strain, and} \\ K_1, K_2 &= \text{fatigue parameters.} \end{aligned}$$

The fatigue relationship developed by Majidzadeh and Ilves (1981) for the FHWA-RII Overlay Design System is used to illustrate 'typical' K_1 , and K_2 parameters:

$$N_f = 7.56 \times 10^{-12} (1/\epsilon_t)^{4.68}$$



Source: MonSmith and Finn 1984

Figure 18.26 Overlay design based on mechanistic analysis

Analogous criteria have been developed for rutting failure, whereby the number of load repetitions to failure is generally made a function of vertical strain in the sub-grade (in place of tensile strains as for asphalt concrete fatigue).

In practice, flexible pavements are subjected to a variety of loads. Miner's rule is used for evaluating cumulative damage. The rule states that the condition at failure is given by :

where,

- n_i = actual number of cycles of stress or strain applied to the pavement,
- N_i = allowable number of cycles to failure based on failure criteria (such as fatigue or rutting), and
- r = number of loading conditions considered.

In this example of mechanistic design, the CHEVPC computer programme has been used. Stress sensitivity is not considered for sub-grade and base course. The failure criteria for fatigue and rutting as per Finn's Model (see Section 18.5.7) have been used to calculate the failure loads from the strain obtained from the CHEVPC programme.

Table 18.22 shows the material properties adjusted by matching the observed deflection with the calculated deflection (by CHEVPC). The considerable variation between the adjusted material properties and test data might be indicative of the inadequacy of test data. Table 18.23 shows the remaining life of the existing pavement and Table 18.24 shows the failure loads for different trial thicknesses of the overlay.

The results from this method indicate a much higher overlay thickness compared to other methods. It should be remembered that the reliability in most other methods is fifty per cent only compared to more than 50 per cent in this method. The deflection with mean plus two standard deviation, adopted as measured deflection for matching calculated deflection, further renders the design more conservative. The poor reliability of test results (obvious from the inconsistencies among material type, CBR field, and CBR lab [see Table 18.15]), and the uncertainty of the measured thickness of existing pavement, all tend to render the design more conservative, leading to a great deal of over-calculation in the thickness of the overlay.

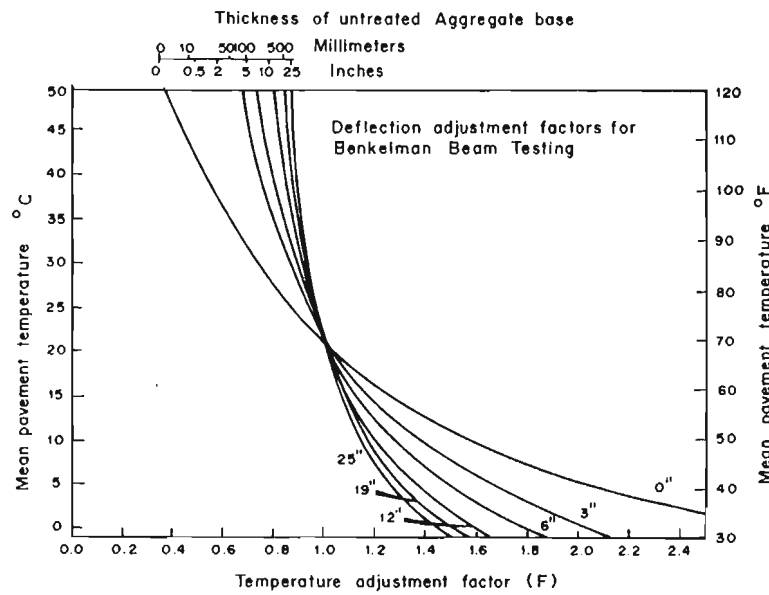
Table 18.19 Overlay design by deflection analysis based on the Asphalt Institute

Case-1, traffic 3.08×10^6 ESA (1988 - 1997)

Case-2, traffic 1.28×10^6 ESA (1988 - 1982)

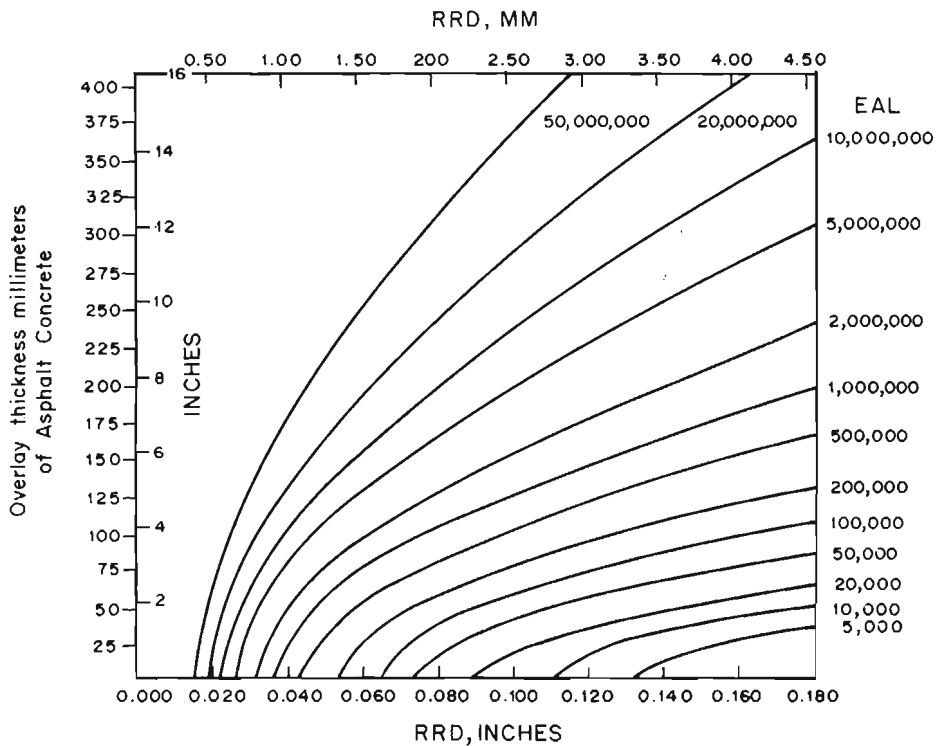
Description	Section-I	Section-II	Section-III	Section-IV	Section-V
RRD(dc in terms of 1800 lb. dual wheel load x 103 in. (from Table 18.15)	14.27	49.70	53.15	45.27	60.52
Designed thick. of overlay (from Figure 18.28) AC Nr = 400 ksi					
Case - 1	nil	3.70	4	3.80	5.60
Case - 2	nil	3.10	3.20	2.30	4.50

Source: Asphalt Institute 1983



Source: Asphalt Institute 1983

Fig. 18.27 Asphalt Institute temperature adjustment factors for Benkelman Beam deflections



Source: Asphalt Institute 1983

Fig. 18.28 Asphalt concrete overlay thickness required to reduce pavement deflection from a measured to a design deflection value

Table 18.20 Overlay design by allowable deflection criteria

Case - 1, traffic 3.08×10^6 ESA (1988 - 1997)Case - 2, traffic 1.28×10^6 ESA (1988 - 1982)

Assumed Allowable Deflection under 18 K - axle :

	<u>Lister 1972</u> (Fig. 18.29)	<u>Cox 1981</u> (Fig. 18.30)
Case - 1	33 x 10-3in.	39 x 10-3in.
Case - 2	46 x 10-3in.	50 x 10-3in.

Allowable Deflection under 14K-axle based on Lister, 1972

For case - 1	-	23 x 10-3in.
For case - 2	-	28 x 10-3in.

Description	Section I	Section II	Section III	Section IV	Section V
Design define before overlay x 10" - 3 in.	11.42	38.76	42.62	36.22	48.42
Designed thick. of Overlay, inches (Figure 18.31)					

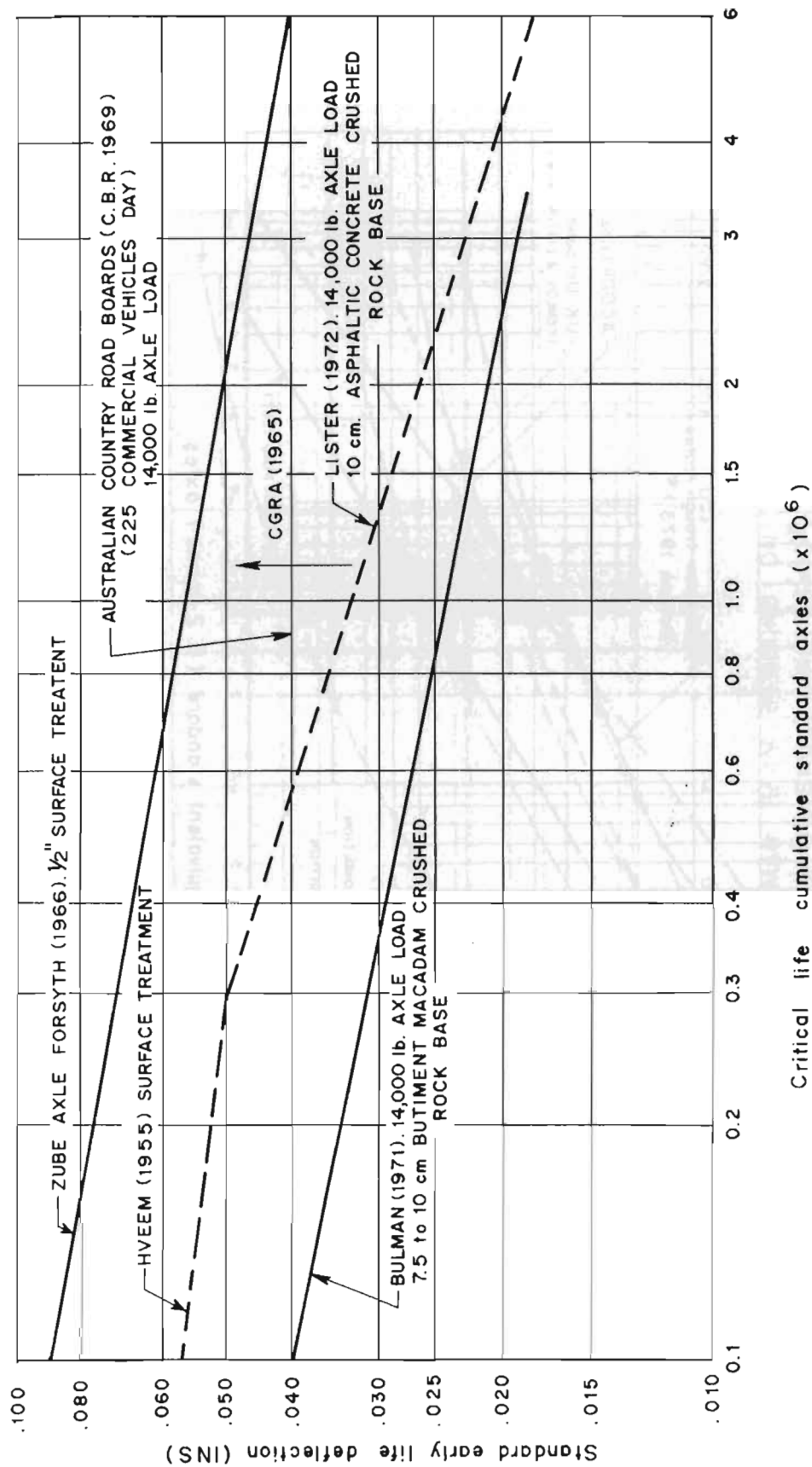
a) *Alternative-1, Granular BC*

Case - 1	nil	10.70	12	8.70	14.20
Case - 2	nil	9	8	4.40	8.80

b) *Alternative -2, AC, M, 400 ksi (Assumed 1 AC = 3" gravel)*

Case - 1	nil	3.57	42.90	4.73	
Case - 2	nil	3	2.67	1.47	2.93

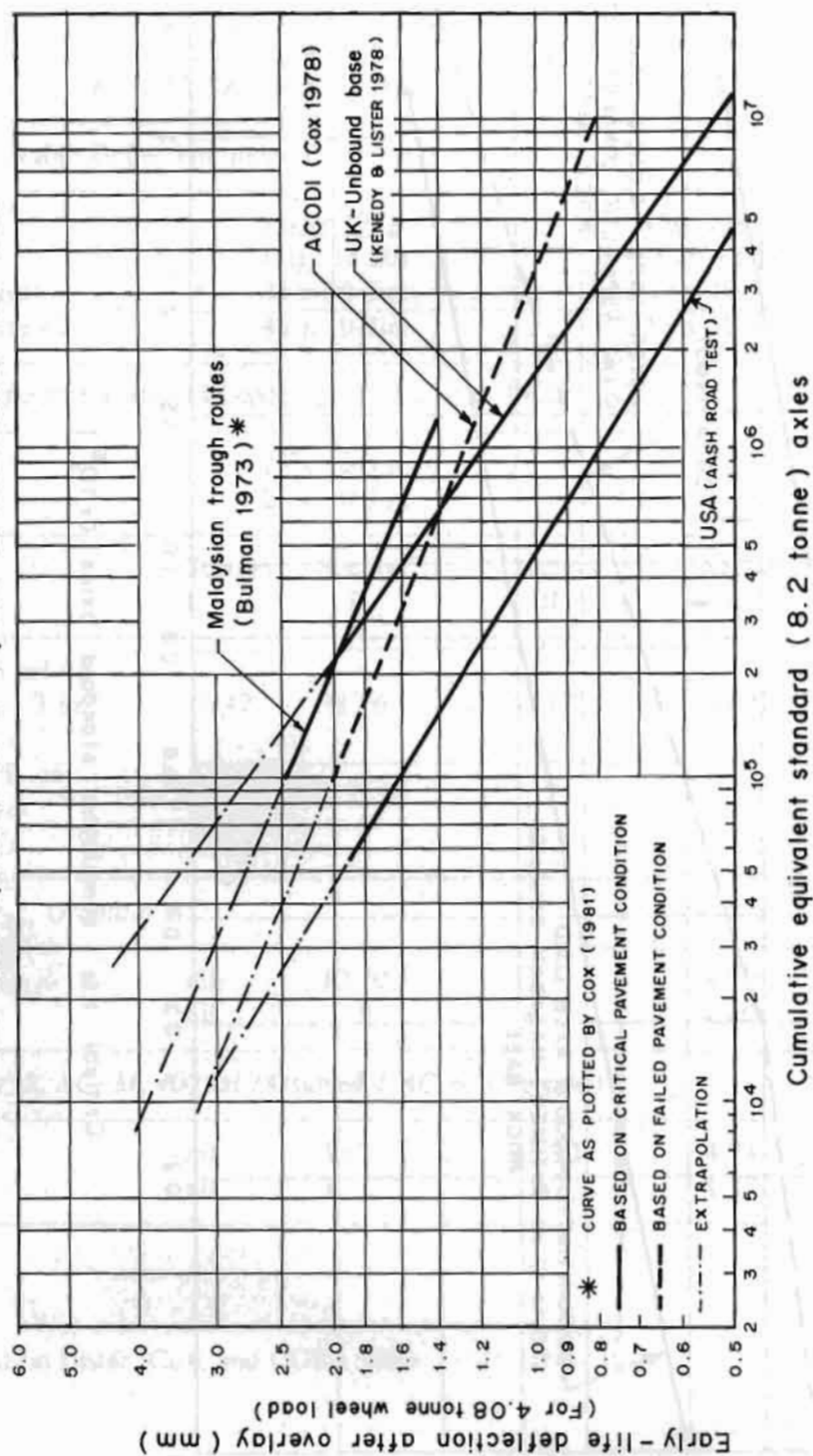
Source: Based on Lister, Cox, and CGRA 1981



Source: Adapted from Lea and Associates 1977

Fig. 18.29 Design deflection curves

Note: All curve equivalent to a 18,000 lb. (8.2 tonne) axle load

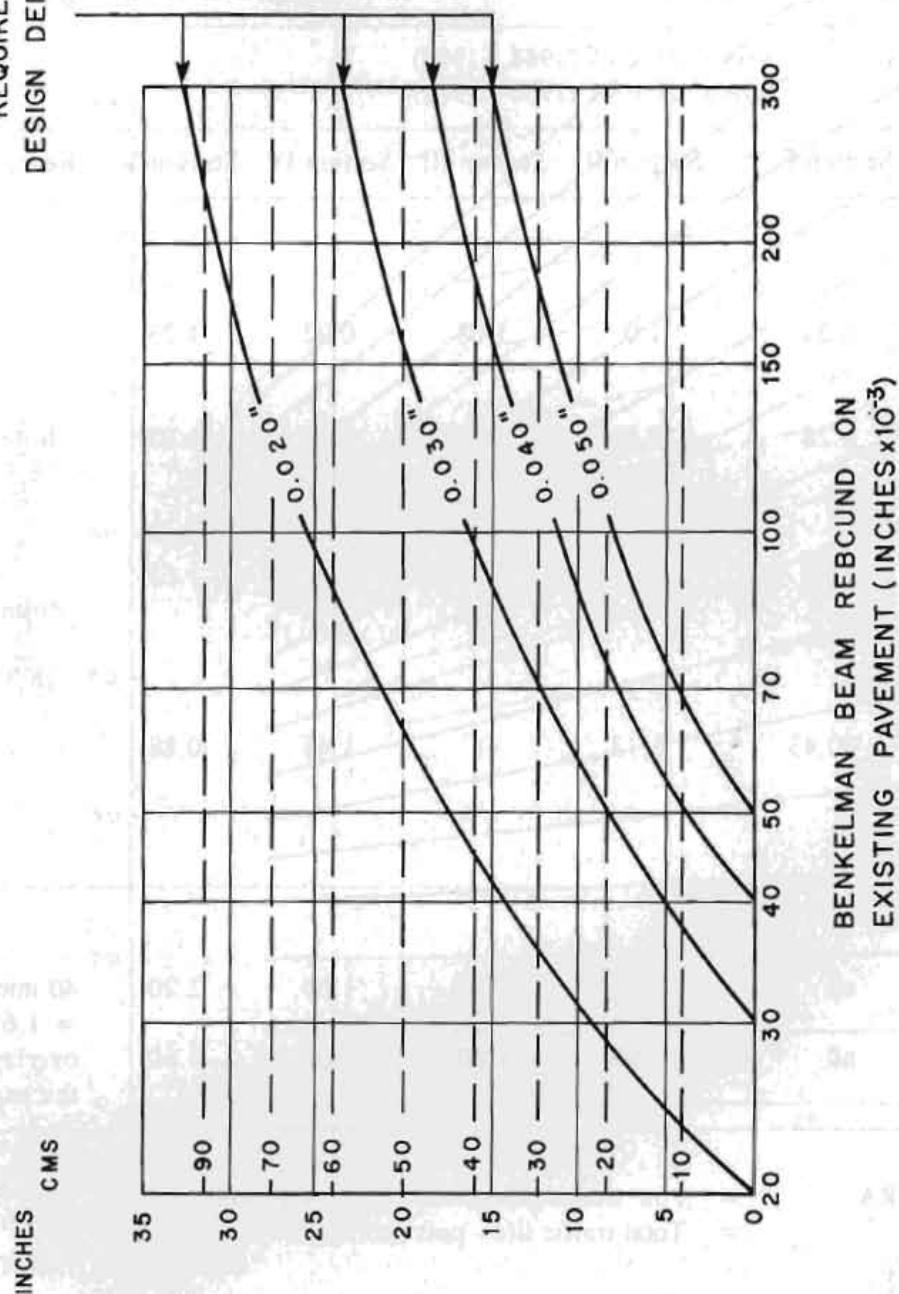


Source: Adapted from Corne 1983

Figure 18.30 Deflection/life relationships for dense plant-mix asphalt overlays

REQUIRED ADDITIONAL THICKNESS OF GRANULAR BASE COURSE

REQUIRED FINAL
DESIGN DEFLECTIONS



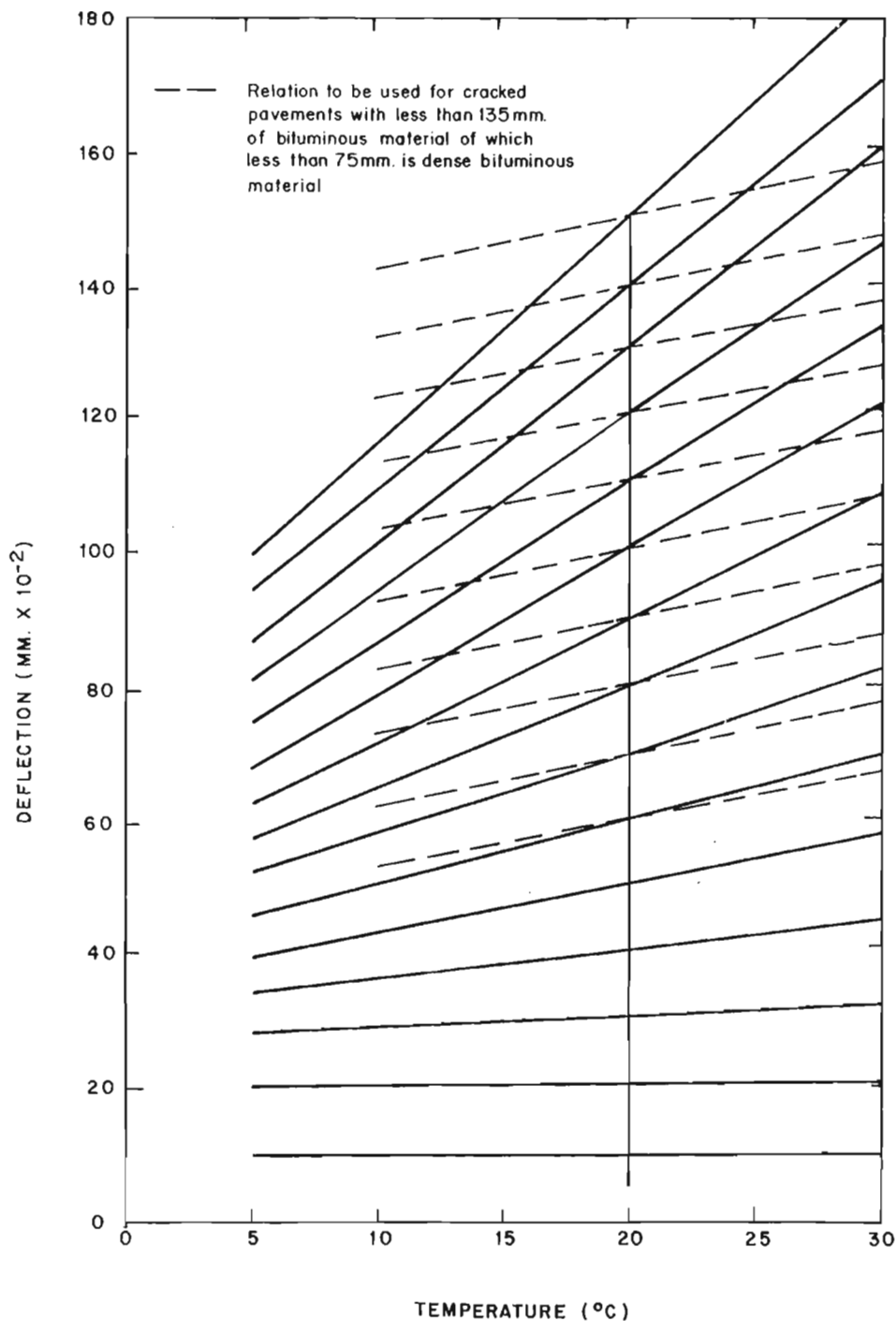
Source: Adapted from Lea and Associates and the Department of Roads (DOR) 1977

Figure 18.31 CGRA overlay design chart by deflection (after reference)

Table 18.21 Overlay design

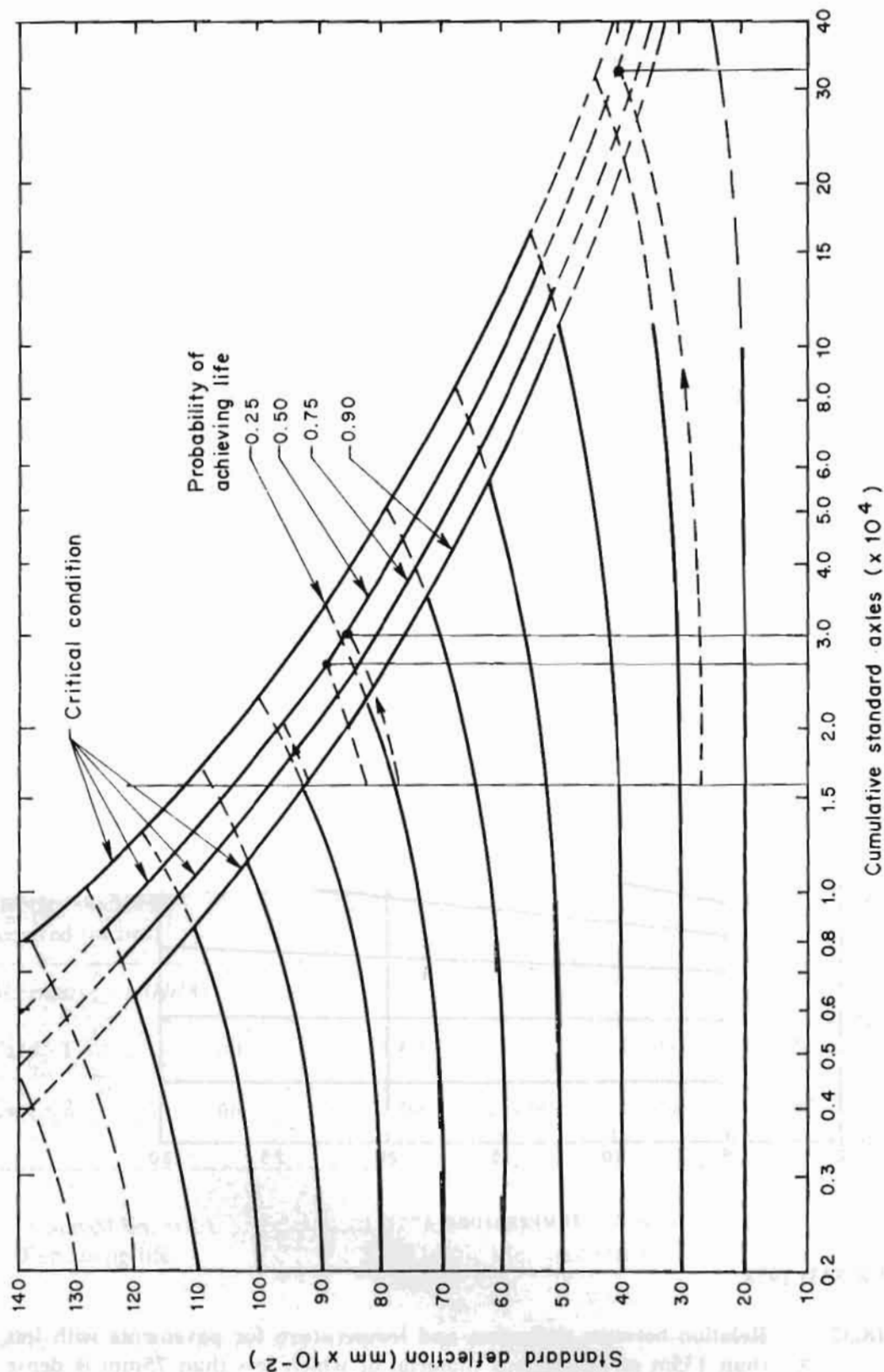
Past traffic assuming probability of achieving life			= 1.57 x 10 ⁶ ESA, = 50 % (base year assumed - beginning of 1988).			
Case - 1, traffic :		3.08 x 10 ⁶ ESA (1988 - 1987)				
Case - 2, traffic :		1.28 x 10 ⁶ ESA (1988 - 1982)				
Description	Section-I	Section-II	Section-III	Section-IV	Section-V	Remarks
1) Design deflection for 14R-axle at 30°C mm	0.29	1.0	1.08	0.92	1.23	
Standard defl. at 20°C mm	0.28	0.83	0.92	0.78	1.03	- from Fig. 18.33, 18.34
2) Total life (x 10 ⁶ ESA)	32.0	2.7	2.05	3.0	1.65	- from Fig. 18.33, 18.34
3) Beginning life (x 10 ⁶ ESA)	30.43	1.13	.48	1.43	0.88	
Overlay thickness required (inches)						
Alternative - 1 (HRA)						
Case - 1	nil	1.60	1.60	1.60	2.20	40 mm. = 1.6" min. overlaying thickness
Case - 2	nil	1.60	1.60	1.60	1.60	
Assumed lin. HRA		= 1 in. dense graded AC. 3 in. of gravel				
Remaining life		= Total traffic life - past traffic.				

Source: TRRL Lab Report 833, 1978



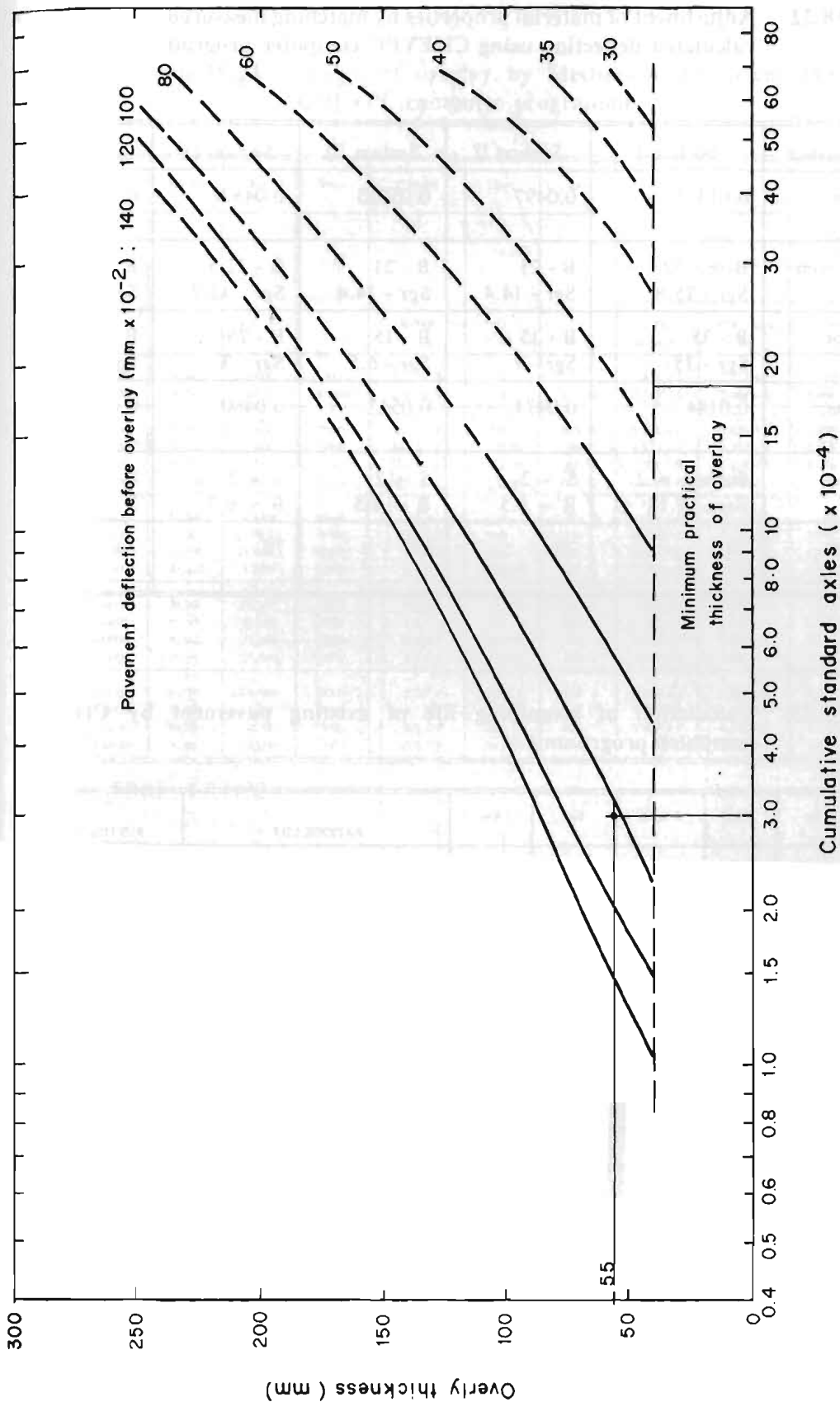
Source: TRRL (LR 833) 1978

Fig 18.32 Relation between deflection and temperature for pavements with less than 135mm of bituminous material of which less than 75mm is dense bituminous material



Source: TRRL 1978

Fig 18.33 Relation between standard deflection and life pavements with non-cementing granular road bases



Source: TRRL (LR 833) 1978

Figure 18.34 Overlay design chart for pavements with non-cementing granular road bases (0.50 probability)

Table 18.22 Adjustment of material properties by matching measured deflection with calculated deflection using CHEVPC computer programme

Pavement Characteristics	Section I	Section II	Section III	Section IV	Section V
Measured Deflection, inches	0.01428	0.0497	0.05315	0.04528	0.0605
Material Properties from field CBR	Base - 22 Sgr - 15.8	B - 21 Sgr - 14.4	B - 21 Sgr - 14.4	B - 22.5 Sgr - 12.7	B - 20.5 Sgr - 12
Adjusted Material for Properties	B - 35 Sgr - 35	B - 15 Sgr - 7	B - 15 Sgr - 6.5	B - 25 Sgr - 7	B - 18 Sgr - 5
Calculated Deflection, inches	0.0144	0.0474	0.0532	0.0460	0.06000
Thickness of Existing Pavement (inches)	Surface = 2 Base 13.18	S = 2 B = 8.5	S = 2 B = 8.5	S = 2 B = 6.7	S = 2 B = 7.9
Assumed Stiffness of Existing Surface, (ksi)	70	70	70	70	70

Table 18.23 Calculation of remaining life of existing pavement by CHEVPC computer programme

Section	Eex, ac, psi	Eb _i	Eagr	T-layers Inches	Eac	Eva	FATIGUE LIFE			RUTTING LIFE	
							Finn model		TRRL model	Finn model	TRRL model
							A.C.		HPA		
							10% crack Nf	45% crack Nf	Nf	Nr	Nr
I	100,000	35000	35000	2,13.78	319	302	9.98E+5	1.09E+6	2.11E+5	8.15E+6	4.94E+6
II	70,000	15000	7000	2,11.8	1385	248.30	1.08E+4	1.18E+4	3.71E+2	1.96E+7	1.07E+7
III	70,000	15000	6500	2,8.5	735.60	1958	8.65E+4	9.47E+4	5.70E+3	1.87E+3	3.07E+3
IV	70,000	25000	7000	2,6.7	365	1878	8.69E+5	9.50E+5	1.18E+5	2.25E+3	3.62E+3
V	70,000	18000	5000	2,7.9	566	2288	2.05E+5	2.24E+5	1.77E+4	9.28E+2	1.66E+3

Table 18.24 Design of overlay by Mechanistic-Empirical Method (MEM) using CHEVPC computer programme

Section	Eac	Eex.ac	Eb _i	Esgr	T-layers	Eac	Evs	FATIGUE LIFE		RUTTING LIFE		
								Finn model		TRRL mode	Finn model	TRRL model
								A.C.		HRA		
								psi			Inches	
I	400000	100,000	35000	35000	2,2,13.78	370	225	1.87E+5	2.05E+5	1.11E+5	3.05E+7	1.58E+7
	400000	100,000	35000	35000	6,2,13.78	174	130.40	2.24E+6	2.46E+6	2.89E+6	3.52E+8	1.36E+8
II	400000	70,000	15000	7000	2,2,11.8	748	918.70	1.85E+4	2.02E+4	5.13E+3	5.55E+4	6.10E+4
	400000	70,000	15000	7000	6,2,11.8	292.30	200.70	4.07E+5	4.45E+5	3.07E+5	5.09E+7	2.48E+7
	400000	70,000	15000	7000	7,2,11.8	205.60	368.60	1.30E+6	1.42E+6	1.41E+6	3.33E+6	2.25E+6
	400000	70,000	15000	7000	8,2,11.8	159.40	248.30	3.00E+6	3.28E+6	4.22E+6	1.96E+7	1.07E+7
III	400000	70,000	15000	6500	2,2,8.5	777	1249	1.63E+4	1.78E+4	4.50E+3	1.40E+4	1.81E+4
	400000	70,000	15000	6500	4,2,8.5	469	810	9.59E+4	9.40E+4	3.99E+4	9.77E+4	1.00E+5
	400000	70,000	15000	6500	6,2,8.5	304	545	3.58E+5	3.91E+5	2.53E+5	5.77E+5	4.80E+5
	400000	70,000	15000	6500	8,2,8.5	164.60	384	2.70E+6	2.95E+6	3.67E+6	2.78E+6	1.91E+6
IV	400000	70,000	25,000	7000	2,2,6.7	572.60	1244.40	4.45E+4	4.07E+4	1.63E+4	1.42E+4	1.84E+4
	400000	70,000	25,000	7000	4,2,6.7	377	826	1.76E+5	1.93E+5	1.02E+5	8.95E+4	9.29E+4
	400000	70,000	25,000	7000	6,2,6.7	256.60	563	6.25E+5	6.94E+5	5.40E+5	4.99E+5	4.22E+5
	400000	70,000	25,000	7000	8,2,6.7	152.40	400.40	3.47E+6	3.80E+6	5.12E+6	2.30E+6	1.62E+6
V	400000	70,000	18,000	5000	2,2,7.9	720	1458	2.10E+4	2.29E+4	6.26E+3	7.00E+3	3.84E+3
	400000	70,000	18,000	5000	4,2,7.9	452	949	9.70E+4	1.06E+5	4.68E+4	4.08E+4	5.37E+4
	400000	70,000	18,000	5000	6,2,7.9	298	400	3.82E+5	4.18E+5	2.83E+5	2.31E+6	1.63E+6
	400000	70,000	18,000	5000	8,2,7.9	165.30	445	2.66E+6	2.19E+6	3.61E+6	1.43E+6	1.07E+6

Source: TRRL, LR1132

Failure Criteria:

Finn,

Fatigue:

$$\leq 10\% \log N_f = 15.947 - 3.291 \times \log \epsilon_i / 10^{-6} 854 \times \log MR/1000 \text{ Fatigue:}$$

TRRL LR1132

$$\log N_f = -9.78 - 4.32 \times \log \epsilon_i$$

$$\leq 45^\circ \log N_f = 15.986 - 3.291 \times \log \epsilon_i / 10^{-6} 854 \times \log MR/1000$$

Rutting:

$$\log N_r = -7.21 - 3.95 \times \log \epsilon_{vs}$$

Rutting:

$$N_r = 1.077 \times 10^{18} \left(\frac{1}{10^6 \times \epsilon_{vs}} \right)^{4.4843}$$

Table 18.25 and 18.26 present a summary of thickness of overlay in terms of asphalt concrete of about 400,000 psi modulus. The considerable variation in thickness obtained, from different methods of design, suggests the need for exercise of engineering judgement to select the method that is most appropriate to the actual conditions. For the purpose of this example, the results from the AASHTO Method are suggested for adoption because the assumptions of design and material properties made are likely to represent actual conditions. The deflections and material properties revealed from Table 18.15 are not consistent for meaningful applications. The results from the TRRL LR 833 Method are not recommended because the design charts are applicable to HRA, sub-grade CBR not greater than 15 per cent, and involve past traffic (which is difficult to assess accurately).

The use of equivalencies may be made in order to convert the overlay of AC in terms of other choices such as emulsified AC, DBST + untreated aggregate, or lower stiffness AC. The following equivalencies are suggested for the purpose of this exercise.

1" AC (400 ksi)	=	1.43" Emulsified AC of Asphalt Institute Type II,
	=	3 " untreated gravel,
	=	1.53 " AC of 175 ksi, and
1" DBST	=	1" AC of 175 ksi.

It may be noted that the probability of achieving designed life in methods other than mechanistic are based on 50 per cent. The mechanistic method may be assumed to give a probability of achieving a designed life of more than 90 per cent.

Recommendations

In view of the variation in the design thickness from different methods, it is suggested that more than one method be tried and the selection be made by experienced judgement. A systematic design method should always be adopted rather than *ad hoc* judgements in deciding overlay thickness for pavement improvements.

The decisions concerning the type of overlay depends on available technology, materials, time, and cost economy. Asphalt concrete or hot, rolled asphalt overlay may not always be possible in developing countries. Emulsified concrete may, in some instances, be more desirable because of considerations of fuel for heating. Overlays of DBST with untreated aggregate may sometimes be feasible and desirable because of equipment and material constraints. In the absence of detailed analysis for a specific type of overlay, it should still be possible to design the overlays in terms of asphalt concrete used in most design charts and subsequently adjusting to the desired type can be done by using equivalencies from the available literature.

The field and laboratory tests for material properties, including the deflection test, should not only be adequate in numbers but also be consistent and acceptable to experienced judgement before they are used for design inputs. Each user agency should, wherever possible, try to develop design charts or methods appropriate to their own conditions.

Table 18.25 Summary of designs - Case 1 (10 year design life - 3.08×10^6 ESA)
(Thickness in inches)

S.No.	Design Method	Section 1	Section 2	Section 3	Section 4	Section 5
Type - 1 Dense Graded Asphalt Conc., $M_r = 400,000$ psi						
1.	Component Analysis	3.57	4.50	5.55	6.39	6.03
2.	AASHTO Design Guide 1985	0.2	1.50	2.70	3.6	4.7
3.	Asphalt Institute Deflection	nil	3.70	4	3.8	5.60
4.	Allowable Deflection Criteria, Cox & CGRA	nil	3.57	4	2.90	4.70
5.	TRRL Lab Report 833, 1978	nil	1.6	1.6	1.6	2.2
6.	Mechanistic Method	6.5	8	8.5	8.0	8.5

Table 18.26 Summary of designs - case 2 (5 yr. design life - 1.28×10^6 ESA)
(Thickness in inches)

S. No.	Design Method	Section 1	Section 2	Section 3	Section 4	Section 5
Type - 1 Dense, Graded Asphalt Conc., $M_r = 400,000$ psi						
1.	Component Analysis	1.87	2.8	3.85	4.59	4.23
2.	AASHTO Design Guide 1985	1.0	0.8			
3.	Asphalt Institute Deflection	nil	3.10	3.20	2.9	4.50
4.	Allowable Deflection Criteria, Lister & CGRA	nil	3	2.70	1.47	2.90
5.	TRRL Lab Report 833, 1978	nil	1.60	1.60	1.60	1.60
6.	Mechanistic Method	nil	7	7.5	7.0	7

DRAINAGE

19.1 INTRODUCTION

Drainage is the single most important factor in the design of infrastructures in mountainous areas. Infrastructures, such as roads, involve design of surface drains, sub-surface drains, drainage crossings, and erosion control measures.

Considerable damage to road pavements, retaining walls, and the surrounding hill slopes occurs from concentrated runoffs from drainage structures which are not properly designed according to hydrologic and hydraulic considerations. Designs of side drains and culverts, which are normally numerous along a road, based on guesswork, do save time and effort in the design process but, in many instances, create problems that subsequently involve more time, efforts, and resources.

This chapter, therefore, presents brief theoretical concepts on hydrology and hydraulics, followed by some simple methods for designing culverts. Practical aspects of designs for side drains and gully control are briefly dealt with in Chapter 24, Section 24. 5.

19.2 HYDROLOGY

The branch of hydrology which is of particular concern to road engineers deals with the following:

- frequency, intensity, and duration of rainfall,
- runoff peaks and their frequencies, and
- distribution of precipitation throughout the seasons, influencing the moisture under the road pavement, and growth of vegetation for erosion control.

19.2.1 *Intensity, Frequency, and Duration of Rainfall*

The intensity of rainfall is the rate of rainfall, usually measured in millimeters per hour. However sometimes it is measured as total precipitation in millimeters for a certain time period, e.g., total millimeters of rainfall in 24 hours.

Rainfall frequency is a term used to denote the probability that a rainfall event of T-yrs' recurrence interval will be equalled or exceeded in any one year. It is derived by:

The Weibull Formula is used to calculate frequency of rainfall from the available rainfall data.

* Tables and Figures without credit lines in this chapter are compiled by the author.

$$F = \frac{1}{T}$$

$$F = \left(\frac{m}{n+1} \right) \times 100 \quad (19.1)$$

where,

- F = percentage of years during which the precipitation is equalled or exceeded, the precipitation of order number m, and
 n = total number of precipitation values.

The recurrence interval (T) is given by,

$$T = \frac{1}{F} = \frac{n+1}{m} \quad (19.2)$$

First, the available rainfall data are tabulated and ranked according to order of magnitude (Table 19.1). The return periods, T, are calculated by using the above formula. The data are then plotted on a semilog paper with 24 hour maximum rainfall on a normal scale at Y axis and return period on a logarithmic scale at X axis or the inverse of return period ($\frac{1}{T}$) in the upper x-axis from right to left as shown in Figure 19.1. Rainfall intensity for the desired return period can be read out or extrapolated from this graph. Alternatively, the frequency of rainfall, that is the probability that rainfall of the given intensity will be equalled or exceeded in any one year, is obtained from the graph by reading $1/T$ in the upper x-axis.

Table 19.1: Frequency analysis of 24 hours rainfall (Nuwakot)

Year	Precipitation, mm	Rank, m	Return Period (Year), T
1972	98	6	2.67
1973	135	2	8.00
1974	75	12	1.33
1975	80	10	1.60
1976	93	8	2.00
1977	69	13	1.23
1978	94	7	2.29
1979	178	1	16.00
1980	69	13	1.23
1981	60	14	1.14
1982	120	5	3.20
1983	77	11	1.45
1984	85	9	1.78
1985	128	4	4.00
1986	132	3	5.33

Source: Environmental Impact Study of the Mahendra Raj Marg - Gaighat Road and Trisuli - Sordang Road, Department of Roads, Nepal, 1991.

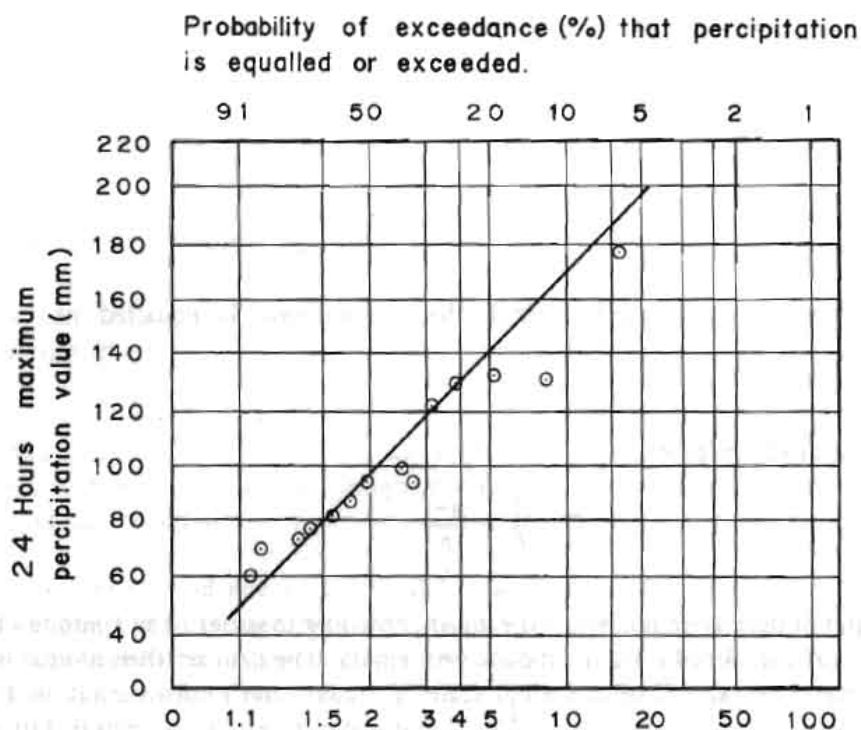


Fig. 19.1 Frequency of rainfall

Frequency analysis of rainfall data can be carried out by two methods.

- The annual series, for which only the maximum rainfall intensity of each year is plotted and other rainfall data of the year are ignored.
- The partial series, for which all the high rainfall intensities are considered regardless of the number occurring within a particular year.

The difference between two methods is insignificant for return periods greater than 10 years. For less than a 10 year return period, the partial series is generally used.

19.2.2 Design Flood and Its Frequency

The first step in designing drainage facilities is to estimate the quantity of water likely to be drained. Drainage facilities should have sufficient capacity to carry off safely not only peak runoffs, which occur frequently, say several times a year, but also larger runoffs, occurring less frequently, say on average once in 10 or more years. For a major highway linking major economic centres, where disruption of traffic, caused by damage to or washout of culverts, may not be acceptable, a peak runoff that recurs less frequently needs to be considered. In contrast, for a rural highway, where some minor traffic disturbances can be tolerated, a peak runoff that recurs frequently might be sufficient.

However, where serious damage would result from erosion caused by the inadequate capacity of drainage facilities, and where large drainage facility costs are involved, the less frequent peak runoffs would have to be used.

It is not practicable to design for a maximum probable flood to cater for the worst possible flood, as the capital costs increase rapidly with the increment of the peak runoff. In order to economise on construction costs, frequency of flood is selected for longer or shorter return periods, depending upon the importance of the structure. The design flood is a flood corresponding to the selected return period.

The **California Culvert Practice**, 1953, recommends a 10 year flood for the culvert to just pass the flood without static head at entrance and a 100 year flood for design of culvert and appurtenances to avoid serious damage from head and velocity.

Regarding the design of road surface drainage, the U.S. Bureau of Public Roads insists that all drainage facilities, other than culverts and bridges, be designed for a 10 year flood.

It should be kept in mind that a 25 year flood does not in any way mean that the flood will occur once in 25 years, rather there is only a 64 per cent probability that it will occur within a 25 year period. However, this flood has a 1 in 25 or 4 per cent chance of occurrence in any one year. The following example illustrates this point.

Let return period of a flood $T = 25$ yrs

Probability of exceeding $P = 1/T$
 $= 0.04$.

Probability that the flood will not occur in 25 years $= (1-P)^{25}$
 $= 0.36$.

Probability that the flood will occur in 25 years $= 1 - (1-P)^{25}$
 $= 1 - 0.36$
 $= 0.64$
 $= 64$ per cent.

19.2.3 Method of Runoff Prediction

Current methods for estimating peak runoffs are discussed below.

(a) Rational Formula

This method is applicable to small catchments (1 to 2 sq.km) only. The peak runoff is given by:

$$Q = \frac{C I_c A}{360} \quad (19.3)$$

where,

- Q = Peak runoff in m^3/sec
- I_c = critical intensity in mm/hr, corresponding to time of concentration of catchment,
- A = catchment area in hectares, and
- C = dimensionless constant, the runoff coefficient (see Table 19.2).

The peak runoff frequency is assumed to be identical to the rainfall intensity frequency.

The critical intensity of rainfall I_c is determined as follows:

$$I_c = \frac{P(T+1)}{T(t_c+1)} \quad (19.4)$$

where,

- I_c = critical intensity of rainfall corresponding to time of concentration, in mm per hour
- P = precipitation of a storm in mm,
- T = duration of storm in hours, and
- t_c = time of concentration in hrs.

The time of concentration (t_c) is given by the formula below (The Indian Roads Congress, 1986):

$$t_c = [0.87 \frac{L^3}{H}]^{0.385} \quad (19.5)$$

where,

- t_c = concentration time duration of a storm corresponding to the maximum rate of runoff (in hrs),
- L = length of the watercourse from the farthest point in the catchment to the outlet, (in km), and
- H = height difference between the farthest point and the outlet, m.

Table 19.2 Maximum values of runoff coefficient C for various soil covers

Steep, bare rock, also city pavements	0.90
Rocks steep, wooded	0.80
Plateau, lightly covered	0.70
Clayey soils, stiff and bare	0.60
Clayey soils, lightly covered	0.50
Loam, lightly cultivated or covered	0.40
Loam, predominantly cultivated	0.30
Sandy soil, light growth	0.20
Sandy soil, covered, heavy brush	0.10

(b) *U.S. Soil Conservation Service Curve Number Method*

The U.S. Soil Conservation Service has developed a method of estimating runoff from small watersheds of up to about eight hundred hectares based on soil and vegetative covers and moisture levels.

The runoff Q is expressed by the following formula:

$$Q = \frac{(P - I_a)^2}{(P + 4I_a)} \quad (19.6)$$

where,

- Q = runoff in mm,
- I_a = initial abstraction or loss due to infiltration, interception, and surface storage, and
- P = design rainfall in mm.

The initial loss (I_a) is defined by a curve number (CN):

$$I_a = 0.2 S \text{ where, } S = \text{potential infiltration:}$$

$$I_a = 5.08 \left(\frac{1000}{CN} - 10 \right) \text{ mm} . \quad (19.7)$$

The curve number (CN) represents the hydrological soil group, the land use type, and the antecedent moisture conditions. The range of C values for normal conditions is presented in Table 19.3.

The CN values obtained from Table 19.3 are for average moisture conditions and should be modified, if necessary, for relatively wet or dry conditions. The antecedent moisture condition levels and CN conversion for other moisture conditions can be taken from Tables 19.4 and 19.5.

The runoff can be directly read off from Figure 19.2, once the appropriate curve number and the design storm rainfall have been chosen.

(c) *California Culvert Practice for Estimating Design Discharge*

Figure 19.3 is a nomograph for estimating the design discharge. The following example illustrates the use of this chart:

Given:

- o distance of the culvert from the critical point (furthest point in the watershed). $L = 3$ miles,
- o elevation difference between farthest points in the catchment and the culvert site, $M = 900$ ft.,
- o area of catchment $A_c = 2$ square miles,
- o one hour rainfall,
(precipitation in 60 minutes over a 100 yr. return period) $P_{60} = 1.9$, inches and
- o K for deciduous timberland = 60.

Table 19.3 Hydrological soil groups and on values for different types of land use

(for antecedent moisture condition II and Ia = 0.25)

Type of Soil		Infiltration Rate	Class			
Deep sandy		High	A			
Shallow sandy and medium textured		Moderate	B			
Shallow with medium heavy texture		Slow	C			
Clay and shallow/hard pans		Very slow	D			

Land Cover	Land Use Type	Surface Runoff	Hydrological Soil Class			
			A	B	C	D
Fallow		Rapid	77	86	91	94
Row crops e.g., maize	Sloping cultivated land	Rapid	72	81	88	91
	Terraced land	Slow	67	78	85	89
Broadcast crops, e.g., upland Rice	Sloping cultivated land	Rapid	65	76	84	88
	Terraced land	Slow	63	75	83	87
Pasture or range	Heavily grazed, no plant cover	Rapid	68	79	86	89
	Moderately grazed, more than 50% plant cover	Moderate	49	69	79	84
	more than 75% plant cover	Lightly grazed, Slow	39	61	74	80
	grazed, some litter present	Moderate	36	60	73	79
Forest	litter and shrubs cover the soil	Slow	25	55	70	77
		Rapid	72	82	87	89
Dirt roads Roads, hard surface		Rapid	74	84	90	92

Source : Adapted from the U.S. Soil Conservation Service (3)

Table 19.4 Runoff curve number (CN), conversions, and constants

CN for Condition		CN for AMC		S Values in**	Curve starts where P = (in)
II	I	III			
(1)	(2)	(3)	(4)	(5)	
100	100	100	0.000	0.0	
98	94	99	0.204	0.04	
96	89	99	0.417	0.08	
94	85	98	0.638	0.13	
92	81	97	0.870	0.17	
90	78	96	1.11	0.22	
88	75	95	1.36	0.27	
86	72	94	1.63	0.33	
84	68	93	1.90	0.38	
82	66	92	2.20	0.44	
80	63	91	2.50	0.50	
78	60	90	2.82	0.56	
76	58	89	3.16	0.63	
74	55	88	3.51	0.70	
72	53	86	3.89	0.78	
70	51	85	4.28	0.86	
68	48	84	4.70	0.94	
66	46	82	5.15	1.03	
64	44	81	5.62	1.12	
62	42	79	6.13	1.23	
60	40	78	6.67	1.33	
58	38	76	7.24	1.45	
56	36	75	7.86	1.57	
54	34	73	8.52	1.70	
52	32	71	9.23	1.85	
50	31	70	10.00	2.00	
48	29	68	10.8	2.16	
46	27	66	11.7	2.34	
44	25	64	12.7	2.54	
42	24	62	13.8	2.76	
40	22	60	15.0	3.00	
38	21	58	16.3	3.26	
36	19	56	17.8	3.56	
34	18	54	19.4	3.88	
32	16	52	21.2	4.24	
30	15	50	23.3	4.66	
25	12	43	30.0	6.00	
20	9	37	40.0	8.00	
15	6	30	56.7	11.34	
10	4	22	90.0	18.00	
5	2	13	190.0	38.00	
0	0	0	Infinity	Infinity	

Source : U.S. Soil Conservation Service, 1957

** S values for CN in column 1

Table 19.5 Rainfall limits for establishing antecedent moisture conditions

Antecedent moisture conditions class	5-day total antecedent rainfall mm	
	Dormat season	Growing season
I	Less than 12	Less than 35
II	12 to 28	35 to 54
III	Over 28	Over 54

Source: U.S. Soil Conservation Service 1957

To find:

- o Design discharge for a 100 year return period:

from the nomograph (Figure 19.3)

- o time of concentration, $T = 41$ min,
- o for $T = 41$ min, and $P_{60} = 1.9$ inches, critical intensity, $i = 2.2$ inches per hour,
- o for $i = 2.2$ in/hr and $A = 2$ sq.m total precipitation for a flood of 100 year return period, $P = 2800$ cu ft per sec, and
- o for $k = 60$, and $P = 2800$ ft/sec, design discharge = 1700 cu ft per sec for 100 year flood.

This nomograph is convenient provided the one hour rainfall records are available. However, the one-hour precipitation for the desired return period in the design can be obtained from Equation 19.4 also.

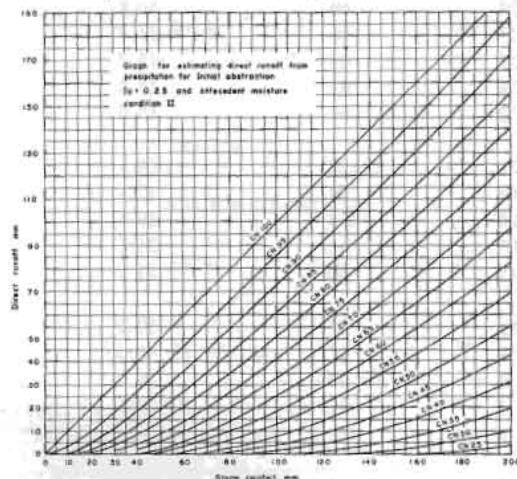


Fig. 19.2 Graph for estimating direct runoff from precipitation for initial abstraction $I_a = 0.25$ and antecedent moisture condition II

19.3 HYDRAULICS

19.3.1 *Hydraulics of Drainage Channels (Adapted from Compendium 5, Roadside Drainage, Transportation Research Board, 1979)*

Most highway drainage facilities such as roadside and catch drains, chutes, and culverts, flowing partially full, are designed according to principles of flow in open channels.

Flow in open channels is classified as steady and unsteady. Unsteady flow occurs when the quantity of water, cross sections of flow, and the slope of the carrying channels are changing. However, for simplicity of hydraulic calculations, flows in road drainage channels are treated as if occurring under steady conditions.

Steady flow can either be uniform or non-uniform (varied).

a) *Uniform Flow*

Uniform flow will take place when the cross section, roughness, and slope of the channel remain constant over the stretch under consideration. The errors involved in assuming uniform flow in drainage channels are relatively small compared to errors in establishing design peak flows, hence drainage channels with constant cross-section, roughness, and slope are often designed as uniform flow channels.

The most widely used equation for uniform flow is the following Manning Equation:

$$V = \frac{1}{n} R^{\frac{2}{3}} S^{\frac{1}{2}} \quad (19.8)$$

where,

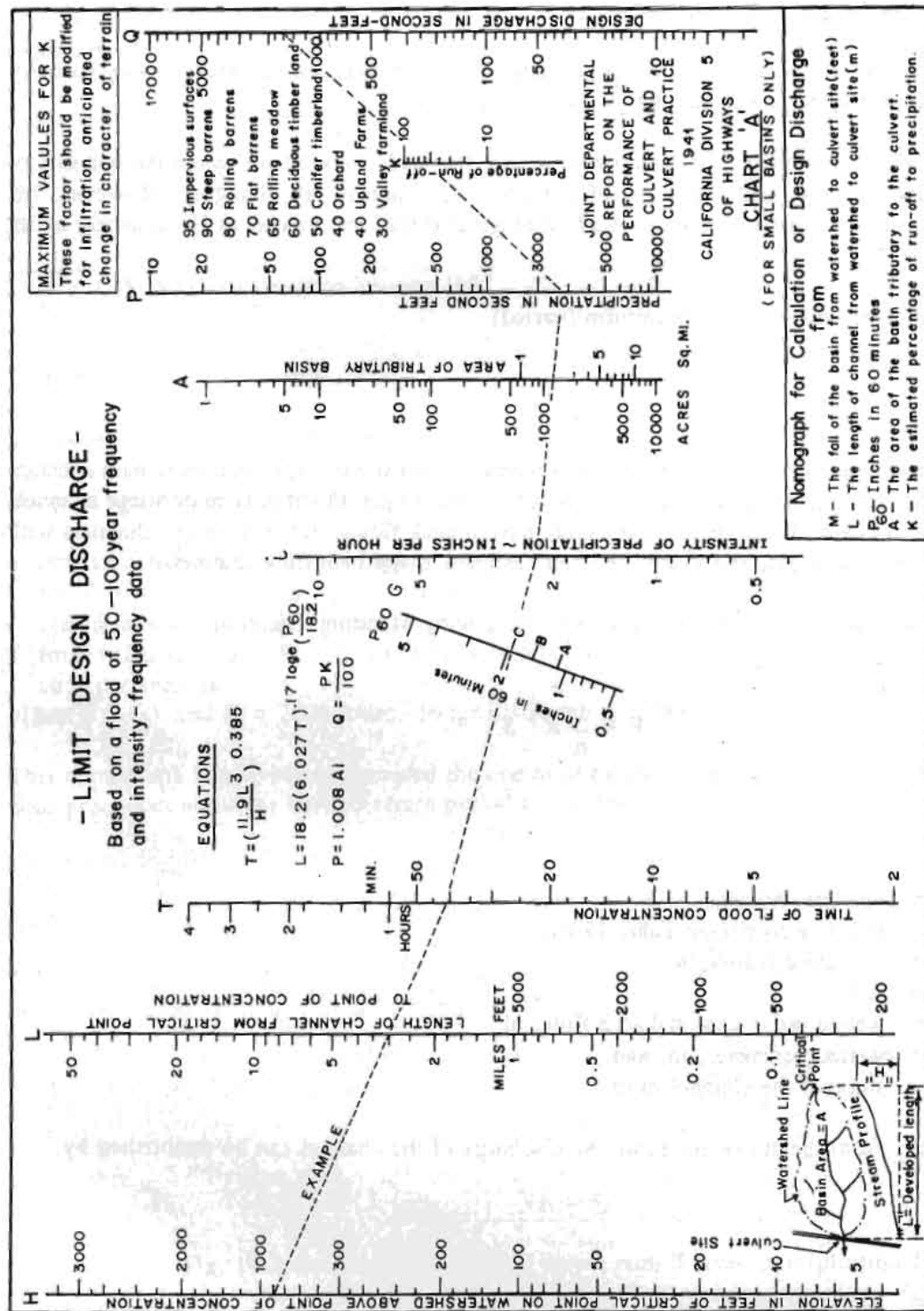
V	= velocity, m/sec,
n	= rugosity coeff (see Table 19.6),
R	= hydraulic radius, m,
R	= A/P,
A	= wetted cross sectional area flow, m ²
P	= wetted perimeter, m, and
S	= slope of the channel m/m.

After finding velocity from the above equation, the discharge of the channel can be established by:

$$Q = AV$$

where,

Q	= flow, m ³ /sec,
A	= cross-sectional area of flow, m ² , and
V	= velocity of flow, m/sec.



Source: Adapted from California Culvert Practice 1957

Fig. 19.3 Nomograph for calculation of design discharge

Table 19.6 Manning roughness coefficient

<u>Closed Conduits</u>	
Concrete Pipe	0.011 - 0.018
Corrugated metal pipe	0.024
Cast iron pipe	0.013
Brick	0.014 - 0.017
Cement rubble masonry with natural floor	0.019 - 0.023
<u>Open Channels</u>	
Earthen, clean, recently completed	0.016 - 0.018
Earthen with short grass and weeds	0.022 - 0.027
Gravelly soil, clean, uniform	0.022 - 0.025
Earthen fairly uniform tides, clean cobble bottom	0.030 - 0.040
Concrete formed no finish	0.013 - 0.017
Concrete bottom, dressed stone sides	0.015 - 0.017
Cement rubble masonry	0.030 - 0.025
Brick	0.014 - 0.017
Mountain stream, no vegetation in channel, steep banks, trees and brush along bank submerged at high stage	
Bottom of gravel, cobbles, few boulders	0.04 - 0.05
Bottom of cobbles, with large boulders	0.05 - 0.07

Source : Compendium 5, Road Drainage, Transportation Research Board, 1979

Table 19.7 Typical safe velocities for different materials

S.No.	Bed Material	Safe velocity (m/s)
1.	Loose clay or fine sand	up to 0.5
2.	Coarse sand	0.5 - 1.0
3.	Fine gravel, sandy or stiff clay	1.0 - 1.5
4.	Coarse gravel, rocky soil	1.5 - 2.5
5.	Boulders, rock	2.5 - 5.0

Source : Sharma 1985.

b) *Non-Uniform or Varied Flow*^{***}

Varied steady flow occurs when the quantity of water remains constant, but the depth of the flow, velocity, or cross-section changes from section to section. The relation of all cross-sections will be:

$$Q = A_1 V_1 = A_2 V_2 = A_n V_n . \quad (19.9)$$

Equation 19.9 is sometimes called the Equation of Continuity.

Velocity of uniform flow in open channels can be computed by the Manning Equation, using the slope of the channel bed as the slope of the energy line but non-uniform steady flow computations require other methods.

The hydraulic design engineer needs a knowledge of varied flow in order to determine the behaviour of the flowing water when changes in channel resistance, size, shape, or slope occur. A discussion of varied flow properly begins with a discussion of the energy of the flowing water.

c) *Energy of flow*

Water flowing in an open channel possesses energy of two kinds - **potential energy** and **kinetic energy**. The potential energy is due to the position of the water above a specific datum and kinetic energy is due to the velocity of the flowing water. In channel problems, energy is conveniently expressed in terms of **head**. Thus, a column of water 20 feet high has a potential (static) head of 20 feet with respect to the bottom of the column. Flowing water has both **potential head** and **velocity head**, the velocity head being equal to :

$$\frac{V^2}{2g}$$

where,

- V = the mean velocity in feet per second, and
g = acceleration of gravity or 32.2 feet per second².

A useful hydraulic concept of the energy of flowing water within one vertical cross-section of the channel is that of **specific head** (also called **specific energy**).

$$\text{Specific head } (H_s) = d + \frac{V^2}{2g} \quad (19.10)$$

^{***} This section up to and including the sub-heading section entitled, The Froude Number, is extracted from Text 1 of Compendium 5 of the Transportation Research Board of the National Academy of Sciences, pp 16-20, Washington D.C. 1978.

If the potential head is related to a datum (Figure 19.5) at or below the bed of the channel at the outlet, energy can be expressed in terms of total head. If Z is the elevation of the channel bottom, total head at any section is:

$$\text{Total head } (H) = d + \frac{V^2}{2g} + Z \quad (19.11)$$

The energy losses due to friction, channel contractions, changes in alignment, and other factors are termed head losses (h_L). The law of conservation of energy, (Bernoulli's Theorem), states that the total head at any section is equal to the total head at any section downstream plus intervening head losses, or, for the channel in Figure 19.5, is equal to the total head at Section 2, plus head loss between Sections 1 and 2, or:

$$d_1 + \frac{V_1^2}{2g} + Z_1 = d_2 + \frac{V_2^2}{2g} + Z_2 + h_L \quad (19.12)$$

In Figure 19.5, the head loss, in a channel of uniform cross-section, equals the change in Z or $(Z_1 - Z_2)$. Thus, the water surface is parallel to the streambed, and

$$d_1 + \frac{V_1^2}{2g} = d_2 + \frac{V_2^2}{2g}$$

Thus the flow is uniform and can be computed by the Manning Equation. The head loss is:

$$(Z_1 - Z_2) = LS_o \quad (19.13)$$

where,

L = horizontal distance between Section 1 and Section 2, and

S_o = channel slope or $\frac{Z_1 - Z_2}{L}$.

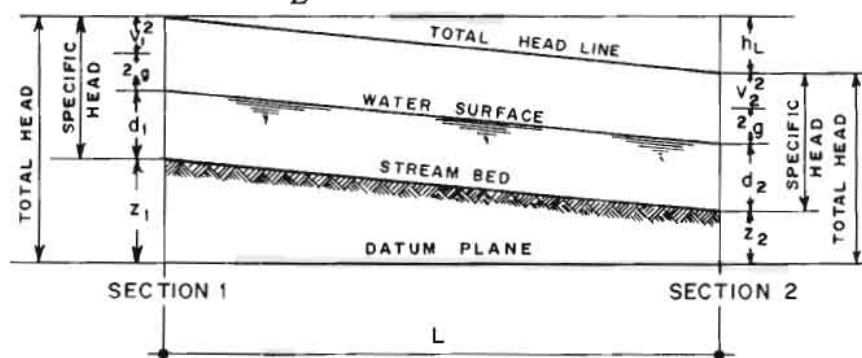


Fig. 19.4 Water-surface profiles of channel with uniform flow

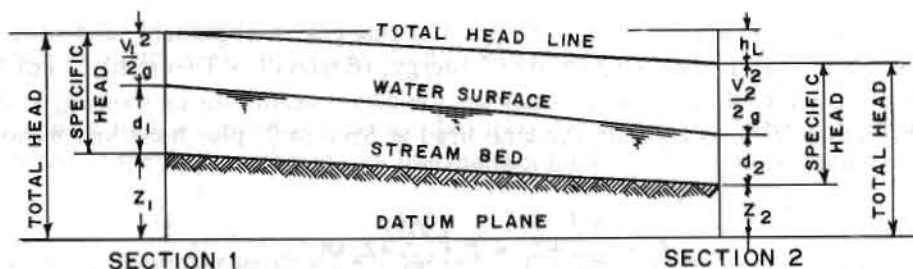


Fig. 19.5 Water-surface profile of channel with non-uniform flow

S_o in uniform flow is sometimes called the **friction slope**. For uniform flow, the Manning Equation can be computed for $S(= S_o)$.

$$S = \left(\frac{V_n}{1.49 R^{2/3}} \right)^2 \quad (19.14)$$

When the head loss does not equal the change in Z , non-uniform flow occurs and the depth of the flow either increases or decreases in a uniform channel. In Figure 19.6, flow takes place with decreasing depth.

Between Sections 1 and 2, the velocity is increasing and the rate of energy loss is, therefore, not constant. This condition could be caused by a channel slope steeper than that needed to overcome frictional resistance or by a change in channel cross-section. Thus, the total head line (also called the energy line or energy gradient) is not a straight line. The water surface line in an open channel is sometimes called the hydraulic grade line.

d) Critical Flow.

With a constant discharge passing a cross-section, changing the depth of flow causes a different specific head for each depth. If specific head is plotted against depth of flow, the result is a specific head (energy) diagram (Figure 19.6).

The specific head curve is asymptotic to the line representing the energy caused by depth and the vertical line of zero depth. Examination of Figure 19.6 reveals several important facts. Starting at the upper right of the curve with a large depth and small velocity, the specific head decreases with decrease in depth, reaching a minimum value at depth d_c known as **critical depth**, sometimes called the depth of the

minimum energy content. Further decrease in depth results in rapid increase in specific head. For any value of specific head, except that corresponding to **critical depth**, there are alternate depths at which the flow could occur. These alternate depths are sometimes referred to as **equal energy depths**.

When the flow occurs at depths greater than critical depth (velocity less than critical), the flow is called sub-critical or tranquil. When the flow occurs at depths less than critical depth (velocities greater than critical), the flow is called supercritical, rapid, or shooting. The change from supercritical to subcritical flow is often very abrupt, resulting in the phenomenon known as hydraulic jump. Flow at the critical depth is called **critical flow** and the velocity at critical depth is the **critical velocity**. The channel slope which produces critical depth and critical velocity for given discharge is the **critical slope**.

Critical depth for a particular discharge is dependent on channel slopes and roughness. Critical slope depends upon the channel roughness, the channel geometry, and the discharge. For a given critical depth and critical velocity, the critical slope for a particular roughness can be computed by the **Manning Equation**.

Supercritical flow is difficult to control because abrupt changes in alignment or in cross-section produce waves that travel downstream, alternating from side to side, and sometimes cause the water to overtop the channel sides. Changes in channel shape, slope, or roughness cannot be reflected upstream except for very short distances (upstream control). Supercritical flow is common in steep flumes and in mountain streams. Pulsating flow can occur at depths as great as 8 feet.

Subcritical flow is relatively easy to control. Changes in channel shape, slope, and roughness affect the flow for some distances upstream (downstream control). Subcritical flow is characteristic of the streams located in the plains and valleys, regions where stream slopes are relatively flat.

Critical depth is important in hydraulic analyses because it is always a hydraulic control. The flow must pass through critical depth in going from one type of flow to the other. Typical locations of critical depth are:

- (1) at abrupt changes in slope when a flat (subcritical) slope is sharply increased to a steep (supercritical) slope;
- (2) at a channel constriction such as a culvert entrance under some conditions;
- (3) at the unsubmerged outlet of a culvert or flume on a subcritical slope, with discharge into a wide channel or with a free fall at the outlet; and
- (4) at the crest of an overflow dam or weir.

Distinguishing between the different types is important in channel design, thus the location of critical depth and the determination of critical slope for a cross-section of given shape, size, and roughness becomes necessary. When flow occurs at critical depth:

$$\frac{A^2}{T} = \frac{Q^2}{g} \quad (19.15)$$

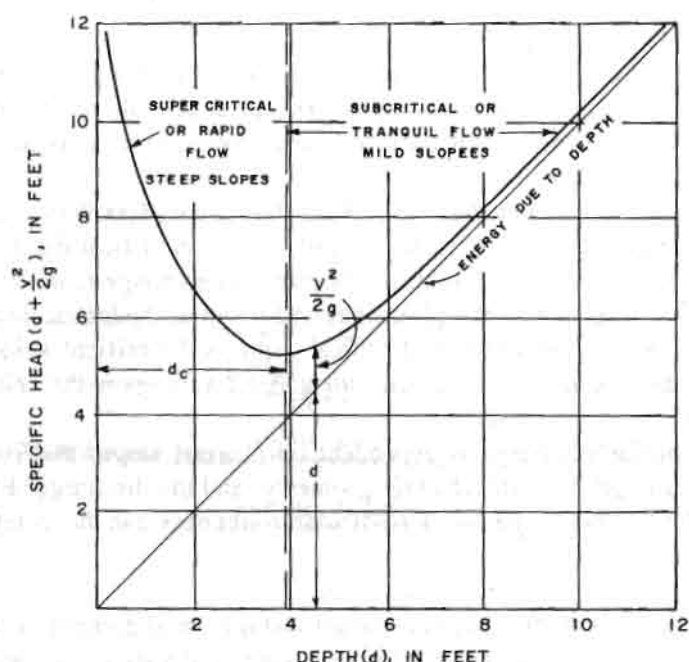


Fig. 19.6 Specific head diagram for constant Q

Critical depth (d_c) can be found from the design charts or computed for various channel cross-sections by the following equations:

Rectangular sections

$$d_c = 0.315 \sqrt[3]{\left(\frac{Q}{B}\right)^2} \quad (19.16)$$

Trapezoidal sections

$$d_c = \frac{4z H_o - 3b + \sqrt{16z^2 H_o^2 + 16z H_o b + 9b^2}}{10z} \quad (19.17)$$

The tables in King's Handbook (1976) provide a much easier solution for critical depth than Equation 19.17.

Triangular sections

$$d_c = 0.574 \sqrt[5]{\left(\frac{Q}{z}\right)^2} \quad (19.18)$$

Circular section, approximate solution:

$$d_c = 0.325 \left(\frac{Q}{D} \right)^{\frac{2}{3}} + 0.083D \quad (19.19)$$

accurate only when d_c/D lies between 0.3 and 0.9

where,

- A = area of cross-section of flow, in square feet,
- B = the width of a rectangular channel, in feet,
- b = bottom width of a trapezoidal channel, in feet,
- D = diameter of a circular conduit, in feet,
- g = acceleration of gravity, 32.2 feet per second²,
- T = top width of water surface, in feet,
- V = mean velocity of flow, in feet per second, and
- x = slope of sides of a channel (horizontal to vertical).

Problems in Non-uniform Flow

Problems in non-uniform flow include computing the water surface profile, design of channel transitions, and dissipation of energy of the flowing water. A case that must be considered in the design of chutes is discussed briefly. This is a case of a sudden change in channel grade from one less than critical to one greater than critical (Figure 19.7).

The depth of flow at Section 1 can be computed using the Manning Equation. The flow at Section 2 (which for practical purposes can be assumed to occur at the change in grade) passes through critical depth (d_c). If the channel grade downstream from Section 2 is equal to the critical slope, the flow will become uniform at a depth equal to d_c . However, when a drainage channel discharges into a chute, the chute grade is steeper than critical slope and the flow is uniform and accelerating. Section 2 becomes the control section for both the flow in the channel (downstream control) and the flow in the chute (upstream control).

Knowing the specific head (H_o) in the approach channel, the capacity of the chute entrance, such as Section 2 (Figure 19.7) for a rectangular channel can be computed by a weir formula.

$$Q = 3.09 k_c B H_o^{3/2} \quad (19.20)$$

For a trapezoidal channel the capacity can be computed by the formula:

$$Q = 8.03 k_c (H_o - d_c)^{\frac{1}{2}} (d_c) (b + zd_c) \quad (19.21)$$

where,

d_c = critical depth at Section 2,

H_o = specific head at Section 1,

K_e = coefficient which represents the entrance loss - varies from 1.0 for perfect entrance of smooth curves and gradual transition to 0.82 for a rectangular shaped-structure with square corners, and

Z = slope of sides of a channel (horizontal to vertical).

The critical depth, d_c , is computed by Equations (19.16 to 19.20).

The usual problem is to determine the size of chute channel required to carry a given discharge. The bottom width at the chute entrance (Section 2, Figure 9.7) can be computed by Equation (19.22) for a rectangular channel,

$$B = \frac{0.324Q}{k_e H_o^{3/2}} \quad (19.22)$$

and approximately by Equation (19.23) for a trapezoidal channel

$$b = \frac{0.324Q}{k_e H_o^{3/2}} - 0.7zH_o \quad (19.23)$$

where,

the symbols are the same as those in Equations 19.20 and 19.17, from which Equations 19.18 and 19.19 were derived.

The flow through the chute must satisfy Equation 19.12. If the head loss (h_L) through the chute is solely from friction, it can be expressed in terms of the hydraulic properties at each end of the chute, the roughness coefficient (n), and the length of chute (L) or:

$$h_L = \frac{n^2}{4.41} \left[\left(\frac{V_1}{R_1^{2/3}} \right)^2 + \left(\frac{V_2}{R_2^{2/3}} \right)^2 \right] L \quad (19.24)$$

If the flow is accelerating ($h_L < LS_o$), the cross-section of a large chute can be gradually reduced in order to provide a more economical section.

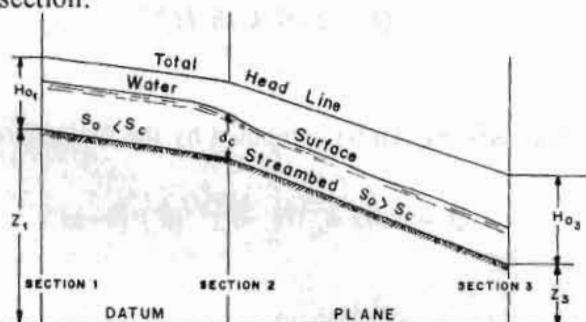


Fig. 19.7 Water-surface profile of a channel with sudden change in grade

The Froude Number

A useful parameter of flow in the Froude Number, one form of which is:

$$F = \frac{V}{\sqrt{gd_m}} = \frac{V}{V_c} \quad (19.25)$$

where,

- d_m = mean depth of flow in feet-in the general expression any characteristic dimension of flow might be used,
- g = acceleration of gravity = 32.2 (fps²),
- V = mean velocity in feet per second, and
- V_c = critical velocity for the channel and discharge.

The Froude Number uniquely describes the flow pattern when gravity and inertia forces are the dominant factor in the flow. For example, in Figure 19.6 each point on the specific head curve has a single value of the Froude Number, although two values on the curve can be found for a particular value of specific head. The Froude number of critical flow is one; values greater than one indicate supercritical flow and values less than one indicate subcritical flow.

19.3.2 Hydraulic Design of Culverts

Flow through culverts occurs under two major conditions of flow (1) flow with inlet control (2) flow with outlet control. To avoid rigorous computations for determining the conditions of flow and headwater depths, the nomograph prepared by the U.S. Federal Highway Administration (Hydraulic Engineering Circular No.5) are used to calculate headwater depths for both inlet control and outlet control. Assuming a trial size culvert, the headwaters are calculated for both inlet and outlet control flow conditions. The condition at higher headwater is assumed to prevail. However, the headwater should not be greater than permitted by site and other design consideration. See 19.3.2 (c) for stepwise details for use of nomographs.

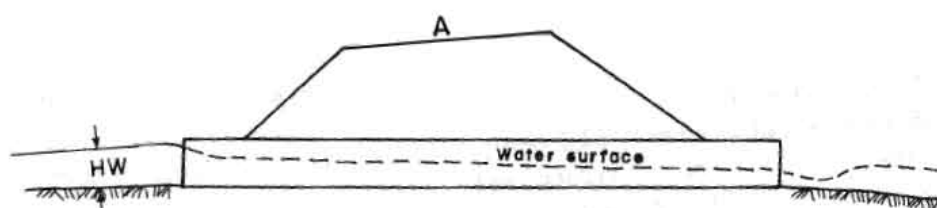
(a) Flow with Inlet Control

A culvert operates with inlet control when the flow capacity is controlled at the culvert inlet by the depth of headwater and the shape of the entrance, including the barrel shape. In inlet control, the roughness and length of the culvert and tailwater depth do not practically affect the culvert capacity.

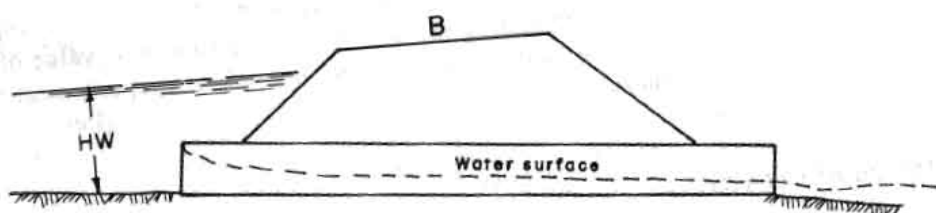
Various inlet flow conditions are shown in Figures 19.8 (a) to 19.8 (c).

(b) Flow with Outlet Control

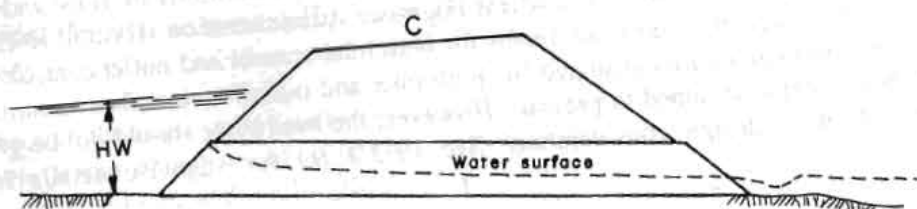
Flow in culverts flowing with outlet control can be full or partially full for part of the barrel length or for the full length. Various types of outlet control flows are shown in Figure 19.9(a-d). In a culvert operating with outlet control, flow capacity is affected by tail water elevation, the length, roughness, and the slope of the culvert in addition to inlet conditions. However, outlet conditions are the determining factors controlling flow capacity.



(a) Projecting end — Unsubmerged



(b) Projecting end — Submerged

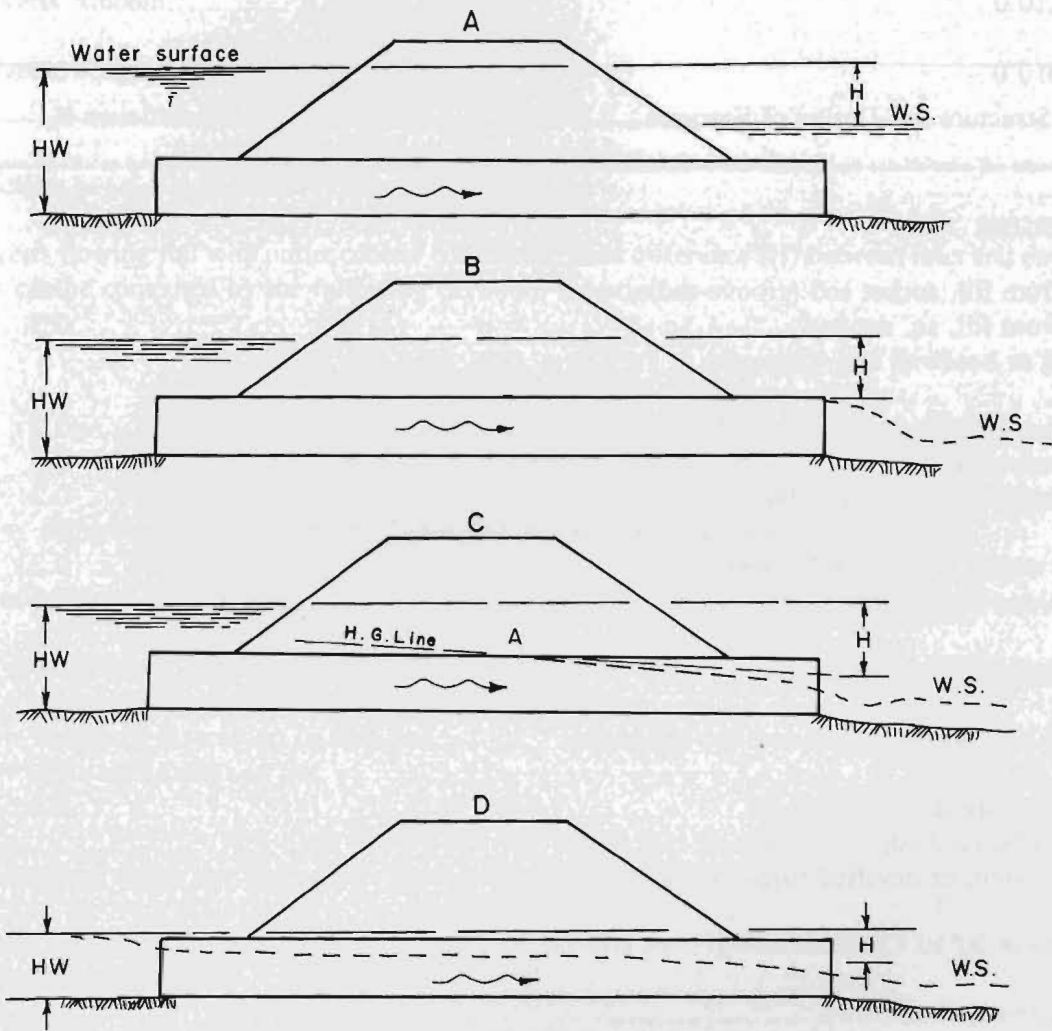


(c) Mitered end — Submerged

INLET CONTROL

Source: U.S. Federal Highway Administration 1977

Fig. 19.8: Culverts with inlet control



OUTLET CONTROL

Source : U.S. Federal Highway Administration 1977

Fig. 19.9: Culverts with outlet control

Table 19.8 Entrance loss coefficients

Outlet control, full or partly full

$$\text{entrance head loss } H_e = k_e \frac{V^2}{2g}$$

Type of Structure and Design of Entrance	Coefficient K_e
<u>Pipe, Concrete</u>	
Project from fill, socket end (groove-end)...	0.2
Project from fill, sq. cut end	0.5
Headwall or headwall and wingwalls	
Socket end of pipe (groove-end).....	0.2
Square-edge.....	0.5
Rounded (radius = 1/12D).....	0.2
Bevelled edges, 33.7° or 45° bevels.....	0.2
Side-or slope-tapered inlet.....	0.2
<u>Box, Reinforced Concrete</u>	
Headwall parallel to embankment (no wingfalls)	
Square-edged on 3 edges.....	0.5
Rounded on 3 edges to radius of 1/12 barrel dimension, or bevelled edges on 3 sides.....	0.2
Wingwalls at 30° to 75° to barrel	
Square-edged at crown.....	0.4
Crown edge rounded to radius of 1/12 barrel dimension, or bevelled top edge.....	0.2
Wingwall at 10° to 25° to barrel	
Square-edged at crown.....	0.5
Wingwalls parallel (extension of sides)	
Square-edged at crown.....	0.7
Side or slope-tapered inlet.....	0.2

Source: Transportation Research Board Commission on Sociotechnical Systems (TRBCSS) 1978

Table 19.9 Value of n for commonly used culvert materials

Concrete pipes.....	0.012
Box culverts, smooth.....	0.012
Box culverts, rough, with sediment deposits...	0.016

The Equation 19.26 can be readily solved for H by the use of the nomograph for full flow. The nomograph can be used for other values on n also by modifying the culvert length.

For culverts flowing full with outlet control conditions, head difference (H) between inlet and outlet water surfaces can be computed by the following Bernoulli Equation:

$$H = \left[1 + K_e + \frac{29n^2L}{R^{1.33}} \right] \frac{V^2}{2g} \quad (19.26)$$

where,

H = difference of levels between headwater and tail water surfaces in feet,

$\frac{V^2}{2g}$ = velocity head in feet,

K_e = coefficient of entrance loss (see Table 19.7),

n = Manning roughness coefficient (see Table 19.8),

L = length of the culvert in feet, and

R = hydraulic radius in feet.

(c) *Stepwise Detail for Use of the Nomograph to Design a Culvert*

Figures 19.10 and 19.11 illustrate flow through pipe culverts and Figures 19.12 to 19.15 are nomographs for determining culvert size.

1. The following design data are required for computation of the culvert size with the nomograph:
 - a. design flood or discharge, Q_n of n years return period (cfs),
 - b. length of the culvert, L (feet),
 - c. slope of the culvert, S, (ft per ft),
 - d. allowable headwater depth, HW, from culvert invert to the permissible water surface elevation at the entrance (feet), and
 - e. mean and maximum velocities in natural drains.

2. Culvert type, including culvert material, shape, and entrance type, is selected. The approximate size of the culvert is determined by the equation:

$$\frac{Q}{10} = A$$

Alternatively, the inlet control nomograph can be used assuming an approximate

$$\frac{HW}{D} = 1.5 \text{ using } Q_a$$

3. For the trial size culvert, headwater depths are determined for inlet control and outlet control conditions of flow as described below.

For Inlet Control Flow,

- Find HW/D for the trial size culvert from the nomograph and establish HW by multiplying obtained HW/D by trial size D .
- If HW is more or less than permissible, another trial size is assumed until HW is acceptable for inlet control.

For Outlet Control Flow

- Assume the depth of tailwater TW , in feet, above the invert at the outlet for the design flood in the outlet channel.

An approximate depth of flow in a natural stream at the outlet can be made by calculating with the Manning Equation, if the channel at the outlet has a uniform cross-section, slope, and roughness. However, most outlet channels are wider and steeper than the culvert; tailwater depth being less than critical depth does not affect the flow and therefore, channel depth calculations are not required.

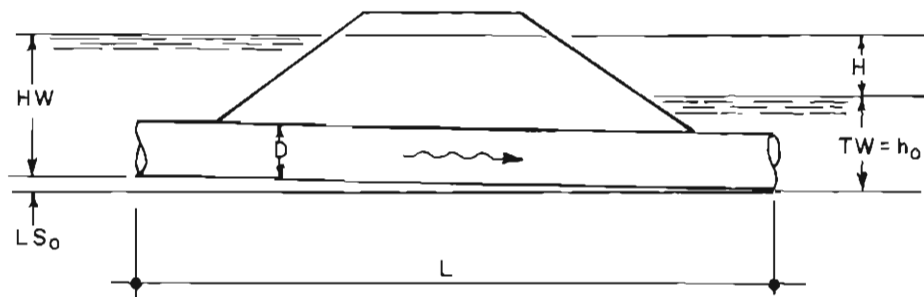
- Establish headwater, HW , by the following equation:

$$HW = H + h_o - LS_o \quad (19.27)$$

where,

- H = headloss from the nomograph (Figures 19.14 and 19.15) for outlet control (ft),
 S_o = slope of culvert invert (ft per ft), and
 L = length of culvert (ft).

However, if the tailwater, TW , elevation is equal to or greater than the top of the culvert at the outlet;
 $h_o = TW - (\text{tailwater depth [feet]})$.



Source : U.S. Federal Highway Administration 1977

Fig. 19.10 Flow through pipe culvert

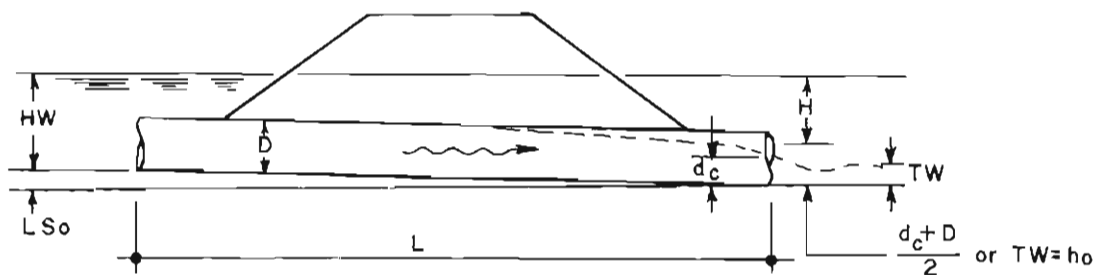
If tailwater elevation is lower than the crown of the culvert at the outlet:

$$h_o = \frac{d_c + D}{2}, \text{ or TW, whichever is greater}$$

where,

d_c = critical depth in feet, and

D = height of culvert in feet.



Source : U.S. Federal Highway Administration 1977

Fig. 19.11 Flow through pipe culvert

4. Compare the headwaters, HW, obtained for inlet control and outlet control flows. The higher headwater governs and indicates flow control for the selected size.
 5. If outlet control governs and gives headwater, larger than permissible headwater, select a larger sized culvert. Only outlet control calculations need to be revised, as inlet control has been satisfied already by the previous smaller sized culvert.
 6. Compute outlet velocities for the finally selected culvert size, to determine the channel protection needs.
- a) If outlet control governs, then outlet velocity $V = \frac{Q_n}{A_o}$, where A_o is the area of flow in the culvert barrel at the outlet:

where,

A_o = the area corresponding to d_c or TW, if d_c or TW is lower than the culvert barrel top at the outlet. A_o is always less than the total cross-sectional area of the culvert barrel.

- b) If inlet control governs, outlet velocity can be taken to be equal to mean velocity in open channel flow, computed with the help of the Manning Equation.

For n or K_c values different from those shown in the nomograph, the following procedure is applied.

For the n of the nomograph and a K_c intermediate between the scales given, connect the given length on adjacent scales by a straight line and select a point on this line spaced between the two chart scales in proportion to the K_c values.

For a different roughness coefficient n_1 from that of the chart n , use the length scales shown with an adjusted length L_1 , calculated by the formula:

$$L_1 = L \left[\frac{n_1}{n} \right]^2 \quad (19.28)$$

- c) Examples on the use of the nomograph (Figures 19.12 to Figure 19.15) for hydraulic design of culverts:

given,

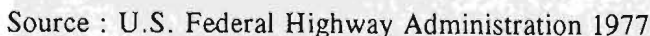
- o 25 year return period flood, $Q = 70$ cu ft/sec,
- o stream-bed slope, $S = 75\%$,
- o culvert type = concrete pipe,
- o length of pipe = 30ft,
- o road formation width = 23ft,

- o culvert diameter
- o culvert slope

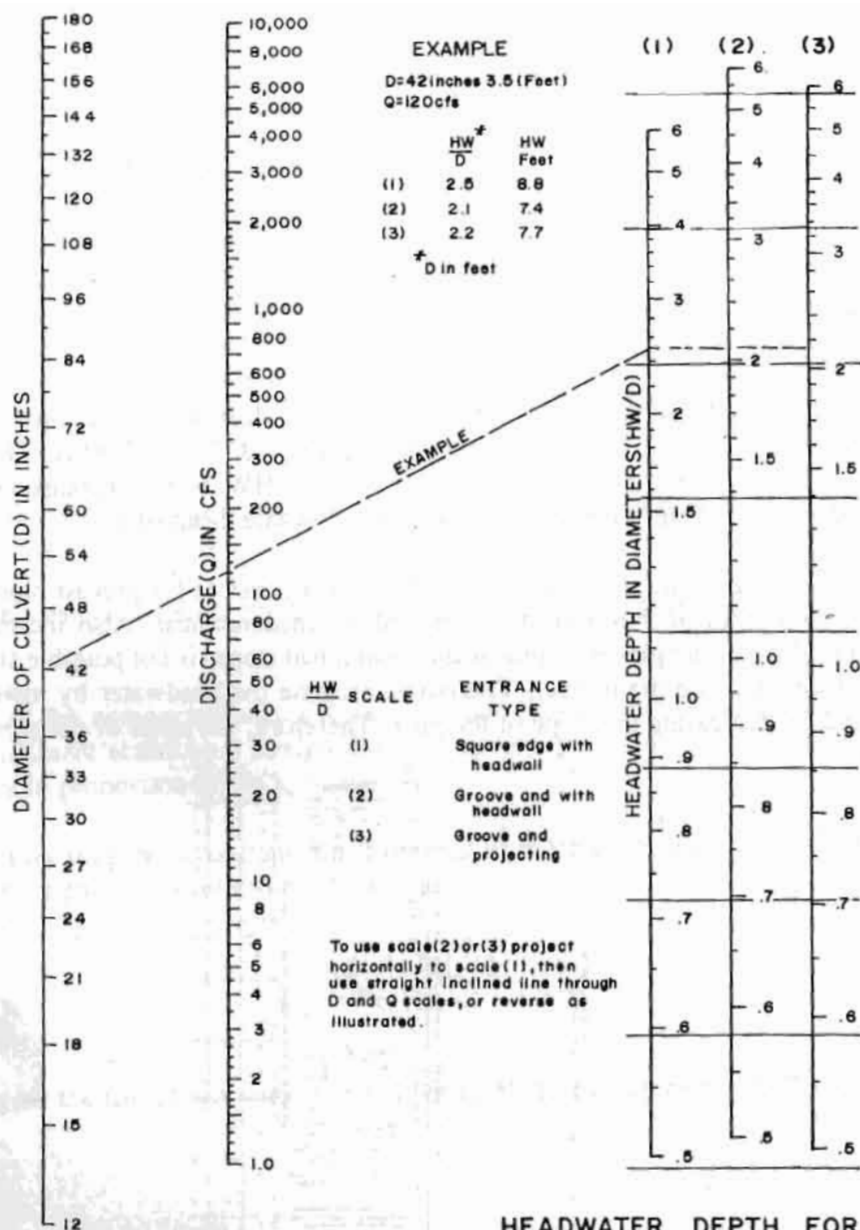
- o assume slope of culvert = 70%,
- o assume size of culvert = 3ft diameter, and
- o assume allowable headwater = 5ft.

o Approximate size of pipe required:
 $= Q/10 = 70/10 = 7 \text{ sq ft.} = \text{one 3ft diameter pipe}$

o Increasing the size of the slope by a few inches is not possible for precast pipes 3 feet in diameter. Providing two pipes of 3 feet in diameter will be uneconomical. Also increasing the headwater, keeping the slope of the pipe the same as the natural bed slope, is not possible since this will increase the road level and side drain level. Therefore, increase the headwater by lowering the inlet of the culvert and by decreasing the slope of the pipe. Therefore, the slope of the pipe = $70 - 4.5 = 65.5$ per cent.

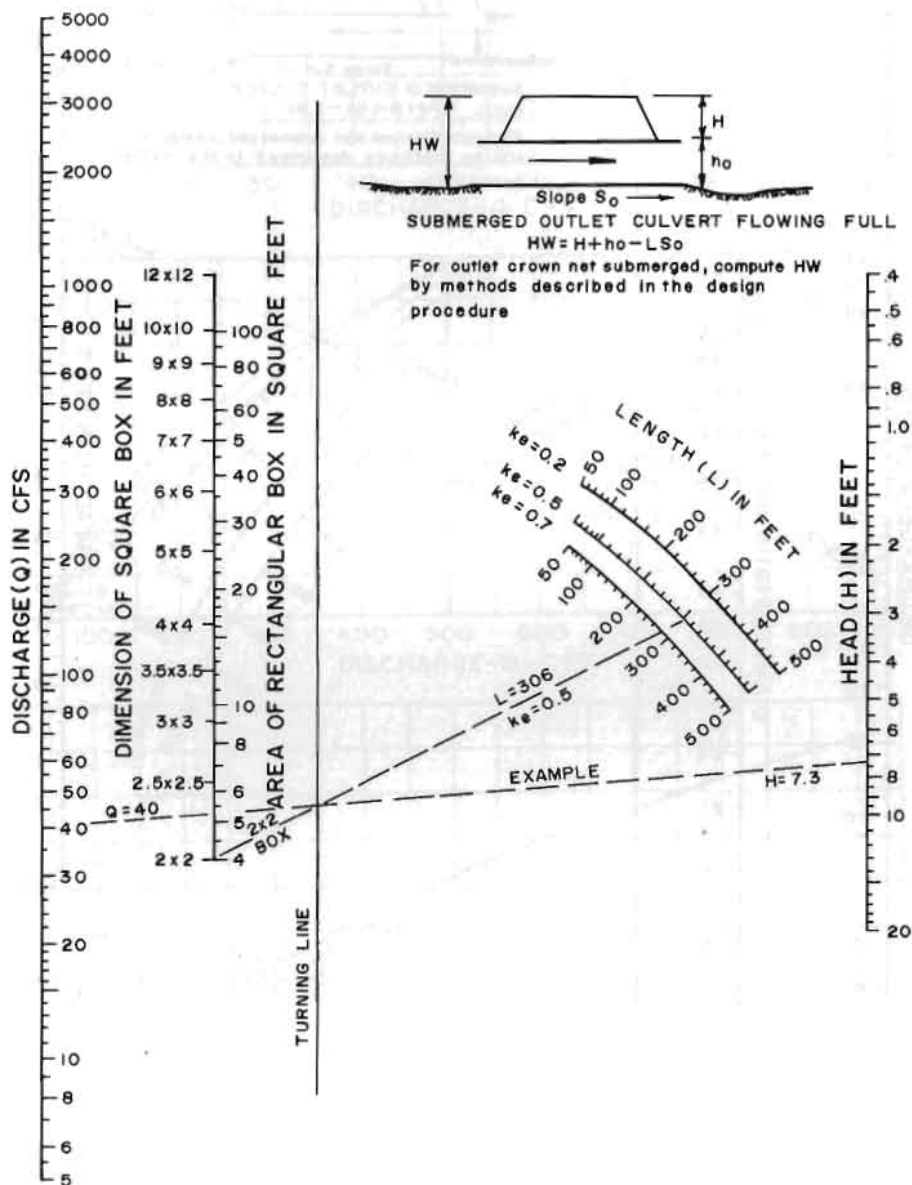


513



Source : U.S. Federal Highway Administration 1977

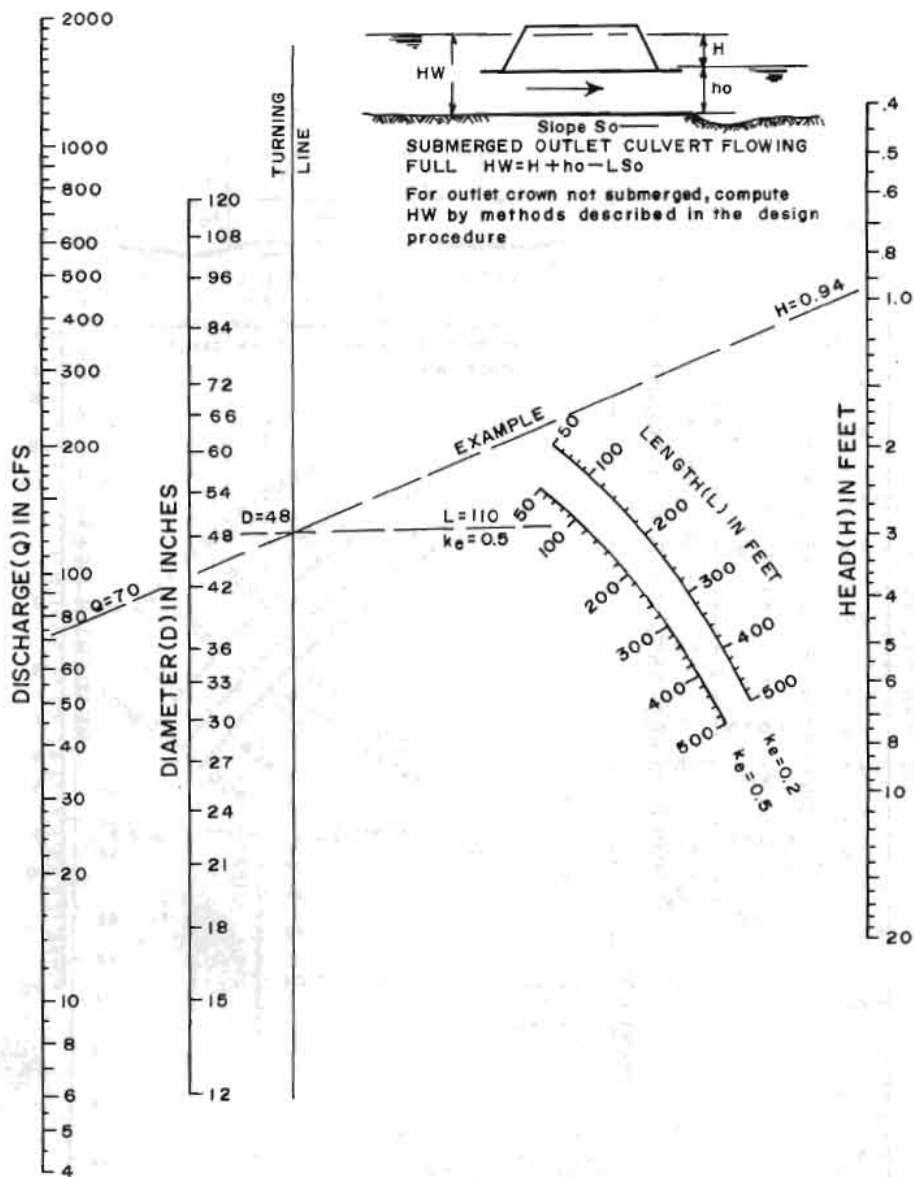
Fig. 19.13 Hydraulic chart



HEAD FOR
 CONCRETE BOX CULVERTS
 FLOWING FULL (OUTLET CONTROL)
 $n = 0.012$

Source : U.S. Federal Highway Administration 1977

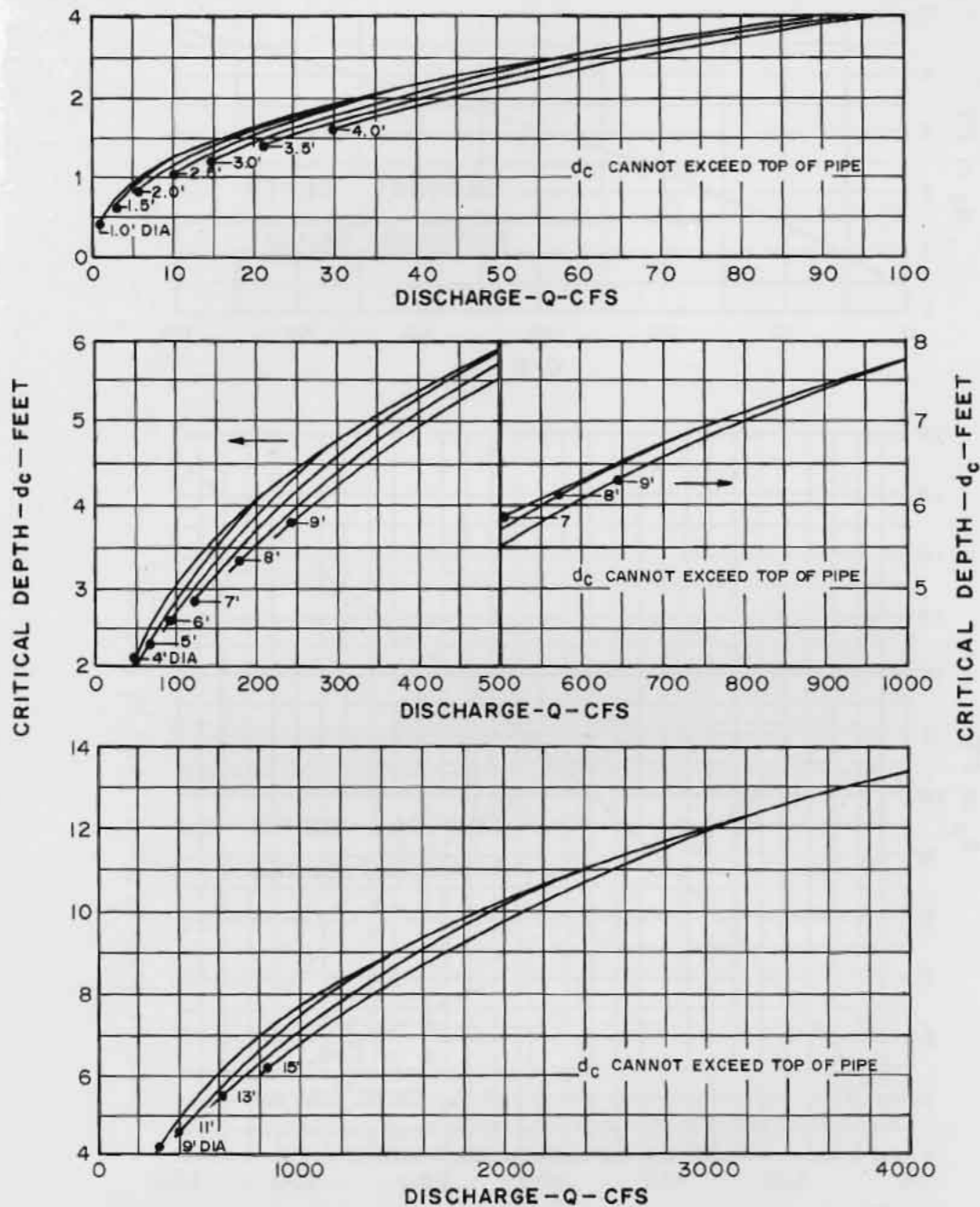
Fig. 19.14 Hydraulic chart



HEAD FOR
 CONCRETE PIPE CULVERTS
 FLOWING FULL
 $n = 0.012$

Source : U.S. Federal Highway Administration, 1977

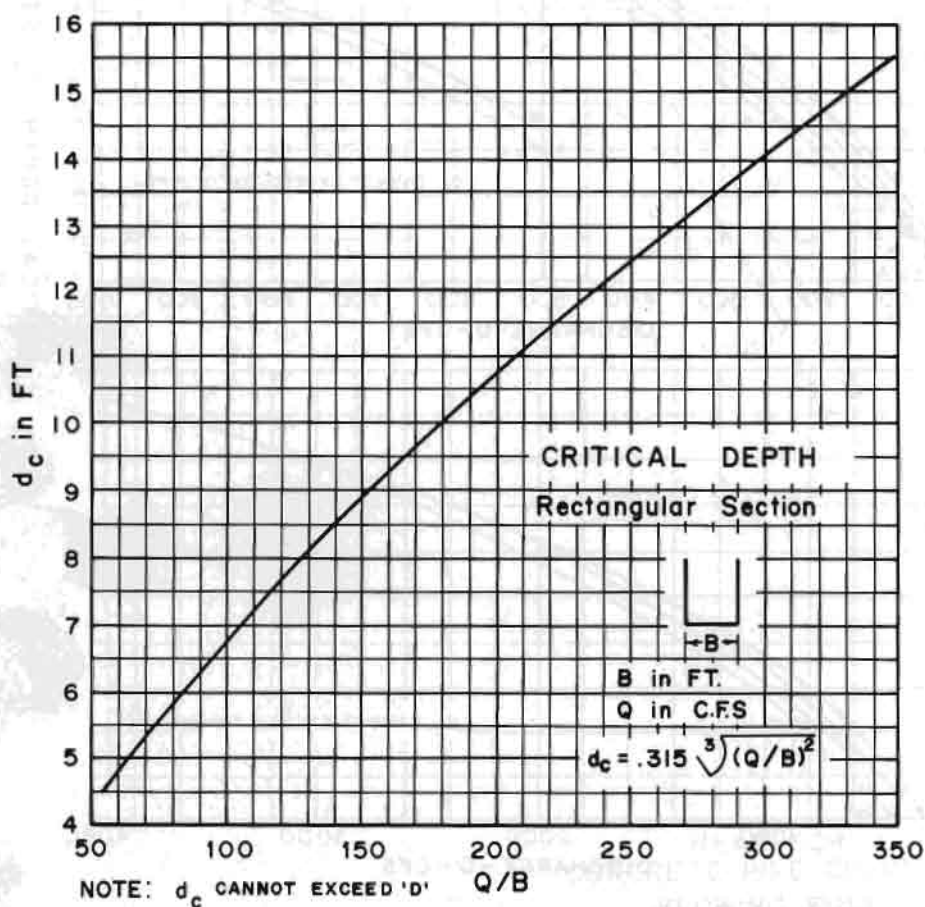
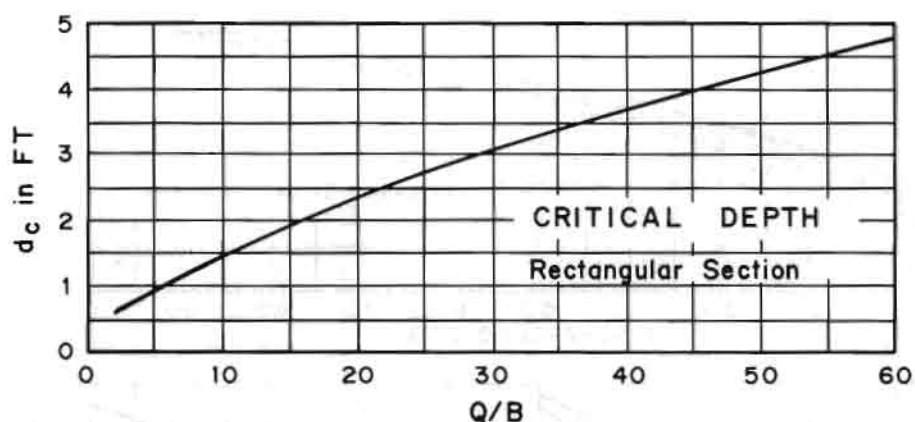
Fig. 19.15 Hydraulic chart



CRITICAL DEPTH FOR CIRCULAR PIPE

Source : Compendium 3, TRB, 1978

Fig. 19.16 Critical depth for circular pipe



CRITICAL DEPTH FOR RECTANGULAR SECTION

Source : Compendium 3, TRB, 1978

Fig. 19.17 Critical depth for rectangular section

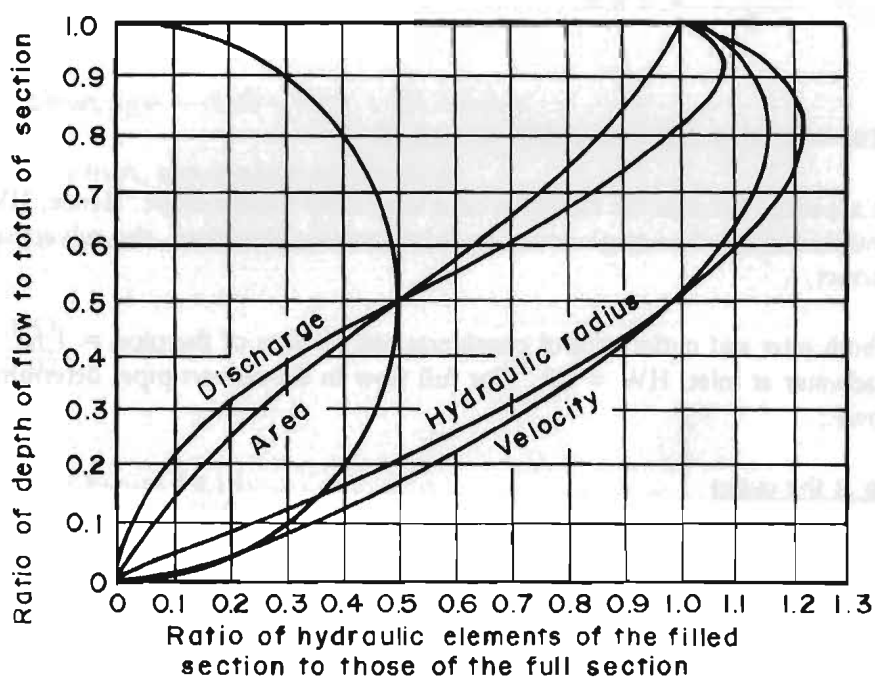


Fig. 19.18 Hydraulic elements of a circular pipe

Checking for Outlet Control

From the outlet control nomograph (Figure 19.14) head loss $H = 2.6$ ft for 50 ft culvert, and $K_e = 0.5$ from Table 19.7. Hence for a 30 ft culvert:

$$\text{head loss } H = 30/50 \times 2.6 = 1.56 \text{ ft, and}$$

$$\text{headwater for outlet control } HW = H + h_o - Ls_o.$$

Because of the steep slope, assume that the tailwater depth below the pipe top at the outlet is half the pipe diameter:

$$\text{if } TW = 1/2 D \text{ then } h_o = d_c + D/2. \text{ (for } d_c \text{ values, see Figures 19.16 and 19.17)}$$

Find d_c from Figure 19.16:

$$h_o = \frac{2.6 + 3}{2} = 2.8 \text{ ft.}$$

Hence,

$$HW = 1.56 + 2.8 - 30 \times .655 = -15.29.$$

The negative sign appeared because the culvert is on a very steep torrent slope. Hence, HW inlet control $>$ HW outlet control, and the flow is governed by inlet control. Therefore, the culvert size selected by inlet control is correct.

Therefore, from both inlet and outlet control considerations the size of the pipe = 1 no. 3ft dia.; slope = 65.5% and headwater at inlet, $HW = 6$ ft. For full flow in the culvert pipe, determine velocity and discharge as follows :

Check for erosion at the outlet

velocity at full flow

$$\begin{aligned} V_F &= \frac{1.49}{h} R^{2/3} S^{1/3} \\ &= \frac{1.49}{.012} \left(\frac{3}{4}\right)^{2/3} (.655)^{1/3} \\ &= 124.16 \times 0.8247 \times 0.8093 \\ &= 82.8 \text{ ft/sec,} \end{aligned}$$

$$\text{full area of culvert pipe, } A_F = \frac{\pi d^2}{4} = \frac{\pi 3^2}{4} = 7.07 \text{ sq.ft,}$$

full flow,

$$Q_F = V.A = 82.8 \times 7.07 = 585 \text{ cfs},$$

$$\frac{Q \text{ of culvert flow}}{Q_F} = 70/585 = 0.1197,$$

from Figure 19.18

$$d/d_f = 0.22, \text{ and}$$

depth of flow in culvert pipe for design flow, $d = 0.22 \times 3' 0" = 0.66'$.

From Figure 19.18,

$$V/V_f = 0.6$$

hence,

$$\text{velocity in the culvert pipe} = 0.60 \times 82.8 = 49.7 \text{ ft/sec.}$$

The velocity is very high, hence adopt milder slope.

Now, limiting the culvert velocity to 20ft/sec for $Q = 70$ cfs, required area = 3.53 sq ft

if,

$$A/A_f = \frac{3.53}{7.07} = 0.5,$$

then,

$$d/d_f = 0.5 \text{ (see Figure 19.18)}$$

$$\text{and for } d/d_f = 0.5; R/R_f = 1.0.$$

Therefore,

$$R = 1.0 \times 3/4 = 0.75 \text{ ft},$$

therefore,

$$P = A/R = 3.53/0.75 = 4.71 \text{ ft.}$$

$$V = \frac{1.49}{n} R^{2/3} S^{1/2}$$

now,

$$S = \sqrt{\frac{V.n}{1.49 R^{2/3}}} = \sqrt{\frac{20 \times 0.012}{1.49 \times 0.75^{2/3}}} = 0.4419,$$

therefore, adopt a culvert pipe slope of 44 per cent.

The inlet control flow is not affected by change in slope. The change in outlet control L_{40} value from the original 19.65 to 13.2 after the change in slope also does not affect the governing inlet flow control. Because of the pipe outlet above the gully bed and the milder slope of pipe, scour protection would be needed at the outlet. The protection measures can be based on the following calculations.

The energy of water will be dissipated by the water falling freely out of the culvert pipe into a water pool lined with at least d_{50} size riprap obtained in the following calculations. Calculate maximum scour depth and riprap gradation required by the following formulas for cohesionless soil:

$$1) \quad \frac{D_{sm}}{D_o} = 0.80 \left(\frac{Q}{D_o^{5/2}} \right)^{0.375} t^{0.10}$$

$$D_{sm} = 0.80 \left(\frac{70}{3^{5/2}} \right)^{0.375} (60)^{0.10} \times 3$$

$$= 6.34 \text{ ft}$$

where,

- D_{sm} = maximum scour depth in ft,
- D_o = diameter of culvert in ft,
- Q = flow in cfs, and
- t = duration of flow in minutes.

The x,y coordinates of the flow trajectory can be approximately calculated as follows :

$$X = V \sqrt{\frac{2y}{g}}$$

where,

- V = velocity at pipe outlet (ft/sec),
- x,y = trajectory coordinates (ft), and
- g = 32.2 ft/sec².

x (ft)	8.5	12	15.7	19
y (ft)	3	6	10	15

For half full flow at outlet and elevation difference of about 6 ft between the top of the flow at the outlet and the ground level below the outlet, the distance (x) requiring protection is 12 ft.

The protection measures can be gabion or masonry cascade or a heap of flow stable, large boulders.

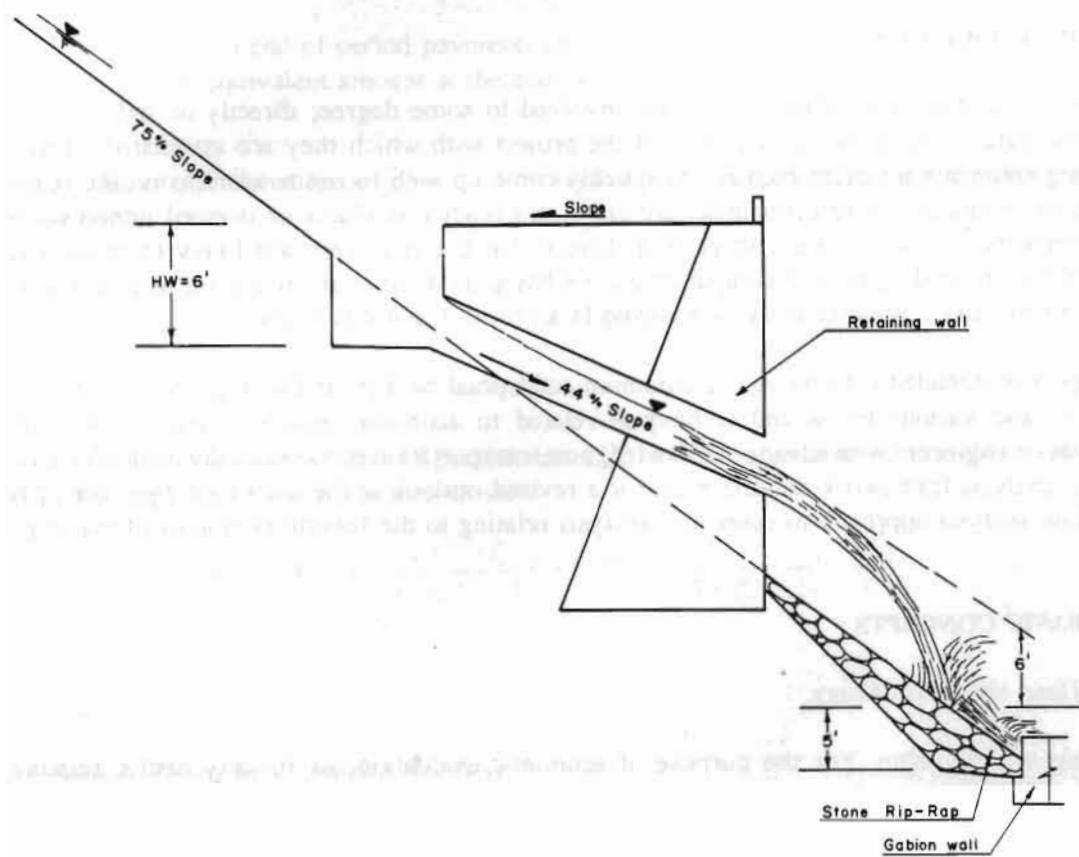


Fig. 19.19: Design example of pipe culvert

TRANSPORTATION ECONOMICS

20.1 INTRODUCTION

Engineers concerned with infrastructure are involved to some degree, directly or indirectly, with the costs, time value, and economic viability of the project with which they are associated. Engineers in developing countries are often required to quickly come up with recommendations on the feasibility of a project in situations where economists are either not readily available or deemed unnecessary by the decision-makers. In such cases, there is a danger that the engineers are likely to present technical feasibility recommendations with comparative costs based on constant monies alone as a substitute for the various criteria and economic analysis involved in a proper feasibility study.

This chapter is intended i) to provide a minimum conceptual background to engineers on the time value of money, and various terms and techniques related to economic analysis, and ii) to highlight, to economists or engineers with advanced knowledge on transportation economics, the methods of a long-run economic analysis framework and the need for a revised outlook at the use of internal rate of return in a cash flow analysis approach to economic analysis relating to the feasibility studies of major projects.

20.2 BASIC CONCEPTS

20.2.1 *Time Value of Money*

Money has a time value. For the purpose of economic evaluation, or for any matter relating to the management of money, it is essential to understand the time value concept. The future value of a single amount or present single amount is given by:

$$F = P (1+i)^n$$

where,

- F = future amount,
- P = present amount,
- i = interest rate, usually per one year, and
- n = number of periods of times, usually in years.

The present amount of P of a future amount F is then given by:

$$P = \frac{F}{(1+i)^n}$$

Often, payments or receipts occur at regular intervals. The future value of a series of uniform payments at equal intervals can be expressed by:

$$F = A \left[\frac{(1+i)^n - 1}{i} \right]$$

where,

- A = uniform end-of-period payments or receipts at a rate of interest i , and
 F = total equivalent amount at the end of the n periods.

The present value of a series of end-of-period uniform payments can be derived from the above equations and is given by:

$$P = A \left[\frac{(1+i)^n - 1}{i (1+i)^n} \right]$$

The equivalent uniform series of end-of-period values A can, for a present value p or future value F , be obtained from the above equations as follows:

$$A = P \left[\frac{i (1+i)^n}{(1+i)^n - 1} \right] = F \left[\frac{i}{(1+i)^n - 1} \right]$$

20.2.2 Common Terms in Economic Analysis

Prices

For economic analysis, it is necessary to bring the streams of costs or benefits at different times over the life of a project to one common unit or base line.

Inflation

The issue of incorporating inflation (differential or general) is an extremely complex matter. Some authorities have recommended the use of differential prices only when there is overwhelming evidence that certain inputs, such as land costs, are expected to experience significant changes relative to the general price level. The inflation, price changes, or interest rates should not be confused with the discount rate.

Because of the uncertainty associated with predicting future rates of inflation, it has been the practice usually to remove the effect of inflation in economic analysis for road projects. Road project costs or

prices estimated for future years are normally expressed in constant monetary terms for the first, or base year, of analysis. In most cases, it can be assumed that future inflation will affect both costs and benefits equally and hence its effects can be ignored. However, there may be exceptions to this and, in these cases, differential rates of inflation will need to be assumed for different elements in the project.

Discounting

The discount rate is used to bring back all future expected costs or benefits to the base line (usually present day value) to allow comparison of alternatives.

Discount rate is the opportunity cost of capital. Money used to invest in the project in one sector could be invested elsewhere and earn a dividend. The loss of this opportunity to earn a dividend by using the capital in a project is accounted for by use of a discount rate in the economic analysis. The choice of discount rates considerably influences the outcome of economic analysis. The discount rates for economic evaluation are normally those provided by the planning authority responsible for the project.

Shadow Prices

Resource costs for a project aimed at economic growth could be exaggerated or underestimated when the market prices are used in economic evaluation. The market prices, which include taxes, fees, and duties imposed by the public agencies to generate revenues, do not reflect a real demand on resources. There could be other distortions such as quotas, subsidies, and imperfect competition in a regulated economy. The real resource required is reflected by using the concept of economic price:

where,

$$\text{economic price} = \text{market price} - \text{transfer charges} + \text{effect of other distortions}.$$

20.2.3 *Costs and Benefits*

Economic evaluation, irrespective of the method used, requires determination of costs and benefits. The approach to costs and benefits differs for the type of project under evaluation. The consumer surplus approach is a traditional approach and is adopted in situations where considerable economic activity already exists and traffic levels are relatively high. For rural roads with low existing economic activity and low traffic levels an integrated approach may be necessary. The developmental effect is a focus of the analysis by this approach. Figure 20.1 illustrates the demand curve for the consumer surplus approach and Figure 20.2 illustrates the supply curve for the producer surplus approach.

Direct Costs or Road Costs

Direct costs may be divided as follows.

1) Agency Costs

- a. Initial construction costs.
- b. Future construction, rehabilitation, or upgrading costs.
- c. Maintenance costs recurring throughout the design period.
- d. Salvage return or residual value at the end of the design period.
- e. Engineering and administration costs.
- f. Traffic control costs.
- g. Land acquisition costs.
- h. Agricultural production costs.

2) User Costs

- a. Travel time costs.
- b. Vehicle operation costs.
- c. Accident costs.
- d. Discomfort costs.
- e. Time delay and extra vehicle operation costs during resurfacing, major improvements, or reinstatements.

Indirect Costs or Non-Road Costs

These are additional costs normally incurred in constructing roads based on an integrated development approach and may include the following.

1) Agency Costs

- a. Agricultural production costs.
- b. Costs of other development infrastructures, e.g., tourism and other industries, education, and health.

2) User Costs

- a. Agricultural transport (vehicle operation) costs.
- b. Other vehicle operation costs.

3) Environmental Costs

- a. Loss of physical resources such as top soil, land value, forests, minerals, and quality of water and air.
- b. Loss of ecological resources such as wildlife, fisheries, plants, and vegetation.
- c. Loss of quality of life resources such as culture, monuments, public health, and safety.

Benefits

Benefits may accrue from a road project, either as road benefits that are of direct benefit to the road user, as a result of the improved transportation facility, or as non-road benefits that are indirect benefits contributing to the integrated development of the areas under the influence of the road. Benefits are nothing but the difference in costs and value of production between, with, and without the proposed road situations.

Assessment of Costs and Benefits

Road construction and maintenance costs are dependent upon the standard of the road and the terrain through which the road passes. Several road costing models such as the HDM (Highway Development Manual) developed by the World Bank (1987) and the RTIM (Road Transport Investment Model) developed by the Transport and Road Research Laboratory (TRRL 1982), U.K., are available. Care must be exercised in using the existing models so that the conditions specific to the project are represented properly. Hill roads in mountain areas have to pass through terrain that is steep and of marginal stability and this means that special factors such as instability hazards should be considered.

Vehicle operation costs, travel time costs, and accident costs are influenced by road standards and type and condition of vehicle. Parameters such as roughness of the road and vehicle speed are used to determine fuel consumption, tire wear, vehicle maintenance, oil consumption, vehicle depreciation, parts' replacement, user travel time, total accidents, non-fatal accidents, and property damage.

Determining indirect costs is a complex and uncertain task. Currently, no method exists to quantify appropriately the environmental costs for use in economic analysis. The assessment of the costs of agricultural production and transportation is done currently for agricultural roads in developing countries by several methods. Literature produced by the World Bank or other appropriate literature may be followed for details of cost and benefit assessments of rural roads.

Stream of costs and benefits for each year and for each alternative throughout the design life of the proposed projects is calculated at constant money. These are converted to base year using an appropriate discount factor. Further analysis using the cash flow method to determine internal rate of return (IRR), benefit cost ratio (B/C), or the long-run economic planning method to determine the lowest unit cost that can be adopted.

The analysis for the appraisal of rural road projects of considerable size should take into account the current and predicted levels of economic activity in the area of influence. For low or non-existent traffic or new road in areas where the level of economic activity is low, a producer-surplus approach to analysis is adopted. Figure 20.2 illustrates the supply curve for this approach. The developmental effect is a focus of the analysis by this approach. Base line data for agricultural or other rural sectors must be collected. These data include such items as crop areas, yields, production costs, farmgate prices, marketed output, and local consumption.

The consumer surplus approach to analysis is the traditional method and is adopted in situations where considerable activity already exists and traffic levels are relatively high. See Figure 20.1 for the demand curve for the consumer surplus approach.

The following discussions give a background that is more specific to the traditional aspects of the economic analysis of road projects.

Economic analysis of a project involves some or all of the following:

- assessment of costs,
- assessment of benefits,
- calculation of benefit-cost ratio, internal rate of return, first year rate of return, and net present value,
- sensitivity analysis, and
- risk analysis.

Costs include construction costs, maintenance costs, and user costs. Benefits include savings in vehicle operation costs, reduction in accident costs, and time costs. Environmental costs and benefits, such as those accruing from noise, vibration, air pollution, socio-cultural changes, plant and animal life, changes in land use pattern, and soil loss due to erosion and landslides, are not yet built into a model for economic analysis. This shall, for the present, fall under the domain of environmental impact assessments.

Assessment of Costs

Several methods exist for calculating road costs. The TRRL Road Investment Model and the World Bank Highways' Design and Maintenance Standards' Model are the prominent models currently available. However, for fragile mountain areas such as in the Hindu-Kush Himalayan Region these models need to be supplemented and modified for specific conditions such as stability of hill slopes, flexibility in design standards, landslide and erosion control works, and environmental protection measures, for example, control of deforestation and indiscriminate cutting and blasting of hills.

20.2.4 Methods of Economic Evaluation

The purposes of economic evaluation are:

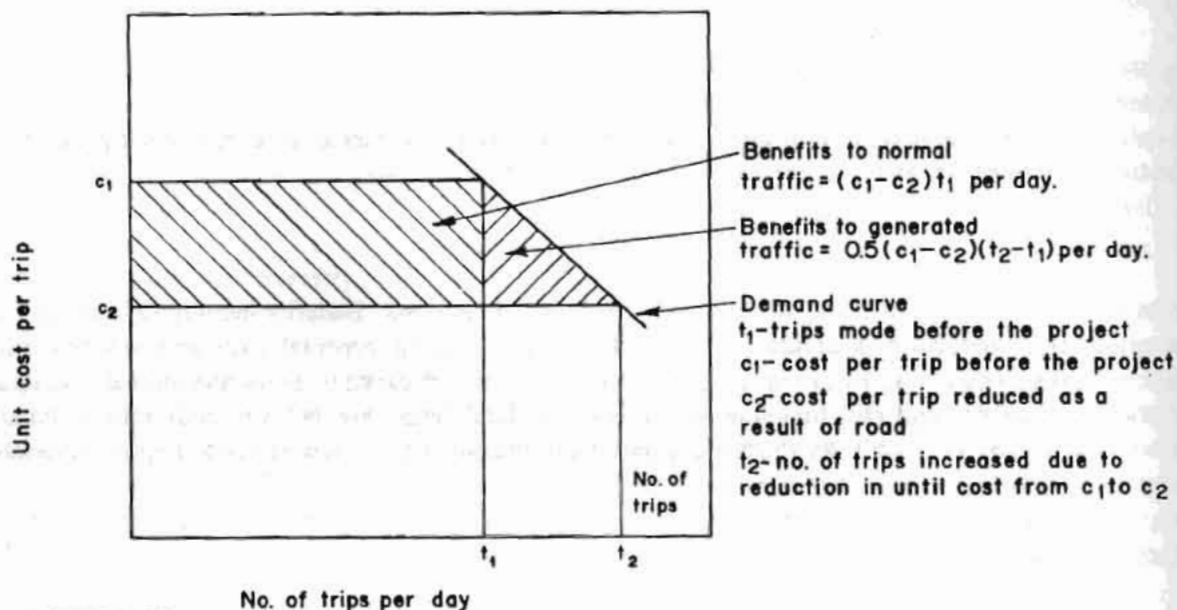
- to ensure that an adequate return in terms of benefits results from making a capital investment, and
- to ensure that the investment option adopted gives the highest return in terms of such things as choice of route, the design and structural standards, and the timing of the project.

The methods of evaluation depend on:

- planning level,
- management levels,
- agency, and
- size of project.

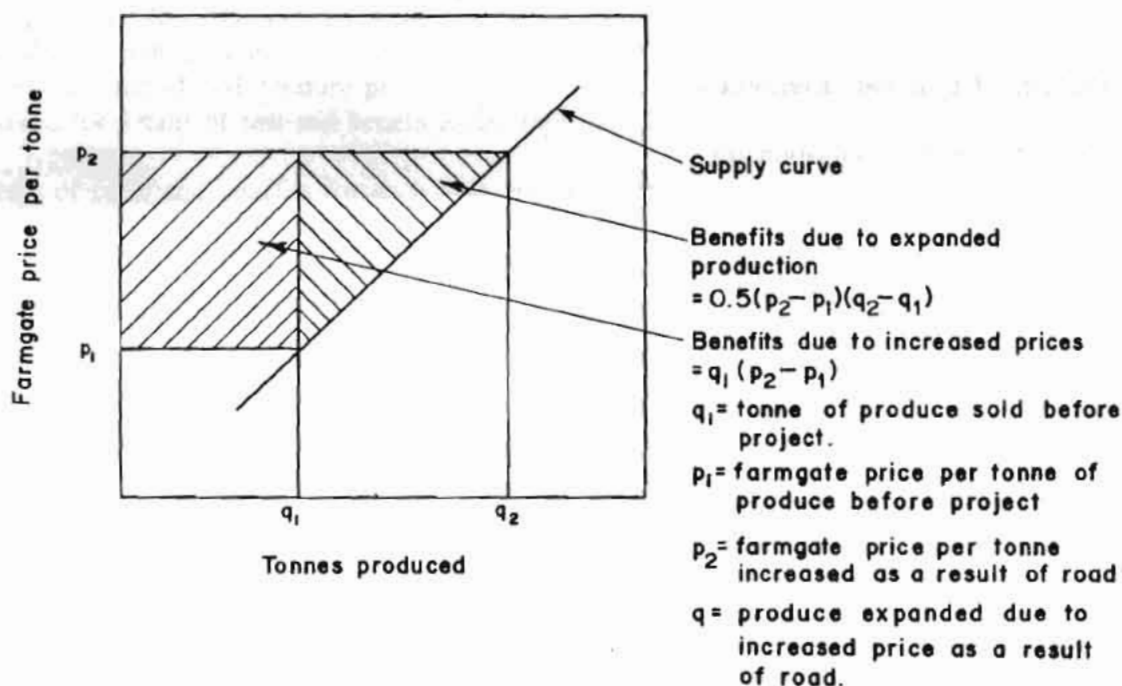
The private agencies are concerned with economic costs and benefits rather than financial ones, whereas public agencies would like to assess the net contribution that the investment will make to the country as a whole.

At the network level, the aim is to compare several investments in terms of their ability to contribute to the national economy, whereas at the project level the aim is to maximize cost effectiveness from the choices available for the given project.



Source: TRRL 1988

Fig. 20.1 Benefits measured as consumer surplus



Source: TRRL 1988

Fig. 20.2 Benefits measured as producer surplus

Since the level of resources required is related to the size of the work, the costs and manpower or equipment required to investigate, analyze, and interpret the economic evaluation become increasingly important and simpler methods become more desirable for smaller works.

There are different methods of economic analysis that are applicable to road projects for selection of investment options and design strategies. They are cited below.

1) *Cash Flow Method*

- a) Equivalent Uniform Annual Cost Method, often simply treated as "annual cost method".
- b) Present Worth Method for:
 - o costs,
 - o benefits, or
 - o benefits minus cost, usually termed the "net present worth" or "net present value method".
- c) Rate-of-Return Method for:
 - i) first year rate of return,
 - o economic, and
 - o financial.
 - ii) Internal rate-of-return,
 - o economic, and
 - o financial.
- d) Benefit-Cost Ratio Method

2) *Long-Run Economic Planning*

In long-run economic planning, the relationship between supply and demand is analysed over a longer period by examining the implications of changes in traffic flow under changing impacts and inputs.

3) *Generalized Heuristics*

The cash flow method of economic analysis is generally followed in most economic analysis. The cash flow analysis method of economic evaluation is suited to roads where the alternatives are not likely to be subject to major variations in terms of size of investments, technological levels, road standards, and demand growth.

A long-run economic planning method is desirable for comparing alternatives where the implications of change in traffic level, at various costs; because of differences in technology, alignment, expansion, maintenance, and economic growth; are likely to be considerable.

For smaller rural road projects, it may not be justifiable to carry out either cash flow or long-run methods of analysis because of the amount of work involved, in comparison to the size of investment and available facilities, and also because of several indirect benefits that need to be considered. A generalized heuristics' method of evaluation should be adequate for such projects. Section 20.4 discusses revised rules relating to the use of the IRR in the Cash Flow Analysis Method. Section 20.3 discusses the Long-Run Economic Planning Method.

20.2.5 Terms Related to Cash Flow Analysis Method

Net Present Value (NPV)

This is simply the difference between the discounted benefits and costs over the analysis period.

$$NPV = \sum_{i=0}^{n-1} \frac{b_i - c_i}{\left(\frac{1+r}{100}\right)^i}$$

where,

- n = analysis period in years,
- i = current year, with i=0 in first year,
- b_i = sum of all benefits in year,
- c_i = sum of all costs in year i, and
- r = planning discount rate in percentage.

Use of net present value is possible only when there are alternatives to be compared and discount rates are given.

Benefit-Cost Ratio (BCR)

This is the ratio between discounted total costs and discounted total benefits:

$$BCR = \frac{\sum_{i=0}^{n-1} \frac{b_i}{\left(\frac{1+r}{100}\right)^i}}{\sum_{i=0}^{n-1} \frac{c_i}{\left(\frac{1+r}{100}\right)^i}} = 0.$$

Internal Rate of Return (IRR)

This is the discount rate at which the present value of costs and benefits are equal; in other words the NPV=0:

$$\sum_{i=0}^{n-1} \frac{b_i - c_i}{\left(\frac{1+r}{100}\right)^i} = 0$$

where, $r = \text{IRR}$.

The solutions are normally obtained graphically or by iterations. IRR gives an indication of the profitability of investment and does not provide any idea of the size of profit.

First Year Rate of Return (FYRR)

The FYRR is simply the sum of benefits, in the first year of trafficking after project completion, divided by the present value of capital cost, grossed up by the discount rate to the same year, and expressed as a percentage:

$$\text{FYRR} = \frac{100 \ b_j}{\sum_{i=0}^{j-1} c_i \left(\frac{1+r}{100}\right)^{j-1}}$$

where,

j = first year of benefits, with $j = 0$ in the base year.

The FYRR assists in deciding the timing of project commencement without sensitivity analysis which, whenever possible, is more desirable. The project is timely if FYRR is greater than the planning discount rate. Figure 20.3 is a diagram for calculating IRR graphically.

20.2.6 Equations Relating to Cash Flow Analysis

A) Equivalent Uniform Annual Cost Method

This method is applied for assessing costs only. All costs at different times are expressed in terms of equal annual payments over the analysis period. This can be expressed by (1):

$$AC_{x_i, n} = Crf_x (ICC)_{x_i} + (AAMO)_{x_i} + (AAUC)_{x_i} - Crf_{i,n} (SV)_{x_i, n}$$

where,

- AC_{x_1} = equivalent uniform annual cost for alternative x_1 , for a service life or analysis period of n years,
- $crf_{i,n}$ = capital recovery factor for interest rate i and n years,
 $= [i(1+i)^n / ((1+i)^n - 1)]$
- $(ICC)_{x_1}$ = initial capital costs of construction (including actual construction costs, materials costs, engineering costs, etc.),
- $(AAMO)_{x_1}$ = average annual user costs for alternative x_1 (including vehicle operation, travel time, accidents, and discomfort if designated), and
- $(SV)_{x_1,n}$ = salvage value, if any, for alternative x_1 at the end of n years.

The above equation considers annual maintenance and operating costs, and user costs, on an average basis. This can be satisfactory for many purposes. Where such costs do not increase uniformly, however, an exponential growth factor can easily be applied.

When additional capital expenditure occurs before the end of the analysis period, i.e., when the service life is less than the analysis period; and future rehabilitation, such as overlays or seal coats, is needed. The equation for this situation may be modified and expressed by:

$$AC_{x_1,n} = Crf_{i,n} [(ICC)_{x_1} + R_1 pwf_i, a_1 + R_2 pwf_i, a_2 + \dots + R_j pwf_i, a_j + (AAMO)_{x_1} + (AAVC)_{x_1} - Crf_{i,n} (SY)_{x_1,n}]$$

where,

- $AC_{x_1,n}$ = equivalent uniform annual cost for alternative x_1 , for an analysis period of n years,
- R_1, R_2, \dots, R_j = cost of first, second, ..., j^{th} resurfacings respectively,
- a_1, a_2, \dots, a_j = ages at which the first, second, ..., j^{th} resurfacings occur respectively,
- pwf = present worth factor $= 1/(1+i)^n$,
- i = discount rate, and
- n = number of years.

BASIS AND DERIVATION OF THE DIAGRAM FOR DETERMINING RATE OF RETURN

The diagram (which is, in effect, a nomogram combined with a family of curves) solves a relatively simplistic model involving:

- (a) a cost, or investment (I);
- (b) the 'base-year benefits' (b) resulting from that investment;
- (c) the annual rate of growth of those benefits (i);
- (d) the number of years considered (n), (i.e., the "economic life"); and
- (e) the internal rate of return on the investment (d).

The annual rate of growth of benefits (i) is considered constant over the economic life. For an indication of how to adapt the diagram when the growth rate is not constant, see note 4 across.

Associated with any investment there are, normally, some notional base-year benefits (B_o). In practice there is a lag between the investment being incurred and the first benefits arising from the investment. The model on which the diagram is based assumes that the investment (I_o) is made in year '0', and that the notional first-year benefits materialize only in year 1. In tabular form, the model is as follows:

Year	Investment	Benefits
0	I_o	
1		$B_o (1 + i)$
2		$B_o (1 + i)^2$
3		$B_o (1 + i)^3$
n		$B_o (1 + i)^n$

The rate of return (d) will be such that:

$$I_o = B_o \frac{(1+i)}{(1+d)} + B_o \frac{(1+i)^2}{(1+d)^2} + \dots B_o \frac{(1+i)^n}{(1+d)^n} \dots \quad (1)$$

or,

$$I_o = \frac{(1+i)}{(1+d)} + \frac{(1+i)^2}{(1+d)^2} + \dots \frac{(1+i)^n}{(1+d)^n} \dots \quad (2)$$

that is,

$$\frac{I_o}{B_o} = k + k^2 + k^3 + \dots k^n \dots \quad (3)$$

where,

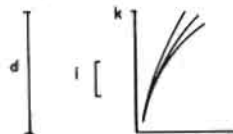
$$k = \frac{1+i}{1+d} \dots \quad (4)$$

Although the family of curves was plotted using the ratio of I_o/B_o (i.e., cost/first year benefits) on the abscissa, in the diagram this has been converted to, and shown as, the reciprocal (first year benefits/cost) since the ratio is more commonly used in this form.

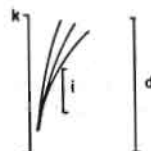
Fig. 20.3 Diagram for calculation of internal rate of return (IRR)

Derivation of the Diagram

The family of curves in the diagram represents the relationship expressed in equation (3), with the right hand side of the equation represented as the sum of a geometrical progression to n terms; ' k ' has been plotted on the vertical axis. The k -axis also forms one of the three axes comprising the three-line nomogram, which 'solves' equation (4), (the other two axes being the ' i ' [or rate of growth] axis, and the ' d ' [or rate of return] axis). The diagram, basically, therefore is as follows:



For the sake of compactness, the nomogram has been 'folded over' the family of curves, thus:



The scale of k -axis is of course common to both the family of curves and the nomogram. Since, in use, the k -axis is only a transfer line, the scale markings of this axis have been suppressed in the diagram.

NOTES

1. The diagram can also be used to examine sensitivity. For example, the straight edge may be rotated about point 'B' to examine the variation in IRR for various values of the growth of benefits; or, in other words, to examine the sensitivity of IRR with respect to change in the rate of growth of benefits. Then again, for a given first year benefit/cost ratio, point 'A' may be located on different curves to examine the sensitivity of the internal rate of return to variation in the economic life.
2. The diagram can also be used "in reverse". For example, if the IRR and the rate of growth of benefits are given, then by working backwards through the diagram the appropriate combinations of economic life and first year benefit/cost ratios can be determined. Quite generally, the diagram uses four variables: if any three are given, the fourth can be determined directly.
3. The diagram indicates certain aspects of the relationship between first year benefit/cost ratio (FYB/C), n , i , and d , which are not readily appreciated from equations (1) and (2), across; the diagram gives one a better "feel" for the relationship. For example, the curves for $n=10$ years and $n=15$ years run together at a point which corresponds to a FYB/C ratio of about one-third. Thus, if the first year benefits are at least one-third of the investment, then there is no advantage in taking an economic life greater than 10 years. Again, the diagram indicates how little is gained (in terms of an increase in IRR) by extending the economic life beyond, say, 30 years; the increase in IRR moving from 30 to 50 years will, under the most favourable circumstances, be at the most about one percentage point.
4. Although the model assumes, as standard, investment in year '0' and the base-year benefits starting in year '1', and just one rate of growth of benefits throughout the economic life considered, non-standard conditions can readily be adapted to conform to these requirements of the model and still give results which are tolerably acceptable. For example:
 - (1) if the rate of growth of benefits is not constant but is i_1 for the first period, followed by a rate of growth of i_2 for the second period, then an 'average' rate of growth should be used, between i_1 and i_2 , but obviously nearer to i_1 since it is the early years that count in the discounting process.
 - (2) if the investment is spread over two years instead of one, with the benefits starting to materialize in the following year, the first year investment should be compounded to the second year using an intelligent guess for the compounding rate and then added to the investment in the second year, and that year then termed year '0'. Thus we would have, effectively, an investment in year '0'. Thus we would have, effectively, an investment in year '0', benefits starting in year '1', and the diagram would apply. If by chance it transpired, having worked out the rate of return, that the intelligent guess for the compounding factor for the initial year's investment was wildly wrong, it would be appropriate to carry out a second iteration using as the compounding factor for the first year investment the rate of return determined in the first 'pass'.
5. Line X-X (near the top of the diagram) has some significance for the relationship between (i) annual rate of growth of benefits, and (ii) internal rate of return. If point 'A' (see "use of the diagram", over) falls anywhere below line X-X, the IRR will always be greater than the rate of growth of benefits; if 'A' falls above line X-X, the IRR will always be less than the rate of growth of benefits. If point 'A' is located anywhere on line X-X, then the IRR will equal the rate of growth of benefits.

Source: Schuster 1973

Fig. 20.3 Diagram for calculation of internal rate of return (IRR) (Cont)

B) *Present Worth Method*

The present worth method can be used to assess costs alone, benefits alone, or the costs and benefits together of all the future streams of costs in terms of the present value by using an appropriate discount rate. The present worth method for costs alone can be expressed in terms of the equation:

$$TWPC_{x_{1,n}} = (ICC)_{x_1} + \sum_{t=0}^{t=n} p w f_{i,t} [(cc)_{x_{1,t}} + (MO)_{x_{1,t}} + (UC)_{x_{1,t}}] - (SV)_{x_{1,n}} p w f_{i,n}$$

where,

$TWPC_{x_{1,n}}$ = total present worth of costs for alternative x_1 ,
for an analysis period of n years,

$(ICC)_{x_1}$ = initial capital costs of construction, etc., for alternative x_1 ,

$(CC)_{x_{1,t}}$ = capital costs of construction, etc., for alternative x_1 , in year t , where t is less than n ,

$p w f_{i,t}$ = present worth factor for discount rate, i , for t years,
= $1/(1+i)^t$

$(MO)_{x_{1,t}}$ = maintenance plus operation costs for alternative x_1 in year t ,

$(UC)_{x_{1,t}}$ = user costs (including vehicle operation, travel time accidents, and discomfort if designated) for alternative x_1 , in year t ,

$(SV)_{x_{1,n}}$ = salvage value, if any, for alternative x_1 , at the end of
the design period, n years,

where,

$$TPWB_{x_{1,n}} = \sum_{t=0}^n p w f_{i,t} [(DUB)_{x_{1,t}} + (IUB)_{x_{1,t}} + (NUB)_{x_{1,t}}]$$

$TPWB_{x_{1,n}}$ = total present worth of benefits for alternative x_1 for
an analysis of n years,

$(DUB)_{x_{1,t}}$ = direct user benefits accruing from alternative x_1 in year t ,

$(IUB)_{x_{1,t}}$ = indirect user benefits accruing from alternative x_1 in year t , and

$(NUB)_{x_{1,t}}$ = non-user benefits accruing from project x_1 in year t .

It is questionable whether or not non-user benefits and indirect user benefits can be measured adequately. Consequently, it is perhaps reasonable to consider only direct user benefits until such time as the state-of-the-art is sufficiently advanced to allow the other factors to be measured.

Net Present Value Method

The net present value method follows on from the foregoing methods, because it is simply the difference between the present worth of benefits and the present worth of costs. Obviously, benefits must exceed costs if a project is to be justified on economic grounds. The equation for net present value is:

$$NPV_{x_1} = TPWB_{x_1,n} - TPWC_{x_1,n}$$

where,

NPV_{x_1} = net present value of alternative x_1 (and $TPWB_{x_1,n}$ and $TPWC_{x_1,n}$ are as previously defined).

However, for road projects' alternative, x_1 , this equation is not applicable directly to x_1 itself, but rather to the difference between it and some other suitable alternative, say x_0 . Considering only direct user benefits, these are then calculated as the user savings (resulting from lower vehicle operating costs, lower travel time costs, lower accident costs, and lower discomfort costs) realized by x_1 over x_0 .

Thus, the net present value method can be applied to projects only on the basis of project comparison, where the project alternatives are mutually exclusive. When a project alternative is evaluated, it needs to be compared not only with some standard or base alternative but also with all the other project alternatives. In the case of roads, the base alternative may be that of 'do-nothing' or 'do-minimum'. The equation form of the net present value method for pavements may then be expressed as:

$$NPV_{x_1} = TPWC_{x_0,n} - TPWC_{x_1,n}$$

where,

NPV_{x_1} , = net present value of alternative x_1 ,

$TPWC_{x_0,n}$ = total present worth of costs, for alternative x_0 (where x_0 can be the standard or base alternative, or any other feasible mutually exclusive alternative x_1, x_2, \dots, x_k) for an analysis period of n years, and $TPWC_{x_1,n}$ is as previously defined.

20.2.7 Sensitivity Analysis and Risk Analysis

Sensitivity analysis is carried out to assess the sensitivity of the economic indicators such as IRR, NPV, and BCR to the variability of important items of the project. The effect of staged constructions and uncertainties of the base line figures of parameters such as traffic, costs, prices, and management inputs

can be assessed by varying the inputs normally one at a time, and determining the total costs, total benefits, IRR, and NPV.

When the combined effect of several variables on the IRR or NPV is to be assessed, risk analysis becomes essential. Risk analysis provides a better basis of judging the relative merits of alternative projects, but it does nothing to reduce the risks. Risk analysis may be carried out by identifying important variables from the sensitivity analysis and specifying the probability of each important variable attaining a range of values. The probability distribution of NPV or IRR can then be obtained. Risk analysis is time consuming for complex projects such as roads. Such an analysis should be considered for highly critical cases such as for roads, which are high cost, and alternates to already existing major traffic diversions or susceptible to them, or washouts. However, the existence of computer facilities and appropriate models for risk analysis can significantly reduce the odds against risk analysis.

20.3 ANALYTICAL FRAMEWORK FOR ECONOMIC ANALYSIS USING LONG-RUN ECONOMIC PLANNING (LREP)

Economic planning of transportation projects consists of exercising basic investment planning principles to determine if any facility is economically desirable and, if so, then which facility is economically most desirable. The economically optimal decisions determined by investment planning are called long-run decisions, which means that the decisions relate to infrastructural changes. Long-run investment planning principles can be applied to compare different modes of transportation (such as roads and ropeways), alternative technologies within a particular mode of transport (such as the use of tunnels or low-volume roads) or both. Social, political, and legal considerations are not within the scope of economic investment planning; they should be brought to bear on the overall investment decision separately.

This section provides an application-oriented explanation of the Long-Run Economic Planning (LREP) approach to investment planning. Part II contains considerations that indicate the specific problem contexts in which the LREP Method, as presented here, is applicable. Further readings are suggested in the references. Figures in this section were extracted from Wohl and Hendrickson (1984).

20.3.1 *Long-Run Economic Planning (LREP)*

Introduction

LREP is based on an analysis of the relationship of the supply, or cost, curve to the demand curve. LREP provides a framework for analysing supply and demand as functions of the quantity of traffic flow over the planning horizon. The LREP model is particularly useful in analysing the implications of changes in traffic flow, at various costs, caused by differences in facilities, technology, alignment, expansion, maintenance, and economic growth. The implications are summarized as the total net benefit or the consumer's surplus.

Definition of Concepts

The cost of a given facility is dependent on the technology and level of usage. Mathematically, costs are defined as a function of technology, capacity, and usage. The time period costs are defined and

differentiated according to the availability of time for adjusting the technology and operation of the facility. Thus, the short-run represents the time horizon in which only minor changes can be made to the technology (i.e., to the existing facility or to the type of operation [such as tolls for trucks]). Over the long run, enough time would be available to alter the technology substantially. Extra costs in the short run arise from increases in usage that cause wear and tear as well as user costs, for example, travel time. Cost changes in the long run arise from changes in either the technology, usage, or both. Long-run cost functions are used to determine which technology should be built and how large it should be. Short-run cost functions can be used to determine optimal operating policies but will only be of interest in this chapter as they relate to working with the long-run cost function.

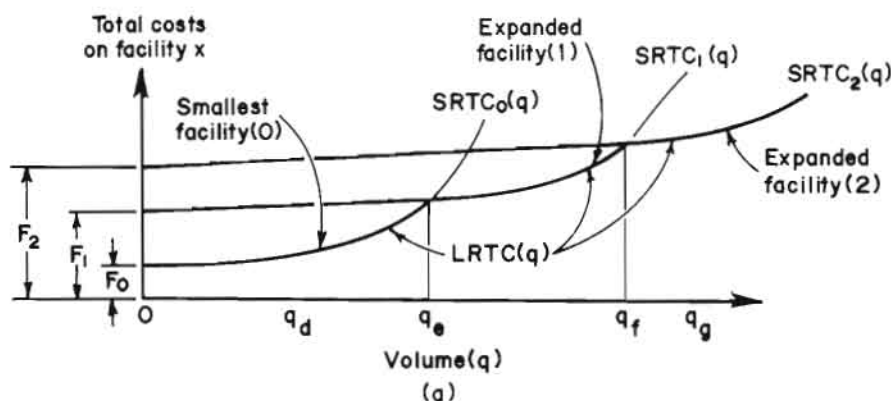
The short-run cost function is as follows:

$$SRTC_{x,t}(q) = F_{x,t} + SRVC_{x,t}(q)$$

where,

- $SRTC_{x,t}(q)$ = the short-run total costs for a volume q (in AADT) using facility x during year t ,
 $F_{x,t}$ = the fixed cost for facility x in year t , and
 $SRVC_{x,t}(q)$ = short-run variable costs for a volume q using facility x in year t .

Fixed costs are usage independent costs for the facility in a given year such as rights-of-way, maintenance facilities, and garages. Variable costs are usage dependent and include such factors as facility and vehicle wear and tear. It should be noted that $SRTC$ include both agency costs as well as user costs (and may be constructed to include external costs incurred, by the environment for example). The long-run cost function, or the planning cost function, represents the minimum cost of serving a given travel volume. This long-run cost function ($LRTC$) represents the envelope of the various short-run cost curves associated with each alternative facility. Figure 20.4 shows the long-run and short-run cost functions.



Source: Wohl and Hendrickson 1984

Fig. 20.4 Long-run and short-run cost functions

Unit cost functions of SRTC and LRTC are the curves of interest during the problem-solving exercise in equilibrium analysis. Regarding the SRTC, three unit cost functions are of interest: the short-run average total cost at flow q - $sratc_{x,i}(q)$, the short-run average variable cost at flow q - $sravc_{x,i}(q)$, and the short-run marginal cost at flow q - $srmc_{x,i}(q)$. Mathematically, these functions are defined as follows:

$$sratc_{x,i}(q) = \frac{SRTC_{x,i}(q)}{q} \quad (1)$$

$$sravc_{x,i}(q) = \frac{SRVC_{x,i}(q)}{q} \quad (2)$$

$$srmc_{x,i}(q) = \frac{\partial SRTC_{x,i}(q)}{\partial q} = \frac{\Delta SRVC_{x,i}(q)}{\Delta q} \quad (3)$$

Similarly, in the long-run, two unit cost curves are of interest: the long-run average total cost for a volume and the long-run marginal cost curve for a volume (lrmc). Mathematically these are:

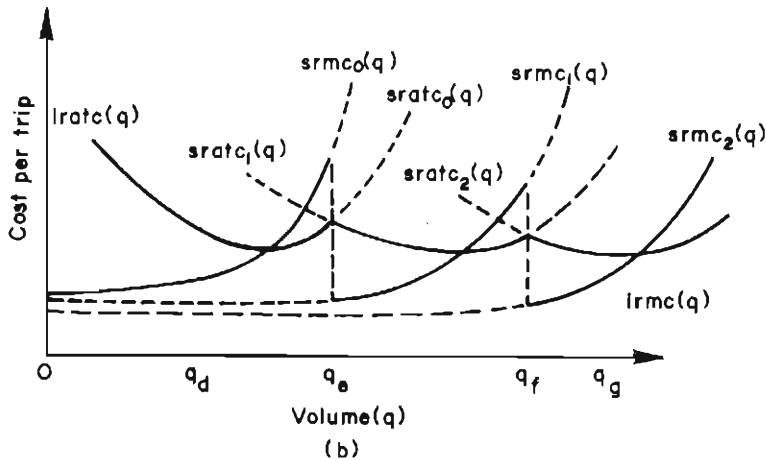
$$lratc(q) = \frac{LRTC(q)}{q} \quad (4)$$

$$lrmc(q) = \frac{\partial LRTC(q)}{\partial q} = \frac{\Delta LRTC(q)}{\Delta q} \quad (5)$$

or,

$$lrmc(q) = LRTC(q) - LRTC(q-1) \quad (6)$$

Figure 20.5, below, illustrates graphically the unit cost curves for the total cost curves shown in Figure 20.4.



Source: Wohl and Hendrickson 1984

Fig. 20.5 Unit cost curves

The benefits of transportation have to be carefully identified and represented mathematically. Proper understanding of the sources of travel benefits is needed to quantify and compare benefits to the costs of travel.

The demand function expresses the dependency of travel desire to the cost (or price) of travel. The price of travel is the total expense incurred by travellers in terms of private time, effort, and money expenses. In other words, the demand function explains the price travellers are willing to pay for travel. The marginal benefit function (mb), which is the inverse of the demand function, is used for analytical purposes here. The value of a trip, which is the price of that trip, is defined as the marginal benefit gained from the trip. Functionally, for a linear demand schedule of the form:

$$q = \alpha - \beta p \quad (7)$$

where,

p = the price of travel, and

α, β = case-specific equation calibration coefficients.

The corresponding price or marginal benefit function is:

$$p(q) = mb(q) = \frac{\alpha}{\beta} - \frac{q}{\beta} \quad (8)$$

where,

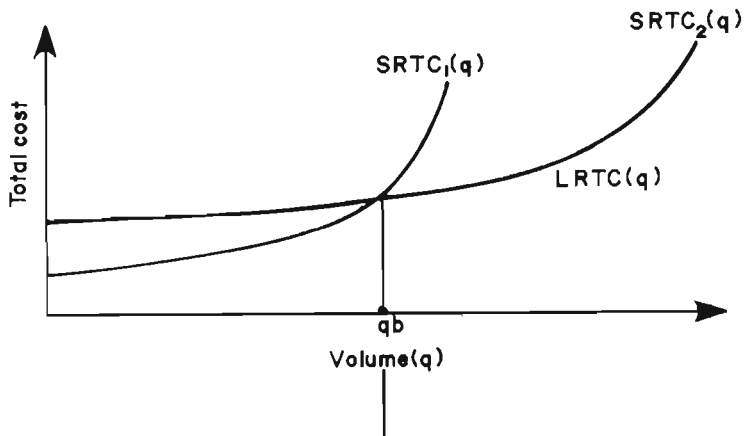
$mb(q)$ = the marginal benefit to travellers by increasing travel volume from $q-1$ to q .

Investment Planning for Economic Efficiency in the Long Run

From the economic perspective, the net social benefit is the parameter of interest in solving the optimal facility. The net social benefit will be measured in monetary terms as expressed by a simultaneous solution of the **lrmc** and **mb** functions. Problems this approach is suited to, as well as guidelines for estimating the parameters, are given in the Section entitled "Considerations for Practice Using LREP".

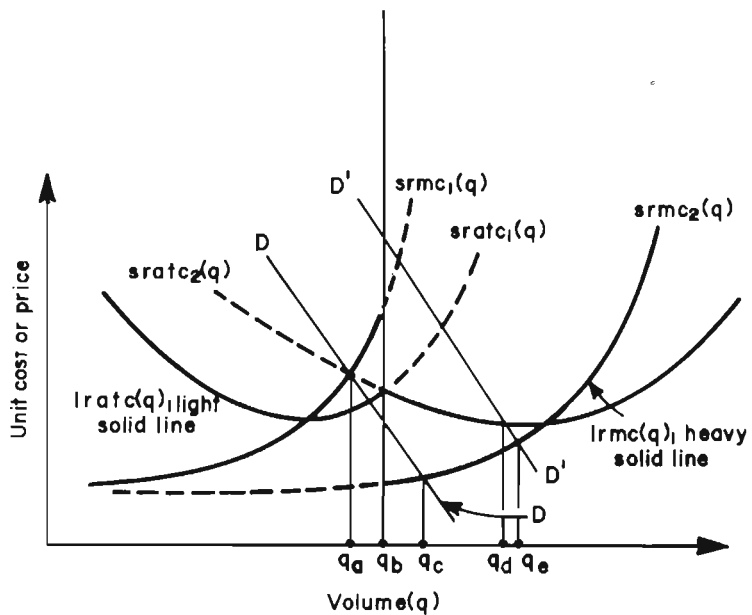
The graph in Figure 20.4 is used to explain the analytical process. The situation shown in Figure 20.4 is a basic problem. Considerations for more involved cases will be elaborated upon in the section on Considerations for Practice.

Figure 20.6 (a) represents the total cost functions of the two facility options while the curves in Figure 20.6(b) are the corresponding unit cost curves. Only two facility options are represented by the cost curves while the travel demand is shown as either low (DD) or high ($D'D'$). The first task is to estimate curves (discussed later) such as those in Figure 20.4 - this will result in a set of curves that are to be analysed as follows.



Source: Wohl and Hendrickson 1984

Fig. 20.6 (a) Total cost functions of two facility options



Source: Wohl and Hendrickson 1984

Fig.20.6 (b) Corresponding unit cost curves

Economically, the optimal pricing policy is to set the $mb = lrmc$. This implies constructing a facility that serves a volume q_0 such that $mb(q_0) = lrmc(q_0)$. It is also necessary that the total benefits must satisfy the equation:

$$\begin{aligned} \sum_{q=1}^{q_a} mb(q) &\geq \sum_{q=1}^{q_a} lrmc(q) + F \\ &\geq LRTC(q_a) \end{aligned} \quad (9)$$

the total costs, to ensure economic efficiency. Analytically, to determine which facility to build at what capacity, the solution can be obtained by solving the above conditions*. In the case of higher demand ($D'D'$) in Figure 20.6(b), $mb > lrmc$ from $q=1$ to q_e ; q_c would set $mb = lrmc$. Furthermore, as $mb = srac_2(q) = ratc(q)$ at q_d and $mb > lrmc$ between q_d and q_e , it can be concluded that:

$$\sum_{q=1}^{q_e} mb \geq LRTC(q_e)$$

Thus, for the higher demand case, the optimal decision would be to construct facility 2 at a capacity of q_e . The lower demand case is less straightforward. Up to q_a , both conditions are satisfied, i.e., $mb > lrmc$ and:

$$\sum_{q=1}^{q_a} mb(q) > LRTC(q_a)$$

Beyond q_a , $mb > lrmc$ on facility 2 but is:

$$\sum_{q=q_a}^{q_e} mb(q) \geq \sum_{q=q_a}^{q_e} lrmc(q)?$$

If this is true then the optimal decision is to construct facility 2 at q_e , otherwise the optimal decision is to construct facility 1 at q_a . To resolve this inequality, it is necessary to know the exact shape of the curves and sum up the quantities of interest numerically.

The considerations made above are typical of the analysis to answer the question concerning which facility to build and how large it should be. Facilities 1 and 2 could represent different road standards, alignments, and technologies in addition to capacity. The demand curves in Figure 20.6 could represent expected growth in traffic over the road's life.

* Conditions of very low land demand, where no such condition exists will be discussed in the section on Considerations for Practice.

1. It is important to realize that problem definitions make implicit assumptions. The application of any approach to solving the problem will have to account for such assumptions to provide valid results. Two specific problems to illustrate this point are given below.
 - i. The decision whether or not to build a road between two points can be made on one or more of economic, social, political, and legal grounds. Often, it is only social or political considerations that effectively have a bearing on the decision. In such situations, the engineering community is handed the task of making a road between two points and not asked to decide if it is economically advisable to make a road (or any other transport facility). In such cases, investment planning must determine the economically most desirable transport facility in the long run, between the pre-determined terminal points. The determination of the most desirable transport facility would involve options such as alternative alignments, road standards, road technologies, and rural development components.
 - ii. Whereas the previous problem considers the economic efficiency of investing in a single project, this problem addresses the economic efficiency in deciding to invest in a number of alternative projects. Decisions, regarding which of several alternative terminal points to build a road across, tend to involve terminal points with similar characteristics of development potential (such as natural resource endowment, population, production patterns, and income levels). In such cases, it is desirable to base the selection of one alternative on economically cognizant social and political considerations. Long-run investment planning needs to determine the prioritization of the alternatives from an economic point of view as well as to determine the corresponding transport facilities.

The first problem assumes that the decision to build a transportation facility has already been made. This means that indirect benefits (i.e., those benefits that arise as a secondary impact of a road - such as higher income from the establishment of industries) are irrelevant to deciding the type of facility to be constructed. The travel demand function will define all benefits that accrue to road users and it is for this group above that investment planning will define benefit and determine the economically efficient transport facility. However, the demand function will include secondary benefits to the extent that they give rise to travel demand (modelled by shifts in the demand curve).

In the second problem, the critical assumption is that of similar terminal points that an economic comparison is made across. Here, the fact that the terminal points are similar makes it possible to assume that indirect benefits will be the same among the alternatives. Thus, we are faced with comparing only the direct benefits of travelling on the road which are captured by the demand function.

If indirect benefits were estimated independently, the LREP approach could be used to account for total benefits. This modified application of LREP would enable more than the two problems given above to be addressed by LREP.

2. The Long-run Total Cost (LRTC) function is the envelope of the lowest cost, Short-run Total Cost (SRTC), curves. For low traffic volumes, a given facility (standard, technology, alignment) might

be the lowest cost alternative, while, at larger flows, the maintenance and user costs may make another facility the cheapest. Thus, a wide range of facilities should be represented by the cost curves to examine the broadest range of investment options. Large investments in slope stabilization, tunnels, express alignments, staged construction, and various road standards are examples of such options. It is also worthwhile to carry out a parallel analysis for alternative modes of transport such as ropeways and electric bus lanes. Moreover, it is important to build rural development investment packages into the cost curves of facility options to study possibilities of enhancing the catalyst role of rural roads for rural development.

3. In estimating a SRTC (thereby estimating part of the LRTC) curve, there are a few categories from which the costs arise. First of all, there are the usage independent, or fixed, costs for the facility. In contrast, there are the usage dependent costs or variable costs. Both fixed and variable costs for a given facility can be experienced by the road-building agency, vehicle-operating agency, or the road user. The categories that the cost function should have are:

- o fixed facility and social dislocation costs,
- o variable facility costs,
- o fixed vehicle ownership costs,
- o variable vehicle costs,
- o variable user costs, and
- o external costs (environmental).

In order to estimate the SRTC, the first task is to estimate these costs in a format such as the one shown below in Table 20.1.

Table 20.1 SRTC costs

Year	Ft Fixed Costs	VARIABLE COSTS (SRVC _j) by TRAFFIC FLOW LEVELS (AADT)						
		Q ₁	Q ₂	Q ₃	Q ₄	Q ₅	Q _{j-1}	Q _j
0								
1								
2								
3								
.								
.								
.								
n-1								
n								

Source: Wohl and Hendrickson 1984

The information tabulated in Table 20.1 has to be transformed into a cost function $\text{SRTC}_i(q) = F_i + \text{SRVC}_i(q)$ to year 0 for all q . Plotting the function $\text{STRC}(q)$ will result in a graph similar to Figure 20.4 Repeated plots of other SRTC functions for alternate facilities will enable the identification of $\text{LRTC}(q)$.

4. Unit cost functions are to be derived in a similar manner. Average costs and marginal costs are to be calculated using relationships (1) and (3). Discounting to year 0 is to be done as for SRTC .
5. The variable user costs consist only of the variable part of the total user costs of travel. Whereas, the user costs of travel, p , consist of the monetary charges for travel as well as user costs. Examples of travel charges are tolls, fares, and vehicle operation costs while user costs are usually taken as the travel time. In other terms, a simple representation of p is:

$$p = vt + f \quad (10)$$

where,

- f = travel fare in monetary terms,
- t = travel time, and
- v = user time cost parameter.

Furthermore, $t = t_0 + \sigma q$, i.e, travel time is a minimum t_0 and time increased by congestion at flow q by σq (σ being the travel time congestion parameter).

Combining the two expressions:

$$p = v t_0 + v \partial q + f = \tau + \xi q + f \quad (11)$$

thus,

the variable user costs are $\tau + \xi q$.

6. The construction of a demand curve requires careful thinking to identify the sources of travel benefits. Some basic concepts are needed to proceed with the construction of a demand and marginal benefit curve.
 - 6.1 The demand function represents the desire, in terms of the willingness to pay under certain circumstances. Mathematically this is expressed as $q = f(p, \text{SE})$, where q is the travel volume demanded under the terms of a function f of the price of travel and socioeconomic conditions SE. This is an aggregate demand function for a population that includes people with high and low demands for travel.
 - 6.2 The construction of a demand curve involves the collection of data and fitting them to a curve using regression analysis. The data needed for the construction of a demand curve are usually of three types: (1) socioeconomic attributes of the origin and destination (income, population, food deficit, etc.), (2) user costs for the facility under consideration, and (3) user costs on

alternative routes (such as walking on trails). The specific variables to be considered within these categories are discussed below. The variables discussed below are meant to be indicative only; it is possible that other variables could give a better explanation of demand under special circumstances.

- 6.3 The estimation of the user costs for either the facility under construction or an alternate mode of travel is based on Equation (11). The user costs, in terms of the costs of travel time or the monetary charges, fall into categories which have to be estimated independently and summed to arrive at the total user costs at various flows, as expressed in Equation (11). At the outset, the travel time congestion parameters have to be estimated by observations of the travel time at various flow levels beyond the flow level that causes no congestion and results in the minimum travel time t_0 .

Estimating:

$$\delta = \sum_{i=1}^n \frac{t_i}{n}$$

for all i observations will suffice.

The traffic flow q is to be measured in average annual daily traffic flow (AADT) as for the cost curves. This and other observations should be made on an existing road with as closely matching facilities and socioeconomic attributes as possible.

- 6.3.1 The user time cost parameter varies for vehicle occupants according to the type of travel undertaken. If the traveller is on official travel, v is the sum of the traveller's wage rate and overheads the employer incurs in the travel of the user. If the traveller is on leisure travel (including commuting), $v = 0$ in Nepal, although studies show $v = 25$ per cent of the traveller's earnings in other developing countries.
- 6.3.2 For freight transportation, v is the sum of the interest rate of the goods and the costs due to spoilage during travel time (and not due to road smoothness). These vary by commodity and a careful study is required to estimate v for freight transportation.
- 6.3.3 The monetary charges, f , are the sum of the fares charged to commercial passengers and to the transport of goods.
- 6.4 The socioeconomic attributes are critical to the construction of a reliable demand function. Various parameters could be relevant such as the total population of the origin, destination, and towns in between; the mean employment or income of the origin, destination, and towns in between, service differentials between nodes, the food deficit in the influence area, and the potentials for expansion of production (tourism, horticulture, mining, forestry, etc). Aside from the care needed to measure such attributes, care should be taken to define the variables to account for the salient features of the major linkages among the socioeconomic factors the demand is likely to be influenced by. Traffic growth estimating heuristics, given in Section 20.5 are useful in this respect.

6.4.1 The test of significance of using various socioeconomic attributes can be done statistically. The estimation of the growth rate of those variables is another problem that requires serious thought. Simple techniques are available, for example, to estimate the income growth rate; one can use the country's GDP growth rate multiplied by the per cent of the national GDP the region accounts for. Such techniques can be very misleading, however, and, given the importance of estimating a realistic growth rate for the socioeconomic variables used in the demand curve, it is worth the effort to consult an economist.

6.5 The data used for developing a demand curve can either be time series or cross-sectional. The choice of which type is used will be dependant on data availability. The choice of the location selected from which to gather the data must be done taking into consideration the similarity of the area where the data are to be gathered to the area where the road is to be built. The similarity is defined by the socioeconomic variables. Finally, a standard text on regression analysis should be consulted for its technique and a computer programme (such as MINITAB or SPSS) should be used for the regression analysis.

20.4 CASH FLOW ANALYSIS AND REVISED RULES FOR THE IRR METHOD

The conventional definition of the IRR Method may lead to ambiguous or incorrect conclusions regarding the economic viability of a project or the most viable alternative. While the Revised Rules for the IRR Method (RIRR) are given below, it should be noted that the RIRR Method requires lengthy calculations which provide the same result as those obtained by using the simpler NPV method. Barring unavoidable circumstances, it is recommended that the NPV or BCR methods be used instead of the RIRR Method. The complete set of rules for the RIRR Method, presented below, were extracted from Wohl and Hendrickson 1984; a critique on the theoretical problems of the IRR Method regarding, among other things, reinvestment implications and Effective Rate of Return (ERR) can be found there.

An appropriate and consistent set of decision rules is outlined below for determining project acceptability when using the IRR Method. The rules widely apply for both single and multiple rates of return, for borrowing or investment situations, and for pure or mixed projects. They are given in the following section.

20.4.1 Revised IRR Decision Rules for Determining Project Acceptability

(a) Determine the sum of undiscounted (net) annual cash flows of the project over the n year analysis period, that is:

$$S = \sum_{t=0}^n [B_{x,t} - C_{x,t}] = [NPV_{x,n}] 0\%$$

where,

S is the sum of (net) annual cash flows; $B_{x,t}$ and $C_{x,t}$ are the benefits and costs, respectively, for project x during year t of the n year analysis period.

- (b) Determine r_x the internal rate of return for project x , i.e., determine the non-negative discount rate or rates at which the discounted benefits just equal the discounted costs over the n -year analysis period). If there are multiple rates of return, list them in ascending order, as follows: $r_x^I, r_x^{II}, r_x^{III}, r_x^{IV}, \dots$; however, exclude all non-positive rates from this list; also, list each positive, repeating the rate separately.
- (c) When there is a single internal rate of return r_x or no positive rate of return and the sum of the annual cash flows is not equal to zero, accept or reject project x according to the following rules:

Condition	Sum of Annual Cash Flows is Positive	Sum of Annual Cash Flows is Negative
MARR < r_x	Accept project	Reject project
MARR > r_x	Reject project	Accept project
No positive r_x	Accept project	Reject project

When Marginal Average Rate of Return (MARR) and the internal rate of return are equal, one would be indifferent between acceptance and rejection.

Applying these rules to the example in Table 20.2 we would reject the project if the MARR was below 20 per cent accept it if the MARR was above 20 per cent, and be indifferent between acceptance and rejection if the MARR was just equal to 20 per cent.

- (d) When there are multiple rates of return and the sum of the annual cash flow is not equal to zero, accept or reject project according to the following rules, where r_x^I is the first positive IRR, r_x^* the second positive IRR, and so on:

Condition	Sum of Annual Cash Flows is Positive	Sum of Annual Cash Flows is Negative
MARR < r_x^I	Accept	Reject
r_x^I < MARR < r_x^{II}	Reject	Accept
r_x^{II} < MARR < r_x^{III}	Accept	Reject
r_x^{III} < MARR < r_x^{IV}	Reject	Accept

Note: Reversal pattern continues for additional rates of return.

Also, when MARR and an internal rate of return are equal, one would be indifferent between acceptance and rejection.

Table 20.2 Third example of the internal rate-of-return

Year	Cash Flow
0	+220
1	-144
2	-144
Sum of annual cash flow	-68
Internal rate of return	20%

Source: Wohl and Hendrickson 1984

For the example in Table 20.3, for which the annual cash flow sum is positive, the project would be accepted for a MARR below 8.52 per cent, rejected for a MARR between 8.52 and 18.66 per cent, accepted for a MARR between 18.66 and 73.57 per cent, and rejected for a MARR above 73.57 per cent. By contrast, for the example in Table 20.4, for which the annual cash flow sum is negative, the project would be rejected for a MARR below 3.85 per cent, accepted for a MARR between 3.85 and 4.99 per cent, and rejected for a MARR above 4.99 per cent.

Table 20.3 Annual cash flows (in \$10,000s) for a bridge improvement

End of Year t	Benefits B_t	Costs C_t	Benefits Less Costs $B_t - C_t$
0	-	50	-50
1	61	55	+6
2	63	0	+63
.	.	.	.
.	.	.	.
.	.	.	.
9	77	0	+77
10	79	70	-626
11	81	610	-529
12	83	495	-412
13	85	0	+85
.	.	.	.
.	.	.	.
.	.	.	.
29	117	0	+117
30	119	0	+119

Source and date: Wohl and Hendrickson 1984

Notes: Rates of return: $r_x' = 8.52\%$, $r_x'' = 18.66\%$, $r_x''' = 73.57\%$
Sum of net annual cash flows = +785

- (e) When the sum of the undiscounted (net) annual cash flows, or S , is zero, a more complex procedure must be adopted. Stated succinctly, we need to know the slope of the discounted cash flow function evaluated for an interest rate of zero. To this end, recall that the discounted value of the project's cash flow stream for an interest rate i is:

$$f(i) = \sum_{t=0}^n \frac{B_{x,t} - C_{x,t}}{(1+i)^t}$$

where,

$f(i)$ is the discounted value of the cash flow stream, expressed as a function of the interest rate i . In turn, the slope of the above discounted cash flow function is simply equal to the derivative of the function with respect to i or:

$$f'(i) = - \sum_{t=1}^n t \frac{[B_{x,t} - C_{x,t}]}{(1+i)^t + 1}$$

where,

$f'(i)$ is the discounted cash flow function for a project, expressed as a function of the interest rate i . When the slope of the function is evaluated at i equal to zero, the slope will be as follows:

$$f'(0) = - \sum_{t=1}^n t [B_{x,t} - C_{x,t}] \quad (12)$$

an expression which can easily be evaluated.

Do not overlook the negative sign for the slope in Equation 12. When there is a single internal rate of return, and thus r_x is equal to 0 per cent, accept the project when the slope, as computed by Equation 12, is positive and reject it when the slope is negative.

When there are multiple rates of return, the acceptance or rejection decision rules for a project, having an undiscounted cash flow stream equal to zero and a slope, as computed with Equation 12, will be as follows:

Condition	Slope of Discounted Cash Flow Function at $i = 0\%$	
	Positive	Negative
$MARR < r_x^I$	Accept	Reject
$r_x^I < MARR < r_x^{II}$	Reject	Accept
$r_x^{II} < MARR < r_x^{III}$	Accept	Reject
$r_x^{III} < MARR < r_x^{IV}$	Reject	Accept

Note: Reversal pattern continues for additional rates of return.

Table 20.4 Annual cash flows (in \$ 10,000s) for a local streetcar extension example

End of Year f	Benefits B_t	Costs C_t	Benefits Less Costs $B_t - C_t$
0	175	-175	
1	0	1265	-1265
2	250	0	+250
3	240	0	+240
4	230	0	+240
5	220	0	+220
.	.	.	.
.	.	.	.
.	.	.	.
19	80	0	+80
20	70	0	+70
21	60	0	+60
22	0	1900	-1900

Source: Wohl and Hendrickson 1984

Note: $r_x' = 3.85\%$, $r_x'' = 4.99\%$
Sum of net annual cash flows = -240

Also, when the MARR and an IRR are equal, one will be indifferent between acceptance and rejection.

For both projects, in Table 20.5 the sum of the undiscounted cash flows is zero and, thus, the above decision rules apply. Accordingly, and using Equation 12, the slope for the discounted cash flow function (at i equal to 0) is -200 for Alternative 1 and +200 for Alternative 2. Thus, Alternative 1 is acceptable when MARR is between 100 and 200 per cent and unacceptable when MARR is below 100 or above 200 per cent. Alternative 2 is acceptable when MARR is between 0 and 81.6 per cent and unacceptable when MARR is above 81.6 per cent. (Recall, however, that when listing and (labeling the internal rates of return any non-positive rates must be excluded.)

Table 20.5 Fourth example of cash flows and the internal rate-of-return method

Year	Alternative 1	Alternative 2
0	-100	-300
1	+600	+900
2	-1100	-700
3	+600	+100
Sum of annual cash flows	0	0
Rate of return r_x	$r_1' = 100\%$ $r_1'' = 200\%$	$r_2' = 81.6\%$
$r_{1/2}' = 85.1\%$		

Source: Wohl and Hendrickson 1984

Table 20.4 Annual cash flows (in \$ 10,000s) for a local streetcar extension example

End of Year f	Benefits B_t	Costs C_t	Benefits Less Costs $B_t - C_t$
0	175	-175	
1	0	1265	-1265
2	250	0	+250
3	240	0	+240
4	230	0	+240
5	220	0	+220
.	.	.	.
.	.	.	.
19	80	0	+80
20	70	0	+70
21	60	0	+60
22	0	1900	-1900

Source: Wohl and Hendrickson 1984

Note: $r'_x = 3.85\%$, $r''_x = 4.99\%$
Sum of net annual cash flows = -240

Also, when the MARR and an IRR are equal, one will be indifferent between acceptance and rejection.

For both projects, in Table 20.5 the sum of the undiscounted cash flows is zero and, thus, the above decision rules apply. Accordingly, and using Equation 12, the slope for the discounted cash flow function (at i equal to 0) is -200 for Alternative 1 and +200 for Alternative 2. Thus, Alternative 1 is acceptable when MARR is between 100 and 200 per cent and unacceptable when MARR is below 100 or above 200 per cent. Alternative 2 is acceptable when MARR is between 0 and 81.6 per cent and unacceptable when MARR is above 81.6 per cent. (Recall, however, that when listing and (labeling the internal rates of return any non-positive rates must be excluded.)

Table 20.5 Fourth example of cash flows and the internal rate-of-return method

Year	Alternative 1	Alternative 2
0	-100	-300
1	+600	+900
2	-1100	-700
3	+600	+100
Sum of annual cash flows	0	0
Rate of return r_x	$r'_1 = 100\%$ $r''_1 = 200\%$	$r'_2 = 81.6\%$
$r_{1/2}' = 85.1\%$		

Source: Wohl and Hendrickson 1984

Note: Zero rates of return have been excluded for r_1, r_2 and $r_{1/2}$

20.4.2 Revised Procedure for Ordering Mutually Exclusive Alternatives

An appropriate procedure for ordering mutually exclusive alternatives is crucial to a proper analysis and determination of the best project. The pitfalls of ordering on the basis of increasing initial costs are all too evident for examples similar to Tables 20.6 and 20.7. To avoid these and other problems, a revised ordering procedure has been developed, and this is given below.

- (a) Determine the sum of the undiscounted (net) annual cash flows for all alternatives.
- (b) List all alternatives in ascending order with respect to their annual cash flow sums (as computed above). However, if the annual cashflow sums for two or more alternatives are equal, determine the slope of each of their discounted cash flow functions evaluated at i equal to zero, as defined in Equation 12, and then list these alternatives in ascending order with respect to the algebraic value of the slopes. Thus, the alternative that has the most positive or least negative slope will be the highest-ordered alternative. Also, it is possible, though highly unlikely, that two or more alternatives would have equal cash flow sums and equal slopes for their discounted cash flow functions; in such a case it would be necessary to use the second or perhaps third derivative of those functions to determine the appropriate ordering.

Using the above rules, the appropriate ordering can differ markedly from the usual ordering rule which calls for ordering alternatives according to the initial year costs or outlays. For instance, the above rules would reverse the ordering of the alternatives as they are shown in Tables 20.6 and 20.7.

Table 20.6 Fourth example of cash flows and the internal rate-of-return method

Year	Alternative 1	Alternative 2
0	-100	-100
1	0	+20
2	+144	+120
Sum of annual cash flow	+44	+40
Rate of return	$r_1 = 20\%$ $r_{1/2} = 20\%$	$r_2 = 20\%$

Source: Wohl and Hendrickson, 1984

Note: r_x is the internal rate of return for alternative x , $r_{1/2}$ is the internal rate of return for the increment in benefits and costs between alternatives 1 and 2.

Table 20.7 Annual cash flows (in \$10,000s) for oil pump alternatives

Year t	Alternative 1		Alternative 2		Difference $\Delta B_t - \Delta C_t$
	$B_{1,t}$	$C_{1,t}$	$B_{2,t}$	$C_{2,t}$	
0	0	100	0	110	-10
1	70	0	115	0	+45
2	70	0	30	0	-40
Sum of net annual flows	+40		+35		-5
Rate of return					$r_{1/2}' = 21.92\%$
$r_1 = 25.69\%$					$r_{1/2}'' = 228.08\%$
$r_2 = 26.16\%$					

Source: Wohl and Hendrickson 1984

Note: $\Delta B_t = B_{2,t} - B_{1,t}$ and $\Delta C_t = C_{2,t} - C_{1,t}$. r_x is the internal rate of return for alternative x , $r_{1/2}'$, and $r_{1/2}''$ are the internal rates of return for the increment in benefits and costs between alternatives 1 and 2.

20.4.3 Revised Decision Rules for Determining the Best Alternative

The decision rules for using the IRR Method, to properly and consistently determine the best among a set of mutually exclusive alternatives, are described below. Of equal importance, is the necessity for a proper ordering of the alternatives for subsequent analysis; thus, it is mandatory that the ordering procedure described in Section 20.4.2 (or some variation thereof) be adopted as part of the project selection process. The overall set of rules is as follows:

- put all mutually exclusive alternatives in ascending order according to the procedure described in Section 20.4.2;
- beginning with the two lowest-ordered alternatives, determine $r_{1/2}$, the IRR for the increments in benefits and costs between the two alternatives; if there are multiple rates of return, list them in ascending order as follows: $r_{1/2}', r_{1/2}'', r_{1/2}''', \dots$; however, exclude all non-positive rates from this listing and list each positive repeating rate separately;
- when there is a single positive rate of return, the higher-ordered alternative of the two being compared will be preferable when MARR is less than r ; when MARR exceeds $r_{1/2}$ the lower-ordered alternative will be better; neither alternative is better when MARR just equals $r_{1/2}$; however, when there is a single rate of return which is equal to zero, the higher-ordered alternative will be preferable for any MARR value; and
- when there are multiple rates of return, the better of the two alternatives being compared can be determined from the following rules.

Condition	Preference Rule for the Better of Two Alternatives
$MARR < r_{1/2}^I$	Higher-Ordered Alternative
$r_{1/2}^I < MARR < r_{1/2}^{II}$	Lower-Ordered Alternative
$r_{1/2}^{II} < MARR < r_{1/2}^{III}$	Higher-Ordered Alternative
$r_{1/2}^{III} < MARR < r_{1/2}^{IV}$	Lower-Ordered Alternative

Note: Reversal pattern continues for additional rates of return.

Also, when MARR is equal to one of the rates of return, neither alternative is preferable.

- (e) Apply the above preferability test (i.e., in rule (d) shown above) to successively higher-ordered alternatives found to be preferable to lower-ordered ones. That is, if Alternative 2 is preferable to Alternative 1, then apply the test to Alternative 3 as compared to Alternative 2, and so forth. But if Alternative 1 is preferable to Alternative 2, then apply the test to Alternative 3 as compared to Alternative 1, and so forth.
- (f) Whenever all internal rates of return are non-positive or indeterminate, the higher-ordered alternative will be preferable.

Let us apply these rules to the examples in Table 20.5, 20.6, and 20.7.

For example, in Table 20.5, is first necessary to determine the slope of the discounted cash flow function (evaluated at i equal to zero) to properly order the alternatives. In this case, the slope for Alternative 1, as determined by Equation 12, was -200 and that for Alternative 2 was +200. Therefore, using the ordering rules in Section 20.4., Alternative 2 is the higher-ordered Alternative among the two and thus the ordering shown in Table 20.5 is correct. Accordingly, if MARR is less than 85.1 per cent, Alternative 2 is preferable, and if MARR is above 85.1 per cent, Alternative 1 is preferable.

For example, in Table 20.6, we first note that the two projects should be reordered with Alternative 1 being the higher-ordered one. Accordingly, we conclude that Alternative 1 is preferable if MARR is less than 20 per cent and that Alternative 2 is preferable if MARR is greater than 20 per cent.

For example, in Table 20.7 we again see that the two Alternatives should be reordered with Alternative 1 being the higher-ordered one. In turn, we conclude that Alternative 1 is preferable if MARR is less than 21.92 per cent or if MARR exceeds 228.08 per cent; Alternative 2 is preferable if MARR is between 21.92 and 228.08 per cent.

20.4.4 Determining the Best Acceptable Alternative

In the interest of brevity, no comprehensive treatment of this obviously important aspect of economic analysis is included here. Suffice it to say, however, that to jointly consider the aspects of acceptability and preference one simply follows the following procedure: (1) order all mutually exclusive alternatives,

using the procedure described in Section 20.4.; (2) determine the lowest-ordered acceptable alternative, using the rules described in Section 20.4.; and (3) determine the highest-ordered alternative, using the rules described in Section 20.4., that is found to be preferable to all lower-ordered acceptable alternatives.

20.5 GENERALIZED HEURISTICS

Educated guesses of likely traffic growth are important to the site-selection process of a road during the prefeasibility stage. Limitations of time, funds, and manpower rule out an economic analysis to forecast traffic growth. On the other hand, a first approximation of traffic growth is essential during the prefeasibility site-selection process to eliminate certain alternatives. The heuristics presented below are oriented to enable the development of broad, but sound, judgements regarding traffic growth. The conclusions from the application of the heuristics are useful in formulating the demand function for the LREP Method during the feasibility stage of a project.

- (a) Traffic growth is influenced by two categories of economic activity: potential growth areas and the existing patterns. Furthermore, the influence of growth areas on existing patterns can result in negative impacts that reduce the traffic demand from existing activities. All three systems are important for estimating the traffic growth.
- (b) Growth areas include the following:
 - o tourism,
 - o mining of new materials (minerals and forests),
 - o future exports (agriculture, horticulture, and cottage industry), and
 - o development projects (imports and exports).
- (c) Regarding the existing pattern, food deficits or surpluses will be important to travel demand, other existing imports (such as utensils) and exports (hides for example) will play a role in travel demand as well.
- (d) Negative impacts on the existing activities may result as a consequence of the road and/or growth of new activities. Impacts such as loss of cottage industry products, as well as the corresponding loss of employment, may occur due to cheaper and higher quality imports. Such imports give rise to traffic growth. Similarly, the displacement of porters due to the road facility will cause a readjustment of that labour force that may reduce or increase the traffic growth depending upon the possibilities for readjustments.
- (e) Experiences of traffic growth in other regions with similar characteristics are the substance that make educated guesses possible. Some typical experiences are given below for illustrative purposes. Impact studies on similar projects should be consulted in estimating traffic growth during the prefeasibility stage. Chapter 22.1 presents examples of some generalized heuristics' methods.

Founding of ICIMOD

The fundamental motivation for the founding of the first International Centre in the field of mountain area development was widespread recognition of the alarming environmental degradation of mountain habitats, and consequent increasing impoverishment of mountain communities. A coordinated and systematic effort on an international scale was deemed essential to design and implement more effective development responses to promote the sustained well-being of mountain communities.

The establishment of the Centre is based upon an agreement between His Majesty's Government of Nepal and the United Nations Educational, Scientific, and Cultural Organisation (UNESCO) signed in 1981. The Centre was inaugurated by the Prime Minister of Nepal in December, 1983, and began its professional activities in September, 1984.

The Centre, located in Kathmandu, the capital of the Kingdom of Nepal, enjoys the status of an autonomous international organisation.

Director : Dr. E. F. Tacke
Deputy Director : Dr. R. P. Yadav

Participating Countries of the Hindu Kush-Himalayan Region

o Afghanistan	o Bangladesh
o Bhutan	o Myanmar
o China	o India
o Nepal	o Pakistan



**INTERNATIONAL CENTRE FOR
INTEGRATED
MOUNTAIN DEVELOPMENT (ICIMOD)**
4/80 Jawalakhel, G.P.O. Box 3226,
Kathmandu, Nepal

Telex : 2439 ICIMOD NP
Cable : ICIMOD NEPAL
Telephone : 525313
Fax : 524509

